The 13th International Workshop on Targetry and Target Chemistry Proceedings

Risø-R-Report

WTTCXIII

Edited by :
Samar Haroun , SFU, TRIUMF; Alex Givskov and
Mikael Jensen , Risø DTU
Risø-R-1787(EN)
June 2011

Risø DTU
National Laboratory for Sustainable Energy

Author: Samar Haroun, SFU, TRIUMF; Alex Givskov and Mikael Jensen, Risø DTU
Title: The 13th International Workshop on Targetry and Target Chemistry Proceedings
Division: Division

Risø-R-1787(EN)
June 2011

Abstract:
This report contains the complete proceedings of the 13th International Workshop on Targetry and Target Chemistry. The Workshop was held at Risø National Laboratory for Sustainable Energy on July 26-28 2010.

The workshop deals with the development of methods and systems for efficient production of radioactive isotopes with accelerators. The WTTC series of workshops was initiated for the purpose of exchanging information about the problems and solutions associated with the production of radioisotopes for biomedical research and their applications to the diagnosis and treatment of disease. The goal of the WTTC is to advance the science associated with radioisotope production targetry. The Workshops are designed to bring experienced targetry scientists together with newcomers to the field, both from industry and academia, to discuss issues of targetry and target chemistry and approaches to exploring in situ target chemistry and the engineering required to optimize production yields. In the workshop, experience, ideas and information are freely and openly shared; learning and collaborations are fostered, with active participation by all attendees. This participation includes both formal and informal sessions. The present proceedings captures both submitted abstracts and the actual presentations showed during the very successful workshop meeting number 13 in the row, the WTTC13.

ISSN 0106-2840
ISBN 978-87-550-3920-9

Contract no.:

Group's own reg. no.:
(Føniks PSP-element)

Sponsorship:

Cover :

Pages:
Tables:
References:

Information Service Department
Risø National Laboratory for Sustainable Energy
Technical University of Denmark
P.O.Box 49
DK-4000 Roskilde
Denmark
Telephone +45 46774005
bibl@risoe.dtu.dk
Fax +45 46774013
www.risoe.dtu.dk

The WTTC13 is grateful for the support from the following sponsors without whom the workshop would have been impossible:

SIEMENS www.siemens.com/healthcare	GE Healthcare www.gehealthcare.com/tracercenter

Von Gahlen VON GAHLEN www.vongahlen.nl	**Arizona Carbon Foils** ACF METALS www.techexpo.com/firms/acf-metl.html	**Canberra** CANBERRA www.canberra.com
Best Cyclotron Systems Inc. Best www.teambest.com	**Bruce Technologies, Inc.** BRUCE TECHNOLOGIES High Performance Radionuclide Production Solutions www.brucetech-targets.com	**IBA** iba www.iba-worldwide.com/gateway
	Comecer COMECER www.comecer.com	

ACKNOWLEDGEMENTS

The workshop has been organised by the following "regional" cross boundary group of cyclotronists:

Mikael Jensen (Chairman), Hevesy Lab, Risø-DTU
Anders Sandell, Skaane Sygehus, Lund
Holger Jan Jensen, Rigshospitalet, Copenhagen
Søren B. Hansen, Århus PET Center, Århus

Our Institutions have contributed effort to the benefit of this meeting.

TABLE OF CONTENTS

Extending a Scintillation Counter's Dynamic Range

Lewis Carroll
Carroll & Ramsey Associates
Berkeley, CA, USA

Introduction Our compact, solid-state scintillation probes are widely used as HPLC / GC radiation detectors for quality assurance in PET/nuclear medicine research labs and radio-pharmacies. The detector probes operate in AC-coupled*, pulse-counting mode*, with a threshold discriminator to exclude noise and to minimize baseline fluctuation and drift.

The threshold discriminator is followed by an analog ratemeter to produce a voltage signal that is proportional to the time-rate of photon-induced pulses which exceed the pre-set threshold. Using this scheme, the ability to discern and evaluate the smallest radio-chromatography peaks – the minimum detectable signal – is governed by fluctuations in the base-line from ambient radiation background in the lab which, in turn, requires that the detector probe be well shielded so that it 'sees' only the radiation emanating from a loop of flow-tubing placed in tight proximity to the probe.

While this scheme is optimum for detection at low-to-moderate levels of radioactivity encountered in a typical quality-assurance radio-assay, pulse-counting detectors generally suffer from saturation effects due to counting system *dead-time* when exposed to high levels of radioactivity. In an effort to broaden the potential application of our scintillation detector products, we are engaged in an ongoing development program to enhance detector system linearity and dynamic range by reducing saturation effects at the 'high-end' while preserving system sensitivity at the 'low end'.

Stress-Testing at high count-rates To facilitate our development, we use home-made random pulse generators [1] operating in parallel. Each pulse generator drives its own light-emitting diode to simulate scintillation pulses (pulse width ~ 200 nsec) from a CsI(Tl) scintillator crystal. The fixed-amplitude, random light-pulses are pre-set to match the 511 KeV principal peak in our 1 cm^3 crystal, and are directed at a 1 cm^2 Si PIN diode + charge-integrating preamplifier (to include the effects of electronic noise inherent in a room-temperature semiconductor diode detector) all placed inside a light-tight enclosure to emulate our scintillation detector probe's 'front end'. Each generator delivers pulses at Poisson random intervals with an adjustable mean rate covering a range of ~100 pulses per second up to ~125K pulses per second. A pair of generators can produce a mean rate up to ~250K pulses per second, providing a convenient, readily-controllable source of detector system excitation over a wide range of count-rates, without having to handle large quantities of radioactive material. The 'Poisson-ness' of our random pulse generators was validated by recording the distribution of inter-pulse waiting times for various mean rates, using a calibrated time-to-amplitude converter plus multi-channel analyzer.

Extending Dynamic range In a radiation *counter*, input pulses which exceed a pre-determined threshold generate corresponding output pulses of fixed amplitude which, in turn, are either counted digitally or time-averaged in an analog rate-meter circuit. A different solution, now under development, entails giving up on the notion of pulse 'counting', *per se*, and replacing the standard threshold discriminator with a new circuit combining the functions of a threshold discriminator, a *pedestal generator,* and a *linear gate* [2]. The sketch below compares the input-output characteristic of a standard discriminator versus our new circuit.

The output of a standard discriminator circuit is zero for input pulses less than the threshold, and steps to a fixed, pre-determined value for input pulses which exceed the threshold. In the new circuit, the output is again zero for input pulses which are less than the threshold; when the input pulse exceeds the threshold, the output steps*, then linearly follows the amplitude of the input.*

The analog time-averaged (analog rate-meter) output signal from this circuit is proportional to the time-average of energy absorbed (i.e., dose-rate) in the detector probe. The new circuit retains the noise-reducing and drift-reducing advantages of a standard threshold discriminator at low count rates, but with the added advantage that integrated energy/amplitude information contained in

---

[1] G.H. White "The Generation of Random-Time Pulses at an Accurately Known Mean Rate and Having a Nearly Perfect Poisson Distribution" J. Sci Instrum. 1964, Vol 41

[2] W.R. Leo; Chapter 14.6 in Techniques for Nuclear and Particle Physics Experiments: A How-To Approach, Springer Verlag, ISBN 0-387-57280. New York, Berlin, Heidelberg, 1994

signal pulses which overlap and 'pile up' is preserved over a substantially greater range of input excitations. Our useful range now extends well beyond the point where a standard discriminator's output has 'flat-lined'.

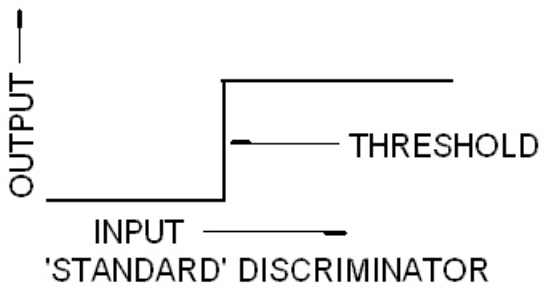

The plots below compare three different detector outputs versus input count rate excitation. The vertical scales are normalized so that all the curves are tangent at low input count rates. In our present system, 'busy time' for a single event is governed by the shaping-amplifier's pulse-width, which is on the order of ~25 micro-seconds – in our case a necessary but reasonable compromise between low dead-time and low noise floor. A wider system band-width (shorter shaping time-constant) would allow a narrower pulse which, in turn, would yield a higher maximum count rate, but that would come at the cost of a higher noise floor, requiring a correspondingly higher threshold setting, potentially compromising performance for lower-energy photon-emitters.

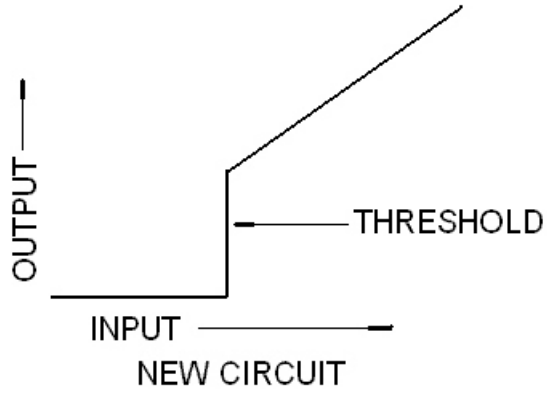

As shown below, the *digital* output count-rate peaks at ~17 kHz for 50 kHz input, then gradually declines due to a 'paralyzing dead-time' component [3] and finally plateaus at ~13 kHz . However, the analog-rate-meter – or analog average – of that same time-over-threshold discriminator signal has a significantly greater dynamic range, since the discriminator's output pulses vary in duration, staying 'high' when responding to multiple, overlapping input pulses as long as they are of sufficient amplitude to exceed the pre-set threshold. Of course the time-over-threshold analog-rate-meter's output eventually saturates as well, but with a gradual and asymptotic, 'non-paralyzing' characteristic.

New Circuit Our new discriminator circuit significantly extends the useable range of the detector. With this circuit, saturation effects begin to set in at ~150 kHz input count-rate, but the analog output is monotonic – still increasing – up to the present limit of our test apparatus.

The simplest, most common means to achieve detector system DC base-line stability – absolutely vital at low count-rates – is to employ capacitive AC coupling with base-line restoration at the input to the discriminator. That, however, combined with the shaping amplifier's constrained bandwidth, leads to a loss of 'DC-average' information, ultimately causing the apparent signal drop-off at high count rates.

We are currently revisiting many of our prior circuit design assumptions. At the time of this submission, we are seeing preliminary, albeit intriguing and very encouraging test-bench results suggesting there is reason to expect significant improvement over the results posted here.

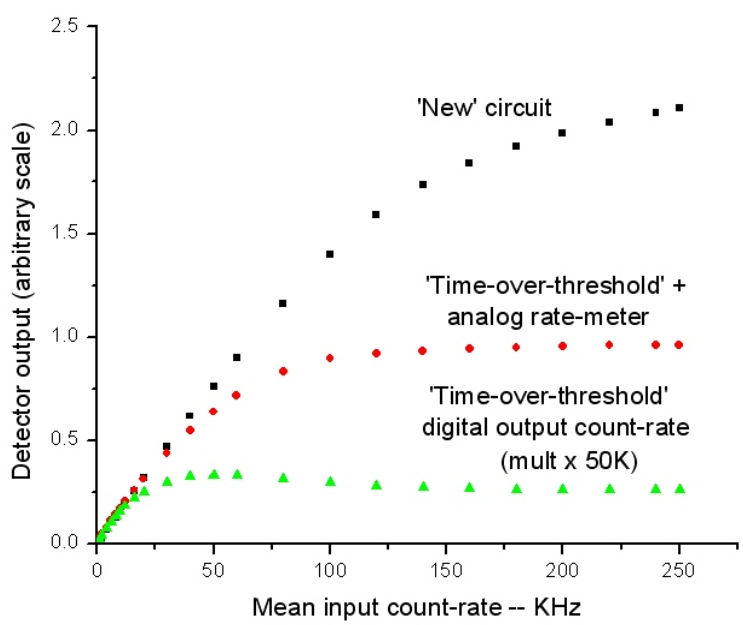

[3] Knoll, Glenn F; Chapter 3, sec. VII in Radiation Detection and Measurement; John Wiley and Sons New York, 1979.

Extending a Scintillation Counter's Dynamic Range

By
Lewis Carroll
Carroll & Ramsey Associates
Berkeley, CA USA
For
XIII Workshop on Targetry and Target Chemistry
Roskilde, Denmark July, 2010

Our solid-state radiation detector products are categorized according to two distinct modes of Signal Processing:

1)Pulse mode
2)DC-current mode

<u>Pulse mode</u> entails processing each detected photon event – pulse by pulse.

This permits the use of a *<u>threshold discriminator</u>* to eliminate noise and to minimize base-line fluctuation and drift.

Pulse mode is preferred for low to moderate levels of activity (e.g., analytic HPLC).

DC current mode integrates or averages the radiation-induced photo-current produced in the semiconductor diode.

There is no threshold discriminator in DC mode.

Hence this mode is more subject to base-line fluctuation and drift.

But since there is no processing of individual pulses, *there is no inherent saturation effect.*

DC Current mode is therefore preferred for use with higher activities (e.g., 'prep' HPLC).

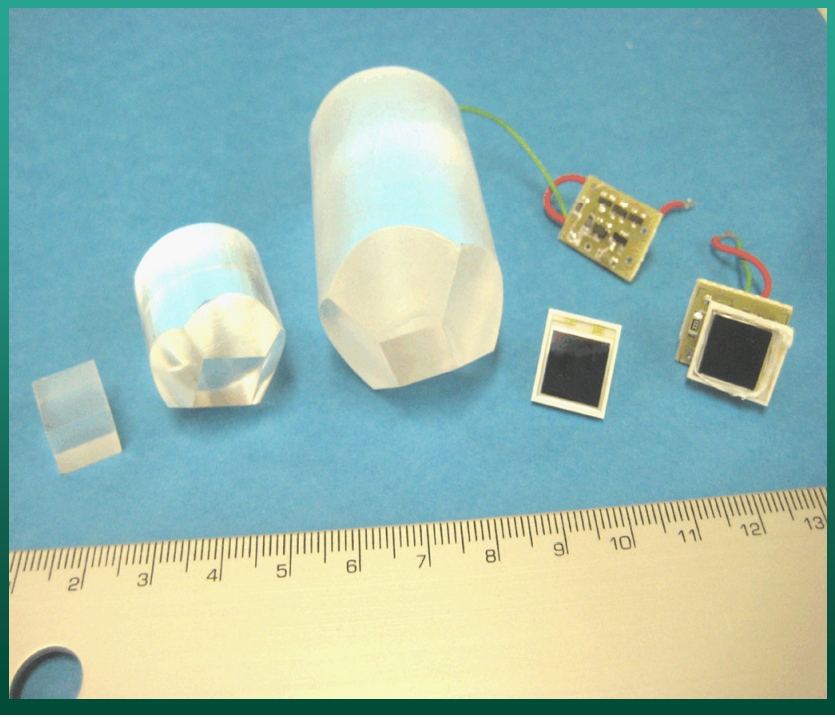

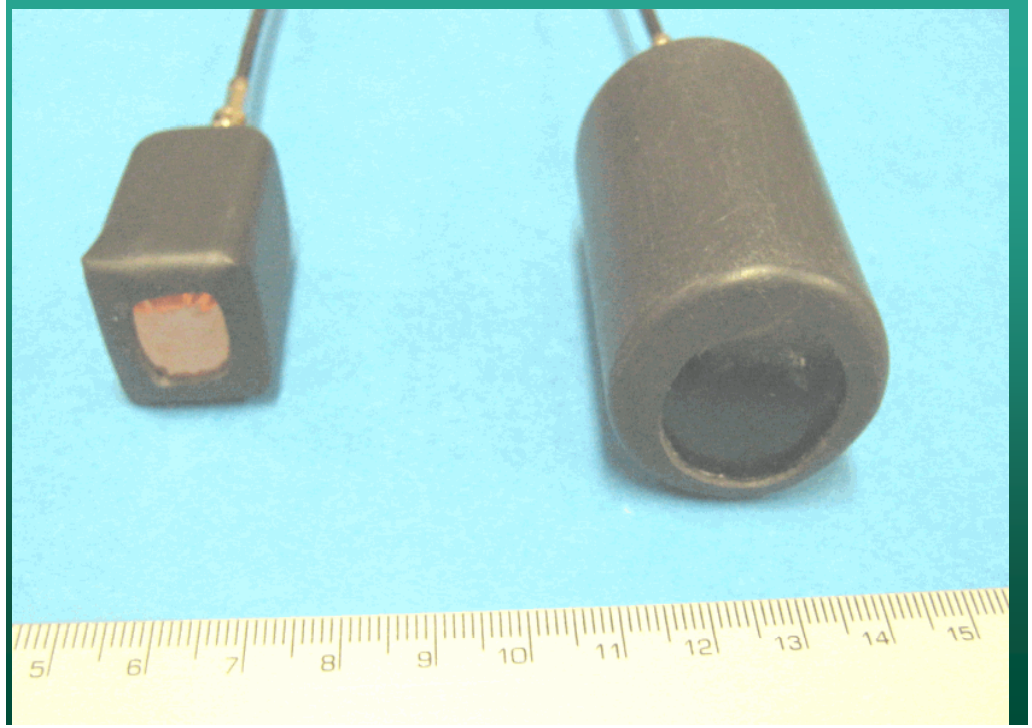

For low to moderate activity levels, we are committed to pulse mode for detection and quantitation of the smallest chromatography signal peaks.

Count rate in peaks is ~100 counts per Second (0.4 pA)

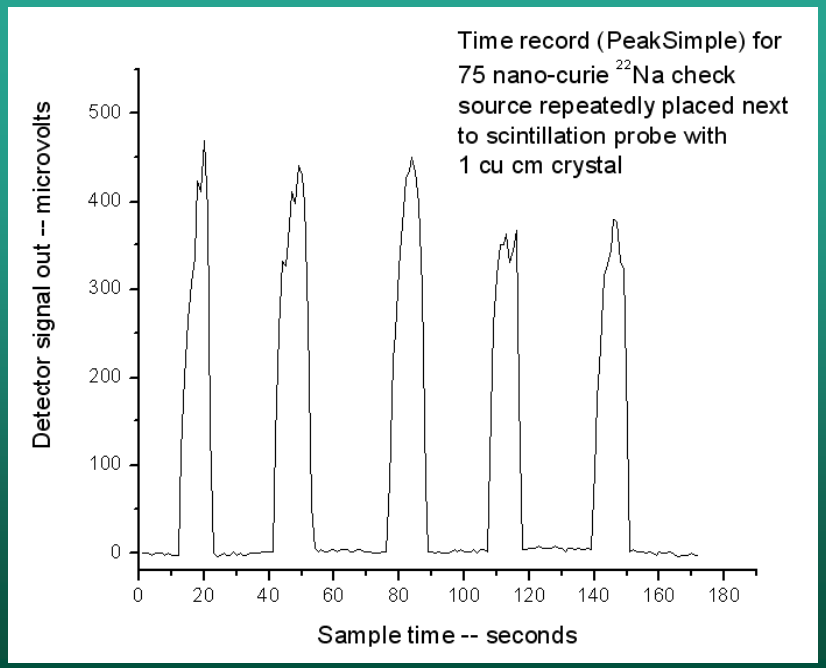

Same size crystal + photo-diode in DC current mode

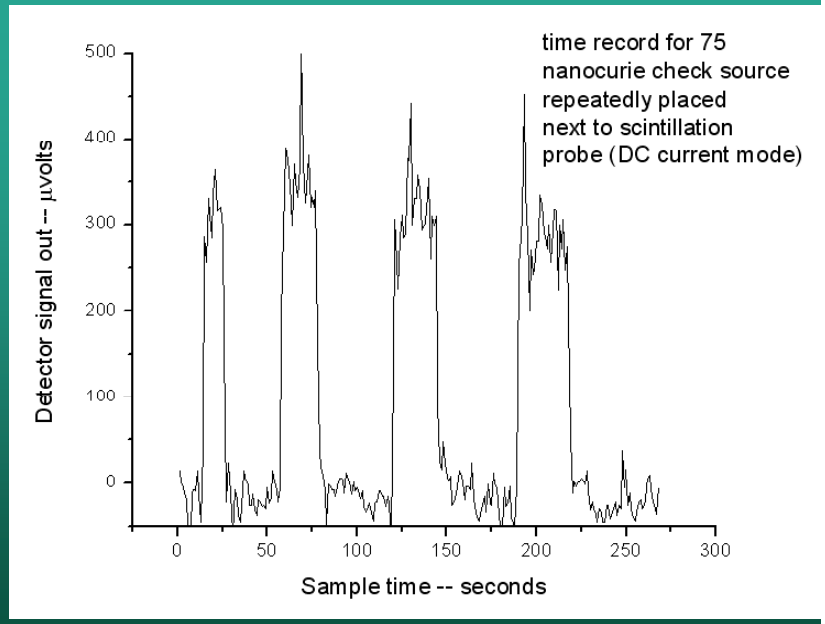

What happens at much higher levels of activity?

Any *pulse counting system* is subject to count-rate saturation effects at high activity levels.

‘Raw’ signal pulses from our semiconductor diode probe are approximated by $e^{(-t / (4\ \mu sec))}$

The ‘raw’ signal pulses are quite noisy and must be ‘shaped’ (smoothed and stretched) to ~25 μsec wide gaussian pulse to optimize signal-noise ratio.

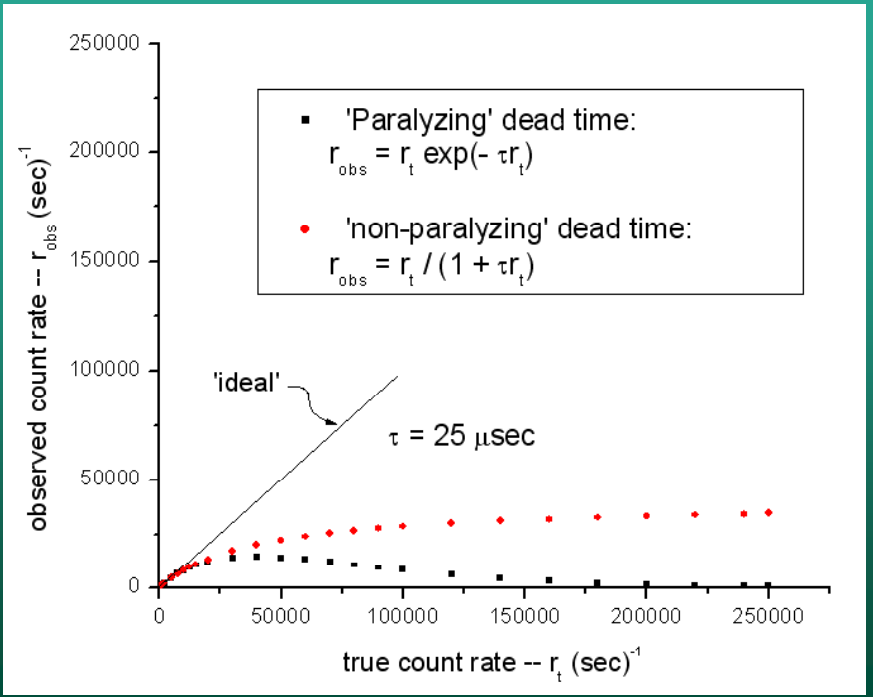

Is it possible to exploit the noise-rejecting properties of pulse-mode for low-to- moderate activity, and the inherent linearity of DC current mode for high activity?

Suppose we give up the notion of pulse ‘counting’, *per se*, and simply measure the mean value of the detector’s analog wave-form* to read radiation intensity.

* proportional to dose rate in the crystal volume

Introduce a new type of threshold discriminator circuit

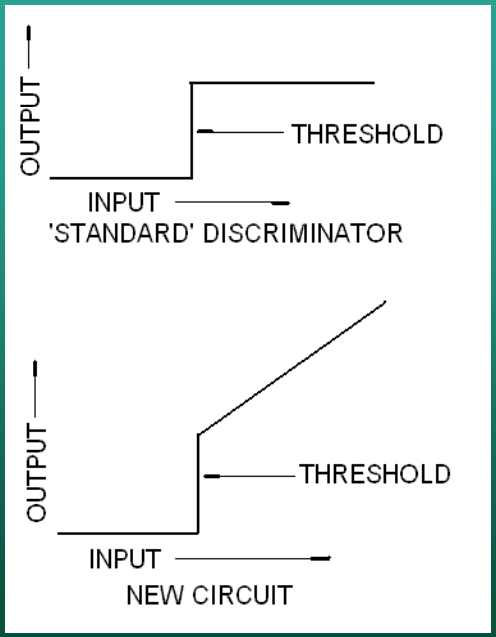

To facilitate our bench tests, we employ an ensemble of *Poisson* random pulse generators driving LED's to stimulate our scintillation detector at high count-rates.

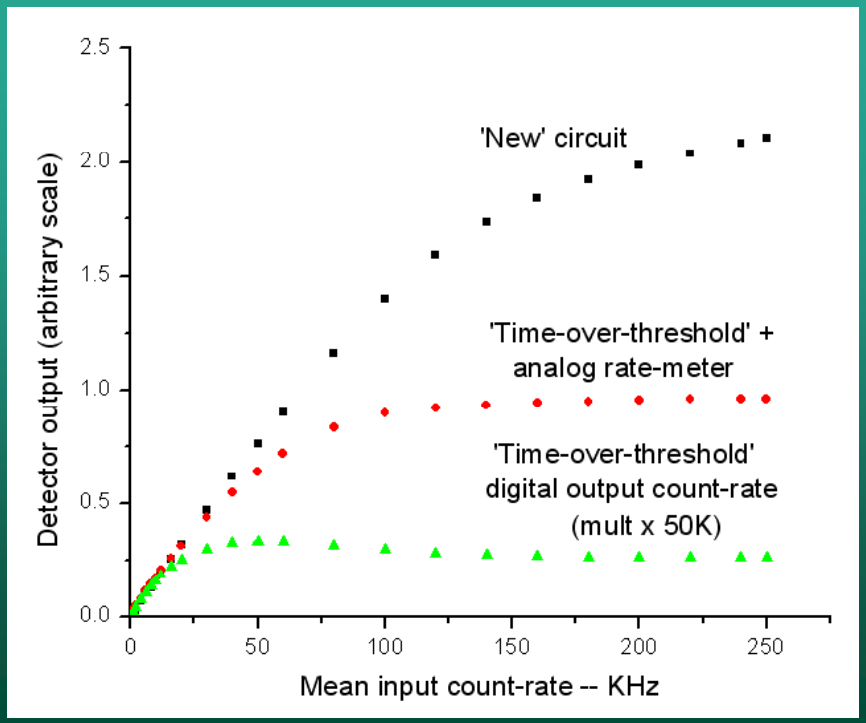

The saturating trend still evident with the 'new' discriminator circuit results from loss of 'DC-level' information due to capacitive interstage coupling.

While satisfactory for moderate count rates, capacitive interstage coupling, combined with our shaping amplifier's constrained band-width, is not well-suited for conditions of extreme count-rate overload.

Time for a major circuit revision!

Introduce DC interstage coupling.

At the input to the post-amplifier, we lock the signal base-line to a fixed reference, and let the signal envelope at the output of the post amplifier do what it will.....

(What does this mean?)

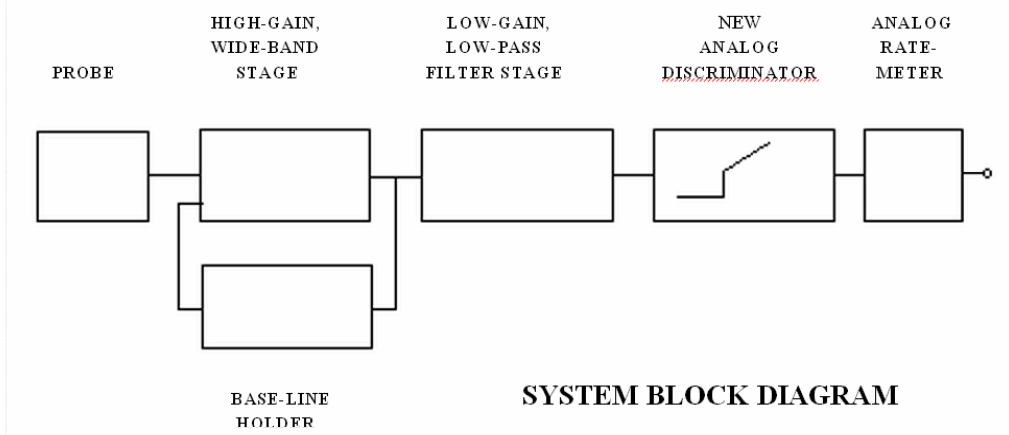

SYSTEM BLOCK DIAGRAM

Observe the signal at the output of the shaping amplifier

100 KHz

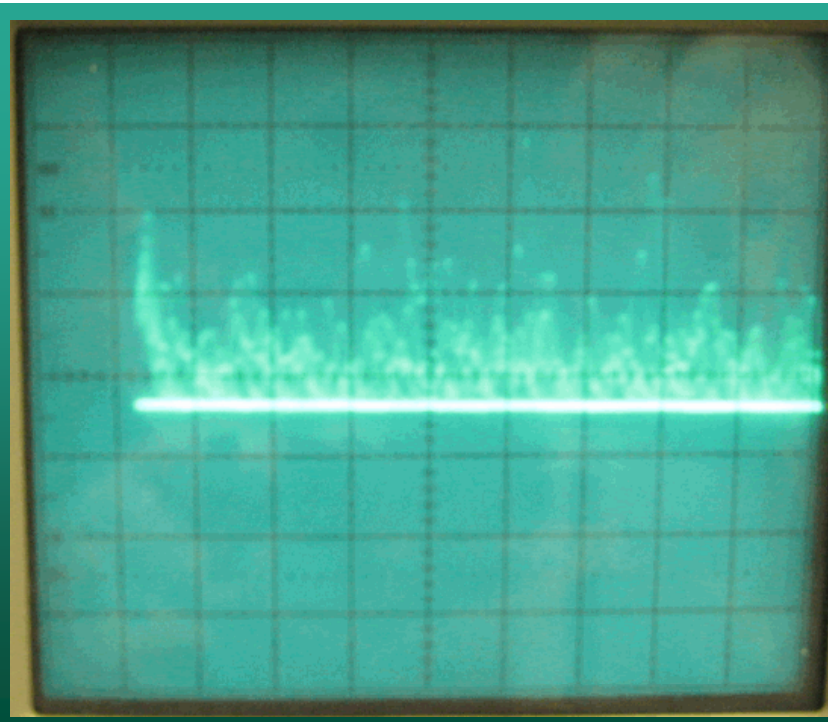

400 KHz

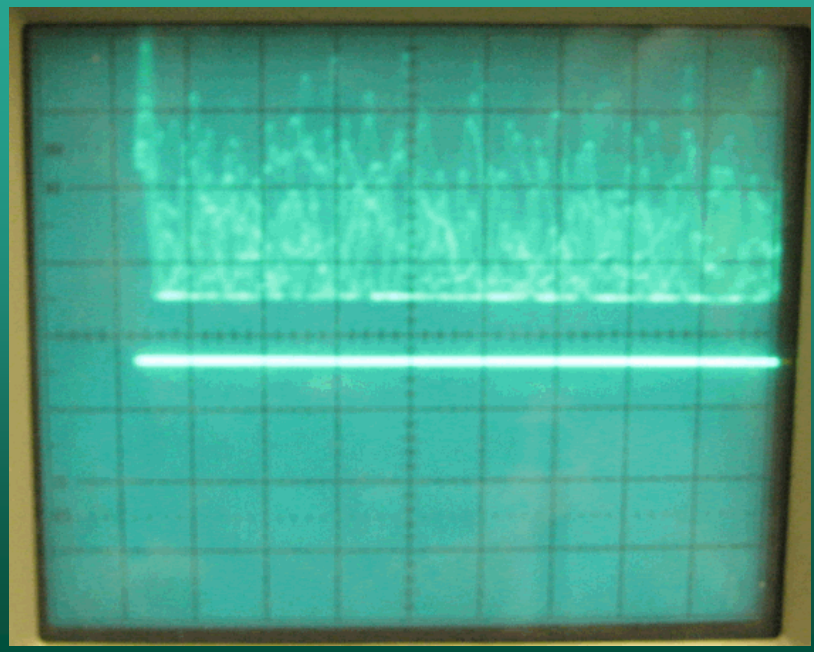

600 KHz

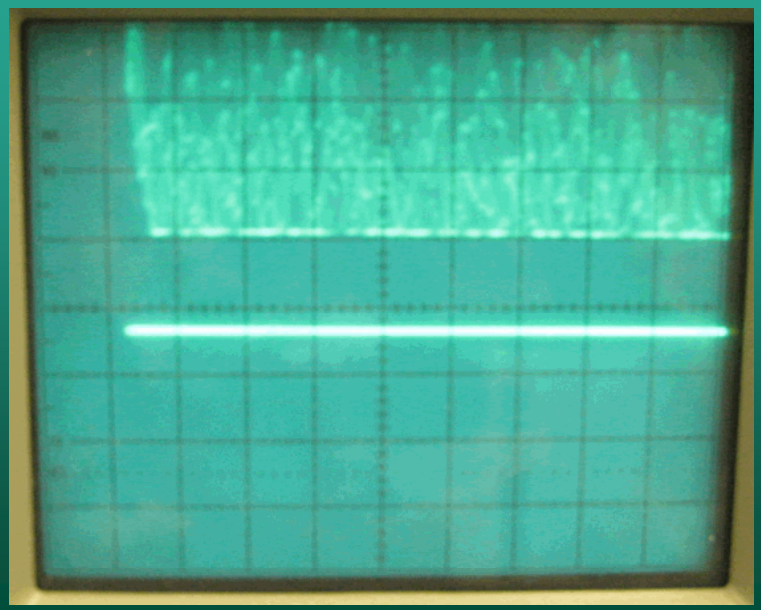

800 KHz

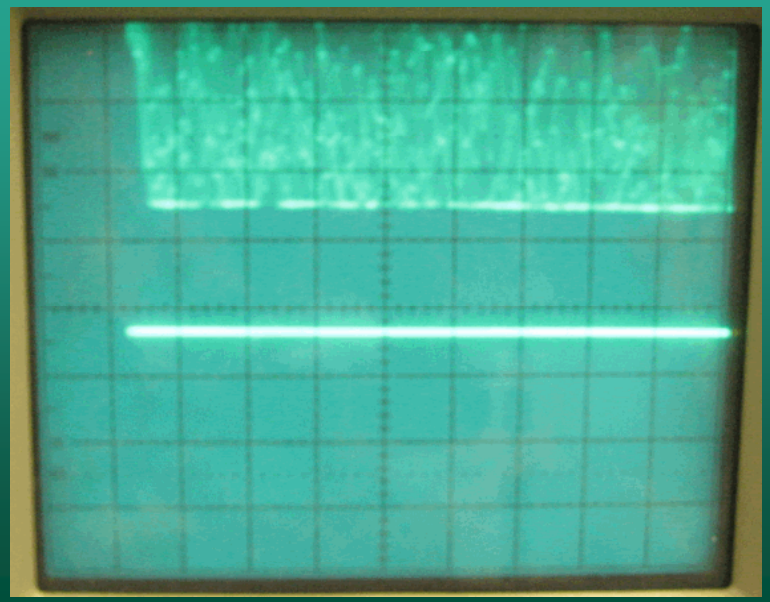

Under conditions of extreme pulse-rate overload, the entire signal envelope observed at the output of the shaping amplifier appears to ‘levitate’ relative to the fixed base-line reference.

Our new discriminator circuit accepts this as a valid signal.

As the signal base-line exceeds the discriminator threshold, the discriminator’s output is a *linear replica* of the input, yielding a proper measure of the signal’s mean value....

...As if we are operating in DC current mode !*

* A "stabilized base-line" and "DC current mode" are mutually exclusive….

A stabilized base-line, in conjunction with a threshold discriminator, is essential for noise-free detection at low excitations, but it is not compatible with true DC current mode operation.

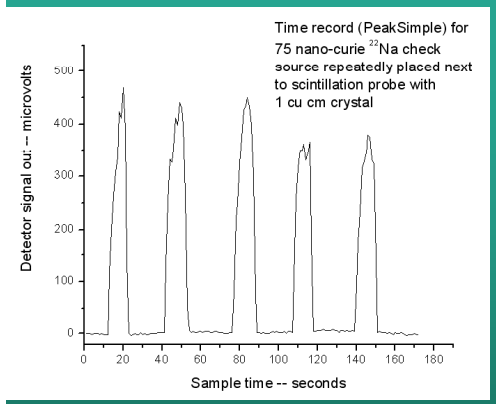

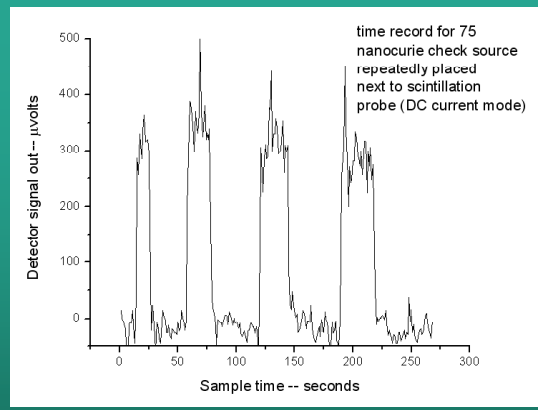

Recap: **Pulse mode**, including a threshold discriminator, is preferred at very low excitations due to 'cleaner' base-line and better detectability for weak signal peaks. **DC current mode** doesn't saturate, and is therefore preferred for very high excitations.

Our new scheme combines the best features of both modes of operation.

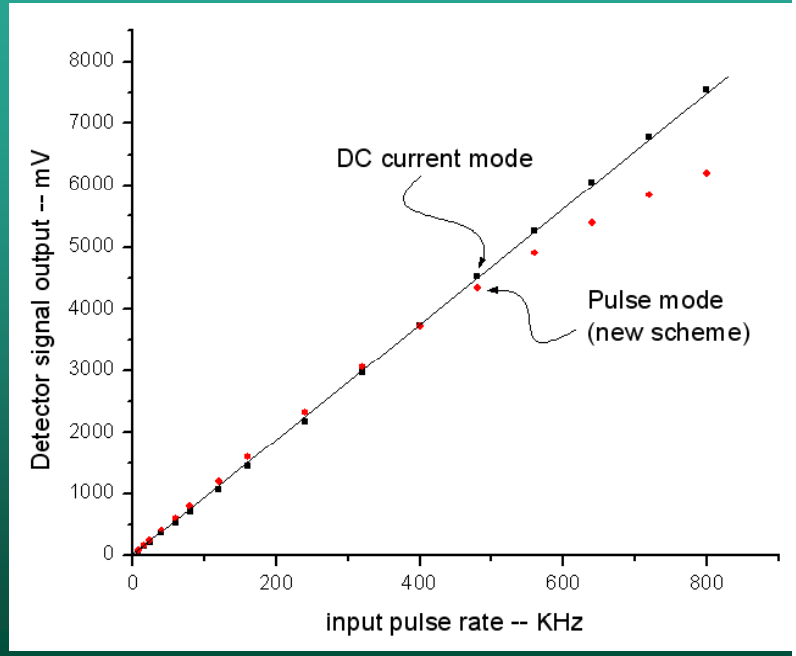

CONCLUSION: We have demonstrated a scintillation detector operating in sensitive pulse-mode at low excitation, having a linear dynamic range from a few tens of pulses per second to more than 500K per second ! *

*USA Patent Pending

WTTC XIII – Presentation Discussions

1. QC systems shall be validated
2. Good, effective, SOP must be implemented

Development of a target system at the baby cyclotron BC1710 for irradiation of solids and gases and the adaptation of existing target systems to the external beamline at the injector of COSY

B. Scholten, S. Spellerberg, W. Bolten, H. H. Coenen

Institute of Neurosciences and Medicine, INM-5: Nuclear Chemistry,
Forschungszentrum Jülich GmbH, 52425 Jülich, Germany

In former years most of our radionuclide development studies were done at the compact cyclotron CV 28 of the Forschungszentrum Jülich. Several dedicated target systems were constructed to irradiate solid and gaseous targets, either for cross section measurements or for production of radionuclides [1-16].

Due to the decommissioning of the compact cyclotron CV 28 in 2006 new target systems had to be developed at our baby cyclotron BC1710. This cyclotron is used to produce the light PET isotopes (^{18}F, ^{11}C, ^{13}N) in special gas chambers and in water targets. These specialized target systems are arranged in a target changing system with six positions. There was no target system at our BC1710 for the irradiation of solid targets and gas cells. So a beam line extension at the lowest position of the target changing system was constructed with a water cooled beam collimator and electrical insulation of the targets for beam current measurement. The front plate allows inserting different target holders close to the main end of the beam line. Target holders were constructed for the irradiation of foils and pellets in the stacked foil technique, which also allows irradiating powders in aluminum capsules. Furthermore, it is also possible to insert a slanting target for the production of radionuclides (i.e. ^{124}I, $^{120g+m}$I, ^{48}V) at higher currents. All target systems are water cooled. A special front plate was constructed for the external irradiation of gas cells. During the development of the target system several optimizations had to be done to collimate the beam and to increase the beam efficiency on the target.

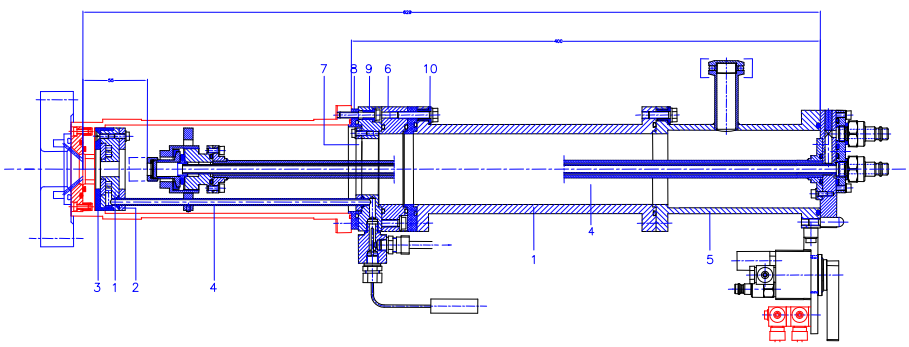

Fig. 1: Drawing of the beamtube extension at the BC 1710 with inserted stack foil holder.

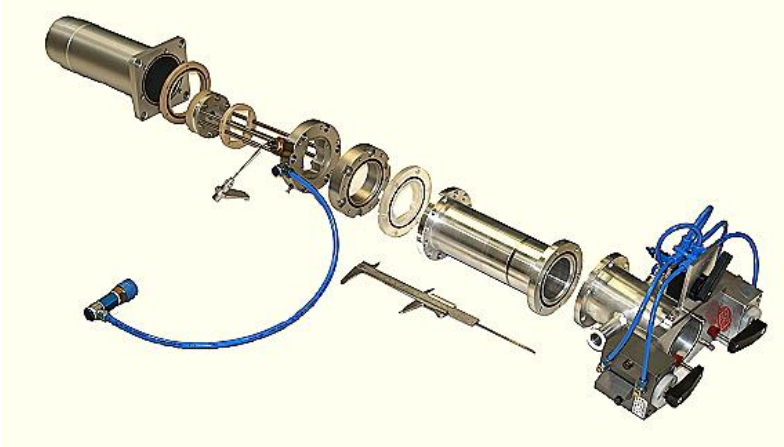

Fig. 2: Picture of the component parts of the BC1710 beamline extension before assembling.

At the injector of COSY an internal target system exists for the irradiation of targets in the stacked-foil mode using the just extracted beam of the cyclotron [17]. At this position there is a geometrical limitation for the target system and special care has to be taken that no contamination of the internal part of the cyclotron can happen. Intense water cooling of the targets is not possible there. Therefore an adaptation system at the end of an external beamline of the injector of COSY was developed which allows using all former target holder systems and dedicated targets developed earlier for the CV 28. In the adapter four adjustable water cooled sector absorbers are built in to collimate the beam. The beam windows are cooled by a helium gas stream. Manual remote control of the system is possible from outside the cyclotron vault and a PC based remote system is projected.

References:

[1] H. Michael et al., Int. J. Appl. Radiat. Isot., 32 (1981) 581 [2] G. Blessing et al., Int. J. Appl. Radiat. Isot., 33 (1982) 333 [3] K. Suzuki et al., Int. J. Appl. Radiat. Isot., 33 (1982) 1445 [4] S. M. Qaim and G. Stöcklin, Radiochim. Acta 34 (1983) 25 [5] G. Blessing and S. M. Qaim, Int. J. Appl. Radiat. Isot., 35 (1984) 927 [6] Z. Kovács et al., Int. J. Appl. Radiat. Isot., 36 (1985) 635 [7] S. M. Qaim, Progress in Radiopharmcy, Martinus Nijhoff Publishers, Dortrecht, The Nederlands (1986) 85 [8] G. Blessing et al., Int. J. Appl. Radiat. Isot., 37 (1986) 1135 [9] S. M. Qaim et al., Proc. 2nd Workshop on Targetry and Target Chemistry, Heidelberg 1987, DKFZ, Heidelberg (1988) 50 [10] S. M. Qaim, Proc. Second International Symposium on Advanced Nuclear Energy Research - Evolution by Accelerators, Mito, Japan1990, JAERI (1990) 98 [11] G. Blessing and S.M. Qaim, Appl. Radiat. Isot., 41 (1990) 1229 [12] G. Blessing et al., Appl. Radiat. Isot., 43 (1992) 455 [13] G. Blessing et al., Appl. Radiat. Isot., 48 (1997) 37 [14] S. Spellerberg et al., Appl. Radiat. Isot., 49 (1998) 1519 [15] E. Hess et al., Appl. Radiat. Isot., 52 (2000) 1431 [16] S. M. Qaim et al., Appl. Radiat. Isot., 58 (2003) 69 [17] G. Blessing et al., Appl. Radiat. Isot. 46 (1995) 955

Mitglied der Helmholtz-Gemeinschaft

JÜLICH FORSCHUNGSZENTRUM

Development of a target system at the baby cyclotron BC1710 for irradiation of solids and gases and the adaptation of existing target systems to the external beamline at the injector of COSY

B. Scholten, S. Spellerberg, W. Bolten, H. H. Coenen

Institute of Neurosciences and Medicine, INM-5: Nuclear Chemistry, Forschungszentrum Jülich GmbH, 52425 Jülich, Germany

JÜLICH FORSCHUNGSZENTRUM

Accelerators at FZ Jülich

- **BC1710: 17 MeV p, 10 MeV d**
- GE PET Trace: 16.5 MeV p, 8.4 MeV d
- **Injector of COSY: 45 MeV p, 75 MeV d (IKP)**
- IBA 18/9: 18 MeV p, 9 MeV d (ICG)
- IBA C30a: 15-30 MeV p, 7-15 MeV d , 30 MeV ^{4}He

Cooperations:

- Vrije Universiteit Brussel, CGR-560 Cyclotron: 42 MeV p, 22 MeV d, 50 MeV ^{3}He, 43 MeV ^{4}He
- iThemba LABS, Faure, SA: 200 MeV p

JÜLICH FORSCHUNGSZENTRUM

Baby Cyclotron BC 1710

Japan Steel Works, installed in 1986

Dedicated to the production of short-lived PET radioisotopes:

- ^{14}N(p,α)^{11}C (gas target)
- ^{18}O(p,n)^{18}F (water target)
- ^{16}O(p, α)^{13}N (water target)

Vertical target changer unit with 6 target positions

No research targets existed for solid and gas samples so far

JÜLICH FORSCHUNGSZENTRUM

BC 1710 Target Changer

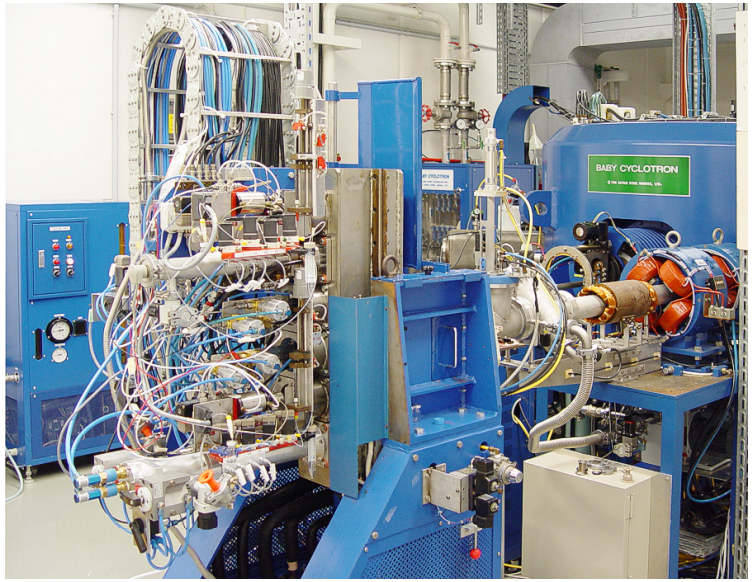

Beam Line Extension at BC 1710

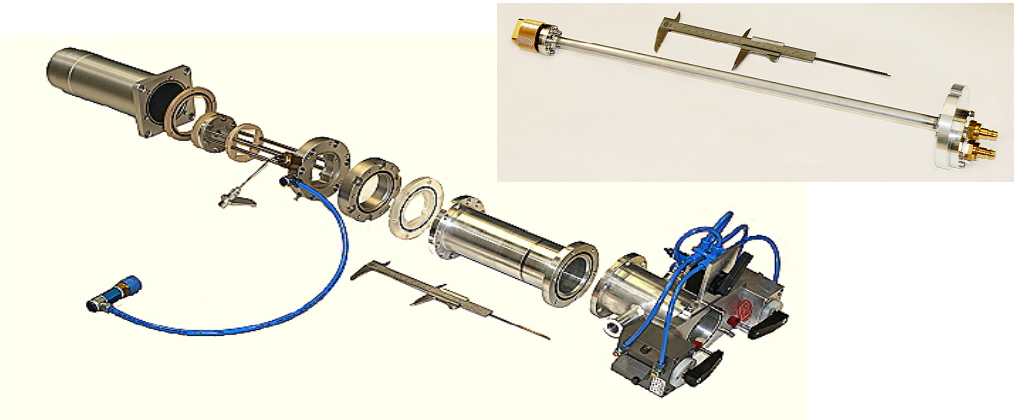

- A beamline extension was constructed for lowest target changer position.
- Water cooled collimator, insulators from peek or plexiglas
- Target vacuum separate from cyclotron vacuum
- Long target rod for solid target systems with water cooling

Target Systems at BC 1710

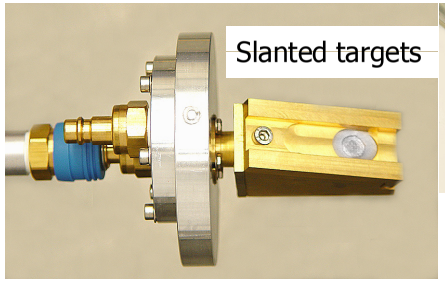

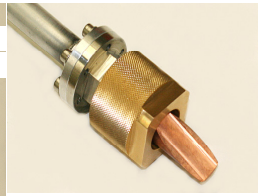

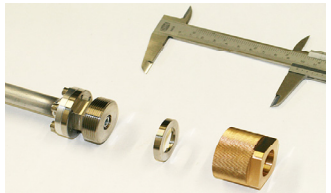

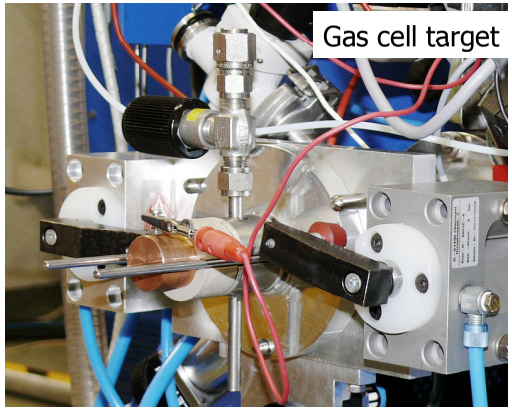

Stacked-foil target holder

Injector of COSY

- Isochronous cyclotron JULIC commissioned in 1968
- Positive light and heavy ions up to 45 MeV/nucleon.
- 1990/91 converted as COSY injector (76 MeV H_2^+)
- 1996 H^- (45 MeV) / 2000 D^- (75 MeV)

- Internal radiation possible
- External beamline was used by other groups so far

- Existing sophisticated target systems for CV28 should be adapted to external beamline
- Remote control from outside the cyclotron vault required

Beamline at JULIC

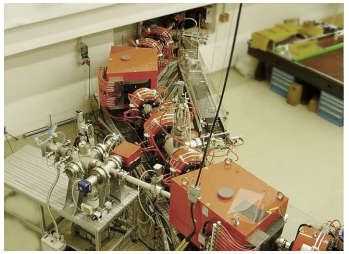

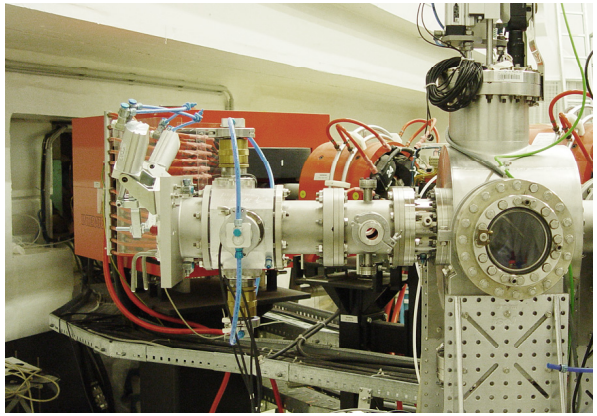

- Adapter with water cooled 4 sector collimators
- Vacuum separated from cyclotron
- Possiblity to adapt existing target holder systems (stacked-foil, Kr-target, slanting target, etc.)
- Electrical beam current measurement
- Remote controlled by hand, forseen by PC

IBA C30a

Replacement for CV28 and BC 1710

- Protons: 30 - 15 MeV, 1 - 350 µA
- Deuterons: 15 - 7 MeV, 50 µA
- Alpha particles: fixed 30 MeV, > 50 µA

- Dual beam mode for protons and deuterons

- New building with cyclotron vault and GMP PET laboratory (2011)
- Two external beamlines in separate vault
- New institute building (2014)

WTTC XIII – Presentation Discussions

1. Production of 74As?
   - Dependent on demand, although more production=more demand

Search for the ideal cyclotron stripper foil

John O. Stoner, Jr.

ACF-Metals, The Arizona Carbon Foil Co., Inc.
2239 E. Kleindale Road
Tucson, Arizona 85719-2440 U.S.A.
<metalfoil@cox.net>

Although carbon stripper foils can now be obtained in any thickness desired by the cyclotron user, it is still necessary to replace foils occasionally because of their finite lifetimes. Limits on lifetime occur because of poor mounting, vacuum disasters, mechanical shock, nuclear collisions (causing violent atomic displacements), thickening, nuclear and electronic heating with resulting evaporation and diffusion, erosion by residual gas, and many other effects. Beam currents are increasing steadily; this trend is expected to continue. Most problems are accentuated at higher beam currents. ACF-Metals is searching through foil compositions, allotropes and mounting methods to identify promising routes to obtaining longer-lasting foils.

Carbon Foils:

feature

Thickness <1 nm to >20 µm

Amorphous, graphitic, or pyrolytic

Low Z, High strength

Withstand high temperature

ACF-Metals

2239 E. Kleindale Road

Tucson AZ 85719

<metalfoil@cox.net>

Why ACF-Metals?

High quality foils; experienced personnel.

Flexible production of unusual types.

Quantity production of standard foils.

Continuing research to improve:

- **Materials & frames**
- **Foil longevity**
- **Operation in extreme conditions**

SNS

(Oak Ridge)

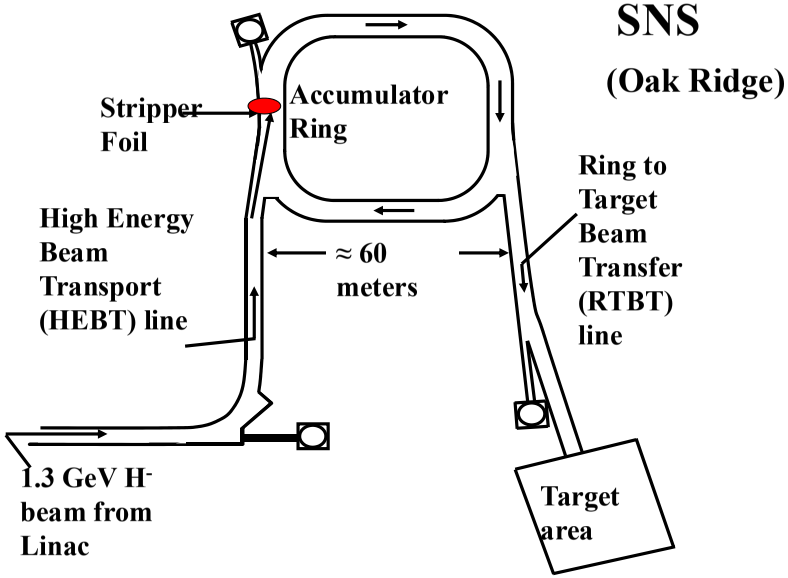

Accelerator Cost: approx. 1B $ (1 G$)
Stripper foil ~1 cm x 5 cm
One carbon stripper foil cost: approx. $300

Research:

Better mountings for longer lifetimes

Example: Fiber-mounted foils for SNS and other accelerators.

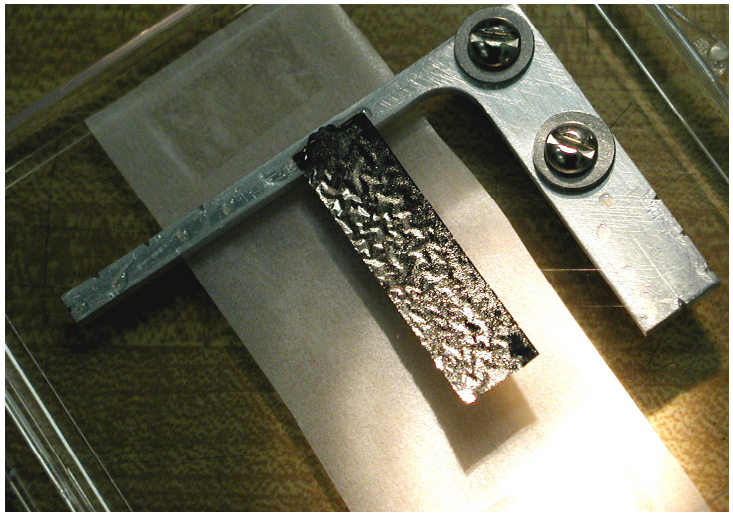

3-micron C foils on tungsten frames

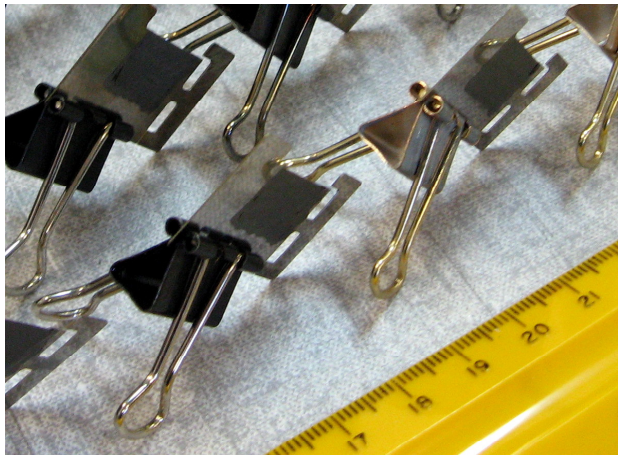

IMG_5572_1.JPG

Carbon foil, 1/2 micron thick, on cyclotron fork

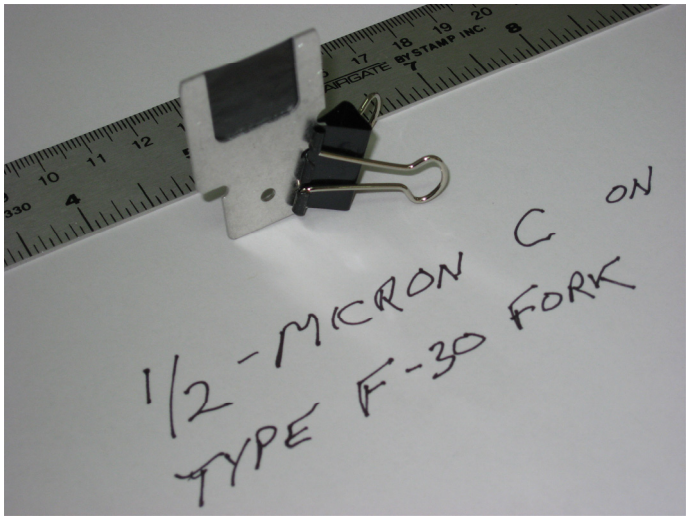

One-piece aluminum foil, 10 μg/cm^2 (40 nm thick) on supporting mesh, ready for shipment.

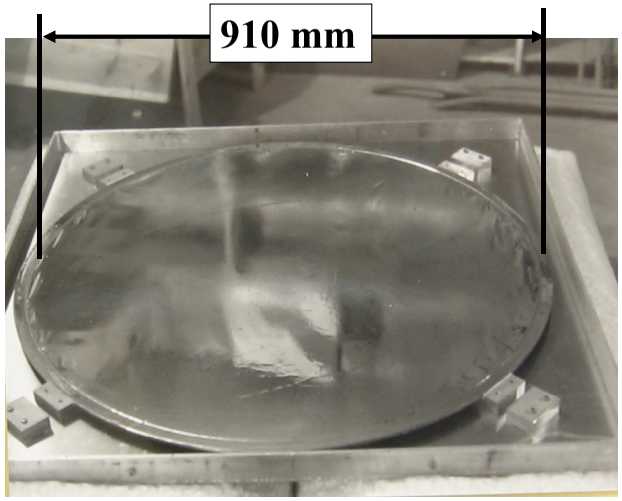

IMG_9162.JPG

<u>Research:</u>

<u>The frontier:</u> Foils to withstand the highest temperatures, the largest beam currents, in corrosive environments, for the longest times.

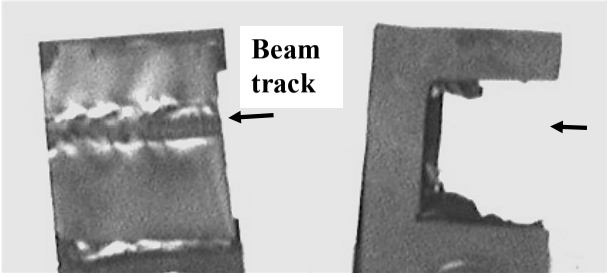

Hotspot™ ACF foil withstood 3500 K !

The other foil didn't.

Carbon Foils:

feature

Thickness <1 nm to >20 µm

Amorphous, graphitic, or pyrolytic

Low Z, High strength

Withstand high temperature

ACF-Metals

2239 E. Kleindale Road

Tucson AZ 85719

<metalfoil@cox.net>

WTTC XIII – Presentation Discussions

1. Foil maintenance
   - Ramp up beam slowly
   - Storage: Desiccators/refrigerators not needed

New Gaseous Xenon Target for ^{123}I Production

Jožef J. Čomor[1], Đuro Jovanović[1], Jean-Michel Geets[2], Bernard Lambert[3]

[1]ELEX Commerce, Hilandarska 28, 11000 Belgrade, Serbia
[2]IBA Molecular, Chemin du Cyclotron 3, 1348 Louvain-la-Neuve, Belgium
[3]IBA Molecular Europe, Le christ de Saclay B.P. 32, 91192 Gif-Sur-Yvette, France

^{123}I is one of the best suited radionuclides for SPECT (Single Photon Emission Computed Tomography) due to its short half life (13.2 h) and low absorbed dose in patients for its low energy gamma emission (154 keV), which is ideal for detection by common scintillation detectors. It is most commonly produced in gaseous Xe targets irradiating highly enriched ^{124}Xe by 30 MeV protons and exploiting the indirect production path via ^{123}Xe. This technology is well established and performed in several cyclotron centers; however radiation safety aspects and the danger of losing the expensive target material are always a concern. Thus, every effort is needed to ensure that the target remains tight during irradiation, while the service and maintenance should be quick and reliable in order to reduce the dose received by the personnel.

The most critical part of every gaseous target is the double window system, there are two possible approaches in handling this issue: hard bolting the windows via flanges and metal seals to the target body, or using window packages, which can be remotely replaced prior failure of elastomer seals. The first approach allows for long periods between scheduled replacements of the target assembly (approx. once in 12 months); however the radiation dose received by the operator during this maintenance is substantial. Moreover, one needs at least two complete targets for uninterrupted production (one in operation while the other is cooling down for maintenance). The second approach requires more frequent replacement of the window package (approx. once in 3 months) without any radiation hazard for the operators.

It is obvious that this second approach is more favorable, thus the new target station has been developed following this concept, with the aim to provide more reliable operation than what the existing target stations can provide. To this end a new mechanism for window foil package replacement has been designed. Unlike the previous target stations, it has no robotic arm. Moreover, there are no sliding seal based connections for compressed air and helium, thus the reliability of the window package replacement mechanism is greatly increased and in the same time the possibility of losing the target material from the helium cooling loop in case of window burst is negligible.

In addition, the target locking mechanism has been also improved: previous designs relied on uninterrupted compressed air supply, thus in case of accidental burst of supply tubing during the irradiation the enriched target material would be lost and the vault would be heavily contaminated. The new locking mechanism keeps the target chamber normally locked. Compressed air is needed only for unlocking the target chamber for window package replacement, i.e. the safety of the target station does not depend on external factors.

The target is patent pending and detailled design will be presented later on (at time of conference).

iba & ELEX COMMERCE

New Gaseous Xenon Target for ^{123}I Production

Jožef Čomor
Đuro Jovanović
Jean-Michel Geets
Bernard Lambert

State of the art

- **Irradiation of gaseous ^{124}Xe is the most cost effective way for large-scale ^{123}I production**
- **There are two common approaches to the target design:**
  - Hard bolted flanges fixing the windows to the target body (R. Robertson, D.C. Stuart, US4,622,201; W.Z. Gelbart, R.A. Pavan, S.K. Zeisler, CA2691484)
  - Windows pre-assembled into remotely exchangeable packages (V. Bechtold, H. Schweickert, US4,945,251 and the KIPROS target station)

Nordion/Triumf/ACSI approach

- **The good:**
  - Very high current acceptance and yield
  - Infrequent (annual) target maintenance
- **The bad:**
  - At least two target sets are needed for normal operation
  - Very high dose delivered to the operators during maintenance

KIPROS approach

- **The good:**
  - High current acceptance and yield
  - Remote target maintenance – minimum dose to the operators
  - Affordable replacement window packages
- **The bad:**
  - The sliding seals used in the robotic arm might fail unexpectedly due to radiation damage

What if a new system is to be designed?

- **The remote exchange of window packages is a great advantage (ALARA principle)**
- **Therefore, follow this principle and in addition:**
  - Simplify the window package replacement mechanism
  - Design a fool-proof insertion principle (the orientation of the double window insert is crucial)
  - Design a fool-proof target locking mechanism

The basic idea

- **… was in fact in the backyard:**

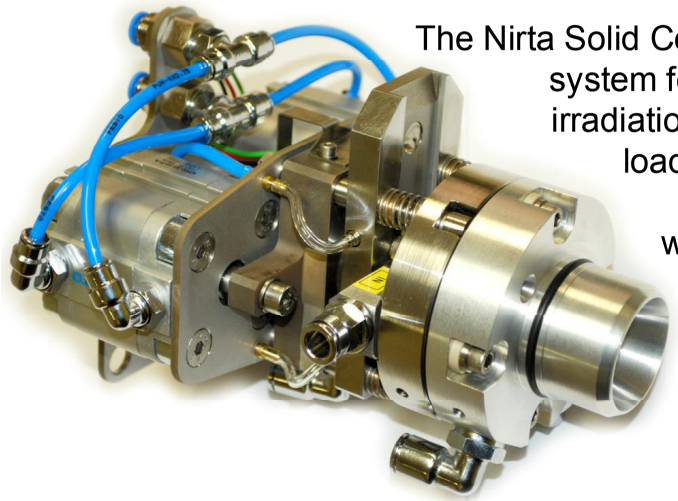

The Nirta Solid Compact target system for solid target irradiation can be pre-loaded with three target disks, which are then irradiated one by one

The concept

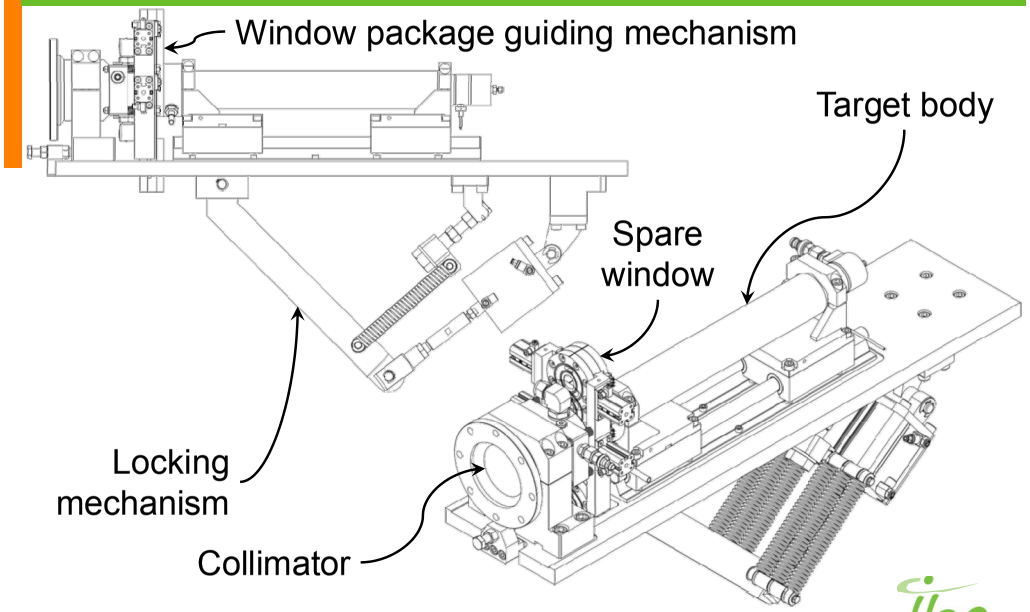

Principle of operation (1/2)

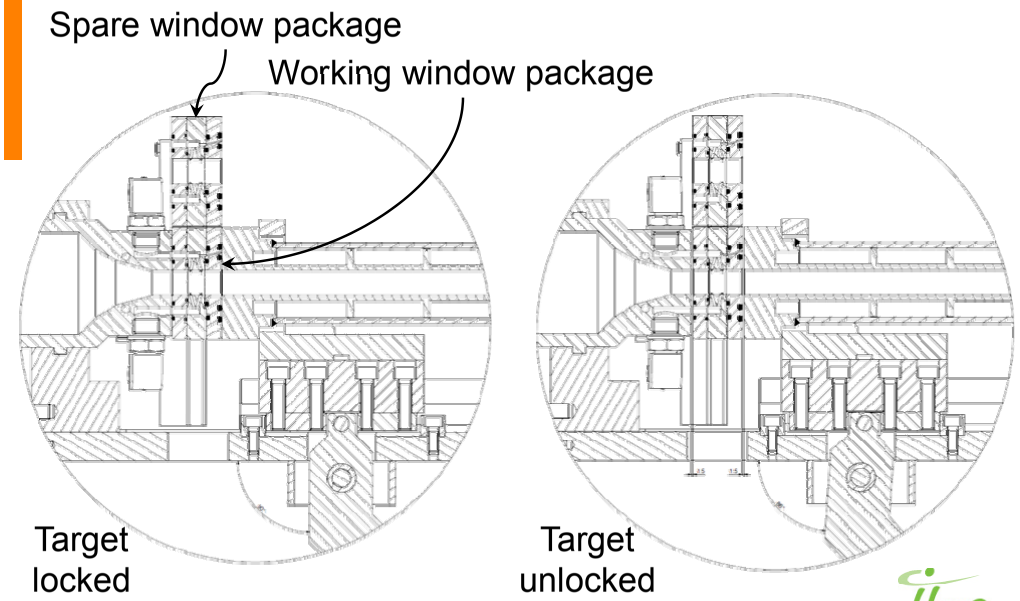

Principle of operation (2/2)

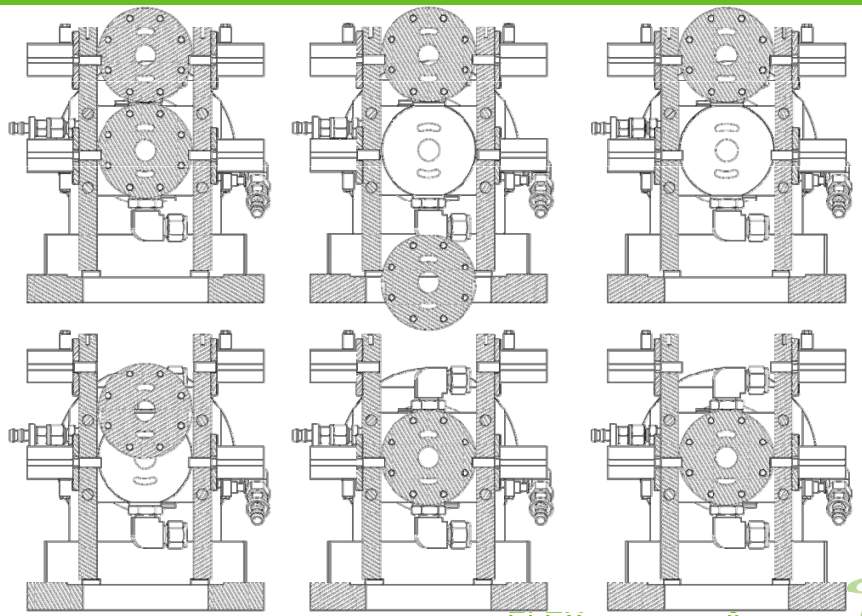

The real hardware (1/4)

The assembled window package

The real hardware (2/4)

Parts of the window package

The real hardware (3/4)

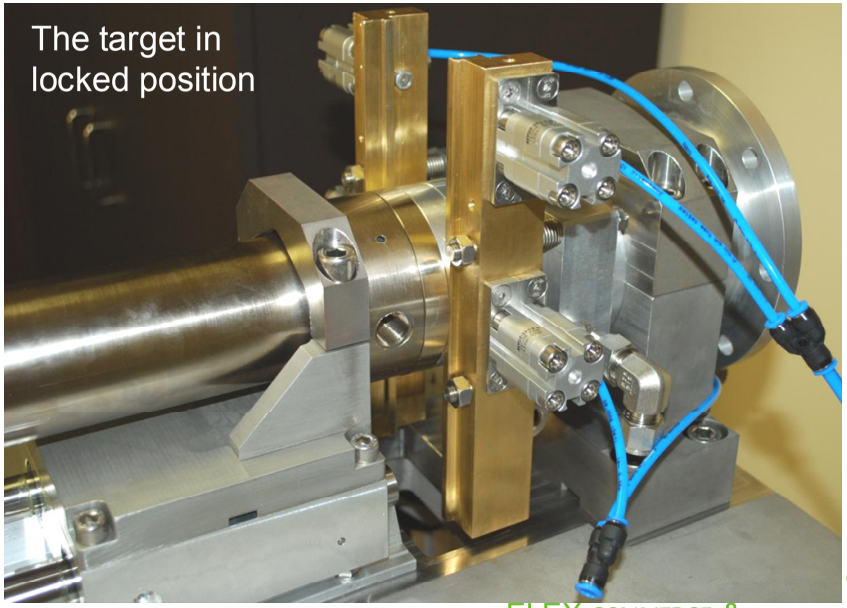

The real hardware (4/4)

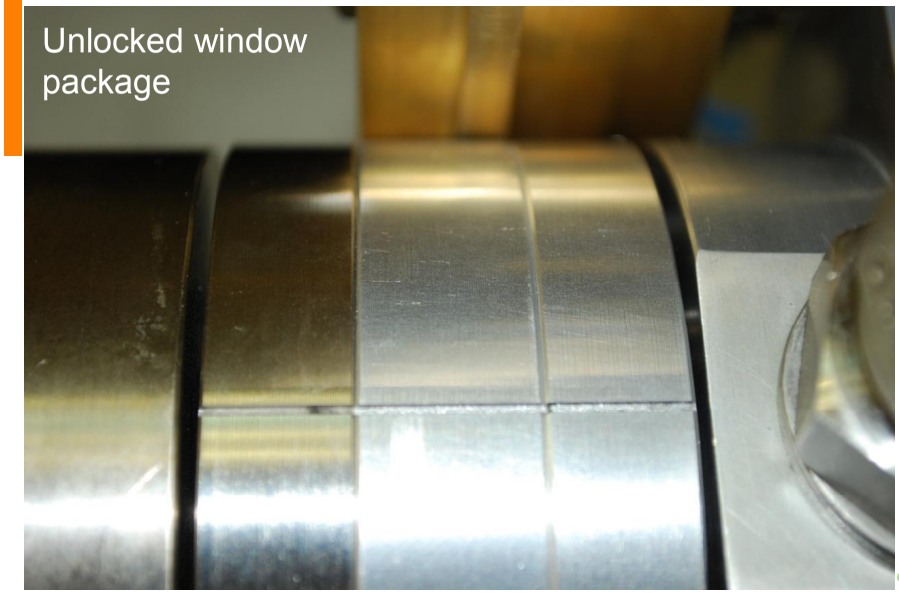

The complete scheme of operation

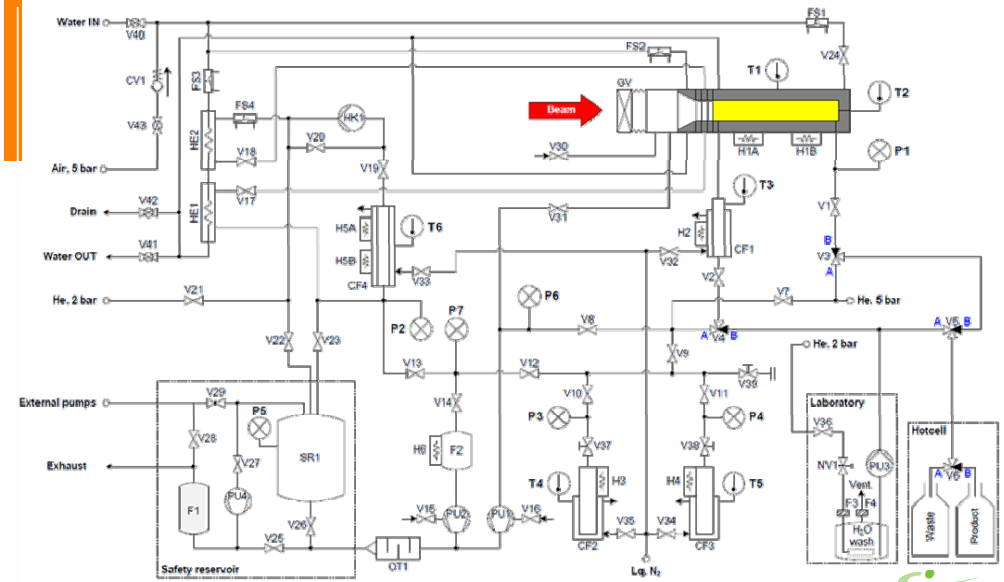

WTTC XIII – Presentation Discussions

1. Target experience
   - Windows changed every 3rd month
   - "Kyros" material to handle temperature
   - Diagnostic system for window holes?
   - Why not use 18F experience?

Mass Production of ^{64}Cu with ^{64}Ni(p,n)^{64}Cu Nuclear Reaction

Kwon Soo Chun*, Hyun Park, Jaehong Kim

Korea Institute of Radiological and Medical Sciences, Seoul, Korea

*** Corresponding author: kschun@kcch.re.kr**

Introduction

^{64}Cu ($T_{1/2}$ = 12.7h, β^- decay: 40%, β^+ decay: 19%, E.C. decay: 41%) is one of the most useful radioisotope in nuclear medicine due to its multiple decay mode and the intermediate half-life. Several nuclear reactions, i.e., ^{64}Ni(p,n)^{64}Ni, ^{68}Zn(p,αn)^{64}Cu and ^{64}Ni(d,2n)^{64}Cu have been investigated for ^{64}Cu production[1,2]. The highest production yield could be obtained with proton irradiation on the enriched ^{64}Ni target. Therefore for mass and routine production, the ^{64}Ni target fabrication by using electroplating[3], the reliable chemical separation of ^{64}Cu from the irradiated ^{64}Ni target and the effective recovery process for the recycling of very expensive enriched material (^{64}Ni enrichment : 96%, $20,000/g) and so on are absolutely necessary to be established. In this work, we report our mass production method of ^{64}Cu with enriched ^{64}Ni and Cyclone-30 accelerator.

Methods

^{64}Cu was produced with high current cyclotron via ^{64}Ni(p,n)^{64}Cu nuclear reaction at 200μA, 18MeV proton beam. Nickel target was prepared by electro-plating of enriched ^{64}Ni (25% of enrichment) on Au coated Cu cooling plate. After proton beam irradiation, Ni target was dissolved with circulation of 50ml of 5N HCl on the dissolving device (home made) and 90°C heating. Water was added to ^{64}Ni solution to dilute the normality of hydrochloric acid to 0.5N. Radiochemical separation of ^{64}Cu from Ni target solution was performed with 0.01% dithizone in CCl_4 solvent extraction and back extraction with 7N HCl[4]. Purification of back extracted ^{64}Cu solution was carried out with AG1-x8 (Bio-Rad) anion exchange resin. For ^{64}Ni recycling, ^{64}Ni from the aqueous phase of solvent extraction and the electrolyte of electroplating was recovered by using AG1-x8 anion and AG50w-x8 (Bio-Rad) cation resin[5].

Results

With the electroplating cell designed by ourselves and the electrolyte, consisting of 1.5g ^{64}Ni(25% enrichment), 1.0g boric acid and 2.0g NaCl in 90ml distilled water, the smooth and uniformed Ni target (thickness : > 50mg/cm^2, area: 1 x 10cm^2) was obtained with applying 200mA of constant current on the cathode for 5hrs. The cathode current efficiency was about 50%. There was no damage on Ni surface during more than 200μA proton beam irradiation. The chemical separation yield of ^{64}Cu with solvent extraction and anion exchange resin was more than 90% and the radionuclidic purity was more than 99% 1 day after bombardment. The ^{64}Ni recovery yield was quantitative and measured with ^{57}Ni activity produced with ^{58}Ni(p,2p)^{57}Ni nuclear reaction and AA spectroscopy.

Conclusion

^{64}Cu production yield was about 9mCi/μAh corrected on 96% enrichment at EOB with ^{64}Ni(p,n)^{64}Cu nuclear reaction and Cyclone-30. The chemical separation yield and the radionuclidic purity of the final ^{64}Cu solution was more than 90% and 99%, respectively. The ^{64}Ni recovery yield performed with ion exchange resin was more than 98%.

References

[1] V.S. Smith, Molecular Imaging with Copper-64, J. Inorg. Biochem., Vol. 98, p.1874-1901, 2004

[2] F. Szelecscenyi, G. Blessing and S.M. Qaim, Excitation Functions of Proton Induced Nuclear Reactions on Enriched ^{61}Ni and ^{64}Ni: Possibility of Production of No-carrier-added ^{61}Cu and ^{64}Cu at a small Cyclotron, Appl. Radiat. Isot., Vol.44, p575-580, 1993

[3] IAEA Technical Report Series No. 432. “Standardized High Current Solid Targets for Cyclotron Production of Diagnostic and Therapeutic Radionuclieds” IAEA, Vienna, 2004

[4] A.K. Dasgupta, L.F. Mausner and S.C. Srivastava, A New Separation Procedure for 67Cu from Proton Irradiated Zn, Appl. Radiat. Isot. Vol. 42, p.371-376, 1991

[5] N. Saito, Selected data on ion exchange separations in Radioanalytical Chemistry, Pure & Appl. Chem., Vol. 56, p.523-539, 1984

Mass production of ^{64}Cu with $^{64}Ni(p,n)^{64}Cu$ Nuclear Reaction

Korea Institute of Radiological and Medical Sciences (KIRAMS), Seoul, Korea

Kwon Soo Chun, Hyun Park, Jaehong Kim

2010. 7. 26

• Cu radioisotopes

Physical properties and potential application of Cu radionuclides

nuclide	Half-life	Decay mode(%)	Major γ (keV)	Major β-/ β+ (keV, %)	application
^{60}Cu	23.7m	β+(93),EC(7)	826(22),1332(88)	872(49)	
^{61}Cu	3.32h	β+(61),EC(39)	282(12),656(10)	523(51)	PET
^{62}Cu	9.74m	β+(97),EC(3)	1173(0.34)	1316(97)	PET
^{64}Cu	12.7h	EC(43.9), β^-(38.5) β^+(17.6)	1345(0.5)	β+:278, β-:190	Therapy PET
^{66}Cu	5.4m	β-(100)	1039(9)	1112(91)	
^{67}Cu	61.83h	β-(100)	184(48.7),93(16),91 (7)	121(57)	Therapy

• ^{64}Cu physical properties

^{64}Cu : Therapeutic RI with monoclonal antibody and PET radionuclide

^{64}Cu nuclidic properties (from NNDC)

Decay mode: E.C.(43.9%), β^-(38.5%), β^+(17.6%)
Half-life: 12.701h
γ-ray energy(keV): 511(35.2%), 1345.8(0.47%)
$\beta^+_{max.}$ energy(keV): 653.03(17.6%)
$\beta^-_{max.}$ energy(keV): 579.4(38.5%)

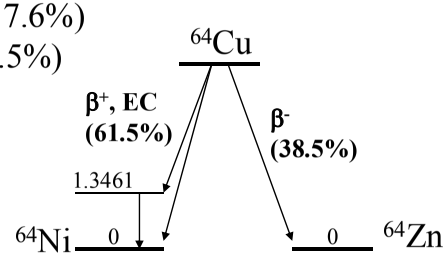

• ^{64}Cu production method

Table. Possible production routes of ^{64}Cu in NCA form.

Production route	Target material	Energy (MeV)	Yield (mCi/μAh)	Expected Yield per batch(mCi)
$^{64}Ni(p,n)^{64}Cu$	^{64}Ni(>95%) $20,000/g	15.5	2-10	800-4,000 (200μA x 2h)
$^{64}Ni(d,2n)^{64}Cu$	″	19	10	
$^{Nat.}Ni(p,n)^{64}Cu$	Natural Ni	20	0.2	80 (200μA x 2h)
$^{68}Zn(p,\alpha n)^{64}Cu$	^{68}Zn(>95%) $3,000/g	30	0.7	280 (200μA x 2h)
$^{66}Zn(d,\alpha)^{64}Cu$	^{66}Zn	12	0.18	

• Excitation functions of ^{64}Cu production

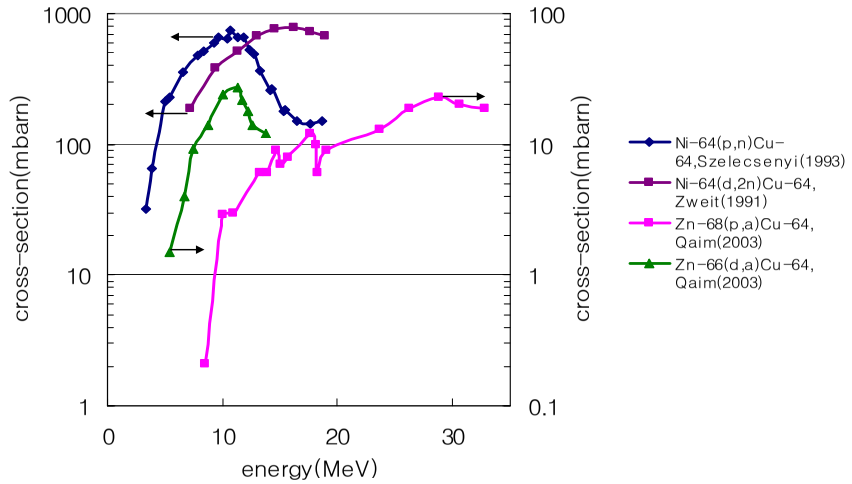

Fig. Excitation functions of ^{64}Ni(p,n)^{64}Cu and ^{64}Ni(d,2n)^{64}Cu, ^{68}Zn(p,αn)^{64}Cu, ^{66}Zn(d,α)^{64}Cu. From Szelecsenyi, Zweit, Qaim

• Schematic procedure for ^{64}Cu mass production

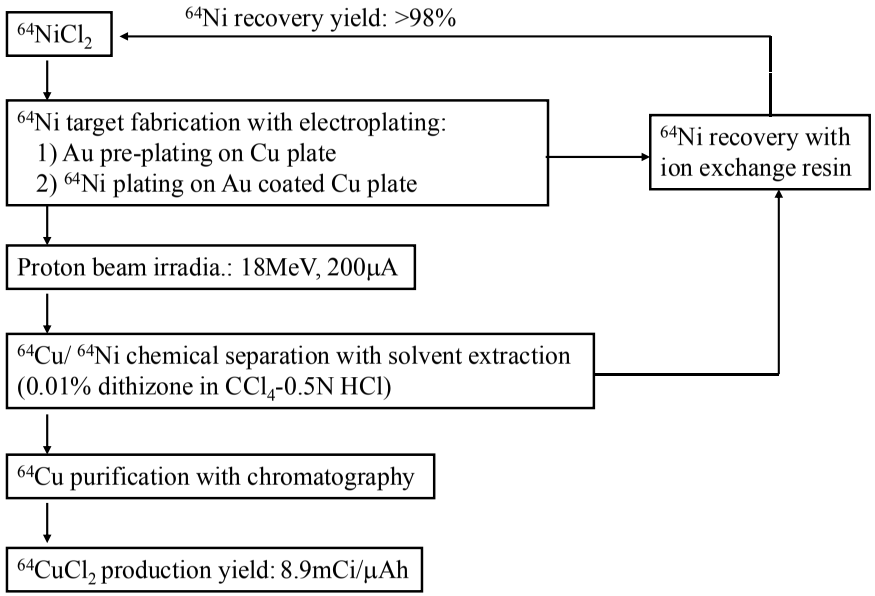

• Target fabrication with electroplating method

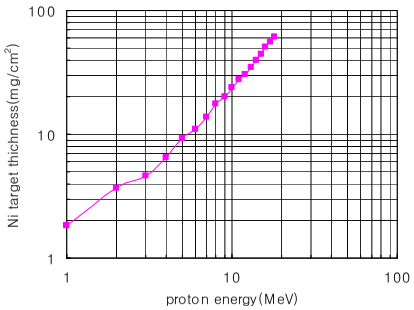

Fig. Range of protons in the Ni target tilted 6° compared to the proton beam line.

Watt = ΔE x I
(18MeV x 200μA =3.6kwatt)
Target area: 1x10cm²

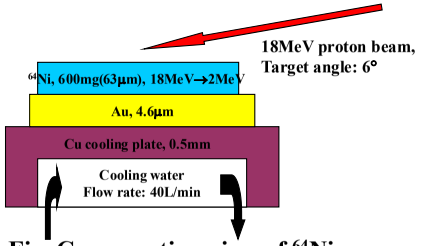

Fig. Cross-section view of ^{64}Ni target assembly

• ^{64}Ni isotope composition

nuclide	abundance		
	nat. Ni	96.1% ^{64}Ni	26.4% ^{64}Ni
^{58}Ni	68.08	1.95	50.4
^{60}Ni	26.22	1.31	19.6
^{61}Ni	1.14	0.13	0.9
^{62}Ni	3.63	0.51	2.8
^{64}Ni	0.93	96.10	26.4

• ^{64}Ni target (Au, ^{64}Ni) electroplating system

1) Au plating : 0.3g $KAu(CN)_2$/3g EDTA/ 2g phosphate buffer in 500mL H_2O
thickness: ≈ 8mg/cm²
target area: 12cm²(=1.2cm x 10.2cm)

2) ^{64}Ni plating: 1.5g ^{64}Ni/1g boric acid /2g NaCl in 90mL H_2O
- **constant current: 200mA,**
- **stirrer: 650rpm**
- **^{64}Ni cathode current efficiency : >30%: 60μm**
- **target area: 10cm²(=1cm x 10cm)**
- **recovery: cation and anion resin**

• ^{64}Ni electro-plating device

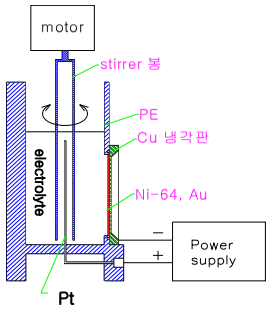

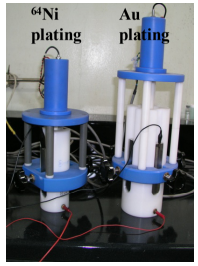

• Au plating

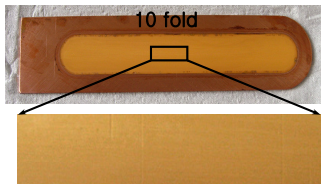

• ^{64}Ni target

•Power supply and rotor controller

• Proton beam irradiation

- Cyclotron: IBA Cyclone-30
- Particle, Energy: p^+, 18MeV
- Current: 200μA
- Irradiation time: 2hr
- Coolant: water 40L/min

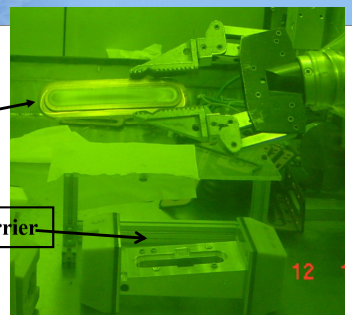

Table. Radionuclides in the proton beam irradiated ^{64}Ni target

nuclide	Nuclear reaction	Half-life	Decay mode	γ-ray energy (intensity)
^{55}Co	Ni(p,x)	17.5h	β^+:100%	803(2),931(75),1316(7),1408(17)
^{57}Ni	^{58}Ni(p,2p)	35.6h	β^+:100%	127(17),1377(75),1919(12)
^{57}Co	^{57}Ni→	271d	E.C :100%	122(86),136(11)
^{61}Cu	^{61}Ni(p,n) ^{62}Ni(p,2n)	3.3h	β^+:100%	656(11),1185(4)
^{64}Cu	^{64}Ni(p,n)	12.7h	β^+, EC, β^-	1346(0.5)

• Solvent extraction of ^{64}Cu with dithizone

Solvent extraction with 0.01% dithizone in CCl_4-HCl (vol. ratio, aq:org=1:1/10)

HCl molarity	Distribution ratio of ^{64}Cu	Distribution ratio of ^{57}Ni, ^{55,57}Co
7.5M	>10%	
2M	19.5%	
1M	41%	
0.5M	95%	>0%

Distribution ratio were measured with the activities of radioisotopes in each phase.

$D_{Cu} = [^{64}Cu]_{org.}/[^{64}Cu]_{aq.}$

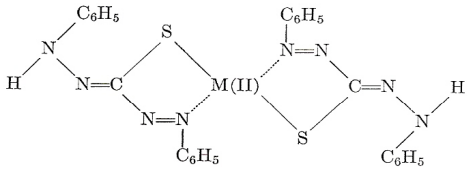

Fig. Structure of metal-dithizone complex.

• Ion chromatogram of ^{64}Cu

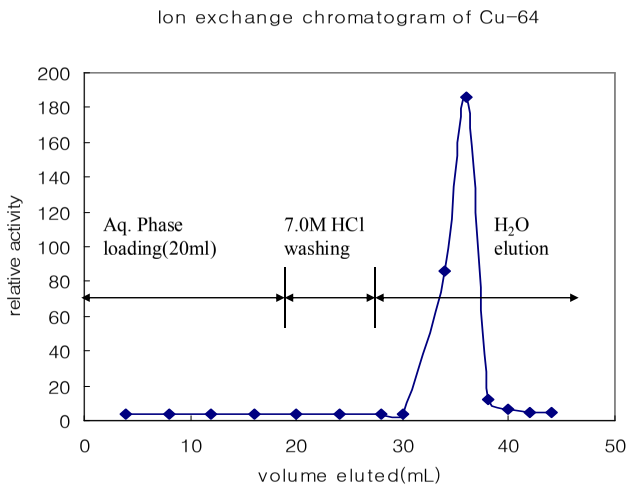

Fig. Ion exchange chromatogram.
- Resin: AG1X-8(100-200mesh, Cl^-form)
- Preconditioning: 15ml 7.0M HCl
- Column size: ϕ 1.0cm x 6 cm (vol. ≈ 5ml)

• Flow chart of chemical processing for ^{64}Cu production

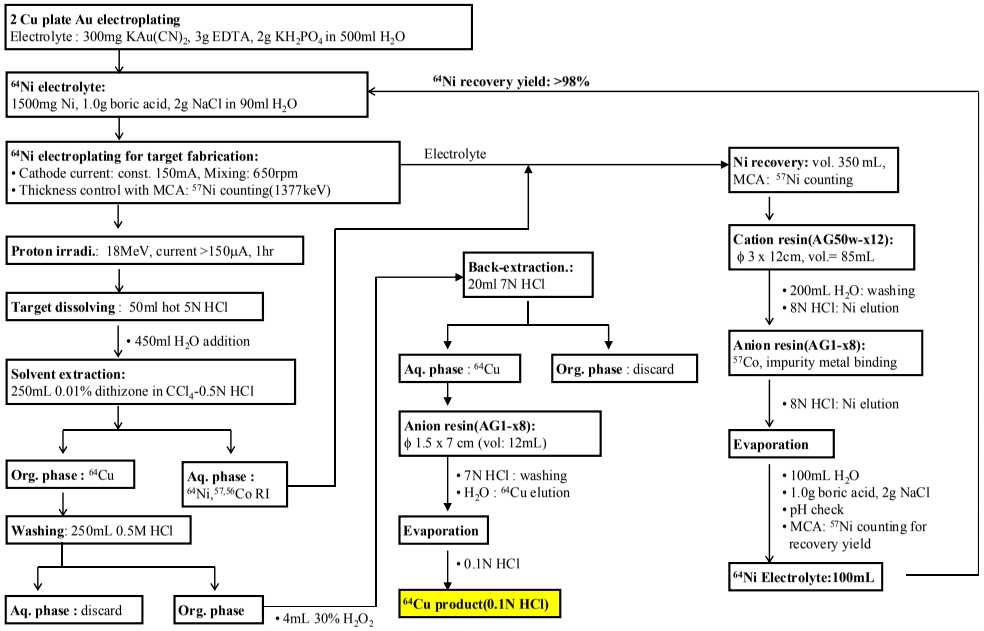

• Chemical separation system for ^{64}Cu production

^{64}Ni target dissolution system

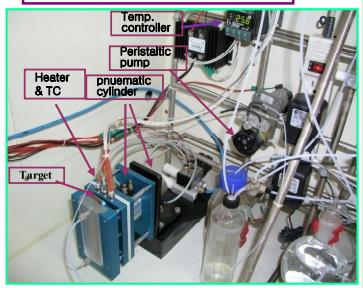

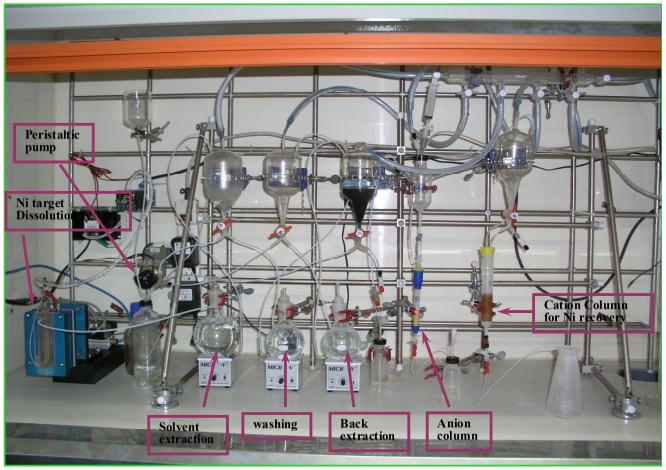

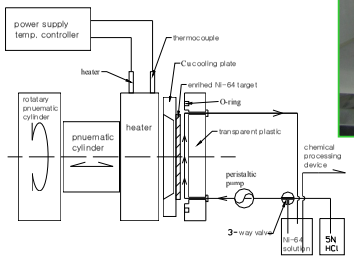

Schematic drawing of dissolution system

• Ni target after dissolution with 50ml of 5N hydrochloric acid (flow rate: 1ml/min, temp.: 90℃)

• Quality control of ^{64}Cu(γ-ray, metal impurity)

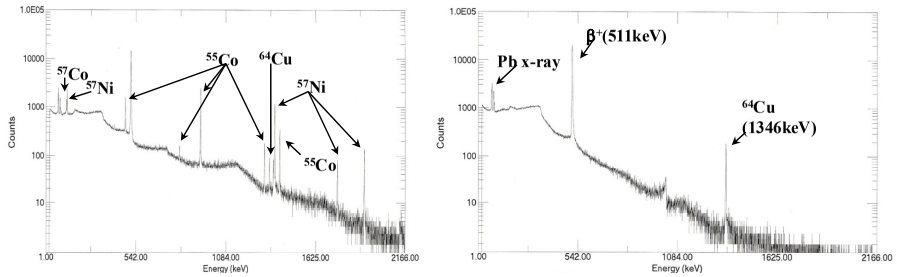

Fig. γ-ray spectrums of the proton beam irradiated ^{64}Ni target and final ^{64}Cu product.

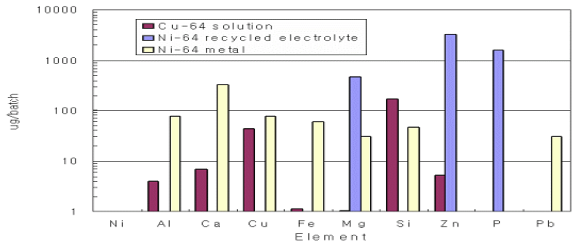

Fig. Metallic impurities in the final ^{64}Cu solution and ^{64}Ni electrolyte measured by ICP-MS.

• Conclusions

- Target material : 26% ^{64}Ni
- ^{64}Cu production yield : 8.9mCi/μAh (96% enrichment, at EOB)
- Proton energy and current: 18MeV, 200μA
- Separation method:
  - solvent extraction: 0.01% dithizone in CCl_4-HCl
  - ion chromatography: AG1x-8
  - separation yield of ^{64}Cu : >90%
  - radionuclidic purity: >99%
- ^{64}Ni recovery method:
  - cation, anion resin
  - recovery yield: > 98%

WTTC XIII – Presentation Discussions

1. 24% 64Ni: is it worth?
   - 400mCi/batch
   - 9mCi/uA (= 90% theoretical value)
2. Absence of front cooling
   - No problems found
3. Why not radiochromatography separation?
   - Not good, only resin method

Activity Delivery System

D.B.Mackay[1], C.Lucatelli[1], R. van Ham[2], M. Willemsen[2], P. Thoonen[2], B. Kummeling[2], J.C.Clark[1]

[1]CRIC, University of Edinburgh, [2]Von Gahlen, Nederland B.V

The CRIC radio-chemistry facility requires that radio-nuclides produced on a GE PETtrace 8 cyclotron are delivered to 4 hot cells in a GMP production lab and to 3 hot cells in a R&D lab. CRIC is working closely with Von Gahlen to develop a comprehensive radionuclide delivery system. The ADS is capable of supplying radioactive gases and liquids safely and reliably from the cyclotron to all of the points of use. The switching valves also have the possibility of directing the radio-nuclides to waste.

The route possibilities are shown in figure 1.

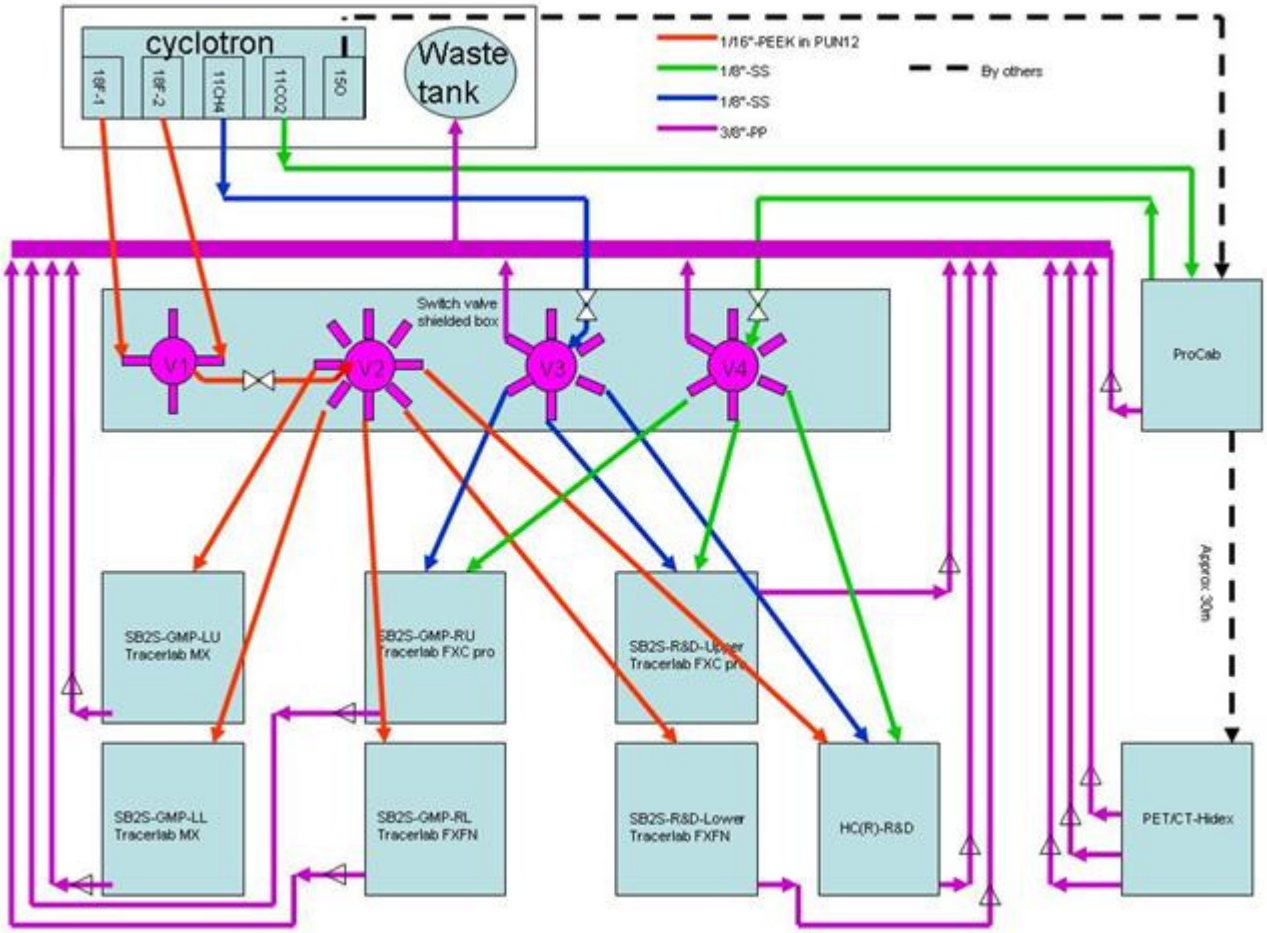

Figure 1: Delivery system routes.

The switching valves and isolation valves have all been selected for their proven reliability and adequate performance characteristics.
The system will be controlled by a plc. Software will be validated to GAMP 5.
The operator can control the delivery from one of three touch screen panels.
The system has been designed with a high level of safety both for the operators and the environment. The whole system is enclosed in a stainless steel box. The box has separate compartments for the valves and the control equipment. The valves and filters are housed in an airtight lead-shielded compartment (75mm) which is ventilated. The extract air is filtered with HEPA/charcoal filters.
Access inside the shielded compartment is not possible while delivery is in progress or when the radiation level is above a pre-set threshold. This is achieved by interlocking the door lock to an internally mounted radiation detector.
Delivery along the chosen route can only occur when safe pre-conditions have been met (e.g. hot cell doors closed).
The lines to the hot cells are run in floor trenches under the hot cells. The trenches are shielded with 75mm of lead and provided with hatches to facilitate replacement of lines.

Views of the box are shown below.

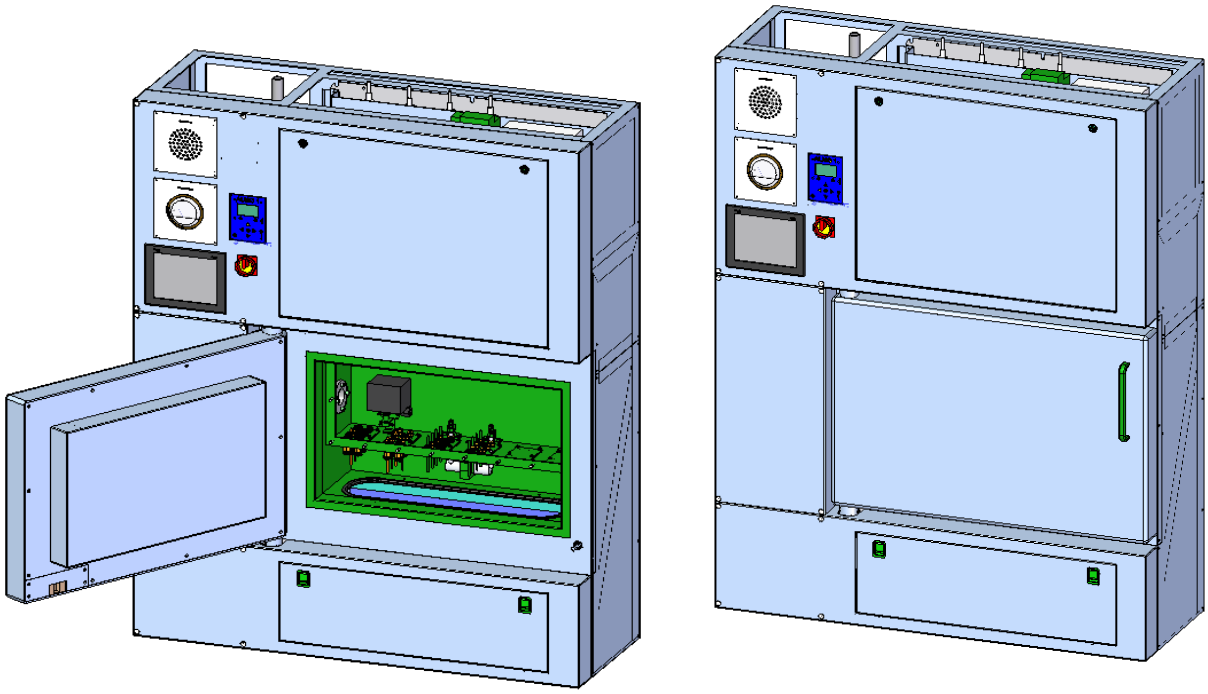

Figure 2: Activity delivery system shielded box

Activity Delivery System

D.B. Mackay

Risoe, 27 July 2010

The CRIC Facility, Edinburgh

- GE PETtrace 8 cyclotron in a vault.
- GMP lab with 4 hot cells.
- Facilities for dispensing and sterilising either by autoclave or aseptic filtration.
- Separate R&D lab with 3 hot cells.
- PET/CT, CT and 3T MRI scanners.

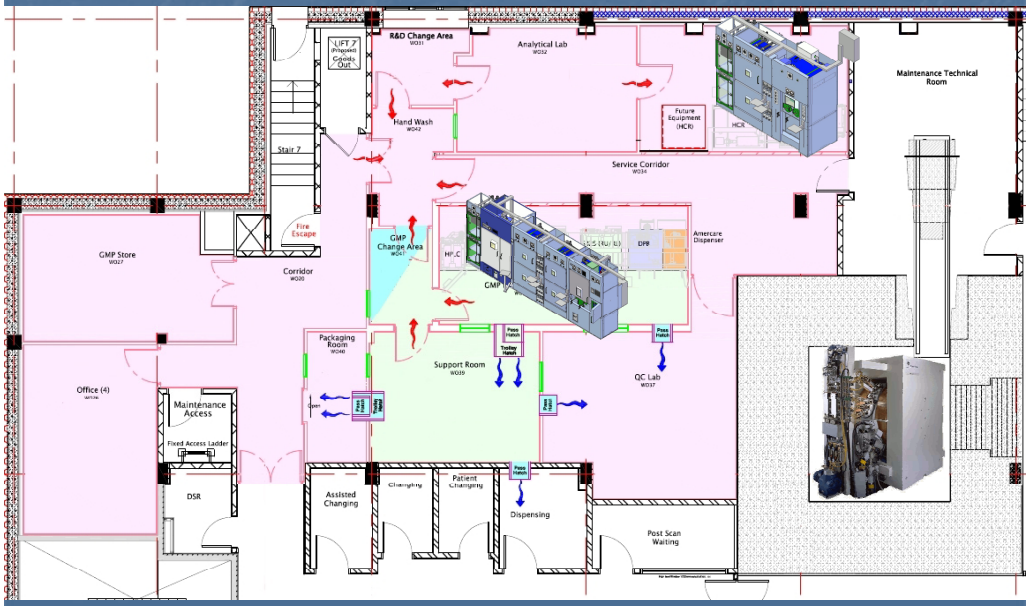

The GMP hot cell lab

- 4 Production hot cells (2xVon Gahlen SB2S)
- Cells equipped with GE synthesisers (2x Tracerlab MX,1x FXC Pro, 1x FXFN
- GE Fastlab dispenser/sterilizer
- Aseptic dispensing facility (Von Gahlen DPB)
- Integrated filter integrity test
- Products from all 4 hot cells can be transferred to either dispensing cell
- HPLC cabinet

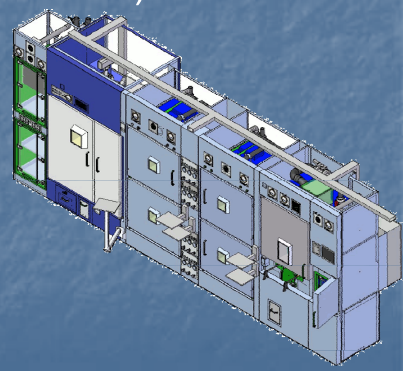

The R&D hot cell lab

- 3 Von Gahlen hot cells (1x SB2S and 1xHC(R))
- Cells equipped with GE synthesisers (1x FXC Pro, 1x FXFN)
- All 3 hot cells are interconnected
- HPLC cabinet

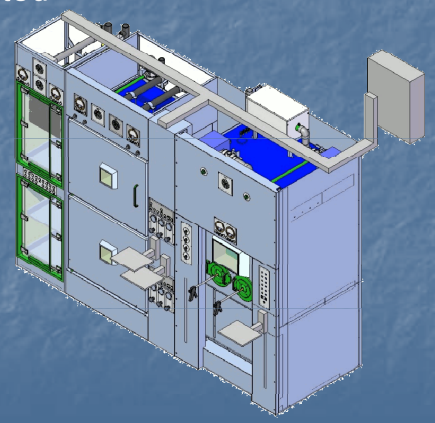

The HPLC support cabinet

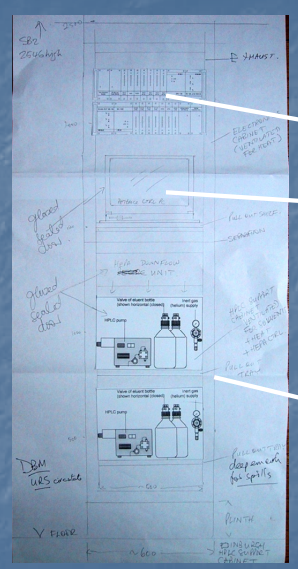

Concept drawing

GE FX control electronics 2X

GE PETtrace control PC

HPLC pumps and solvents 2X

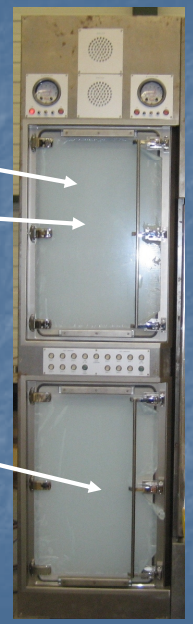

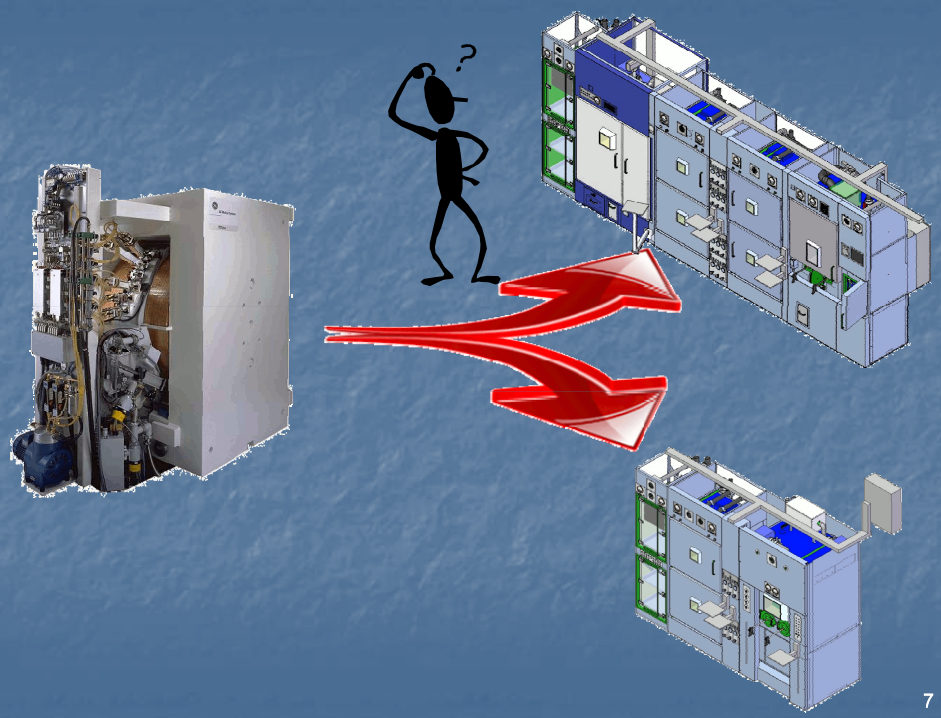

The Activity Delivery System Schematic

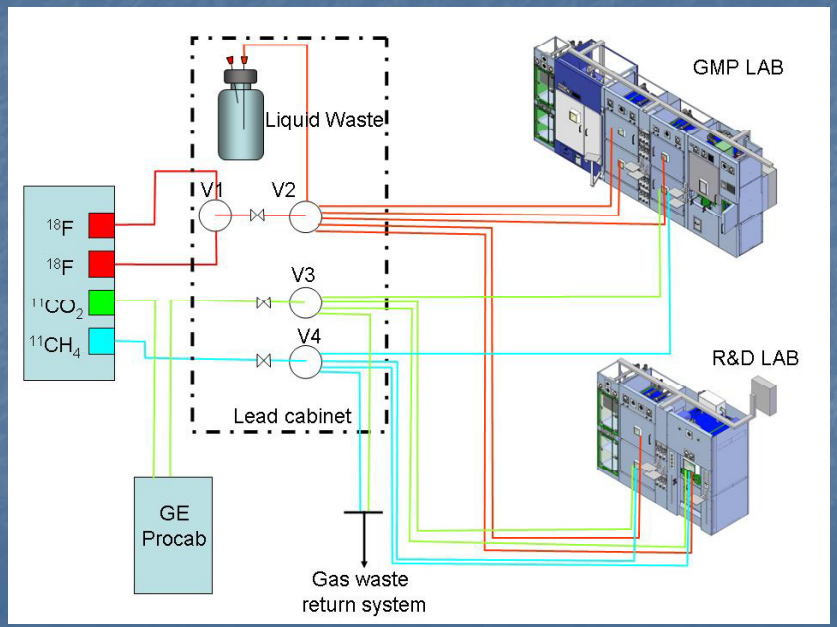

The Activity Delivery System Hardware

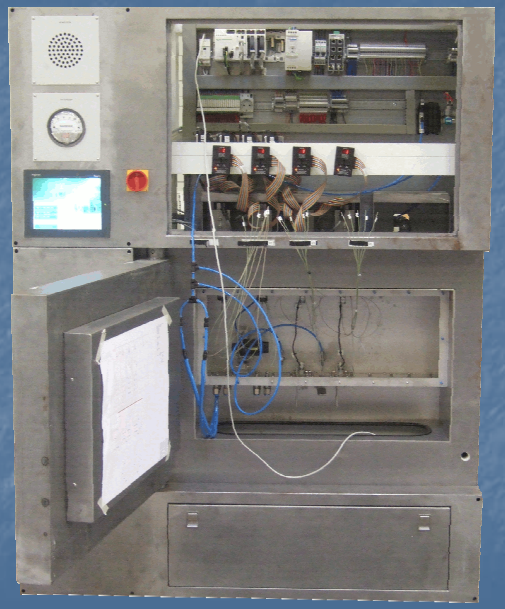

Valves

- Different valves for gases and liquids
- High pressure specs
- Separate routing valves (rotary) and safety valves (on/off)
- Safety valves default to closed
- Cleanliness for C-11 – factory clean, lubricant-free valves
- Helium specified for route testing
- Wetted path materials checked
- Low dead volume for liquids

V1	*Valve, VICI C5-2344EMT8-485-VGA [4-way] [1/16" Fittings] [8" standoff]*
V2	*Valve, VICI C5H-2348EMT8-485-VGA [8-way] [1/16" Fittings] [8" standoff]*
V3	*Valve, VICI EMT8SD6MWE-485-VGA [6-way] [1/8" Fittings] [8" standoff]*
V4	*Valve, VICI EMT8SD6MWE-485-VGA [6-way] [1/8" Fittings] [8" standoff]*
V7	*Multimedia valve, Parker 009-1513-900*
V8	*Multimedia valve, Parker 009-1513-900*
V9	*Check valve, Swagelok SS-6C-1/3*
V11	*On - off valve, Swagelok SS-41GS1-31CC*

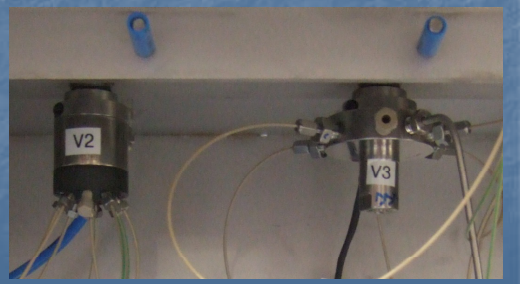

Control

- Plc control Modicon M340 Type 2020
- Touch screen with user log in and access levels
- Delivery only possible if cyclotron status, door interlocks and radiation levels ok.
- Software to GAMP 5

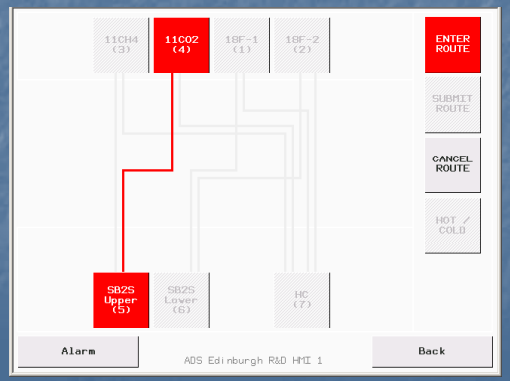

Safety

- Log in with user levels and password control.
- 75mm lead shielding.
- Sealed valve compartment
- Valves separate from actuators
- Rotary valve position feedback
- Inlet air HEPA filtered
- Box ventilated (negative pressure)
- Exhaust air HEPA/Charcoal filtered
- Radiation monitor built-in.
- Door lock
- Door interlocks
- All lines run in 75mm lead-shielded floor trenches
- FMEA analysis conducted

Conclusion…

- Flexible
- Expandable
- Safe
- Reliable
- Affordable

Authors and acknowledgements

University of Edinburgh
Prof J.C. Clark
Dr. C. Lucatelli
K. Wilson

Von Gahlen
R. van Ham
M. Willemsen
P. Thoonen
B. Kummeling

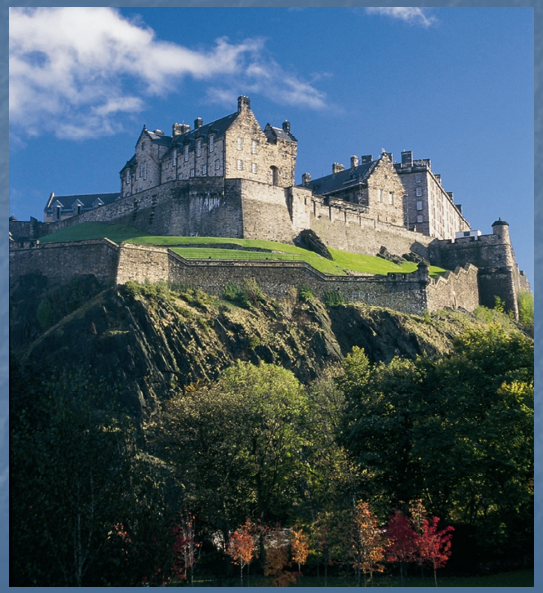

Integrated GMP PET Radiotracer Production and Dispensing Facility

C. Lucatelli[1], D. B. Mackay[1], G. Mokosa[2], C. Arth[2], R.C. van Ham, M.A.B. Willemsen[3], J. C. Clark[1]

[1]University of Edinburgh, CRIC, [2] Millipore France, [3]Von Gahlen Nederland B.V

Dispensing of PET radiopharmaceuticals can be done either by final thermal sterilization or by sterile filtration. If thermal sterilization is the recommended method, it is very often impractical (short half-life, tracer thermo-sensitive) and many PET radiotracers are therefore dispensed by sterile filtration.

Among all the Quality Control tests required, prior to batch release, by Good Manufacturing Practice and European Pharmacopeia standards, the integrity of the membrane filter used during the final dispensing is to be checked. This activity is relatively time consuming and is the main source of analyst finger radiation doses.

To overcome this problem, we decided that this test should be automated and “in line” to avoid manual handling of this highly active filter, and to allow other activities to be performed as the filter is being tested.

The University of Edinburgh is currently setting up a brand new PET radiotracer production facility, as part of its new Clinical Research Imaging Centre (CRIC) and wants to achieve a state of the art uncluttered integrated facility.

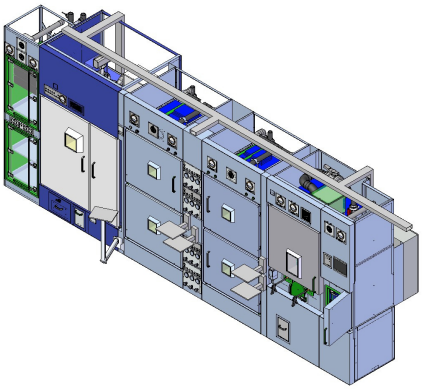

Figure 1: GMP production lab hot cells assembly. From left to right: ventilated HPLC cabinet; GE FASTLab dispenser and sterilizer; 2 VG SB2S hot cells; 2 VG SB2S hot cells; VG Grade A DPB-LF dispenser.

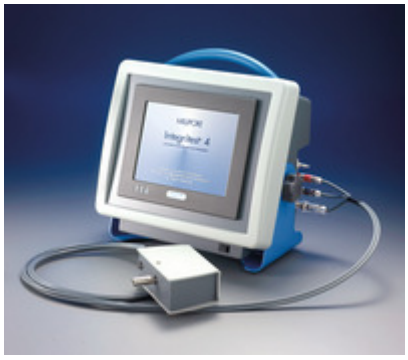

Figure 2: Millipore Integritest® 4

This facility will operate a GE PETtrace 8 cyclotron equipped with 5 targets: 2 Niobium for ^{18}F production, 1 ^{11}C-CO_2, 1 ^{11}C-CH_4 and 1 ^{15}O-target. The 4 first targets will be connected to 2 independent labs, a GMP production housing 4 hot cells and a R&D lab housing 3 hot cells. The target will be routed to the right destination using a specially designed Activity Delivery System. A specialy designed ventilated HPLC cabinet, integrated within the row of hot cells will house 2 GE

syntheziser module electronic racks, 2 semi-preparative HPLC pumps and a computer controlling the cyclotron.

In addition to the 4 production hot cells, the GMP production lab will be equipped with 2 dispenser hot cells, a GE FASTLab dispenser and autoclave for thermal sterilisation and a Grade A Von Gahlen DPB-LF hot cell for the aseptic dispensing of radiotracers sensitive to heat or with a short half-life. Each of the production hot cells will be connected via shielded ducts to both dispensers.

As part of the design of the lab, we investigated the possibility of integrating a filter integrity test facility into our aseptic dispensing hot cell.

We decided to use the “off the shelf” Millipore Integritest 4 (Networked version) as a basis for this system, due to its modular design. We worked jointly with Millipore and Von Gahlen to achieve a solution which would allow the filter to be directly and automatically tested as part of the dispensing process.

The challenge was to integrate this tabletop system into the hot cell without compromising the Grade A laminar flow and the radioprotection. To achieve this integration, the commercial system needed to be disassembled. The touch screen computer panel is located on the front face of the hot cell. The part connected to the filter (External Valve Array) is fitted into the shielded environment and the remaining parts are located in a shielded enclosure on the top of the hot cell. A solenoid valve protects the Millipore External Valve Array during the filtration of the product . The filter is connected to product transfer line and to the Millipore Integritest® 4 by a sterile single use Vygon tubing assembly equipped with a check valve.

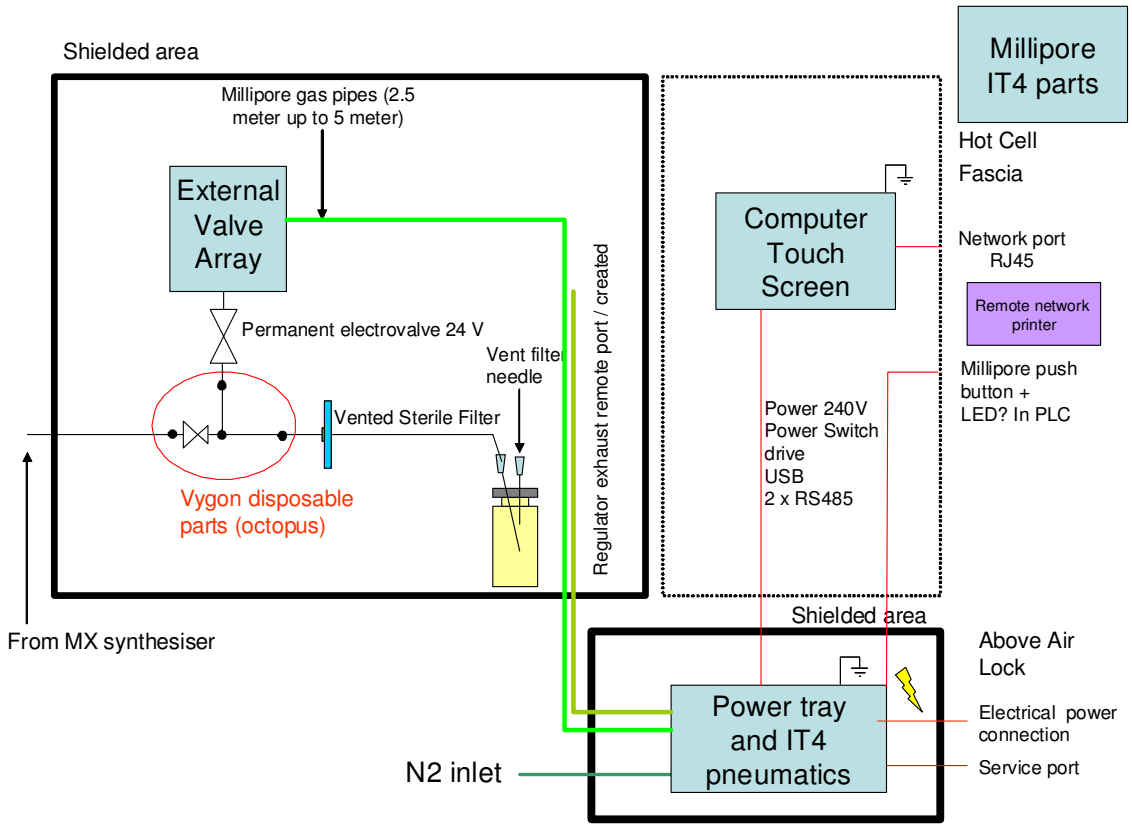

Figure 3: Integration of the Millipore Integritest®4 into the Von Gahlen DPB-LF hot cell.

Integrated GMP PET Radiotracer Production and Dispensing Facility

C. Lucatelli[1], B. Mackay[1], G. Mokosa[2], C. Arth[2], R.C. van Ham[3], M.A.B. Willemsen[3] and J. C. Clark[1]

1CRIC, University of Edinburgh,
2 Millipore, France
3 VonGahlen, Netherlands

Introduction

Dispensing and sterilisation of PET radiopharmaceuticals can be done either by terminal thermal sterilization or by aseptic sterile filtration. Although thermal sterilization is the recommended method, it is very often impractical (short half-life, thermo-sensitive tracers) and many PET radiotracers are therefore dispensed by aseptic sterile filtration.

Among the Quality Control tests required, prior to batch release, by Good Manufacturing Practice and European Pharmacopoeia standards, the integrity of the membrane filter used during the terminal sterilisation and dispensing must to be checked. This activity can be cumbersome time consuming and is the main source of analyst finger radiation doses.

To overcome this problem, we decided that this test should be automated and “in line” to avoid manual handling of this highly active filter, and to allow other activities to be performed as the filter is being tested.

As part of the design of our new lab, we investigated the possibility of integrating a filter integrity test facility into our aseptic dispensing hot cell.

The University of Edinburgh is currently setting up a brand new PET radiotracer production facility, as part of its new Clinical Research Imaging Centre (CRIC) aiming to achieve a state of the art integrated uncluttered Licensed GMP facility.

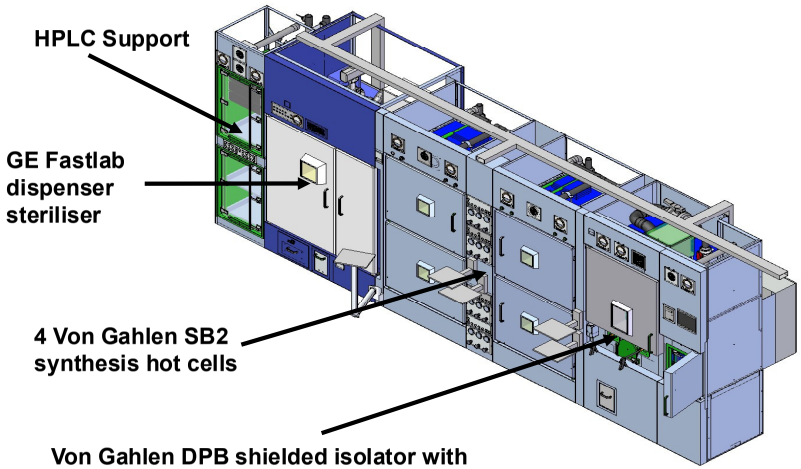

As part of the design of the lab, we investigated the possibility of integrating a filter integrity test facility into our aseptic dispensing hot cell.
We decided to use the "off the shelf" Millipore Integritest 4 (Networked version) as a basis for this system, due to its modular design.

We have worked jointly with Millipore and Von Gahlen to achieve a solution which would allow the filter to be directly and automatically tested as part of the dispensing process

Integration

The challenge was to integrate this tabletop system into the hot cell without compromising the Grade A laminar flow and the radioprotection.
To achieve this integration, the commercial system needed to be disassembled. The touch screen computer panel is located on the front face of the hot cell. The part connected to the filter (External Valve Array) is fitted into the shielded environment and the remaining parts are located in a shielded enclosure at the back of the hot cell.

A solenoid valve protects the Millipore External Valve Array during the filtration of the product. The filter is connected to product transfer line and to the Millipore Integritest® 4 by a sterile single use Vygon tubing assembly "Octopus" equipped with check valves.

A solenoid valve protects the Millipore External Valve Array during the filtration of the product. The filter is connected to product transfer line and to the Millipore Integritest® 4 by a sterile single use Vygon tubing assembly equipped with a check valve.

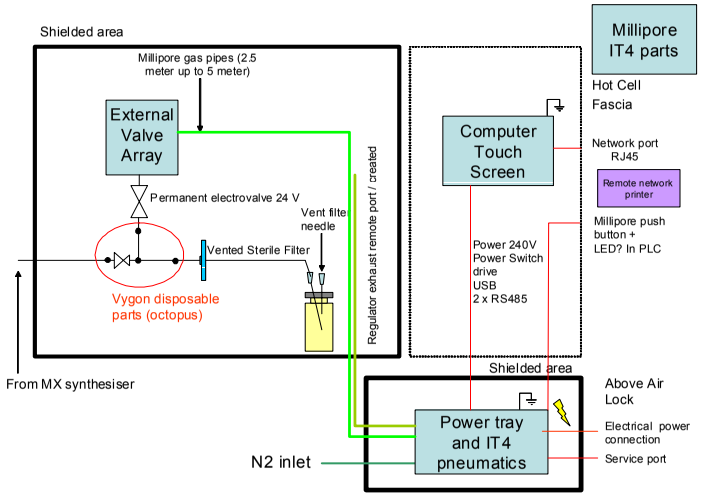

The facility remains to be validated but we are quite confident that all will be well!

It is an example of the williness of commercial partners to engage with a user to arrive at a solution to a common problem.

Our thanks go to Millipore and Von Gahlen

WTTC XIII – Presentation Discussions

1. Tests used
   - Pressure
   - Flow rate
   - Bubble test not used

Synthesis of 4-[^{18}F]Fluorobenzaldehyde in a CPCU for Peptide Labeling

V.M. Lara-Camacho, J.C. Manrique-Arias, E. Zamora-Romo, A. Zarate-Morales, A. Flores-Moreno, M.A. Avila-Rodriguez

Unidad PET/CT-Ciclotrón, Facultad de Medicina, Universidad Nacional Autónoma de México, México, D.F., México

Objetives: Implement the synthesis of 4-[18F]fluorobenzaldehyde ([^{18}F]FB-CHO) in a CTI/Siemens Chemistry Process Control Unit (CPCU) for peptide labeling.

Methods: No-carrier-added [^{18}F]FB-CHO was prepared by radiofluoridation of 4-formyl-*N,N,N*-trimethylanilinium triflate precursor in two reaction vessels. Reagents used in the synthesis are summarized in table below. After elution of $^{18}F^-$ from QMA cartridge and azeotropic distillation at 110°C in reaction vessel #1, precursor was added, bubbled for a few seconds, and transferred to reaction vessel #2. Fluorination reaction was performed at 60°C for 10 min [Speranza et al., Appl. Radiat. Isot. 67 (2009) 1664] and the residue mixture was diluted with 3 mL of H_2O. The product was trapped in a Sep-Pak C18 cartridge and washed with 10 mL of H_2O. [^{18}F]FB-CHO was eluted with 0.5 mL of EtOH. For peptide labeling HYNIC-peptide conjugates were incubated with [^{18}F]FB-CHO at 50°C, 25 min, pH 4.5. Purification was performed by gradient-HPLC in a semi-prep C18 reverse phase column with EtOH/H_2O 10-80% in 20 min [Lee et al., Nucl. Med. Biol. 33 (2006) 667]

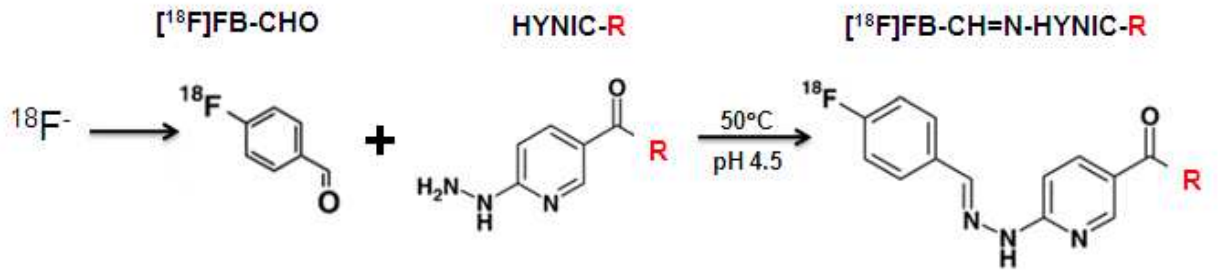

Vial #	Reagents Vessel # 1	Reagents Vessel #2
1	K222/K_2CO_3	Vial empty
2	2 mL CH_3CN	Vial empty
3	5 mg precursor in 1 mL DMSO	Vial empty
4	Vial empty	3 mL H_2O
5	Vial empty	10 mL H_2O

Results: [^{18}F]FB-CHO was obtained in a decay corrected RCY of 30% within 50 min with a RCP>95%. The peptides Try^3-Octreotide (TOC) and c-RGDyK (RGD) were labeled with 60-90 efficiencies with RCP>99% after HPLC purification, independently of the peptide used. MicroPET studies were performed with [^{18}F]FB-CH=N-NYNIC-RGD using C6 glioma xenografts in nude mice.

Conclusions: After the CPCU was replaced with a modern FDG-maker in our institution, to this chemistry module was given a second chance for the synthesis of other tracers taking advantage of its simplicity and versatility. In this work, [^{18}F]FB-CHO was successfully prepared and used for peptide labeling with a RCY highly enough for clinical applications.

Synthesis of 4-[^{18}F]Fluorobenzaldehyde in a CPCU for Peptide Labeling.

V.M Lara-Camacho, J.C. Manrique-Arias,
E. Zamora-Romo, A. Zarate-Morales,
A. Flores-Moreno, M.A. Ávila-Rodríguez.

Unidad PET, Facultad de Medicina-UNAM, México D.F.

The 13Th International Workshop on Targetry and Target Chemistry, Denmark July 27th 2010

Objective

- The aim of this work is:

  To implement the synthesis of [^{18}F]FB-CHO in a CTI/Siemens Chemistry Process Control Unit (CPCU) for peptide labeling.

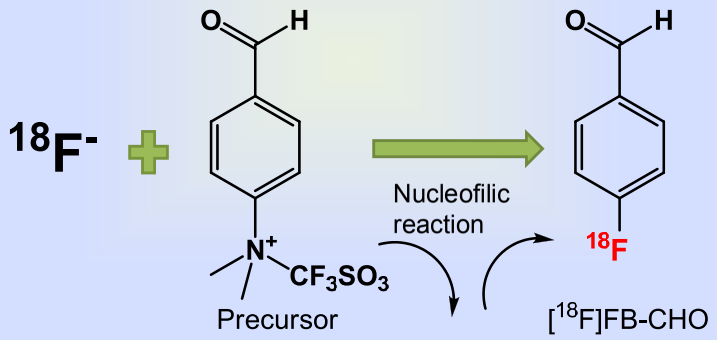

4-formyl-N-N-N-trimethylanilinium triflate precursor

Steps of [^{18}F]FB-CHO

Reaction Vessel # 1

$[^{18}F]F^-_{(aqueous)} + K_2^+CO_3^- / K\text{-}222 \xrightarrow{CH_3CN} (K / K\text{-}222)^+ / [^{18}F]F^-_{(aqueous)}$

$(K / K\text{-}222)^+ / [^{18}F]F^-_{(aqueous)} \xrightarrow[110\ ^\circ C]{\text{Azeotropic distillation}} (K / K\text{-}222)^+ / [^{18}F]F^-_{(anhydrous)}$

Reaction Vessel # 2

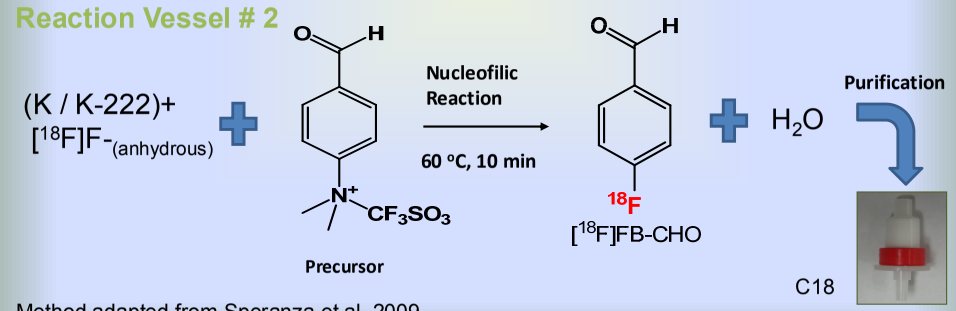

Method adapted from Speranza et al. 2009

Materials and Methods

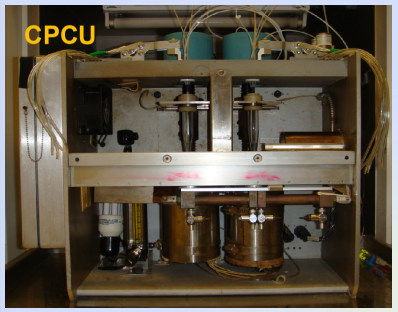

Arrangement

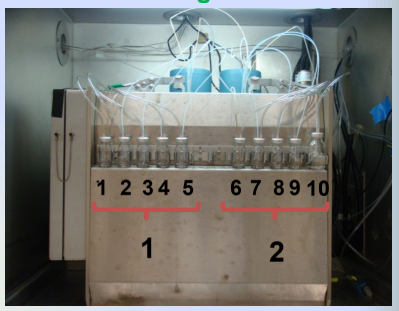

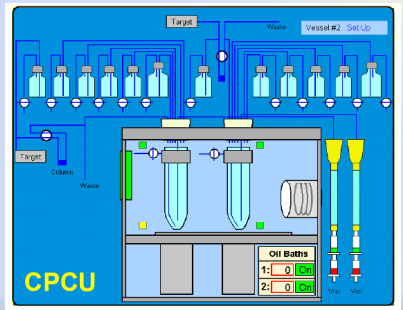

# Vial	Reagents
1	1.5 mL K-222/K_2CO_3
2	2.0 mL CH_3CN
3	5.0 mg precursor in 1.0 mL DMSO
9	3.0 mL H_2O
10	10 mL H_2O
4, 5, 6, 7, 8	Empty vials

Peptide-radiolabeling

- After elution from C18 with 0.5 ml of EtOH , the [^{18}F]FB-CHO was incubated with peptide conjugated.

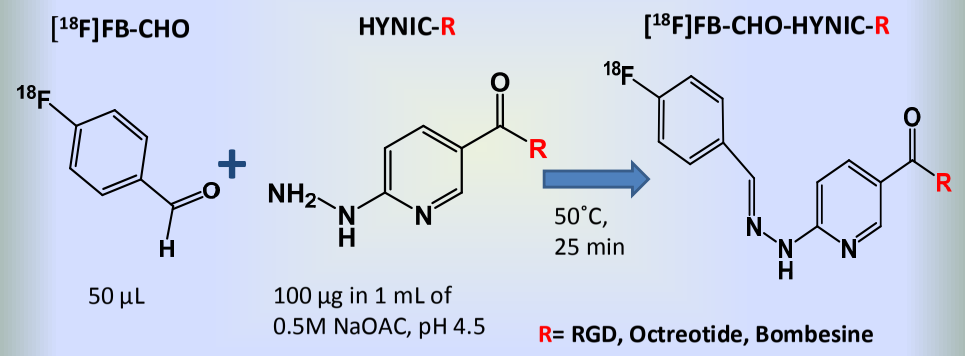

- Gradient-HPLC in a semi-prep C18 reverse phase column with EtOH/H_2O, 10-80% in 20 min [Lee et al. 2006].

Results

YMC-Pack Pro C18 column, 10 µm, 250 mm x10 mm, EtOH:H_2O 10-80% EtOH, 3 mL/min

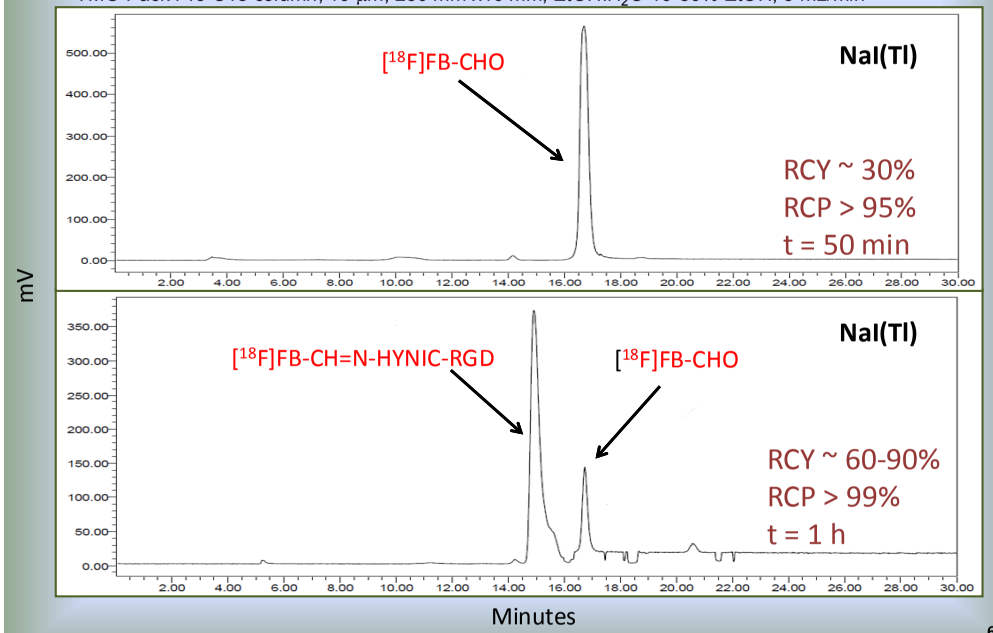

Targeting Tumor Expression of $\alpha_v\beta_3$ Integrin with [^{18}F]FB-CH=N-HYNIC-RGD

C6 glioma xenograft in nude mice

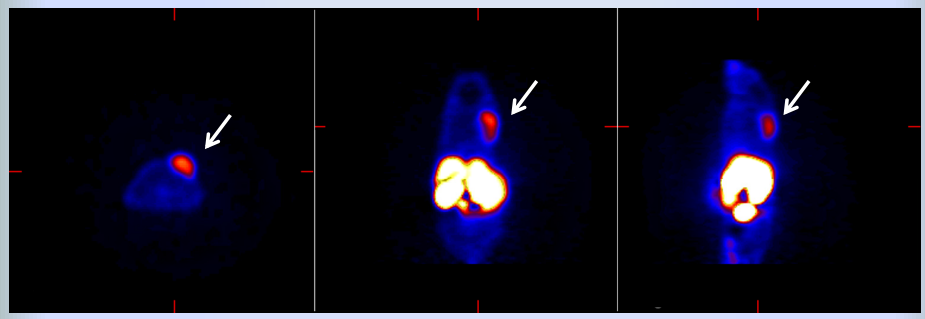

Axial **Coronal** **Sagittal**

MicroPET Focus 120

Receptors Blocking Method

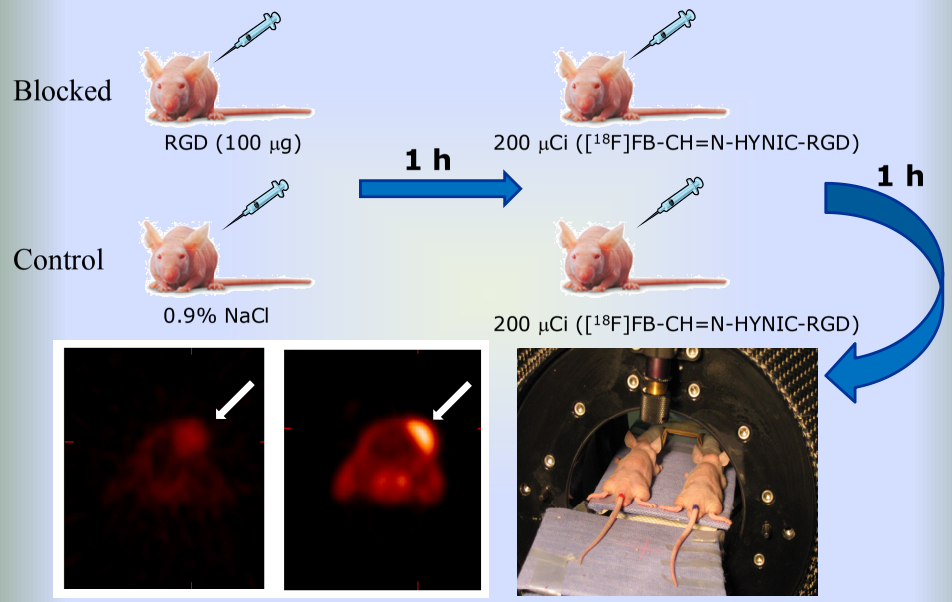

Conclusions

- The synthesis of [^{18}F]FB-CHO was successfully achieved in the CPCU.
- [^{18}F]FB-CHO was used for peptide labeling.
- The synthesis of [^{18}F]FB-CHO represents a second chance for the CPCU module in the preparation of other tracers.
  - [^{18}F]Fluorothymidine is another tracer synthesized in the CPCU with a RCY >30%, with 10 mg of BOC-precursor.

A comparison of Nb, Pt, Ta, Ti, Zr, and ZrO_2-sputtered Havar foils for the high-power cyclotron production of reactive [^{18}F]F$^-$

K. Gagnon, J.S. Wilson, and S.A. McQuarrie

Edmonton PET Centre, Cross Cancer Institute, University of Alberta, Edmonton, AB, CANADA

Introduction: Previous studies performed at the Edmonton PET Centre (EPC) have demonstrated that the use of Nb-sputtered Havar foils during [^{18}F]F$^-$ production via proton irradiation of [^{18}O]H_2O decreases the radionuclidic and chemical impurities within the irradiated water[1]. Given the improved [^{18}F]F$^-$ reactivity, increased [^{18}F]FDG yield consistency, and decreased need for target rebuilding noted for Nb-sputtered Havar, these sputtered foils were adopted as the standard practice for [^{18}F]F$^-$ production at our facility in mid-2006. Following prolonged use of the Nb-sputtered foils however, degradation of the niobium film has been noted, with Havar impurities, FDG yield consistency and [^{18}F]F$^-$ reactivity returning over time to levels comparable with that of non-sputtered Havar.

Aim: The goal of this current work was to find a film that demonstrates increased longevity with regards to [^{18}F]F$^-$ reactivity when compared with niobium.

Methods: All film sputtering (Nb, Pt, Ta, Ti, Zr, and ZrO_2) was performed on 30 µm Havar at the University of Alberta's NanoFab micro and nanofabrication research facility (Edmonton, AB). Film thicknesses were verified through profilometer measurements and SEM micrographs.

To test the Havar impurity reducing properties of the sputtered foils (thicknesses = 250–450 nm), test irradiations were performed using 2.8–3.0 mL Barnstead 18MΩ-cm $^{nat}H_2O$. Multiple (N = 9–15) test irradiations (of 1,000 µAmin and 5,000 µAmin) were performed on all foils at 17.5 MeV using the EPC's TR 19/9 cyclotron to achieve total integrated currents of approximately 20,000–30,000 µAmin (weighted average currents of 69–81 µA). To ensure consistent irradiation conditions and complete sample transfer, both the ^{13}N saturated yield and the recovered $^{nat}H_2O$ mass were measured following all irradiations. Following ^{13}N decay, all water samples were assayed for radionuclidic impurities using an HPGe detector (dead time < 5%). Chemical analysis for extractable metals was also performed for a subset of the water samples via inductively coupled plasma mass spectroscopy (ICP-MS) at the Exova Lab (Edmonton, AB).

As tantalum was the only film which demonstrated Havar impurity-reducing properties comparable to niobium, the foil above was further irradiated to a total integrated current of 80,000 µAmin. Given the excellent continued performance noted via radionuclidic contaminant analysis, our next step was to install a new Ta-sputtered foil on our main production target for the purpose of testing both the [^{18}F]F$^-$ reactivity and evaluating the tantalum film's longevity performance. Prior to installation of the Ta-sputtered Havar on our production target, a series of five 1,000 µAmin (65 µA) $^{nat}H_2O$ test irradiations were performed on the existing (previously irradiated to ~980,000 µAmin) 400 nm Nb-sputtered Havar foil to establish a baseline to which the tantalum results could be compared. A new 900 nm Ta-sputtered Havar foil was installed and the produced [^{18}F]F$^-$ used for routine production of [^{18}F]FDG, [^{18}F]FAZA, and [^{18}F]FLT. Periodically (every 75,000–100,000 µAmin), a series of four test irradiations (1 @ 5,000 µAmin followed by 3 @ 1,000 µAmin) were carried out at 65 µA on $^{nat}H_2O$. All test irradiations were assayed for radionuclidic impurities.

---

[1] Avila-Rodriguez, et al., *Appl. Radiat. Isot.* (2008) 66: 1775 [2] Wilson, et al., *Appl. Radiat. Isot*. (2008) 66: 565

Results: The following figure summarizes the Havar-associated radionuclidic impurities measured for the initial (approx. 20,000–30,000 μAmin) test irradiations, and the Ta-sputtered sputtered foil to 80,000 μAmin ("Ta (80k)"). With a clear dependence noted on the integrated current, the reported values are given as the average and standard deviation of the end-of-bombardment (EOB) radioactivity normalized to the integrated current for each irradiation. It is important to note that since the radionuclidic impurities showed a marked decrease for the first few irradiations on all new foils before reaching a relatively constant value, the first three 1,000 μAmin irradiations were omitted when producing the figure below. Evaluation of this figure reveals that tantalum is the only film which demonstrates radionuclidic impurity reducing characteristics similar to that of niobium. Based on strong correlations observed between the radionuclidic and ICP-MS measurements, we have concluded that trends noted in the radionuclidic impurities are reflective of trends in the ionic impurities.

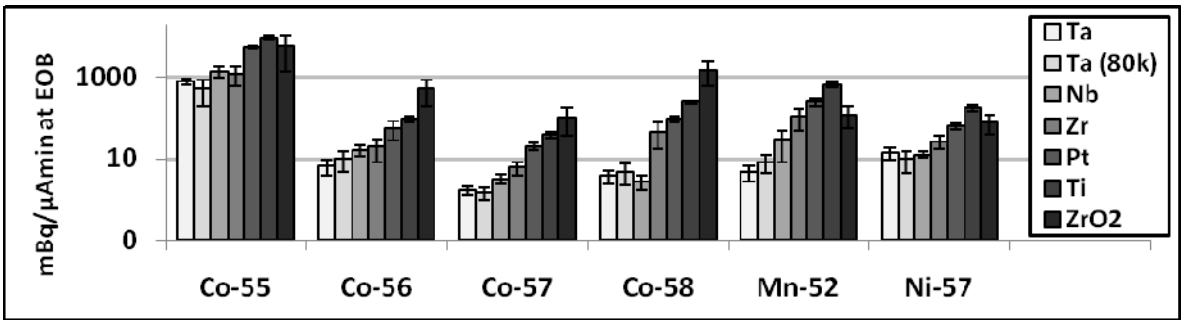

Table 1 summarizes the radionuclidic impurities (in units of mBq/μAmin at EOB) measured for the previously employed Nb-sputtered foil and the Ta-sputtered foil used on the production target. All values are reported as the average and standard deviation of the normalized activities. The integrated current (C) is reported as the total current on target prior to the test irradiations.

Table 1 C [μAmin]	Nb 979,307	Ta 473,696	Ta 1,0002,546
Co-55	9748 ± 1621	37 ± 48	721 ± 238
Co-56	2038 ± 237	75 ± 27	171 ± 56
Co-57	807 ± 98	5 ± 1	13 ± 4
Co-58	9248 ± 1097	42 ± 6	120 ± 35
Mn-52	9035 ± 1476	98 ± 41	111 ± 48
Ni-57	2708 ± 394	18 ± 9	73 ± 18

Table 2 summarizes the [^{18}F]FDG decay-corrected (DC) yields and end-of-synthesis (EOS) activities (A) obtained on the EPC's GE TracerLab MX synthesis unit for all syntheses performed up to the reported integrated current. A comparison of the average [^{18}F]FDG DC yield (for comparable total integrated currents) demonstrates a 6.4 percent improvement (one-tailed t-test, $p = 0.0025$) with the Ta-sputtered foil when compared with the previously employed Nb-sputtered foil.

Table 2 C [μAmin]	Nb 936,802	Ta 922,113
N	38	35
Mean DC yield [%]	60.9 ± 11.7	67.3 ± 6.1
EOS $A_{average}$ [GBq]	123 ± 26	139 ± 19
EOS A_{max} [GBq]	171	184
EOS A_{min} [GBq]	64	109

Conclusions: Compared with our current Nb-sputtered Havar standard, the Ta-sputtered Havar demonstrates a significant reduction in the Havar-associated impurities following prolonged use up to ~1,000,000 μAmin. In addition to decreased Havar-associated impurities, we have also noted an improvement in the [^{18}F]FDG yields and yield consistency. Studies are currently underway to further evaluate this Ta-sputtered foil to a total integrated current of ~1,500,000 μAmin.

Acknowledgements: This project was supported by the University of Alberta's MicroSystems Technology Research Initiative (MSTRI). The authors would like to thank Dr. Chris Backhouse and Ms. Eva Sant for their helpful discussions in film selection, and for performing the film sputtering.

A comparison of Nb, Pt, Ta, Ti, Zr, and ZrO_2-sputtered Havar foils for the high-power cyclotron production of reactive $[^{18}F]F^-$

K. Gagnon, J.S. Wilson, D. Robinson, S.A. McQuarrie

WTTC 13, July 2010

Background

- Ionic contaminants in irradiated $[^{18}O]H_2O$ have been attributed to decreases in the reactivity of $[^{18}F]F^-$
- Early 2006, Nb-sputtered Havar foils were first introduced at the Edmonton PET Centre
- Nb-sputtered Havar reduced the radionuclidic and chemical impurities and showed improved $[^{18}F]$FDG yields and yield consistency

Challenge

- Following prolonged irradiation, the Nb film oxidizes over time

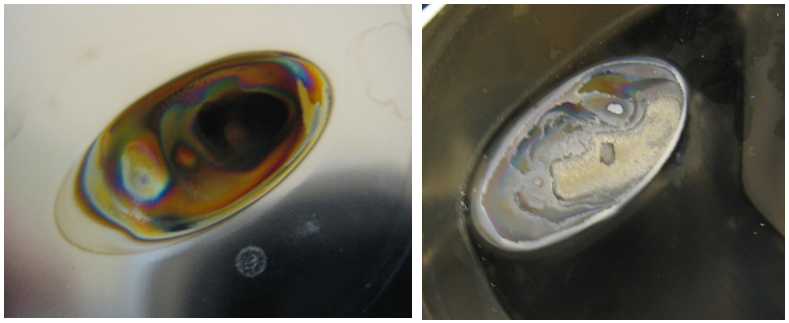

- Goal: Investigate alternative sputtering materials

Irradiations performed

- $^{nat}H_2O$ irradiations to:
  - Assess radionuclidic impurities (both Havar and non-Havar)
  - Measure conductivity of irradiated water
  - Perform ICP-MS (small sample subset)
- $[^{18}O]H_2O$ irradiations to:
  - Assess $[^{18}F]$FDG yield using TracerLab MX

$^{nat}H_2O$ irradiations

- Care taken to ensure consistent sample handing:

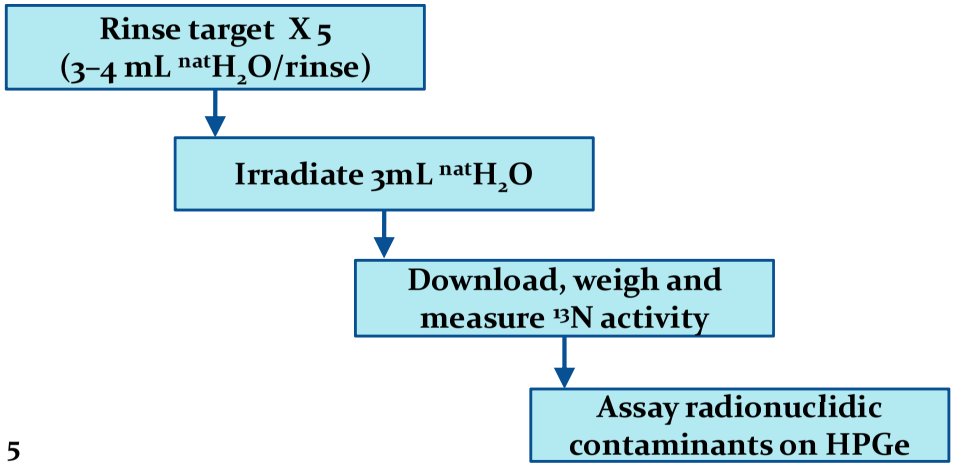

Initial test irradiations on $^{nat}H_2O$

Film	Approx. Thickness [nm]	N	Total Current [µAmin]	Average Current [µA]	^{13}N Yield [MBq/ µA]
Nb	400	12	28001	81	1255 ± 36
Pt	360	11	24029	69	1068 ± 131
Ta	350	13	32505	78	1261 ± 42
Ti	250	9	17047	74	1150 ± 80
Zr	375	15	31001	79	1257 ± 32
ZrO_2	450	13	29000	80	1219 ± 39

Results of initial irradiations

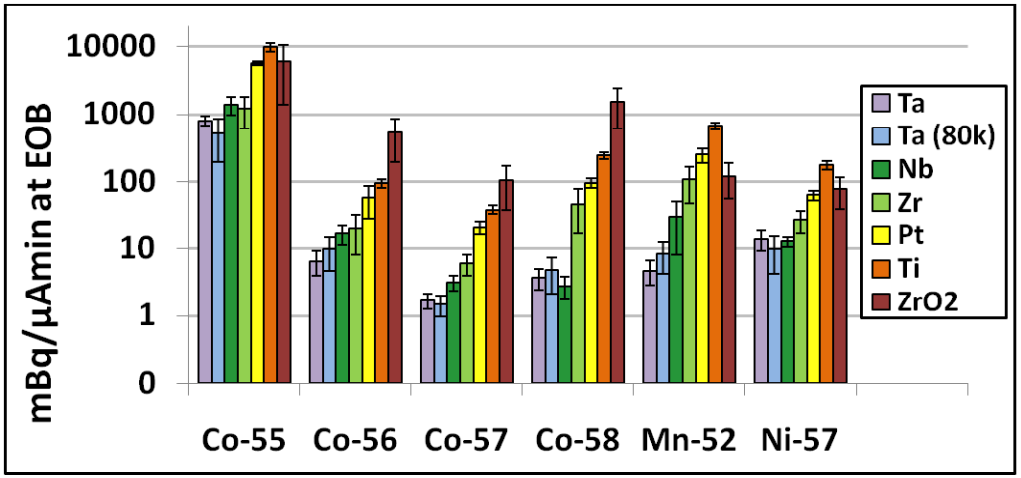

- Information from film radioactive contaminants was also useful

Tantalum – a promising candidate?

- Plan:
  - Setup Ta-sputtered Havar on main production target
  - Use [^{18}F]F$^-$ for clinical [^{18}F]FDG, [^{18}F]FAZA, and [^{18}F]FLT
  - Periodically measure the radionuclidic contaminants by irradiating $^{nat}H_2O$
- But first…
  - Irradiate $^{nat}H_2O$ on existing Nb-sputtered foil before removal (~1,000,000 µAmin) to establish baseline

Nb vs. Ta impurities [mBq/µAmin]

	Niobium 979,307 µAmin	Tantalum 473,696 µAmin	Tantalum 1,0002,546 µAmin	Tantalum 1,517,223 µAmin
Co-55	9748 ± 1621	37 ± 48	721 ± 238	545 ± 454
Co-56	2038 ± 237	75 ± 27	171 ± 56	329 ± 159
Co-57	807 ± 98	5 ± 1	13 ± 4	21 ± 11
Co-58	9248 ± 1097	42 ± 6	120 ± 35	194 ± 107
Mn-52	9035 ± 1476	98 ± 41	111 ± 48	206 ± 156
Ni-57	2708 ± 394	18 ± 9	73 ± 18	72 ± 50

[^{18}F]FDG yield comparison

	Niobium 936,802 µAmin	Tantalum 922,113 µAmin	Tantalum 1,534,025 µAmin
N	38	35	57
Mean decay corrected yield [%]	60.9 ± 11.7	67.3 ± 6.1	68.6 ± 6.3
Mean EOS Activity [GBq]	123 ± 26	139 ± 19	143 ± 20
Max EOS Activity [GBq]	171	184	202
Min EOS Activity [GBq]	64	109	109

Statistically significant (p = 0.0025) improvement in the [^{18}F]FDG yield for comparable total integrated currents when using Ta vs. Nb

Summary

- Pt, Ti, Zr, and ZrO_2 were not viable sputtering materials for coating Havar
- Ta-sputtered Havar has been extensively tested to ~1,500,000 µAmin
- Ta-sputtered Havar was shown to outperform Nb-sputtered Havar for prolonged irradiations:
  - Reduced impurities
  - Improved [^{18}F]FDG yields
  - Improved [^{18}F]FDG yield consistency

Trends for Ta-Havar

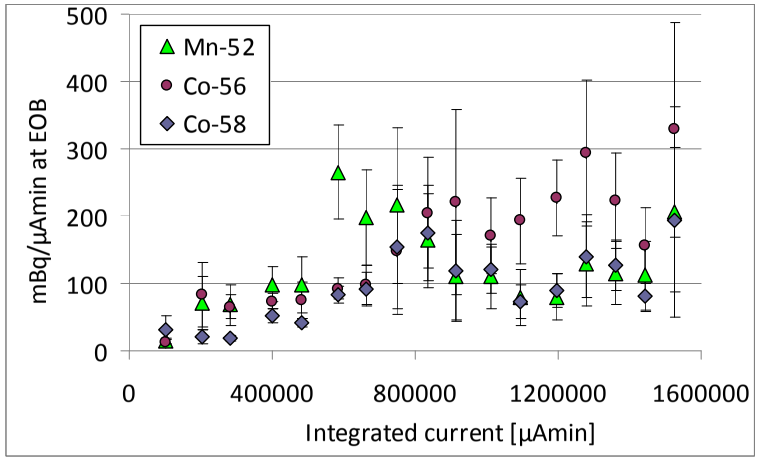

Note: Nb @ ~1,000,000 uAmin:

^{52}Mn = 9035, ^{56}Co = 2038, ^{58}Co = 9248

A simple calibration-independent method for measuring the beam energy of a cyclotron

K. Gagnon[1], M. Jensen[2], H. Thisgaard[2+], J. Publicover[3++], S. Lapi[3+++], S.A. McQuarrie[1] and T.J. Ruth[3]

[1]Edmonton PET Centre, Cross Cancer Institute, University of Alberta, Edmonton, AB, CANADA
[2]Hevesy Laboratory, Risoe-DTU, Technical University of Denmark, Roskilde, DENMARK
[3]TRIUMF, Vancouver, BC, CANADA
[+]Presently at PET and Cyclotron Unit, Odense University Hospital, Odense, DENMARK
[++]Presently at University Health Network, Toronto, ON, CANADA
[+++]Presently at Mallinckrodt Institute of Radiology, Washington University, St. Louis, MO, USA

Introduction: When used for medical radionuclide production, both new and old cyclotrons need to have their beam energy checked periodically. This is not only part of good manufacturing practice and quality assurance but is also necessary for optimising target yields and minimising the radiation dose overhead of radionuclide production. As the production targets for most medical cyclotron configurations sit more or less straight on the vacuum tank with no room for beam diagnostics, an off-line approach for evaluating the beam energy of a medical cyclotron is required. Although beam monitor reactions have been extensively published, evaluated, and used for many years, the reliable use of these methods, at present, requires access to and knowledge of a well calibrated (typically HPGe) detector system.

Aim: Develop a simple method for evaluating the beam energy of a cyclotron to an accuracy of a few tenths of an MeV without using complex data analysis methods or sophisticated equipment.

Theory: To overcome the need for gamma spectroscopy and high quality efficiency calibrations, this study suggests the irradiation of two thin monitor foils of the same material interspaced by a thick energy degrader. By carefully selecting both the monitor foil material and degrader thickness, the differential activation of the two monitor foils may be used to determine the beam energy. The primary advantage to this technique is that by examining the ratio of two identical isotopes produced in the two monitor foils (e.g. ^{63}Zn/^{63}Zn) as opposed to, for example, the ^{62}Zn/^{63}Zn ratio resulting from proton irradiation of a single copper monitor foil, all detector efficiency calibration requirements are eliminated. The energy can thus be monitored by experimentally measuring the activity ratio and comparing this value with activity ratios predicted using published cross section data (σ) as given by: $\frac{A_{Foil1}}{A_{Foil2}} = \frac{\sigma_{Foil1}}{\sigma_{Foil2}}$. A sample plot of the predicted ^{63}Zn activity ratio is given [right] for a 350 μm aluminum degrader, 25 μm copper monitor foils, and a 25 μm aluminum vacuum foil.

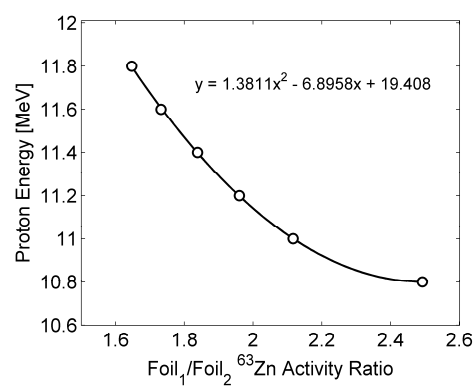

Methods: The proposed strategy was evaluated using 25 μm ^{nat}Cu monitor foils, a 25 μm aluminum window, and an aluminum energy degrader for protons in the 11–19 MeV range on the Edmonton PET Centre's (EPC) TR 19/9 cyclotron and the tandem Van de Graaff at Brookhaven National Lab (BNL). As the sensitivity of this technique depends upon the degrader thickness employed, this technique assumes prior knowledge of the beam energy (within ~ 1 MeV). The

degrader thicknesses employed in this study are given in the table [top right]. For the blind BNL measurements, the energy range was specified so that an appropriate degrader thickness could be selected.

Assumed Energy Range [MeV]	Al Degrader Thickness [μm]	A	B	C
10.8 – 11.8	350	1.3811	-6.8958	19.408
12.0 – 12.8	500	0.7058	-4.0449	17.795
13.0 – 13.8	625	0.5352	-3.1150	17.527
14.0 – 14.8	750	0.5223	-2.7947	17.696
15.0 – 15.6	875	0.5254	-2.5192	17.837
15.8 – 16.4	1000	0.7218	-2.8021	18.380
16.6 – 17.2	1125	1.1060	-3.3724	19.029
17.4 – 18.0	1250	2.1607	-4.7938	19.934
18.2 – 18.8	1375	4.5682	-7.3352	21.028

Prior to irradiation, the predicted activity ratios were determined using the IAEA recommended $^{nat}Cu(p,x)^{63}Zn$ cross sections (www-nds.ipen.br/medical/) and simulations performed in the TRIM module of SRIM (www.srim.org), v.2008.04. From these predicted ratios, we present in the above table the coefficients (A, B, and C) necessary for determining the proton energy incident on the aluminium vacuum window, $E(MeV) = Ar^2 + Br + C$, where r is the experimental ^{63}Zn activity ratio measured between the front and back copper foil. In obtaining these coefficients we have assumed the presence of a 25 μm Al vacuum window, the Al degrader, and two 25 μm Cu monitor foils.

Following irradiation, the ^{63}Zn activity ratios were measured using Capintec™ CRC-15PET (EPC) and CRC-15W (BNL) dose calibrators set to an arbitrary calibration setting of 100. As ^{62}Cu and ^{62}Zn production is also possible during irradiation of ^{nat}Cu, activity measurements were made at: (i) a single time-point roughly 1-hour post-EOB to ensure minimal ^{62}Cu contribution, and (ii) multiple time-points from 20 minutes to 3 hours post-EOB where the ^{63}Zn activity reading contribution was determined through exponential curve fitting to account for both the ^{62}Cu and ^{62}Zn contributions.

Results: The table [bottom right] summarizes the incident energies evaluated using the ^{63}Zn activity ratio measured using either the single 1-hour post-EOB time-point or exponential stripping of the ^{63}Zn activity contribution via curve-fitting. All energies are reported as the energy incident on the vacuum foil and were calculated using the coefficients provided above. The excellent agreement noted with the nominal energy for the 1-hr measurements up to 17 MeV suggests that half-life discrimination is not necessary below this energy.

	E [MeV] Nominal	E [MeV] 1 hr	E [MeV] Curve
EPC	10.9	10.9	10.9
EPC	11.1	11.2	11.2
EPC	11.3	11.4	11.4
EPC	11.6	11.6	11.7
EPC	11.8	11.9	11.9
EPC	13.8	13.8	13.9
EPC	14.6	14.5	14.6
EPC	15.4	15.4	15.5
EPC	16.2	16.2	16.4
EPC	17.0	16.9	17.2
EPC	17.8	17.5	17.9
EPC	18.6	18.1	18.5
BNL	11.00	10.93	10.96
BNL	13.50	13.47	13.45
BNL	16.00	15.92	16.10
BNL	18.00	17.56	18.17
BNL	Blind (12.3)	12.32	12.32
BNL	Blind (14.4)	14.36	14.42

Conclusions: The new, simple, calibration-independent method proposed for measuring the beam energy of a cyclotron was found to provide an accurate determination of proton energies in the 11–19 MeV range without the need for sophisticated equipment. To facilitate the adoption of this technique into routine evaluation of the cyclotron beam energy, we have included a look-up table of recommended aluminum degrader thicknesses as well as a list of the corresponding curve fit data for evaluation of the proton energy using the measured ^{63}Zn activity ratio.

Acknowledgements: The authors would like to thank Drs. Chuck Carlson, Michael Schueller, and David Schlyer for helpful discussions and organizing the experiments at BNL. This work was supported through a grant from NSERC.

A simple calibration-independent method for measuring the beam energy of a cyclotron

K. Gagnon, M. Jensen, H. Thisgaard, J. Publicover,
S. Lapi, S.A. McQuarrie and T.J. Ruth

WTTC 13, July 2010

Proposed Method

- Irradiate two monitor foils interspaced by an energy degrader
- Compare the activation of the same isotope for both foils

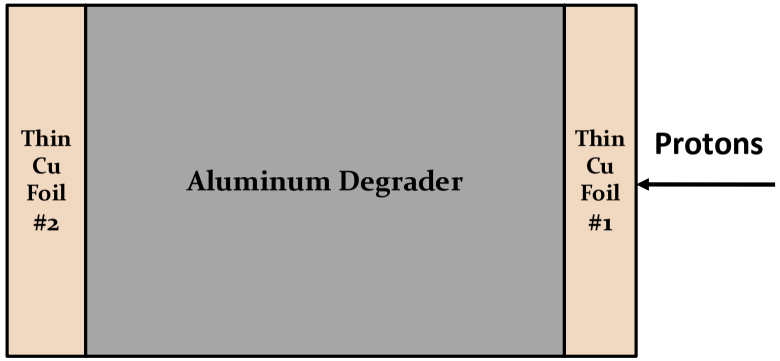

* Not to scale

Proposed Method:

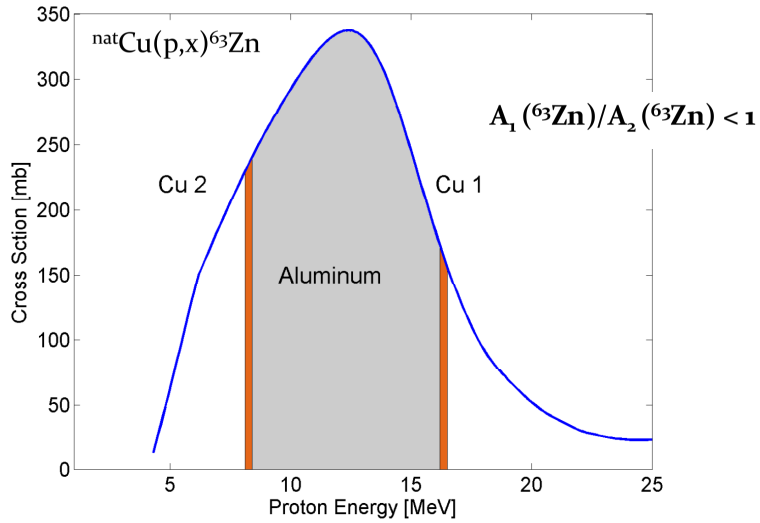

Proposed Method:

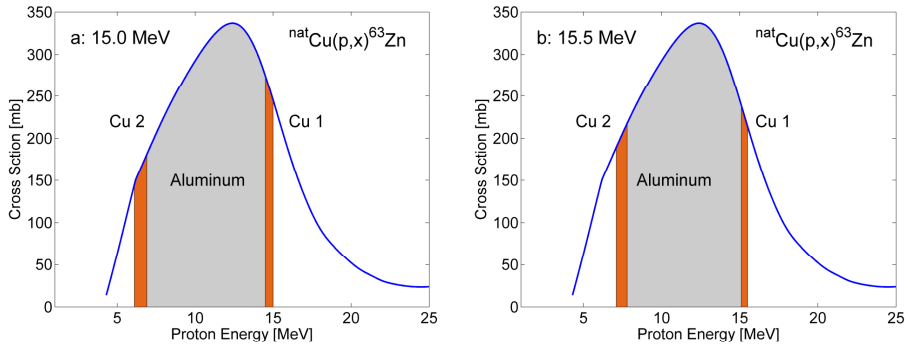

- Example given for 875 μm Al degrader and two 25 μm Cu foils

Predicting the ratio:

$$\frac{A_i}{A_j} = \frac{nI\sigma_i(E)\left(1-e^{-\lambda_i t_b}\right)}{nI\sigma_j(E)\left(1-e^{-\lambda_j t_b}\right)} = \frac{\sigma_i(E)\left(1-e^{-\lambda_i t_b}\right)}{\sigma_j(E)\left(1-e^{-\lambda_j t_b}\right)} = \frac{\sigma_i(E)}{\sigma_j(E)}$$

- Benefits of examining the ratio of <u>the same isotope</u>:
  - Ratio is independent of irradiation length
  - Ratio is independent of time post-EOB
  - Ratio depends only on the shape of the cross section curve (error in magnitude will not impact the results)

Implementation

- <u>Step 1 - Before experiment:</u>
  - Produce graph of energy vs. ^{63}Zn activity ratio.
  - Note: One degrader isn't optimal for all energies.
- <u>Step 2 – After experiment:</u>
  - Measure the activity ratio and use the plot to determine the irradiation energy.

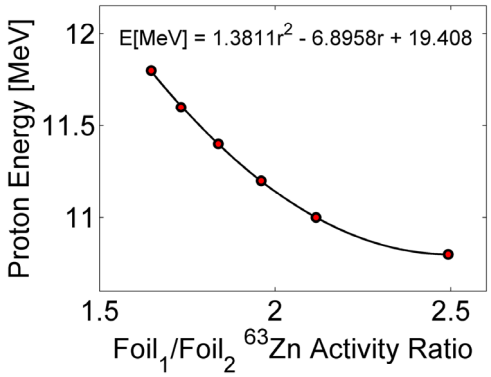

- Example above: Al = 350 μm, Cu = 25 μm, Vacuum window = 25 μm Al

Efficiency calibration independent!

- Since we are examining the ratio of <u>the same isotope</u>, detector efficiency calibration factors will cancel!

$$\frac{A_i}{A_j} = \frac{Rdg_i}{Rdg_j}$$

<u>Consequently:</u>

- Can use arbitrary calibration factor
- Simplifies use of a dose calibrator
- Do not have to wait 5+ hours
- Spectrum analysis is not required

Competing reactions?

- Said that: $\frac{A_i}{A_j} = \frac{Rdg_i}{Rdg_j}$
- Only true if ^{63}Zn is the only contribution to the reading

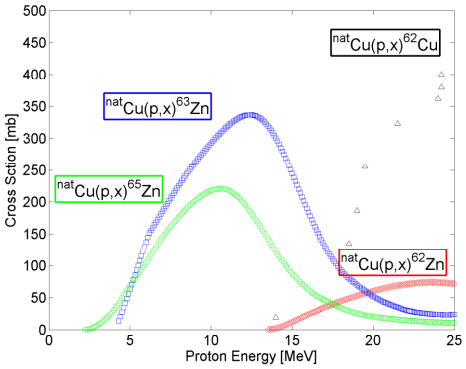

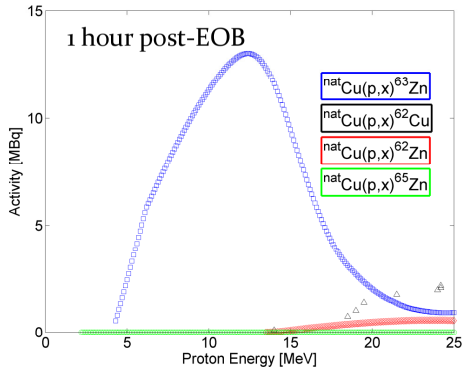

Results EPC:

Incident energy [MeV]	Measured energy [MeV]		
	Nominal Thickness	Measured Thickness	Maximum Δ from nominal E
10.9	10.9	10.9	--
11.1	11.2	11.2	0.1
11.3	11.4	11.4	0.1
11.6	11.6	11.6	--
11.8	11.9	11.9	0.1
13.8	13.8	13.8	--
14.6	14.5	14.5	0.1
15.4	15.4	15.4	--
16.2	16.2	16.2	--
17.0	16.9	16.9	0.1
17.8	17.9*	17.9*	0.1
18.6	18.5*	18.5*	0.1

Tandem Van de Graaff at BNL:

Incident energy [MeV]	Measured energy [MeV]		
	Nominal Thickness	Measured Thickness	Maximum Δ from nominal E
11.00	10.93	10.98	0.07
13.50	13.47	13.51	0.03
16.00	15.92	15.94	0.08
18.00	18.17*	18.18*	0.18
Blind (12.0-12.8) 12.30	12.32	12.36	0.06
Blind (14.0-14.8) 14.40	14.36	14.37	0.04

Reproducibility at EPC:

Attempt	E [MeV] 1 hour	E [MeV] 2 hours
1	14.43	14.49
2	14.37	14.40
3	14.27	14.31
4	14.41	14.44
5	14.43	14.48
6	14.38	14.42
7	14.43	14.49
8	14.43	14.50
9	14.34	14.36
10	14.40	14.44
Average	**14.39**	**14.43**
Standard Deviation	**0.05**	**0.06**

Summary

- Evaluated a new method for measuring E_p
- Method is independent of detector calibration
- Method is simple to perform using equipment on hand
- Method is insensitive to small variations in nominal foil thickness and shows good reproducibility and agreement with the nominal energies
- Future work: Other energy ranges? Deuterons?

WTTC XIII – Presentation Discussions

1. Careful with Foil thickness error

Thermal modelling of a solid cyclotron target using finite element analysis: An experimental validation

K. Gagnon, J.S. Wilson, and S.A. McQuarrie

Edmonton PET Centre, Cross Cancer Institute, University of Alberta, Edmonton, AB, CANADA

Introduction: Although radioisotope production yields may be increased by elevating the irradiation current, the maximum allowable irradiation current is often dictated by the thermal performance of a target. This limitation is commonly observed for solid targets as these materials often demonstrate poor thermal conductivities and low melting points. As we are interested in improving the power rating of solid targets by optimizing the shape and location of the cooling channels, we have investigated the use of finite element analysis to model both heat transfer and turbulent flow. Before cooling optimization can be performed however, we needed to first validate our initial model. Such an experimental validation is the focus of this work.

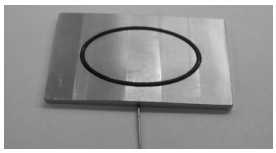

Methods: For the purpose of validating the finite element model, we have designed a target plate with a simplistic geometry. In order to perform on-line real-time temperature measurements, this target plate is equipped with a thermocouple that extends to the centre of the plate [upper right]. Target plates of both copper and zirconium were constructed. These materials were selected for their markedly different thermal properties: copper is an excellent thermal conductor with a thermal conductivity, *k*, of 401 $Wm^{-1}K^{-1}$ (@ 300 K), while zirconium is a relatively poor thermal conductor with *k* equal to 22.6 $Wm^{-1}K^{-1}$ (@ 300 K). The target plate and thermocouple were mounted into the water/helium cooled target assembly [lower right]. Irradiations were performed with proton currents up to 80 μA (17.5 MeV) for the copper plate and 50 μA (15.5 MeV) for zirconium. Both the beam tuning[1] and target positioning were optimized to maximize the temperature readout. In calculating the power on the target plate, we have assumed a 10 percent beam loss to the target nosepiece/helium cooling chamber. Several low current measurements were also obtained without helium cooling as this source of cooling is not yet incorporated into the finite element model.

The 3D heat transfer and turbulent flow of the cooling water were modelled using the COMSOL Multiphysics® v. 3.5a. steady-state general heat transfer and k-ε turbulence models, respectively. Experimental input parameters to the model include the cooling water temperature, cooling water flow rate, target plate/cooling water channel geometry, and a sample proton beam profile obtained using radiochromic film[2]. The temperature dependent material properties (i.e. thermal conductivity, density, heat capacity, etc.) were defined using COMSOL's built-in material library.

One of the primary challenges in developing the model was to accurately define the convective heat transfer at the water/plate boundary. Although COMSOL has built-in heat transfer coefficients for various geometrical configurations, at present these coefficients are limited exclusively to air cooling applications. To this end, three user-defined strategies were employed for evaluating the convective heat transfer coefficient at the water/plate interface.

---

[1] See WTTC13 abstract: J.S. Wilson et al., A Simple Target Modification to Allow for 3-D Beam Tuning

[2] Avila-Rodriguez et al., Appl. Radiat. Isot., 2009, 67: 2025

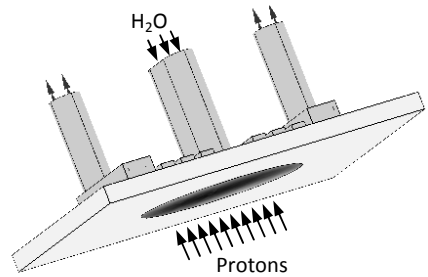

The cooling geometry under consideration consists of a single central-inlet water-cooling channel and two water-outlets, all of which are perpendicular to the target plate [upper right]. Although the Dittus-Boelter and Sieder-Tate heat transfer formalisms are used to describe turbulent forced convection within long straight pipes (which is not representative of our geometric configuration), these two strategies were nevertheless investigated as both formalisms have been previously implemented and recommended for targetry applications[3,4,5]. The third model employed for evaluating the heat transfer coefficient (selected for its geometric similarity to our configuration) was a method characterized by Chang et al. for turbulent submerged liquid jets[6]. In all three strategies the Reynolds number was calculated from the temperature dependent water properties, the hydraulic diameter of the inlet water-cooling channel and the inlet water velocity, while the Prandtl number was calculated from the temperature dependent water properties. COMSOL's non-linear, direct (UMFPACK) parametric segregated solver was employed to evaluate beam powers ranging from 50–1300 W.

Results: Three models were employed for characterizing the heat transfer at the water/plate boundary. Although all three strategies give rise to heat transfer coefficients whose magnitude increases as the cooling-water flow rate increases, when comparing the model predictions with experimental data [graphs, right], the results of this work suggest that the heat transfer in our geometric configuration is best described by the method proposed by Chang et al[6]. The poor performance of the Dittus-Boelter and Sieder-Tate correlations has been attributed to the underlying geometric assumptions of these models.

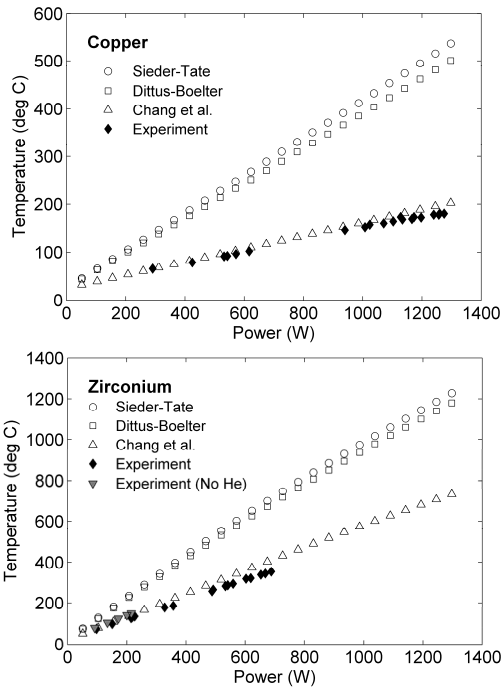

Conclusion: The experimental measurements performed in this study have allowed us to select a convective heat transfer model which is capable of accurately predicting the target plate temperature for materials with widely varying thermal properties. Future finite element investigations will include the introduction of helium cooling and the optimization of the cooling channel geometry for the purpose of improving the solid target power rating.

Acknowledgements: The authors would like to thank Dr. Avila-Rodriguez for early development of the 3D target model. This project has been made possible through a grant from the Alberta Health Services and the Alberta Cancer Foundation.

[3] Pavan et al., J. Radioanal. Nucl. Chem., 2003, 257: 203
[4] Avila-Rodriguez et al., Proceedings of the COMSOL Conference, 2007, 359.
[5] IAEA Technical Reports Series no. 465, Vienna, 2008
[6] Chang et al., Int. J. Heat Mass Transfer, 1995, 38: 833

Thermal modelling of a solid cyclotron target using finite element analysis: An experimental validation

K. Gagnon, J.S. Wilson, D. Robinson, S.A. McQuarrie

WTTC 13, July 2010

Motivation

- Although increased beam currents are desired, production is often limited by the thermal performance of the target
- Finite element analysis can be employed to model heat transfer and turbulent flow within the target
- Desire to use models to improve target thermal performance
- Goal of this work: Experimentally validate a finite element analysis based heat transfer/turbulent flow model

Modeling the thermal performance

- Modelling of the heat transfer and cooling flow using COMSOL Multiphysics (finite element analysis)
- Input parameters to model include:
  - Geometry (plate/cooling)
  - Target materials
  - Cooling flow/temperature
  - Convective heat transfer coefficient
  - Proton current
  - Experimental beam profile and scaling as a function of depth (to account for non-uniform dE/dx)

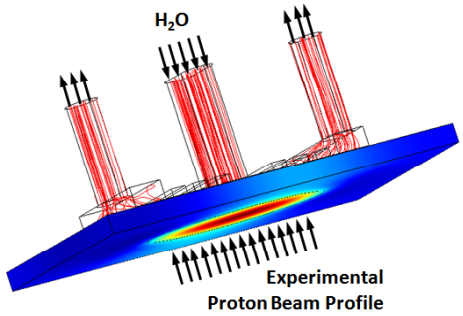

Heat transfer coefficient

- Difficulty: How to define the convective heat transfer coefficient?

Chang:

$$h=\left(\frac{k}{D}\right)(\mathrm{Re})^{0.574}(\mathrm{Pr})^{0.4}\left(\frac{z}{D}\right)^{-0.106}\left[0.66\left[1+0.1147\left(\frac{r}{D}\right)^{1.81}\right]^{-1}\left(\frac{r}{D}\le 1.25\right)+0.7017\left(\frac{r}{D}\right)^{-0.62}\left(\frac{r}{D}>1.25\right)\right]$$

Sieder-Tate:

$$h=0.023\left(\frac{k}{D}\right)(\mathrm{Re})^{0.8}(\mathrm{Pr})^{0.33}\left(\frac{\mu_b}{\mu}\right)^{0.14}$$

Dittus-Boelter:

$$h=0.023\left(\frac{k}{D}\right)(\mathrm{Re})^{0.8}(\mathrm{Pr})^{0.4}$$

Re = Reynolds Number
Pr = Prandtl Number
D = hydraulic diameter
k = thermal conductivity
μ = kinematic viscosity
μ_b = bulk kinematic viscosity
z = plate spacing
r = radial distance from jet

Experimental validation

- Compared experimental measurements with the three strategies for defining the heat transfer coefficient at the water/plate interface
- Examined Cu and Zr

Material	m.p. (K)	k @ 300 K [$Wm^{-1}K^{-1}$]
Copper	1357	401
Gold	1337	318
Rhodium	2237	150
Molybdenum	2896	139
Nickel	1728	90.9
Platinum	2041	71.6
Tantalum	3290	57.5
Niobium	2750	53.7
Zirconium	2128	22.6

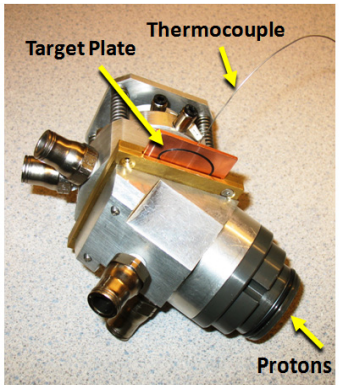

Experimental validation (results)

- Model is capable of accurately predicting temperature for materials with markedly different thermal properties

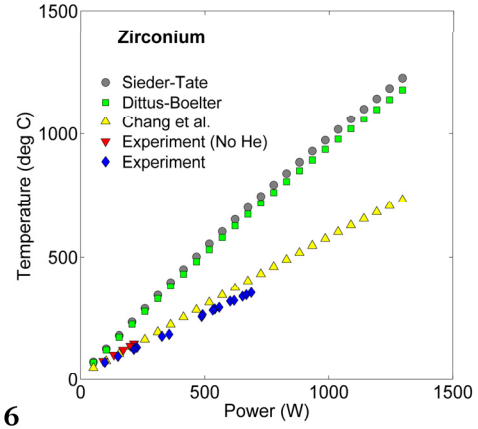

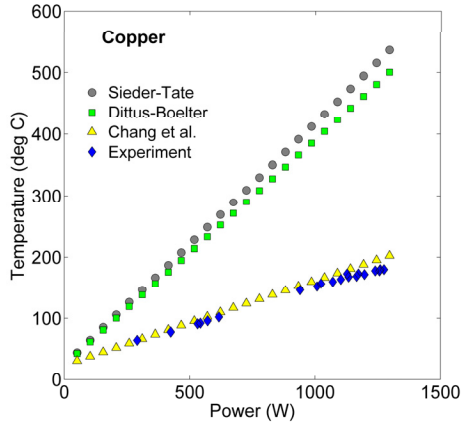

Mo on Ta, E_p = 24→10 MeV

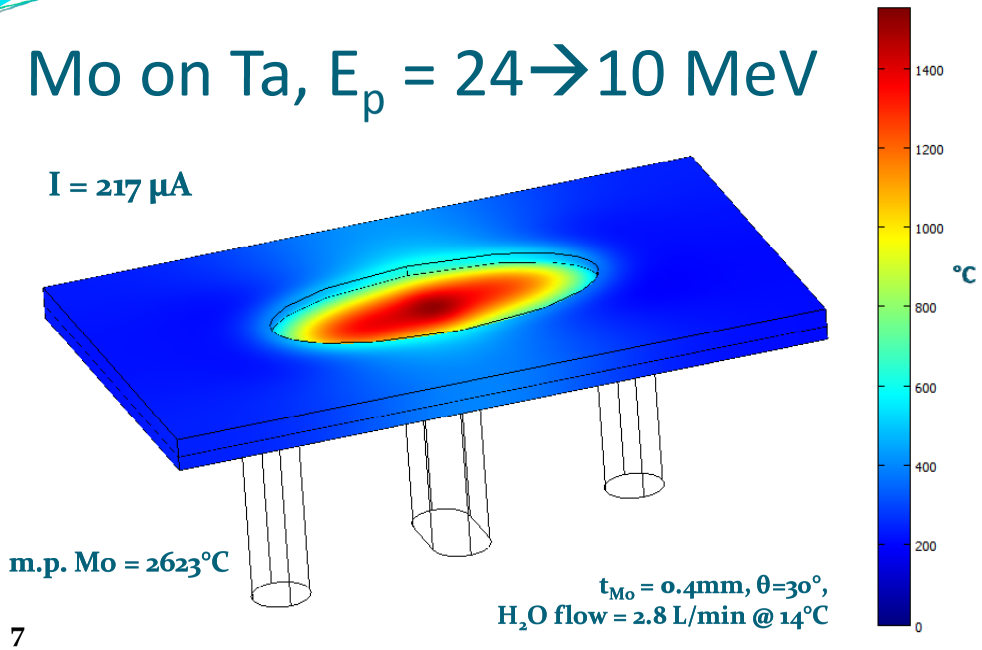

Mo on Cu vs. Mo on Ta @ 217 μA

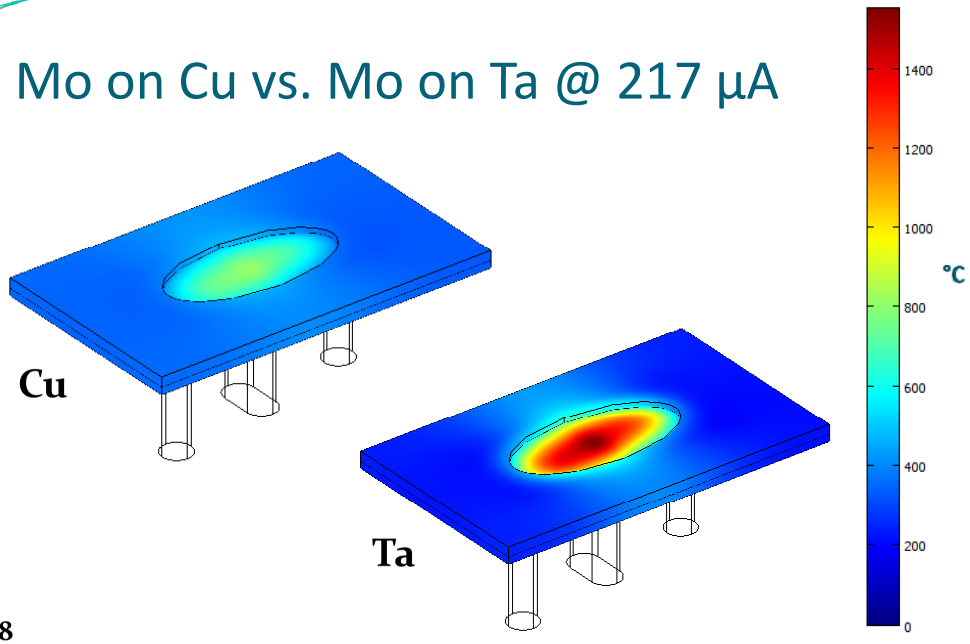

Areas for optimization?

- Target plate material
- Water flow rate
- Input water temperature
- Cooling channel/fin geometry
- Helium cooling geometry

Summary

- Experimental temperature measurements (on Cu and Zr) were compared with model predictions.
- The experimental measurements have led to the selection of the heat transfer coefficient described by Chang et al.
- Model allows us to explore methods for improving the thermal performance of the target

Beam profile & scaling with depth

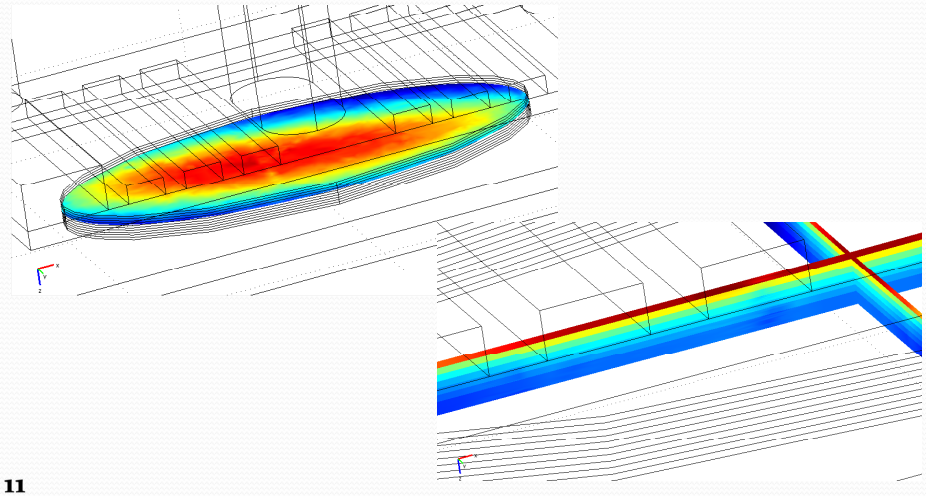

WTTC XIII – Presentation Discussions

1. Simulation conditions
   - Simulation starts on influx
   - Will water get out symmetrically?
   - Non-symmetric and finite element model can improve cooling

RDS-111 to Eclipse HP Upgrading with Improvement in ^{18}F Production

A. Zarate-Morales, A. Flores-Moreno, J.C. Manrique-Arias, E. Zamora-Romo, M.A. Avila-Rodriguez

Unidad PET/CT-Ciclotrón, Facultad de Medicina, Universidad Nacional Autónoma de México, México, D.F., México

The first PET Center in Mexico was inaugurated in 2001 at the School of Medicine of the National Autonomous University of Mexico (UNAM). In that time a self-shielded CTI RDS-111 cyclotron with targetry for the production of the main sequence CNOF radionuclides was installed. Nowadays, there are 3 compact cyclotrons in the country and 11 PET/CT cameras in different hospitals. UNAM´s cyclotron produces FDG for 6 of the 8 PET scanners located in hospitals and clinics of Mexico City, and more hospitals are planning to install more PET/CTs. To satisfy this increased demand of FDG, one of the beam lines of our RDS-111 cyclotron was recently upgraded to an Eclipse HP configuration. In this way, now we have a hybrid cyclotron with BL1 as Eclipse HP and BL2 as RDS-111.

The main features of the upgrade include a new ion source that increased the beam current from 40 to 60μA, a new four-position target carrousel capable to handle 60μA, high power gridded-targets designed to be operated under high pressure conditions (>1000 psi), target body of refractory material (Ta) for the production of ^{18}F, and installation of high vacuum butterfly valves to the diffusion pumps. In addition, the Eclipse HP beam line has no vacuum window, and therefore no helium recirculation cooling system. With this upgrade we practically double the yield of ^{18}F with the same time of bombardment. Table 1 shows the yield of the different radionuclides in both versions while Table 2 summarizes our experience regarding ^{18}F production.

Table 1. Comparison of yields (EOB) obtained in RDS-111 *vs.* Eclipse HP targets.

Radionuclide	RDS-111 (40 μA)	Eclipse HP (60 μA)
$^{18}F^-$	1187 mCi (1h, 1200 μL $H_2{}^{18}O$)	2300 mCi (1h, 2400 μL $H_2{}^{18}O$)
^{13}N	146 mCi (10 min)	213 mCi (10 min)
^{11}C	1547 mCi (40 min)	1902 mCi (40 min)

Table 1. Comparison of ^{18}F production runs in RDS-111 *vs.* Eclipse HP targets.

	Bombardment time	A_{EOB} of $^{18}F^-$	A_{EOS} of FDG	Production runs
RDS-111	747.2 h	536.4 Ci	271 Ci	506
Eclipse HP	393.3 h	839.2 Ci	455 Ci	455
HP/RDS	0.53	1.56	1.68	0.90

The benefits of the upgraded BL were immediate for the production of ^{18}F. The high volume Ta target produces more activity of highly reactive n.c.a. [^{18}F]fluoride compared with the traditional Ag target of the RDS-111 configuration. We are still producing ^{18}F in both targets using the Ta target for the heavy morning-production run, and the Ag target for the second and less heavy production run at midday. Other benefits of the upgrade include a faster (0.5 h *vs.* 4 h) recovery of the vacuum in case of the rupture of a window, and lengthened the maintenance intervals of the ^{18}F target decreasing the radiation exposition to the cyclotron staff. Our plans for this year are to upgrade the second BL to the Eclipse HP configuration with the option for the irradiation of solid targets.

RDS-111 To Eclipse HP Upgrading with Improvement in ^{18}F

A. Zarate-Morales, A. Flores-Moreno, J.C. Manrique-Arias, E. Zamora-Romo, M.A. Avila- Rodriguez

Unidad PET/CT-Ciclotrón, Facultad de Medicina, Universidad Nacional Autónoma de México,
México, D.F., México

The first PET Center in Mexico was inaugurated in 2001 at the School of Medicine of the National Autonomous University of Mexico (UNAM). In that time a self-shielded CTI RDS-111 cyclotron with Targetry for the production of the main sequence CNOF radionuclides was installed.

Nowadays, there are 3 compact cyclotrons in the country and one TRACE (GE) and 11 PET/CT cameras in different hospitals. UNAM´s cyclotron produces FDG for 6 of the 8 PET scanners located in hospitals and clinics of Mexico City, and more hospitals are planning to install more PET/CTs.

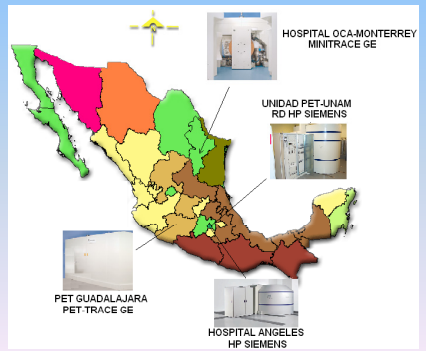

To satisfy this increased demand of FDG, one of the beam lines of our RDS-111 cyclotron was recently upgraded to an Eclipse HP configuration. In this way, now we have a hybrid cyclotron with BL1 as Eclipse HP and BL2 as RDS-111. In 2005 our facility provided 10 unidoses diary, today produce 35 unidoses per day in average. In 2006 increased the unidoses and was neccesary make two or three runs per day.

Some reasons for upgrade the RDS were:

a) Trouble with carusel system . The target position was non-reproducible when the carusel moved to F-18-N-13 and F-18.

b) RF and magnet are not stable.

c) When the window target was broken, the recovery of the accelarator consuming four hours

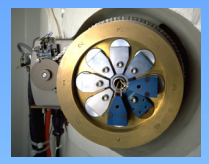
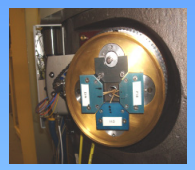


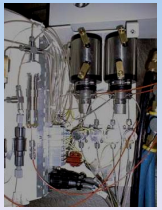


With this upgrade we practically double the yield of F-18 with the same time of bombardment. Table 1 shows the yield of the different radionuclide in both version.

Table 1. Comparison of yields (EOB) obtained in RDS-111 *vs.* Eclipse HP targets.

Radionuclide	RDS-111 (40 µA)	Eclipse HP (60 µA)
$^{18}F^-$	1187 mCi (1h, 1200 µL $H_2{}^{18}O$)EOB	2300 mCi (1h, 2400 µL, $H_2{}^{18}O$)EOB
^{13}N	146 mCi (10 min)	213 mCi (10 min)
^{11}C	1547 mCi (40 min)	1902 mCi (40 min)

RESULTS

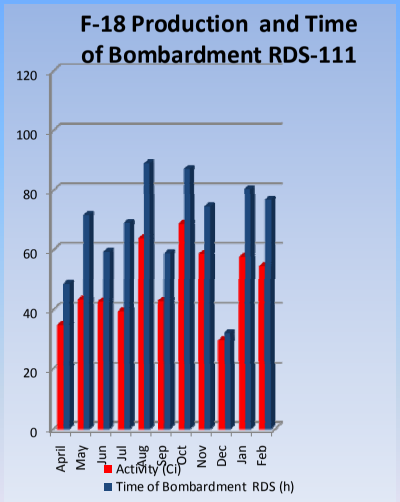

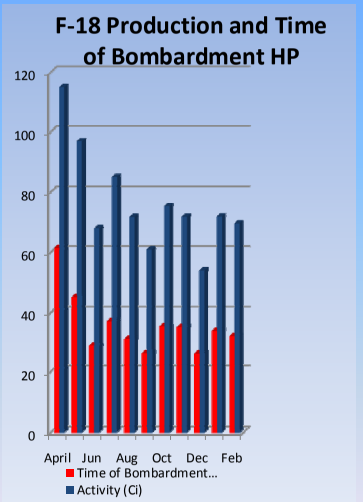

The doses obtained before and after upgrade. In the data are not included the doses applied in our nuclear medicine laboratory

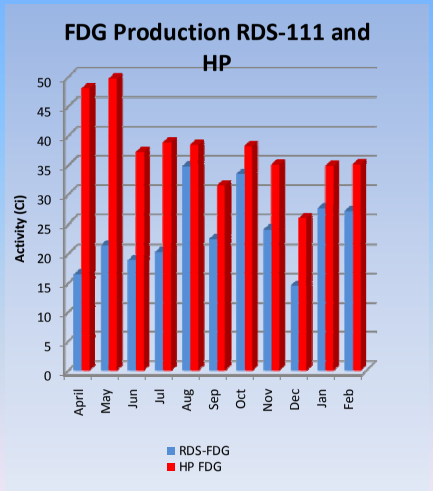

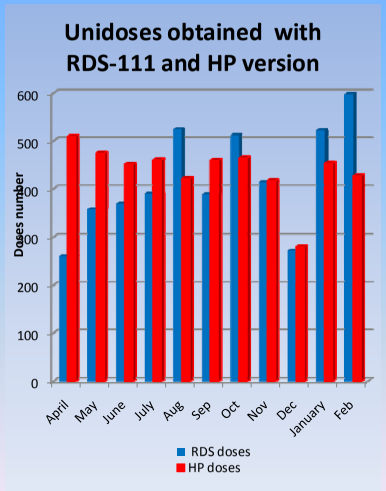

Comparison of F-18 production runs in RDS-111 *vs.* Eclipse HP targets. Bombardment time AEOB of F-18. AEOS of FDG Production runs

	Bombardment time	AEOB of $^{18}F^-$	AEOS of FDG	Production runs
RDS-111	747.2 h	536.4 Ci	271 Ci	506
Eclipse HP	393.3 h	839.2 Ci	455 Ci	455
HP/RDS	0.53	1.56	1.68	0.90

Conclusion: Benefits of the RDS Eclipse

The benefits of the upgraded BL1 were immediate for the production of F-18:

- The high volume Ta target produces more activity of highly reactive n.c.a. [F18]fluoride compared with the traditional Ag target of the RDS-111configuration.
- We are still producing F -18 in both targets using the Ta target for the heavy morning-production run, and the Ag target for the second and less heavy production run at midday.
- Other benefits of the upgrade include a faster (0.5 h vs. 4 h) recovery of the vacuum in case of the rupture of a window, and lengthened the maintenance intervals of the F-18 target decreasing the radiation exposition to the cyclotron staff.
- The RDS Eclipse upgrade allows the routine production of 40 unidoses of FDG with a high degree of success, added of production of (N-13) Amonia and (C-11)- Acetate and (F-18)FLT.

Upgrade of 2nd Beam Line in 2011

With solid target irradiation option

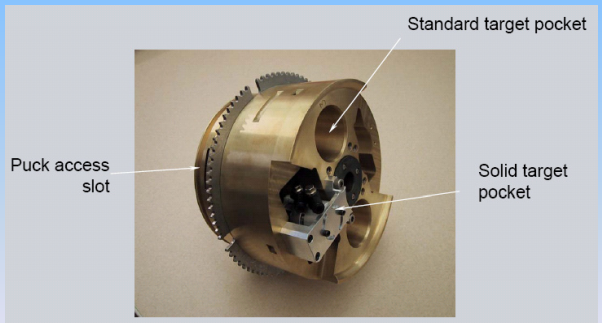

Abstract 013

Title: **CYCLOTECH – A method for Direct Production of ^{99m}Tc using Low Energy Medical Cyclotrons**

Authors: **Johnson RR[1], Wm. Gelbart[2], Benedict M[3], Cunha L[4], Metello LF[4]**

1 – Best Cyclotrons Systems Inc (BSCI - Team BEST), Ottawa, Canada and University of British Columbia, Vancouver, Canada;

2 – Advanced Systems Design (ASD), Garden Bay, Canada;

3 - Molecular Diagnostics and Therapeutics Inc. (MDTI), Longmont, Colorado, USA;

4 – Isótopos para Diagnóstico e Terapêutica SA (IsoPor SA), Porto, Portugal and Nuclear Medicine Department of the High Institute for Allied Health Technologies of Porto, Polytechnic Institute of Porto (ESTSP.IPP), Porto, Portugal.

Introduction:

This paper presents work in progress, to develop an efficient and economical way to directly produce Technetium 99metastable (^{99m}Tc) using low-energy – so-called "medical" – cyclotrons. Its importance is well established and directly relates to the increased global trouble in delivering ^{99m}Tc to Nuclear Medicine Departments relying on this radioisotope. Since the present delivery strategy has clearly demonstrated its intrinsic limits, our group decided to follow a distinct approach that uses the broad distribution of the low energy cyclotrons and the accessibility of Molybdenum 100 (^{100}Mo) as the Target material. This is indeed an important issue to consider, since the system here presented it is not based on the use of HEU (or even LEU) 235 Uranium, so entirely complying with the actual international trends and directives concerning the use of this potentially critical material.

The production technique is based on the nuclear reaction ^{100}Mo (p,2n) ^{99m} Tc whose production yields have already been documented.

The object of the system is to present ^{99m} Tc to Nuclear Medicine radiopharmacists in a routine, reliable and efficient manner that, remaining always flexible, entirely blends with established protocols.

Material and Methods:

We have developed a Target Station that can be installed on most of the existing PET cyclotrons and that will tolerate up to 400 µA of beam by allowing the beam to strike the Target material at an adequately oblique angle. The Target Station permits the remote and automatic loading and discharge of the Targets from a carriage of 10 Target bodies.

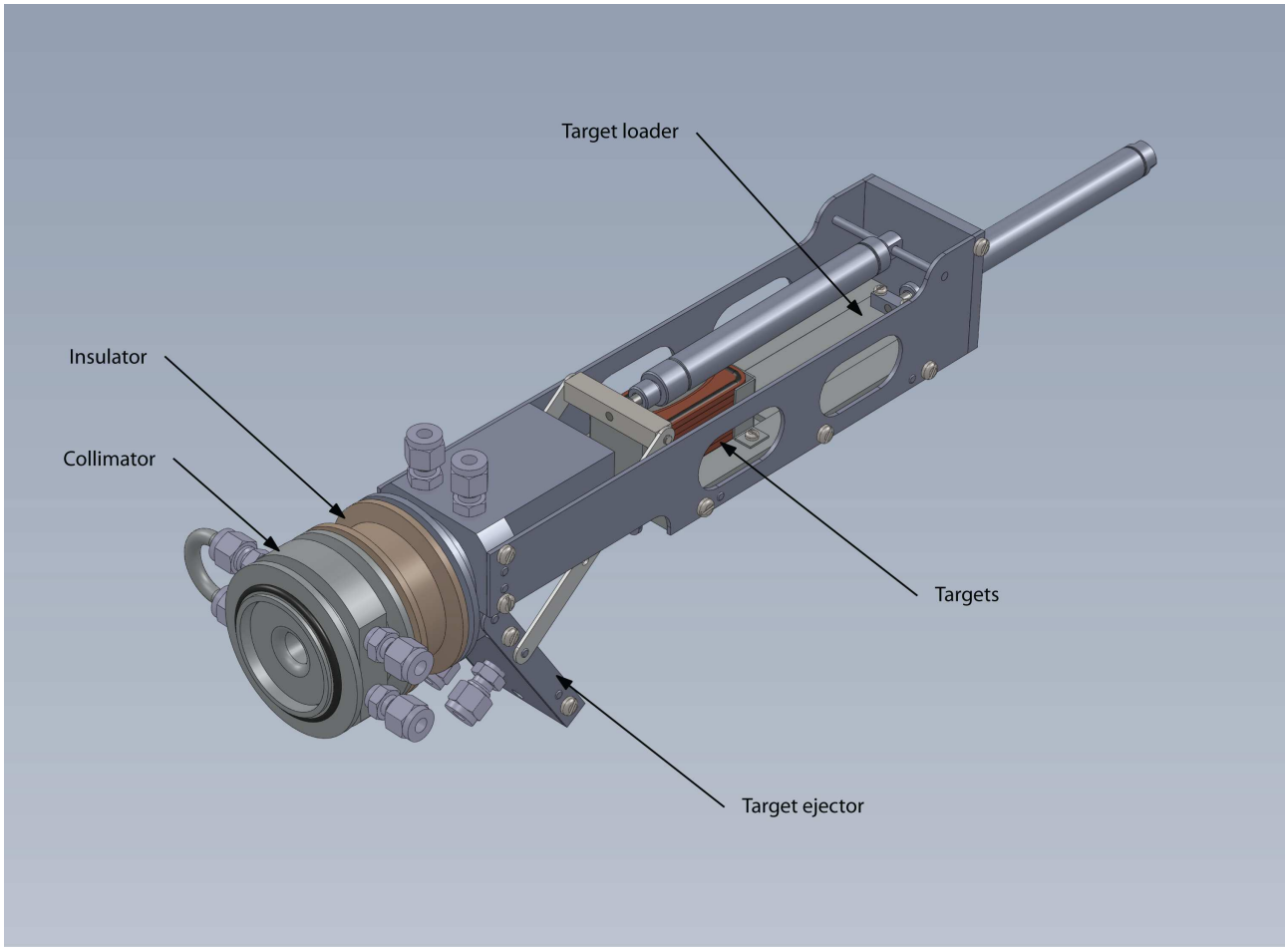

Fig1. The remotely controlled Target Changer ejects the irradiated Target (to a Transfer System that transports it to a Processing Unit –inserted in a dedicated Hot Cell) and loads a new one. Up to 10 Targets can be pre-loaded in the Target Changer.

Several methods of Target material deposition and Target substrates are presented. The object was to create a cost effective means of depositing and intermediate the target material thickness (25 - 100µm) with a minimum of loss on a substrate that is able to easily transport the heat associated with high beam currents.

The separation techniques presented are a combination of both physical and column chemistry. The object was to extract and deliver ^{99m}Tc in the identical form now in use in radiopharmacies worldwide. In addition, the Target material is recovered and can be recycled.

WTTCXIII

The 13th International Workshop on Targetry and Target Chemistry

WTTC13

DTU - Risoe (Denmark)
26 to 28 July 2010

CYCLOTECH – a Method for Direct Production of 99mTc using Low Energy - medical – Cyclotrons

(L.F. Metello, Wm Gelbart, M. Benedict , L. Cunha , F. Alves, V. Sossi, R. R. Johnson)

IsoPor S.A.

ESTSP POLITÉCNICO DO PORTO

Best healthcare for everyone

WTTCXIII

^{99m}Tc ROLE IN NUCLEAR MEDICINE

July 26 – 28th 2010

ESTSP POLITÉCNICO DO PORTO

IsoPor S.A.

Best healthcare for everyone

Nuclear Medicine...

… is a Medical Speciality in which low doses of radioactive materials are used for diagnosis, by imaging and non-imaging techniques, as well as for therapy in many disease processes. (WHO, 1960)

^{99m}Tc-Technetium is used in over 85% of NM Procedures

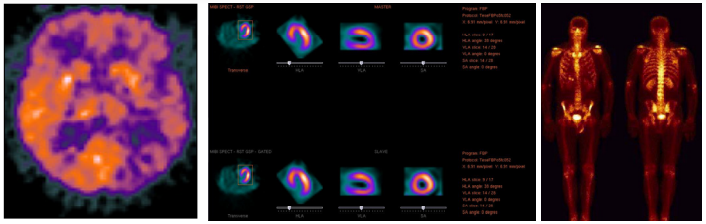

Neurology (10%) Cardiology (30%) Oncology (60%)

WTTCXIII

July 26 – 28th 2010

ESTSP POLITÉCNICO DO PORTO

IsoPor S.A.

Best healthcare for everyone

US Demand for Nuclear Medicine Procedures and ^{99m}Tc Generators

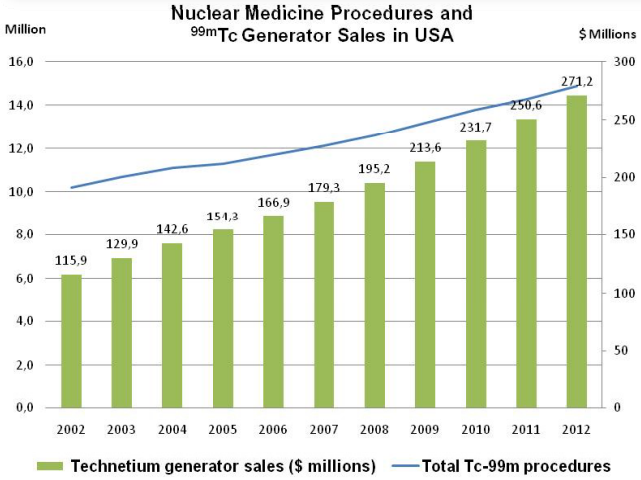

Minimal Annual Growth Rate: 6% (average: 12,3%)

Reference: Committee on Medical Isotope Production Without Highly Enriched Uranium, National Research Council (2009).

WTTCXIII

July 26 – 28th 2010

ESTSP POLITÉCNICO DO PORTO

IsoPor S.A.

Best healthcare for everyone

Cascade of Technetium-99m Production

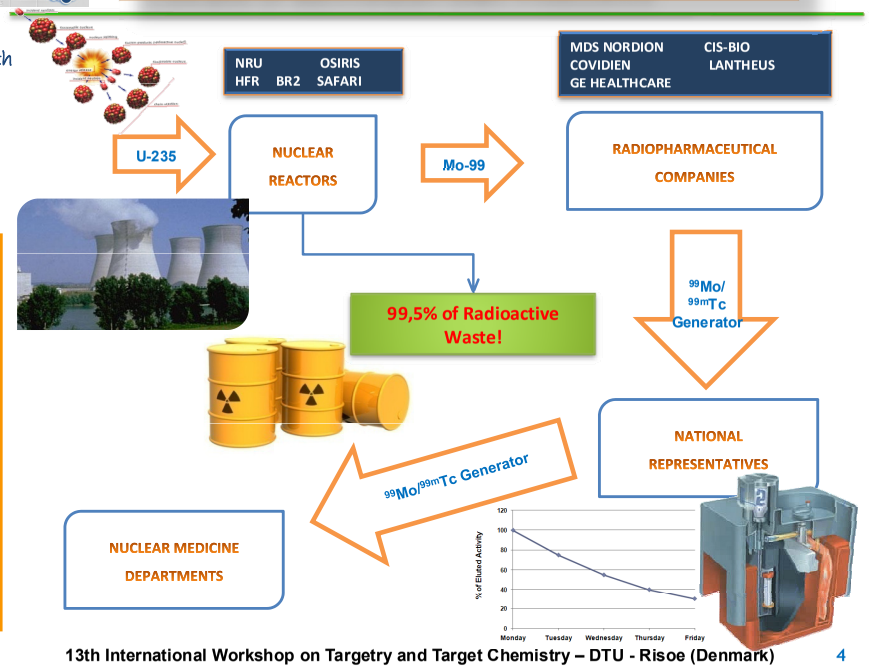

July 26 – 28th 2010

ESTSP
POLITÉCNICO DO PORTO
IsoPor S.A.
Best healthcare for everyone

Cascade of Technetium-99m Production

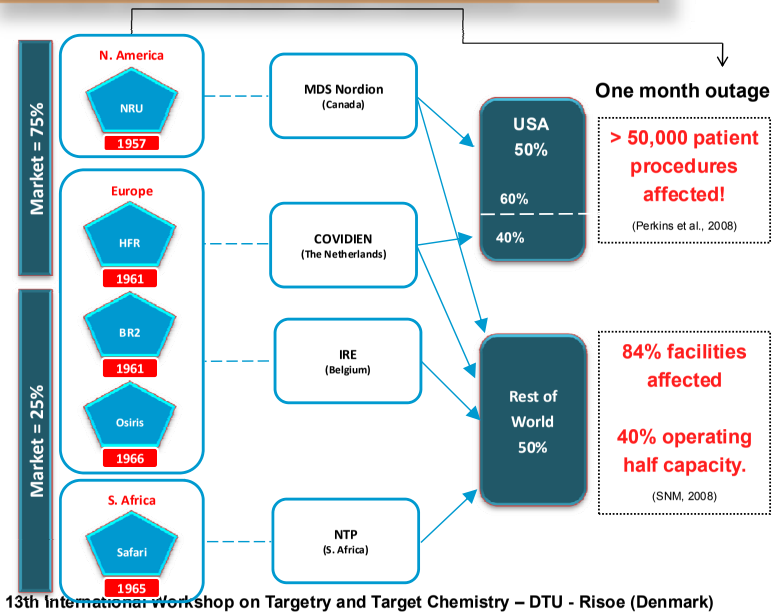

July 26 – 28th 2010

ESTSP
POLITÉCNICO DO PORTO
IsoPor S.A.
Best healthcare for everyone

Definitely…

Nuclear Medicine

Community needs a

reliable and **regular**

source of ^{99m}Tc!!

July 26 – 28th 2010

ESTSP
POLITÉCNICO DO PORTO
IsoPor S.A.
Best healthcare for everyone

Value System of the ^{99m}Tc Production (following CYCLOTECH)

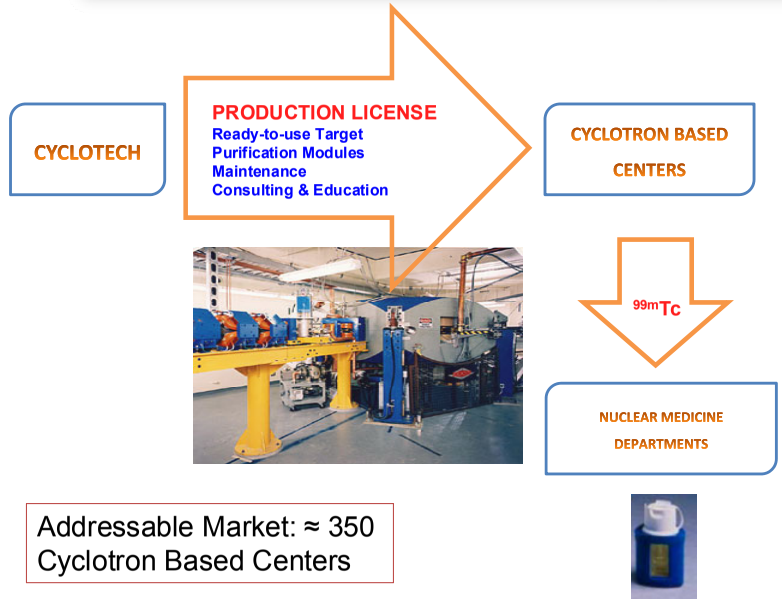

July 26 – 28th 2010

ESTSP
POLITÉCNICO DO PORTO
IsoPor S.A.
Best healthcare for everyone

For the Cyclotron Owners

- Cyclotron value chain optimization (actual occupation rate: only 15%);
- Additional service;
- Small extra investment;

For NM Departments

- Reliable and daily-based delivery;
- Workflow optimization;
- Increase in number of Procedures;
- Less storage of radioactive material on site/ less waste;
- Cost Reduction;

For the Environment

- Unlike NR production, Cyclotron based 99mTc production process is safer, cleaner and easier to spread worldwide in a short term

...in the meanwhile.....

July 26 – 28th 2010

ESTSP

POLITÉCNICO DO PORTO

IsoPor S.A.

Babcock & Wilcox Technical Services Group (B&W TSG)

has been awarded $9 million from the **National Nuclear Security Administration** (NNSA) for further development of **reactor technology** for **medical isotope** production using **low-enriched uranium**.

(Aunt Minnie, 29 Jan 2010)

……..

……..

….. (EANM Paper Position)……

July 26 – 28th 2010

ESTSP

POLITÉCNICO DO PORTO

IsoPor S.A.

Report of the Expert Review Panel on Medical Isotope Production

Presented to the Minister of Natural Resources Canada

30 November 2009

The cyclotron option has the potential to be the timeliest option. Commercial production of Tc-99m could begin between 2011 and 2014, depending primarily on results of R&D and health regulatory issues.

July 26 – 28th 2010

ESTSP

POLITÉCNICO DO PORTO

IsoPor S.A.

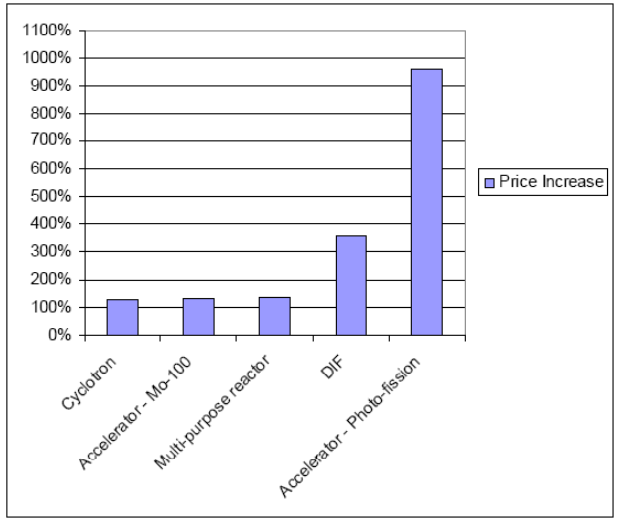

Extracted from: "**Report of the Expert Review Panel on Medical Isotope Production**" – presented 30th November 2009 (pag 39)

Direct ^{99m}Tc Production by a Low Energy - Medical - Cyclotron

July 26 – 28th 2010

ESTSP

POLITÉCNICO DO PORTO

IsoPor S.A.

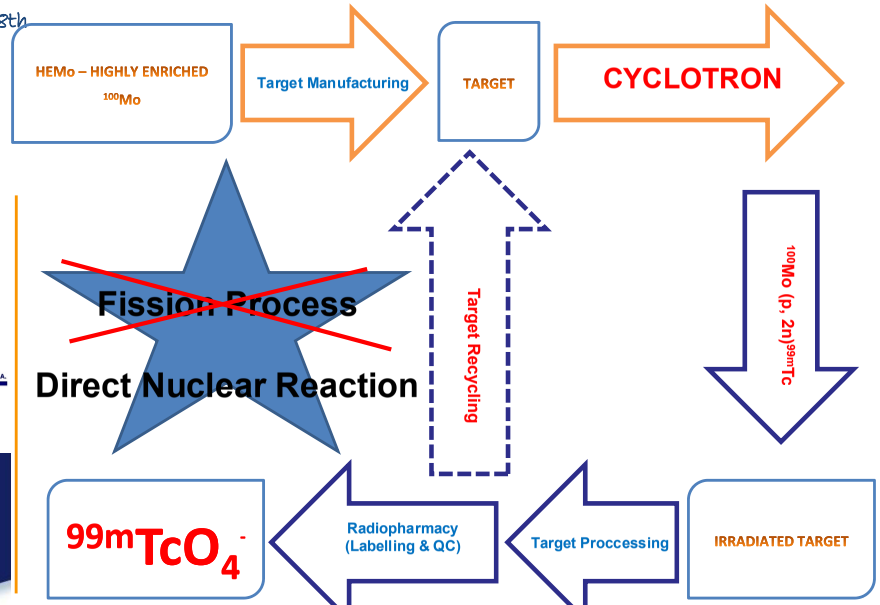

WTTCXIII

Production cross section for the reaction $^{100}Mo(p,2n)^{99m}Tc$

July 26 – 28th 2010

ESTSP

POLITÉCNICO DO PORTO

IsoPor S.A.

Best healthcare for everyone

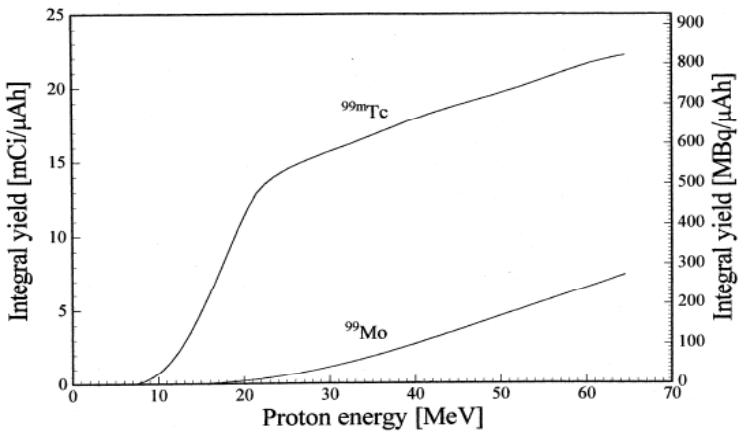

The thick target yield for the reaction 100Mo(p,2n)99mTc as it as been presented by *B. Schloten et al.Applied Radiation and Isotopes 51 (1999) 69*

Note that 99Mo begins to appear as a contaminant in the target material at 18 or 19 MeV (must be removed in processing steps).

WTTCXIII

PRODUCTION YIELDS FOR VARIOUS PET CYCLOTRONS

July 26 – 28th 2010

ESTSP

POLITÉCNICO DO PORTO

IsoPor S.A.

Best healthcare for everyone

Production Yields for Various Cyclotrons
with 100uA internal ion source and (400uA) external ion source

Cyclotron	Energy on Target (MeV)	Yield (mCi)	Mo99:Tc99m Activity Ratio at EOB
BEST 14p	14	2000 (8000)	0.010
GE PETtrace	16	2600	0.011
IBA Cyclone 18	18	3000	0.036
ACSI TR19	19	4000 (16000)	0.038
ACSI TR24	24	5600 (22400)	0.270

Tc99m estimated yields for a production run of 4 hours at 100 and (400) uA

WTTCXIII

The inner workings of a High Current Isotope Production Target

July 26 – 28th 2010

ESTSP

POLITÉCNICO DO PORTO

IsoPor S.A.

Best healthcare for everyone

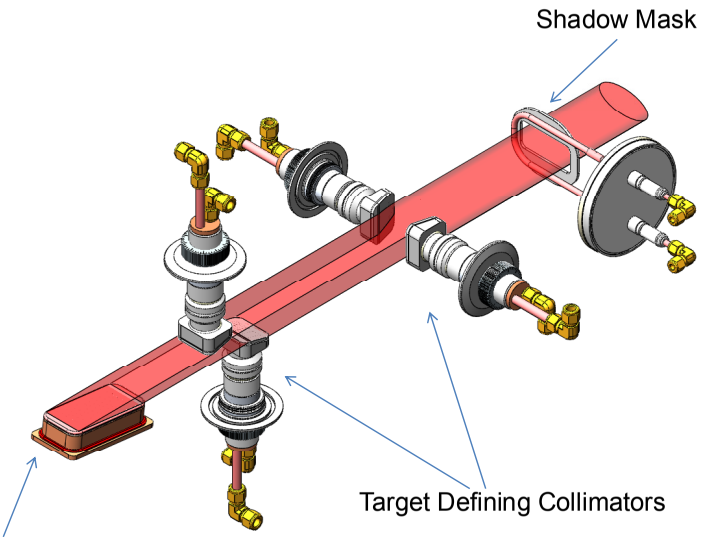

Targets have been **operated up to 1 mA of Proton Beam and 30 kW of heat dissipation**

WTTCXIII

Target Material comparisons for distinct bombarding energies

July 26 – 28th 2010

ESTSP

POLITÉCNICO DO PORTO

IsoPor S.A.

Best healthcare for everyone

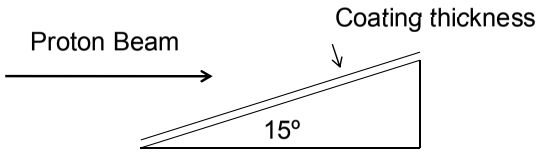

Cyclotron Energy	Target thickness	Target coating
MeV	um	um
14	96.8	25
16	204	53
19	383	100
24	673	174

Target Material: some Considerations

July 26 – 28th 2010

ESTSP

POLITÉCNICO DO PORTO

IsoPor S.A.

Best healthcare for everyone

The preferred Target material would be ^{100}Mo metal, though most processes now use $^{100}MoO_3$

(The Oxide is not preferred, because the extra Oxygen atoms reduce the yield of the Technetium and contribute with an additional radioactive contaminant background of ^{13}N.)

The Target Material will be a metal sheet converted from a metal powder. Solid metal foils must be laid down on the Target Body. The thicknesses of ^{100} Mo-foil differ according to accelerator energy. (Note that the Target is inclined at 15^0 so that the actual Target coating is thinner.)

As the Target coating becomes thicker, the Molybdenum becomes brittle and has a tendency to flake. Thinner foils are much more malleable. (The metallic foil development is underway, after studying the various options to produce foils in the 25 to 100 um range.)

One key starting point is that separated Molybdenum is supplied as a powder and the foil must be prepared from that.

Molybdenum plating on Carbon substrate

July 26 – 28th 2010

ESTSP

POLITÉCNICO DO PORTO

IsoPor S.A.

Best healthcare for everyone

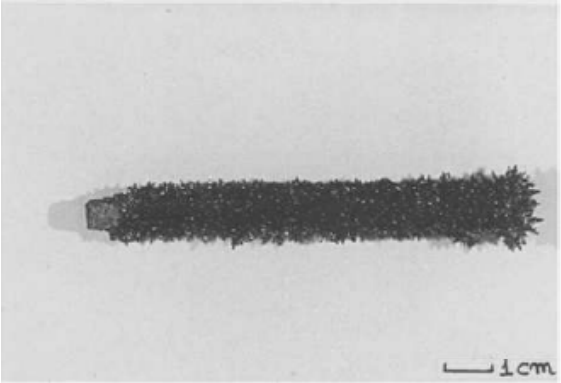

The electro plating creates needle-like structures.

(From: *Kipouros et.al. J. Appl Electrochemistry 18 (1988) 823)*

Molybdenum Deposition

July 26 – 28th 2010

ESTSP

POLITÉCNICO DO PORTO

IsoPor S.A.

Best healthcare for everyone

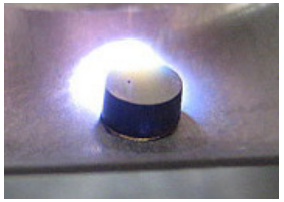

A

Molybdenum is first pressed (A).

B

Then, it is melted using an arc or electron gun into a pellet (B).

C

Finnally, it is pressed or rolled into a foil (C).

(The presence of oxides results in the fragmenting and layering of the foils).

Molybdenum Deposition

July 26 – 28th 2010

ESTSP

POLITÉCNICO DO PORTO

IsoPor S.A.

Best healthcare for everyone

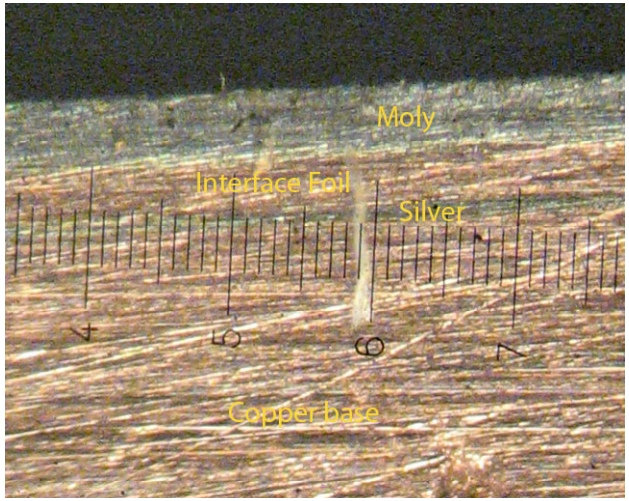

D

Molybdenum foil is bonded by a surface brazing technique that joins the copper base substrate to the target foil (D). The first step in the target processing leaves the bonding materials with the base substrate.

WTTCXIII

Model of High Current Target used on CYCLOTECH

July 26 – 28th 2010

ESTSP

POLITÉCNICO DO PORTO

IsoPor S.A.

Best healthcare for everyone

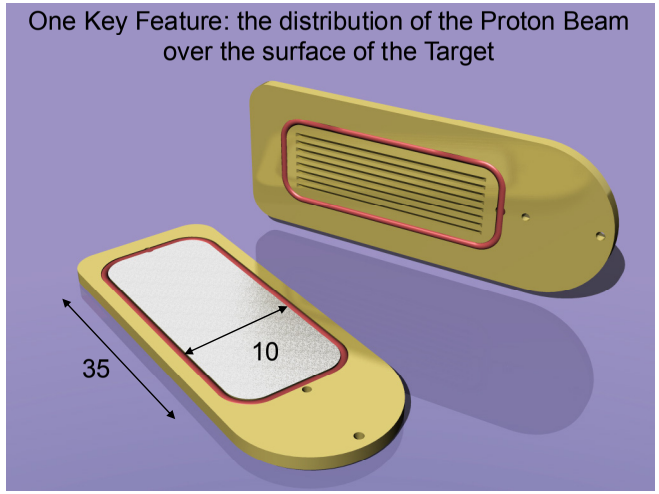

Irradiation Target view. The back of the Target (top picture) incorporates water cooling channels. The irradiated material is deposited on the front face. An O-ring acts as the vacuum seal.

WTTCXIII

Finite element analysis of Production Target at 200 μA

July 26 – 28th 2010

ESTSP

POLITÉCNICO DO PORTO

IsoPor S.A.

Best healthcare for everyone

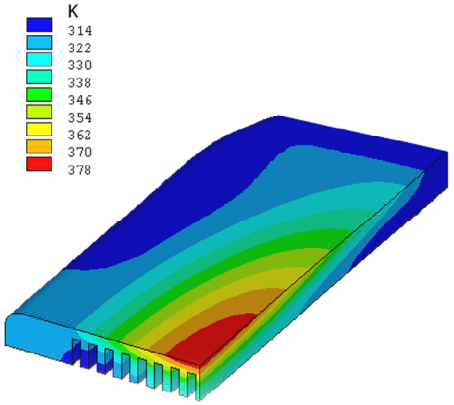

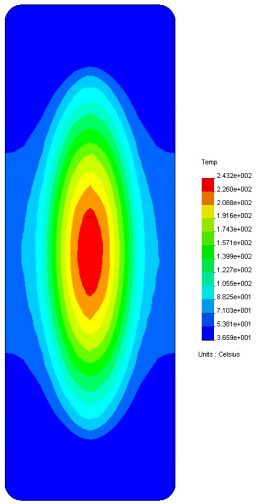

FEM analysis of the temperature distribution of the Molybdenum Target Body for a 4,3 kW beam striking the Target face. The beam is Gaussian and 20% of the total Beam is deposited on the collimator. The hot spot at the centre is about 250 degrees Celsius.

WTTCXIII

TARGET IRRADIATION SYSTEM

July 26 – 28th 2010

ESTSP

POLITÉCNICO DO PORTO

IsoPor S.A.

Best healthcare for everyone

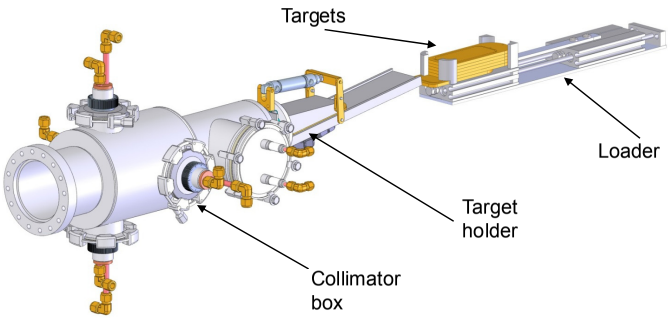

Target Holder mounted on Collimator Box.

Target Loader inserts new Targets into the Holder

WTTCXIII

TARGET IRRADIATION SYSTEM CROSS-SECTION

July 26 – 28th 2010

ESTSP

POLITÉCNICO DO PORTO

IsoPor S.A.

Best healthcare for everyone

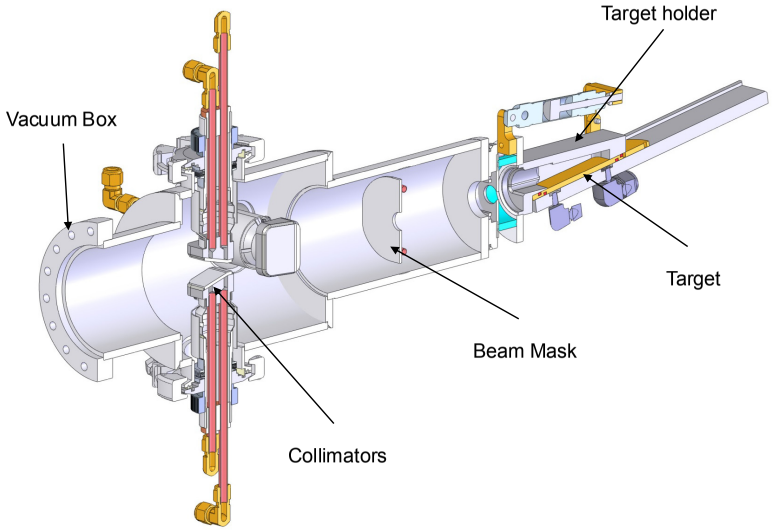

WTTCXIII

SEQUENCE OF LOADING

July 26 – 28th 2010

ESTSP

POLITÉCNICO DO PORTO

IsoPor S.A.

Best healthcare for everyone

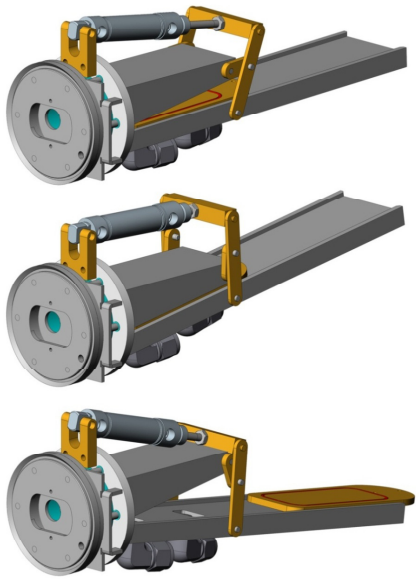

Loading

Closed

Ejecting

WTTCXIII

TARGET ASSEMBLY

July 26 – 28th 2010

ESTSP

POLITÉCNICO DO PORTO

IsoPor S.A.

Best healthcare for everyone

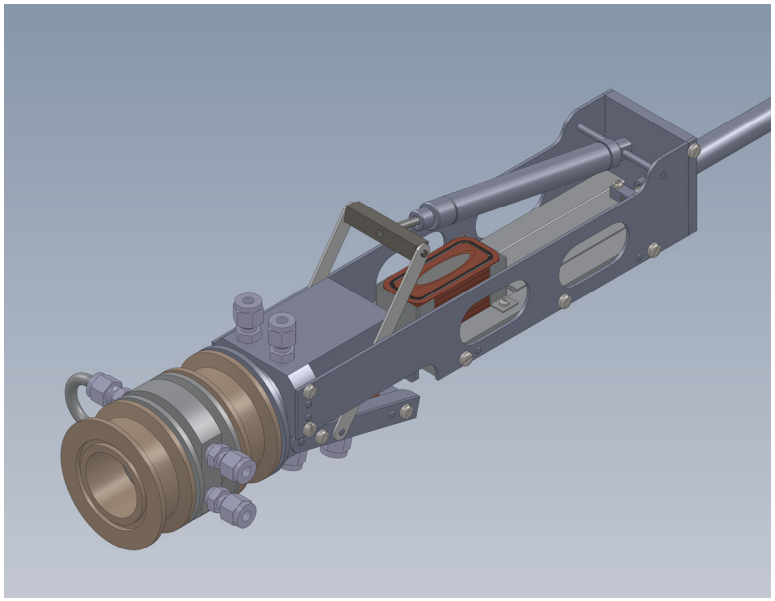

WTTCXIII

TARGET ASSEMBLY

July 26 – 28th 2010

ESTSP

POLITÉCNICO DO PORTO

IsoPor S.A.

Best healthcare for everyone

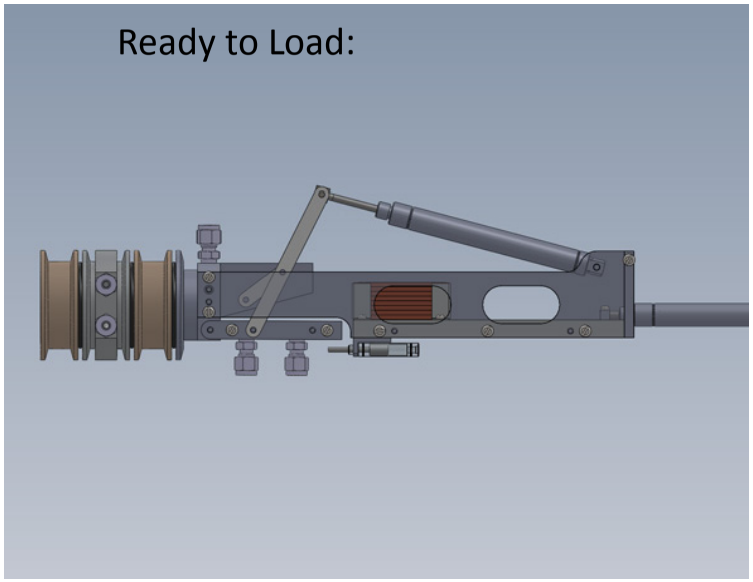

WTTCXIII

TARGET ASSEMBLY

July 26 – 28th 2010

ESTSP

POLITÉCNICO DO PORTO

IsoPor S.A.

Best healthcare for everyone

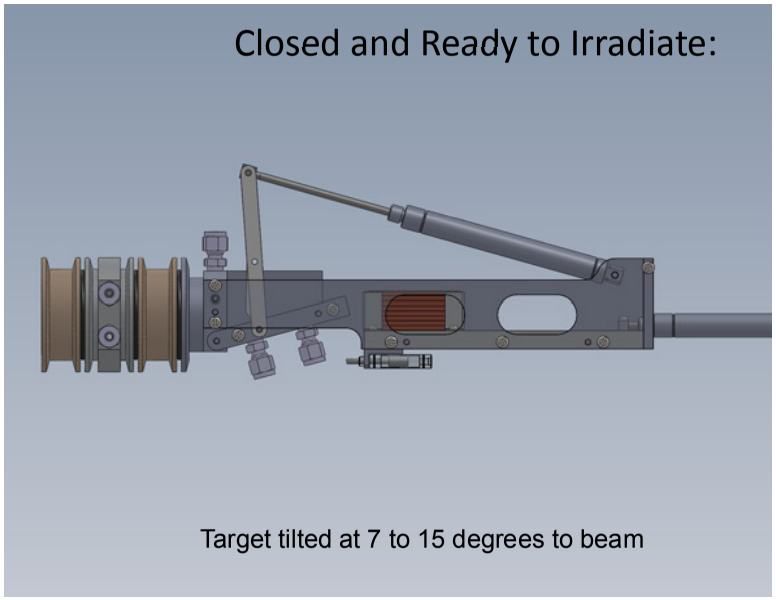

TARGET ASSEMBLY

July 26 – 28th 2010

ESTSP

POLITÉCNICO DO PORTO

IsoPor S.A.

Best healthcare for everyone

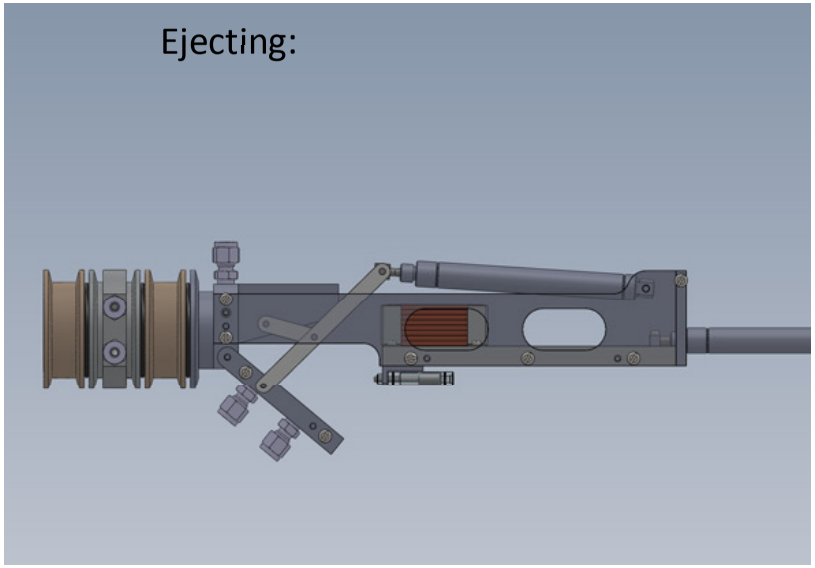

Processing Module Scheme

July 26 – 28th 2010

ESTSP

POLITÉCNICO DO PORTO

IsoPor S.A.

Best healthcare for everyone

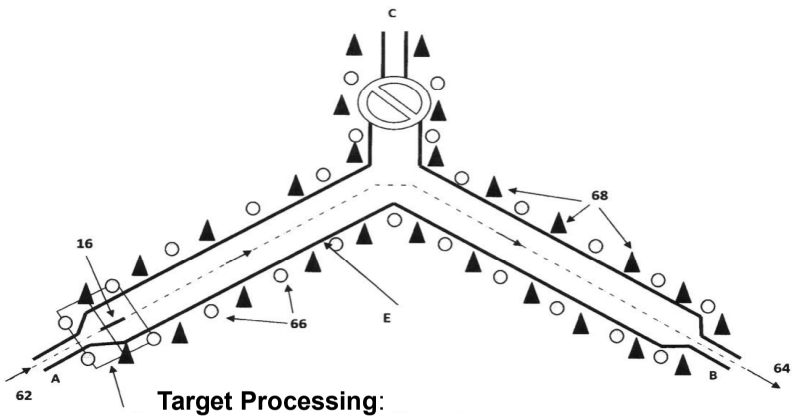

Target Processing:

16. Target 62. **Carrier gas** 66. **heaters**

C. **elution input** 64. **$^{99m}TcO_4$ elute**

COLD TEST APPARATUS

July 26 – 28th 2010

ESTSP

POLITÉCNICO DO PORTO

IsoPor S.A.

Best healthcare for everyone

HEATER OVEN

DISTILLATION COLUMN

CARRIER GASES

COLD TEST APPARATUS

July 26 – 28th 2010

ESTSP

POLITÉCNICO DO PORTO

IsoPor S.A.

Best healthcare for everyone

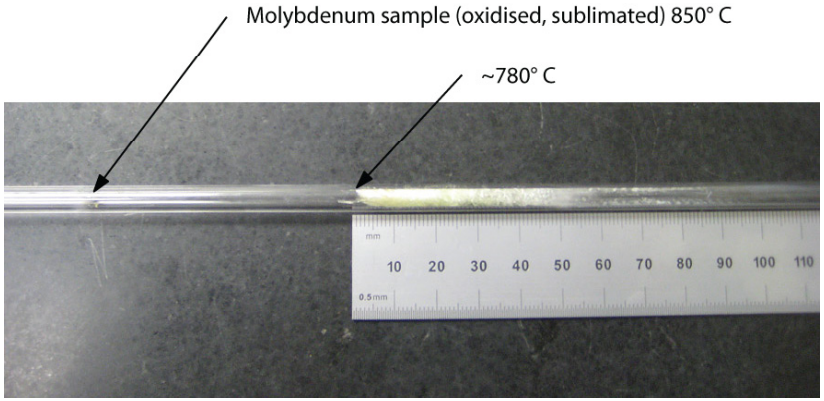

First Processing Stage development:

Mo is oxidized in an O_2 environment and then transported until it is condensed at 780^0 C

All Target Substrate contaminants are left behind and one has pure MoO_3 for subsequent processing.

COLD TEST APPARATUS

July 26 – 28th 2010

ESTSP

POLITÉCNICO DO PORTO

IsoPor S.A.

Best healthcare for everyone

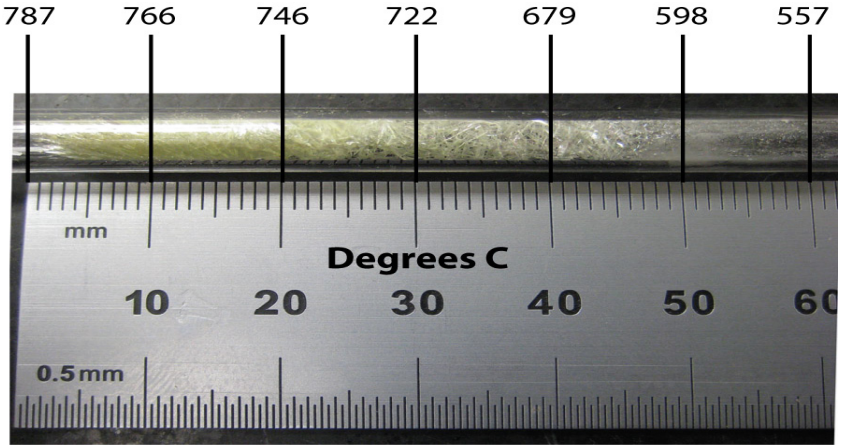

The MoO_3 is deposited in a band corresponding to about 40 ^{0}C.

Since Condensation Temperatures of Molybdenum and Technetium Oxides are very different, a form of fractional distillation in such a column can be incorporated into the process. (Physical and Wet Chemistry under study)

Target Processing System

July 26 – 28th 2010

ESTSP

POLITÉCNICO DO PORTO

IsoPor S.A.

Best healthcare for everyone

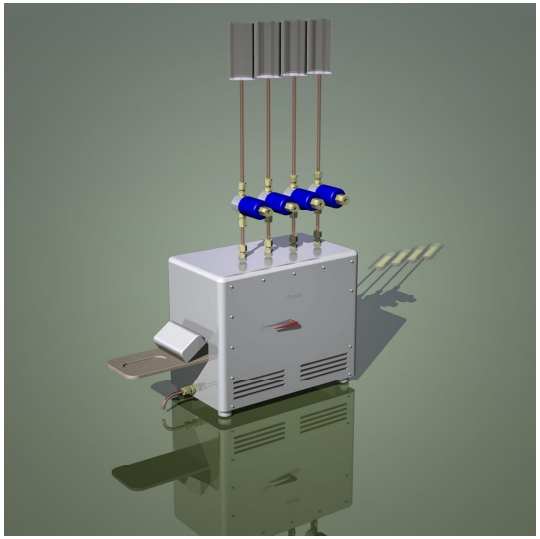

Fully automated system for the processing of irradiated targets.

The high processing temperature requires good thermal insulation and fully mechanized loading of the Targets.

Processing Unit in a Hot Cell

July 26 – 28th 2010

ESTSP

POLITÉCNICO DO PORTO

IsoPor S.A.

Best healthcare for everyone

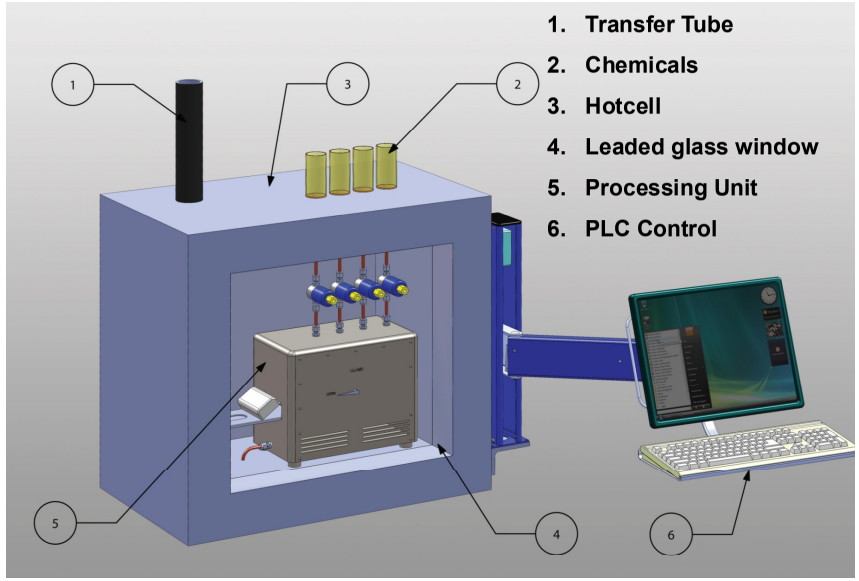

1. Transfer Tube
2. Chemicals
3. Hotcell
4. Leaded glass window
5. Processing Unit
6. PLC Control

Status and Summary

July 26 – 28th 2010

ESTSP

POLITÉCNICO DO PORTO

IsoPor S.A.

Best healthcare for everyone

1 - Technical Feasibility

- Cross Section, Process X

2 - Economics X

3 - Development

- Target Assembly under construction X
- Separation Process tested X
- Prototyping X

Yet To Come,

- Entire System Integration
- Conclusion of Accelerator & Optimization Tests
- Pharmaceutical Validation and Regulatory Issues

WTTC XIII – Presentation Discussions

1. MoO_3 to Mo reduction
   - In H environment

2. Production of 99 Mo? Production in positive ion machine?
   - More energy and high currents needed

3. Target deposition techniques
   - Sputtering only good for too thin… 25um needed!
   - Plasma deposition does not work

4. Financing
   - 99Tc from cyclotron: 3 or 4 x more expensive than today
   - 99Tc prize: not the ultimate factor
   - Actual chemistry and imaging equipment can be used directly

Effects of the Tantalum and Silver Targets on the Yield of FDG Production in the Explora and CPCU Chemistry Modules

J.C. Manrique-Arias, E. Zamora-Romo, A. Zarate-Morales, A. Flores-Moreno, M.A. Avila-Rodriguez

Unidad PET/CT-Ciclotrón, Facultad de Medicina, Universidad Nacional Autónoma de México, México, D.F., México

Ionic contaminants in water have generally been considered to influence the reactivity of n.c.a. [^{18}F]fluoride decreasing the yield in the synthesis of radiopharmaceuticals by nucleophilic fluorination. Until a few years ago the most widely used material for target chamber in ^{18}F-production was silver. However, more recently, the use of refractory materials such as tantalum and niobium has been shown to provide highly reactive fluoride.

The PET Center at the National Autonomous University of Mexico (UNAM) produces [^{18}F]fluoride ion for FDG synthesis in two different targets: a high volume (2.4 mL) gridded tantalum-target and a low volume (1.2 mL) double-foil silver-target capable to withstand 660 and 440W of beam power at 11 MeV, respectively. Chemistry modules for FDG production at this facility include an Explora recently acquired to replace a CPCU in use since 2001. The Explora module is used primarily for the routine production of FDG while the CPCU serves as a backup for the Explora and for the production of other non-FDG tracers. Figure below shows the yields of FDG in six-consecutive months using a tantalum and a silver target for fluoride production. The FDG yields when using the silver target range from 60 to 70% compared to 70 to 80% when using the tantalum target, clearly showing the superiority of tantalum vs. silver to produce highly reactive fluoride.

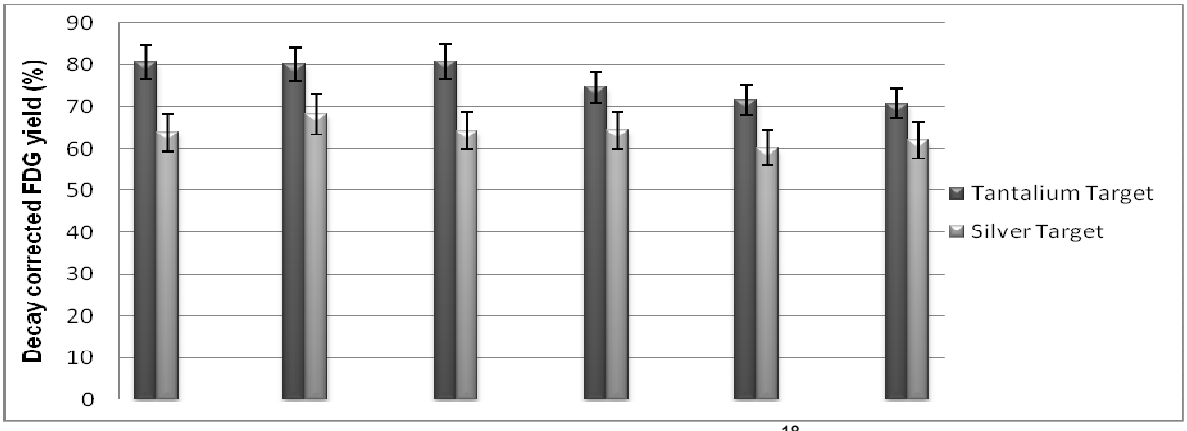

Figure 1. Six-month FDG yields in the Explora module using ^{18}F from two different targets.

Regarding the use of the Explora and CPCU modules, we found no significant difference in their FDG yields, independently of the target used for fluoride production, and their synthesis time is practically the same (~45 min). However, the Explora features a single closed reaction vessel with heating/cooling by forced convection including temperature, pressure and radiation sensing. Performs up to four sequential runs of FDG without intervention. On the other hand, the CPCU features two open reaction vessels heated by two independent oil baths that can be used for back-to-back synthesis, but it lacks of any kind of sensors to monitor the performance of the synthesis.

Effects of the Tantalum and Silver Targets on the Yield of FDG Production in the Explora and CPCU Chemistry Modules

J.C. Manrique-Arias, E. Zamora-Romo, A. Zarate-Morales,
A. Flores-Moreno, M.A. Avila-Rodríguez

Unidad PET, Facultad de Medicina, Universidad Nacional Autónoma de México, MÉXICO

Cyclotrons in Mexico

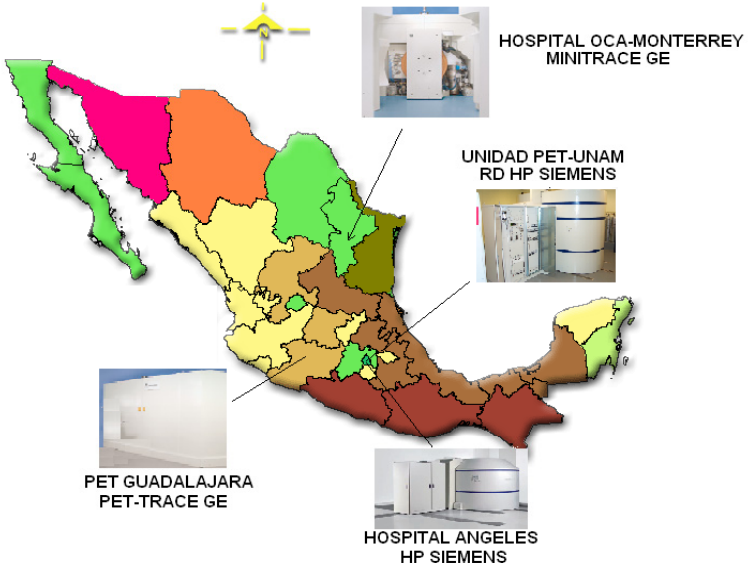

PET in Mexico (2001-2010)

4 Cyclotrons
- Facultad de Medicina, UNAM (México, D.F)
- Hospital Ángeles (México, D.F.)
- Oca Hospital (Monterrey, N.L)
- Guadalajara PET (Zapopan, Jal.)

12 PET/CT
- Facultad de Medicina, UNAM (México, D.F)
- Instituto Nacional de Cancerología (México, D.F.)
- Hospital de Marina (México, D.F.)
- Hospital Médica Sur (México, D.F.)
- Hospital ABC (México, D.F.)
- CT Scanner de México (México, D.F.)
- Hospital Ángeles Pedregal (México, D.F.)
- Hospital Ángeles Lomas (México, D.F.)
- Hospital Ángeles Puebla (Puebla, Puebla)
- Oca Hospital (Monterrey, N.L.)
- Guadalajara PET (Zapopan, Jal.)
- **Hospital San José (Monterrey, N.L.)**

3 Coincidence detection
- ISSEMYM (Toluca, Edo. México)
- Hospital General M.G.G. (México, D.F.)
- Instituto Nacional de Cardiología (México, D.F.)

Production of FDG at UNAM´s PET Center

Produces FDG from Monday to Saturday

Produces FDG for 9 of the 11 PET Centers in México City

More than 8,000 unidoses/year

Two production runs per day

Other tracers:
- [^{18}F]FLT
- [^{18}F]NaF
- [^{11}C]Acetate
- [^{13}N]Ammonia

Water Targets

HP Target:

Type: Gridded

Target Body: Tantalum

Volume: 2.4 mL (60 μA)

Window: Havar

RD Target:

Type: Double foil

Target Body: Silver

Volume: 1.2 mL (40 μA)

Window: Havar

Chemistry Module CPCU

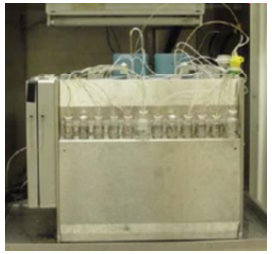

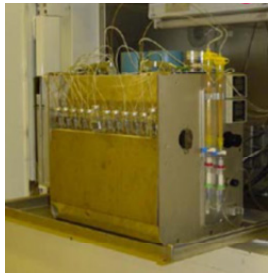

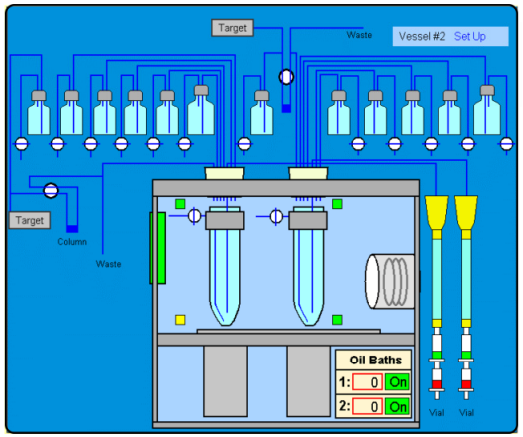

Chemistry Module Explora FDG_4

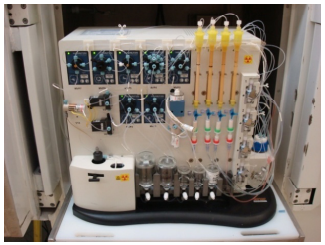

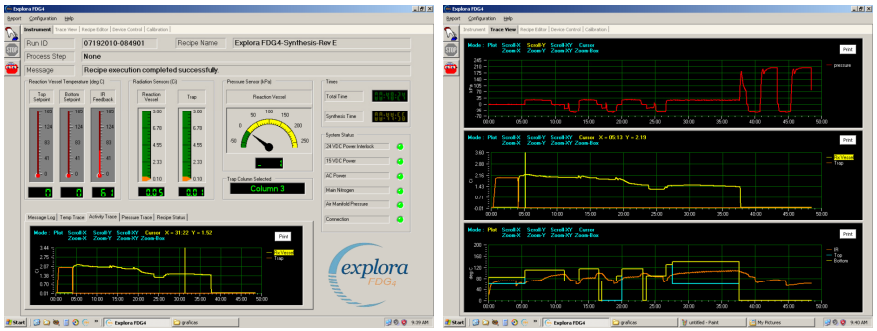

Characteristics of the Modules

Explora FDG_4	CPCU
One-closed reaction vessel	Two-open reaction vessels
Up to four production runs/day	Two production runs/day
Synthesis time ~45 min	Synthesis time ~45 min
Heating/cooling by forced convection	Heating by conduction (oil baths)
Precise addition of reagents from reservoirs	Exact amount of reagent need to be added in each vial
Temperature, pressure and radiation sensing	Easy of maintenance

Six-month FDG Yields in the Explora Module Using ^{18}F from Two Different Targets

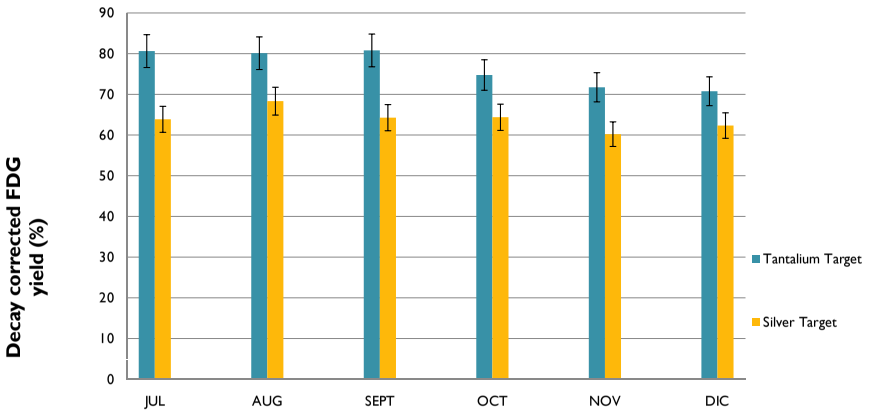

RESULTS

- The FDG yields when using the silver target range from 60 to 70% compared to 70 to 80% when using the tantalum target, clearly showing the superiority of tantalum vs. silver to produce highly reactive fluoride.
- No difference in the FDG yield was noticed when using the CPCU or Explora Modules

Undergoing Projects

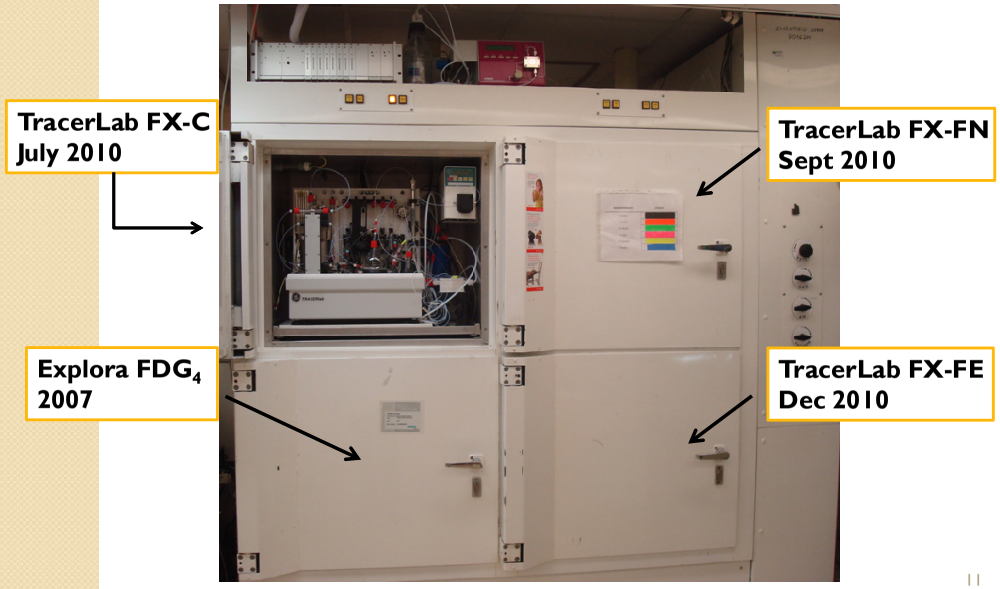

FULLY AUTOMATED SYSTEM FOR THE PRODUCTION OF [^{123}I] AND [^{124}I]-IODINE LABELLED PEPTIDES AND ANTIBODIES.

P. Bedeschi[a], S. Bosi[a], M. Montroni[a], G.Brini[b], S.Caria[b], M.Fulvi[b], G. Calisesi[b]

a Comecer, Castel Bolognese (RA), Italy

a Nuclear Specialists Associated, Ardea (Roma), Italy.

Radiolabelled amino acids, peptides and monoclonal antibodies are certainly a useful non-invasive diagnostic tools to detect malignant tumours, infectious and inflammatory lesions[1,2]. In combination with the potential of Positron Emission Tomography (PET), the aim of the present study was to develop a fully automated system for the radiolabelling of these new tracers, that avoids any direct manipulation by operators from target production and recovery, to synthesis and purification of the final product.

Nowadays radionuclides used for PET-imaging are generally short-lived isotopes, such as [^{18}F]-fluorine ($t_{1/2}$ = 110 min), but recently the growing need for alternative positron emitters focuses the attention on the long-lived radiohalogen [^{124}I]-iodine ($t_{1/2}$ = 4.17 d). [^{124}I]-Iodine, is a suitable radionuclide for both diagnostic, such as Positron Emission Tomography and therapeutic applications, it decays by positron emission (23.3%) and electron capture (76.7%). Its long half-life permits this isotope to be imaged for more than 4 days, which makes it possible to study the labeled molecule over a longer time period. Furthermore the promising clinical aspect of [^{124}I]-iodine leads research institution and commercial company seeking to produce multi-millicurie quantities for distribution purposes[3], that means a wider geographical area.

A variety of radioiodination methods is supported by a large amount of literature[4,5], preferentially a radioiodine atom is incorporated in a vinylic or aromatic moiety, due to the high strength of the carbon-iodine bond. Therefore, the radioiodination is often implemented by nucleophilic or electrophilic substitution and is more or less predicted by the structural feature of the molecule[6]. Obviously this kind of chemistry is applicable to any iodine isotopes, therefore in addition to [^{124}I]-iodine, our attention is focused on [^{123}I]-iodine too.

[^{123}I]-Iodine has a half-life of 13.2 h, decays by electron capture and its medium energy (E_γ = 159 keV) is ideal for planar imaging and for Single Photo Emission Computed Tomography (SPECT), a lower cost diagnostic tool compared to PET.

The production of both [^{123}I] and [^{124}I]-iodine radionuclides is based on a low-energy (p, n) reaction at a small-sized (14 MeV) cyclotron, using TeO_2-target technology and dry distillation

[1] Journal of Labelled Compdounds & Radiopharmaceuticals, 2008, 51, 48-53
[2] International Journal of Cancer, 19991, 47, 3, 344-347
[3] Applied Radiation and Isotopes, 2007, 65, 407-412
[4] Bolton, 2002; Glaser et al., 2003; Adam & Wilbur, 2005
[5] Bioconjugate Chem., 1990, 1, 154-161
[6] Journal of Labelled Compounds and Radiopharmaceuticals, 2005, 48, 241-257

method of radioiodine separation[7,8,9,10]. The collected radioiodide is then delivered to a fully-automated module for the product labeling. The module is built with the concepts of the "disposable cassette", so all the components that get in contact with the product are disposable; this structure avoids the module contamination. Finally the labeled compounds are allowed to pass through an HPLC purification system connected at the end of the synthesis module. The figure 1 below shows a schematic illustration of the fully automated process.

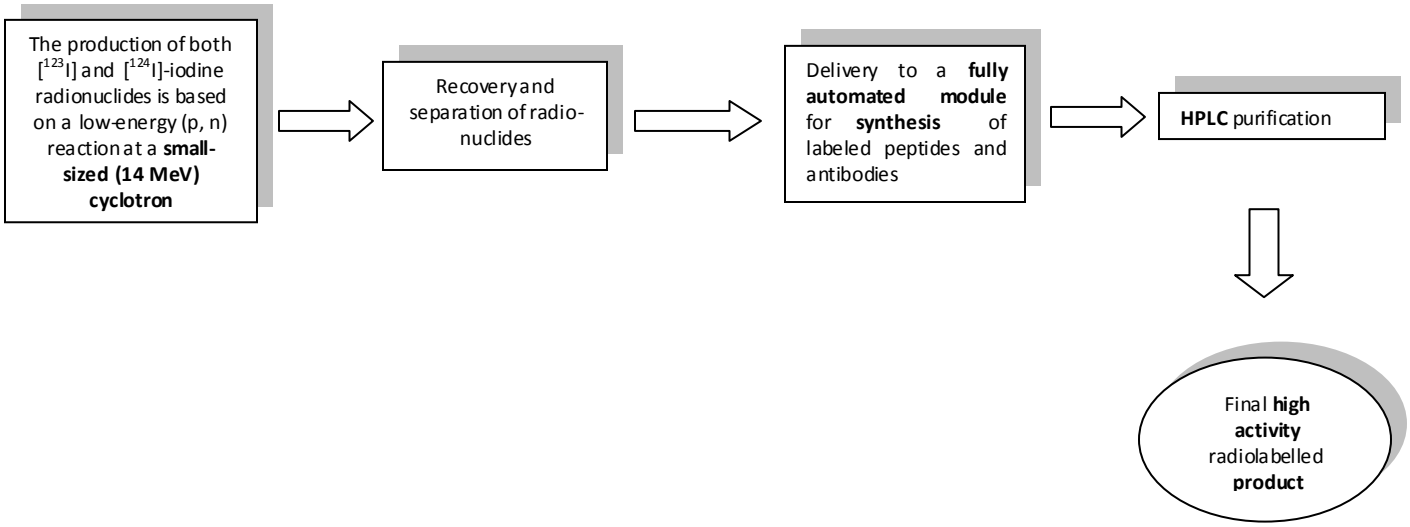

Figure 1 Schematic illustration of the fully automated system

In conclusion we develop a fully automated system for the high activity production of iodo-labelled peptides and monoclonal antibodies, high-lived pharmaceuticals for PET and SPECT imaging. Due to the automated process applied from the radio-isotopes production and separation to the synthesis and purification of the final products, the operators are completely shielded from radiation. The use of [^{123}I] and [^{124}I]-iodine, medium and high -lived radionuclides permits longer term studies and a wider geographically distribution.

[7] Applied Radiation and Isotopes, 2003, 58, 69-78
[8] Radiochim. Acta, 2000, 88, 169-173
[9] Applied Radiation and Isotopes, 2007, 65, 407-412
[10] Journal of Radioanalytical & Nuclear Chemistry, 1996, 213, 2, 135-142

WTTCXIII

Fully Automated System for the Production of [^{123}I] and [^{124}I]-Iodine labeled peptides and antibodies

Montroni[1] , Caria[2] , Fulvi[2] , Brini[2], Bosi[1], Calisesi[2], Bedeschi[1]
Comecer SpA, Castel Bolognese (RA), Italy
NSA Nuclear Specialists Associated, Ardea (RM), Italy

Marco Montroni
R&D dept.
Comecer, ITALY

AIMS

The purposes of an automated system for radio-iodine production are:

- to increase radioprotection standards of the operator during the process
- to obtain high production yields for small cyclotrons and to assure the process reproducibility
- to assure a good product quality in terms of chemical and isotopic purity
- to establish a background for a future GMP production

the study has considered…

- development of a bi-directional pneumatic transfer system between the cyclotron and the dry distillation module
- development of a specific irradiation module for the automated target positioning with a high efficiency water and helium cooling system
- application of an industrial HF heating system on the dry distillation device in order to improve traditional harvesting methods
- development of a labeling procedure on an automated multipurpose synthesis module

TeO_2 Solid Target

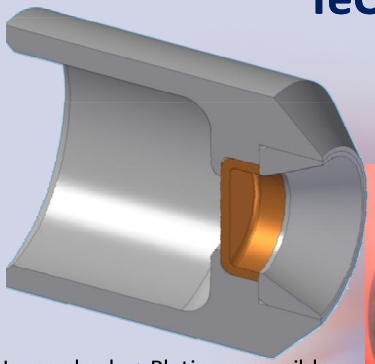

Haynes body + Platinum crucible shuttle dimension: Ø28x35mm

Platinum pit: Ø8x3mm

Alumina and enriched TeO_2 powders loading

a High RadioFrequency heater quickly drives the melting …

500 mg of green glassy TeO_2 ready for irradiation

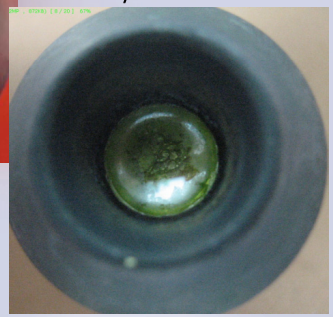

ALCEO - irradiation unit

ALUMINIUM DEGRADER FOIL
with
EXAGONAL SUPPORTING GRID

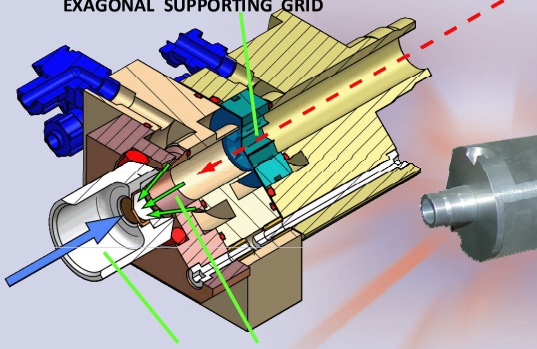

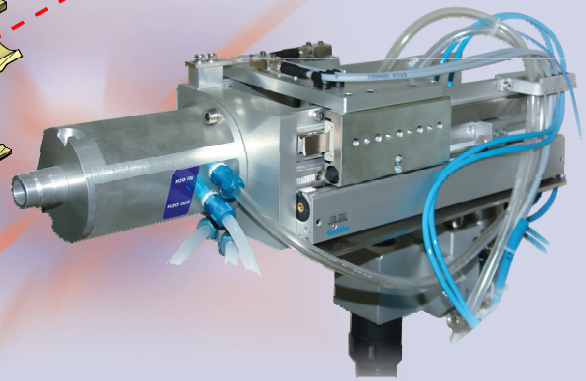

double WATER and HELIUM
indipendent cooling system

Water flow: 3 l/min, 850 W
Helium flow: 15 kg/min, 100W

ALCEO - target processing module

- target automatic transfer from/to the cyclotron
- plating of target with TeO_2
- dry distillation and harvesting of radio-iodine

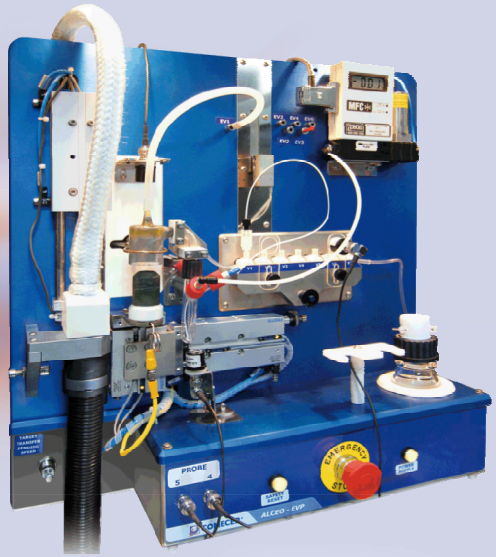

Connected to:

ALCEO PTS module (irradiation unit)

TADDEO synthesis module

Iodine Harvesting

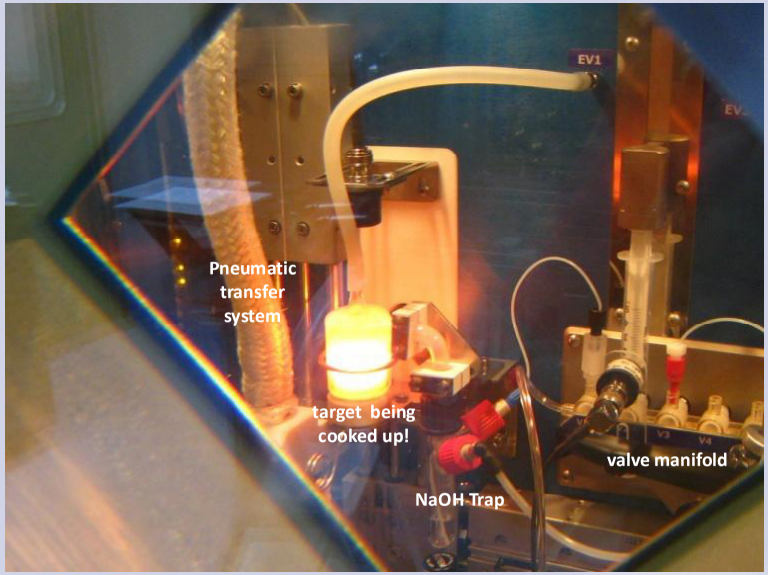

Sustainable Iodine Production

Prepare enriched Te powders

(500 mg of TeO_2+ Alumina 5%)

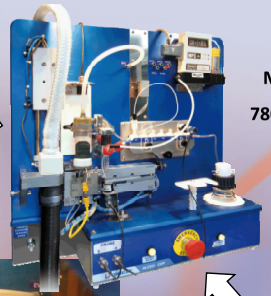

Melt (plating)

780°C for 15 min

14 MeV (p,n) reaction
4 hours @ 12 uA

Dry Distillation
(iodine harvesting)

780°C for 45 min
2ml 0.1 M NaOH
bubbling system
trap

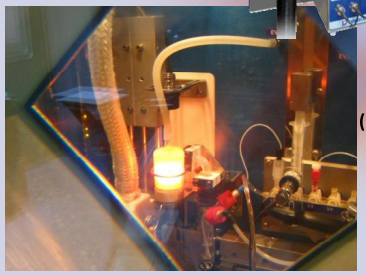

Sustainable Iodine Production

Alceo Halogen / Production Data

Target transfer speed: 2 m/s

Beam Energy 14 MeV, typical current 12-20 µA

Typical beam duration: from 4 to 6 hours

Typical production yield with 500 mg of $^{124}TeO_2$ (99.5% enriched): 40/50mCi ^{124}I EOB

Production yield: ~ 0,5 mCi/uAh

Target can be irradiated multiple times (5 to 10)

TADDEO - labeling module

multipurpose research module equipped with…

- Open software in order to allow the user to customize and perform his own labeling recipe
- 15 valves disposable cassette kit
- 2 syringe precision drawing stations
- 2 reactors with cooling system
- 5 activity detector probes
- 12 tech gas outlets
- 1 membrane pump

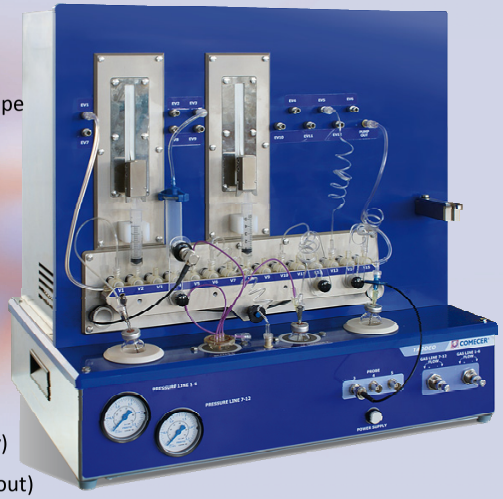

Connected to:

ALCEO EVP module (iodine inlet capillary)

HPLC purification module prototype (in/out)

THEODORICO dispensing system (product outlet)

Automated Radio-iodination

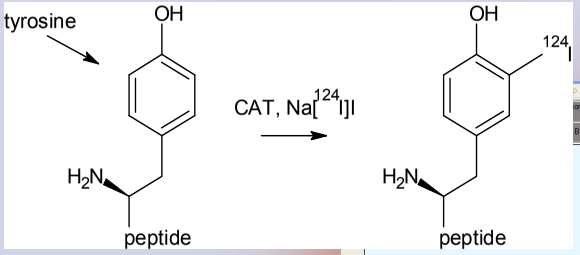

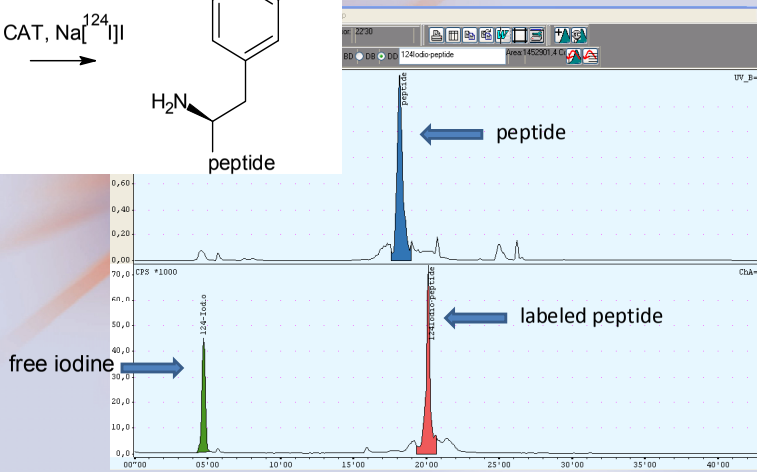

And of course…

Radiopharmaceutical is finally ready to be injected

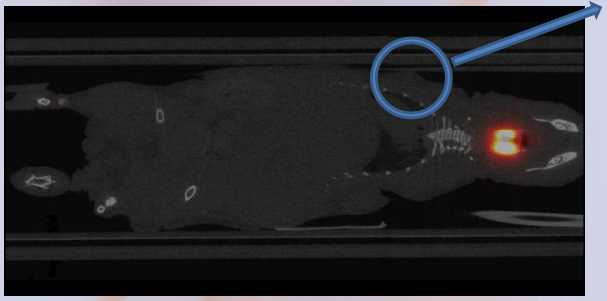

tumor

u-PET image courtesy of NSA, Rome

u-PET image 48 hours after injection

124I-peptide seems not being uptaked in the tumor

Conclusions

- **We developed a fully automated system for iodine target handling**
- **We developed a fully automated system to label a peptide with iodine-124**
- **We applied this system to a biodistribution study with micro-PET**
- **Future developments will involve iodine-123 and GMP production**

special thanks to…

Giorgia Brini, Saverio Caria, Marcello Fulvi, Gianni Calisesi
NSA Rome

Stefano Bosi, Paolo Bedeschi
Comecer SpA

Prof. Robert J Nickles and his cyclotron gang
University of Wisconsin, Madison (WI)

Prof. Jacek Koziorowski
Herlev University, Denmark

WTTC XIII – Presentation Discussions

1. System characteristics and running experience
   - TeO2 target material
   - Haynes stainless steel
   - Very low loss of iodine during transport, temperature not high
   - Use Te123 to reduce I125 contaminant

Accepted for ORAL presentation during 13th WTTC 2010 in RISOE/Denmark

Routine Automated Production of ^{18}F-Labelled Radiopharmaceuticals on IBA Synthera® Multi-Purpose Platform

Bernard Lambert[1] ; Jean-Jacques Cavelier[1], Guillaume Gauron[1], Christophe Sauvage[2], Cécile Kech[2], Tim Neal[3], M. Kiselev[3], David Caron4, Anat Shirvan4, Ilan Ziv[4]

[1]BP 32 91192 Gif sur Yvette Cedex France. [2]IBA RI SA, rue de l'Esperance, 1 6220 Fleurus Belgium. [3]IBA Molecular, 100 Executive Dr. Sterling VA USA; [4]Aposense Ltd, 5-7 Odem St., P.O Box 7119, Petach-Tikva 49170, Israel e-mail: christophe.sauvage@iba-group.com.

Although FDG provides most of the clinical PET imaging today its low specificity limits its use. In molecular imaging technology, highly specific probes for clinical applications are crucial justifying the development of non-FDG radiopharmaceuticals such as: [^{18}F]-NaF, for bone metastasis detection; [^{18}F]-F-Choline ([^{18}F]-FCH=methylcholine) for diagnosis/staging of prostate cancer; [^{18}F]-FLT, for cell proliferation imaging, and [^{18}F]-ML-10 (α-methyl 18F-alkyl-dicarboxylic acid), for apoptosis imaging. This work will present automated and optimized processes developed on IBA Synthera® platform for the routine production of [^{18}F]-NaF, [^{18}F]-FCH, [^{18}F]-FLT, [^{18}F]-ML-10.
The synthesis of each radiotracer takes place on single-use IFP™ system (integrated fluidic processor) which comprises appropriate pre-defined synthesis hardware and plumbing. [^{18}F]-NaF manufacturing is straightforward and employs IFP™ Chromatography. For the [^{18}F]-FCH, two synthesizers as well as two interconnected IFP™ (IFP™ Distillation & IFP™ Alkylation) are necessary for the two-step synthesis (fig.1). In synthesis of [^{18}F]-FLT and [^{18}F]-ML-10 IFP™ Nucleophilic is used. The product obtained is purified in Synthera® HPLC unit. In none of the applications hardware changes are required compatible with a multipurpose platform.

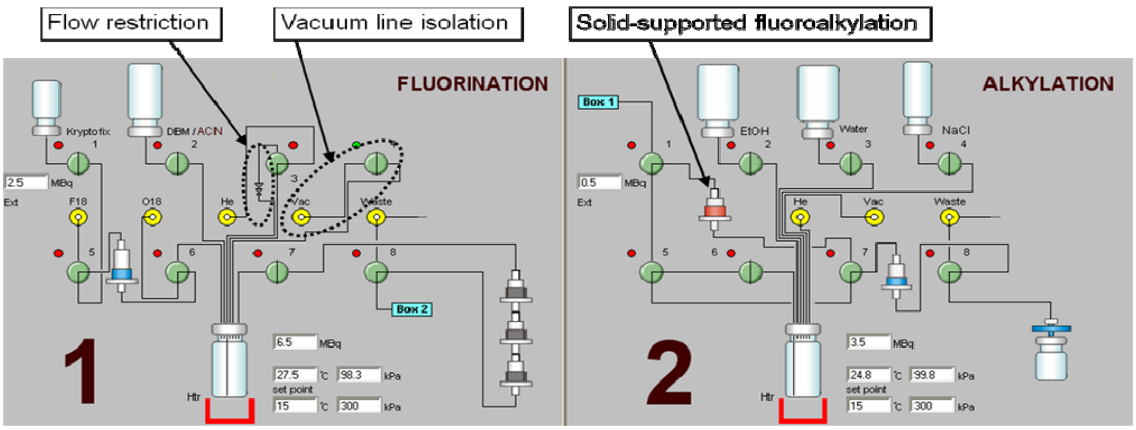

Fig 1-Synthera® graphical user interface screen-shots for [^{18}F]-FCH highlighting main features.

The synthesis of [^{18}F]-NaF is obtained by washing trapped [^{18}F] with water followed by elution with saline solution. [^{18}F]-FCH is produced in two steps according to published method[1]. The first step, performed in IFP™ Distillation, includes the fluorination of dibromomethane (DBM) and purification of fluorinated volatile by distillation through silica cartridges. Next, in the IFP™ Alkylation, fluoromethylation of N,N-dimethylaminoethanol takes place resulting in [^{18}F]-FCH which is purified through a cation exchange cartridge. [^{18}F]-FLT is produced according to adapted methodology[2].

The synthesis is realized within IFP™ Nucleophilic. [^{18}F]-fluorination of 3-N-Boc-5'-O-dimethoxytrityl-3'-O-nosyl-thymidine (Boc-FLT-Precursor) as well as subsequent acid hydrolysis with diluted HCl are carried out at 100°C. These steps take 10 min. and 5 min., respectively. Crude product is buffered and loaded into reversed-phase HPLC column in Synthera® HPLC for final purification. Ethanol/water is used as mobile phase. Synthesis of [^{18}F]-ML-10 also employs IFP™ Nucleophilic. Both fluorination of the tosylated precursor and consecutive hydrolysis with aqueous HCl were performed at 110°C for 10 min. Buffered reaction mixture was then purified in Synthera® HPLC by reversed-phase HPLC with phosphate buffer/ethanol as mobile phase.

[^{18}F]-NaF is obtained in less than 10 minutes with RCY (radiochemical yield) > 90% EOS. Analytical data show it complies with European Pharmacopoeia. Average RCY for [^{18}F]-FCH >20% EOS. The total synthesis time is < 50 minutes. Final product shows high radiochemical purity (99%) and chemical purity (>95 %). [^{18}F]-FLT total synthesis time is 45 minutes (including HPLC purification) with average RCY>20%. Final product presents high radiochemical purity (>95%) and high chemical purity (>95 %). [^{18}F]-ML-10 RCY > 40 % after 60 min of total synthesis time including HPLC purification. Final product presents high radiochemical and chemical purity (> 99%) (fig 2).

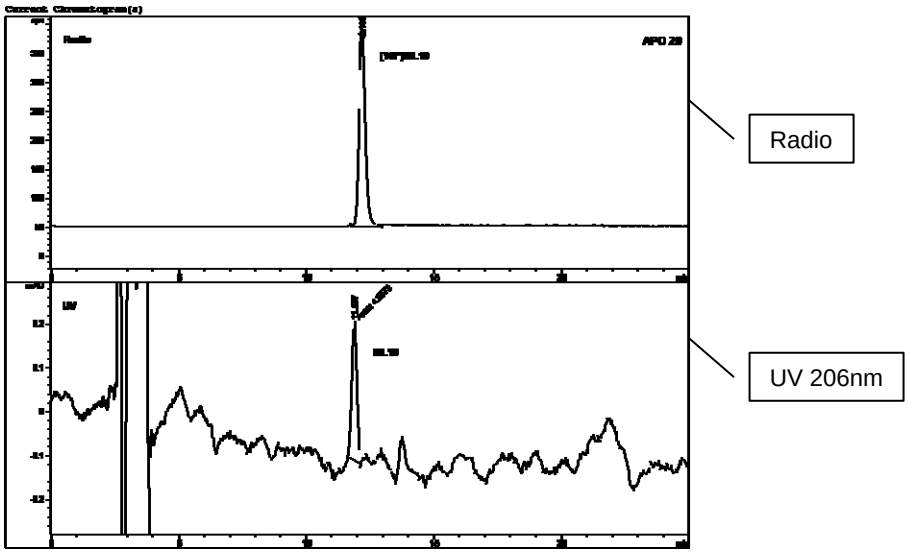

Fig. 2- Typical chromatogram of [^{18}F]-ML10 after HPLC purification

The automated platform has proven to be robust and reliable when it comes to routine production of promising radiopharmaceuticals such as [^{18}F]-NaF, [^{18}F]-FCH, [^{18}F]-FLT and [^{18}F]-ML-10 for clinical applications. The radiochemical yields obtained are reproducible and final products show high radiochemical and chemical purity. All of the radiopharmaceutical syntheses are carried out within dedicated IFP™ systems (Chromatography, Distillation, Alkylation and Nucleophilic) in one single platform set up with open software for customized applications. The IFP™ is a disposable, preventing cross-contamination, which is line with GMP. The modules are fully interchangeable underpinning the platform multipurpose capability (do-all-in-one platform) and flexibility.

References:

[1]Kryza D et al Nuc.Med.Bio. 35:255 – 260 (2008)
[2]Oh SJ, et al Nuc.Med. Bio. 31:803–809 (2004).

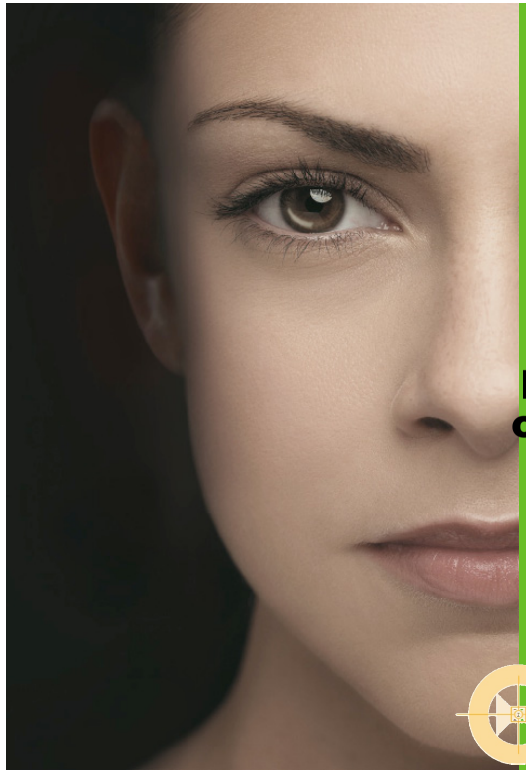

Routine Automated Production of ^{18}F-Labelled Radiopharmaceuticals on IBA Synthera® Multi-Purpose Platform

C. Gameiro

We Protect, Enhance and Save Lives.

Synthera® — Innovative concept

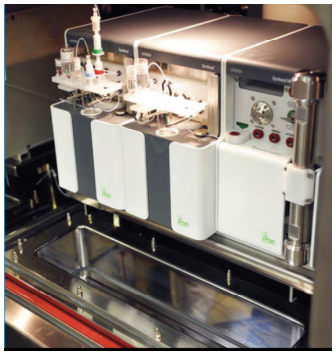

- IFP™ (Integrated Fluidic Processor)
- Most compact
- Multi-run operation
- Multi-tracers system
  - Integrated Synthera® HPLC
  - Modular concept (single interface)
  - Palette of IFP™

Synthera® — Multi-tracers platform

- Whatever you need, …

A palette of commercial IFP™ gives access to most synthesis steps:

- IFP™ Nucleophilic
- IFP™ Distillation
- IFP™ Akylation
- IFP™ Chromatography
- IFP™ Reformulation

Synthera® — Multi-tracer Platform

- IFP™ Nucleophilic : FLT, ML10, FDG, FMISO,

F-18 trapping and activation

Precursor addition

Hydrolysis

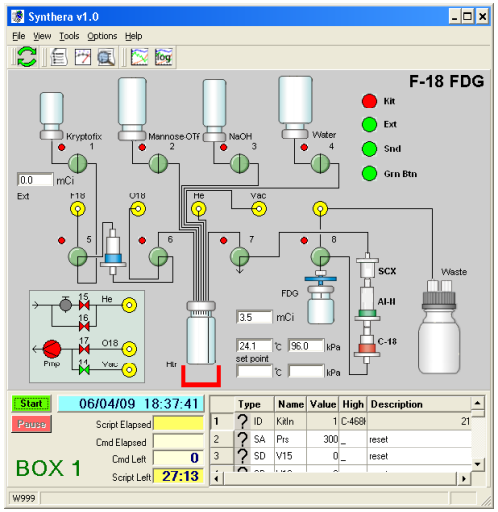

Dilution / neutralization/ buffering

Synthera® HPLC

Example of proprietary compound Parallel with FDG

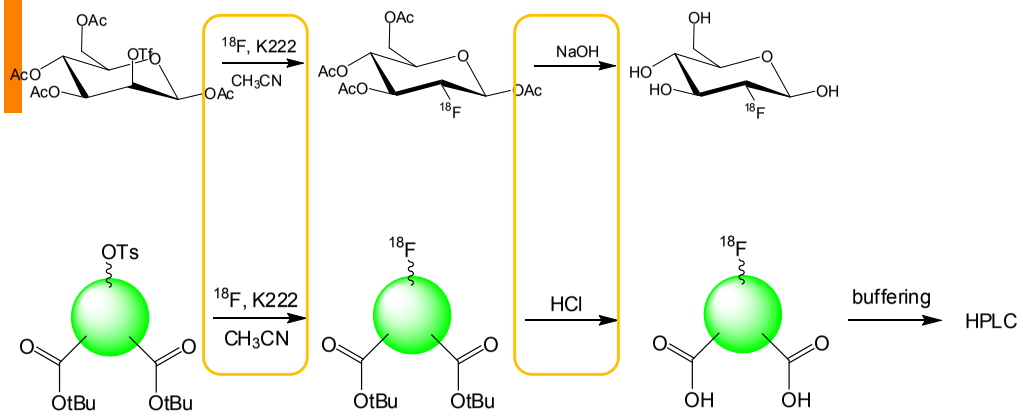

ML10 precursor

BOC-Nosyl precursor

HCL 1M

acetate buffer

^{18}F-ML10 Quality Control

- **Fully validated process**
- **Analytical methods validated according to ICH**
  - RCP and chemical purity > 99 %
  - Residual solvents below ICH limits

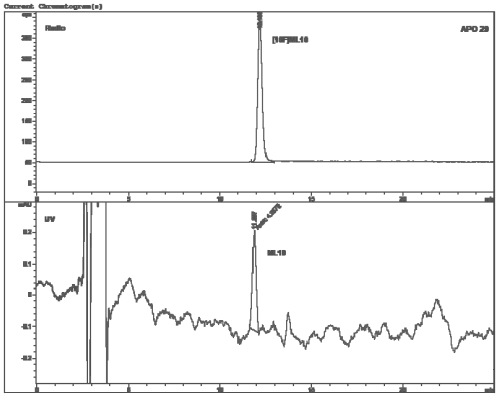

radiodetection

UV 206 nm

^{18}F-FLT Quality Control

- **Fully validated process**
- **Analytical methods validated according to ICH**
  - RCP and chemical purity > 95 %
  - Residual solvents below ICH limits

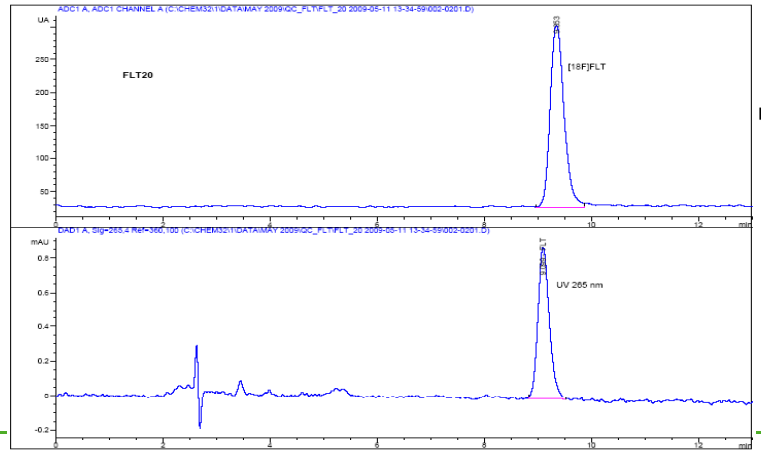

radiodetection

UV 206 nm

Specifications

^{18}F-ML10

- **Radiochemical yield:**
  - (40± 5) % EOS
- **Radiochemical purity:**
  - > 95 %
- **Chemical purity:**
  - Ts-OH< 0.25 ppm
  - ML-10-OH < 5 ppm
  - K222 & Residual solvents: USP & Eur. Ph. Compliant

^{18}F-FLT

- **Radiochemical yield:**
  - (20± 5) % EOS
- **Radiochemical purity:**
  - > 95 %
- **Chemical purity:**
  - Stavudine< 0.1 ppm (LOD)
  - [^{19}F]-FLT < 0.2 ppm
  - K222 & Residual solvents: USP & Eur. Ph. Compliant

Synthera® Multi-tracer Platform

IFP™ Chromatography

Washing trapped [^{18}F]F$^-$ with water & final elution with saline

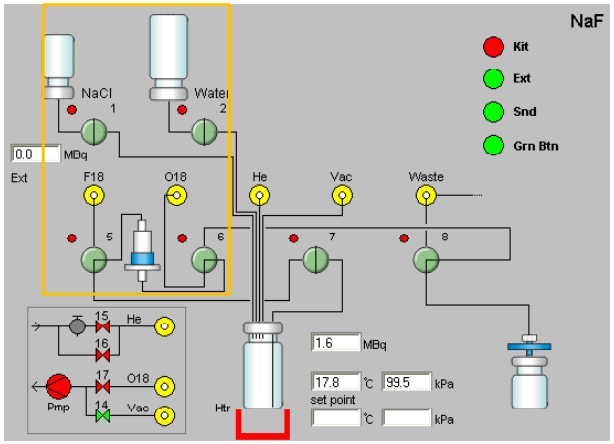

Example of the synthesis of [^{18}F]NaF

Specifications

^{18}F-NaF

- **Radiochemical yield**
  - 95 % EOS
- **Radionuclidic purity**
  - ^{18}F > 99.9 %
- **Radiochemical purity: Eur. Ph. Compliant**
  - [^{18}F]-fluoride> 98.5 % of total activity
- **Chemical purity: Eur. Ph. Compliant**
  - [^{19}F]-NaF < 4.52 mg/V

Synthera® Multi-tracer Platform

IFP™ Distillation & IFP™ Alkylation

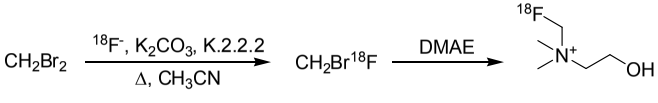

Synthera® 1
Preparation of FBM

Synthera® 2
Alkylation of DMAE

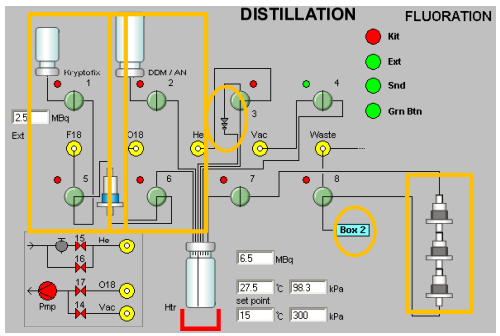

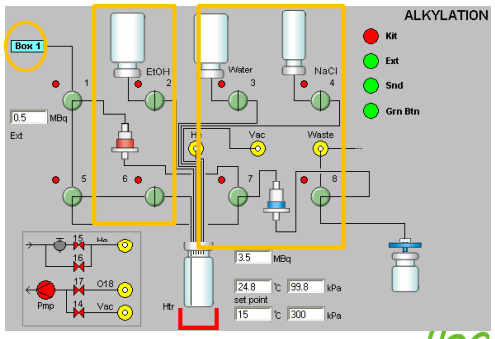

Example of the synthesis of [^{18}F]methylcholine

^{18}F-FCH Quality Control

- **Fully validated process**
- **Analytical methods validated according to ICH**
  - RCP and chemical purity > 95 %
  - Residual solvents below ICH limits

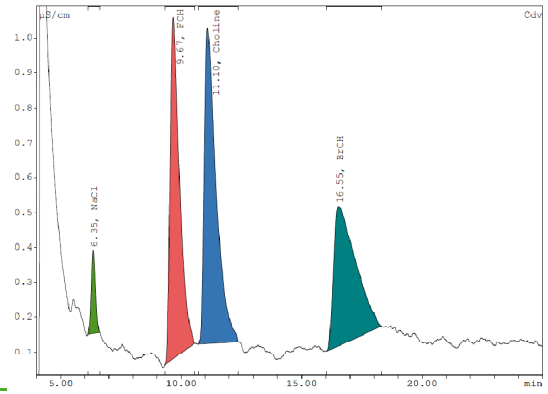

^{19}FCH and Choline 15 ppm

Bromocholine 25 ppm

Specifications

^{18}F-FCH

- **Radiochemical yield:**
  - (20± 2) % EOS
- **Radiochemical purity:**
  - > 95 %
- **Chemical purity:**
  - DBM < 0.1 ppm
  - [^{19}F]-FCH < 4 ppm
  - DMAE < 1500 ppm
  - Choline < 20 ppm
  - Bromocholine < 0.1 ppm
  - K222 & Residual solvents: USP & Eur. Ph. Compliant

Synthera® Multi-tracers Platform

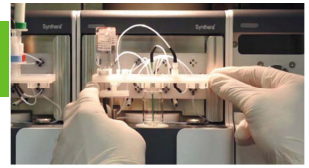

Extend your capabilities

IFP™ Nucleophilic	• FDG, **FLT**, FMISO, FES,**ML10**…
IFP™ Distillation	• **FBM**, click-chemistry precursor
IFP™ Alkylation	• **FCH**,…
IFP™ Chromatography	• **NaF**,…
IFP™ Reformulation	• More complex tracers, AV-45

Routine Production of Cu-61 and Cu-64 at the University of Wisconsin

Jonathan W Engle, Todd E Barnhart, and Robert J Nickles

University of Wisconsin, Madison, USA

The application of copper isotopes in PET research has undergone a dramatic rise, driven by their versatile chelation chemistry, favourable decay characteristics, and national distribution potential. The (p,n) reaction has long been used to produce ^{61}Cu and ^{64}Cu from ^{61}Ni and ^{64}Ni with reported yields of 21.4 ± 2.2 mCi/uA/hr and 8.7 ± 0.4 mCi/uA/hr at 11 MeV, respectively.[1] The ^{64}Ni(p,n)^{64}Cu reaction in particular necessitates careful consideration of incident particle energy. Electrodeposition of enriched ^{61}Ni and ^{64}Ni target material onto high purity gold or silver blanks has been described previously and appears to be limited to approximately 80-120 mg/cm^2, by time and cost concerns.

Using the pooled cross section data σ(E) for the ^{64}Ni(p,n)^{64}Cu reaction,[2] the end of saturated (EoSB) yield of ^{64}Cu can be predicted as a function of ^{64}Ni thickness and incident beam energy, shown below. This family of yield curves strongly suggests that very thick targets (≈ ½ gram/cm^2; ≈$10,000 in ^{64}Ni inventory) are needed to take advantage of proton energies above 11 MeV, being prohibitive both in cost and plating time. We have degraded the 16 MeV incident proton energy of the PETtrace to approximately 12 MeV with a 0.23 mm tantalum foil to improve the efficiency of our production runs. However, it is apparent that our legacy CTI RDS 112 is still far better suited for the weekly production of ^{64}Cu at the 0.5 Ci level for our own needs, as well as national distribution of the excess.

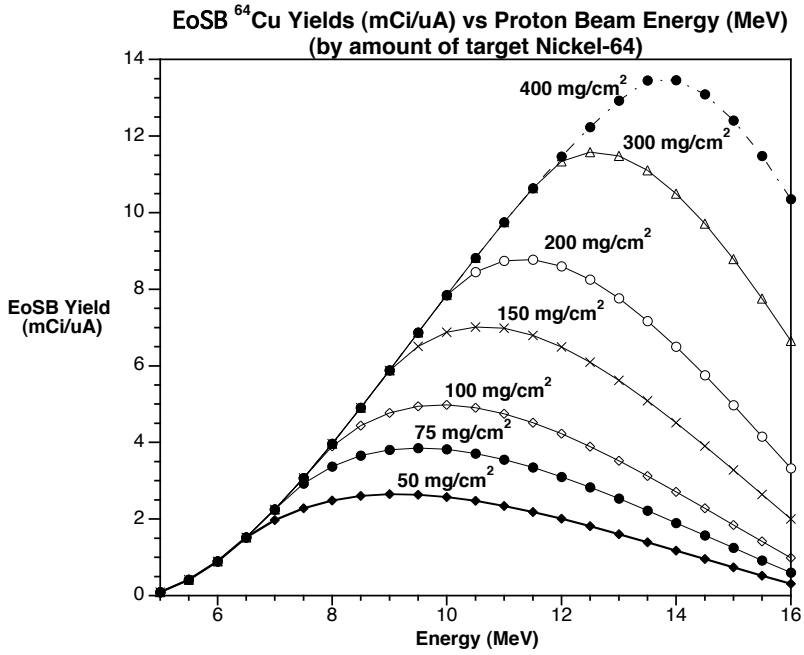

Copper-61 offers several advantages over ^{64}Cu for PET imaging, namely 61% vs 20% β^+ branching and a 3.4 hr vs 12.7 hr half-life, which combine to result in a three-fold greater useful β^+ flux to absorbed radiation dose ratio for trapped agents. Three reactions present themselves for cyclotron facilities without alpha beams: ^{61}Ni(p,n)^{61}Cu, ^{60}Ni(d,n)^{61}Cu, and ^{64}Zn(p,α)^{61}Cu. With the

recent three-fold price increase of enriched ^{61}Ni, we have reverted to the $^{60}Ni(d,n)^{61}Cu$ reaction for protocols needing Cu-ATSM for hypoxia imaging in human and veterinary patients.[3] Human studies use enriched ^{60}Ni plated on gold discs. Animal studies, with more relaxed specific activity requirements (>300 mCi/µmole), can utilize the deuteron irradiation of ^{nat}Ni targets, obviating the need for recycling of enriched target stock. The HPGe spectrum below testifies to the radionuclidic purity of the ^{61}Cu. Electroplated and foil targets are dissolved in HCl at 100^{s} C, accelerated with H_2O_2. Alternatively, biasing the Ni foil (10 volts, 1 amp) in unheated concentrated HCl removes approximately 40 mg of the foil and >90% of the activity in 3 minutes.[4] The dissolution apparatus is identical to the electroplating setup. These platers have been recently improved, adding flow, temperature control, pulsed voltage and current regulation under LabView control.

As more subtle targeting strategies develop, the chelation of copper radionuclides to molecular imaging candidates will permit PET to determine the best lead compound, significantly shortening the time to achieve diagnostic utility. Any improvements in the supply of ^{61}Cu and ^{64}Cu will greatly serve that end.

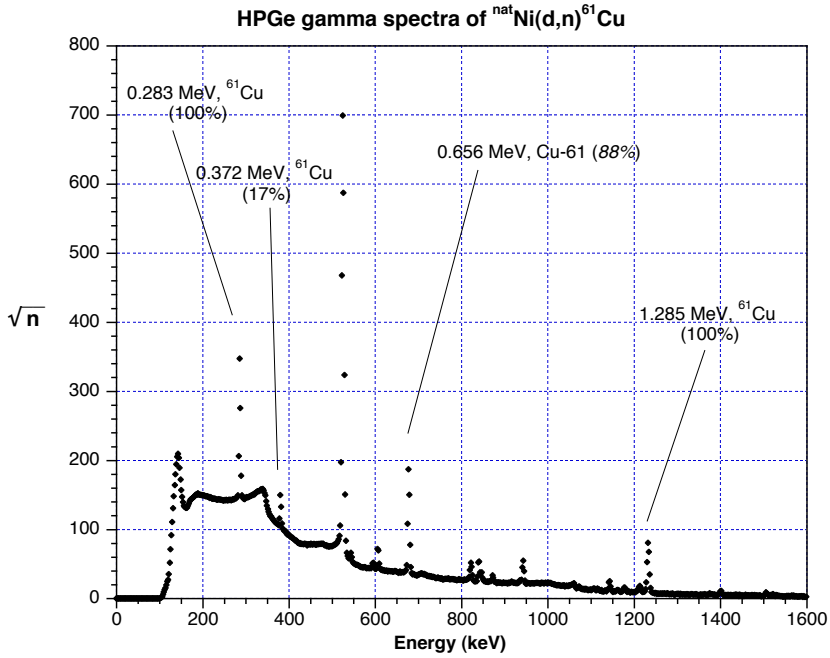

---

[1] Avila-Rodriguez M A (2007). Low energy cyclotron production of multivalent transition metals for PET imaging and therapy. Ph.D. Dissertation University of Wisconsin Press, Madison, WI.

[2] Cyclotron Produced Radionuclides: Physical Characteristics and Production Methods (2009). IAEA Technical Reports Series No. 468. IAEA Press, Vienna, Austria.

[3] Tolmachev V, Lundqvist H, Einarsson L (1998). Production of 61Cu from a natural nickle target. Applied Radiation Isotopes, 49(1-2), 79-81.

[4] Martin C C, Oakes T R, Nickles R J (1990). Small Cyclotron Production of Cu-60 PTSM for PET Blood Flow Measurements. J Nucl Med 31, p815.

Routine production of ^{61}Cu and ^{64}Cu at Wisconsin

Jon W Engle, Todd E Barnhart, Miguel A Avila-Rodriguez and Jerry Nickles




A cottage industry

OR

A sweatshop

Range = $\{(t_{1/2}/\ln 2)/\text{velocity}\} \times \ln(A_o/A_{needed})$

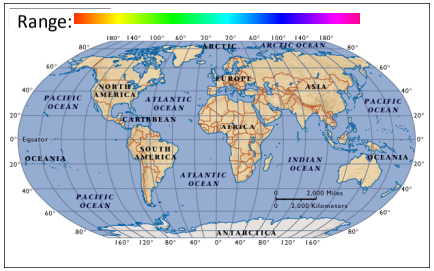

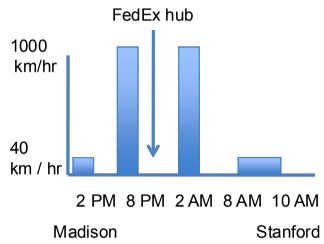

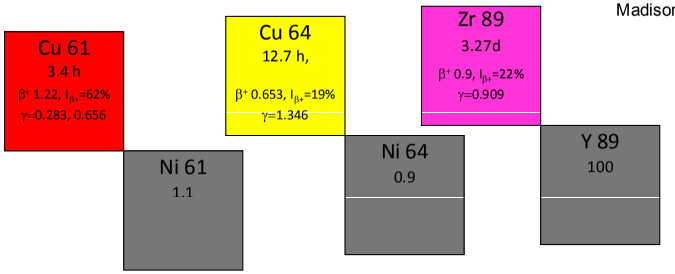

^{61}Cu = hundreds km
^{64}Cu = thousands km
^{89}Zr = international

^{64}Cu DECAY

Lederer & Shirley (1978)

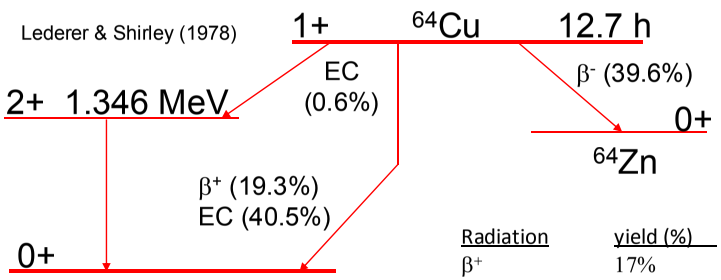

$E_{\beta+max}$ = 0.656 MeV

Radiation	yield (%)	E_{av} (keV)
β^+	17%	278
γ^+	35%	511
γ	0.5%	1346
$K\alpha_1$	10%	7.4
$K\alpha_2$	5%	7.4
$K\beta$	2%	8.2
L	0.5%	0.8
Auger-K	22%	6.5
Auger-L	57%	0.84
β^-	39%	190

UW Medical Physics Cyclotron(s)

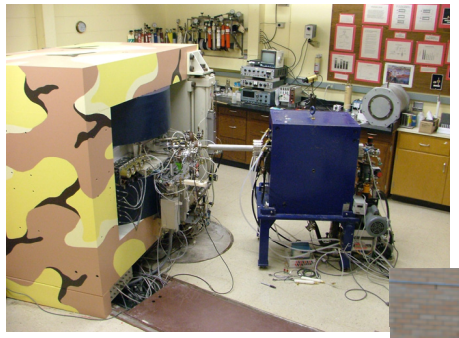

RDS 112 #1 - 1985 - to - ∞
Mother of All RDS's

PETtrace 144
2008 - to - ∞

^{64}Cu yield at EoSB (mCi/μA)

$$Y = \frac{N_A \rho}{A_w} f\, I(1-e^{-\lambda t}) \int_{E_1}^{E_2} \left(\frac{dE}{dx}\right)^{-1} \sigma(E)\, dE$$

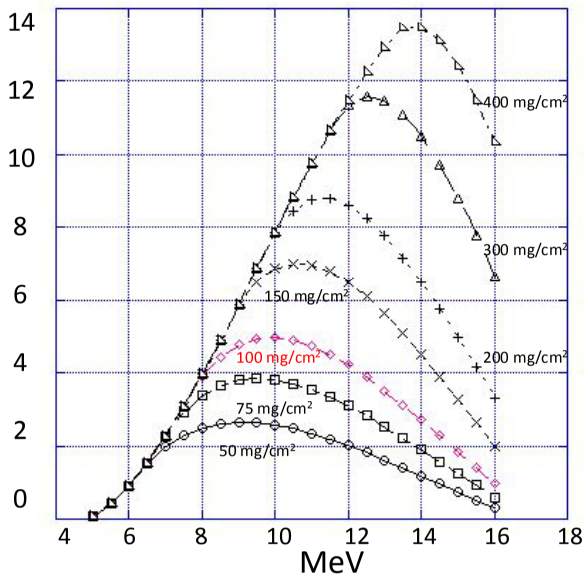

Optimum scaling

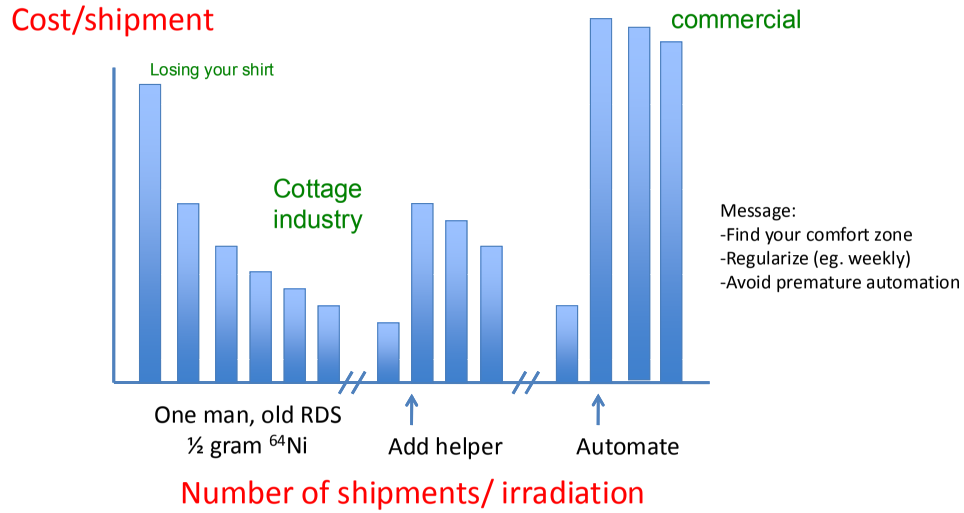

Shipments / quarter

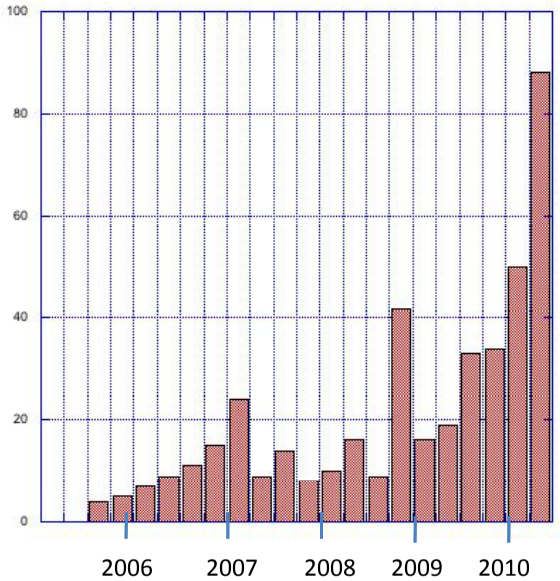

ignition

Materials Needed for the Production of High Specific Activity ^{64}Cu

The production of high specific activity ^{64}Cu for clinical applications requires at least 15 k$ of startup investment

- Enriched (>95%) ^{64}Ni ($20/mg)

Natural abundance of ^{64}Ni = 0.9%

- High-purity Au disks (99.999%)
- Ultra high-purity solvents (ppt Cu)

Nickel Target Preparation and Recovery

^{64}Ni > 96%

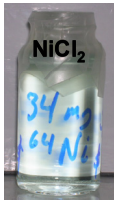

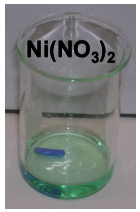

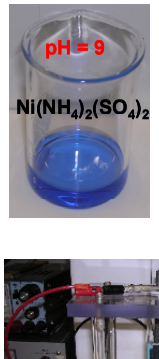

The Challenge

Recovery Efficiency =96.9±1.8%

More than 130 production runs using and recycling 500 mg of ^{64}Ni

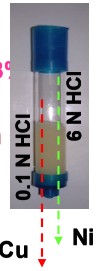

11 MeV p

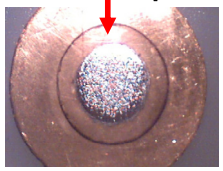

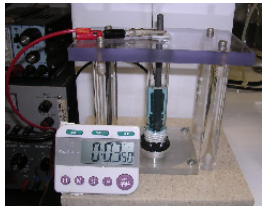

Anode: graphite rod
Cathode: Au disk
I = 15-25 mA, (2.4-2.6 V)

Piel *et al.* Radiochimica Acta 57 (1991) 1-5.

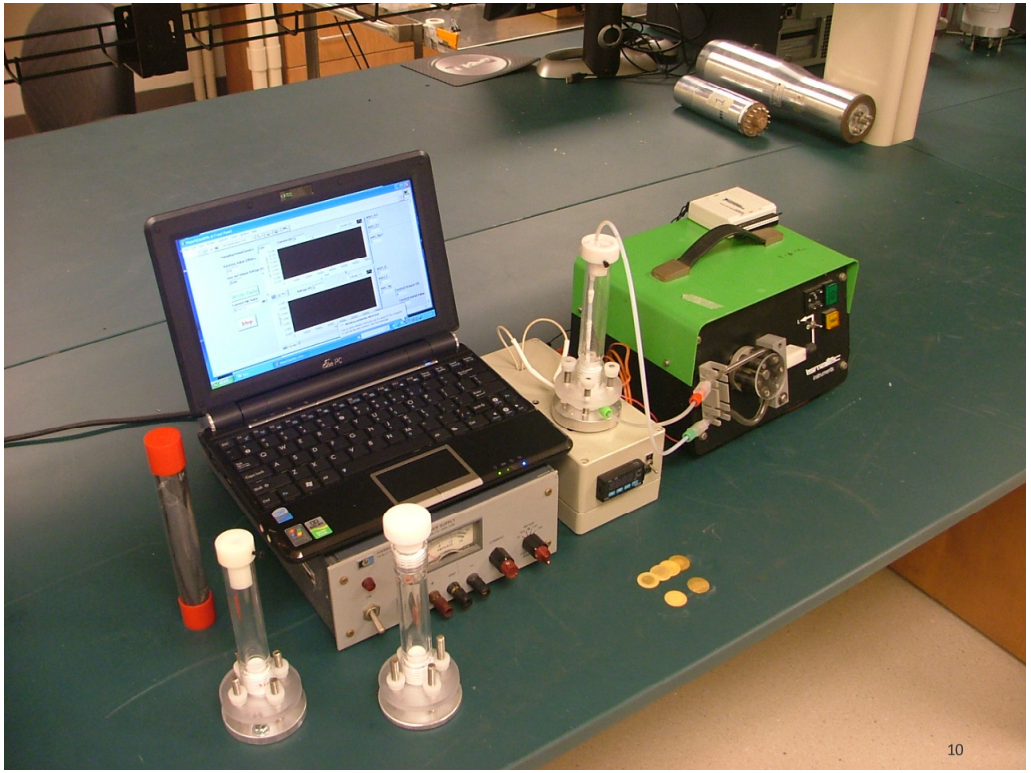

Target Holder and Proton Beam Profile

Target : Windowless water cooled mounting

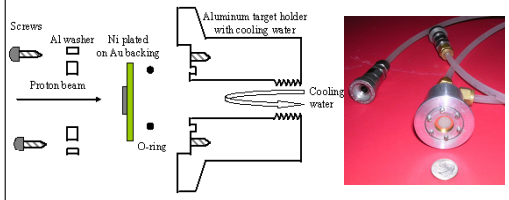

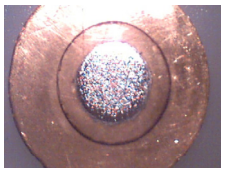

Pre-shot

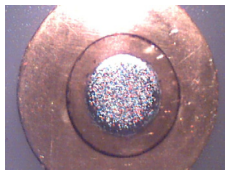

Post-shot (30 μA x 7.5 h)
~1 Ci ^{64}Cu

Imaging Apparatus:
Asahi Pentax K-1000
1:2:8 macro lens (Sigma X)
Micro-meter stage mount
3/4" PMT as light meter

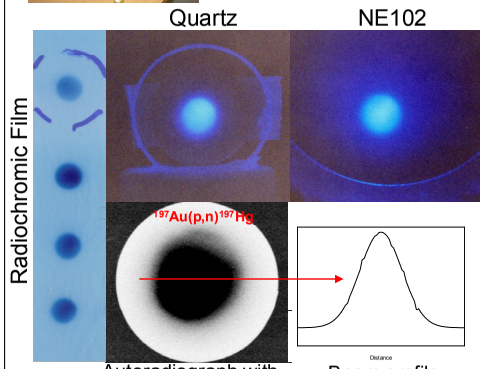

Autoradiograph with X-ray co-registration

Beam profile FWHM ~ 8 mm

Radiochemical Separation of Ni and Cu

Target dissolved in 2 ml 12 N HCl + heat + 2 ml H_2O

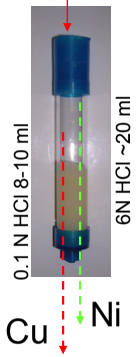

Anion Exchange AG1-X8 resin

^{nat}Ni(d,n) reaction

Key reactions (6 MeV)

^{60}Ni(d,n)^{61}Cu
^{64}Ni(d,p)^{65}Ni

Half-lives:
^{61}Cu: 3.4 h
^{65}Ni: 2.5 h

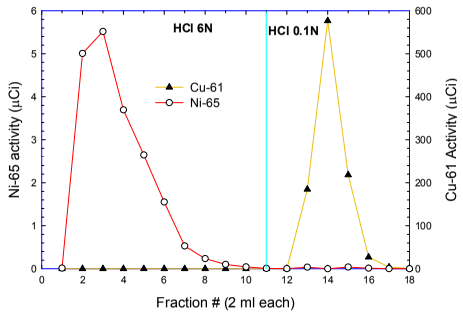

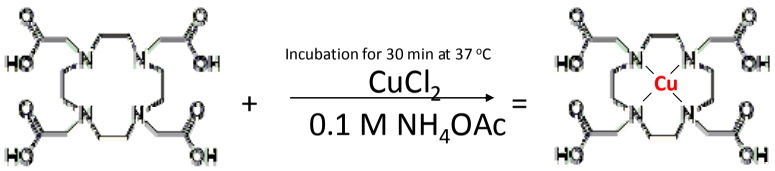

TETA titration

Carrier – free => 245 Ci / µmole

64 ppb = 1 nanoMol / ml => 245 mCi / ml CF

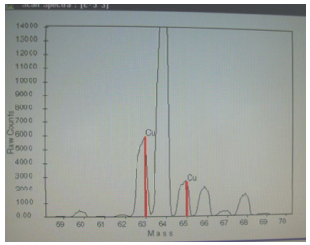

specific ion electrode
[Cu^{++}] > 60 ppb

ICP - mass spec
[Cu] ≈ 50 ppb

One copper does NOT fit all

Cu	60	61	62	64	67
$t_{1/2}$	23 m	3.4 hr	10 m	12.7 hr	78 hr
mode	β^+(93%)	β^+(62%)	β^+ (98%)	$\beta^\pm$(19%),EC	β^-
E_{β^+}(max)	2-4	1.2	2.9	0.6	0.4
A (EOSB 11 MeV) p)	40	86	gen	160	-
Abs Dose useful β^+	1	5	3	20	-

^{61}Copper ($t_{1/2}$=3.4 h, $I_{\beta+}$=62%, $E_{\beta+max}$=1.22 MeV)

Experimental target yields of ^{61}Cu from 86% ^{61}Ni targets

Thickness (mg/cm^2)	Irradiation (µAh)	Experimental batch yield at EOB (mCi)	Yield at EOB (mCi/µAh) Experimental	Yield at EOB (mCi/µAh) Theoretical	% of predicted
65	31.6	164	5.2	6.8	76
62	22.5	110	4.9	6.5	75
54	27.5	105	3.8	4.9	78

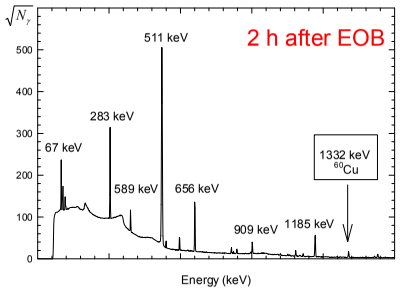

Thick target yield for 100% enrichment with 11.4 MeV protons:

21.4 ± 2.2 mCi/µAh

Production Pathways

Reaction	target $	recycle?	mCi/µA-hr	Problems
^{61}Ni(p,n)^{61}Cu	$17->$50/mg	YES	21 (@ 11 MeV)	costly target
^{60}Ni(d,n)^{61}Cu	≈ $/mg	yes	4 (@8 MeV)	need deuterons
^{nat}Ni(d,n)^{61}Cu	-	no	1	need d + time
^{nat}Zn(p,α)^{61}Cu	-	no	4 (@16 MeV)	^{66,68}Ga
^{64}Zn(p,α)^{61}Cu	≈ $/mg	yes	8	
^{64}Ni(p,n)^{64}Cu	$17/mg	YES	160	costly target
^{67}Zn(p,α)^{64}Cu	≈ $10/mg	YES	1	low yield, “

PET Imaging Performance of Copper Radionuclides

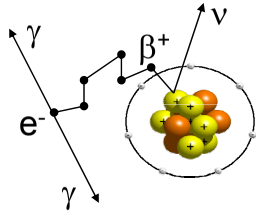

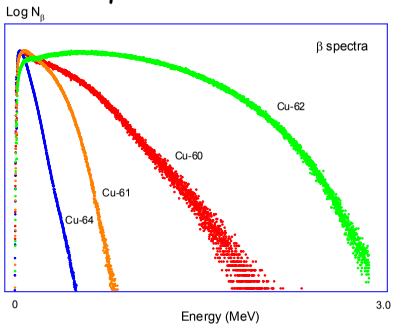

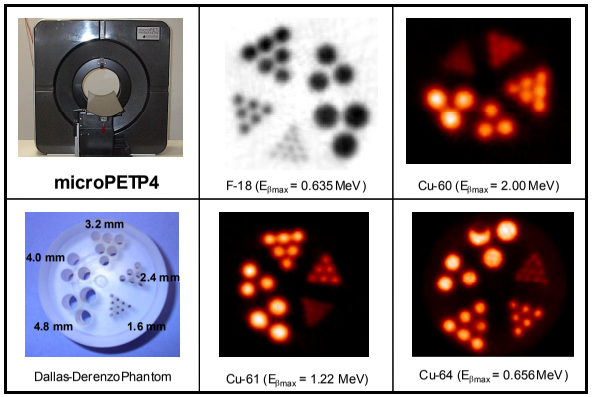

Imaging at Keck Lab, P4 Concorde microPET

Now with deuterons

$^{nat}Ni(d,n)^{61}Cu$

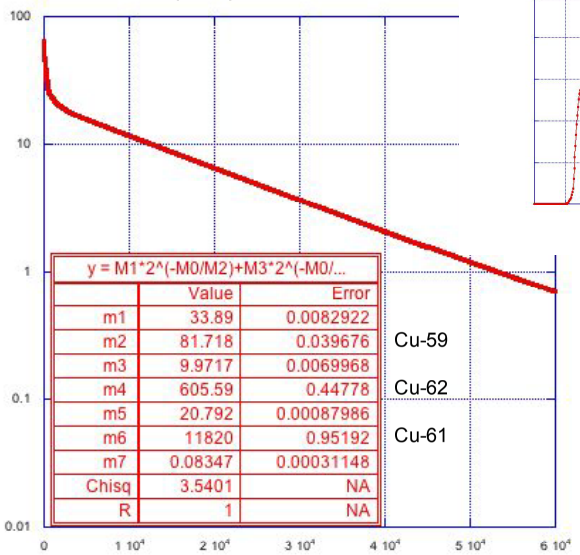

y = M1*2^(-M0/M2)+M3*2^(-M0/...		
	Value	Error
m1	33.89	0.0082922
m2	81.718	0.039676
m3	9.9717	0.0069968
m4	605.59	0.44778
m5	20.792	0.00087986
m6	11820	0.95192
m7	0.08347	0.00031148
Chisq	3.5401	NA
R	1	NA

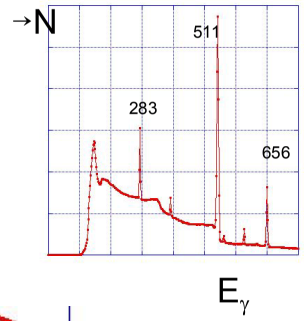

Slow, but free from recycling

In vivo Quantification of Hypoxia (Cu-ATSM)

Cu(II)-diacetyl-bis(N^4-methylthiosemicarbazone)

Because its low redox potential Cu-ATSM is retained only in oxygen-depleted tissues

$^{64}Cu(II)$-ATSM

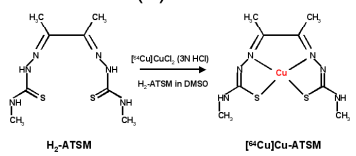

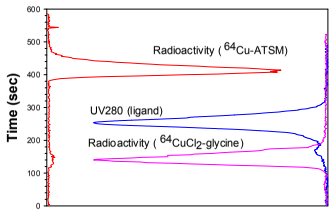

Radiochemical Purity > 98%

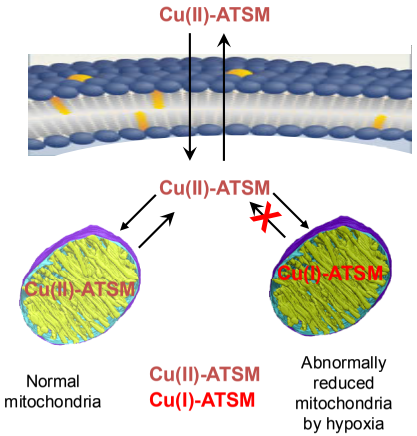

Adapted from Fujibayashi et al. (1997)

PET Molecular Imaging of Hypoxia (^{61}Cu-ATSM)

Now routinely used at UW-Madison Hospital and Clinics (Human trials)

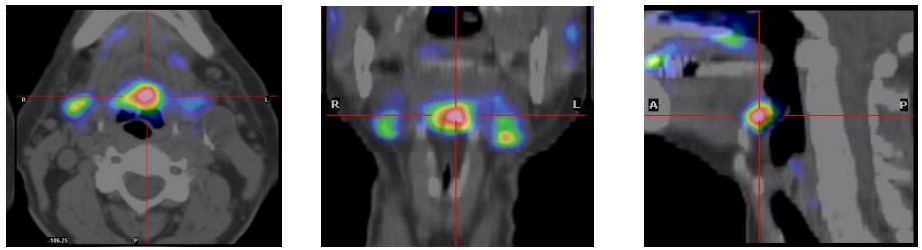

Hypoxic head and neck tumor in a human subject
UW-Madison Hospital and Clinics (GE PET/CT)

UW Medical Physics PETtrace beamline extension

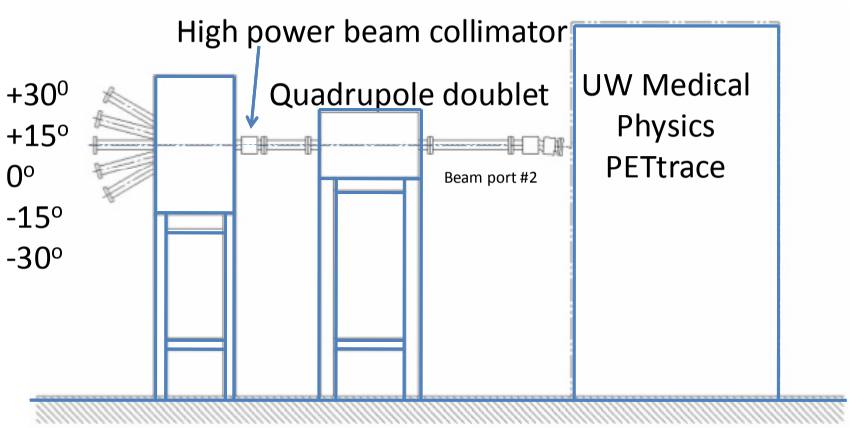

MIZZOU – SMITH

Long Island Jewish Hospital

Univ Texas SW

Stanford

MD Anderson

Mizzou - Lewis

MPI

Univ Texas - San Antonio

Mizzou - Deutscher

USC

Johns Hopkins

Univ North Carolina

Univ Texas - Houston

UW – Weibo Cai

UW- Sarah Mudd

Univ California – San Francisco

WTTC XIII – Presentation Discussions

1. Cu production setup implementation
   - Avoid premature automation
   - "specific ion electrode" to measure specific activity
2. Production/distribution in the USA
   - Saturation not achieved yet
   - Industry not yet interested on distribution
3. Cobalt contamination
   - Ni purity is important!
   - Co trapped in ion exchanger

Sustainable PET tracer production at Wisconsin

Todd E Barnhart[1], Jonathan W Engle[1], Peter Larsen[2], Bradley T Christian[3], Dhanabalan Murali[1], Dustin Wooten[1], Onofre T DeJesus[1], Ansel Hillmer[1], and Robert J Nickles[1]

[1]University of Wisconsin, Madison, USA

[2]Scansys, Copenhagen, Denmark

[3]Waisman Institute for Brain Imaging and Research, Madison, USA

Introduction

The University of Wisconsin PET tracer production facility has evolved over four decades, progressing from an EN tandem (1971), the first CTI RDS 112 (1985), an NEC pelletron (1998) and now, a GE PETtrace, bunkered in a new facility. Balancing a mixed assignment of graduate training, basic and clinical research, our emphasis has centered on achieving a *sustainable* campus-wide resource, free from unrealistic expectations or crippling service contracts. The foundation of this self-support is inherent in the state-audited charge-back account within the autonomy of the Medical Physics Department, where users cover the fair share for the development and production of the tracers that they request.

Targetry

We have continued the Wisconsin tradition of making our own cyclotron targets on the new GE PETtrace. Helium cooling has been cast aside in favour of single, gridded entrance windows. The [^{18}F]-fluoride target's niobium body houses a 1.1 mL target volume behind a havar window with a water-cooled grid support described previously.[1] The [^{13}N]NH_3 target is a 304 stainless steel volume of 2.5 mL also behind a havar foil and grid. A 3 mL/min flow of 5 mM EtOH provides a steady state production of [^{13}N]NH_3 trapped on an Alltech IC-Na Plus cartridge. [^{11}C]CO_2 and [^{11}C]CH_4 targets are electropolished 304 stainless steel tubes (25 cm x 1.6 cm dia.), TIG welded inside the water-jacket. These targets are also sealed to the vacuum by the same havar foil /grid system. All grids are approximately 2.5 cm deep with hexagonal holes (2.5 mm across the flats, 0.3 mm septa) electric discharge-machined into aluminum.

Automated chemistry

[^{18}F]-fluoride, [^{13}N]-NH_3, [^{11}C]-CO_2, and [^{11}C]-CH_4 are transported to shielded radiochemistry equipment in the lab adjacent to the vault through narrow bore lines. Aqueous fluoride and C-11 carbon dioxide or methane are remotely unloaded via FEP and stainless steel lines, respectively, and sent to two Capintec (New Jersey) hot cells, each containing a Labview-controlled Scansys (Copenhagen) automated radiochemistry module. [^{11}C] activity can also be piped to the Waisman Institute for Brain Imaging and Research via a "tuned"[2] 300 meter underground PTFE pipeline. Each Scansys module contains a syringe pump-fed 2-dimensional robot with access to reagent vials, two thermally heated, air-cooled reactors, and a microwave module. Customized inserts permit reaction vessels to range in size from 500 uL to 7 mL. Robotic access is provided to additional reagents through 4 banks of 3-way valves, a needle cleaning station, and HPLC injection loop. Three Rheodyne TitanEX 7-port selector valves direct flow through cartridges for in-line separations and filtration, all monitored by miniature Centronix ZP1300 GM tubes. The HPLC

system supports up to 5 separate columns via additional switching valves and includes a column heater as well as a linear scanner gamma viewing any column with one of 8 included ZP1300 (Centronic) GM tubes. Following HPLC purification, the Scansys module also includes a custom evaporator which is capable of removing 10 mL water in ~ 1 min. for reconstitution in appropriate solvents. Drydown, as well as fluid movement throughout the module, can be accomplished with 4 MFC-regulated gas channels, currently plumbed and calibrated for argon, nitrogen, and helium flow. Each module also contains two vacuum pumps capable of pulling approximately 50 mL/min through 1 m of 1/16" ID tube.

To date, we have successfully automated syntheses of [^{18}F]FLT, [^{18}F]FES, [^{11}C]MHED and [^{11}C]DTBZ for animal studies on these systems. Yields are comparable to those obtained with our prior manual chemistries. For [^{18}F]FLT, yields average 10.1 ± 5.1% (decay corrected to QMA trapping, using 10 mg 3-N-Boc ABX precursor) with specific activities of 3.7 ± 1.8 Ci/umol (n=30). [^{18}F]FES yields average 16.9 ± 4.2% (decay corrected to QMA trapping, using 2 mg ABX precursor) with 3.8 ± 1.5 Ci/umol (n=4). Syntheses of [^{18}F]FMISO are planned to follow.

Conversion efficiency from [^{11}C]CH_4, produced in-target, to [^{11}C]MeI by recirculating loop in the new module is 70.0 ± 0.4% (n=28). Automated syntheses of [^{11}C]MHED and [^{11}C]DTBZ on the Scansys module average yields of 16.0 ± 5.8% (n=11) and 36.3 ± 11.6% (n=3) respectively (decay corrected to methylation). Specific activities for both syntheses, decay corrected to EoB, are 8.4 ± 0.3 Ci/umol. [^{11}C]WAY, produced manually from the [^{11}C]CO_2 target, averages 1.4 ± 0.6 Ci/umol at end of synthesis (n=8); decay correction puts EoB specific activity from this target at 9.8 ± 3.3 Ci/umol.

Conclusion

The natural evolution of production capacity at Wisconsin has been driven by the increased demand for PET tracers for molecular imaging, both in basic research and in the clinic. The new PETtrace, bunkered in new facilities, easily handles the call for conventional radionuclides, freeing up the legacy prototype CTI RDS 112 for a new life concentrating on the production of ^{64}Cu for distribution,$^{18}F_2$ for electrophilic fluorination (F-DOPA, FMT), and target development for the production of orphan isotopes.

---

[1] Roberts A D, Armstrong I S, Kay B P, Barnhart T E (2004). Improved strategies for increased [^{18}F]F^- yield via the ^{18}O(p,n)^{18}F reaction with thin target windows and bodies. Presentation at the 10th Semi-Annual Workshop on Targetry and Target Chemistry, Madison, WI.

[2] Hichwa R D and Nickles R J (1979). The tuned pipeline: A link between small accelerators and nuclear medical needs. IEEE Transactions on Nuclear Science 26, 1707-1709.

Sustainable PET tracer production at Wisconsin

Todd E Barnhart[1], Jonathan W Engle[1], Peter Larsen[2], Bradley T Christian[1], Dhanabalan Murali[1,3], Dustin W Wooten[1], Onofre T DeJesus[1], Ansel Hillmer[1], and Robert J Nickles[1]

[1]University of Wisconsin, Madison USA
[2]Scansys, Copenhagen DK
[3]Waisman Institute for Brain Imaging and Research, Madison, USA

^{11}C gas targets

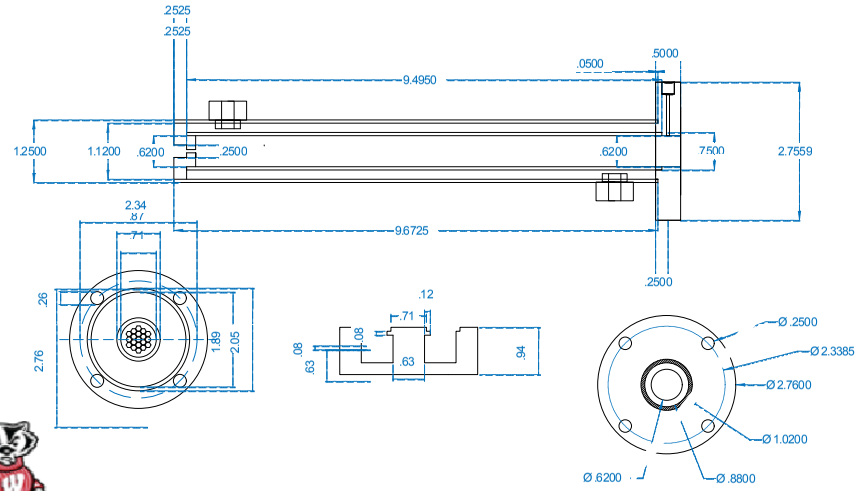

^{18}F water target

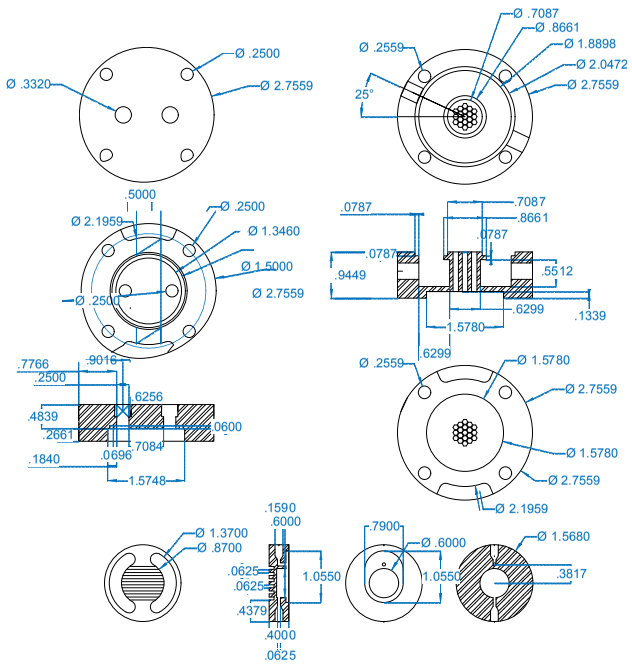

^{13}N target

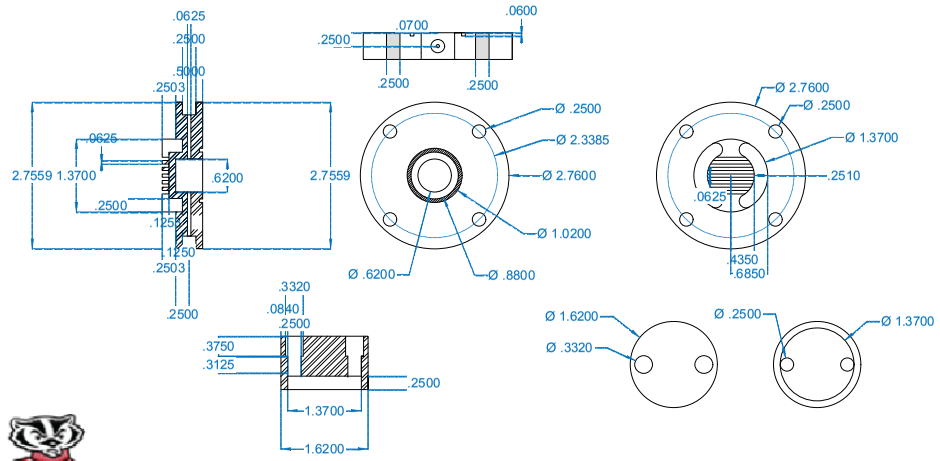

Targets mounted on the UW PETtrace

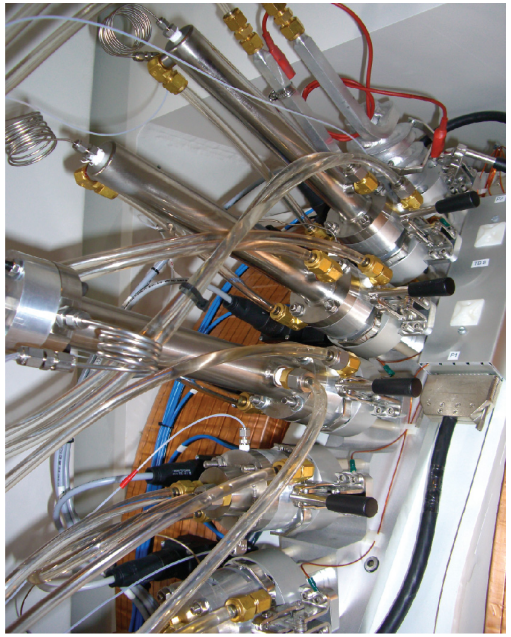

Capintec Hot Cells

Scansys Radiochemistry Box

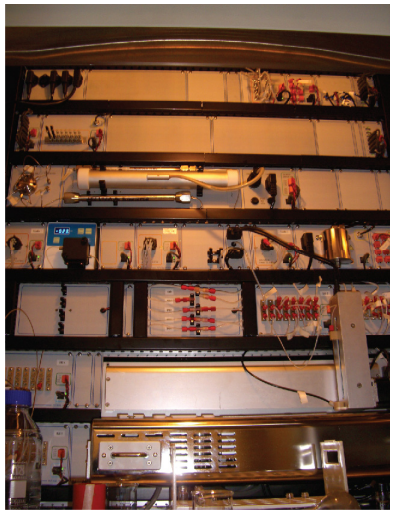

Scansys box and interface

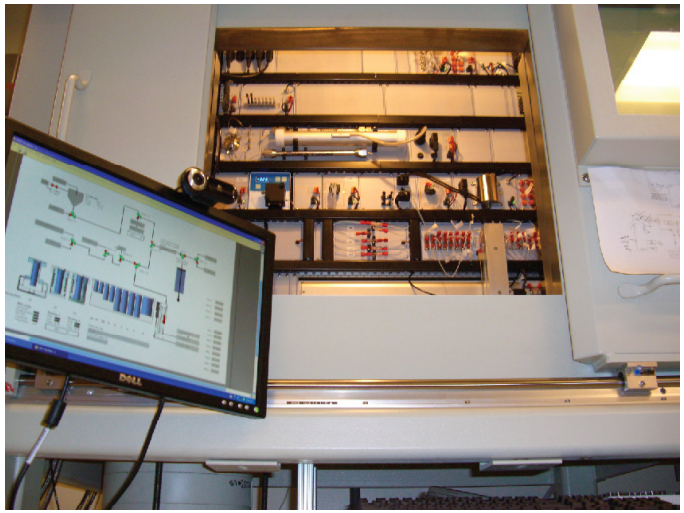

WTTC XIII – Presentation Discussions

1. Manufactured targets
   - Cheaper
   - Same yields
   - Stainless steel target experience

Production of Cl-34m via the (d,α) reaction on Ar-36 gas at 8.4 MeV.

Jonathan W. Engle, Todd E. Barnhart, Onofre DeJesus, and Robert J. Nickles

University of Wisconsin, Madison, USA

Introduction

The radioisotope ^{34m}Cl (β+, $t_{1/2}$=32.2 m) is of interest to the medical community, especially in drug development. However, ^{34m}Cl production is currently limited to facilities capable of accelerating alpha particles.[1] Proton-only accelerators can make use of reasonable yields for enriched ^{34}S targets, but must contend with the poor thermal and electrical properties of sulphur and its compounds, which reach the molten state at even limited beam currents. The utility of the ^{20}Ne(d,α)^{18}F reaction[2] suggests an alternative route to ^{34m}Cl via the corresponding noble gas, argon. The excitation function and yield measurements for ^{36}Ar(d,α)^{34m}Cl near 8.4 MeV, the nominal deuteron energy on a PETtrace cyclotron, elude a careful search of the literature.

Test Irradiations of ^{nat}Argon

A gas target (21 cm x 1.4 cm ID) was built with removable endplates for rapid removal of a quartz tube with trapped ^{38,34m}Cl- from ^{40,36}Ar(d,α). Exploratory deuteron irradiations were conducted on a thick target of ^{nat}Ar 130 psig. Following irradiation, the target was “cooled” briefly to allow the overwhelming 511 keV gammas from ^{16}O(d,n)^{17}F in the quartz tube to decay and then flushed twice into a 1 L syringe to remove ^{41}Ar prior to target disassembly and analysis. The quartz tube was removed and assayed with an HPGe detector (spectra shown below). Gamma spectroscopy revealed the production of 0.9 ± 0.1 mCi/uA of ^{38}Cl ($t_{1/2}$=37.2 m) and 5.1 ± 0.4 mCi/uA of ^{41}Ar ($t_{1/2}$=109 m) at end of saturated bombardment (EoSB). More importantly, the production of ^{34m}Cl in approximately 1:300 ratio with ^{38}Cl mirrors the abundance ratios of their target isotopes.

Yield Measurements with ^{36}Argon

Enriched ^{36}Ar (99.993%, 1 L at STP) was obtained from Isoflex (San Francisco). The high cost (~$5000/L) of the target material necessitated cryotrapping ^{36}Ar post-irradiation in a 50 mL stainless steel vessel.[3] Vacsorb greatly improved the cryorecovery of argon at -196°C (<1 mm Hg) compared to vapor pressures achievable in its absence (0.3 atm), in agreement with the Clausius-Clapeyron relation’s prediction. A second target (21 cm x 1.9 cm ID) better accomodated the width of our deuteron beam, albeit at some cost in target pressure. The ^{36}Ar-filled target was irradiated at an initial pressure of 68 ± 1 psig by beam currents between 5 and 20 uA for 30 minutes. After the run, 10 minutes of cryotrapping recovered >99.5% of target material at -196°C. The target was vented and the quartz insert removed for analysis. To date, 12 irradiations have been completed, revealing radionuclidically clean production of desired ^{34m}Cl trapped in the quartz tube. EoSB yields and decay over more than 3 decades are shown below, averaging 1.8 ± 0.2 mCi/uA for thick-target runs, reflecting the larger ID target’s accomodation of the PETtrace deuteron beam. The target appears to thin beyond 10 uA, reducing effective yield. Phosphor plate imaging of the quartz tubes’ adsorbed activity confirms this hypothesis, as the activity peak progresses steadily towards the back of the target with increased beam currents.

Conclusion

These results suggest the possibility of subsequent labeling with ^{34m}Cl; nucleophilic test reactions to confirm the reactivity of the product will follow.

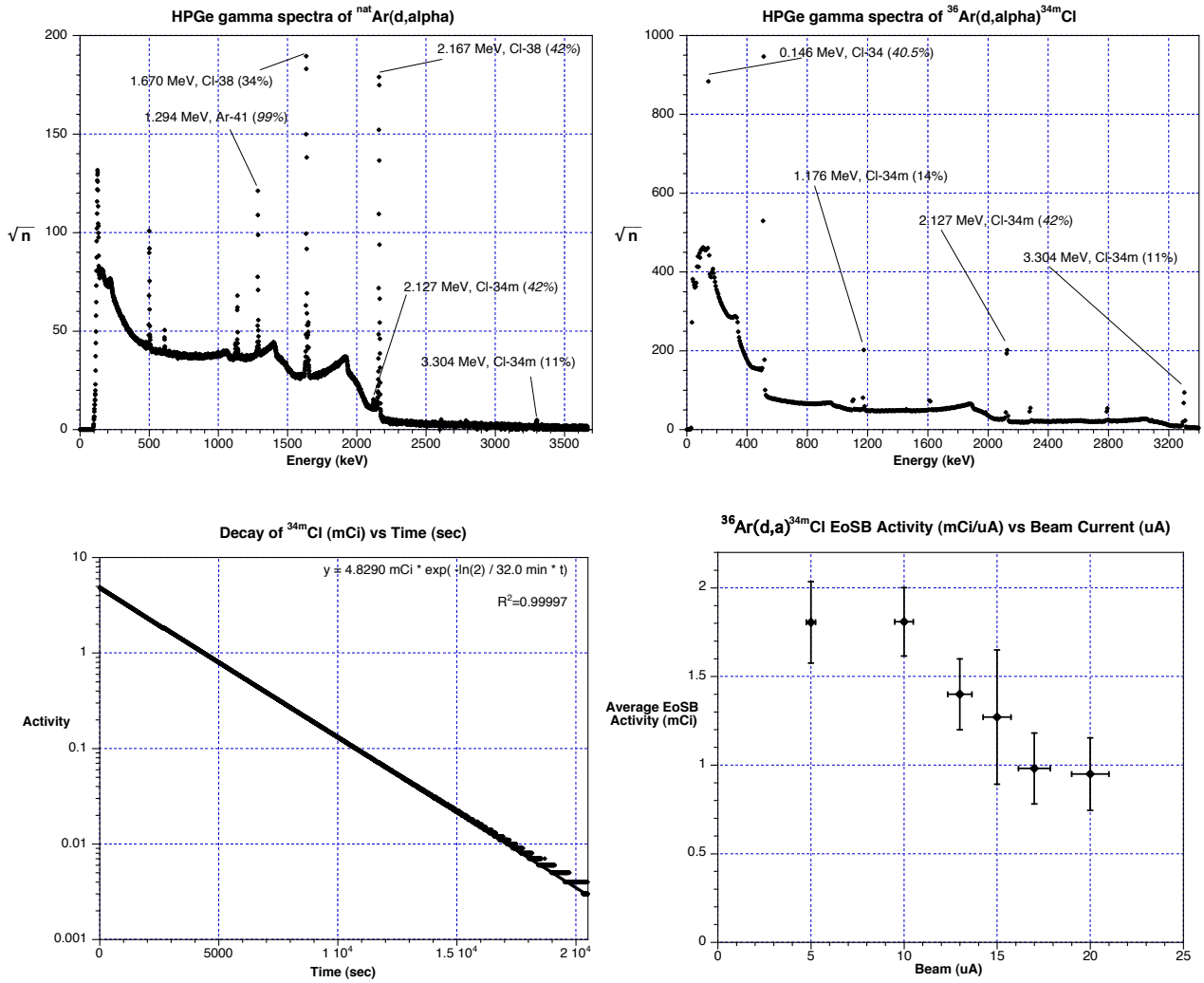

---

[1] Takeia M b, Nagatsua K, Fukumuraa T, Suzuki K (2007). Remote control production of an aqueous solution of no-carrier-added $^{34m}Cl^-$ via the $^{32}S(\alpha,pn)$ nuclear reaction. Applied Radiation and Isotopes 65(9), 981-986.

[2] Casella V R, Ido T, Wolf A P, Fowler J S, MacGregor R R, Ruth T J (1980). Anhydrous F-18 labeled elemental fluorine for radiopharmaceutical preparation. Journal of Nuclear Medicine, 21, 750-757.

[3] Nickles R J, Daube M E, and Ruth T J (1984). An $^{18}O_2$ target for the production of $[^{18}F]F_2$. International Journal of Applied Radiation Isotopes 35(2), 117-122.

Production of ^{34m}Cl via (d,α) on ^{36}Ar gas at 8.4 MeV

Jonathan W Engle, Todd E Barnhart, Onofre J DeJesus, Robert J Nickles.
The University of Wisconsin, Madison

An introduction to Cl-34m

$t_{1/2}$=32.2 min, β^+ endpoint energy = 4.5 MeV

Reaction	Q Value (MeV)	Approximate Yields (note confusing units)
^{32}S(α,n)^{34m}Cl	-14.66	18 mCi/μA at E_α=50 MeV
^{34}S(p,n)^{34m}Cl	-6.42	12 mCi/μA at E_p=11 MeV
^{34}S(d,2n)^{34m}Cl	-8.64	0.3 mCi/uA/hr at E_d=10 MeV
^{35}Cl(n,2n)^{34m}Cl	-12.79	n/a
^{35}Cl(p,pn)^{34m}Cl	-12.79	2.7 mCi/uA/hr at E_p=15 MeV
^{31}P(α,n)^{34m}Cl	-5.79	8.5 mCi/uA/hr at E_α=20 MeV
^{36}Ar(d,α)^{34m}Cl	-8.38	This work

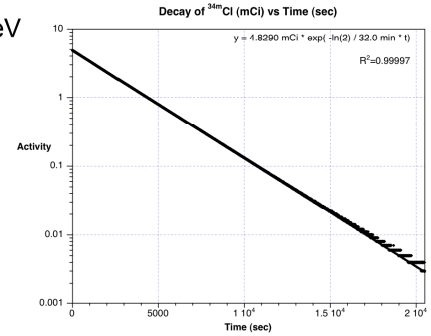

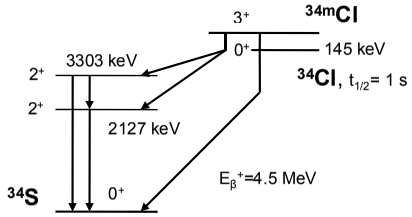

^{nat}Ar(d,α), a test reaction

36K 342 MS ε: 100.00% εp: 0.05%	37K 1.226 S ε: 100.00%	38K 7.636 M ε: 100.00%	39K STABLE 93.2581%	40K 1.248E+9 Y 0.0117% β-: 89.28% ε: 10.72%	41K STABLE 6.7302%	42K 12.321 H β-: 100.00%
35Ar 1.775 S ε: 100.00%	36Ar STABLE 0.3365%	37Ar 34.95 D ε: 100.00%	38Ar STABLE 0.0632%	39Ar 269 Y β-: 100.00%	40Ar STABLE 99.6003%	41Ar 109.61 M β-: 100.00%
34Cl 1.5264 S ε: 100.00%	35Cl STABLE 75.77%	36Cl 3.01E+5 Y β-: 98.10% ε: 1.90%	37Cl STABLE 24.23%	38Cl 37.24 M β-: 100.00%	39Cl 56.2 M β-: 100.00%	40Cl 1.35 M β-: 100.00%

Expected products from a deuteron irradation at 8.4 MeV: ^{41}Ar, ^{38}Cl, $^{34/34m}$Cl.

Yields for both reactions of interest are presently absent from the literature.

Preliminary Experiments with ^{nat}Argon

- Exploratory irradiations at 130 psig, 8 MeV
- Target has removable endplate for extraction of quartz tube with trapped Cl^-
- Tube assayed with HPGE (FWHM @ 1333 keV = 2.5 keV)
- 0.9 ± 0.1 mCi/uA ^{38}Cl (37.2 m) at EoSB, 300:1 with ^{34m}Cl
- 5.1 ± 0.4 mCi/uA ^{41}Ar (1.83 h) at EoSB

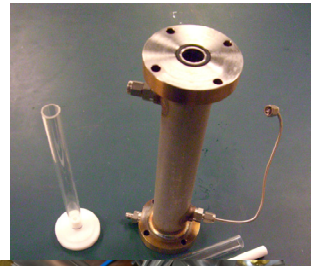

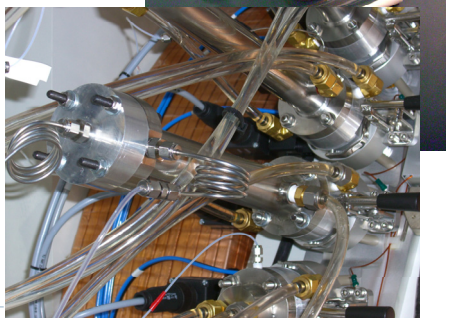

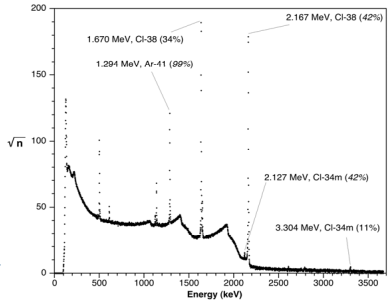

Cryotrapping ^{36}Ar Gas (99.993%)

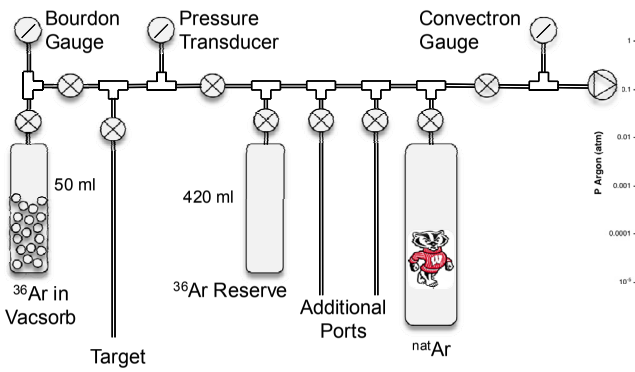

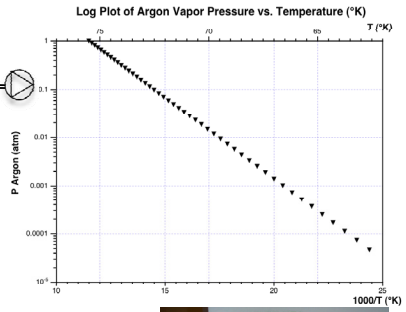

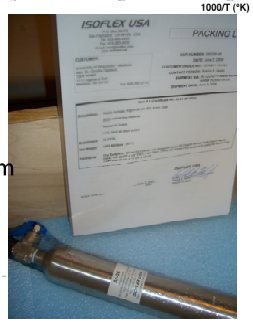

- Exploratory recovery tests using 60 psig in the target…
- Pressure in -196° C Cryotrap 5 min after opening valves… 0.3 atm
- Pressure after addition of Vacsorb … < 1 mm Hg
- Recovery: >99.5% in 10 min after EoB

A Second Target

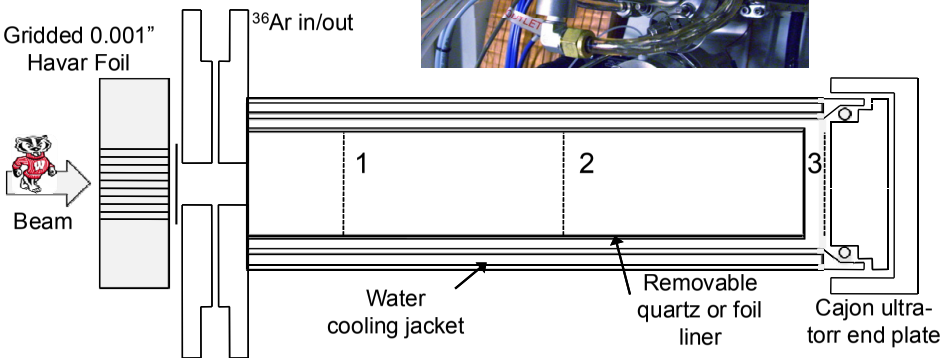

- Built to better accommodate the width of the PETtrace deuteron beam (~ 7 mm FWHM, tailing to 10 mm).
- Target volume increase by ~ factor of 2 (lower pressure)
- Figure shows end-of-range for deuteron beam at 120 psig (1), 60 psig (2), and 30 psig (3)

^{34m}Cl Yields with Quartz Liners and ^{36}Ar

- 18 irradiations from 5 to 20 uA at 68 ± 1 psig
- Target cryotrapped following irradiation, ^{17}F from ^{16}O(d,n) to decay
- Liner removed and again assayed with HPGE

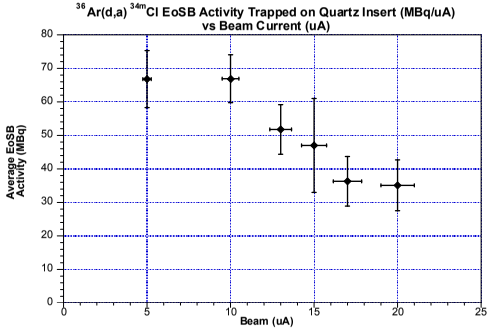

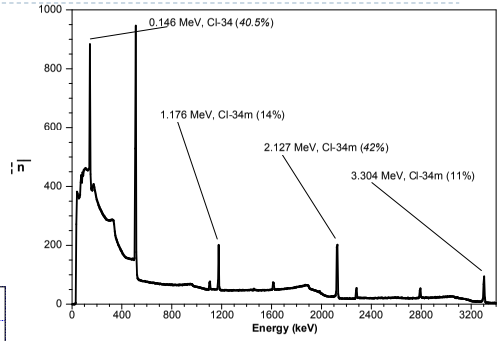

- ^{34m}Cl yields: 1.8 ± 0.2 mCi/uA at EoSB for 5 and 10 uA.
- Drop in yield at higher currents initially attributed to quartz trapping ability – try different liners.
- ^{38}Cl yields increase from initial target to 1.4 ± 0.2 mCi/uA at EoSB (not shown)

Stainless Steel / Phosphor Images

- Stainless and aluminum foils show consistent yields for pressures from 15 to 120 psig and beam currents from 1 to 40 uA.

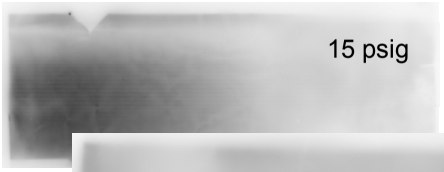

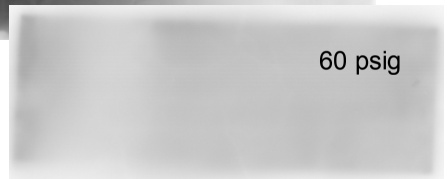

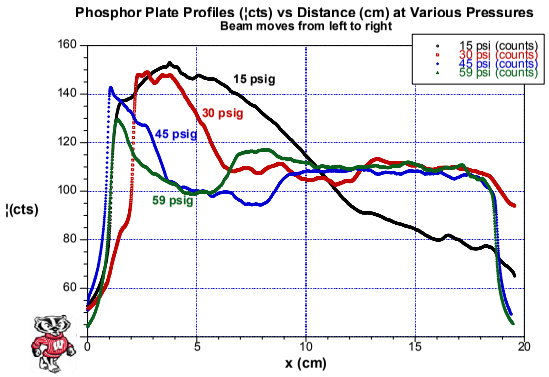

- Electronic energy deposition of beam heating the liner, causing Cl-38 to preferentially trap elsewhere.
- Foils also show activity on the "top" of the target tube, suggesting an upward convective flow of gas within the tube during irradiation.

[$^{38/34m}$Cl]MeCl: A test reaction

- Wash stainless foil with 40 ml water, load onto QMA prepped with 0.6 ml $KHCO_3$ and 5 ml water.
- Elute with 0.5 ml $K_{2,2,2}$, 1 ml MeCN
- Add 0.1 ml 1 N HCl (carrier) and 0.1 ml TEAOH, azeotropically distill with 2 x 1ml MeCN at 90° C
- Cool to < 80° C and add 1 ml MeCN and 0.1 ml MeI
- Flush product into syringes by bubbling low psi argon through sealed vessel. Analyze by GC.
- Poropak Q column (80/100, 6' x 0.125" x 0.085" SS), Shimadzu 8610B running 0.5 ml/min He at 110° C
- Decay Corrected Yield 82 ± 8% (max 9.4 mCi following a 30 min, 20 uA bombardment).

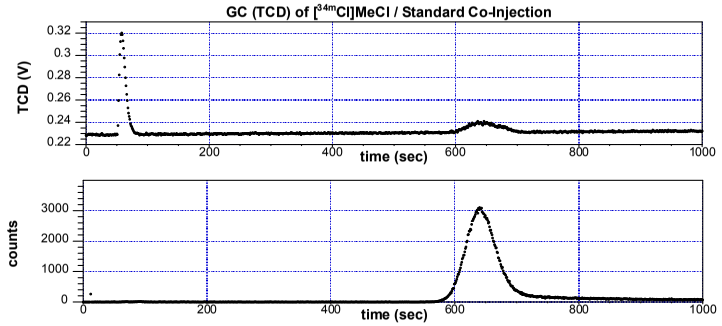

Future Directions

- Electrophilic or In-target chemistry to increase the utility of the cyclotron product immediately?
- Small animal imaging to probe the strength of the Cl-C bond?

Conclusions and Acknowledgements

- To our knowledge, this work is the first demonstration of the ^{36}Ar(d,alpha)^{34m}Cl with useful yields. Using these methods, more than 50 mCi ^{34m}Cl has been produced in radionuclidically clean form suitable for further chemistry.

- We gratefully acknowledge the support of NIH Grant NS054933 (OTD) and NIH Radiological Sciences Training Grant T32 CA009206 (TJH).

WTTC XIII – Presentation Discussions

1. Pros and Cons
   - No [^{34m}Cl]ArCl signs observed
   - Cl chemistry easier than F
   - High ^{24m}Cl positron energy
2. Challenge: cross sections measurement

OPTIMISATION OF AN ELECTROPLATING PROCESS TO PREPARE A SOLID TARGET FOR (p,n) BASED PRODUCTION OF COPPER-64

C. Jeffery[1,2], S. Chan[1], D. Cryer[1], A. Asad[1], RAPID Group[1]; R.I. Price[1,3]

[1]Medical Technology and Physics, Sir Charles Gairdner Hospital; [2]Chemistry & [3]Surgery, University of WA, Perth, Western Australia

Introduction

Research into the production of copper-64 from a nickel-64 solid target utilising a semi-automated solid target assembly coupled to an IBA 18/9 MeV proton cyclotron is ongoing. The target is prepared using an electroplating method adapted from McCarthy et al (1997), which uses a solution of nickel ammonium sulfate (adjusted to pH 9 with ammonium hydroxide) to plate nickel onto a gold substrate. While this method of production is sometimes very successful, it has also proved unreliable, producing poorly plated disks in approximately 50% of experiments. The irregularities observed in the nickel surface include - flaking, crazing, formation of spheres or pits, loose/powdery Ni, poorly adhered Ni, a lack of 'lustre' and a black deposit forming on the anode. An article from Kim et al (2009) described the black anode deposit, and suggested that ammonium hydroxide and/or ammonium sulfate added to counter residual acidity in the nickel ammonium sulphate solution was the cause. Kim et al suggested an electroplating method to resolve this issue. Further work was carried out to optimise our electroplating procedure, based on their method.

Aim

To develop a method that reliably and reproducibly generates a solid target for copper-64 production by electroplating nickel-64 onto gold; and to optimise the electroplating conditions to enable maximum nickel deposition for minimal time and use of nickel-64.

Method

Preparation of purified $NiSO_4$ [adapted from Kim et al (2009)]

Nickel metal is dissolved in nitric acid and evaporated to dryness. The solid is treated with sulfuric acid and dried to a yellow solid. The residue is dissolved in milliQ water and recrystallised by adding acetone. The solid is collected by vacuum filtration, and dried over vacuum for two hours, followed by drying in an oven at 120°C for a minimum of two hours. The resulting yellow-green solid is $NiSO_4$.

Preparation of electroplating solution

Purified $NiSO_4$ (0.13770g to 0.30079g) was dissolved in milliQ water (5mL, 10mL, or 15mL). Ammonium sulfate (~0.06g) was also dissolved into the solution.

Electroplating experimental conditions

Anode: initially carbon rod (rotating), then platinum rod (non-rotating)
Cathode: initially 2mm x 20mm gold disk, then 125µm x 15mm gold foil
Solution: initially nickel ammonium sulfate, pH 9, with ammonium sulfate buffer, Ni concentration ~3mg/mL (McCarthy et al, 1997); then nickel sulfate, pH 4.5, with ammonium sulfate buffer, Ni concentration ~5mg/mL (Kim et al, 2009)
Plating area: 10mm diameter, 78mm^2
Current: Constant 6mA
Time: 12 hours (10 experiments, varying masses of $NiSO_4$), plus 6 experiments with time varied from 12-96 hours (constant mass of $NiSO_4$)

Results

16 experiments were conducted with nickel sulfate - 14 considered were successful.

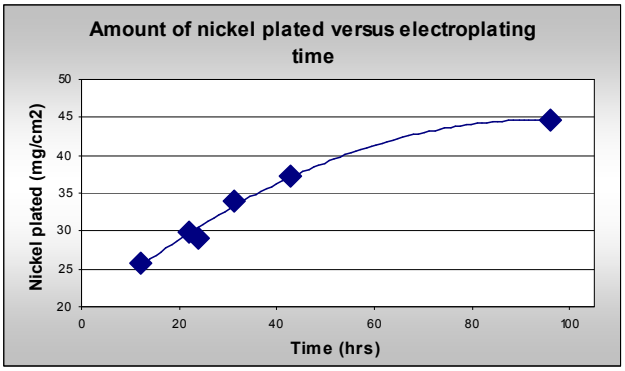

Figure 1: Mass of nickel plated versus electroplating time (constant concentration of nickel in solution, 150mg $NiSO_4$ in 10mL)

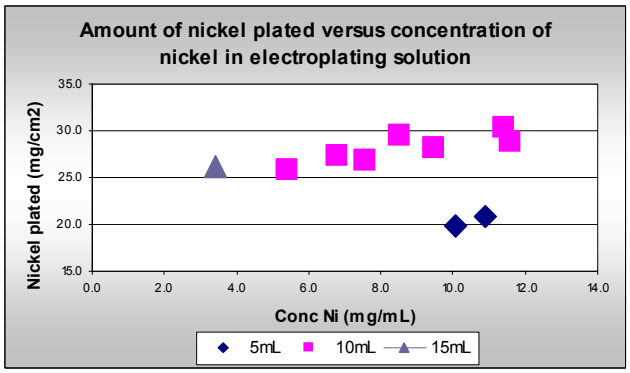

Figure 2: Mass of nickel plated versus concentration of nickel in electroplating solution (for constant electroplating time, 12 hours)

Discussion and Conclusion

Fourteen of the 16 $NiSO_4$ experiments resulted in a lustrous, well-adhered layer of nickel, with no black residue on the platinum anode. The two failures were the result of variation in the constant current applied to the cell, and a change in the volume of water (increased to 15mL). Some divots have been observed in the nickel surface, indicating that bubbles have adhered to the surface during plating, but they are small and not considered a defect. The electroplating solution is stable over time (ie. no precipitate formed), and it is easy to prepare. The average yield of nickel plated using $NiSO_4$ is much lower than that achieved with $Ni(NH_4)_2.2SO_4$ (37-63%, versus ~70-95%), which is a disadvantage.

Effect of time (constant $NiSO_4$ concentration): Figure 1 shows the amount of nickel plated plateaus rapidly. Doubling the time (12 to 24 hours) results in a 1.1x increase in Ni plated, while quadrupling the time (12 to 96 hours) only results in 1.7x more nickel plated. Run times less than 24 hours are therefore most efficient.

Effect of varying $NiSO_4$ concentration (constant time): Figure 2 shows a low yield was achieved using a volume of 5mL. One experiment using 15mL of water resulted in a poor nickel surface despite a reasonable amount of nickel plated. The best yield with minimal amount of nickel in solution was achieved with a 10mL solution of 8.5mg/mL of nickel.

Overall, we are satisfied with the reliability and reproducilbility of our method.

References

Kim, J.Y., Park, H., Lee, J.C., Kim, K.M., Lee, K.C., Ha, H.J., Choi, T.H., An, G.I., Cheon, G.J., A simple Cu-64 production and its application of Cu-64 ASTM. Applied Radiation and Isotopes (2009), vol. 67, pp1190-1194

McCarthy, D.W., Shefer, R.E., Klinkowstein, R.E., Bass, L.A., Margeneau, W.H., Cutler, C.S., Anderson, C.J., Welch, M.J., Efficient Production of High Specific Activity 64Cu Using A Biomedical Cyclotron. Nuclear Medicine & Biology (1997), vol. 24, pp 35-43

Streamlined measurement of the specific radioactivity of in target produced [^{11}C]methane by on-line conversion to [11C]hydrogen cyanide.

1) Jacek Koziorowski and 2) Nic Gillings

1) Herlev Hospital Copenhagen University, Denmark, 2) Copenhagen University Hospital, Rigshospitalet

Abstract

A simple method for the direct measurement of in-target produced [^{11}C]methane specific radioactivity is described. The method is also suitable for the production of [^{11}C]cyanide for radiosynthesis. Specific activities up to 13 000 GBq/µmol are reported.

Introduction

For monitoring and optimization of the specific radioactivity of in-target produced [^{11}C]methane it is desirable to have a simple method for measurement of the mass of carbon without having to performed a complete radiosynthesis. Quantification of [^{11}C]methane using gas chromatography (GC) is rather cumbersome and if using a flame ionisation detector (FID) it is necessary to wait until the activity has decayed before performing the measurement. Such a delay gives rise to the possibility of losses of methane, thus leading to an over-estimation of the specific activity. Furthermore, a reliable measurement of such small masses of methane is challenging.

[^{11}C]hydrogen cyanide can be easily produced on-line from [^{11}C]cyanide by passing over platinum at 1000 °C in the presence of ammonia. Since ammonia is produced in situ during irradiation of the [^{11}C]methane target by the radiolysis of nitrogen in the presence of hydrogen, this further simplifies the procedure. Cyanide can be quantified down to ppb levels by HPLC using an electrochemical detector (1) or by the use of colorimetric methods.

Experimental

Target

The target consists of a water cooled, quartz lined aluminium body (length 250 mm, i.d. 19.8 mm) (2). The target volume is 75 mL.

Irradiations

Irradiations were performed using the Scanditronix MC-32 cyclotron at Copenhagen University Hospital, Rigshospitalet. H- ions were accelerated to 17.2 MeV, giving an target entrance energy of ca. 16 MeV. The target gas consisted of ultra pure gases of 10% hydrogen in nitrogen (AGA, Sweden, grade 6.0 [>99.99995%]) . The target fill pressure was 26 bar giving a gas volume of 2L at NTP.

Analysis

Following irradiations, the gases were released from the target by simply opening a valve and transferred to a hotcell. A mass-flow controller was set at 100mL/min and the gasses were passed over 3.37g of platinum wire (20m L x 0.1mm Ø) in a 6mm ID quartz tube at 1000°C. The produced [^{11}C]cyanide was trapped in a 20mL vial containing 20mL of pure water. After the vial an Ascarite trap (for measuring cyanide trapping efficiency) and a gas collection bag (to prevent the escape of radioactive gasses) was attached. After decay the amount of cyanide was measured using the pyridine-barbituric acid colorimetric test (Koenig reaction, EPA method 335.4-1) (3,4).

Results

Not optimized conversion from [^{11}C]methane to [^{11}C]cyanide were 50%. Trapping was quantitative (no radioactivity was found in the Ascarite trap) and 20GBq (n=4) of activity was trapped and the concentration of cyanide in the solution was below the detection limit (2µg/L = 77nM/L). This corresponds to a specific activity of >13 000 GBq/mol (EOB). For radiosynthesis the residual ammonia is easily removed by a trap filled with Dowex 50W (200-400 mesh) followed by Sicapent (to dry / remove water), for multi-runs, or a smoke tube (Draeger air current tube; silica impregnated with fuming sulfuric acid) for a single run.

Outlook

Experiments to increase the conversion and minimize the trapping volume are planned.

References

1)) Direct determination of free cyanide in drinking water by ion chromatography with pulsed amperometric detection *T*.T. Christison, J.S. Rohrer, *J. Chromatogr. A 1155, 2007, 31–39.*

2) A flexible [^{11}C]methane target,Jacek Koziorowski, Peter Larsen, Holger Jensen and Nic Gillings, *Proceedings of the 12th International Workshop on Targetry and Target Chemistry*, July 21-24, 2008Seattle, Washington

3) Stable reagents for the colorimetric determination of cyanide by modified König reactions, Jack L. Lambert, Jothi Ramasamy and Joseph V. Paukstells, *Analytical Chemistry*, Vol. 47, No. 6, 1975, pp916-8.

4) Method 335.4, Determination of total cyanide by semi-automated colorimetry, Rev.1.0 ,James W. O'Dell (Ed.) Inorganic Chemistry Branch, Chemistry Research Division, August 1993

Streamlined Measurement of Specific Radioactivity of in Target Produced [^{11}C]Methane by On-line Conversion to [^{11}C]Hydrogen Cyanide

Nic Gillings & Jacek Koziorowski

Why Measure Specific Activity?

- High affinity neuroreceptor ligands labelled with carbon-11 require high SA in order to avoid occupancy of binding sites with the cold ligand.
- Less than 5% occupancy is normally used as a cut-off for *tracer* studies.

Neuroreceptor Ligand Binding

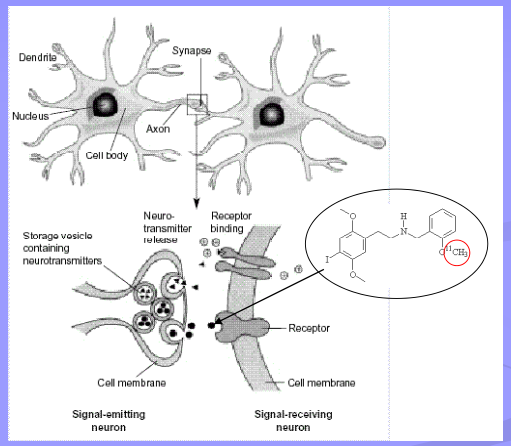

Non-radioactive compound will compete for active binding sites

Specific Activity of [^{11}C]Methane

- Theoretical maximum: 341 TBq/μmol
- Maximum we have measured: 9 TBq/μmol (EOB)
- ^{12}C/^{11}C ratio: 38:1
- Mass of methane: 0.143 μg (based on 50 GBq)

Measurement of Specific Activity

- Direct quantification of methane in target gas at end of bombardment using gas chromatogrphy with FID (Steel et al. 8th WTTC, 1999) or Pulsed Discharge Detector
- Conversion to [^{11}C]methyl iodide and quantification with HPLC
- Conversion to a [^{11}C]-labelled compound and quantification with HPLC

Specific Activity

Specific activity at end of bombardment (EOB) based on measurement of [^{11}C]-labelled tracers using HPLC with UV detection.

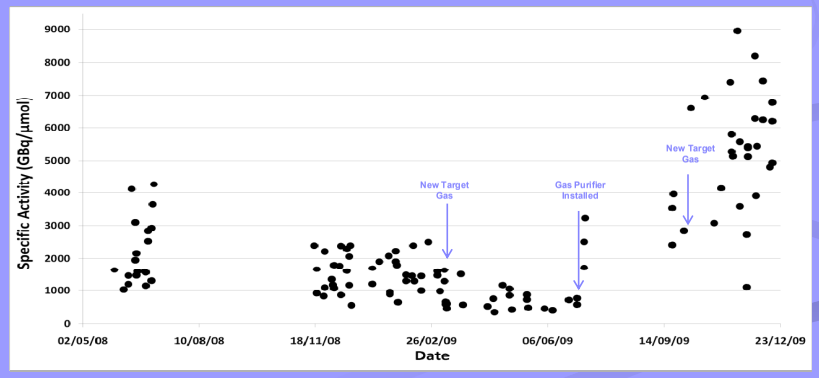

Figure from: Koziorowski J, Larsen P, Gillings N. A quartz-lined carbon-11 target: striving for increased yield and specific activity, *Nucl Med Biol 2010, accepted manuscript*

Measurement of Specific Activity

- Aim: A simple method to determine SA of target gas without the need to perform a full radiosynthesis.
- Solution: On-line conversion to [^{11}C]CN
- Quantification of cyanide: Colorimetric methods or HPLC with fluorometric or electrochemical detection
- Sensitivity:

  Cyanide Test Kit - 2 µg/L
  HPLC (fluorometric) – LOD: 0.05 µg/L
  HPLC (electrochemical) – LOD: 0.27 µg/L

Experimental Set-up

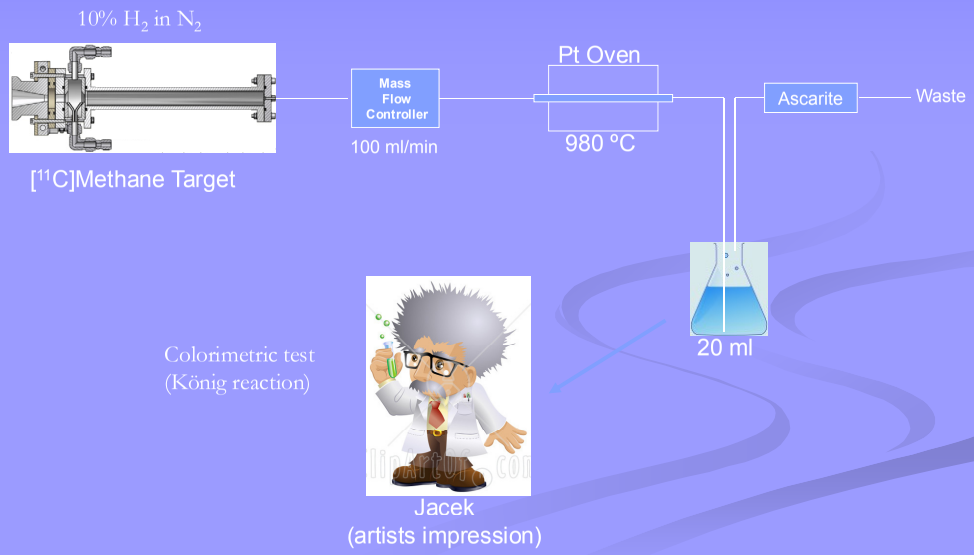

Preliminary Results

- Irradiation 20 μA for 20 min (n=4)
- [^{11}C]CN yield: 20 GBq (EOB) in 20 ml water (ca. 50% conversion, quantitative trapping)
- Cyanide concentration: <2 μg/L (<0.04 μg total)
- Specific Activity: >13000 GBq/μmol

Conclusions

- On-line conversion to cyanide is a simple and convenient method for determination of specific activity
- Specific activity of target gas appears to be very high (>13000 GBq/μmol)
- More sensitive methods for analysis of cyanide are required to truly quantify SA of target gas

Perspectives

- Trapping [^{11}C]cyanide in a smaller volume can be achieved by trapping first in a cryotrap then transferring to a small vial with a low helium flow
- A more quantitative estimation of specific activity may then be possible
- Repeat experiments to test the effect of different target paramters (e.g. beam current) on specific activity may be possible with this method

WTTC XIII – Presentation Discussions

1. Production of oxides
   - Important factor affecting conversion rate
   - Go through the system to avoid it
2. UV vs visual inspection?
   - Results always bellow detection limit

Recent advances and developments in IBA cyclotrons

Jean-Michel Geets, Benoit Nactergal, Michel Abs, Claudy Fostier, Eric Kral

IBA Molecular, IBA Technology group, www.iba-group.com

Various development and enhancement to the existing IBA cyclotron range were accomplished last year including the launch of new cyclotrons and the revival of the oxygen machine.

To reply to the strong demand of F-18 radiopharmaceuticals in PET nuclear medicine, IBA has achieved a development program on the Cyclone® 18/9 PET cyclotron with the aim of increasing beam current and reliability. The strippers were replaced by a 'drop-in-place' designed to ease the maintenance. The uncritical internal ion source system was doubled so as to provide redundancy and lower maintenance schedule in the Cyclone® 18 TWIN with two proton sources. Since almost all of the PET tracers are today produced by protons, the same concepts were reused to develop the Cyclone 11 TWIN compact self-shielded machine for hospital-scale production of PET tracers.

The well-know Oxygen generator, a positive deuteron machine known as Cyclone® 3d, is under redesign for installation in Japan in early 2011. The aim is to provide a continuous flow of $^{15}O_2$ without disrupting the PET production schedule of the main hospital cyclotron. The production is carried out on natural nitrogen as target with 3.6 MeV deuteron.

In the high energy range, following the Cyclone® 70 XP multiparticules machine installation in Nantes (France), a small brother was designed in the 30 MeV proton-alpha range, the Cyclone® 30 XP for Jülich (Germany). While proton (15-30 MeV) and deuteron (8-15 MeV) are produced and extracted in the well-known negative ion mode with stripping extraction in the Cyclone® 30, the positive alpha beam (nucleus of helium atom He^{+}) is accelerated and extracted in positive ion mode using an electrostatic deflector. The He^{2+} acceleration needs specific external source and adjustments to the cyclotron magnetic field and acceleration frequency (RF). The energy of the alpha beam will be fixed in the 29-30 MeV range to maximize At-211 production. Redesign of the magnet system was needed in order to leave free space for the alpha deflector and to reuse magnetic 'flaps' for field correction as it is done on the IBA-Cyclone® 18/9. Some technical challenges were solved to fit the two RF acceleration modes in the same machine with external ion sources platform for the different ions species. The innovative new RF design was patented by IBA.

The well-know Cyclone® 30 used by most of the SPECT producers worldwide was upgraded to higher current mainly to deal with the Tl-201 needs. A new external powerful H^{-} ion source was used, a redesigned injection line and central region was installed onto a standard 30 MeV cyclotron. The acceleration power (RF) was upgraded to 100 kW using the IBA in-house expertise giving the power extra supply for acceleration of 2mA of proton beam. Auxiliaries systems were upgraded (extraction, collimators,..) to handle the new beam power. Consequently, the high power solid target system is proposed with an optimized full process (plating, separation and recovery of isotope).

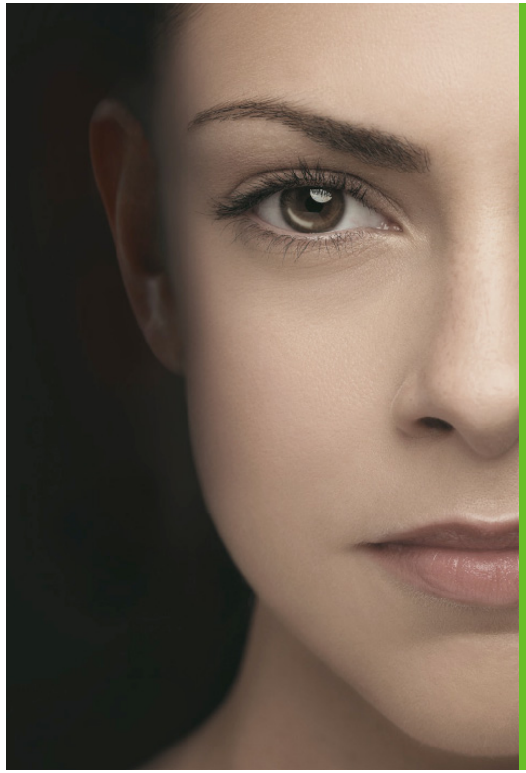

WTTC #13
Risoe, Dk

Recent advance and development in IBA cyclotrons

Geets Jean-Michel

WTTCXIII

The Oxygen generator

- **Revival of the Cyclone® 3D**
  - 3.6 MeV D+ beam , ESD extraction
  - One gaz target
    - 14N(d,n)15O
- **Improvements from the old design (ref. Turku)**
- **4 machines sold – > discontinued in 90's**

^{15}O generator : Main specifications

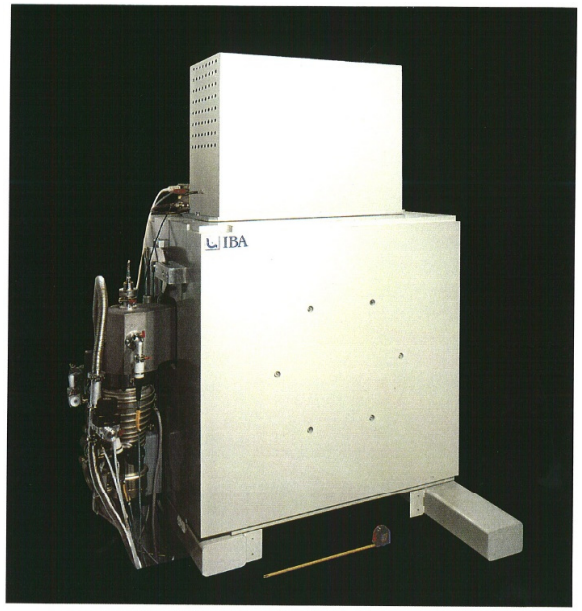

Specifications

Ions	Deuterons
Energy	3,6 MeV
Beam Current	50 µA
Power Consumption	35 kW
Weight	6 tons

Redesign of the main systems

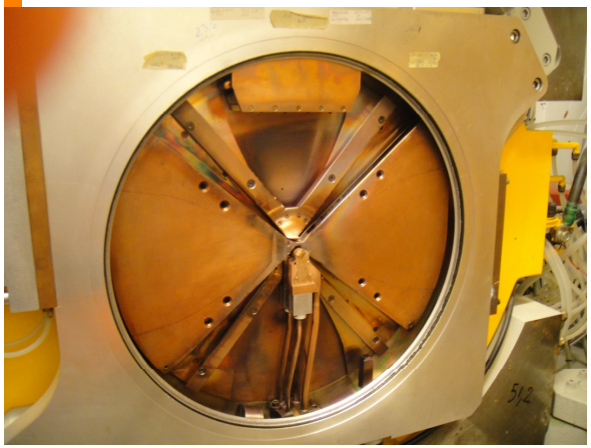

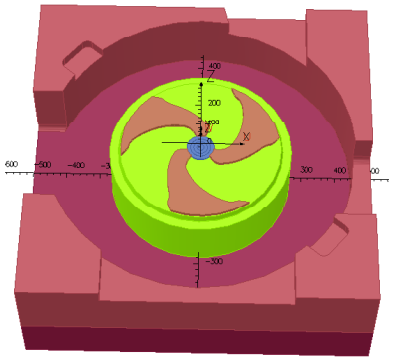

Machine with vertical plane, self resonating RF on top, no valleys

Cyclone® 18 – model 2010

- **Redundancy**
  - 8 targets with 8 extractors (x 2 foils)
  - TWIN proton sources system
- **I.S. Extended lifetime**
- **Maintenance**
  - Drop-in-place strippers

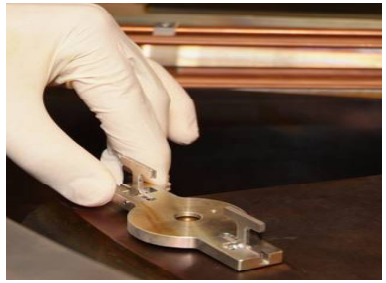

Central region redesign, TWIN sources

Introduction of the Cyclone® 11

- **The self-shielded « little brother »**
- **11.5 MeV proton TWIN source**
  - 8 targets, 8 extractors (x 2 foils)
  - Using Cyclone 18 components & parts

Zephiros® control system for PET cyclotrons

- **More automation**
  - Full automatic production mode
  - Self-tests ; before batch & after maintenance
- **More feedback and datalogging**
- **Extended Remote diagnostics**

Main page – overview cyclotron-targets (manual)

Main page overview – automatic recipe followup

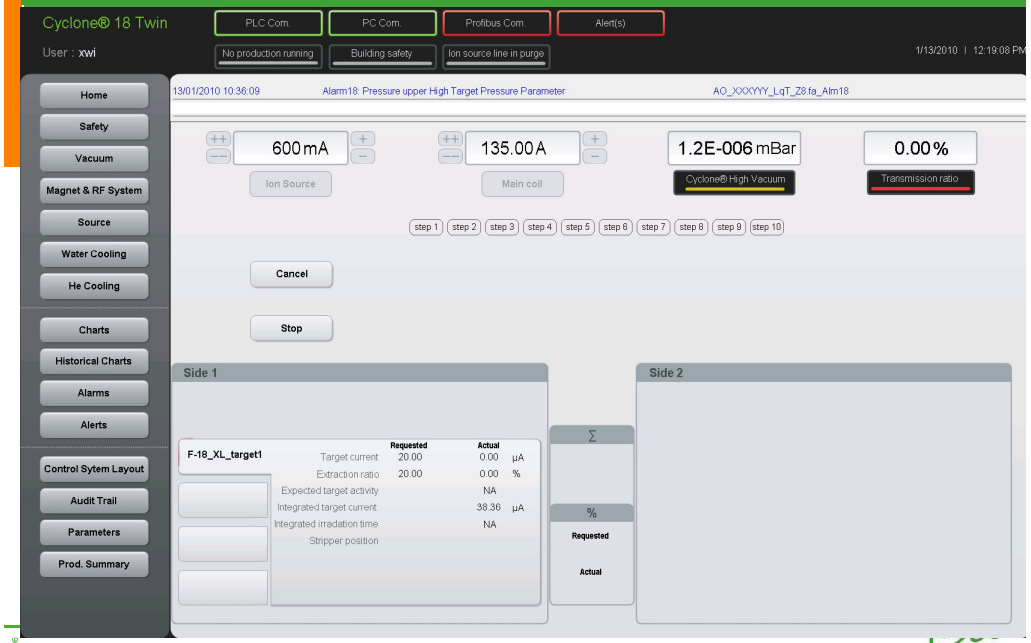

Target parameters + auto test (post maintenance)

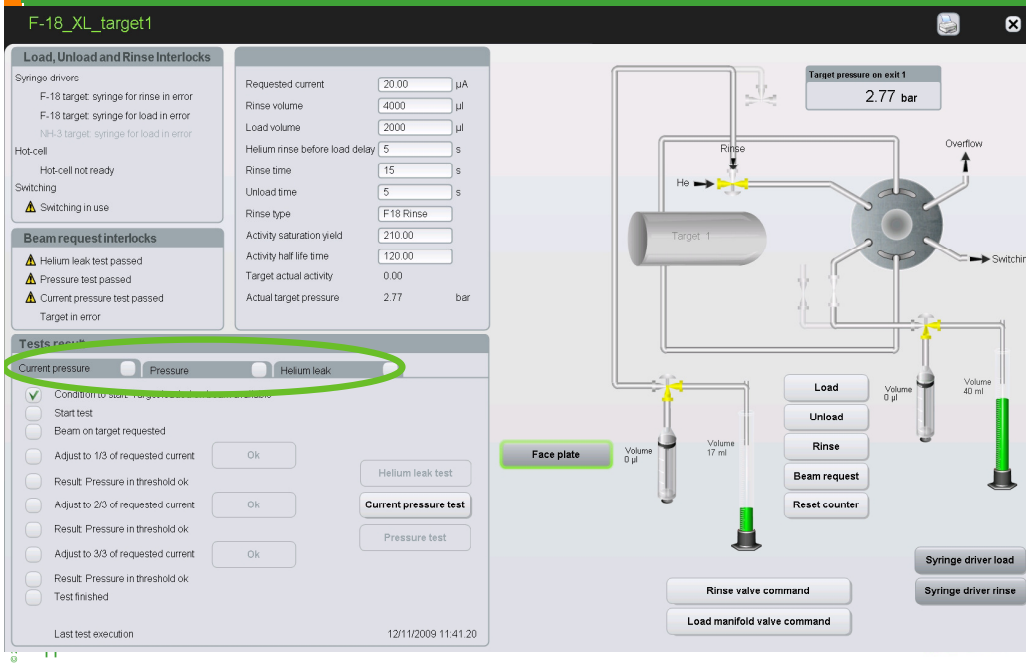

Cyclone® 70 in Arronax, Nantes

- Operating at specs
- We learned a lot of interesting things above the 30 MeV

Particule	Energy	Current
Proton	30- 70 MeV (stripper)	400 µA
Deuteron	15- 35 MeV (stripper)	50 µA
Alpha	70 MeV (ESD)	70 µAe
HH+	35 MeV (ESD)	50 µA

What's inside the vaults

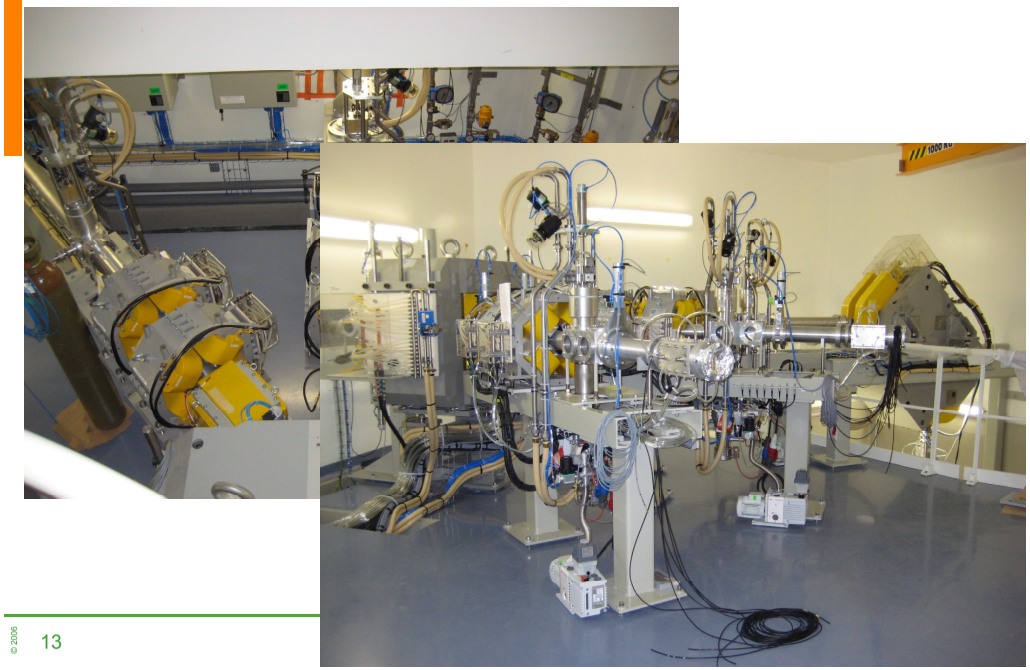

30 MeV alpha beam on the Cyclone® 30 XP

- Multiparticule machine for research & ^{211}At production

Particule	Energy	Current	Beam port
Proton	15- 30 MeV (stripper)	400 µA (700µA)	Dual
Deuteron	8- 15 MeV (stripper)	50 µA	Dual
Alpha	30 MeV (ESD)	50 µAe	Single

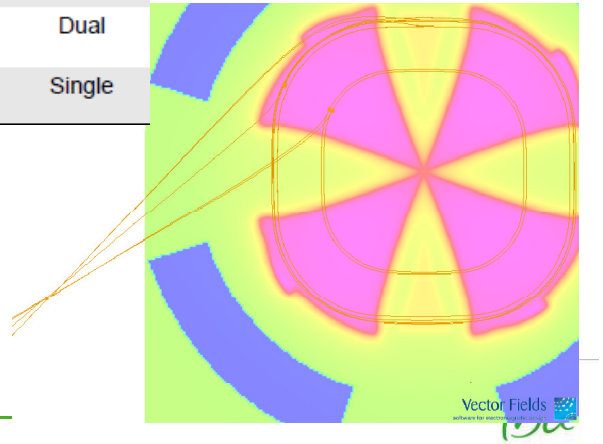

Design of Cyclone 30 XP

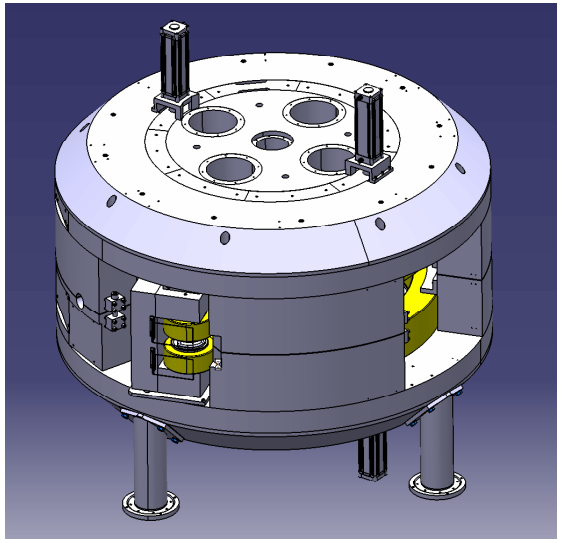

- Use standard magnet with modifications
- New internal switching
- New main coils
- Opening in median plane
- Flaps for field adjustment
- bi-frequency RF system

w/o moving contacts

Deep Valley with flaps and pole extensions

The high current Cyclone® 30

- **Finally the 1.5 mA proton beam – 30 MeV machine**
  - Powerfull external ion source
  - Optimisation of central region inflector
  - Higher RF power for 2mA beam

External source + injection line

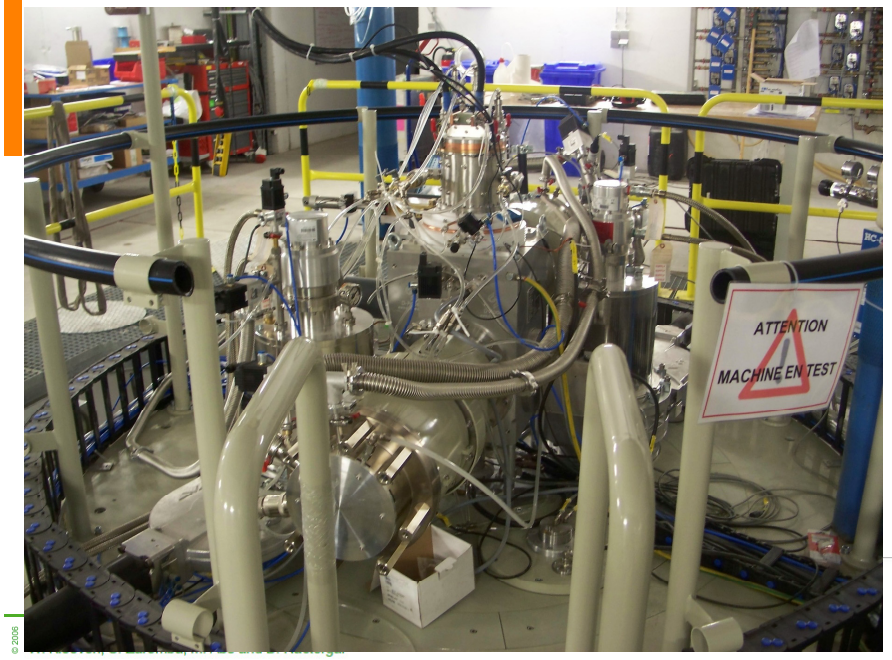

OUH Odense Universitetshospital

Risø DTU
National Laboratory for Sustainable Energy

Production of therapeutic quantities of ^{64}Cu and ^{119}Sb for radionuclide therapy using a small PET cyclotron

H. Thisgaard[a], M. Jensen[b], D. R. Elema[b]

[a] Odense PET Centre, Dept. of Nuclear Medicine, Odense University Hospital, Sdr. Boulevard 29, DK-5000 Odense C, Denmark.

[b] The Hevesy Laboratory, Radiation Research Department, Risoe National Laboratory for Sustainable Energy, Technical University of Denmark, P.O. 49, DK-4000 Roskilde, Denmark.

Introduction

In the recent years the use of radionuclides in targeted cancer therapy has increased. In this study we have developed a high-current solid target system and demonstrated that by the use of a typical low-energy medical cyclotron, it is possible to produce tens of GBq's of many unconventional radionuclides relevant for cancer therapy such as ^{64}Cu and ^{119}Sb locally at the hospitals.

Materials and methods

The irradiations were performed using a slightly modified GE PETtrace cyclotron equipped with a beam line. The PETtrace is originally specified to deliver > 75 µA 16.5 MeV protons or > 60 µA 8.4 MeV deuterons on target but has been shown to be capable of accelerating > 200 µA protons by careful adjustment of the central region and with much attention to vacuum conditions.

The target consists of a 2 mm thick silver plate with 8 cooling fins (height 2 mm, width 1 mm) which is mounted on top of an aluminium base with a stainless steel mounting ring (see figures). The back side of the silver plate is cooled by water flow through the rectangular channels between the cooling fins (1 mm × 2 mm) with a water flow rate of 14 l/min and a water inlet temperature of ~3°C.

Two different target materials were used for the irradiations. Either enriched ^{64}Ni for the direct production of ^{64}Cu via the

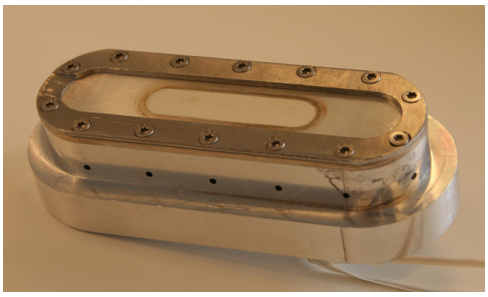

Target body with electroplated Sn

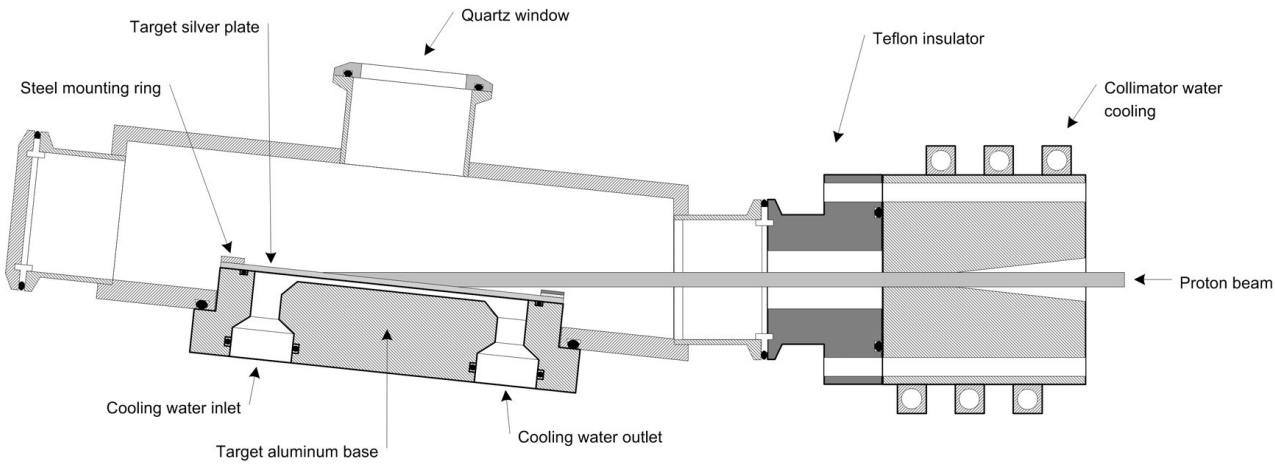

Schematic drawing of the 6° grazing incidence target design with irradiation chamber and Ø5 mm circular collimator (right). For illustration purposes the Ø5 mm collimated proton beam is shown.

^{64}Ni(p,n)^{64}Cu reaction or ^{nat}Sn to demonstrate the capability of producing high amounts of the Auger-electron-emitter ^{119}Sb via the ^{119}Sn(p,n)^{119}Sb reaction. The electroplating of the ^{64}Ni targets were done using a ^{64}Ni ammonium sulphate plating solution and the ^{nat}Sn targets were made according to our newly developed method (Thisgaard and Jensen, Appl. Rad. Isot. 67, 2009) with a hot ^{nat}Sn potassium hydroxide solution.

The targets were irradiated several times with the 16 MeV proton beam collimated to Ø5 mm. Both target materials were initially irradiated with a net target current of 180 µA with a collimator spill between 10–15%, i.e. with approximately 200–210 µA beam current before the Ø5 mm collimator to test the thermal performance of the targets. After the irradiations the targets were stored for a few days to let the produced activity decay and then inspected with a microscope and weighted. For production yield measurements, the targets were irradiated several times with peak target currents of 150 µA, again with a collimator spill between 10–15%, with irradiation times up to 76 minutes.

The temperature profile and the thermal induced stress (data not shown) in the silver plate were modelled using Comsol Multiphysics 3.3. The code uses a finite-element analysis (FEA) of the silver plate with 24096 mesh elements.

Results

The target was capable of withstanding the 180 µA Ø5 mm proton beam with both target materials tested. No sign of melting was seen on the target surfaces and no losses of target material were found from weighing the targets after EOB. This means that the surface temperature had not been above 231.93 °C during the Sn irradiations (the melting point of Sn) and probably not during the Ni irradiations either due to the higher thermal conductivity of Ni – in good agreement with the modelled results (see figure below).

From the 150 µA peak current irradiations the produced ^{64}Cu activity was measured to be 8.2 ± 0.7 GBq at EOB for the 76 min. irradiation (mean current of 121 µA), corresponding to 54 ± 5 MBq/µAh using 98% enriched ^{64}Ni with a plated target thickness of 8.5 mg/cm^2. This corresponds to the proton energy interval of 16.0 → 14.3 MeV, i.e. well above the maximum cross section of the excitation function for the ^{64}Ni(p,n)^{64}Cu reaction at approximately 11 MeV.

By increasing the plated target thickness to e.g. 30 mg/cm^2 of enriched ^{119}Sn or ^{64}Ni (resulting in a surface temperature increase of less than ~25 °C) , it will be possible to produce ~46 GBq of ^{119}Sb or ~174 GBq of ^{64}Cu, respectively, in 3 hours using 150 µA target current as above. In both examples, the total amount of enriched target material required to obtain the 30 mg/cm^2 thickness will be less than 60 mg due to the extremely focused proton beam (Ø5 mm), thus keeping the specific activity high and the metal impurities low.

Conclusion

In the current study we have developed a high current solid target system and shown that by the use of a typical low-energy, medical cyclotron, it is possible to produce tens of GBq's of unconventional therapeutic radionuclides locally at the hospitals.

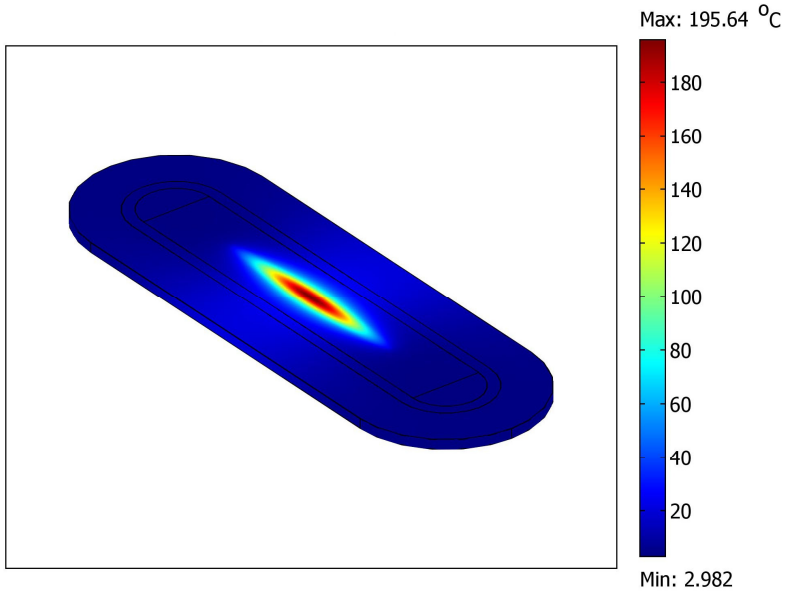

The calculated temperature profile on the target face for a 203 µA beam corresponding to 180 µA on the target.

Production of therapeutic quantities of 64Cu and 119Sb for radionuclide therapy using a small PET cyclotron

Presentation for WTTC 13

Helge Thisgaard , Mikael Jensen
and Dennis Ringkjøbing Elema
Hevesy Laboratory,
Risoe National Laboratory and
Odense Universitetshospital

Region Syddanmark
Risø DTU
National Laboratory for Sustainable Energy

Matching the beam to the target:
Targets for isotope production

With compound nuclear reactions (dominated by one exit channel)
When $T_{\frac{1}{2}} \approx T$ irradiation:

1 kBq ≈ 1 pA
1 MBq ≈ 1 nA
1 GBq ≈ 1 μA
1 TBq ≈ 1 mA

If (p,n) is available, it gives:
smallest target (High SA, low volume chemistry)
highest power efficiency (Ci/kwh)

The nuclear "battery" in our vials

16 MeV 50 μA delivers 800 Watts of kinetic energy to the target

-only a small fraction is stored as nuclear energy

Energy efficiency of a cyclotron : 800W/ 80kW = 1%
Energy efficiency of target: (200 GBq*1.5 MeV)/800W=0,006%
Overall energy efficiency 0,00006%

The rest goes into heat.

"A beamline for the PETtrace cyclotron"

Why ? Isotope production !

1) **Solid targets with HIGH CURRENTS and "optimal" beam spot**
2) **Get the "long lived" stuff away from the cyclotron**
3) **Neutron production (for (n,p) and (n,gamma) reactions)**

GE Pettrace with beam line

3 m driftspace

2 Q pole pairs
Vertical stering

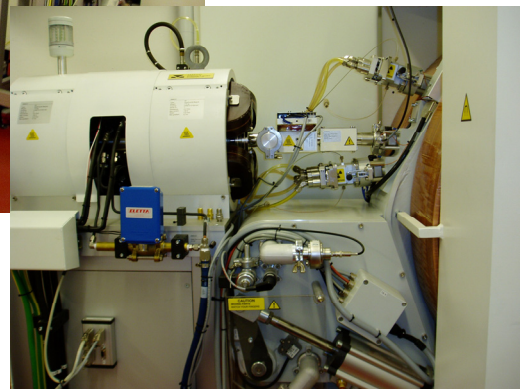

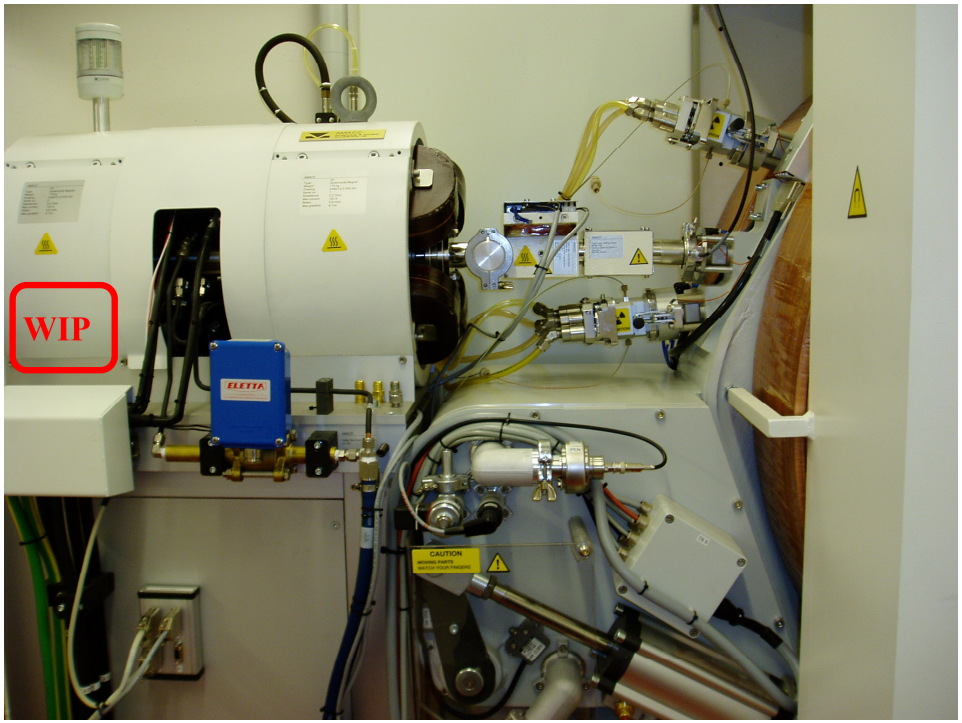

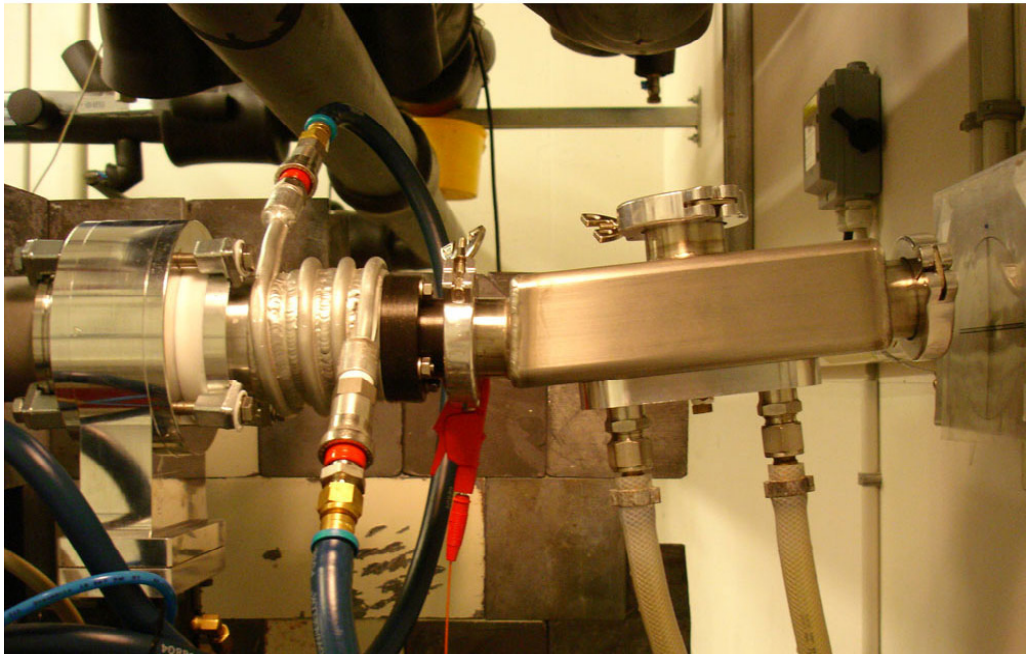

6 degrees grazing incidence of a Ø 10 or Ø 5 mm beam

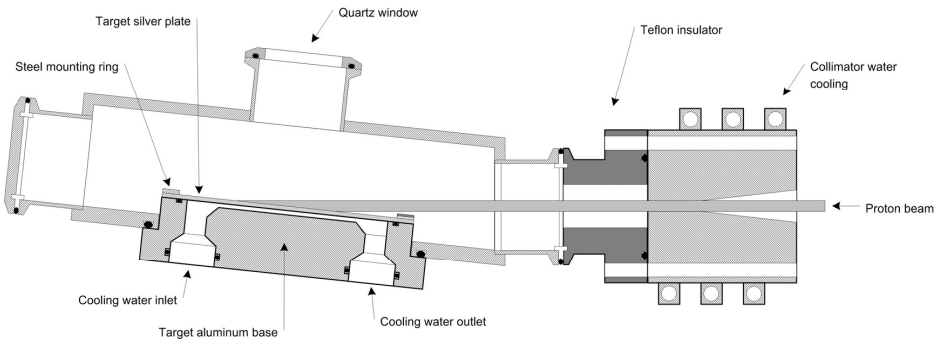

Target base is Silver 2 mm thick , with fins
Water flow is 14 liters / minute , 6 deg. C inlet

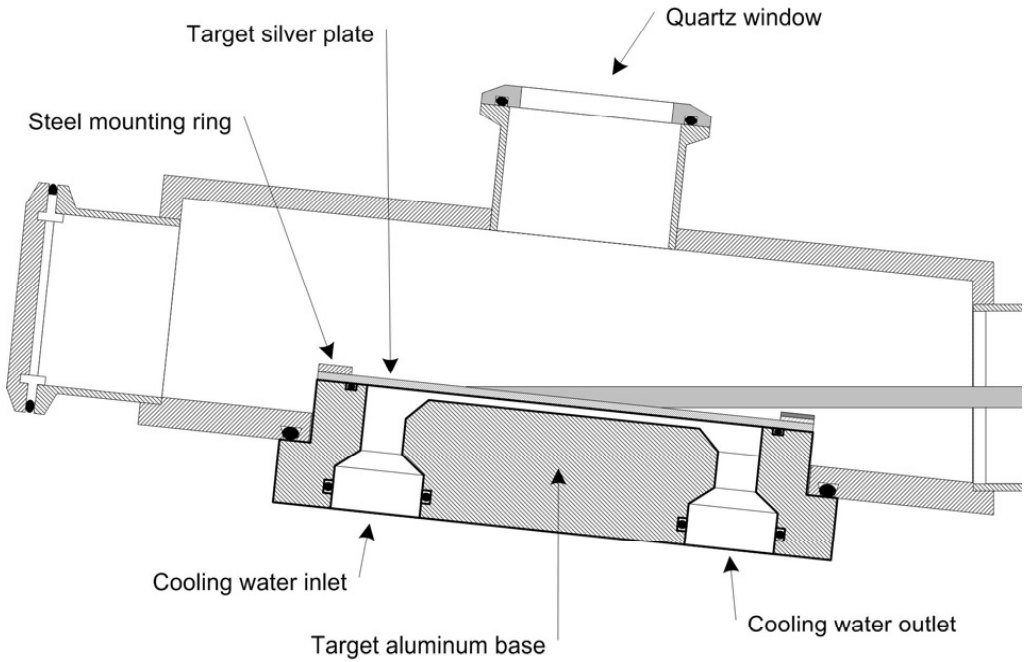

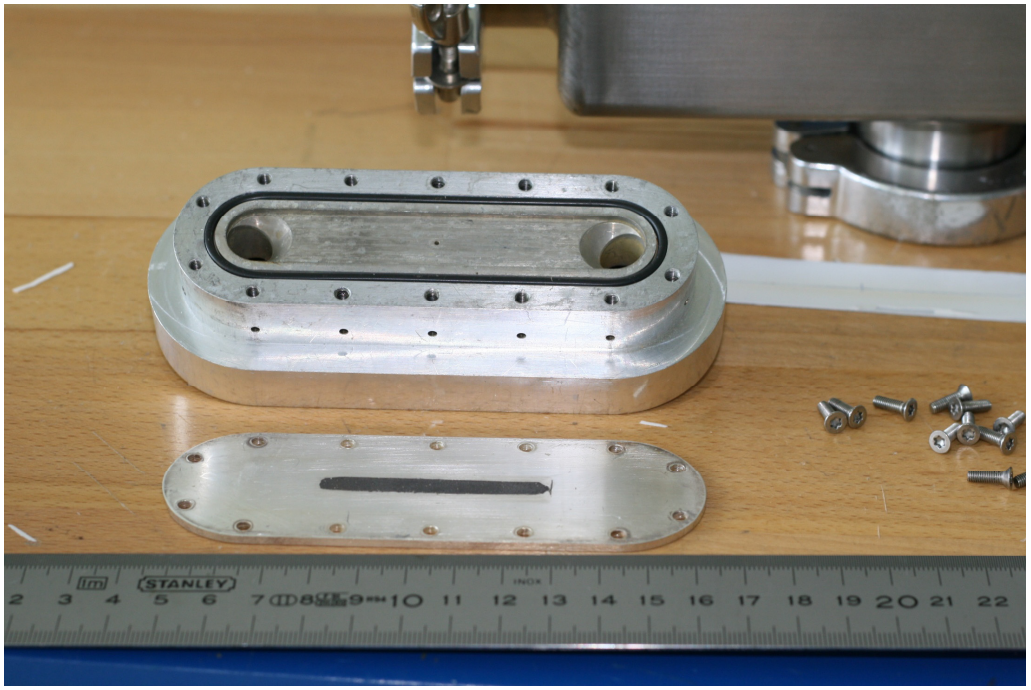

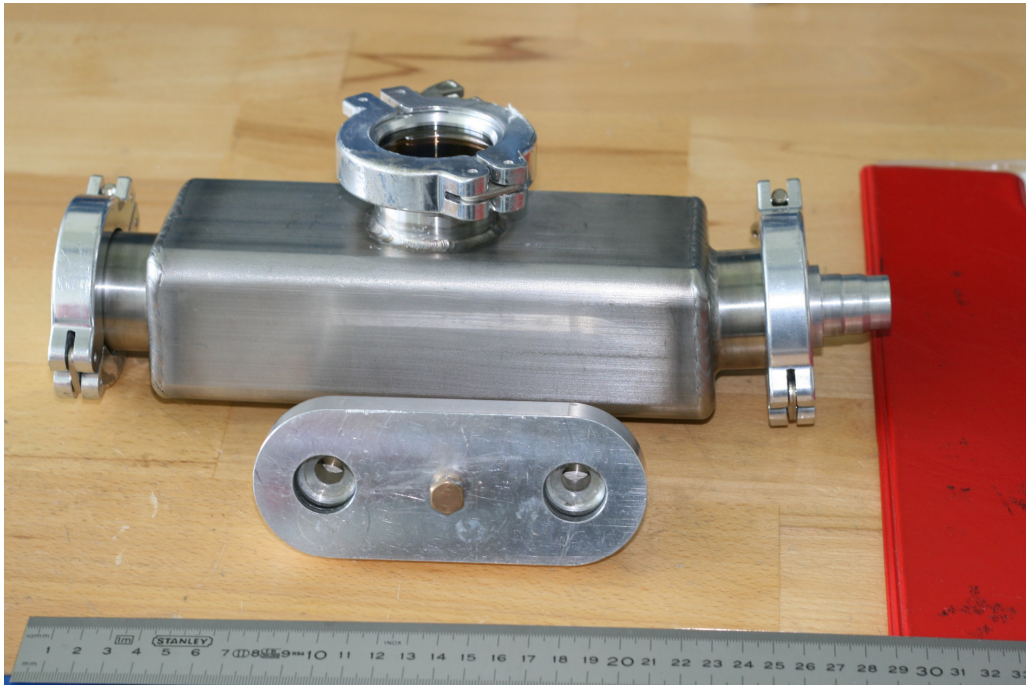

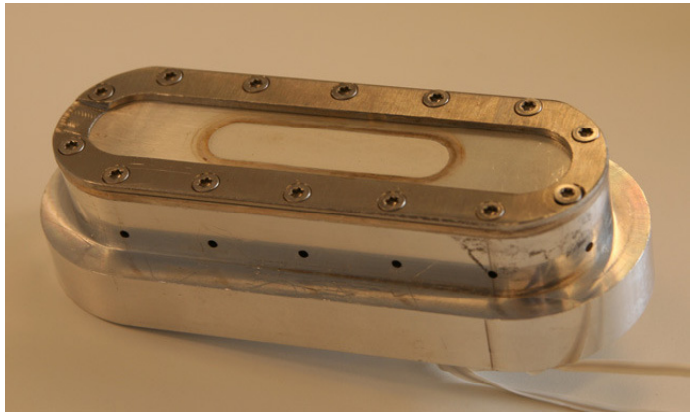

Target with electroplated Tin,- survives 200 uA

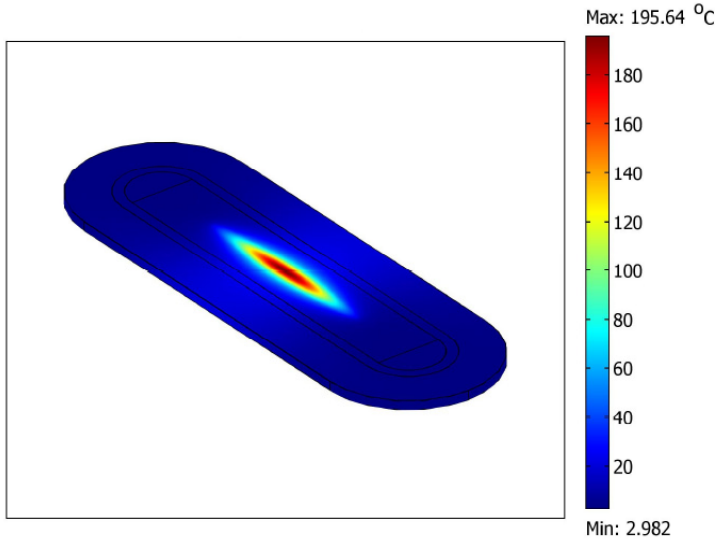

The calculated temperature profile on the target face for a 203 μA beam corresponding to 180 μA on the target.

At present we are hitting the target with 16.5 MeV

That is to High ! We could use thick Ni-64 targets

Degrade or strip at lower radius ?

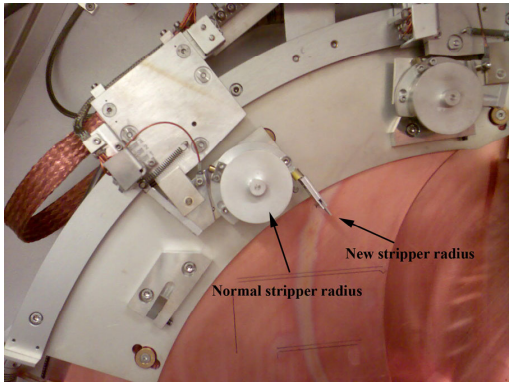

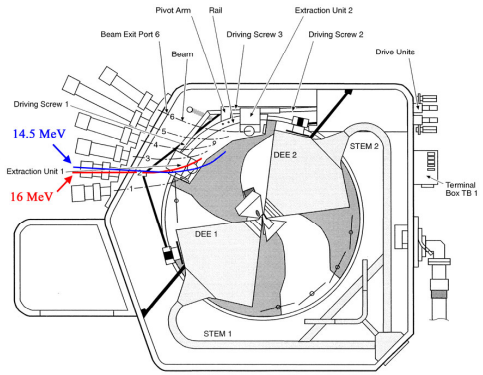

174 GBq of 64Cu,in 3 hours using 150 μA

What do we want that for ?

Therapy ?

WTTC XIII – Presentation Discussions

1. Ag target: materials
   - May force all materials (even) screws to be Ag
   - Anodized Al as isolator: no scratches = no problems
   - Ge window + infrared thermocouple
2. Collimator?
   - 10mm, 30% loss, good cooling necessary
3. Purification
   - Identification of residuals is important
   - Be careful with benzenes, etc

The chemistry of high temperature gas phase production of methyliodide

L. van der Vliet, G. Westera*
Veenstra Instruments, Joure, The Netherlands, *University Hospital, Center for Radiopharmaceutical Science , Zurich, Switzerland,

A methyliodide system was set up to react iodine and methane at high temperature in the gasphase (Larsen).

$CH_4 \uparrow + I_2 \uparrow \rightarrow CH_3I \uparrow$

The apparatus consists of an iodine vaporizer, a high temperature (about 700º C) reactor and a Porapak-N methyliodide trap. The lenght of the tube which is heated to the high temperature can be varied.
A known quantity of methane is added from an injection loop or from a methaniser which is fed with carbon dioxide from the injection loop. The methane is transported by a controlled flow of helium through a carbosphere column, which is needed to remove hydrogen from the methane (which is present when starting with methane from a cyclotron and after methanisation). Behind the iodine oven a UV spectrometer is positioned to measure the absorbance in the glastube and the iodine absorbance is used as feedback to regulate the temperature of the vaporizer and thus control the iodine concentration (Link, Clark).

Scheme:

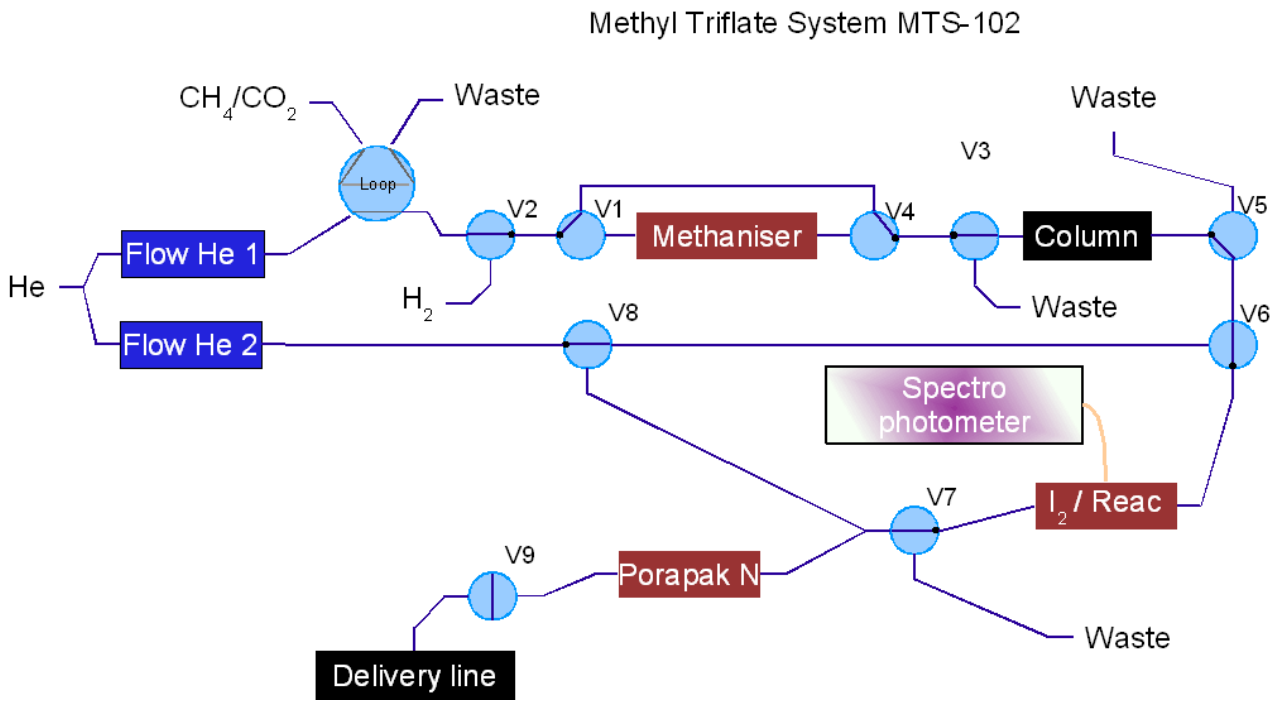

This way all relevant parameters are under control and known quantitatively. The initial amount of methane was choosen as 9 µl, which is the amount of carbon delivered from a cyclotron when producing carbon-11 of moderate specific activity.

The relation between the iodine concentration and the absorbance was calibrated, by collecting the iodine at a stable absorbance during a defined time and weighing the absorbed iodine.

The MeI is collected in methanol (> 90 % is known to be trapped in the first bottle) and analysed by HPLC over an ACE 5 C18 column (15 x 4.6 mm, particle size 5 µm) eluting with methanol / water 60/40 (v.v.) and UV detection (240 nm). A standard solution containing Methyliodide (MeI) and diiodomethane (MeI_2) was used for calibration.

Results

The results given here are preliminary and have to be more precisely calibrated

Transport flow (He)-flow) dependence:

The MeI yield decreases at high and low transport flow. Over a broad flow range, the variation in yield was not significant.

Various flows with a I2 abs of 0.10					
Flow [ml/min]	15	23	30	38	45
Peak area	0.38	0.61	0.39	0.50	0.38
MeI [uMol]	0.026	0.042	0.027	0.035	0.026
Yield [%]	7	10	7	8	7

Iodine concentration dependence:

The MeI yield increases with increasing iodine gas concentration, the maximum concentration still has to be determined:

Various flows with and I2 concentrations resulted in the following yields			
	0.10 I2abs	0.15 I2 abs	0.20 I2 abs
23 ml/min	10	13	17
30 ml/min	7	11	16
38 ml/min	8	13	16

References

Larsen P., Ulin J. and Dahlstrom K. (1995) A new method for production of ^{11}C-labelled methyliodide from ^{11}C-methane. *J. Lab. Comp. Radiopharm.* **37**, 76-78
Linl, J.M., Krohn K.A., Clark J.C. (1997) Production of $[^{11}C]CH_3I$ by single pass reaction of $[^{11}C]CH_4$ with I_2. *Nucl. Med. Biol.* **24**, 93-97

The chemistry of the high temperature gas phase production of methyliodide (MeI)

L. van der Vliet, G. Frederiks, G. Westera *Veenstra Instruments, Joure, The Netherlands, *University Hospital, Center for Radiopharmaceutical Science , Zurich, Switzerland,

Aim

- Better understanding of the chemistry
- Better Device

Better Device

- Longer usage of the Iodine
- Low heat dissipation
- Dimensions of the reaction oven
- Small footprint
- Robust in usage

Better Understanding Chemistry

- Critical points
  - H_2
  - Parameters: I_2,T_r,Flow, ...
  - Concentration methane
  - Specific activity
- Single pass
- Multi pass

Reactions

- Methaniser

  $CO_2 + 2H_2 \rightarrow CH_4 + H_2O$
- Cold trap

  CH_4
- Reaction oven

  $2CH_4 + I_2 \Leftrightarrow 2CH_3I + 2HI$

  $2CH_3I + I_2 \Leftrightarrow 2CH_2I_2 + 2HI$

Methods

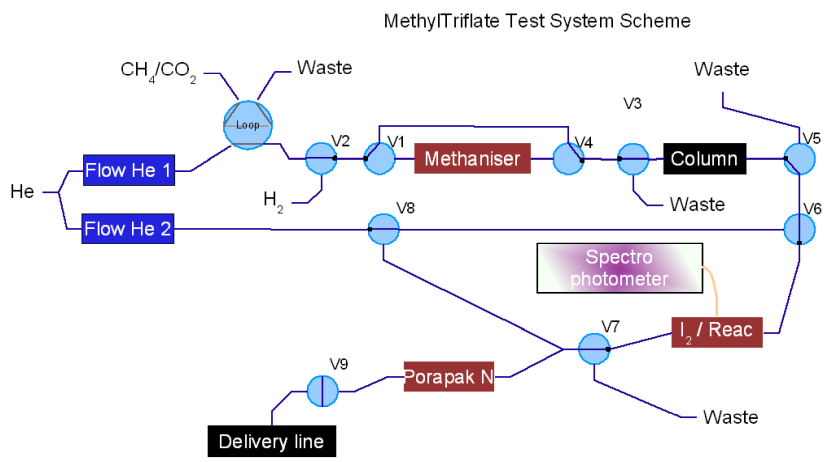

Methods

- Test set up
  - Two flow controllers
  - Spectrophotometer
  - Methane Injector
  - Trap product in pure MeOH
- HPLC
  - C18 column
  - Eluens: $MeOH:H_2O$/60%:40%

Methods

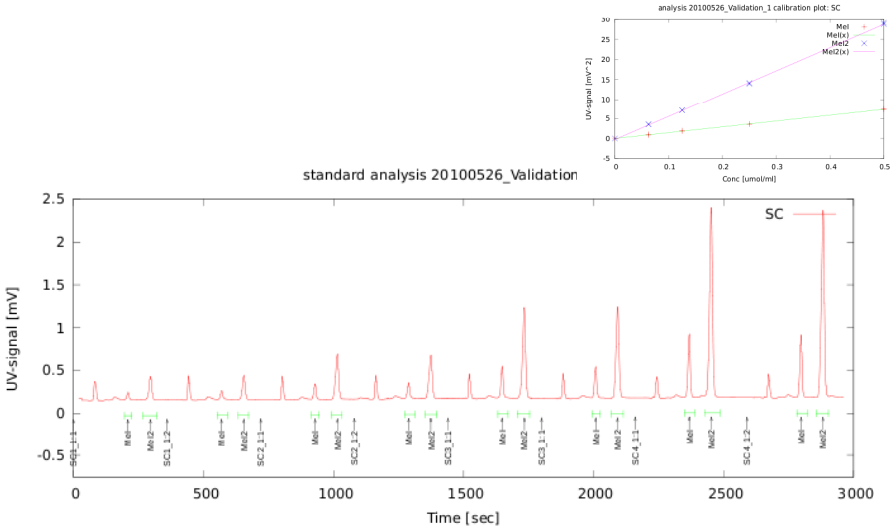

Results

Parameters compared: I_2, Flow and Me concentration

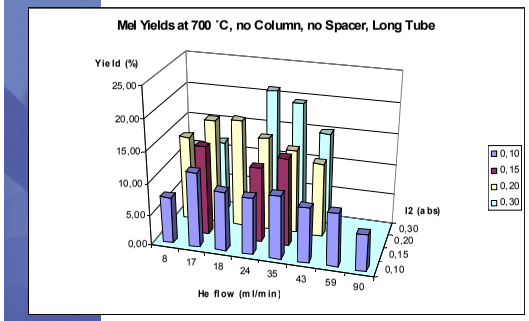

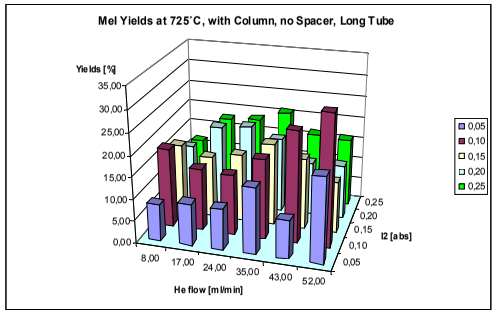

Results

Temperature dependance:

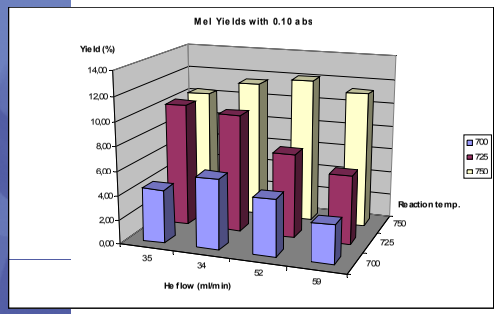

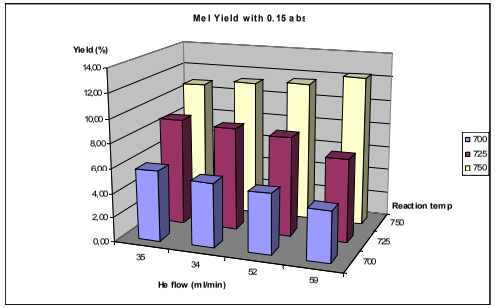

Results

Short tube:

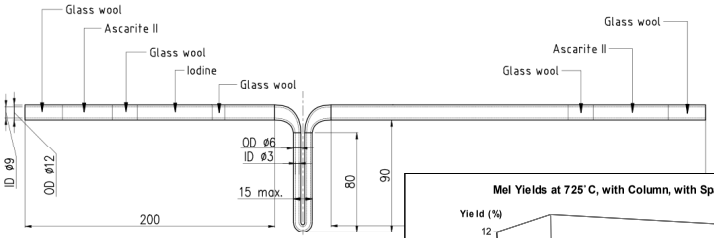

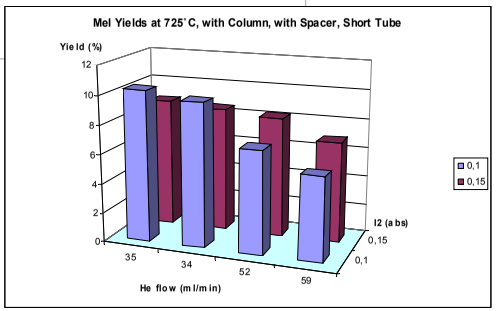

Acknowledgement

- Calle Sjoberg
  from COSAB enginering
- Jaring Huitema
- Teake Bijkerk
- And others collegues
  from Veenstra Instruments

WTTC XIII – Presentation Discussions

1. Challenge: Why not make a nano-reactor?

Target Performance – [^{11}C]CO_2 and [^{11}C]CH_4 Production

Semi Helin[1], Eveliina Arponen[1], Johan Rajander[2], Jussi Aromaa[2], Olof Solin[1,2]

Turku PET Centre, University of Turku[1] and Åbo Akademi University[2], Turku, Finland

Introduction

A systematic investigation on N_2 (0.1 % O_2) and N_2 (5 % H_2) target performances is presented in terms of saturation yields as function of target body temperature and irradiation current.

Materials and methods

Identical aluminium target bodies were used for both [^{11}C]CO_2 and [^{11}C]CH_4 productions. The conical chambers measured 11.2 x 90.0 x 19.4 mm (front I.D. x length x back I.D.) and 16.9 cm^3. The inlet foil was supported by a metallic grid having a transparency of ~ 70 %. In all irradiations the chambers were loaded at 20 °C to 35 bar pressure and irradiated for 20 minutes. Variable parameters were the target body temperature (10, 40, 70 °C), regulated with a cooling fluid circuit and a heat exchanger, and the irradiation current (10, 20, 30, 40 µA). For the data points n = 2. The proton beam was generated with a fixed energy (17 MeV) negative ion cyclotron (CC 18/9, D.V. Efremov Scientific Research Institute of Electrophysical Apparatus, St. Petersburg, Russia).

The irradiation product was directed to a hot cell via a capillary and valve arrangement and a mass flow controller. The main ^{11}C-species was first separated from the target gas using a selective trap: Porapak N column in Ar(Liq) for the [^{11}C]CH_4 and an Ascarite column at room temperature for the [^{11}C]CO_2. The traps were placed in a dose calibrator and the irradiated gas that passed a trap was collected as gas. The collected volume was readable from the gas trap and an aliquot could be taken for radioactivity measurement.

The ^{11}C main product yield was thus measured on-line with the dose calibrator containing the first trap. The content of ^{11}C and ^{13}N in the second trap was determined by iterating the decay curve fitting to the radioactivity values at early and late time points. Yields for the ^{11}C main product and ^{11}C and ^{13}N by-products were calculated as saturation activities (A_{sat} [GBq/microA]).

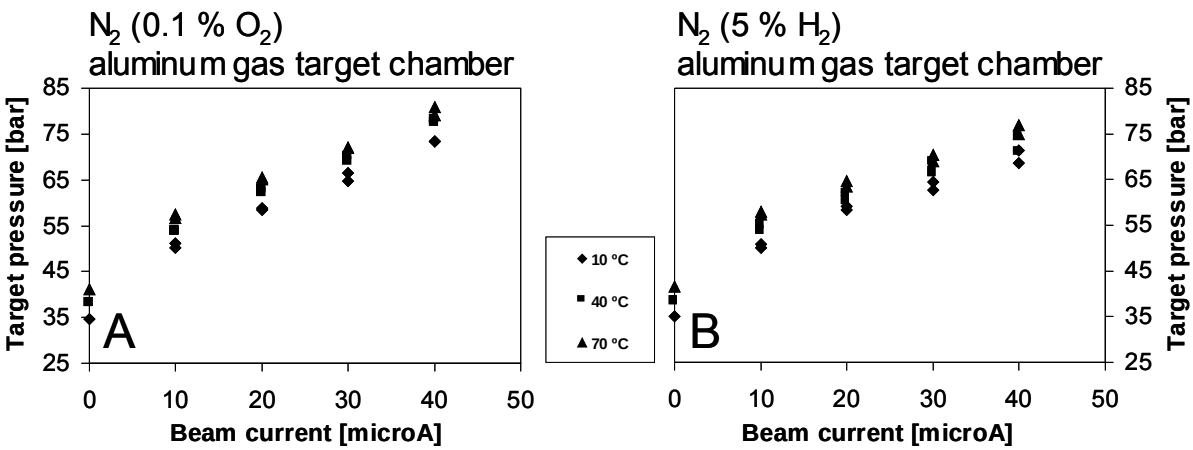

Figure 1. Pressure versus irradiation current at different target body temperatures

Results

The pressure increase as function of beam current was similar for both targets (figure 1). A slight difference was observed at higher currents.

The main component yield is practically constant for the [^{11}C]CO_2 (figure 2, pane A) across the range of varied target body temperature and irradiation current. The [^{11}C]CH_4 yield (figure 2, pane B) is directly proportional to the temperature and inversely proportional to the current.

[^{11}C]CO generation in the N_2 (0.1 % O_2) target is low and inversely proportional to temperature and constant across the investigated current range. [^{11}C]by-product generation is negligible in the N_2 (5 % H_2) target.

^{13}N generation is constant across the range of current and temperature using either N_2 (0.1 % O_2) or N_2 (5 % H_2) target gases. However, ^{13}N production is slightly lower for the N_2 (5 % H_2) target.

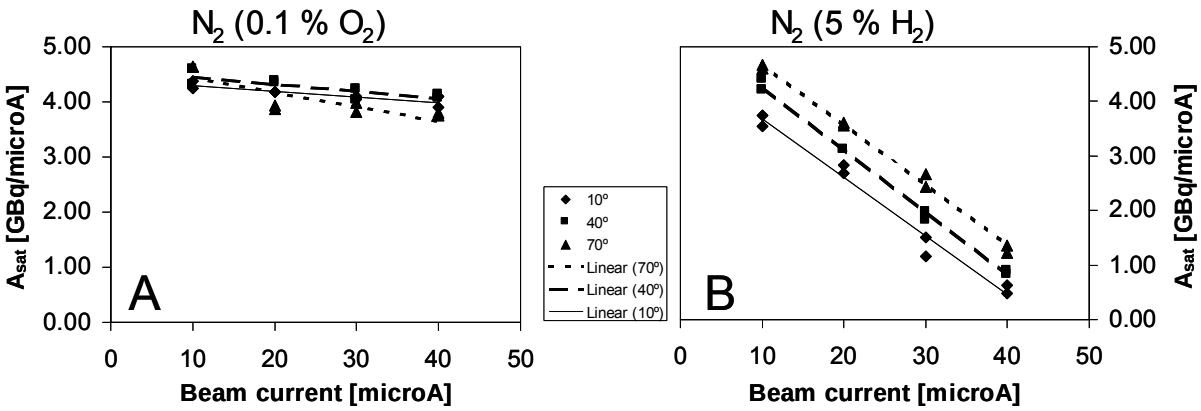

Figure 2. Yield of the main component as a function of irradiation current at 10 – 70 °C.

Conclusions

Production of [^{11}C]CO_2 is practically independent of the irradiation current and the target body temperature, whereas [^{11}C]CH_4 production was found to be strongly dependent on the current and target body temperature.

Acknowledgement

The study was conducted within the "Finnish Centre of Excellence in Molecular Imaging in Cardiovascular and Metabolic Research" supported by the Academy of Finland, University of Turku, Turku University Hospital and Åbo Akademi University.

References

Ache HJ and Wolf AP, (1966), Reactions of energetic carbon atoms with nitrogen molecules, *Radiochim Acta,* 6, pp. 32-33.

Ache HJ and Wolf AP, (1968), The effect of radiation on the reactions of recoil carbon-11 in the nitrogen-oxygen system, *J Phys Chem*, 72, pp. 1988–1993.

Buckley KR, Huser J, Jivan S, Chun KS and Ruth TJ, (2000), ^{11}C-methane production in small volume, high pressure gas targets. *Radiochim Acta*, 88, pp. 201–205

Buckley KR, Jivan S, Ruth TJ, (2004), Improved yields for the in situ production of [^{11}C]CH_4 using a niobium target chamber, *Nucl Med Biol*, 31, pp. 825-827

Target Performance – production of $[^{11}C]CO_2$ and $[^{11}C]CH_4$

WTTC XIII, Risø, 28.7.2010, #25

Semi Helin, Eveliina Arponen, Johan Rajander, Jussi Aromaa, Olof Solin

Turku PET Centre, Finland

Introduction

- Background
  - Measured $[^{11}C]CO_2$ and $[^{11}C]CH_4$ vs. theoretical ^{11}C yields

    Buckley KR, *et al.*, ^{11}C-methane production in small volume, high pressure gas targets. *Radiochim Acta,* 88 (2000) 201–205

    Buckley KR, *et al.*, Improved yields for the in situ production of $[^{11}C]CH_4$ using a niobium target chamber, *Nucl Med Biol,* 31 (2004) 825-827
  - Better yields with higher body temperature
- Aim
  - Systematic investigation of selected parameters
    - Varied: *I*, *t*, *T*
    - Fixed: *E*,target composition, *p,* etc.

Experimental setup

- Efremov CC18/9 cyclotron
  - $E(H^+)$ = 17.0 ± 0.1 MeV
  - $I(H^+)$ up to 40 µA
- Conical aluminium target chambers
  - 11.2 x 90.0 x 19.4 mm = (16.9 cm^3)
  - Grid(ca. 70% transparency) and 25 µm foil (SS 321)

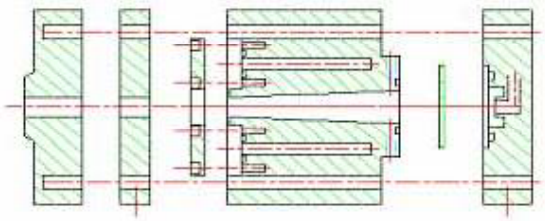

Experimental setup, target chamber temperature control

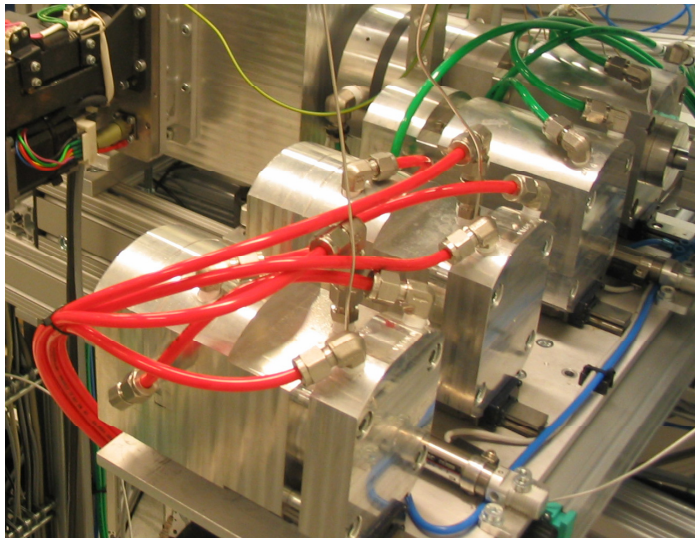

Experimental setup, Measurements & data collection

- Irradiation log file
  - Exact actual values for various parameters
- Produced radioactivity
  - 1st trap for the **main** ^{11}C-product inside a dose calibrator
  - 2nd trap for the **unretained** irradiated target gas, sampling available

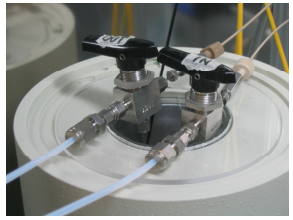

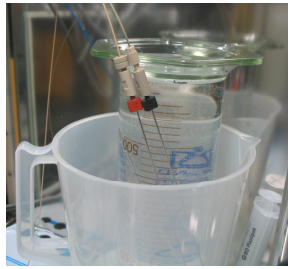

Investigated parameters

Set	Target composition	*p*(load) [bar]	*E*(H⁺) [MeV]	*t*(irr) [min]	*I*(H⁺) [µA]	*T*(body) [° C]
A	N_2(0.1% O_2) N_2(5% H_2)	35	17	10	20	20
B	N_2(0.1% O_2) N_2(5% H_2)	35	17	20	10	10, 40, 70
					20	10, 40, 70
					30	10, 40, 70
					40	10, 40, 70
C	N_2(0.1% O_2) N_2(5% H_2)	35	17	12, 24, 36, 48, 60, 80	10	40
				6, 12, 18, 24, 30, 40	20	
				3, 6, 9, 12, 15, 20	40	

Results, set A
system repeatability

Category A	*I* [µA]	*T* [°C]	*t* [min]	A_{EOB} ([^{11}C]CH_4) [GBq]	A_{calc} (^{11}C) [GBq]
	19.8	21.6	10.0	16.3	*22.8*
	19.7	21.6	10.0	17.2	*22.7*
	19.0	21.7	10.1	18.5	*22.0*
	19.9	21.7	10.0	18.6	*22.9*
	19.6	21.7	10.0	18.2	*22.6*
	19.6	21.6	10.0	17.8	*22.6*
	19.6	21.6	10.0	17.8	*22.6*
	19.6	21.4	10.0	18.2	*22.6*
	19.6	21.4	10.0	18.1	*22.6*
	19.9	20.1	10.0	19.4	*22.8*
	19.9	21.6	10.0	18.5	*22.9*
	19.3	21.4	10.0	17.6	*22.3*
Average	**19.6**	**21.4**	**10.0**	**18.0**	***22.6***
SD	**0.3**	**0.4**	**0.03**	**0.8**	***0.3***
RSD (%)	**1.4**	**2.0**	**0.3**	**4.3**	**1.1**

Results, set B
Saturation yields of **main ^{11}C component** as function of irradiation current at 10-70°C

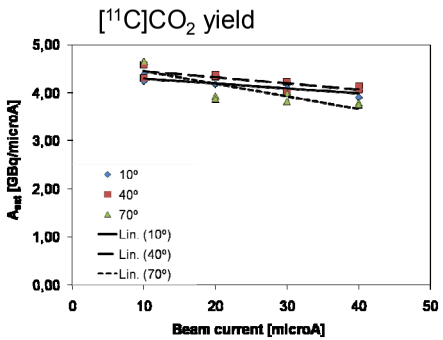

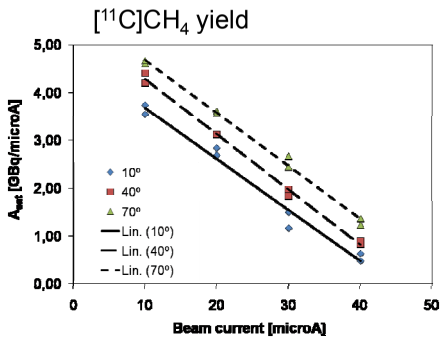

Discussion,

? Current dependent factor;
Reactions competing for H_2

$^{11}C^* + 2H_2 \rightarrow {}^{11}CH_4$ $\qquad$ $N_2^* + 3H_2 \rightarrow 2NH_3$

$^{11}C^* \sim I$ $\qquad$ $N_2^* \sim I^2$

Semitheoretical model of the $A_{predicted}([^{11}C]CH_4)$

$$A_{EOB} = A_{sat} \cdot \left(1 - e^{\ln 2 \cdot t_{irr} / T_{½}}\right) \cdot I$$

$A_{predicted}([^{11}C]CH_4) = A_{sat\text{-}modified}(I,T) * (1 - e^{\ln 2 * t/T½}) * I$

$A_{sat\text{-}modified}$: stemming from nuclear reaction, proton energy, *beam current, temperature of the chamber wall, other factors inherent to the target setting in case.*

Predicted yield of $[^{11}C]CH_4$ as function of temperature and irradiation current

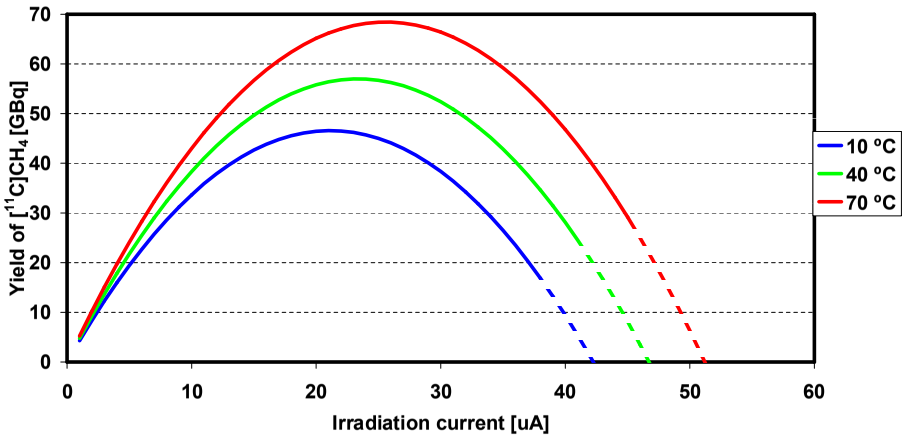

Conclusions

- $[^{11}C]CO_2$ production quite constant within varied range of parameters
- For $[^{11}C]CH_4$ production:
  - temperature dependence
    - wall effect
  - current dependence
    - hydrogen reserve
    - balance of consuming reactions
- Knowledge for optimization and design

Acknowledgements

This study was conducted within the

"Centre of Excellence in Molecular Imaging in Cardiovascular and Metabolic Research"

supported by the
Academy of Finland,
University of Turku,
Turku University Hospital and
Åbo Akademi University.

ACADEMY OF FINLAND
RESEARCH FUNDING AND EXPERTISE

Turun yliopisto
University of Turku

TYKS TURUN YLIOPISTOLLINEN KESKUSSAIRAALA TURKU UNIVERSITY HOSPITAL

Åbo Akademi University

WTTC XIII – Presentation Discussions

1. Low yield
   - Can $^{11}CH_4$ be produced but stay in target walls?
   - Can gas quality/quantity or temperature help?

A Solid ^{114m}In Target Prototype with Online Thermal Diffusion Activity Extraction- Work in Progress

Jonathan Siikanen[a,b] and Anders Sandell[b]
[a]Lund University, Medical Radiation Physics, Barngatan 2:1, 221 85 Lund, Sweden
[b]University Hospital in Lund, Radiation Physics, Klinikgatan 7, 221 85 Lund, Sweden

Introduction

A solid target system is under development for indium isotope production. Pure ^{114m}In ($T_{1/2}$=45 d, Eγ=190 keV, 15.6%) can be produced from proton irradiation on natural cadmium foils if the simultaneously produced ^{110}In-^{111}In activity is allowed to decay several days. ^{114m}In decays to ^{114}In ($T_{1/2}$=71.9 s, β^-=99.5%). This work focuses on ^{114m}In production/extraction.

Material and methods

A target holder was constructed to match a MC 17 Scanditronix cyclotron with a wide beam. The beam fits into a collimator of 40x10 mm^2. The foil holder is a 30° slanted cooling/heating block with a three side frame mounted to the beam strike side (fig 4). On this frame a 25 µm niobium foil is placed to create a water tight cavity, of some ml volume, between the niobium foil and cooling/heating block. In this cavity the cadmium foils are placed. The slanting gives a beam strike area of 40x20 mm^2. This area is cooled with a 1.5 mm thick, 3 l/min water film.

The system was loaded with natural cadmium foils and bombarded with 45 µA protons, under helium flush. After irradiation, the foils were heated to 280-310°C for 1 to 2 hours under argon flush in the cavity. The heating was performed with two heating elements (L=40 mm, ø=6.5 mm, P=160 W each) mounted symmetrically on the long sides to the beam strike area (fig 3). The temperature was measured, with two PT100 sensors (9.5x1.9x1.0 mm, -70…+500°C) mounted on the sides (fig 4), and displayed/controlled with two Shimaden RS32 controllers. The side temperatures were calibrated to the actual temperature under the cadmium foil with another PT 100 sensor.

The activity extraction was made with a thermal diffusion technique [1]. This technique is based on heating close to the melting point of cadmium (320°C). At this temperature, the produced indium isotopes (melting point 150°C) are diffusing in the cadmium matrix. Gradually over time, the indium atoms concentrate on the foil's surface and can then be etched off with a weak acid (0.05 M HCl). The acid was pumped in and out with a peristaltic pump.

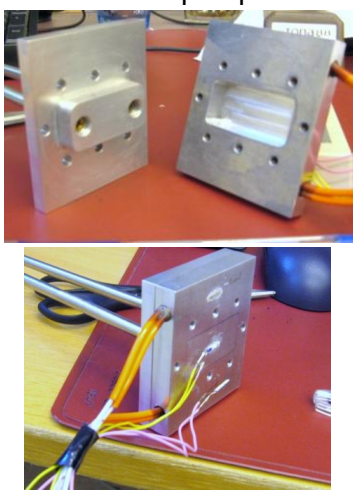

Fig 1. Target cooling/heating block back plate with water cooling in out and two heating elements.

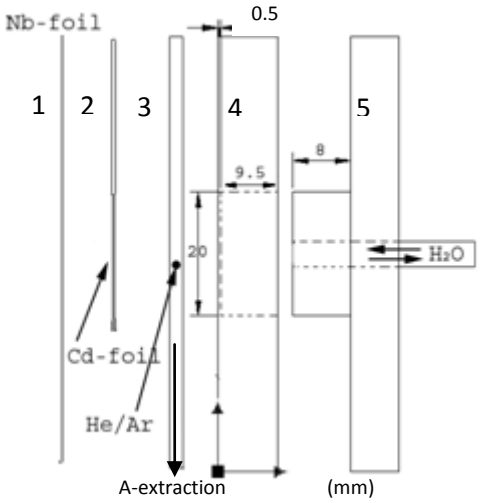

Fig 2. 1: 25 µm Nb foil, 2: Cd-foil-Al-fork (fig 4) 3: Outer frame with He/Ar in/out and a hole in the bottom for activity extraction, 4: back plate 0.5 mm back wall to cooling water, 5: water in/out plate.

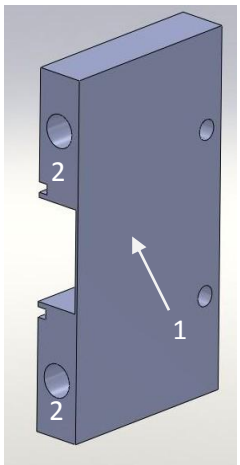

Fig 3. Cross section view of the back plate: 1: Beam strike area. 2: Heat element holes.

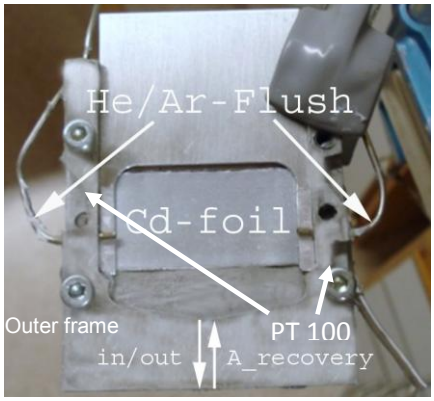

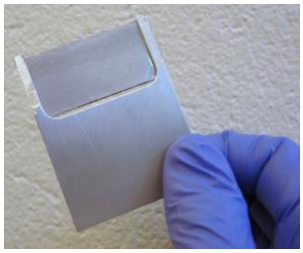

Fig 4. The foil is squeezed and stabilized into place under the flush tubes. This view is covered with a 25 µm Nb foil. HCl is pumped in/out from below, in the cavity between the back plate and the Nb-foil. The Cd-foils are mounted on an Al-fork with a silicone adhesive.

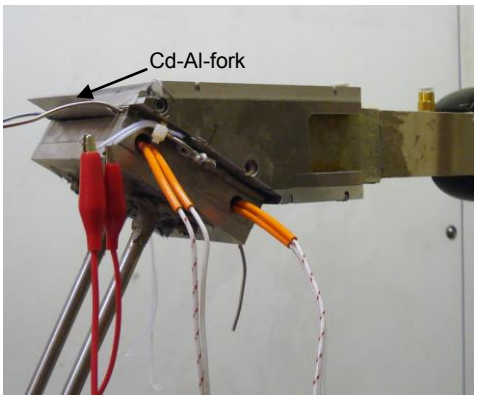

Fig 5: The target is loaded from its rear top simply by sliding down a Cd-Al-fork.

E_p on cadmium foils is ~12.3 MeV. 100 and 50 µm cadmium foils slanted 30° degrades 12.3 → 9.2 and 12.3 → 10.9 MeV. This correspond to theoretical ^{114m}In activity yields of 0.2 MBq/µAh and 0.08 MBq/µAh for natural[1] cadmium foils [2].

Preliminary Results

Low activity yields indicated that a great portion of the beam had missed the actual target, i.e. the cadmium foil. Activity yields will be presented at the conference when new irradiation has been performed. Separation yields on the other hand are valid and are given in table 1.

Table 1: Extraction yields were either measured with a Capintec CRC 120 dose calibrator or a HPGe detector. Etching time was 1-2 min.

Foil #	Thickness (µm)	Irradiation Time (min)	Heating time (min)	extraction (%)
1=T116	100	~6.3	128	41
2=T117	100	~6.8	120	54
3=T118	100	~6.8	60	44
4=T119	50	~6.7	120	41
5=T122	100	~7.0	60	40
6=T123	100	~6.8	120	49
7=T124	50	~6.7	120	56

Discussion

It was found that thermal diffusion extraction of indium from cadmium foils, which only requires temperatures around 300°C, is practically doable direct in the target without any dismounting of foils after irradiation. About 40-50% of produced activity could be extracted with heating times of 1-2 hours. Natural cadmium material for one target cost about 10 Euros.

Acknowledgements:
Thanks to Jan Hultqvist, University Hospital Lund, for machining the target pieces.
Thanks to Professor Hans Lundqvist, Professor Vladimir Tolmachev and Dr Lars Einarsson Uppsala University for the separation technique and discussions.

References:
[1] Lundqvist. H. et al "Rapid Separation of ^{110}In from Enriched Cd Targets by Thermal Diffusion" *Appl Radiat. Isot.* Vol. 46, No. 9, pp. 859-863, 1995
[2] IAEA Recommended cross sections for ^{114}Cd(p,n)^{114m}In reaction (http://www-nds.iaea.org/radionuclides/cd4p4in0.html)

[1] The yields are calculated to correspond to the abundance of ^{114}Cd in natural Cd foil i.e. 28.73 %

A Solid ^{114m}In Target Prototype with Online Thermal Diffusion Activity Extraction - Work in Progress

Jonathan Siikanen[a,b] and Anders Sandell[b]
[a]Lund University, Medical Radiation Physics, Barngatan 2:1, 221 85 Lund, Sweden
[b]University Hospital in Lund, Radiation Physics, Klinikgatan 7, 221 85 Lund, Sweden

The 13th International Workshop on Targetry and Target Chemistry - WTTC 13, Risoe, Denmark, 2010, 25-28 July

Background

- Long lived isotope for therapy. ^{114m}In is listed by IAEA as an emerging therapeutic isotope
- A solid target system for ^{114m}In
- Remote activity handling to decrease dose burden to personnel

Background

- ^{114m}In/ ^{114}In

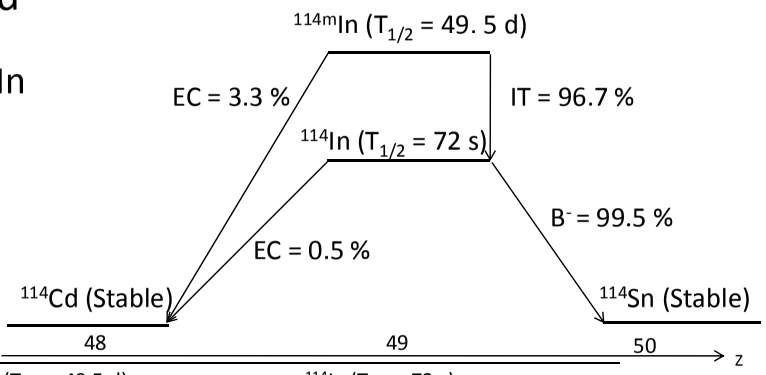

	^{114m}In ($T_{1/2}$ = 49.5 d)		^{114}In ($T_{1/2}$ = 72 s)	
Radiations	Energy (keV)	Intensity (%)	Energy (keV)	Intensity (%)
Auger e K	19-20	6.4		
Auger e L	2.7-2.8	68		
Conversion e	162-190	80		
Beta			779[1]	99.5
X-ray L	23-27	37		
X-ray K	3.1-3.3	5		
γ	190	15.6		
γ	558	3.2		
γ	725	3.2		

Data only given when intensity > 1 %, [1] Average energy, Data is from: Nuclear Decay Data in the MIRD Format (http://www.nndc.bnl.gov/mird/)

Target

- ^{nat}Cd (p,n) ^{114m}In (29 % ^{114}Cd)
- 100 µm cadmium foils
- mounted to an aluminum fork with a high temperature resistant silicon adhesive (316 ° C)
- Target mass ~1 g

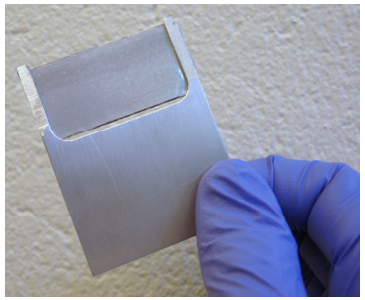

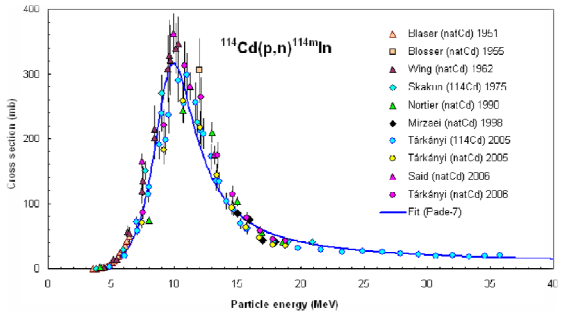

Recommended cross sections for ^{114}Cd(p,n)^{114m}In reaction (http://www-nds.iaea.org/radionuclides/cd4p4in0.html)

Activity extraction

- Remote handling to avoid personnel doses
- Online activity extraction with thermal diffusion[1,2]
- Heating close to 320° C melting point of cadmium
- Meting point of indium is 157° C
- Over time the indium atoms concentrate on the foil's surface and can then be etched off with a weak acid (0.05 M HCl)

Schematic figure over the etching process in a foil

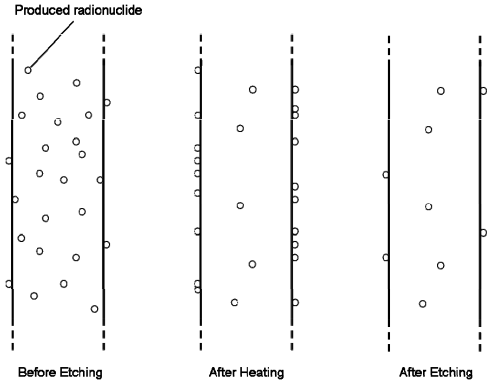

[1]Lundqvist et. al AppL Radiat. Isot. Vol. 46, No. 9, pp. 859-863, 1995
[2]Tolmachev et. al Vol. 27, pp. 183–188, 2000

Target Holder-Cooling/Heating Block

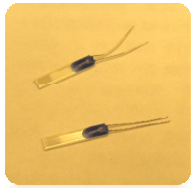

- Cooling block with a 1.5 mm thick 3 l/min water flow
- Two heating elements (L=40 mm, ø=6.5 mm, P=160 W each)
- PT100 sensors (9.5x1.9x1.0 mm, -70 … + 500°C)
- Displayed/controlled with two Shimaden RS32 controllers

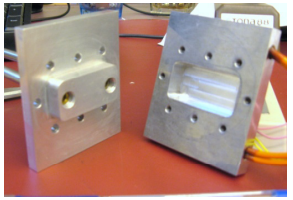

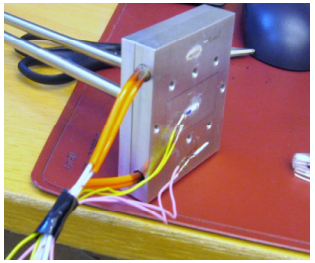

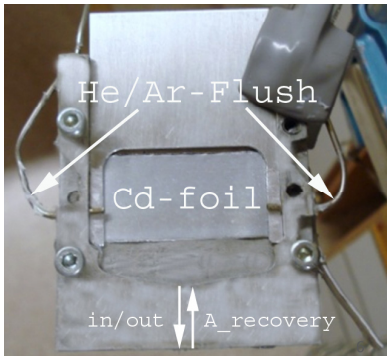

Material

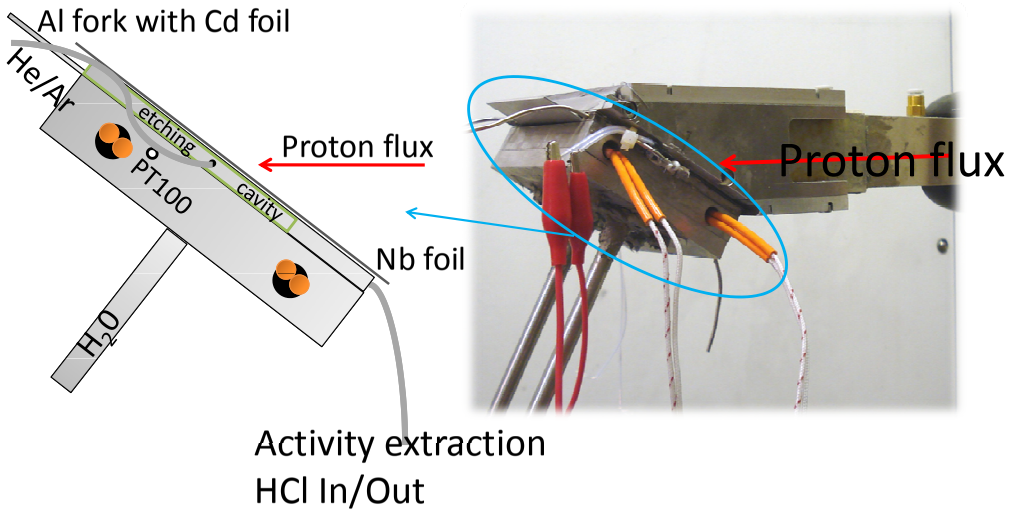

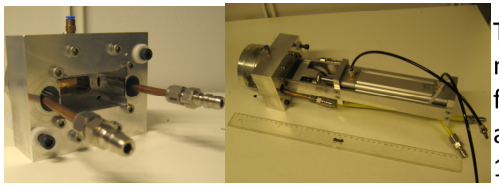

The beam fits into a collimator of 40x10 mm^2 and passes through a double He-cooled foil window (25 µm Havar and 200 µm Ag) and another 25 µm Nb foil → Ep on target 12.3 MeV

Method

Target site

1. Irradiation with 30-40 µA (2-8 µAh) protons under He-flush and water cooling
2. After EOB: Water cooling off and He-flush switched to Ar-flush
3. Heating close to 300 °C for 1-2 h and then cool down to about 30 °C
4. Foil is etched with 5-6 ml 0.05 M HCl for about 2 min. In/out of acid is controlled with peristaltic pumps.

Results

- First set of experiments gave 40-50 % extraction yield (n=7) but very poor A-yields due to bad alignment of holder etc
- Heating 280-310°C (some problems with PT100)

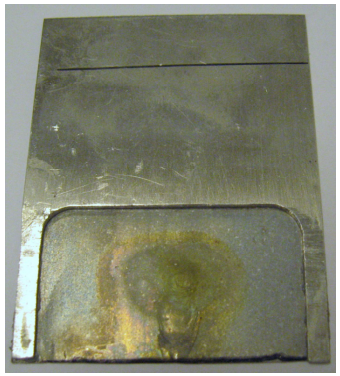

Results

- 100 µm Cd foil slanted 30° , E_p 12.3 → 8.4 MeV[1]
- theoretical ^{114m}In yields of 0.25 MBq/µAh nat-Cd
- In this set all foils were heated for 2 h at 300 °C

Table 2: ^{114m}In activities and separation yields were quantified with HPGe detector. Dead times < 4%

Foil #	I (µA)	Irrad Time (min)	Beam dose (µAh)	Exp A (EOB) (KBq)	Exp A (EOB) (KBq/µAh)	Theo Activity (KBq)	Yield of Theo (%)	Separation Yield (%)
1	45	10	7	155	22	1750	9	43
2	45	7.5	5.1	95	19	1275	7	47
3	45	5.2	3.5	147	42	875	17	48
4	30	6.5	3	130	43	750	17	49
5	30	6.5	3	141	47	750	19	54
6	40	5	3	155	52	750	21	TBD

Discussion

- It was found that thermal diffusion extraction of indium from cadmium foils, which only requires temperatures around 300°C, is practically doable direct in the target without any dismounting of foils after irradiation
- About 40-50% of produced activity could be extracted with heating times of 1-2 hours
- < 2 % of cadmium material losses
- Natural cadmium material for one target cost about 10 Euros
- Low activity yields (about 20 % of theoretical) needs further investigation

In the future

- ^{110}In ($T_{1/2}$=69 min)
  - B^+=62 %
- ^{111}In ($T_{1/2}$=2.8 d)
  - γ=171 keV (90,6 %) and γ=245 keV (94,1 %)

WTTC XIII – Presentation Discussions

1. Why not a Niobium target?
   - Not tried

2. Diffusion/extraction
   - Process known in Russian literature
   - Stack could be used, but difficult to get the acid in there

Upgrade of a Control System for a Scanditronix MC 17 Cyclotron

Jonathan Siikanen[a,b] Kaj Ljunggren[b] and Anders Sandell[b]
[a]Lund University, Medical Radiation Physics, Barngatan 2:1, 221 85 Lund, Sweden
[b]University Hospital in Lund, Radiation Physics, Klinikgatan 7, 221 85 Lund, Sweden

In order to extend the life time of the relatively old Scanditronix MC17 cyclotron (built 1980) an upgrade to the control system was commissioned. The existing system is a PM 550 Texas Instruments. It consist of a Central Control Unit (CCU, 4 KB), a programmer, 6 MT input(170)/output(120) modules (fig 1), 7MT analog input(16)/output(12), a 7MT parallel input(4)/output(4) module and a control consol interface (fig 3). The programming is ordinary ladder logic. The system works well but the lack of spare CCU:s forced an upgrade to the system.

The choice was the CTI 2500 system due the existing special interface card 505-5190 B. This card makes it possible to keep, and avoid rewiring of, all the 6 MT modules. CTI-2558/2562 N analog input/output modules replaced the old ones. The ADC:s were connected in parallel to the old ones. The old DAC:s and the new DAC:s were connected to a toggle switch. This simple rewiring was done in less than five hour. The 7MT parallel input/output were only used for display function and could be omitted in the new system. The installation makes it possible to change between the systems within less than 5 minutes. The CTI system runs under CTI P-SM505-CW N software (505 Workshop Single License). A new interface was written in Visual Basic instead of using a commercial SCADA program. The interface was used on a PC lap top. The upgrade was performed in collaboration with a Danish company Green Matic. Green Matic made the ladder programming. The total cost of the upgrade was less than 20 000 Euros. Testing and debugging of the new system took one day.

Fig 1: The 6MT modules

Fig 2: The new CTI system (In order from left: Power Supply, CPU, Interface card, 4 Analog 8 Channels IN/OUT cards)

Fig 3: The PM550 control consol

Fig 4: New interface written in visual basic

New software for the TracerLab Mx

D. Fontaine[2], D. Le Bars[3], D. Martinot[1], V. Tadino[4], F. Tedesco[1], G. Villeret[4]

1. 49h, 23 Rue du Vieux Mayeur, 4000 Liège, Belgium
2. Eosis, 33 Rue Lefebvre, 7000 Mons, Belgium
3. Cermep, 59 Bvd Pinel, 69003 Lyon, France
4. ORA, 337 Rue de Tilleur, 4420 St Nicolas, Belgium

Introduction: With almost 800 systems installed all over the world, the Coïncidence/TracerLab Mx (General Electric, USA) is still the best seller among synthesizers for [^{18}F]FDG production. This device is approved by relevant Authorities for most of the Marketing Authorizations and used in a GMP environment to produce pharmaceutical grade fluorodeoxyglucose. When FDG started to be commercialized, private laboratories were approved by the Authorities as “mono-product” producers allowed to prepare, sell and deliver only FDG. Further, following the increasing market demand for other radiopharmaceuticals, they were solicited to produce already published tracers under special license and under specific orders for approved clinical protocols. Today, more and more producers are very far in the development of new tracers and on their way to submit Marketing Authorizations.

Objective: On one hand, most of the production laboratories must adapt their license and organization to become “multi-product” and one major step of the file update is the demonstration that in one room, several different synthesis are managed at no risk for the final product (schedule, cross contamination, ….). On the other hand, most of technician teams are trained on the TracerLab Mx and the switch to any other system may easily take up to several months to recover the same reliability. Today, by using the TracerLab Mx in its original configuration, the above mentioned two points are not under control, mostly due to the inadequacy of the original software.

Features:

The purposes of a new software development were:

1) Availability of specific folders for each different produced radiopharmaceuticals
2) Use of kits commercially available from ABX (Dresden, Germany) for NaF, FLT, F-Miso, FET, F-acetate and F-choline
3) Avoidance of sequence problems, with reset of the PLC memory between each run
4) Specific kit test dedicated to the molecule
5) Display a specific flow path layout for each molecule
6) Creation of a specific report corresponding to the name of the molecule
7) Building of data base in order to manage and optimize the preventive maintenance
8) Implementation of different level of users that can log into the system (administrator, operator,...)
9) Safe and secure control of the TracerLab Mx from any computer through secured LAN (cabled and/or wifi) or secured internet connection
10) Open updatable list of compounds

Other useful features added to the software:

11) Addition of a 5th radioactivity detector
12) Possibility to connect a UV detector
13) Control of the 8 outputs still available on the back of the Mx

14) For the user willing to run synthesis including HPLC purification, dedicated screen displaying HPLC UV and radio detection, “Collect” and “Stop collect” button and the possibility to control an “Add On Reform”

Upgrade Procedure:

The upgrade of an existing TracerLab Mx is quite simple:

- Replacement of the RS232 cable by an RJ45 cable
- Replacement of the PLC control board
- Installation of a control server and a WIFI router

From that configuration, any computer loaded with standard browser (Firefox for example), can control the TracerLab Mx.

User Procedure:

Step 1:

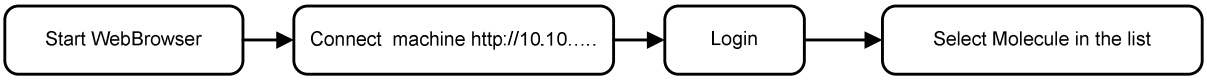

Step 2

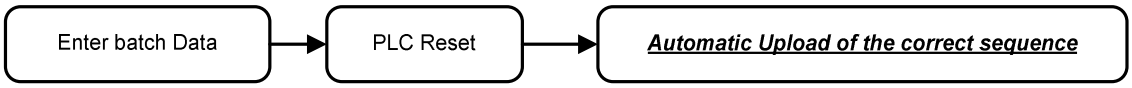

Step 3 :

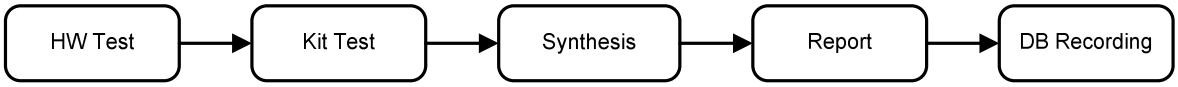

Results:

	Duration	Uncorrected Yield
Kit Only		
NaF	<10 min	Quantitative
FLT	54 min	21%
F-Miso	54 min	22%
F-choline	32min	17%
FET	54	17%
F acetate	42	39%
FDG	26	61%
HPLC		
MPPF	68 min	21%
FLT	40 min	39%
Fallypride	Under Progress	
Licensed 1	Under Progress	

Conclusion:

By using the new software the Tracer Mx has now become a flexible platform dedicated not only to FDG production, but also to most of the fluorinated tracers with clinical demand.

New software for the TracerLab MX

V. Tadino
D. Fontaine
D. Le Bars
D. Martinot
F. Tedesco
G. Villeret

WHY?

- FDG only !
- Other kits available but ...
- New radiotracers ?
- 8 year old software ;-((

HOW?

in less than 1 hr ?

Unplug → Change CPU → Replace 16 I/O by 32 → Router → Black box (server)

AND NOW?

1. web connect
2. select
3. visualize
4. launch synthesis
5. monitoring

AND NOW?

1. web connect
2. select
3. visualize
4. launch synthesis
5. monitoring

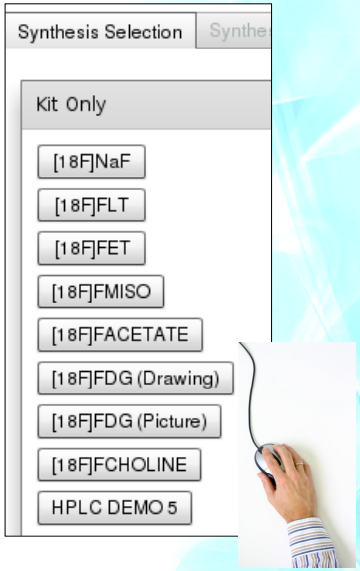

AND NOW?

1. web connect
2. select
3. launch synthesis
4. visualize
5. monitoring

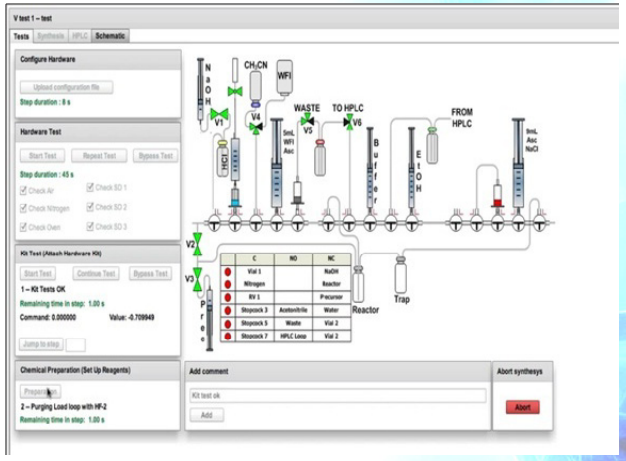

AND NOW?

1. web connect
2. select
3. launch synthesis
4. visualize
5. monitoring

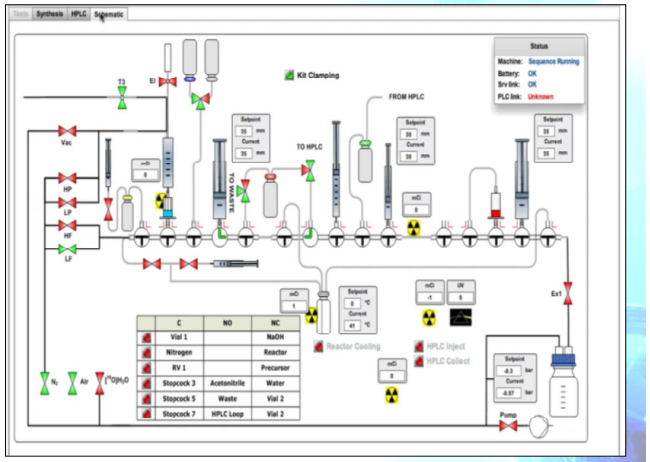

AND NOW?

1. web connect
2. select
3. visualize
4. launch synthesis
5. monitoring

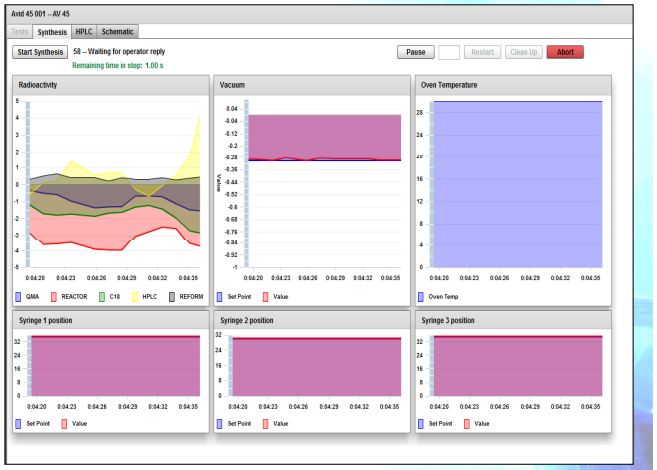

FUNCTIONALITIES?

Specific kit test

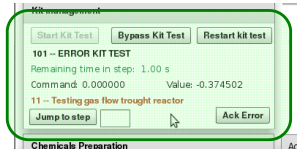

Specific report

Specific follow up

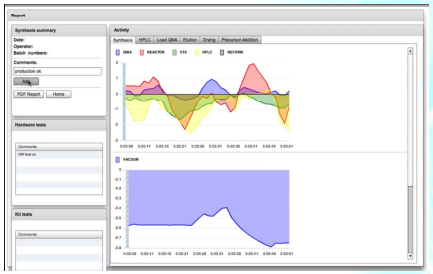

HPLC Collect / Stop collect

Optional UV connection

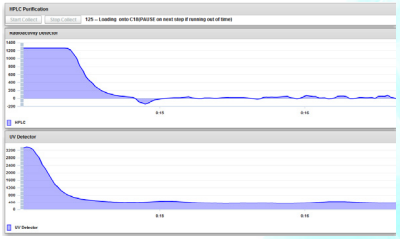

Does it work ?

	Duration	Uncorrected Yield
Kit Only		
NaF	<10 min	Quantitative
FLT	54 min	21%
F-Miso	54 min	22%
F-choline	32min	17%
FET	54min	17%
F acetate	42min	39%
FDG	26min	63%
HPLC		
MPPF	68 min	21%
FLT	40 min	39%
Licensed 01	64 min	25%

WHAT?

NEPTIS network concept

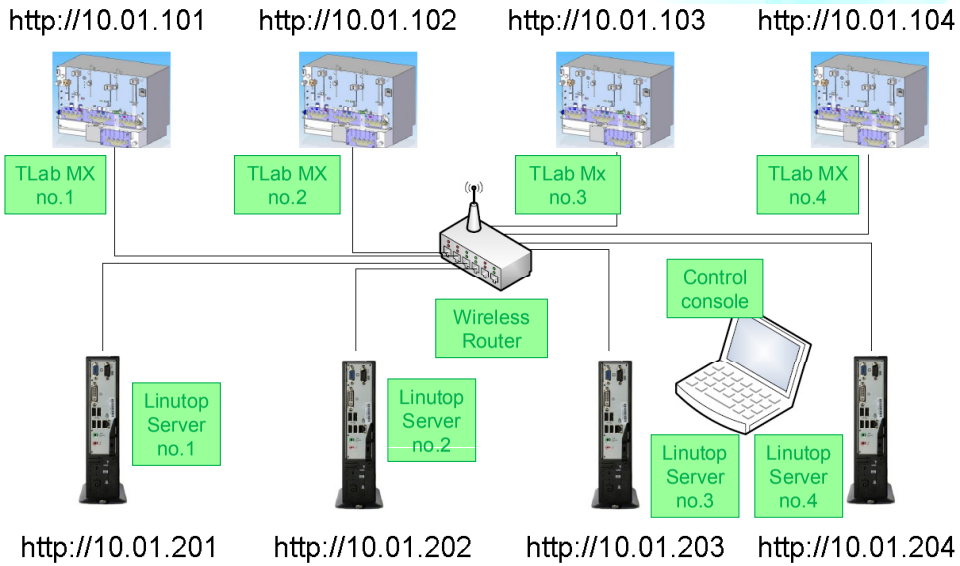

BENEFITS?

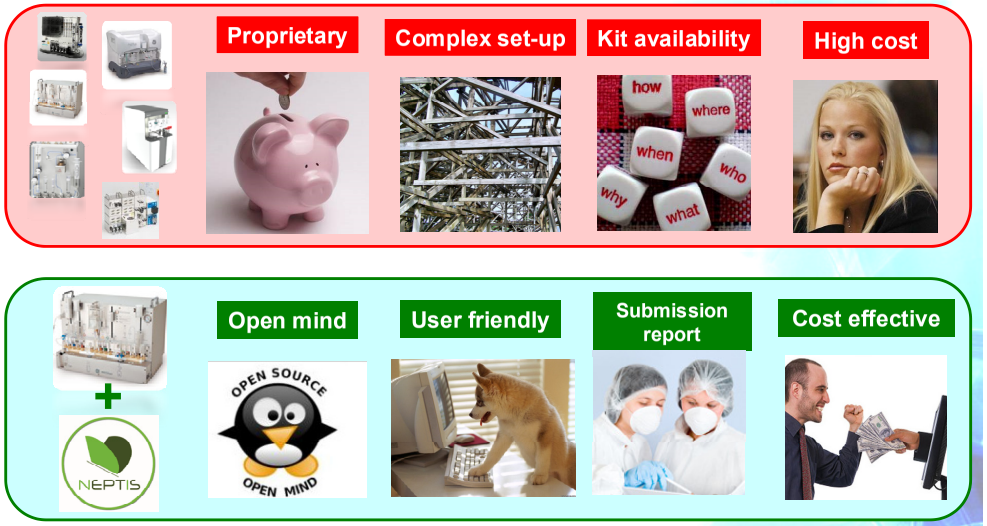

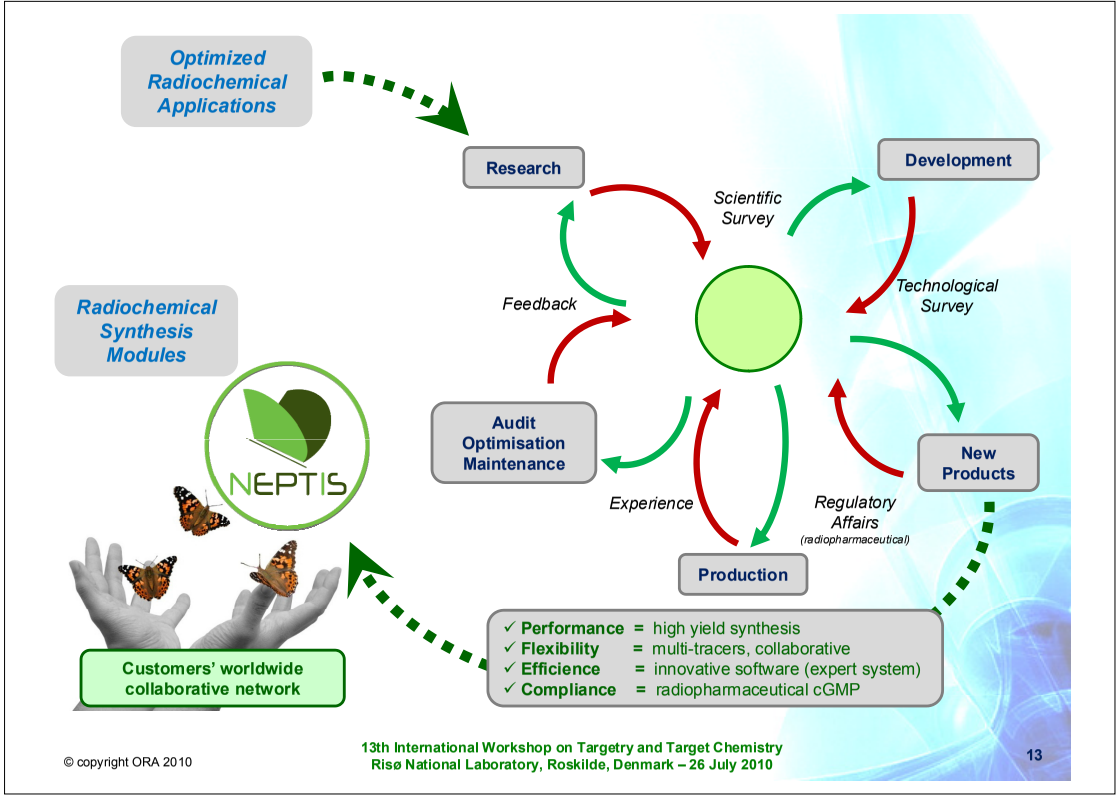
Optimized Radiochemical Applications
Research
Development
Scientific Survey
Technological Survey
Feedback
Radiochemical Synthesis Modules
NEPTIS
Audit Optimisation Maintenance
New Products
Experience
Regulatory Affairs
(radiopharmaceutical)
Production
✓ Performance = high yield synthesis
✓ Flexibility = multi-tracers, collaborative
✓ Efficience = innovative software (expert system)
✓ Compliance = radiopharmaceutical cGMP
Customers' worldwide collaborative network
© copyright ORA 2010
13th International Workshop on Targetry and Target Chemistry
Risø National Laboratory, Roskilde, Denmark – 26 July 2010
13

PRODUCTION OF NO CARRIER ADDED ^{64}Cu & ^{55}Co FROM A NATURAL NICKEL SOLID TARGET USING AN 18MeV CYCLOTRON PROTON BEAM

A. H. Asad[1,2], C. Jeffery[1], S.V. Smith [3], S. Chan[1], D. Cryer[1] & R. I. Price[1,4]

[1]Radiopharmaceutical Production & Development (RAPID) Laboratory, Medical Technology and Physics, Sir Charles Gairdner Hospital, Perth, Australia
[2]Imaging and Applied Physics, Curtin University of Technology, Perth, Australia
[3]Australian Nuclear Science and Technology Organisation (ANSTO), Sydney, Australia
[4]School of Physics, University of Western Australia, Perth, Australia

INTRODUCTION: There is growing interest in the Australian research community for new PET radioisotopes with relatively long half lives. ^{64}Cu is a candidate, since; (i) it can be produced in cyclotrons found in a medical setting; (ii) the translational energy of its emitted positron is moderate (0.65MeV), and; (iii) its half life is sufficiently long (12.7h) to be used to radiolabel a range of molecular targeting agents (including monoclonal antibodies) and for the isotope to be transported across continents.

The RAPID Lab produces [^{18}F]FDG on a daily basis (~4500 doses per year), plus other clinical radiopharmaceuticals based on biogenic PET isotopes. The radioisotopes for these products are produced using standard targetry of an 18/9 MeV IBA cyclotron. As the productions of ^{64}Cu and ^{89}Zr both require an external beam, the RAPID team has devised a purpose built solid targetry system to suit this setting. The new targetry system consists of a 30cm long external beam line fitted with a 50μm Havar vacuum window plus an independent vacuum and cooling system (chilled water plus helium) for the target and beam degrader. Proton energies and currents can be controlled between 4–17.3MeV (using beam degraders) and 10-30μA, respectively.

The preferred approach for the production of ^{64}Cu using a medium-energy cyclotron uses enriched ^{64}Ni as the target in the reaction ^{64}Ni(p,n)^{64}Cu. A yield of 248MBq/μA.h has been reported [2]. However, for a natural nickel (^{nat}Ni) target the yield is considerably less, since the abundance of ^{64}Ni in ^{nat}Ni is only 0.91%. This study investigated the production and purification of the radionuclides ^{64}Cu, ^{55}Co and ^{57}Co, (the latter two arising from ^{58,60}Ni[p,α]^{55,57}Co) using a ^{nat}Ni thin-foil target, as a preliminary 'proof-of-principle' study prior to the bombardment of more expensive isotopically enriched targets formed by electroplating ^{64}Ni onto a gold substrate.

METHODS: A high purity ^{nat}Ni foil (99.99%) of nominal thickness 50μm and 15mm diameter was weighed on a 5-decimal-place balance to determine true average thickness prior to proton bombardment. Three separate runs were performed. The target foil was cooled by both chilled water and helium. The accessible proton beam energy of 17.3 MeV was moderated to 11.7MeV at the target surface by using a 1020μm graphite degrader placed in the collimator of the solid targetry beam line.

Bombardment elapsed times were 8, 19, and 20 minutes with beam currents of 10.4, 19.1 and 14 μA, respectively. Beam currents were uncorrected for secondary electron emission. At end of bombardment (EOB) the irradiated nickel target was left to decay for 3-4 hours to remove the short half-life radioisotopes ^{60}Cu & ^{61}Cu.

The target was then dissolved in concentrated acids at 100°C and then loaded on to either a cation or an anion exchange column (1x 20cm). Nickel from the target plus Cu and Co radioisotopes were separately eluted using a range of solvents mixed with

hydrochloric acid. The fractions containing the radioisotopes of Cu and Co were characterized for radionuclidic purity and activity by calibrated gamma spectrometry (cryo-HPGe gamma spectrometer; Genie2000 software).

RESULTS: The table summarises the activities for ^{64}Cu, ^{57}Co and ^{55}Co for each ^{nat}Ni target for 3 consecutive runs. It compares the activity for each radioisotope (corrected to EOB) with values calculated using reaction cross sections reported in the literature [1, 2 and 3].

Table: Activities for ^{64}Cu, ^{55}Co and ^{57}Co, as a percentage of their respective predicted values calculated using published reaction cross sections plus targetry and beam parameters.

Nickel Foil Thickness	Proton Energy; Current	Irradiation Time	^{64}Cu	^{55}Co	^{57}Co
(μm)	(MeV; μA)	(min)	(% of Predicted Activity) [using ref. 2]	(% of Predicted Activity) [using ref. 1]	(% of Predicted Activity) [using ref. 3]
46	11.7 ; 10.4	8	80.2	94.8	86.4
47	11.7 ; 14.0	20	84.4	84.8	88.7
47	11.7 ; 19.1	19	64.7	78.6	97.2

CONCLUSION: We have performed preliminary 'proof-of-principle' experiments (prior to the use of an enriched target) on the production of Cu and Co isotopes using a ^{nat}Ni target and a medium-energy cyclotron in a medical setting. The activities produced are in reasonable agreement with predicted activities. For the three runs, activities of ^{64}Cu ranged from 64.7 to 84.4% of the predicted values calculated from [2]. Activities of ^{55}Co and ^{57}Co varied from 78.6% to 94.8% and 86.4% to 97.2%, respectively, of those values calculated from [1,3]. Work is proceeding to understand the variability in results between runs, particularly in the ratio of ^{55}Co to ^{57}Co, since these isotopes are eluted under identical chemical conditions.

REFERENCES

1. F.S. Al Saleh et al., Applied Radiation and Isotopes 65 (2007) 104–113
2. Szelecsenyi F et al, Applied Radiation and Isotopes. 44 (1993) 575-580
3. S.Kaufman, et al., Physical Review. 117, 1532 (1960)

Production of No Carrier Added ^{64}Cu & ^{55}Co From a Natural Nickel Solid Target Using an 18MeV Cyclotron Proton Beam

A. H. Asad[1,2], C. Jeffery[1], S.V. Smith [3], S. Chan[1], D. Cryer[1] & R. I. Price[1,4]

[1]Radiopharmaceutical Production & Development (RAPID) Laboratory, Medical Technology and Physics, Sir Charles Gairdner Hospital, Perth, Australia
[2]Imaging and Applied Physics, Curtin University of Technology, Perth, Australia
[3]Australian Nuclear Science and Technology Organisation (ANSTO), Sydney, Australia
[4]School of Physics, University of Western Australia, Perth, Australia

Ali Asad; Radiation Physicist & PhD Candidate in Applied Physics

The 13th International Workshop on Targetry and Target Chemistry - WTTC13

Introduction

- Rapid advances in radioimmuno-diagnosis & -therapy techniques have focused interest on different production strategies for the longer lived PET isotopes such as ^{64}Cu ^{89}Zr & ^{124}I.
- The three decay paths of ^{64}Cu [$t_{1/2}$=12.7hr], namely EC, β^+ and β^- makes it an attractive radionuclide for PET imaging as well as targeted radiotherapy.
- Over the past two decades, cyclotron-based production of ^{64}Cu has been optimized, and ^{64}Cu is now being produced at several medical and research facilities (Szelecsenyi et al., 1993, McCarthy et al., 1997 & Avila et al.,2007).

Excitation Functions (σ) for Selected ^{64}Cu Production Strategies

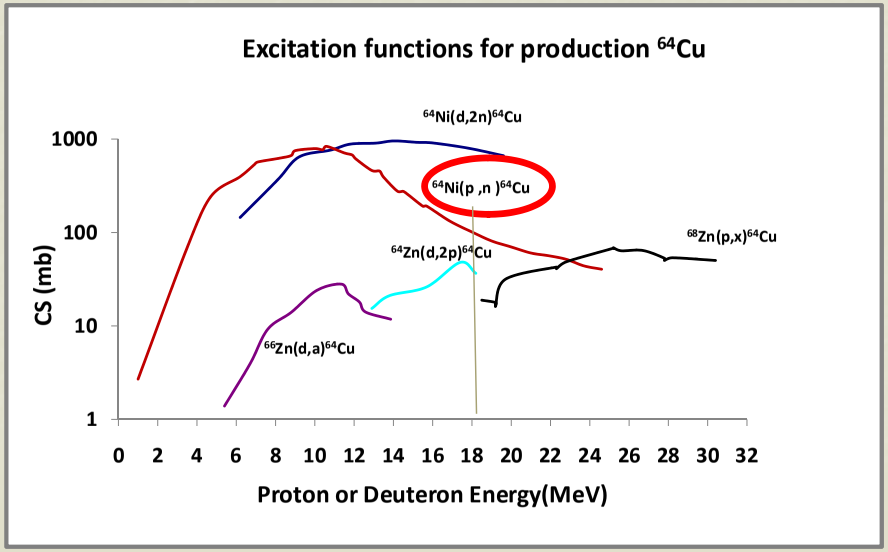

^{64}Cu

^{64}Cu decays via two paths

- ^{64}Ni (stable) with emission of β^+ (17.86%) & EC (42.63%) and
- ^{64}Zn (stable) with emission of β^- (39.03%)

- The most common path for the production of ^{64}Cu is
  - **$^{64}Ni(p,n)^{64}Cu$**
- It requires a medium energy cyclotron; often available in a major hospital
- The ^{64}Ni is of low abundance (1%) and must be enriched prior to use.
- Use of ^{nat}Ni targets yields more complex mixture of radioisotopes.

Characteristics of Products from Reactions $^{nat}Ni(p,x)^{60,61,64}Cu/^{55,57}Co$

Isotope	Half-life	Decay mode	Eγ(MeV)	Iγ(100%)	Contributing reaction	Eth(MeV)
^{60}Cu	23.2 min	EC(7)	826.06	21.7	$^{60}Ni(p,n)^{60}Cu$	7.02
			1791.6	45.4		
		β⁺(93)	1322.50	88.0		
^{61}Cu	3.41 h	EC(38)	282.95	12.2	$^{61}Ni(p,n)^{61}Cu$	3.10
		β⁺(62)	656	10.7		
^{55}Co	17.54h	EC	477	20.2	$^{58}Ni(p,\alpha)^{55}Co$	1.36
			931.30	75.0		
		β⁺(62)	1408.40	16.9		
			1316.40	7.1		
^{57}Co	271 d	EC	122.13	85.6	$^{60}Ni(p,\alpha)^{57}Co$	0.27
			136.40	10.7		
^{64}Cu	12.7 h	β⁺(19)	511		$^{64}Ni(p,n)^{64}Cu$	3.50
		EC(40)	1345			
		β-(41)				

Cross sections (σ) for $^{nat}Ni(p,x)$ reactions

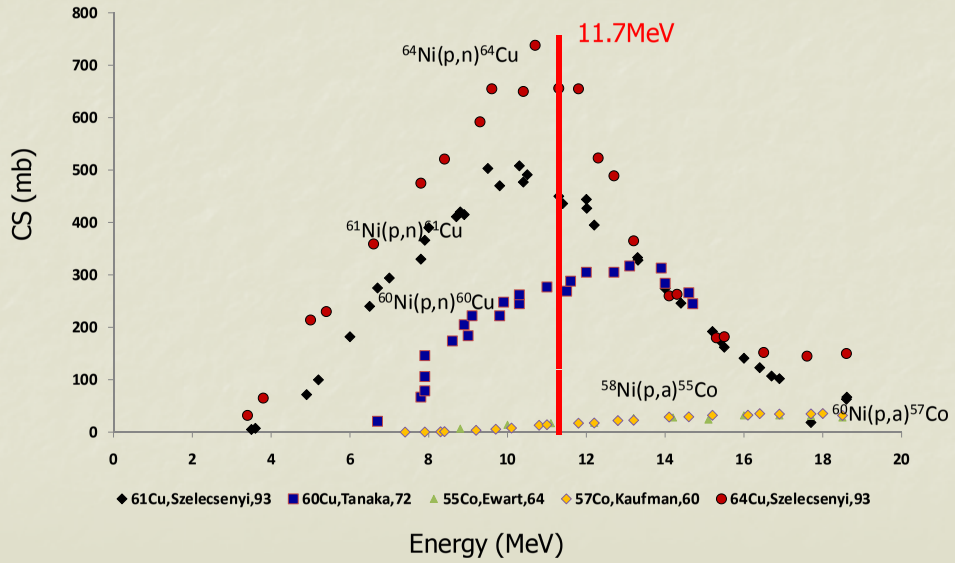

Isotopic Abundances of Ni Targets

Isotope	^{nat}Ni [a]	^{64}Ni [b]
^{58}Ni	68.27	2.67
^{60}Ni	26.10	1.75
^{61}Ni	1.13	0.11
^{62}Ni	3.59	0.67
^{64}Ni	0.91	94.8

a: Supplied by Trace Sciences International Inc., U.S.A

b: Supplied by Goodfellow., U.K

Aims

- To re-evaluate cyclotron based production of ^{64}Cu
- To test feasibility of the co-production & purification of ^{64}Cu & ^{55}Co from proton bombardment of ^{nat}Ni, partly aiming at reducing cost of targetry

Methods: Radionuclides Production

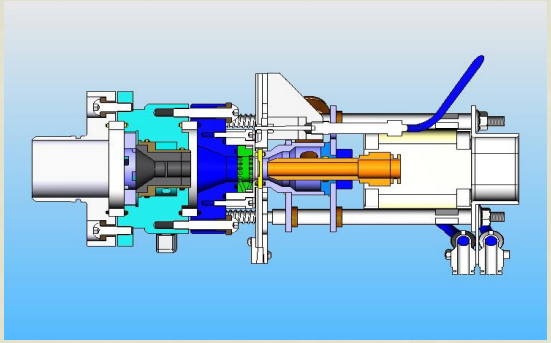

- IBA 18/9 cyclotron provides the primary beam
- In-house built solid targetry system for up to 30μA at 18MeV
- Cooled by chilled water & helium, independent vacuum
- Achievable proton bombardment energy = 17.3 MeV
- Graphite beam-energy collimator & degrader (to 11.7MeV for ^{64}Cu)
- **In these experiments, ^{nat}Ni & enriched ^{64}Ni used as target**

Methods: Experimental Precision of Beam Energies

The mean primary beam energy is **18.08 (0.09) MeV (SD) (0.5% CV).**

Calculated using both EXFOR & IAEA regimes for σ *plus* ^{63}Zn & ^{65}Zn data from replicate stacked Cu-foil runs

Graphite disc of thickness 1020 μm, inserted in front of 50mm Havar window, is used to reduce energy of incident beam to **11.68 (0.18) MeV (1.5% CV)**

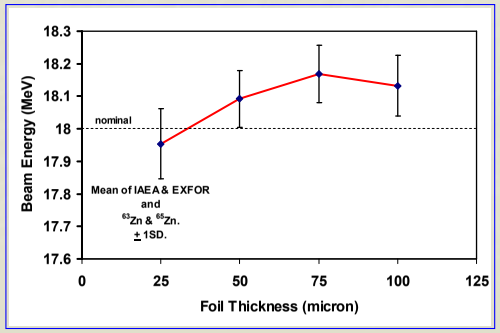

Primary beam energy vs Cu-foil thickness (corrected for Havar foil)

Methods: Experimental σ for ^{64}Ni(p,n)^{64}Cu

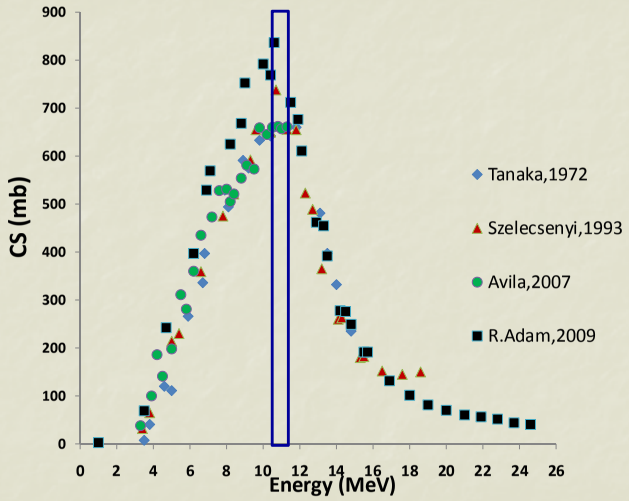

Box shows proton energies within 50μm thick ^{nat}Ni target, where normally-incident (degraded) beam energy = 11.7 MeV

Methods: Schematic Solid Targetry of ^{nat}Ni(p,x)

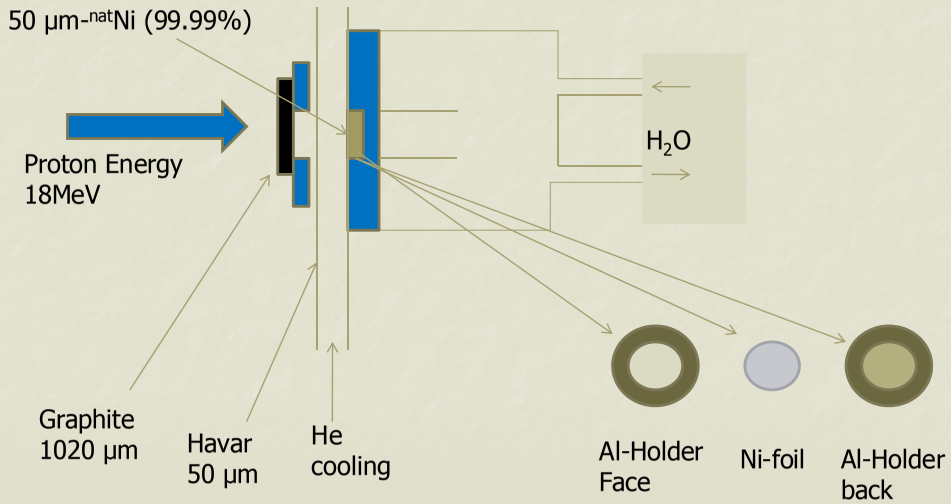

Target diameter =15mm; beam diam. = 10mm

Methods: Production ^{64}Cu from ^{nat}Ni-foil (I)

Principle

- Activation of target ; chemical separations & identification of radioactive products

Methods

- Insert the target in target holder
- Determine beam current (over time of bombardment)
- Measure activities of produced isotopes using calibrated coaxial HPGe cryo-cooled detector
- Calculate projectile energy degradation in graphite degrader, Havar window & (finally) depth-dependent energy in ^{nat}Ni target
- Calculate yields of produced isotopes from experimental production parameters plus literature σ data

Methods: Production ^{64}Cu from ^{nat}Ni-foil (II)

- Irradiate ^{nat}Ni-foil [Diam =15mm,thickness = 50um]
- ^{nat}Ni 100 times lower abundance of ^{64}Ni than enriched ^{64}Ni target
- Place in Al target cradle [thickness= 1.2mm] before inserting into a target holder
- 11.7MeV protons with various current and time
- Target stayed in a cyclotron bunker for 2-3 hours to let short half-life isotopes [^{60}Cu and ^{61}Cu] decay
- Dissolve Ni-target into heated 6M HCl, then transferred to ion-exchange column

Methods: Production ^{64}Cu from ^{nat}Ni-foil (III)

- Elution of Ni ions in 0.3MHCl & Ethanol. [No need to recycled ^{nat}Ni]
- Wash column with 0.3MHCl & Ethanol to extract Co- fraction
- Extract Cu using 0.3MHCl & Ethanol
- Evaporate the 3 fractions Ni, Co and Cu, adjusted to 1ml
- Measure the activities of produced ^{64}Cu, ^{55}Co & ^{57}Co using gamma-spectroscopy

Results: Calculated Comparative Yields

	Calculated yield EOB (MBq/uA.h)		
Target	**^{nat}Ni**	**^{64}Ni**	**Ref**
Produced isotope			
^{61}Cu	**3.1**	**0.3**	**Szelecsenyi, 1993**
^{60}Cu	**365**	**24.5**	**Tanaka, 1972**
^{55}Co	**1.3**	**0.05**	**Ewart,1964**
^{57}Co	**0.002**	**0.000**	**Kaufman,1960**
^{64}Cu	**1**	**102**	**Szelecsenyi,1993**

Results: Experimental – ^{nat}Ni Target

Proton bombardment of ^{nat}Ni. Investigation of production reproducibility of three isotopes

^{nat}Ni thick.	Proton E; A	Irrad. time	^{64}Cu	^{55}Co	^{57}Co
(µm)	(MeV; µA)	(min)	(% Predicted Activity)	(% Predicted Activity)	(% Predicted Activity)
46	11.7; 10.4	8	80.2	94.8	86.4
47	11.7;14.0	20	84.4	84.8	88.7
47	11.7;19.1	19	64.7	78.6	97.2

Results: Experimental – ^{64}Ni Target

- 25 mg of ^{64}Ni (<95%) electroplated on Au-disk for 12 hours; 2.2-2.4 V with 6 mA
- Bombardment of enriched ^{64}Ni target with 10µA for 1 min
- Experimentally determined activity & half-life of ^{64}Cu in good agreement with calculation & literature

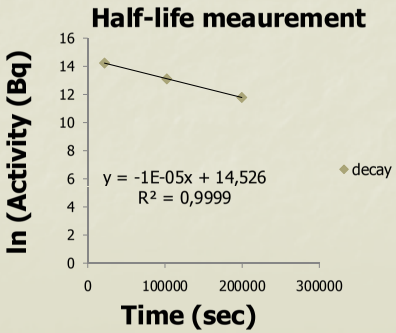

$T_{1/2}$ (Exp) = 12.7 hr

$T_{1/2}$ (Lit) = 12.7 hr

Summary & Discussion

- Production & purified separation of ^{64}Cu, ^{55}Co & ^{57}Co from bombarded ^{nat}Ni in reasonable agreement with calculation. However there is still inter-run variability in our hands
- Electroplating ^{64}Ni on Au-foil has been successful in constructing an enriched target
- Aluminium 'cradle' an easy and cheap material to encapsulate the electroplated foil
- Production of ^{64}Cu from electroplated ^{64}Ni target in good agreement with calculations
- ***Future work*** *aimed at combining the capacity to separate purified Cu & Co isotopes from bombarded (inexpensive) ^{nat}Ni foil, together with prospect of partly enriching ^{64}Ni content of this target foil – aiming at reducing cost of targetry in ^{64}Cu production*

Acknowledgments

RAPID Team,Perth Australia

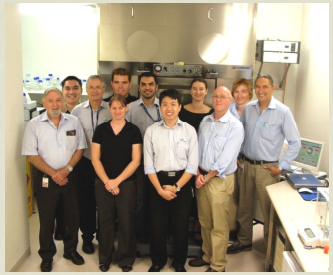

Australian Nuclear Science & Technology Organisation (Dr Suzanne Smith & Co-workers)

Organisers of WTTC13, Rosekilde,Denmark

WTTC XIII – Presentation Discussions

1. (p,n) reaction
   - 11,7 MeV to reduce isotopic impurities
   - Energy degradation by graphite (1020 um)
   - 64Ni electroplated on gold

2. Separation: ethanol method
   - Separates Ni, Co, Cu (checked by gamma spectroscopy)
   - Column as big as 20 x 1

3. Why not (the cheaper) nat Ni?
   - Less production, more problems
   - OK only for testing

4. Graphite degradator? What kind of graphite?
   - Less beam divergence (Monte Carlo)
   - Pyro? Better heat transfer, more expensive

5. Why keep using He flow?
   - Keep oxidation (air!) away

WTTC XIII – Presentation Discussions

6. Target material direct to cyclotron vacuum?
   - Dangerous: Ni is magnetic

7. Target irradiation on line verification?
   - Possible by neutrons, but only to 11MeV (16MeV too much)

Reportback from iThemba LABS: Some tales of broken targets, split beams and particle tracking

C. Vermeulen, G.F. Steyn, N. Stodart, J.L Conradie, A Buffler, I Govender

iThemba Laboratory for Accelerator Based Sciences, Cape Town, South Africa

Introduction

iThemba LABS started 2006 with one bombardment station handling batch targets with 66MeV protons up to a maximum 100uA. In 2010 we have four bombardment stations and the ability to split beam to two stations increasing the total intensity on target to 350uA. We have reported in previous meetings on the vertical bombardment station for large batch targets at high currents as well as the degrading system to produce F-18 on a commercial water target. This report will look at some successes and failures of these systems and highlight the new developments at the lab.

Broken targets etc.

Fig 1: When 66 MeV Strikes

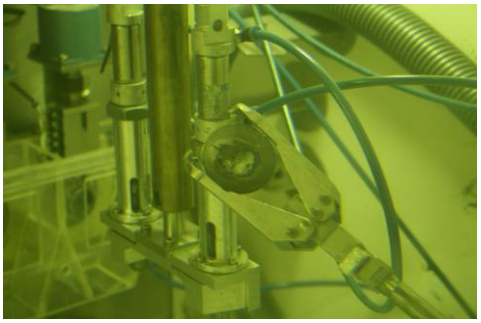

Fig 2: Broken Ga Target

The vertical bombardment station (VBTS) at iThemba LABS has now been in operation for 4 years and has seen just over 1 million micro-amp hours of beam. We have experienced a number of target (Fig 2) and infrastructure (Fig 1) failures, especially of gallium metal targets. We have implemented a number of measures (Fig 3) to reduce the frequency of breakage of these.

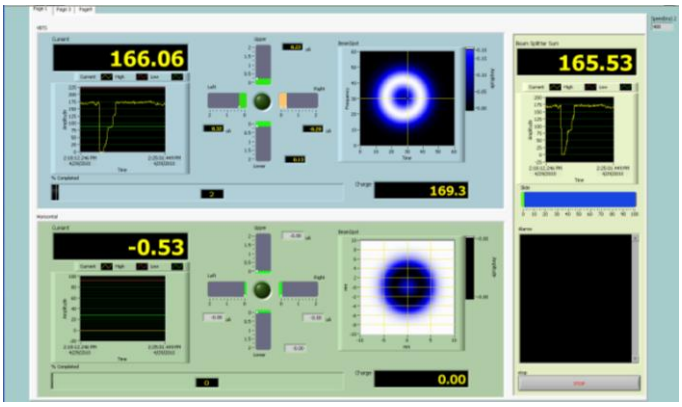

Fig: 3: New Diagnostics

Beam Splitter

We have implemented an electrostatic channel and a septum magnet (Fig 5), to obtain separated but simultaneous beams for the vertical and horizontal bombardment stations. This is based on the system for splitting employed at the Paul Scherrer Institut. (Conradie et al. 2007)

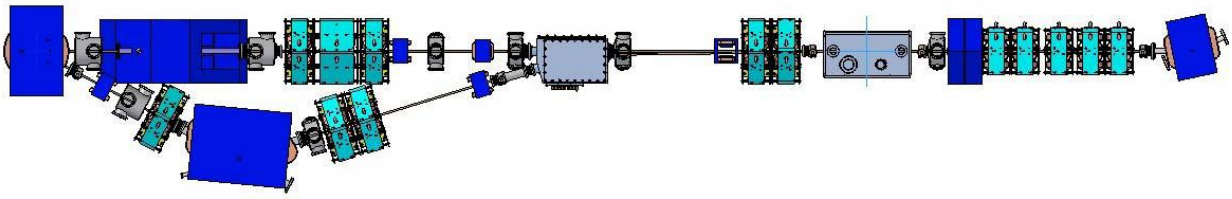

Fig 5: Split Beamline

PEPT

Positron emission particle tracking (PEPT) was developed at the University of Birmingham (Hawkesworth et al., 1991; Parker et al., 1994). Since the arrival of the ECAT 'EXACT3D' (Model: CTI/Siemens 966) PET camera (Fig. 6), from Hammersmith Hospital Cape Town now boasts the second dedicated PEPT lab in the world.

Initial runs (Fig 7) with tumbling mills, flotation cells and even an angle grinder have proven very successfull and development of tracer manufacture using both ion-exchange labelled particles and directly activated particles is continuing well.

Fig 6: EXACT3D in its new home

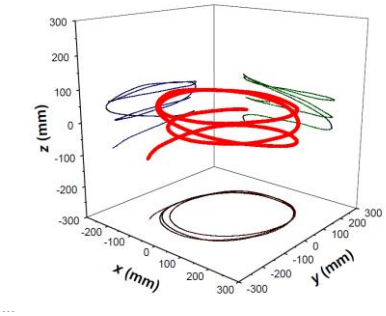

Fig 7: First PEPT run

References

Hawkesworth, M.R., Parker, D.J., Fowles, P., Crilly, J.F., Jefferies, N.L., Jonkers, G., 1991. Non-medical applications of a positron camera. Nucl. Instrum. & Meth. A310, 423-434.

Parker, D.J., Hawkesworth, M.R., Broadbent, C.J., Fowles, P., Fryer, T.D., McNeil, P.A., 1994. Industrial positron-based imaging: principles and applications. Nucl. Instrum. & Meth. A348, 583-592

J.L. **Conradie**, P.J. Celliers, J.G. de Villiers, J.L.G. Delsink, H. du Plessis, J.H. du Toit, R.E.F. Fenemore, D.T. Fourie, I.H. Kohler, C. Lussi, P.T. Mansfield, H. Mostert, G.S. Muller, G.S.Price, P.F. Rohwer, M. Sakildien, R.W. Thomae, M.J. van Niekerk, P.A. van Schalkwyk Improvements to iThemba LABS Cyclotron Facilities. Cyclotrons and their Applications Conference (2007)

iThemba LABS

National Research Foundation

Laboratory for Accelerator Based Sciences

ITHEMBA LABS REPORTBACK

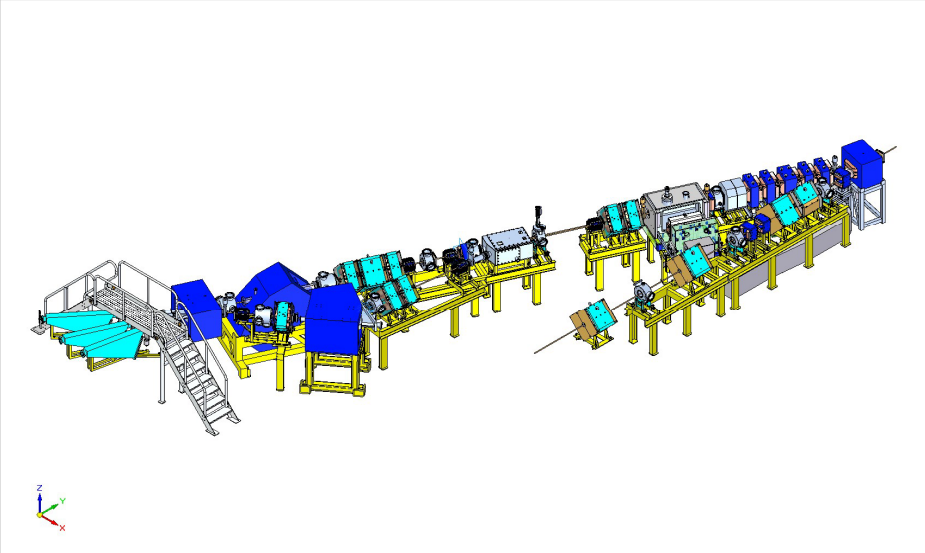

Beam Splitter

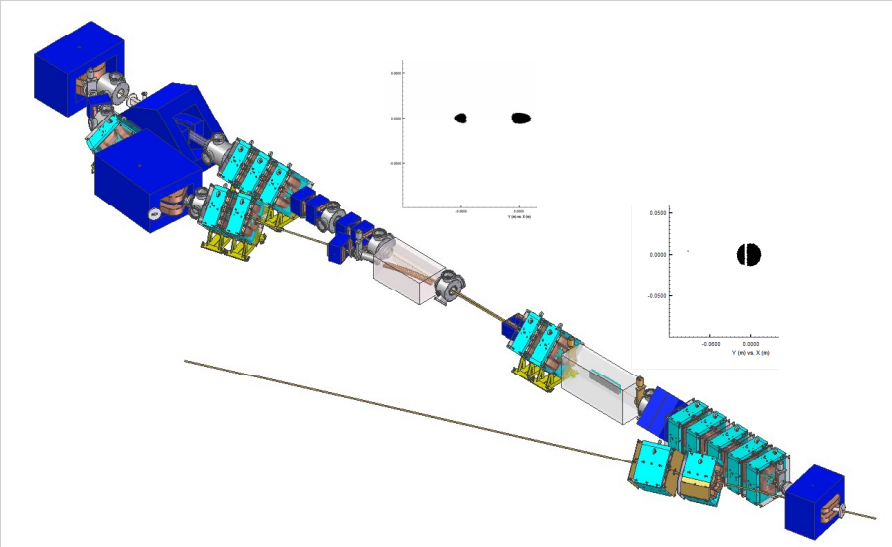

Beam Splitter

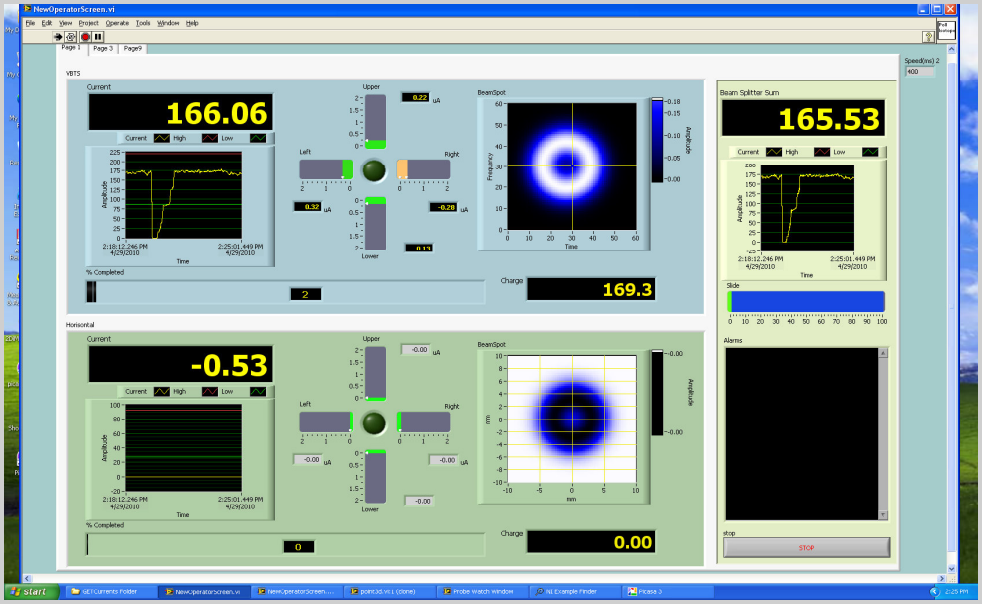

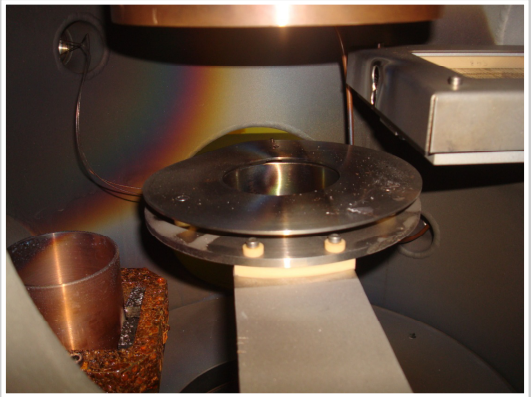

This Beam Bites!!!

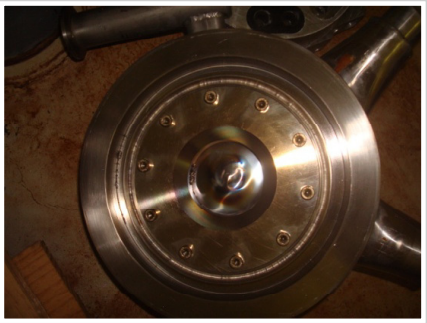

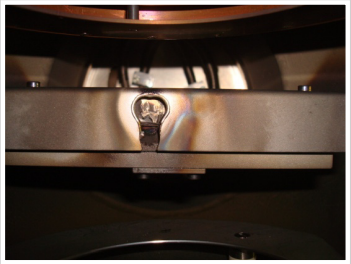

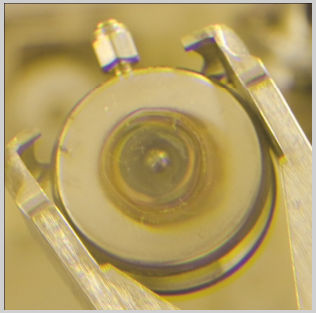

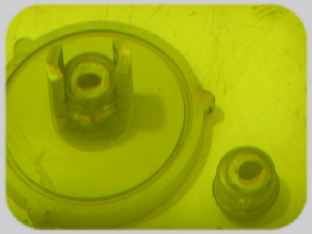

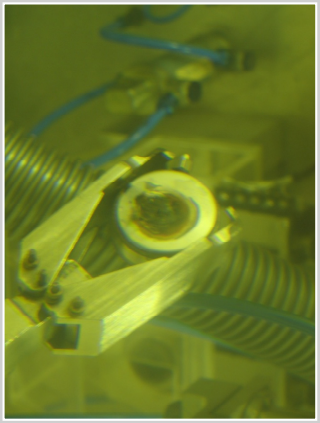

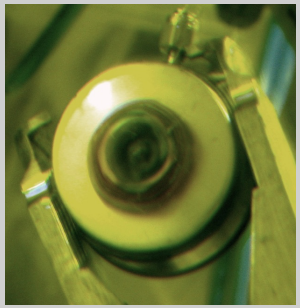

More Holes

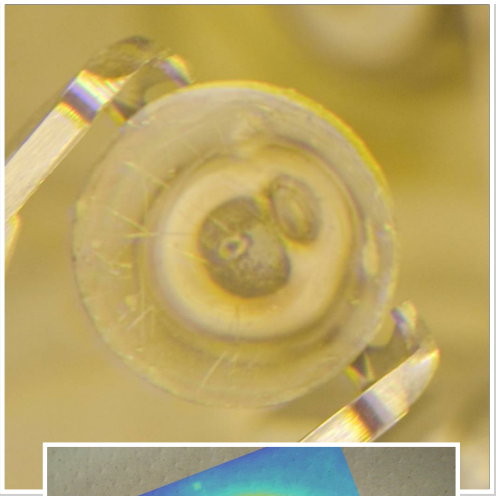

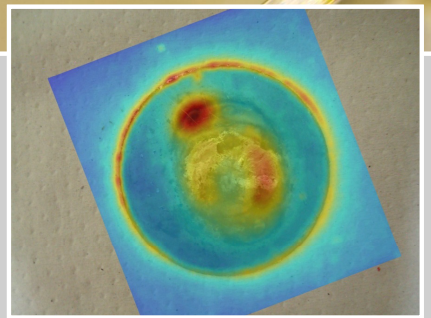

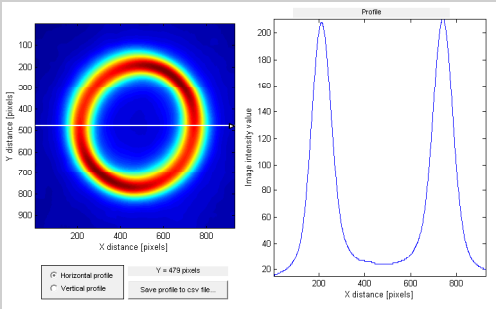

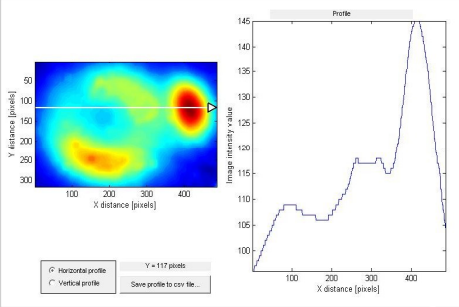

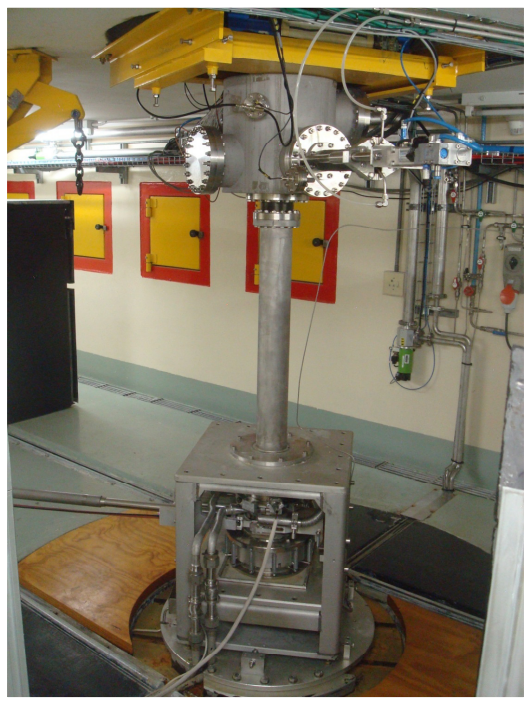

Vertical Target Station

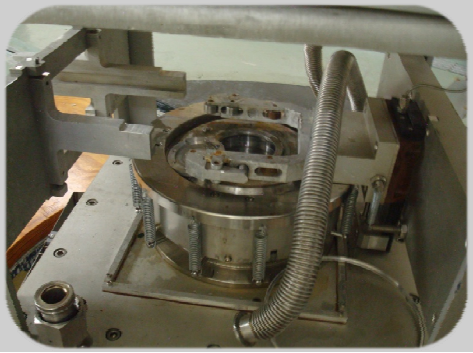

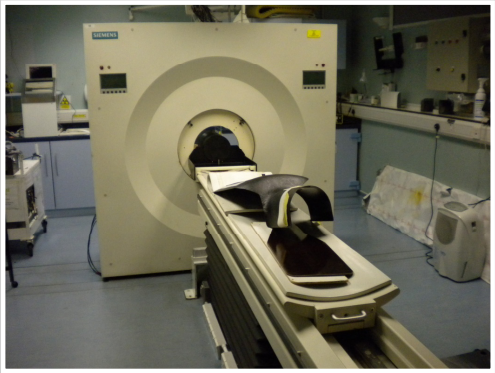

- New Cyclotron Facility

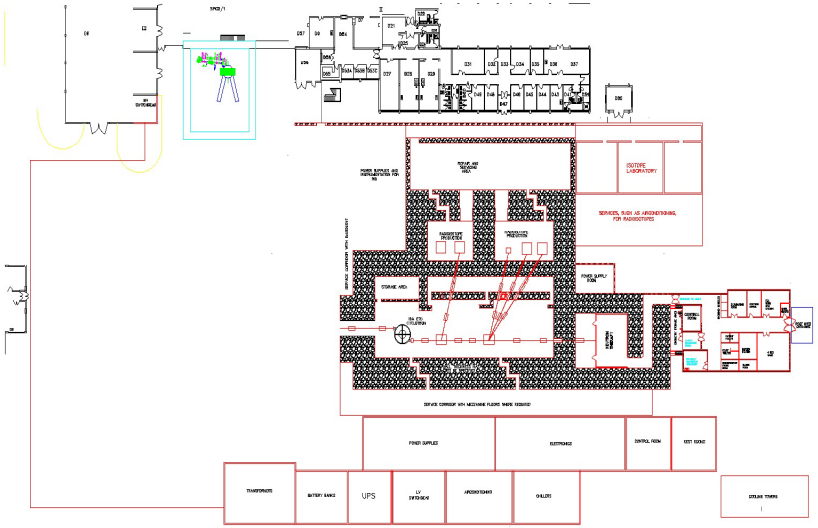

13

Technical pitfalls in the production of ^{64}Cu with high specific activity

J. Rajander[1], J. Schlesinger[1], M. Avila-Rodriguez[1,2] and O. Solin[1]

[1]Turku PET Centre, Turku University and Åbo Akademi University, Finland

[2]Unidad PET/CT-Ciclotrón, Facultad de Medicina, Universidad Nacional Autónoma de México, Mexico-City, Mexico

Introduction

In 2008, we initiated production of ^{64}Cu aiming at high specific activities and high quantities. Routine production of ^{64}Cu as well as the reproducible and economical preparation of the ^{64}Ni target material with ultra-low metal contamination was established. Some technical pitfalls had then to be overcome. We faced a) aggressive corrosion by concentrated acid solutions, b) flaking of the target material during the irradiation, c) contamination of the target material with cooling water, d) formation of insoluble [^{64}Ni]NiO during the irradiation and e) incomplete dissolution of the irradiated target material.

Methods

Using the ^{64}Ni(p,n)^{64}Cu reaction with an optimized beam profile and proton energy (13.0±0.2 MeV), we routinely produce high quantities of ^{64}Cu (10-38 GBq) on our CC 18/9 cyclotron (Efremov Scientific Research Institute of Electrophysical Apparatus, St. Petersburg, Russia) as previously described (Avila-Rodriguez et al., 2008). A semiautomatic processing of the irradiated ^{64}Ni target material and a remote controlled separation of ^{64}Ni and ^{64}Cu has been developed, which yields ^{64}Cu with a high specific activity of 3 TBq/μmol. Using four miniature Geiger-Müller tubes, which are placed within the processing module, we monitor the distribution of activity and control the separation process of ^{64}Cu (Rajander et al., 2009). The recovery of the ^{64}Ni target material and the preparation of the ^{64}Ni electrolyte solution are done in a dedicated rotary evaporator. The computer controlled electrochemical deposition of the ^{64}Ni target material starts with a stepwise increase of the deposition voltage from 2.0 V to 2.5 V within 5 h, followed by a constant voltage of 2.5 V for 40 h.

Results

a) The use of concentrated acid solutions for preparing the ^{64}Ni electrolyte solution as well as for separating ^{64}Ni/^{64}Cu caused serious corrosion problems in the fume hood and in the hot cell. This problem was partly solved by using a closed and remote-controlled module for the processing of the irradiated ^{64}Ni target material, which includes dissolution, separation of ^{64}Ni/^{64}Cu and concentration of the acidic ^{64}Cu fraction. For recovery of the ^{64}Ni target material from the concentrated hydrochloric acid solution, a dedicated rotary evaporator is used inside a fume hood. Acidic vapour from the evaporation process is neutralized by passing the vapours through an alkaline aqueous solution in a flask.

b) Flaking of the ^{64}Ni material from the Au-backing was twice observed during the irradiation. Thus, we included an additional cleaning step for the gold disk in the target preparation procedure. After

cleaning with Deconex®, the gold disk is briefly soaked in 6 M HNO_3 and then rinsed subsequently with DI water to efficiently remove traces of metallic and organic contamination from the gold surface. After this step was included in target processing, no flaking of ^{64}Ni target material from the gold surface during the irradiation has occurred. Also the electroplating process is controlled with a computer program in order to obtain more reproducible results in the target preparation.

c) Due to scratches on the back of the gold disk and thus, insufficient sealing of the O-ring against the cooling water, contamination of the target material with cooling water was twice observed after the irradiation. Due to this, lower specific activities were obtained for ^{64}Cu. In order to solve this problem, the gold disks were henceforth visually inspected and serious scratches were removed by sanding.

d) A first series of targets was irradiated under ambient atmosphere. We then observed twice the formation of insoluble, greenish [^{64}Ni]NiO particles on the target material surface, resulting from an oxidation of ^{64}Ni during the irradiation. In order to avoid oxidation of nickel in the presence of atmospheric oxygen, we henceforth applied a stream of helium on the target material during irradiation. Subsequently, we have not observed formation of [^{64}Ni]NiO.

e) In some cases, a thermal treatment of the irradiated target material with 10 M HCl at 100 °C for 20 min was insufficient to dissolve the target material. This might be a result of a passivation of the ^{64}Ni surface during the irradiation. This problem was solved by applying a stream of helium on the target material during irradiation, and also by extending the period of thermal treatment with concentrated HCl from 20 to 40 min.

Acknowledgement

The study was conducted within the "Finnish Centre of Excellence in Molecular Imaging in Cardiovascular and Metabolic Research" supported by the Academy of Finland, University of Turku, Turku University Hospital and Åbo Akademi University. This work was also supported by the EU-FP7 integrated project BetaImage contract no.: 222980.

References

M.A. Avila-Rodriguez, J. Rajander, S. Johansson, P.O. Eriksson, T. Wickström, S. Vauhkala, E. Kokkomäki, J. Schlesinger, O. Solin, Production of ^{64}Cu on the CC18/9 Cyclotron at TPC, a work in progress, 12th International Workshop on Targetry and Target Chemistry, July 21-24, 2008, Seattle, Washington.

J. Rajander, J. Schlesinger, M. A. Avila-Rodriguez and O. Solin, Increasing specific activity in Cu-64 production by reprocessing the Ni-64 target material, J. Label. Comp. Radioph.**52** (2009) S234

Turku PET Centre

Technical pitfalls in the production of ^{64}Cu with high specific activity

WTTCXIII, Risø, 26-28.7 2010

J. Rajander[1], J. Schlesinger[1], M. Avila-Rodriguez[1,2] and O. Solin[1]

[1] Turku PET Centre, Turku, Finland
[2] Unidad PET/CT-Ciclotrón, Universidad Nacional Autónoma de México, Mexico-City, Mexico

^{64}Cu production

^{64}Cu routine production	• High specific activity • Economical large scale production (>37 GBq)
^{64}Cu-labeling	• High effective specific activity • Post- and prelabeling techniques
Preclinical investigations	• Micro-PET studies *in vivo* • Metabolite analysis • Receptor binding assays
Automated radiosynthesis	• Automated processing/labeling/purification for a future GMP production

Supported by:

Academy of Finland
Research funding and expertise

BetaImage
EU 7th Framework Programme

IAEA
International Atomic Energy Agency

^{64}Cu production

- Reproducible ^{64}Ni-target preparation with ultra-low metal contamination
- Adapted proton energy and beam profile yields ^{64}Cu in high quantities (38 GBq)
- Semiautomated ^{64}Ni/^{64}Cu separation yields ^{64}Cu with high specific activity (3000 GBq/μmol)
- Recycling of ^{64}Ni for an economical ^{64}Cu production (95% recovery rate)

Technical pitfalls

- aggressive corrosion by concentrated acid solutions
- flaking of the target material during the irradiation
- contamination of the target material with cooling water
- formation of insoluble [^{64}Ni]NiO during the irradiation
- incomplete dissolution of the irradiated target material

Corrosion in the fume hood

Flaking of the target material from the gold backing

Cooling water leakage

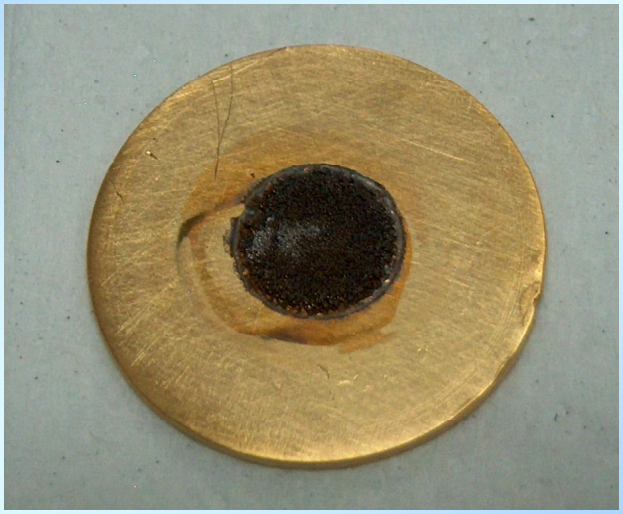

Insoluble NiO on the gold disc

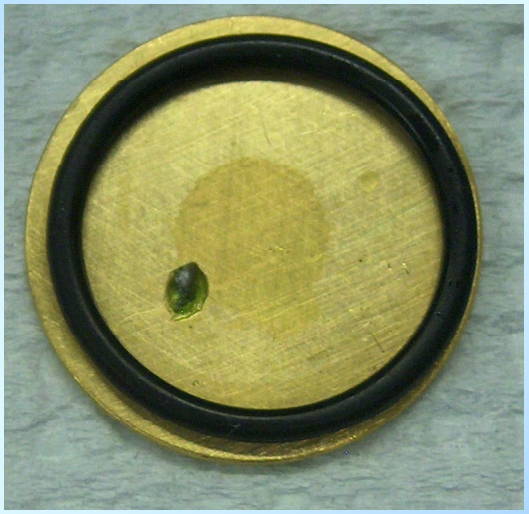

Target holder

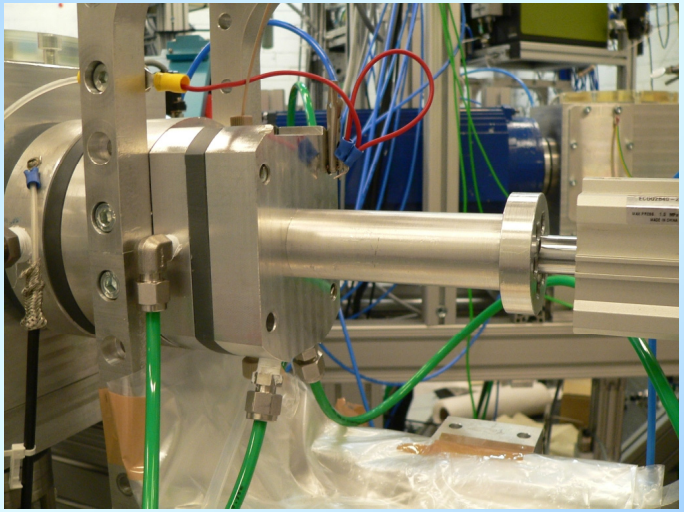

WTTC XIII – Presentation Discussions

1. Problems in Cu production
   - Hotcell oxidation/corrosion caused by acidic environment

2. Target material
   - Gold?
     - NiO found in gold, but removable by He flux
   - Silver?
     - Rust, impurities if not very high quality silver
   - Gold coating?
     - Scratching can be a problem
   - Rhodium?
     - Easy to plate, hard, no problems found by users

3. Energy degradation on target?
   - Just to 13 MeV

Supported Foil Solution for Legacy Helium-Cooled Targets When An Alternative to Havar Foil Material is Desired

Benjamin R Bender and G. Leonard Watkins

PET Imaging Center, University of Iowa Health Care, Iowa City, IA 52242, USA

For any given radionuclide target system, the choice of targetry is often made as a compromise between Quantity and Quality. Quantity refers primarily to higher target yield or in the case of smaller volumes, higher specific activity. Quality, for the purpose of this discussion, refers to radionuclidic and chemical purity. Most recent target system design innovations have been driven by the need for increased target yield per run. In no application is this more evident than in the evolving design of ^{18}F targetry [Eriksson, et al; Zyuzin, et al]. This pursuit of "quantity" has resulted in numerous target design innovations. Most notable are improvements in target geometry, optimization of target cooling thermodynamics and designs modifications intended to reduce proton beam loss due to interceding structures and foils. But for those facilities whose overall production does not require target yields beyond a few Curies, the helium-cooled, two-foil target systems (fig 1) have remained in service, even if only for backup or research ^{18}F production. These legacy targets are characterized as having two foils along the beam path terminating in the target volume (gas or liquid). The front foil separates the tank vacuum from a helium cooling flange. The back foil separates the helium cooling flange from the target volume chamber.

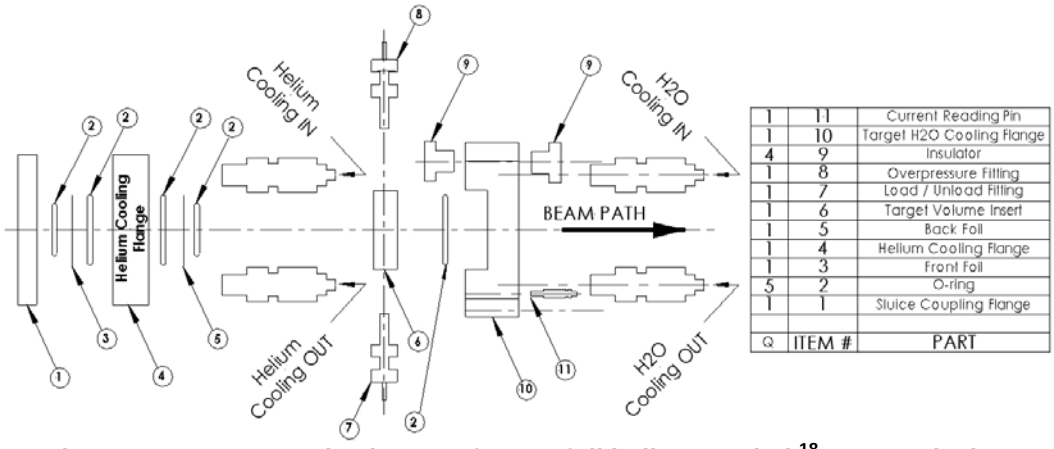

Figure 1. Representative image of a two-foil helium-cooled ^{18}F target design.

Our facility produces ^{18}F and other radionuclides solely for our own clinical and research needs; thus our production needs are modest. But to satisfy our low-level research production needs while also improving the yield of our low-efficiency radiopharmaceutical syntheses (eg. [^{18}F]FLT) we have directed our targetry efforts towards reduction of radionuclidic and chemical impurities. Regardless of target type, improvement in product purity may have significant implications to the efficiency of radiopharmaceutical syntheses as well as patient/participant dosimetry. To achieve this we have retrofitted our two-foil ^{18}F target to utilize Niobium for both the back foil (0.003" thick) and the body material of the target volume chamber [Nye, et al]. The significantly lower strength of Niobium when compared to Havar for the back foil presented an additional hurdle to the retrofit. Additionally, local heating of the Niobium foil by the proton beam further threatens its ability to perform without failure. To address these issues we opted to include another modern target feature, the grid support.

This became the evolution of our novel retrofit grid support solution (fig 2). Support grids in modern targetry are generally made from copper or aluminum and cooled by the same water that cools the target volume chamber. This observation brings to light the final hurdle in our design – grid cooling. The solution is the existing Helium cooling system, but since a grid support, placed to support the Niobium foil, would block the flow of the Helium cooling, the grid must be modified. Therefore, we have included a vent hole through the grid perpendicular to the beam path to allow helium flow which now becomes the grid cooling mechanism of this retrofit design.

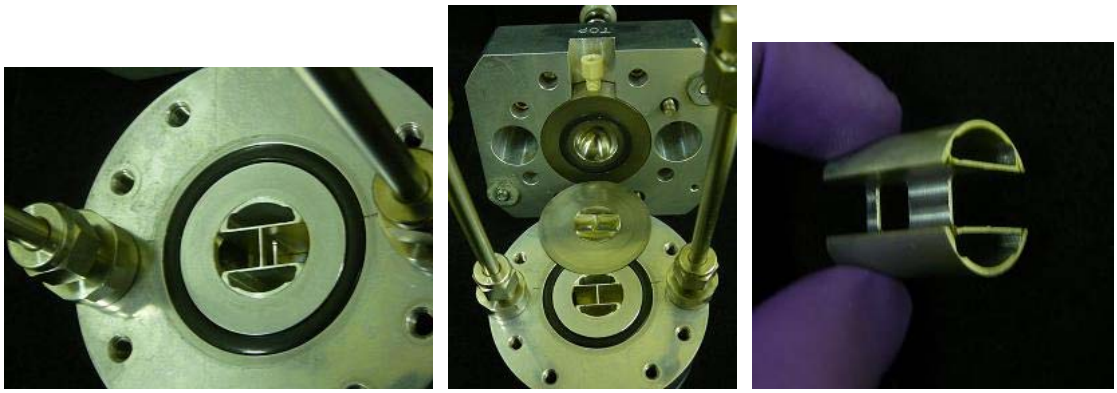

Figure 2. Foil Support Grid representation and placement.

The primary benefit of this design is its low cost. Commercially available targets may cost as much as $50,000, but the direct cost for this design was less than $3,000 for materials and machining. To achieve this inexpensive solution, the aluminum grid foil support we designed requires only that the beam aperture in the helium flange be widened slightly to hold the grid support captive. Additionally, this grid support can be fabricated using standard machining practices and a simpler rectangular grid design. This significantly reduced the expense when compared to the commercial copper or aluminum hex-grid supports which utilize a more expensive EDM machining technology.

A second benefit of this design is its ease of incorporation into the existing target. It may be either slipped or press fit into the widened Helium flange beam aperture.

Yet a third benefit is the utilization of the existing Helium cooling. Where previously the Helium flow was directed to cool both the front and back foils, that flow will now pass through the vented support grid to conduct its heat away. Because the grid is in direct contact with the back foil, it also acts as a heat sink to conduct heat away from the localized point where proton beam heating may weaken it. Also, because we utilize the existing helium cooling, it need not be defeated as a target interlock, as it is on many older cyclotrons. And lastly, there is no need to make additional modifications to the target to cool the grid using the water cooling system as is common in the commercially available systems.

As a final site specific benefit, our older, self-designed target allows easy replacement of the target insert (ie. the target load chamber). This has allowed us to very easily convert this target at any time for the in-target production of [^{13}N]Ammonia [Krasikova, et al] by simply replacing the Niobium insert and foils with Aluminum versions of each and overpressuring with CH_4. Without the support grid, it would likely be impractical to use such thin (0.005" thick) aluminum foils, as they would be far too weak.

In conclusion, this grid foil support design is an economical solution allowing the use of more chemically advantageous, though weaker, foils materials while easily maintaining integrity, even with overpressure in excess of 300 psi. Additionally, no negative impact on the overall yield of the target was observed.

Acknowledgement: University of Iowa Medical Instruments shop and Tim Weaver for design support.

References:

T Eriksson, J Norling, R S Ererl, M Husnu & R Chicoine. "Experiences from using a PETrace cyclotron at 130 µA (2 x 65 µA) with niobium targets producing $^{18}F^-$/FDG.". *Abstract Book: 12th International Workshop on Targetry and Target Chemistry, Seattle,* 2008: pp14-15.

A Zyuzin, E van Lier, R Johnson, J Burbee & J Wilson. "High Current F-18 Water Target with Liquid Spray-Cooled Window". *Abstract Book: 12th International Workshop on Targetry and Target Chemistry, Seattle,* 2008: pp16-18.

JA Nye, MA Avila-Rodriguez & RJ Nickles. "A grid-mounted niobium body target for the production of reactive [^{18}F]fluoride". *Appl. Radiat. Isot.* (2006);64:536-539

RN Krasikova, OS Fedorova, MV Korsakov, B Landmeier Bennington & MS Berridge. "Improved [^{13}N]ammonia yield from the proton irradiation of water using methane gas". *Appl. Radiat. Isot.* (1999);51: 395-401

UNIVERSITY of IOWA HOSPITALS & CLINICS
University of Iowa Health Care

Supported Foil Solution for Legacy Helium-Cooled Targets When An Alternative to Havar Foil Material is Desired

Benjamin R Bender , G. Leonard Watkins

University of Iowa Health Care, Iowa City, Iowa, USA

UNIVERSITY of IOWA HOSPITALS & CLINICS
University of Iowa Health Care

Introduction

Target Selection Criteria

Quantity:
- Higher Target Yields
- Higher Specific Activity

Quality:
- Reduced radionuclidic & nonradionuclidic impurities

UNIVERSITY of IOWA HOSPITALS & CLINICS
University of Iowa Health Care

Introduction

Target Improvements

Quantity:
- Better Target Geometry
- Better Target Cooling
- Fewer Target Foils

Quality:
- Purer Target Load Material
- More Chemically Compatible Target & Foil Materials

UNIVERSITY of IOWA HOSPITALS & CLINICS
University of Iowa Health Care

Introduction

Target Choice

Quantity: (newer target designs) [Eriksson, et al; Zyuzin, et al]
- Commercial Radionuclide Production Facilities
- High Volume In-House Clinical Needs
- Higher Synthesis Production
  - for low-efficiency radiopharmaceutical syntheses
    *** (start with more ==> end with more)*

Quality: (modify existing target)
- Higher Synthesis Production
  - for low-efficiency radiopharmaceutical syntheses
    *** (start with more ==> end with more)*
  - improves efficiency in any synthesis where havar metal ions compete

Introduction

UNIVERSITY of IOWA HOSPITALS & CLINICS
University of Iowa Health Care

Application

Using Two-Foil Target for Research & Backup Clinical Production

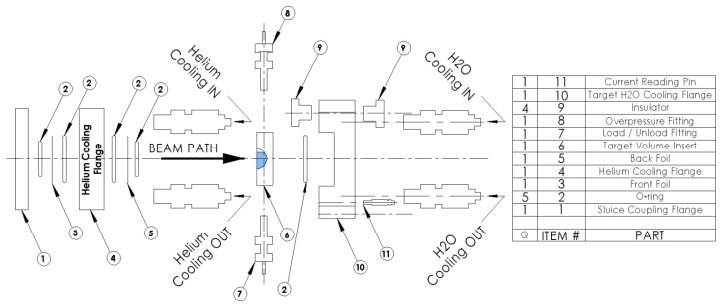

Design Development

UNIVERSITY of IOWA HOSPITALS & CLINICS
University of Iowa Health Care

Application

Problem #1:

- Havar Foils Leave Problematic Contaminants
  ex. [^{18}F]FDG and [^{18}F]FLT syntheses

Solution:

- Niobium Foil Instead of Havar [Nye, et al]
  Niobium target body is also preferred

Problem #2:

- Niobium Is Much Weaker Than Havar

Solution:

- Grid Support for Target Foil
- Thicker Foil

Material	Tensile Strength (MPa)
Havar	1860
Niobium	585
Aluminum	190

Design Development

UNIVERSITY of IOWA HOSPITALS & CLINICS
University of Iowa Health Care

Grid Support Design

Grid Geometry:

- Designed So Grid Walls Avoid Beam
- Outer Walls are Outside Target Aperature
  - Helium flange aperture slightly widened

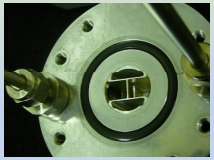

Quality:

- Purer Target Load Material
- More Chemically Compatible Target & Foil Materials

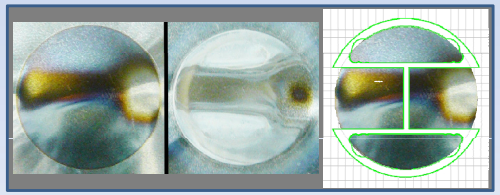

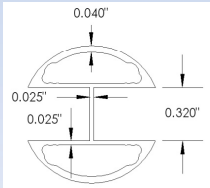

Design Development

UNIVERSITY of IOWA HOSPITALS & CLINICS
University of Iowa Health Care

Grid Support Design

Grid Cooling:

- Conductive Cooling of Target Foil
- Existing Helium System Left Intact
  - Helium flow-through holes
  - Convective cooling of both foils & grid

Target Foil End
(back foil)

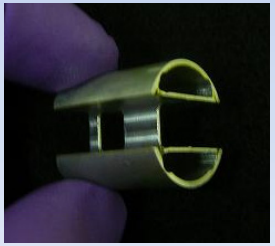

Vacuum Foil End
(front foil)

Results

Foil Considerations

Stopping Power:

- Havar = ~ 157 MeV/cm [Shiomi-Tsuda, et al] **extrapolated*
- Niobium = ~ 144 MeV/cm [Burkig, et al] **based on Al comparative data collected @ 19.8 MeV*
- Aluminum = 60.6 MeV/cm [Janni]

Beam Energy Loss:

Material	Thickness	Beam Energy Loss (keV)
Havar	0.001”	~ 400
Niobium	0.002”	~ 730
	0.003”	~ 1095
Aluminum	0.005”	770

Results

Foil Considerations

Burst Pressure:

Material	Thickness	Burst Pressure (psi) w/ Grid	Burst Pressure (psi) w/o Grid
Havar	0.001”	> 530	360
Niobium	0.002”	300	150
	0.003”	> 530	280
Aluminum	0.005”	430	190

Results

Foil Considerations

Thermal Conductivity:

- Better Heat Transfer to Grid
- Reduced Localized $[^{18}O]H_2O$ boiling
  - Better nuclide conversion

Material	Thermal Conductivity (W/m*K)
Havar	14.7
Niobium	53.7
Aluminum	237.0

Other:

- Niobium-Coated Havar
  - Difficult to get
  - Havar contamination leak-through
  - Delamination

Results

Beam Transmission

Beam Current Blocked by Grid:

- Calculated 3.5%
  ** Assumes beam homogeneity between upper & lower horizontal grid walls*
- Measured < 2.5%
  ** Reflects the 2.5% beam current reading resolution @ 20 uA*

Conclusions

UNIVERSITY of IOWA HOSPITALS & CLINICS
University of Iowa Health Care

Benefits of Grid Design

Cost:

- Low-Cost Machining Techniques Used
  - *vs expensive EDM machining methods used for hex grid in commercial targets*
- Modification Far More Inexpensive Than New Target

Ease of Implementation:

- Simple Design
- Grid Fits in Helium Flange with Slip- or Press-Fit
- Target Not Significantly Modified

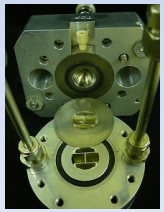

Conclusions

UNIVERSITY of IOWA HOSPITALS & CLINICS
University of Iowa Health Care

Benefits of Grid Design

Better Foil Cooling:

- Conducitve Cooling of Foil *(by contact with grid)*
- Retains Helium Convective Foil Cooling

Adaptation of Design:

- Can Be Adapted to Other Target Types
  - *like [^{13}N]Ammonia [Krasikova, et al] using Al foil & Al target body*

Other:

- Early Testing Shows no Discernable Effect on Production Yields

UNIVERSITY of IOWA HOSPITALS & CLINICS
University of Iowa Health Care

References

T Eriksson, J Norling, RS Ererl, M Husnu & R Chicoine. "Experiences from using a PETrace cyclotron at 130 µA (2 x 65 µA) with niobium targets producing ^{18}F$^-$/FDG". *Abstract Book: 12th International Workshop on Targetry and Target Chemistry, Seattle,* 2008: pp14-15.

A Zyuzin, E van Lier, R Johnson, J Burbee & J Wilson. "High Current F-18 Water Target with Liquid Spray-Cooled Window". *Abstract Book: 12th International Workshop on Targetry and Target Chemistry, Seattle.* (2008): pp16-18.

JA Nye, MA Avila-Rodriguez & RJ Nickles. "A grid-mounted niobium body target for the production of reactive [^{18}F]fluoride". *Appl. Radiat. Isot.* (2006);64:536-539

RN Krasikova, OS Fedorova, MV Korsakov, B Landmeier Bennington & MS Berridge. "Improved [^{13}N]ammonia yield from the proton irradiation of water using methane gas". *Appl. Radiat. Isot.* (1999);51: 395-401

JF Janni,. AFWL-TR-65-150. Kirtland Air Force Base Technical Rep. (1966); (unpublished)

VC Burkig, KR MacKenzie. "Stopping Power of Some Metallic Elements for 19.8-MeV Protons" Physical Review (1957); Vol. 106, No. 5: 848 – 851

N Shiomi-Tsuda, N Sakamoto, H Ogawa, M Tanaka, T Goto, Y Nagata. "Stopping powers of havar for protons from 4.0 to 13.0 MeV". Nuclear Instruments and Methods in Physics Research: (1996); B 117: 343 – 346

WTTC XIII – Presentation Discussions

1. Which one is the best foil?
   - Ni vs. Havar: no yield difference
   - Careful with impurities in foil material
   - Ti can be used, Va trapped in Sep-pak
   - Niobium-Havar preferred to Niobium-Niobium (experience)

A Simple Target Modification to Allow for 3-D Beam Tuning

J.S. Wilson, K. Gagnon and S.A. McQuarrie

Edmonton PET Centre, Cross Cancer Institute, University of Alberta, Edmonton, AB, CANADA

Introduction: The TR19/9 cyclotron at the Edmonton PET Centre (EPC) is a variable energy machine with a proton beam energy range from 13 to 19 MeV and a deuteron beam energy range from 6.5 to 9 MeV. The energy and trajectory of the extracted beam is determined by the orbital at which the beam is intercepted by the extractor foil and it is essential, especially with the longer gas targets, that the beam is being directed down the centre of the target. To ensure optimal beam alignment, more feedback on the angle of beam entry to the target was desired than could be offered by the 2 dimensional target port collimators.

Aim: To provide a means of monitoring the beam position during normal operation. This would allow for interactive real-time target alignment to assure that the beam is centred on target.

Methods: The nosepiece of the target was lengthened to provide a 1 cm cylindrical beam port extending 5 cm prior to the target body. (Extended nosepiece with current pickup and original nosepiece, pictured opposite) The nosepiece was fabricated from anodized aluminum so that with insulated attachment, electrical isolation from the target body was possible. Use of insulated bolts and plastic washers during target assembly enabled separate current pick-ups to be attached to the target body and the nosepiece.

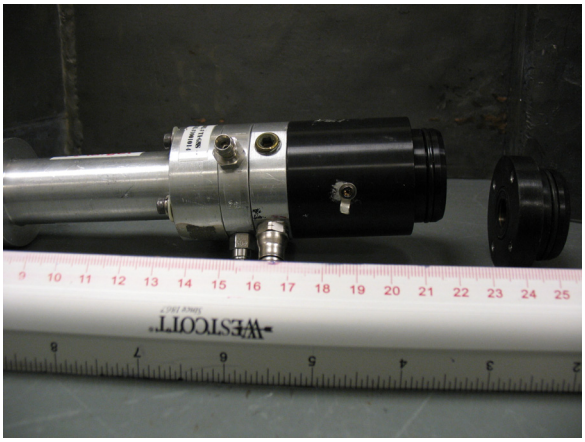

A solid target plate was prepared which had a hole drilled in the top to allow a temperature probe to be inserted to the middle of the plate. This enabled the temperature of the target plate to be monitored between the beam spot and the water cooling on the back of the plate.

Results: Beam alignment was easily achieved on gas targets equipped with the extended nosepiece and the irradiation pressure was readily optimized on true aligned conditions. The effect of varying different ion source, radiofrequency and magnet parameters was also readily observed and all while the beam was at maximum normal operating specifications.

Solid target irradiation (no nosepiece present): We found a very linear relationship between the beam current and the target plate temperature. It became increasingly difficult, however, to maintain this linear relationship at higher beam currents indicating that the registered beam was not hitting the plate. As beam spread is more pronounced at higher currents, it is probable that the 1 cm target aperture was no longer accommodating the entire beam. Use of an isolated nosepiece would maintain alignment and show at what point maximum beam on target had been reached.

Recently the nosepiece has been put onto the high current water targets and we will be evaluating the saturated yields vs observed nosepiece currents to determine the extent of beam expansion.

Conclusions: The isolated nosepiece allows for facile beam tuning and gives useful real time information on beam size and alignment.

A Simple Target Modification to Allow for 3-D Beam Tuning

John Wilson
Edmonton PET Centre
Edmonton, AB, Canada

TR 19/9 Cyclotron

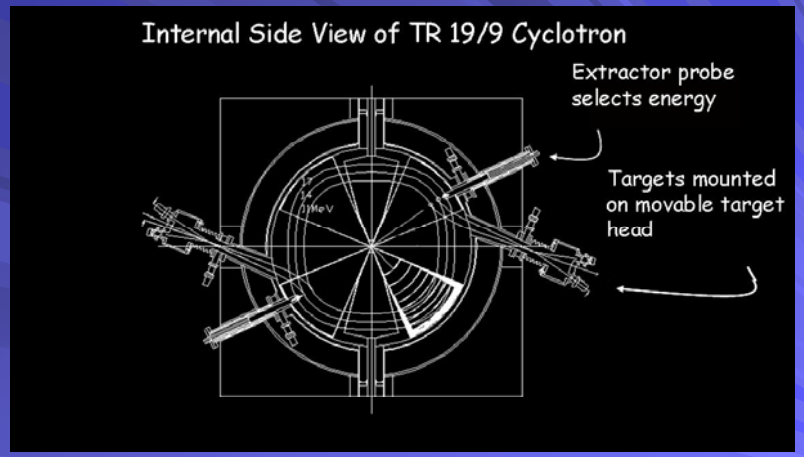

Variable energy extraction determined by depth of extractor probe

Beam Extraction

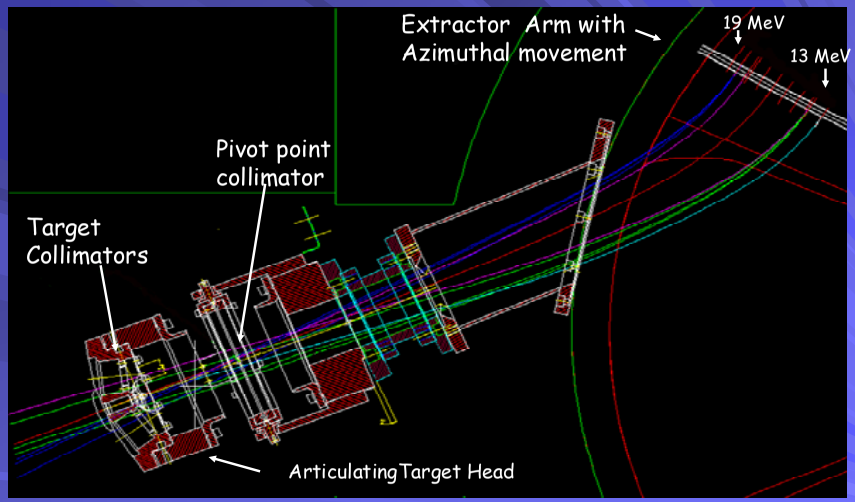

Beam trajectory related to extractor depth

Beam Extraction

Beam trajectory affected by:

- Extractor depth
- Azimuthal angle of extractor
- Extractor foil condition
- Magnetic field (temperature)
- Ion source parameters

Beam Collimation

- Pivot point and target collimators are divided into 4 sectors each with separate current pickup
- Both have a 1 cm circular aperture
- 12 cm between the 2 collimators
- Sufficient beam position monitoring?

Extended Isolated Nosepiece

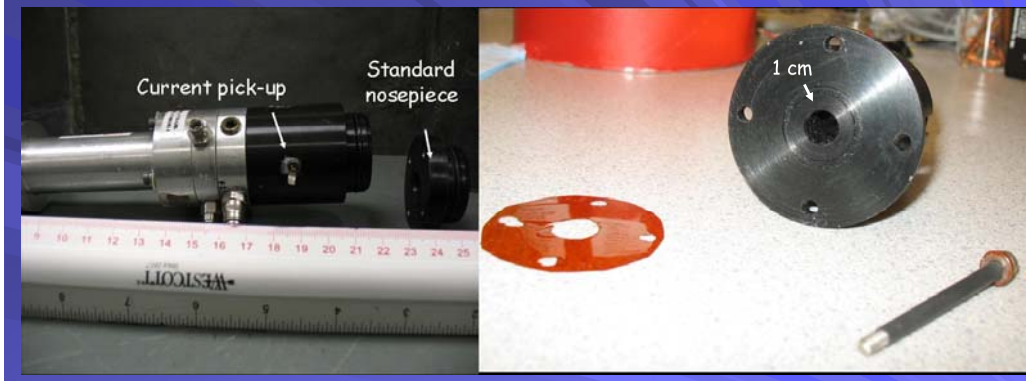

- Target nosepiece extended from 1 cm to 5 cm in length with 1 cm cylindrical hole
- Anodized aluminum for electrical isolation
- Two current pickups used

Extended Nosepiece

- Intended for gas targets to provide more space at target head and to confirm target alignment.
- the effect of varying different ion source, radiofrequency and magnet parameters was also readily observed and all while the beam was at maximum normal operating specifications.
- All targets were subsequently fitted with the extension

Results

- C-11 gas target ruptured
  - Maximized pressure on slightly misaligned target
- Water targets were fairly aligned.
  - routine saturated yield determination
- Beam alignment fast and accurate
- Pressure maximization

Solid targets

- No pressure indicator
- linear relationship between the beam current and the target plate temperature.
- linear relationship not maintained at higher beam currents (100 uA) indicating that not all registered beam was not hitting the plate.
- He window temperature rise

Solid Target Conclusions

- Over collimation results in beam loss.
  - Higher intensity beams – larger not smaller collimator apertures
- Solid target beam indicators desirable at low current, critical at high currents
- Electrically isolated, water cooled, He window best option?

Pivot Point Collimator

Evolution of a High Yield Gas Phase $^{11}CH_3I$ Rig at LBNL

James P. O'Neil, James Powell, Mustafa Janabi
Biomedical Isotope Facility, Lawrence Berkeley National Laboratory, Berkeley CA USA

After working with a home built "wet method" [^{11}C]methyl iodide system for a number of years, an effort was made towards the in-house development of a gas phase rig. This began with personal communication and visits to both TRIUMF and the University of Washington, Seattle PET centers for many helpful discussions, photos, drawings and hints that only years of experience can provide. The culmination of this was the construction of a first iteration single pass, gas phase [^{11}C]methyl iodide system that closely resembled the Seattle system described by Link[1].

The Biomedical Isotope Facility (BIF) at the Lawrence Berkeley National Laboratory houses the prototype CTI RDS111 (E_{proton} = 11MeV) negative ion cyclotron. We run an original 7mL aluminum-body target filled to 300psi with 1% O_2/N_2 to produce [^{11}C]CO_2. Typical production irradiations are 40 minutes in duration at 35uA beam current and provide on average 1.5Ci of [^{11}C]CO_2 that is most often converted to [^{11}C]CH_3I. Operation of the [^{11}C]CH_3I system is as follows: (a) Post irradiation, target gas is rapidly unloaded through a Carbosphere trap (60-80 mesh, 1.4g) at room temperature. Discussions with Bruce Mock led us to choose this trapping medium over molecular sieves for the chromatographic properties providing trapping of the [^{11}C]CO_2 and separation from target gas and side products. (b) After static heating of the trap to >80°C, the trap is swept with helium (50mL/min) and combined with hydrogen (50mL/min). (c) The mixture is passed through a heated (400°C) nickel catalyst (Harshaw) and the resulting [^{11}C]CH_4 is trapped on a PoroPak-Q trap (100mg in aluminum u-tube, 2mm id x 90mm tall) at -196°C. (d) The [^{11}C]CH_4 is released by raising the trap from the liq-N_2 dewar and flushing with helium (80mL/min) directing the gas stream through a quartz reaction tube (10mm id x 350mm). The head of the tube is packed with solid iodine that is heated to provide I_2 vapor which mixes with incoming [^{11}C]CH_4 and is pushed further downstream into a high temperature segment (100mm long) where conversion takes place. (e) The resulting [^{11}C]CH_3I exits the quartz reactor, is passed through a dry ascarite column (7mm id x 150mm), and is trapped on a glass test tube (4mm id x 50mm) immersed in liq-N_2.

Single-Pass Optimization

Significant optimization of the single pass system was initially required to generate useable yields and purity of [^{11}C]CH_3I. There are primarily three parameters that govern the overall conversion of [^{11}C]CH_4 to [^{11}C]CH_3I in the system, namely: (1) Iodine oven temperature (I_2 concentration); (2) flow through the reactor tube (residence time); and (3) temperature of the reactor (energy potential). These three factors are highly interdependent, thus changing any one parameter requires a re-optimization of the other two. For example, higher quartz tube (reactor) temperatures may require a faster flow rate and lower iodine oven temperature to decrease the co-production of [^{11}C]CH_2I_2 and maintain [^{11}C]CH_3I yield. Through this process we experimentally determined a push gas flow of 80mL/min and I_2 oven temperature of 70°C and then re-explored a range of reactor temperatures. Over a range of 625-775°C, the undesired production

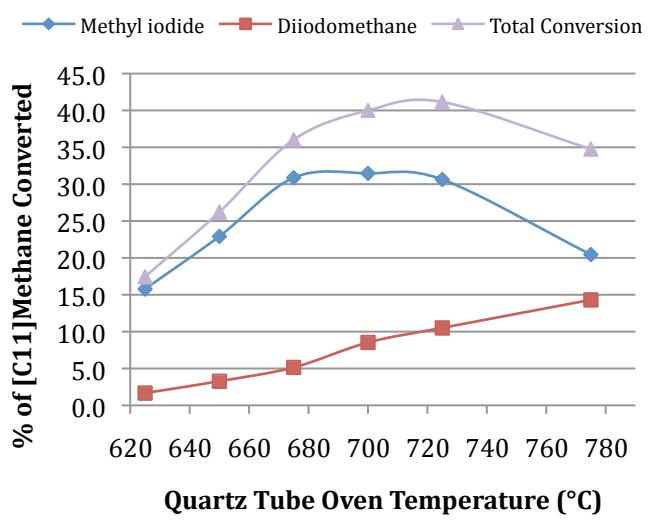

Figure 1: Optimization of reaction temperature for single pass conversion with flow at 80 mL/min and I_2 oven at 70°C.

of [^{11}C]CH_2I_2 increased linearly from 1.5-15%. Over the same temperature range (625-775°C), [^{11}C]CH_3I yield started at 15.5%, peaked at 32% (680°C) and fell back to 21%. Total conversion of methane to iodinated species followed a similar curve as shown in **Figure 1**. Consistent yields of 25-30% were realized for production runs for a number of months.

Recirculation System In order to increase the conversion yield we installed a recirculation pump in the system, passing the unconverted [^{11}C]CH_4 back to the reactor as described by Larsen[2]. In addition, we have separated the conversion oven from the [^{11}C]CH_4 and [^{11}C]CH_3I trapping station allowing vertical placement on the hotcell side wall thus saving space. At the exit of the oven, a vortex chiller (-8°C) rapidly condenses I_2 vapor ensuring nearly complete iodine recovery. Other refinements to the system include a low mass Kapton resistive heater on the I_2 reservoir and a LED/photodiode based I_2 concentration detector.

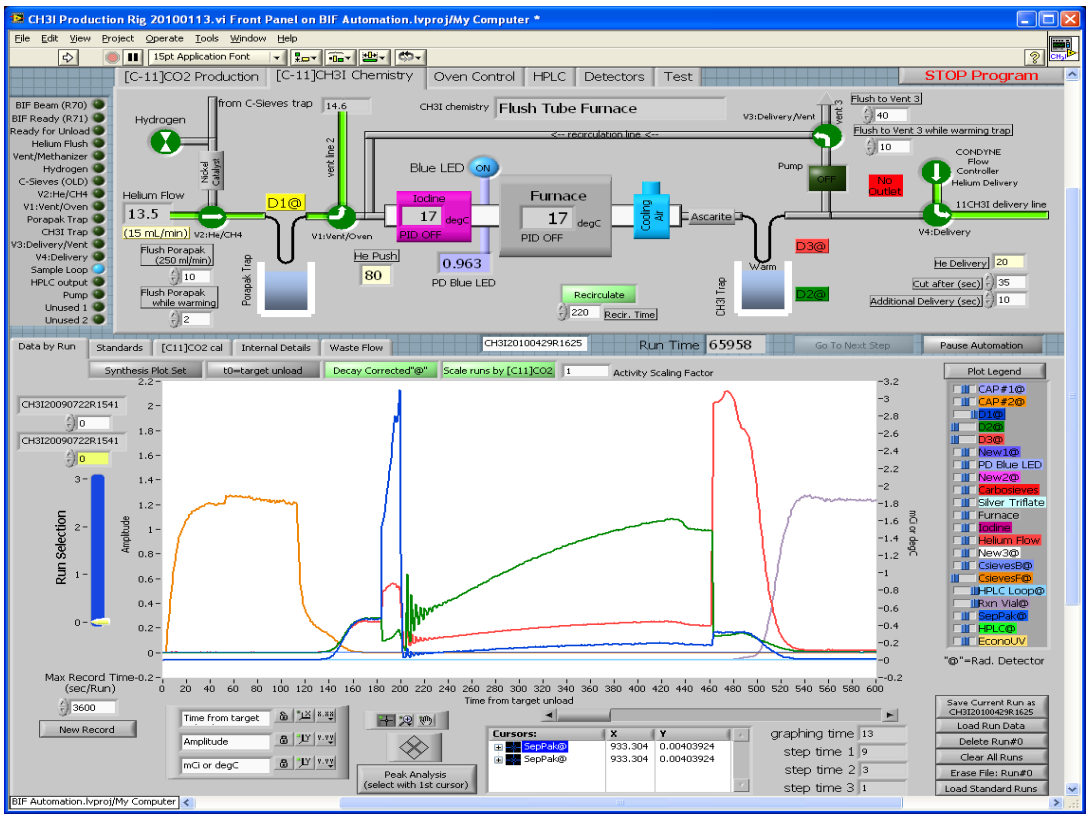

Figure 2: Screenshot of LabVIEW based software control panel on BIF methyl iodide rig.

With very little modification to either equipment or parameters we were able to realize a significant gain in conversion yield as compared to the single-pass setup. Optimized conditions provide 64-73% decay corrected yield of [^{11}C]CH_3I based on trapped [^{11}C]CO_2 with >98% purity. The high purity is attributed to cryogenically trapping the iodinated methane in a glass loop, releasing the [^{11}C]CH_3I while the glass warms, and recooling the glass before the [^{11}C]CH_2I_2 is pushed to the reaction vial.

Over the past 5 years we have seen 50-60% conversions on a daily basis. Maintenance is minimized by having the [^{11}C]CH_4 Poropak trap outside of the recirculation path, trapping iodine at -8°C, and cold trapping the [^{11}C]CH_3I on a glass trap. We have routinely used this system to produce a variety of [^{11}C] labeled PET tracers at or above literature yields and high specific activity (5-12Ci/umol eos).

References:

[1] Link, J., Krohn, K., Clark, J., 1997. Production of [^{11}C]CH_3I by Single Pass Reaction of [^{11}C]CH_4 with I_2. Nucl. Med. Biol. 24, 93-97

[2] Larsen, P., Ulin, J., Dahlstrom, K., Jensen, M., 1997. Synthesis of C-11 iodomethane by iodination of C-11 methane. Appl. Radiat. Isot. 48, 153-157

Evolution of a High Yield Gas Phase $^{11}CH_3I$ Rig at LBNL

James P. O'Neil, James Powell, Mustafa Janabi

Biomedical Isotope Facility, Lawrence Berkeley National Laboratory, Berkeley CA USA

Background

Biomedical Isotope Facility, Lawrence Berkeley National Laboratories

Prototype CTI RDS111 Cyclotron

Original aluminum bodied 7 mL internal volume CO_2 target

Tried our hands a decade ago at wet method methyl Iodide

After discovery trips to Seattle and Vancouver a gas phase rig established
take home message…go to the experts/experienced for advice
…avoid same mistakes they made starting up

Original system single pass modeled after Link's work
optimized for these conditions

LBNL Single Pass Gas Phase Methyl Iodide Rig circa 2004

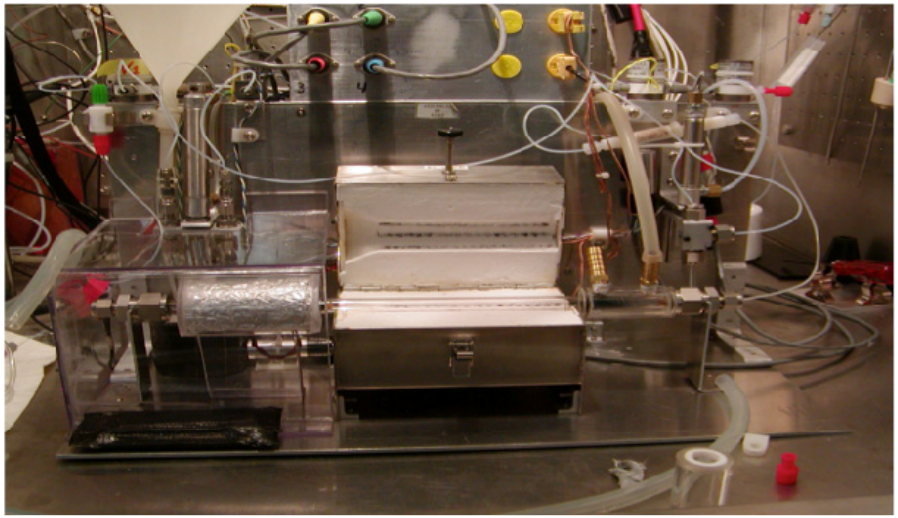

CO_2–Crb Sv–H_2/Ni-PPQ–He–Push–I_2–Heat–Glass/liq N_2–Release–Cool

Link, J., Krohn, K., Clark, J., 1997. Production of $[^{11}C]CH_3I$ by Single Pass Reaction of $[^{11}C]CH_4$ with I_2. Nucl. Med. Biol. 24, 93-97

LBNL Single Pass Gas Phase Methyl Iodide Rig Production Optimization

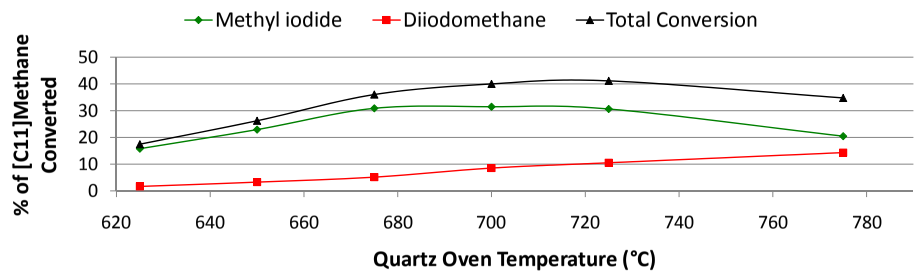

Optimization of $[^{11}C]CH_4$ to $[^{11}C]CH_3I$ conversion in single-pass mode

For a fixed flow rate the production of $[^{11}C]CH_2I_2$ increases steadily

At higher temperature $[^{11}C]CH_3I$ production yield drops rapidly

Conversion to Recirculation

Added KNF micro-diaphragm Pump

CH_4 trap left out of recirculation loop to avoid contamination/trapping of CH_3I

Re-Optimized parameters

- Flow limited by pump capacity (500 mL/min)
- Lower iodine concentration and oven temperature

System separation

Split system for space utility

- cold trap, valves, recirculating pump
- ovens, iodine detector, ascarite trap
  - vertically mounted oven board on cave wall

LBNL Recirculating Path Gas Phase Methyl Iodide Rig

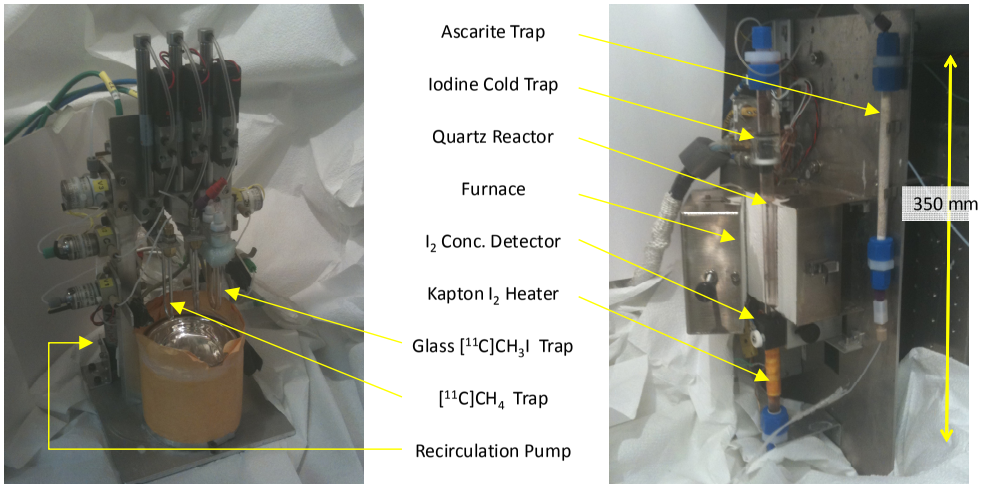

Sequence of Operation as seen by Radiation Detectors

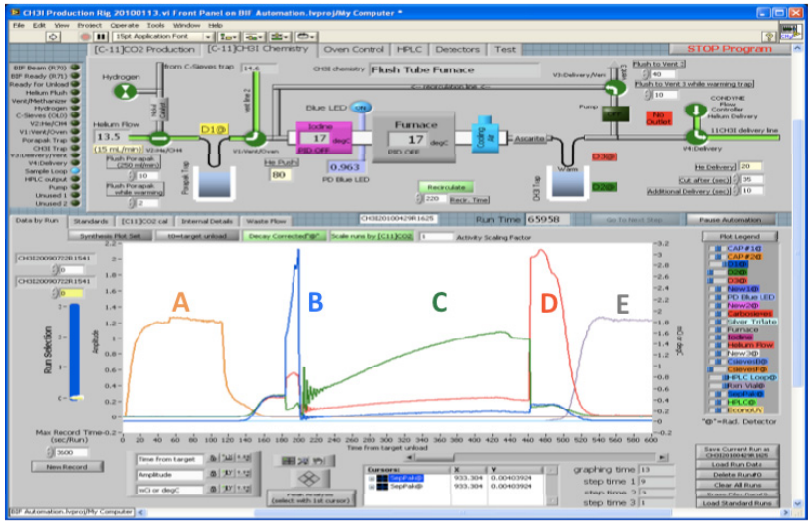

National Instruments FieldPoint Hardware
LabVIEW Software
Time, Temperature and Activity control

Importance of Optimization, Consistency, and Pumping Speed

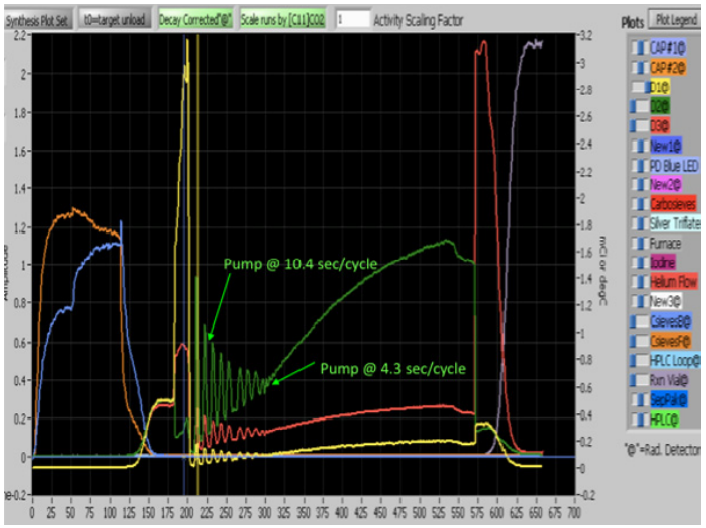

For an optimized set of parameters it is important to maintain consistency

LED – Photo Diode Based Iodine Concentration Detector

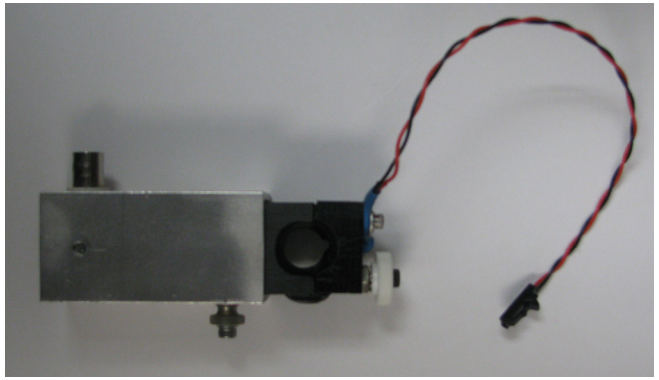

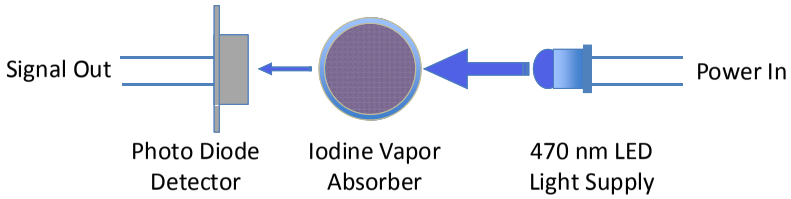

Iodine Concentration Adjustment

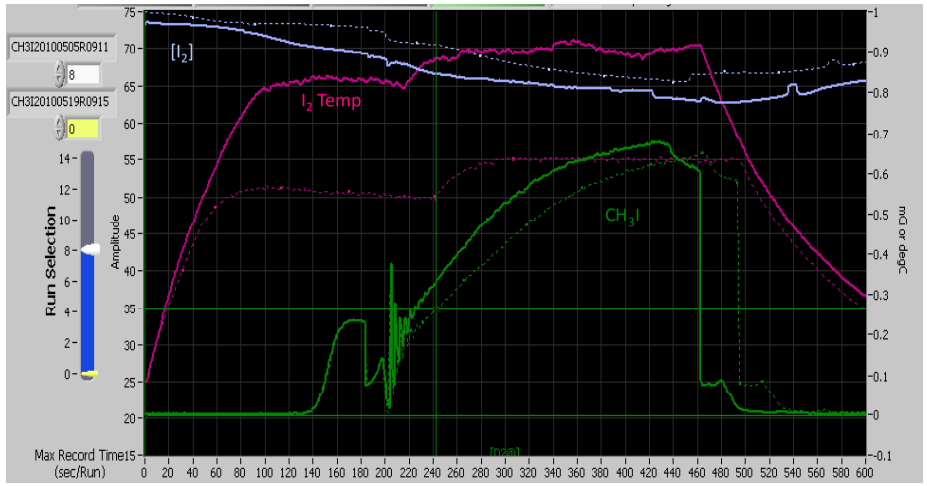

Relatively Consistent Iodine Concentration can be Maintained >25 runs

hatched line run = 3 *solid line run = 27*

Vortex Chiller as Iodine Trap Cooler

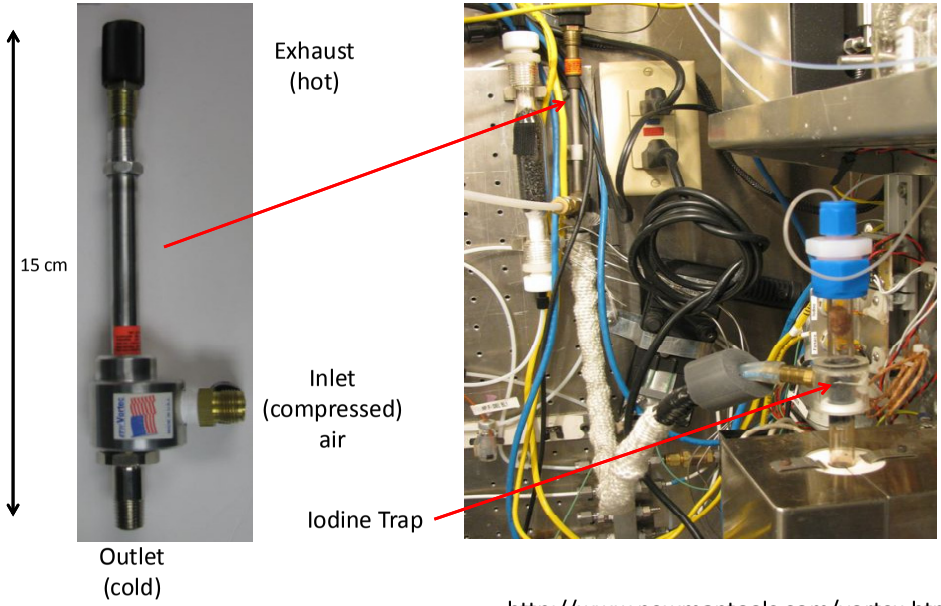

http://www.newmantools.com/vortex.htm

Summary

Key system attributes and components for success:

- low system volume…less contact, more passes, milder reaction conditions
- monitoring iodine concentration quick adjustments
  - low cost LED based absorbance detector
- efficient post oven iodine trapping…reuse of iodine
  - iodine reuse very important for purity
- system separation
  - free up hotcell floor space for chemistry and other clutter

The Numbers

System volume	25-30 mL recirculating path
Recirculation time	4 – 5 sec per pass (3.8 min)
Runs between I_2 driveback	25-30
Time of production	9 min EOB to CH_3I complete delivery
Typical conversion yield (CO_2–CH_3I)	55-65% dc 10 min
Typical tracer specific activities	5-20 Ci/umole (1.5 Ci CO_2)

WTTC XIII – Presentation Discussions

1. System can (also) do, at environment temperature
   - Methane triflate
   - Raclopride

2. System performance
   - Running consistently = better performance on specific activity
   - After long stop, run cold couple of times before going hot

One Year Experience With a IBA 18/9 Cyclotron Operation for F-18 FDG Rutin Production

Nicolini J; Ciliberto J; Nicolini M A; Nicolini M E; Baró G; Casale G; Caro R; Guerrero G; Hormigo C; Gutiérrez H; Pace P; Silva L

Laboratorios Bacon S.A.I.C. Ururuguay 136 –B1603DFD- Villa Martelli, Bs. As. Argentina

This paper tries to encourage those countries that still do not have an industrial production system to supply FDG to PET centers. We show a compilation of performance data, maintenance and production yield. With the statistical analysis of these data we conclude that the whole system is robust and effective. This work also shows graphic performance of the ion source before and after maintenance and repositioning, and also performance of targets and chemical process yields. we include the layout of the installation which was designed to have visual control of the important areas from the control room of the cyclotron.

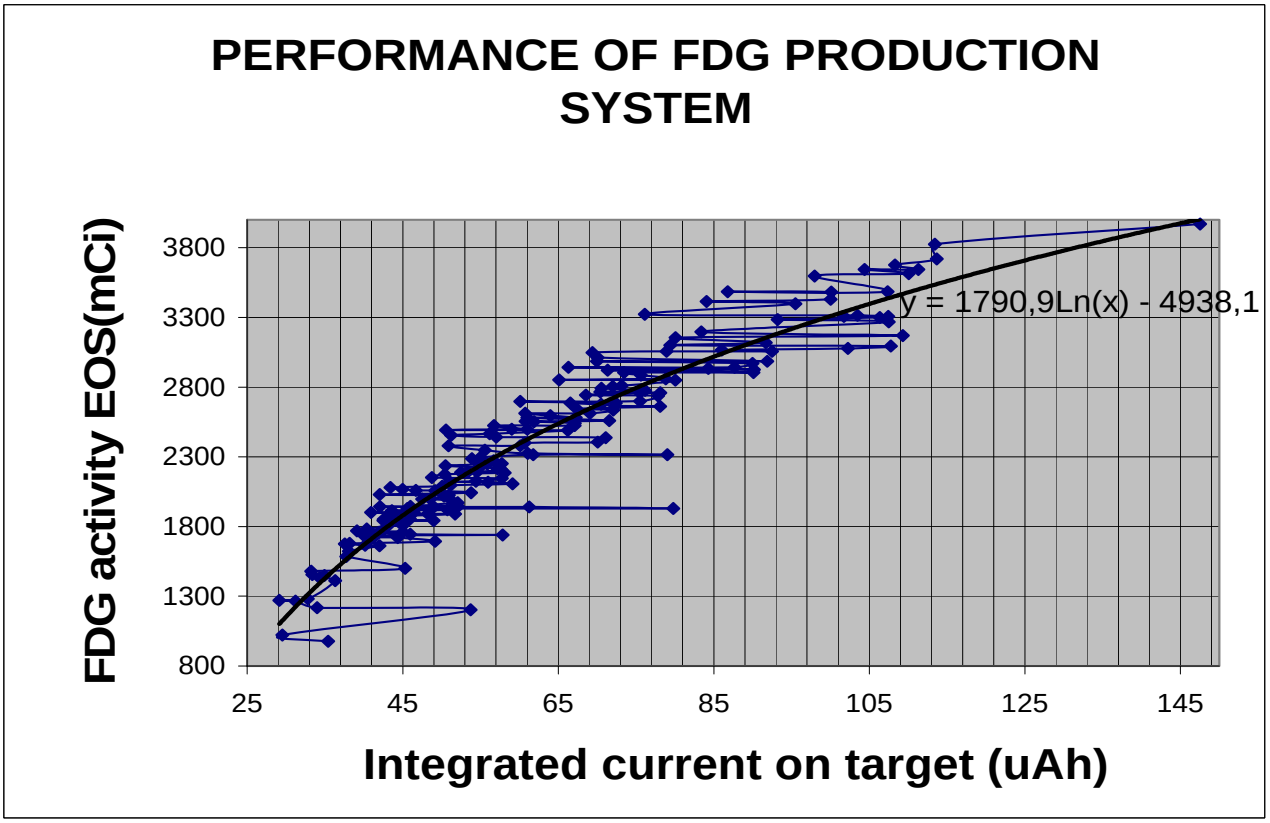

One-Year Experience with an IBA 18/9 Cyclotron Operation for F-18 FDG Routine Production

BACON

18F-FDG Radiofarma

The Cyclotron Facility

- Facility Diagram
- The Bunker
- The Cyclotron
- Hot Cell
- Chemistry Synthesis Unit
- The Target

Ground Layout

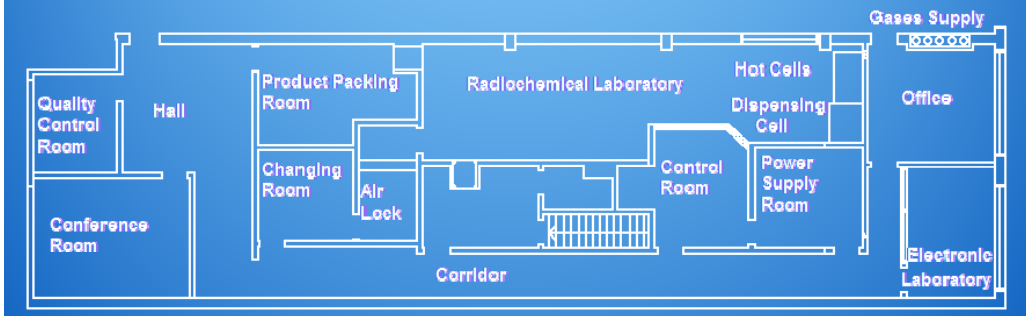

Control Room

- Designed to have visual contact with the Power Unit and Hot cells at the Radiochemistry Laboratory

Underground Layout

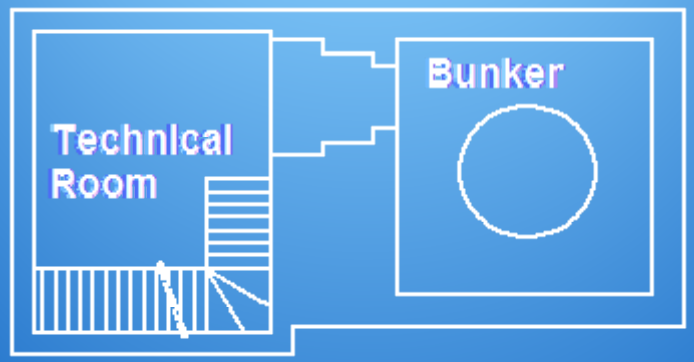

The Bunker

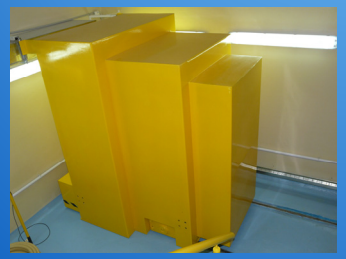

- Designed to shield neutron and gamma radiation. Walls are made of concrete (density 2,35 g/cm^3).
- During the irradiation the bunker is closed by a 14-ton concrete door.

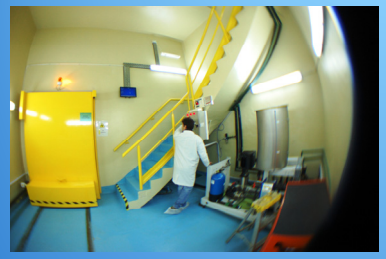

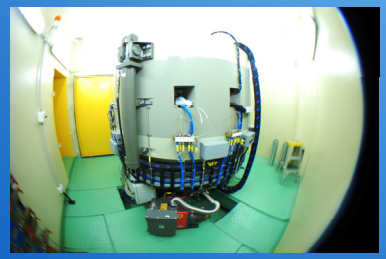

- The shields are designed in order to limit the dose to the workers to 0.5 mSv/year.
- The ventilation system keeps a depression greater than 100 Pa.
- The safety system locks the door if the dose rate inside the bunker is greater than 100 µSv/h

The Cyclotron

- Cyclone® 18/9- HC (high current) model.
- Energy:

  18 MeV Protons

  9 MeV Deuterons.

Synthesizing Hot cell

- The HEPA filter and charcoal filter are built to filter the exhaust air.
- A continuous radiation air monitoring system.
- Front lead shielding 75mm thickness.
- Side and back shielding 60 mm thickness.

Dispensing HOT cell

- Ventilation systems: 70% recycling.
- Completely efficient HEPA filters (HEPA> 99,999).
- 60 mm Pb shield in the front, 50 mm Pb shield at Side, behind, bottom and top

Chemistry Synthesis Unit

- Synthera® nucleophilic sustitucion.
- FDG Syntesis time <25 min.
- Yield EOS 60% (70% corrected yield).
- Integrated Fluidic Prossesor (IFP™)
- Single use

Adjustable Parameters

- Reactor: temperature 30-150℃.
- Pressure: 0-2 bar.
- Timing: each step adjustable

Water Target

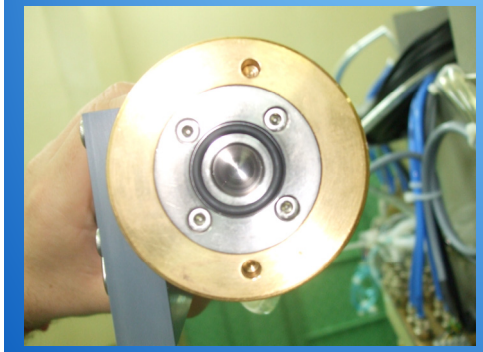

- IBA comercial target
- Niobium body
- Large volume 2,4 ml
- 50 µm Havar foild window
- Filling volume 2 ml 98% enriched water

Target Care

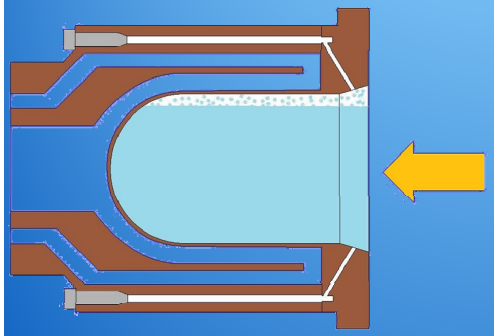

- Keep the pressure between 27-30 Bar
- keep the Tgt/Tgt + Coll current ratio above 90%
- Replace the o'ring and foils windows at 5000 µAh
- Not use recycled enriched water to fill the target

Target Performance

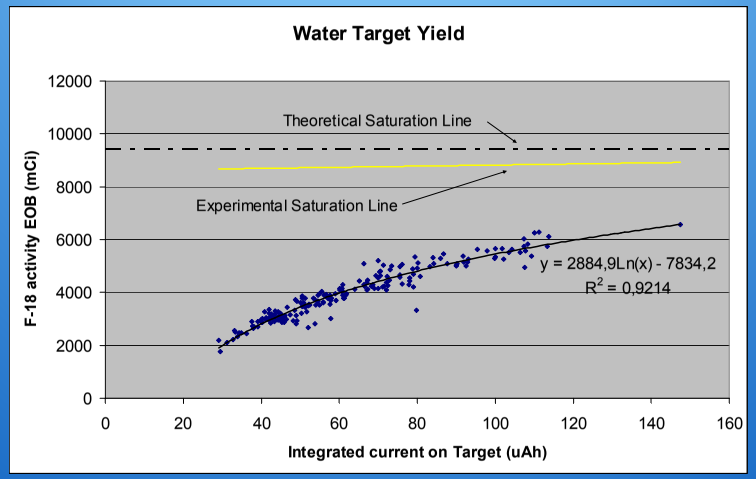

Performance of FDG Production System

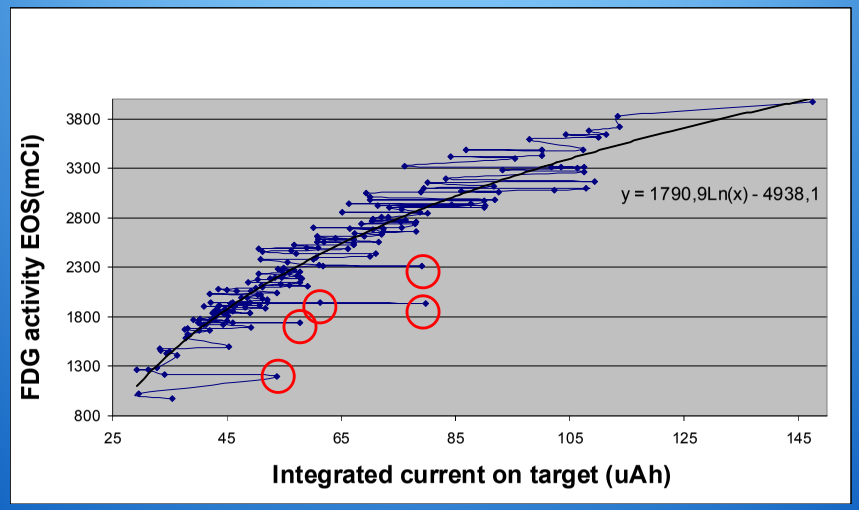

Summary

- More than 200 runs
- Average daily production of FDG: 2300 mCi.
- Maximun FDG activity obtained in one run: 3970 mCi (147,54 μAh in 3,5 h).

17

Comparison of [^{11}C]CH_3I yields from 2 in-house Methyl Iodide Production systems – Does size matter?

Salma Jivan, Ken R. Buckley, Wade English & James P. O'Neil[1]
UBC/TRIUMF PET Program, 4004 Wesbrook Mall, Vancouver, B.C., Canada
[1]Lawrence Berkeley National Laboratory, 1 Cyclotron Road, Berkeley, CA, U.S.A.

The TRIUMF/PET Program is largely reliant on carbon-11 tracers for neurology studies. The reliability and high specific activity radiotracers are key components to the success of the program. Recently, we experienced low in-target [^{11}C]CH_4 yields which prevented us from synthesizing certain low radiochemical yield tracers. To circumvent the problem, a new module was constructed. We report our conversion yields obtained from 2 in-house built CH_3I modules and describe the changes made between the two systems.

[^{11}C]CH_4 is produced in a niobium target as previously described(1). The target contents and helium flushes (approximately 1.5 litres) are transported 50 metres in 3.2 mm stainless steel tubing to a hotcell in the radiochemistry lab that houses the CH_3I module. The target contents pass through phosphorous pentoxide to trap ammonia formed in target and are collected on 2 grams of Poropak N cooled at -196°C. Helium is used to flush nitrogen and hydrogen off the trap upon warming. After flushing, the recirculating pump is started and the [^{11}C]CH_4 is pumped through a 720°C quartz tube containing iodine vapour. An ascarite trap (9.5mm OD x 7mm ID x 12cm length) is placed between the quartz tube and CH_3I trap which is packed with 0.2 grams of Poropak N. Recirculation proceeds until the radiation level on the CH_3I detector levels off. The trap is heated to 180°C and helium elutes the [^{11}C]CH_3I into precursor solution or solvent for quantifying CH_3I.

Methyliodide Systems Description

The first TRIUMF gas phase recirculating [^{11}C]CH_3I system built in 1996 was based on works by Link and Larsen (2,3) with minor modifications. Our first system had a 19mm OD x 16.5mm ID x 30.5cm length quartz tube placed in a 15 cm horizontal oven. The I_2 vapour source was a heated side arm near the head of the quartz tube and temperature was varied from 50°C to 90°C to maintain a constant I_2 concentration. A copper coil with running water was placed at the end of the quartz tube to condense iodine and prevent migration through the system. System pressures during recirculation ranged from 2 to 4 psi and flows were 250-300ml/min for a period of 6 minutes. The [^{11}C]CH_4 trap was in the recirculation loop for this system. The conversion yields of [^{11}C]CH_3I averaged 20% decay corrected based on [^{11}C]CH_4 production. The system worked reliably and made enough dose for injection until we experienced target problems and low yields from our Niobium target. With high demand for scanning tracers to be shared with multiple scanners, the need for another CH_3I system was pushed forward.

The new system was built with the same model oven rotated into a vertical orientation with a 12.75mm OD x 10.5mm ID x 38cm length quartz tube as the reactor and the flow upward through the tube. The I_2 is now inside a heated portion of the quartz tube (2.5 cm band heater set at 50°C) and sees the flow path directly. A Peltier cooler is used to condense and trap the I_2 vapor exiting the oven to prevent migration through the system. The relatively large volume diaphragm Cole Parmer pump from the original system was replaced with a micro diaphragm KNF pump as the recirculation pump. The system volume was further reduced by replacing the 3.2 mm stainless steel tubing to 1.6 mm teflon tubing where possible. Tubing from the outlet of the quartz tube to the ascarite trap was kept to 3.2 mm due to iodine plating out and causing high pressure and plugging of the system. Fittings were changed to PFA from stainless steel where possible to prevent corrosion in the system. The major difference between the two systems was the recirculation path. After CH_4 trapping, the trap contents were pressurized into the quartz tube. The CH_4 trap was isolated from the recirculation path and [^{11}C]CH_4 was recirculated for 3.5 minutes at a flow rate of 300 to 400ml/min. Pressures during recirculation ranged between 9 and 12 psi.

Results and discussion

The original CH_3I system provided conversion yields averaging 20%. Due to poor trapping of I_2 after the oven, the ascarite trap was changed between every run, while the I_2 pot was topped up every 20 runs. The system was given a complete cleaning after 60 runs. Upon cleaning of traps, it was found that the CH_3I Poropak packing appeared light yellow in colour proving the breakthrough of iodine and preventing efficient $[^{11}C]CH_3I$ trapping. It was also noticed that the counts on the CH_4 trap radiation detector would rise during recirculation confirming breakthrough of the formed product. With routine maintenance of the system, high specific radioactivity was maintained and the mass of CH_3I produced ranged from 5 to 10 nmols.

With the new system we find the conversion yields increased close to 2 fold and averaged 40% with measured masses of CH_3I ranging between 15 and 25 nmols. We replace the ascarite trap at the beginning of each production day and can perform up to 6 batches with short turnaround time of 20 minutes. The iodine is scraped down the quartz tube for re-use periodically as the vapor concentration decreases thus avoiding the need to add fresh iodine. The system currently has operated with 100 runs without any intervention or I_2 filling.

A smaller recirculation volume allows for larger number of passes of $[^{11}C]CH_4$ through the reaction chamber over the same time period. The original system had a recirculation cycle time of 40 sec per pass providing approximately 10 to 12 passes for the given 6 to 8 minute recirculation time whereas the new system has a recirculation cycle time of 10 sec per pass providing approximately 18 to 24 passes in the 3 to 4 minute recirculation step. In addition, the removal of the CH_4 trap from the recirculation system avoids buildup, and therefore the loss, of any $[^{11}C]CH_3I$ not trapped or bled from the $[^{11}C]CH_3I$ trap. In conclusion, the changes made to the new system with smaller recirculation volume improved the conversion yield of the system.

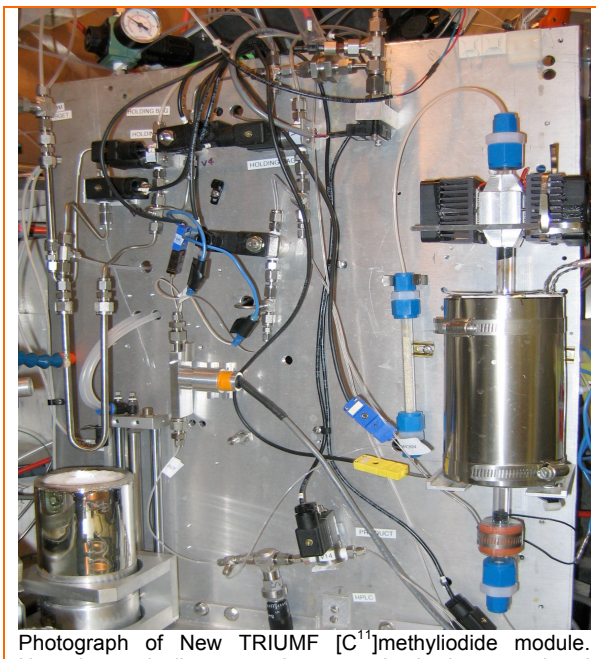

Photograph of New TRIUMF $[C^{11}]$methyliodide module. Note the vertically mounted quartz tube in the oven, band heater for iodine vaporization below and Peltier cooling unit for iodine trapping above.

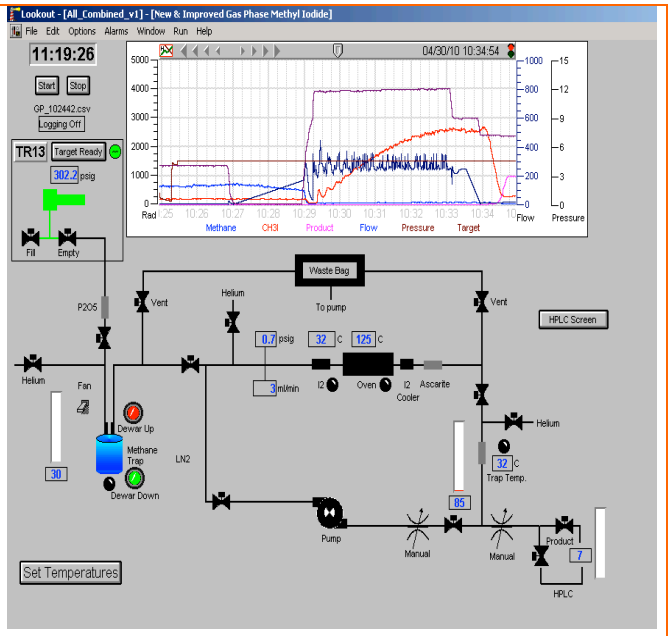

Lookout Screen capture of new system. The graph trends target pressure, flow rate and pressure in recirculating loop, radiation detector values for methane trap, methyliodide trap and product.

References:

1. Buckley, K.R., Jivan, S., Ruth, T.J., 2004. Improved yields for the in situ production of $[^{11}C]CH_4$ using a niobium target chamber. Nucl.Med.Biol. 31, 825-827
2. Link, J., Krohn, K., Clark, J., 1997. Production of $[^{11}C]CH_3I$ by Single Pass Reaction of $[^{11}C]CH_4$ with I_2. Nucl. Med. Biol. 24, 93-97
3. Larsen, P., Ulin, J., Dahlstrom, K., Jensen, M., 1997. Synthesis of $[^{11}C]$Iodomethane by Iodination of $[^{11}C]$Methane. Appl. Radiat. Isot. 48, 153-157
4. Andersson, J., Truong, P., Halldin, C., 2009. In-target produced $[^{11}C]$methane: Increased specific radioactivity. Appl. Radiat. Isot. 67, 106-110

TRIUMF

Canada's National Laboratory for Particle and Nuclear Physics
Laboratoire national canadien pour la recherche en physique nucléaire et en physique des particules

Comparison of [^{11}C]CH_3I Yields from 2 In-house Methyl Iodide Production Systems – Does Size Matter?

Salma Jivan, Ken R. Buckley, Wade English & James P. O'Neil[1]

UBC/TRIUMF, 4004 Wesbrook Mall, Vancouver, BC Canada
[1]Lawrence Berkeley National Laboratory Berkeley, CA USA

Motivation

Original system built 1997
- 15-20 syntheses per week
- reliable but needed frequent maintenance

In-target [^{11}C]CH_4
- low inherent target yield
- target issues

Synthesis of low RC yield tracers
- existing system not adequate, low conversions

TRIUMF

System Schematics

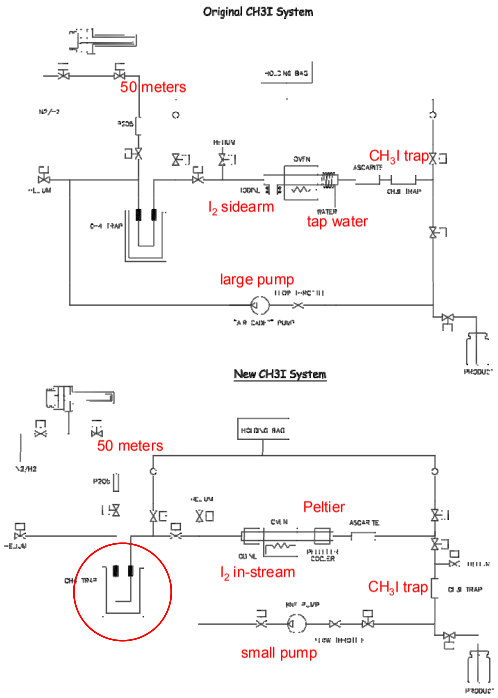

TRIUMF

Original System Hardware

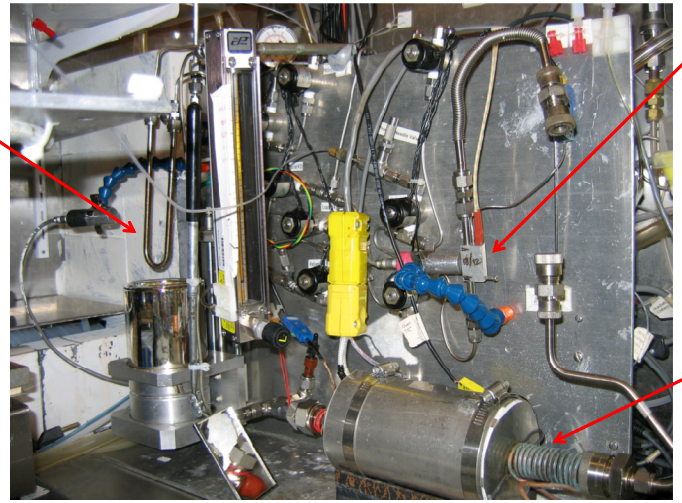

TRIUMF

System Hardware

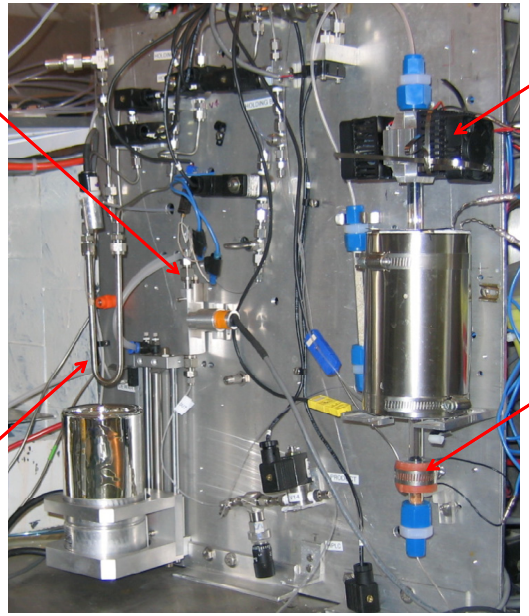

TRIUMF

Radioactivity Trend

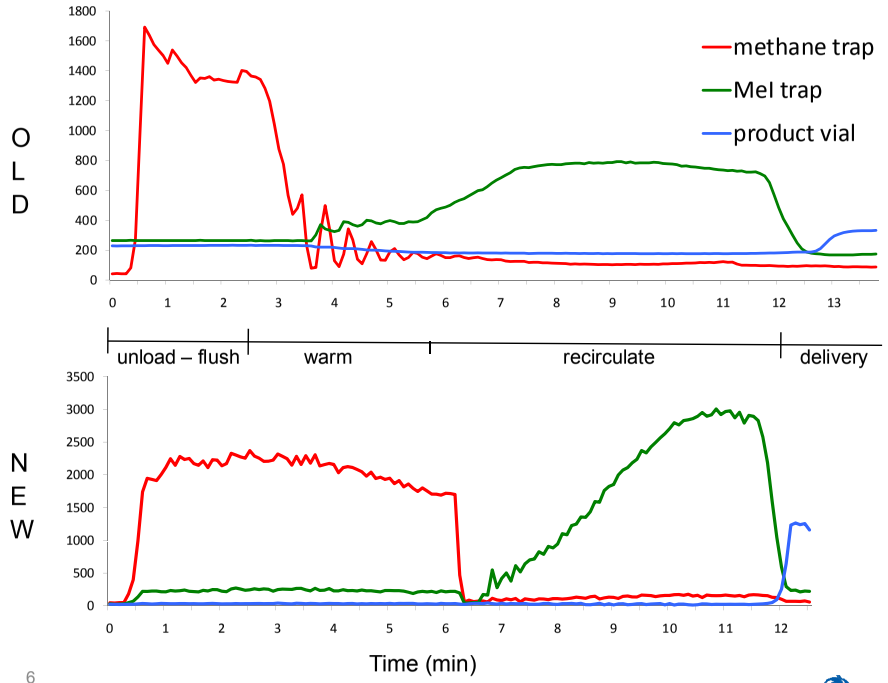

TRIUMF

Summary

	Original	New
Quartz tube volume	65ml	33ml
Recirculation pump	large volume	micro
Recirculation volume	150mL	80mL
Recirculation time	6-8 min	3-4 min
Number of passes	10-12	18-24
Iodine source	Side port	In stream
Cooling source	Water (18-20°C)	Peltier (0°C)
Conversion based on $^{11}CH_4$	15-20%	35-40%

System volume reduction
- removal of CH_4 trap
- increase in number of passes
- increase in conversion yield

Performed 200 runs without needing to replace traps or replenish iodine thus reducing maintenance requirements

TRIUMF

The take home message…

TRIUMF

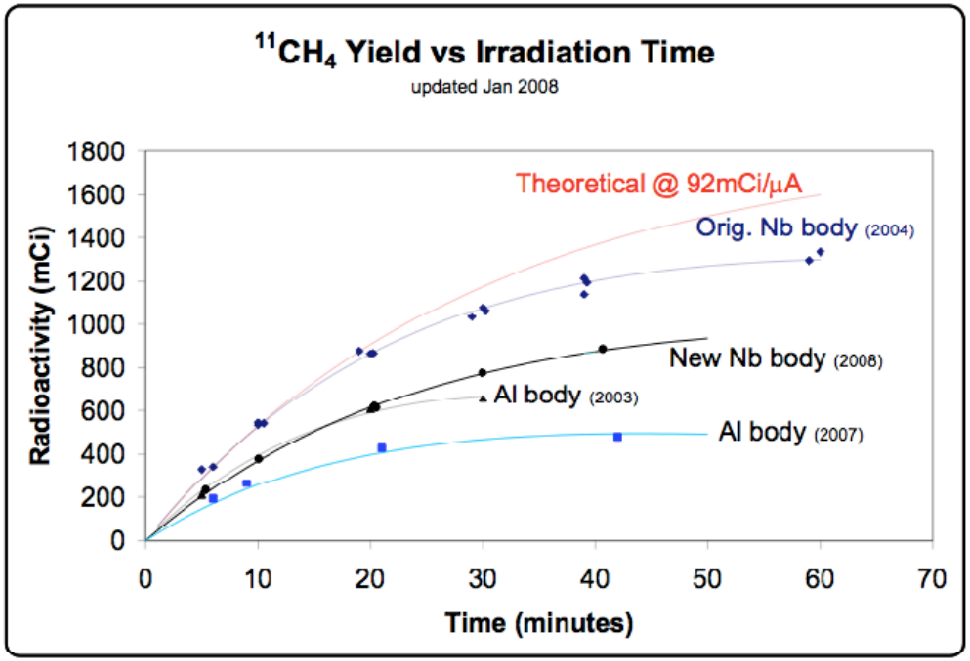

TRIUMF

WTTC XIII – Presentation Discussions

1. Temperature during synthesis
   - 720º C in all synthesis
   - Too high temperature = problems
2. Specific activity
   - 7 Ci / umol
   - No difference observed between systems
3. Cold trap
   - Cold trap outside: decreased volume

Cyclotron production of ^{99m}Tc via the ^{100}Mo(p,2n)^{99m}Tc reaction

K. Gagnon[1], F. Bénard[2], M. Kovacs[3], T.J. Ruth[4], P. Schaffer[4], and S.A. McQuarrie[1]

[1] Edmonton PET Centre, Cross Cancer Institute, University of Alberta, Edmonton, AB, CANADA
[2] BC Cancer Agency, Vancouver, BC, CANADA
[3] Lawson Health Research Institute, London, ON, CANADA
[4] TRIUMF, Vancouver, BC, CANADA

Introduction: In light of the current world-wide shortage of reactor-produced ^{99}Mo/^{99m}Tc, there is a growing interest in exploring the large-scale cyclotron production of ^{99m}Tc via the ^{100}Mo(p,2n)^{99m}Tc reaction (a method first proposed by Beaver and Hupf, *J Nucl Med*, 1971, 12: 739). In producing ^{99m}Tc, knowledge of the cross sections and theoretical yields are essential for optimizing the high-current irradiation conditions and verifying the processing/recovery techniques. A review of the existing published cross section data for the ^{100}Mo(p,2n)^{99m}Tc reaction however reveals large discrepancies in these measured values.

Aim: Given the large cross section discrepancies in the current literature, the goal of this work was to re-evaluate the cross sections for the ^{100}Mo(p,2n)^{99m}Tc and ^{100}Mo(p,pn)^{99}Mo reactions.

Methods: The ^{99m}Tc and ^{99}Mo cross sections were evaluated using both natural abundance (7.5 mg/cm^2) and ^{100}Mo enriched (97.42%, 7.4–11.1 mg/cm^2) foils. Foils were individually irradiated with proton energies up to 18 MeV for 600 seconds on the Edmonton PET Centre's TR 19/9 variable energy cyclotron (Advanced Cyclotron Systems Inc., Richmond, BC). A copper foil was in place for all irradiations for the purpose of monitoring the beam energy and irradiation current. Unless otherwise noted, all decay data were obtained from the NuDat 2.5 database.

The molybdenum foils were assayed multiple times (from a few hours to several days post-EOB) using an HPGe detector (sample distance ≥ 25 cm, dead time < 7%). The detector was calibrated using standard sources of ^{22}Na, ^{54}Mn, ^{57}Co, ^{60}Co, ^{109}Cd, ^{133}Ba and ^{137}Cs. The ^{99}Mo activity was determined using a weighted average of the 181 keV and 739 keV peaks. In determining the ^{99m}Tc activity, the non-resolved 140/142 keV peak (89.06%/ 0.02%) was measured. Two additional contributing sources to the 140 keV peak were subtracted prior to evaluation of the direct ^{99m}Tc cross section. Firstly, as ^{99}Mo decays to ^{99m}Tc, the ^{99}Mo associated ^{99m}Tc activity at the start of counting was determined from the measured ^{99}Mo activity using the radioactive parent-daughter relationship described by Attix (*Introduction to Radiological Physics and Radiation Dosimetry*, 2004, pp. 105–106) with the branching ratio to ^{99m}Tc taken as 87.6% (Alfassi et al., *Appl Radiat Isot*, 2005 63: 37). Next, as ^{99}Mo gives rise to a 140 keV (4.52%) gamma ray upon decay, this peak contribution was calculated from the measured ^{99}Mo activity of each respective foil. Cross sections were calculated using the standard activation formula (Krane, *Introductory Nuclear Physics*, 1988, pp. 169–170) with values normalized to 100 percent ^{100}Mo enrichment.

Thick target yields were calculated from the measured ^{99m}Tc cross sections assuming 100 percent ^{100}Mo and fitting the cross-section data with a 2nd order polynomial. Values are reported for 18→10 MeV, and 22→10 MeV (cross sections extrapolated to 22 MeV from a polynomial curve fit).

Results: The following figures compare the evaluated cross sections for the direct production of ^{99m}Tc and ^{99}Mo to previously published cross section data. For the purpose of comparison, we have normalized the ^{99m}Tc data of Challan et al. (*Nucl Rad Phys*, 2007, 2: 1) to 100 percent ^{100}Mo by dividing by 9.63%. For both reactions, our results are in good agreement to values published by Levkovskij (1991). Good ^{99m}Tc cross section agreement is also noted up to E_p ~12 MeV when

comparing with Lagunas-Solar (*IAEA-TECDOC-1065*, 1999) and Challan et al. We believe that the elevated ^{99m}Tc cross sections for Lagunas-Solar for E_p > ~12 MeV may be attributed to the incomplete subtraction of the ^{99}Mo 140 keV peak contributions due to underestimated ^{99}Mo cross sections. Although Challan et al. mention that they have corrected for the growth and decay of the metastable and ground states, it is unclear if the ^{99m}Tc 140 keV peaks were corrected to account for ^{99}Mo→^{99m}Tc contributions post-EOB. The absence of such a correction would similarly explain the elevated ^{99m}Tc cross sections for E_p > ~12 MeV. While the ^{99}Mo cross sections are in good agreement, the ^{99m}Tc cross sections measured in this work are significantly higher than values published by Takács et al. (*J Radioanal Nucl Chem*, 2003, 257: 195) and slightly higher, by approximately 2σ, than values presented by Lebeda and Pruszynski (to be published in *Appl Radiat Isot*). An overall disagreement was noted for both reactions when comparing with the published cross sections of Scholten et al. (*Appl Radiat Isot*, 1999, 51: 69).

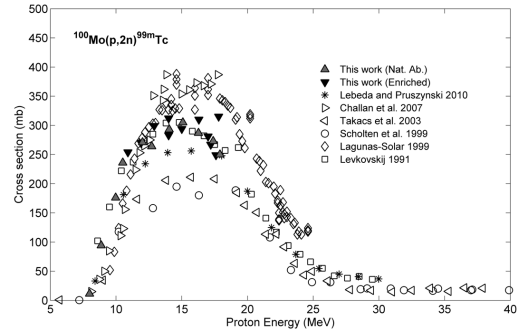

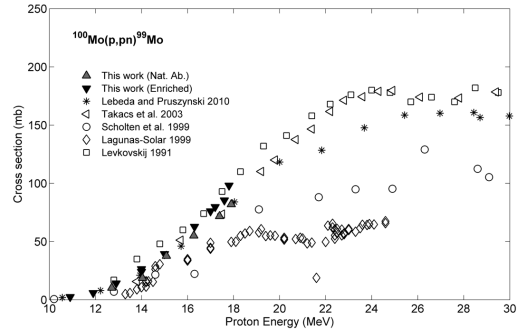

E [MeV]	Foil	^{99m}Tc [mb]	^{99}Mo [mb]
8.0 ± 0.2	Nat. Ab.	11.3 ± 1.2	–
8.9 ± 0.4	Nat. Ab.	94.1 ± 8.3	–
10.0 ± 0.2	Nat. Ab.	176 ± 15	–
10.5 ± 0.6	Nat. Ab.	236 ± 21	–
12.0 ± 0.3	Nat. Ab.	271 ± 24	–
12.7 ± 0.3	Nat. Ab.	264 ± 23	10.3 ± 6.2
14.0 ± 0.3	Nat. Ab.	293 ± 26	18.7 ± 5.4
15.1 ± 0.4	Nat. Ab.	305 ± 27	37.7 ± 6.0
16.3 ± 0.5	Nat. Ab.	287 ± 25	55.1 ± 7.6
17.4 ± 0.7	Nat. Ab.	273 ± 24	71.8 ± 9.6
17.9 ± 0.8	Nat. Ab.	250 ± 22	82 ± 10
10.9 ± 0.6	Enriched	254 ± 22	2.47 ± 0.22
11.9 ± 0.2	Enriched	270 ± 24	5.82 ± 0.51
12.9 ± 0.5	Enriched	299 ± 26	14.1 ± 1.2
14.0 ± 0.2	Enriched	283 ± 25	24.1 ± 2.1
14.0 ± 0.2	Enriched	312 ± 27	26.4 ± 2.3
15.0 ± 0.2	Enriched	294 ± 26	39.4 ± 3.4
16.3 ± 0.2	Enriched	310 ± 27	62.7 ± 5.5
17.0 ± 0.3	Enriched	281 ± 24	76.1 ± 6.6
17.2 ± 0.8	Enriched	267 ± 23	79.8 ± 7.0
17.6 ± 0.8	Enriched	249 ± 22	85.4 ± 7.5
17.8 ± 0.4	Enriched	315 ± 27	98.2 ± 8.6

Throughout this experiment the beam current and detector efficiency were carefully monitored and we are confident with the 140 keV peak area corrections performed in this experiment as the evaluated ^{99m}Tc cross sections were consistent, independent of the time post-EOB upon which they were evaluated (i.e. calculated within a few hours post-EOB or >24 hours post-EOB).

Thick target yields were determined to be 14.2 mCi (526 MBq)/μAh for 18→10 MeV, and 18.2 mCi (674 MBq)/μAh for 22→10 MeV. These yields are higher than the value of 11.2 mCi (415 MBq)/μAh for 22→12 MeV reported by reported by Scholten et al., and are in good agreement with the value of 17 mCi (629 MBq)/μAh for 25→5 MeV given by Takács et al.

As we are not only interested in optimizing the yield of ^{99m}Tc, but also the purity, future work is planned to experimentally evaluate the ^{100}Mo(p,2n)^{99g}Tc cross sections. Preliminary calculations using cross sections modelled with Empire–II suggest that a ^{99m}Tc/$^{99m+99g}$Tc ratio of 18% is possible for a 3 hour irradiation at 22→10 MeV. In comparison, assuming a 24 hour elution frequency and 5% retention, the ^{99m}Tc/$^{99m+99g}$Tc ratio calculated for the standard generator setup is 26% (Alfassi et al., *Appl Radiat Isot*, 2005 63: 37).

Conclusion: We have presented updated cross sections for the ^{100}Mo(p,2n)^{99m}Tc and the ^{100}Mo(p,pn)^{99}Mo reactions. Results of this work suggest that production of large quantities of ^{99m}Tc via a cyclotron may be a viable alternative to the current reactor-based production strategy.

Acknowledgements: The authors would like to thank Advanced Cyclotron Systems, Inc. This work was supported through a grant from NSERC/CIHR (MIS 100934).

Cyclotron Production of ^{99m}Tc via the ^{100}Mo(p,2n)^{99m}Tc reaction

K. Gagnon, F. Bénard, M. Kovacs, T.J. Ruth, P. Schaffer, S.A. McQuarrie

WTTC 13, July 2010

Motivation/Background

- Current /ongoing world-wide shortage of reactor-produced ^{99}Mo/^{99m}Tc
- Growing interest in exploring the large-scale cyclotron production of ^{99m}Tc via the ^{100}Mo(p,2n)^{99m}Tc reaction
- Knowledge of the cross sections and theoretical yields are essential for optimizing the irradiation conditions and verifying the processing/recovery techniques
- Large discrepancy amongst published literature

Reaction scheme:

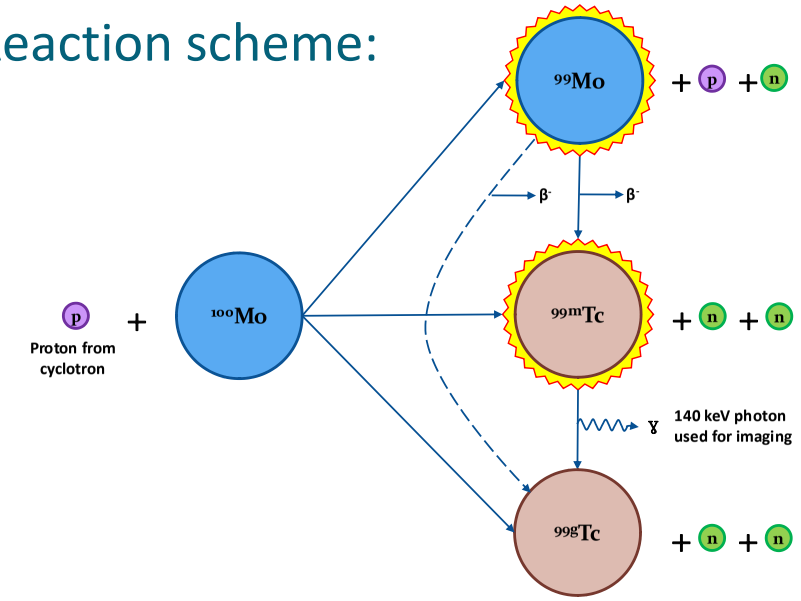

Irradiations:

- Thin foils, both ^{nat}Mo and ^{100}Mo (97.42% enrichment)
- Foils individually irradiated on the TR-19/9 at the EPC
- I ≈ 1 μA, t = 600 seconds
- E_p and current monitored using copper foils

HPGe Assays:

- Foils assayed at multiple time points post-EOB
- To minimize contribution of ^{99}Mo, assays for ^{99m}Tc were performed within a few hours post-EOB. Typical assay times were 300 seconds.
- Note: HPGe calibration sources included ^{57}Co
- Correct for overlapping 140 keV contributions from ^{99}Mo:
  - Direct (I_γ= 4.52%)
  - Indirect (^{99}Mo → ^{99m}Tc) post-EOB

Results

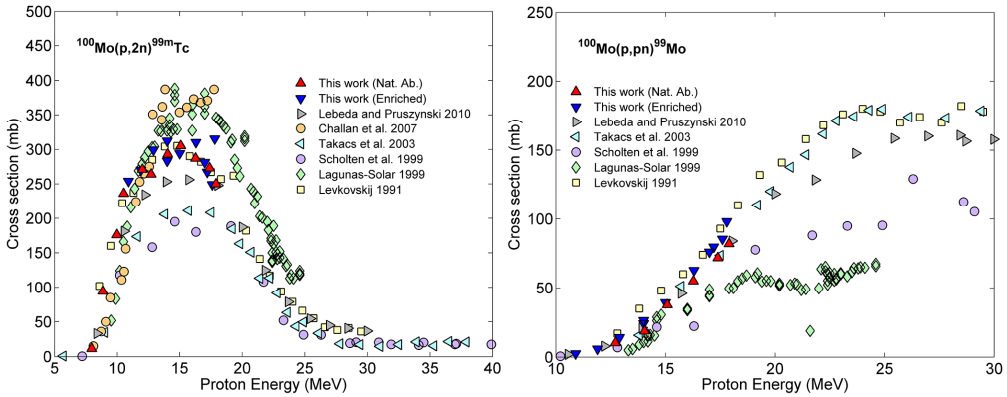

Cross sections for ^{100}Mo(p,x) production of ^{101}Tc, ^{96}Nb, and ^{97}Nb also evaluated for enriched foil irradiations

Thick Target Yields

- Cross sections extrapolated to 22 MeV
- Cross sections used to determine thick target yields

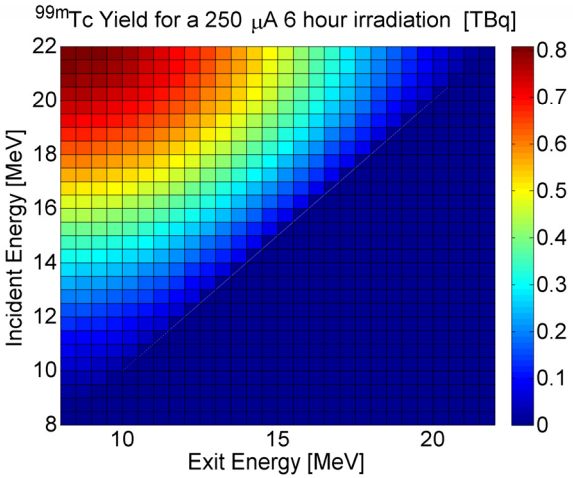

Future/Ongoing

- Planned measurement of the ^{100}Mo(p,2n)^{99g}Tc excitation function.
- Enriched foils were irradiated ~12,000 μAmin (20 μA x 10 hours), June 2010.
- Production of ^{99}Mo and ^{99m}Tc have been measured for these foils.
- Currently awaiting for decay of ^{99}Mo, ^{96g}Tc, etc.
- Foils will be analyzed via ICP-MS at the University of Alberta's Radiogenic Isotope Facility.

Summary

- We have presented updated cross sections for the $^{100}Mo(p,2n)^{99m}Tc$ and $^{100}Mo(p,pn)^{99}Mo$ reactions
- Calculated thick target yields suggest that production of large quantities of ^{99m}Tc via a cyclotron may be a feasible alternative to the current reactor-based strategy
- Experiments are underway to evaluate the $^{100}Mo(p,2n)^{99g}Tc$ excitation function

WTTC XIII – Presentation Discussions

1. Resolve g/m states by neutron counting?
   - Neutron measurements difficult in thin foil methodology

Cyclotron Production of ^{99m}Tc

A. Zyuzin[1], B. Guérin[2], E. van Lier[1], S. Tremblay[2], S. Rodrigue[2], J.A. Rousseau[2], V. Dumulon-Perreault[2], R. Lecomte[2], J.E. van Lier[2]
[1]*Advanced Cyclotron Systems Inc., Richmond, BC, Canada*
[2]*Sherbrooke Molecular Imaging Center, Université de Sherbrooke, QC, Canada*

Introduction. Current global interruptions of ^{99}Mo supply, aging reactors, and the staggering costs of their maintenance have accelerated the search for alternative sources of ^{99m}Tc. Direct production of ^{99m}Tc via ^{100}Mo(p,2n)^{99m}Tc nuclear reaction can be considered as one of such alternatives. The feasibility of ^{99m}Tc production with a cyclotron was first demonstrated in 1971 by Beaver and Hupf[1] and confirmed by a number of researchers.[2,3,4,5] Measured yields indicate that up to 2.1 TBq (56 Ci) of ^{99m}Tc can be produced in 12 h using a 500 µA 24 MeV cyclotron. This amount will be sufficient to cover population base of 5-7 million assuming: 15 % ^{99m}Tc losses, an average injected dose of 25 mCi and a 10 hrs decay. Initial results of the target development and thick target yields are presented in the "Mo-100 development for direct Tc-99m Production" abstract. In this work we compared the chemical and radiochemical properties and *in vivo* behavior of cyclotron- and generator-produced ^{99m}Tc.[6]

Experiment. Targets, 6-mm diameter discs, were prepared by melting ^{100}Mo pellets (99.54% enrichment) onto tantalum backing supports. Targets were bombarded for 1.5–3 h with 15.5–17.0 MeV protons (14–52 µA), using a TR-19 cyclotron (ACSI). After bombardment, ^{100}Mo targets were partially dissolved and purified by the method of Chattopadhyay *et al.*[7] The radionuclide purity of the ^{99m}Tc was >99.99%, as assessed by γ-spectroscopy, exceeding USP requirements for generator-based ^{99m}Tc. Although small peaks corresponding to ^{99}Mo were observed in the initial solute, these were not detectable in the purified ^{99m}Tc-pertechnetate solution. Minute amounts of ^{97}Nb were also quantitatively separated from during target processing. The content of other technetium isotopes was measured after allowing sufficient time (4 days) for ^{99m}Tc decay. The presence of 0.0014% ^{96}Tc and 0.0010% ^{95}Tc at the end of bombardment, was below USP requirements of 0.01% for generator-produced ^{99m}Tc. No other radionuclidic impurities were found. The radiochemical purity of cyclotron-produced [^{99m}Tc]TcO_4^-, as determined by instant thin-layer chromatography was >99.5%, well above the USP requirement of 95%. The content of ground state ^{99g}Tc ($T_{½}$ = 2.1 × 10^5 years) was not determined in these experiments and is one of the tasks for future work. For imaging studies, both cyclotron- and generator-produced ^{99m}Tc were formulated as 3 different radiopharmaceuticals: ^{99m}Tc-pertechnetate for thyroid imaging, ^{99m}Tc-methylene diphosphate (^{99m}Tc-MDP) for bone scanning, and ^{99m}Tc-hexakis-2-methoxy*iso*butyl isonitrile (^{99m}Tc-MIBI) for heart imaging. These radiopharmaceuticals account for more than 75% of all routine ^{99m}Tc scans currently used in diagnostic nuclear medicine. The latter two radiopharmaceuticals were prepared using commercially available kits. Labeling efficiency for the bone imaging agent ^{99m}Tc-MDP and heart imaging agent ^{99m}Tc-MIBI were 98.4% and 98.0%, respectively, well above USP requirements of >90%.

Animal Scans. The bio-distributions of ^{99m}Tc-pertechnetate, ^{99m}Tc-MDP, and ^{99m}Tc-MIBI, prepared with either cyclotron- or generator-produced ^{99m}Tc, were assessed in a healthy rat model. For each experiment 2 animals were simultaneously injected with a 0.3-mL physiologic saline solution containing 34–90 MBq of the selected ^{99m}Tc-radiopharmaceutical, prepared either with cyclotron- or generator-produced ^{99m}Tc. Dynamic acquisitions were continued over a 2 h period. At the end of scanning, the rats were killed and dissected to

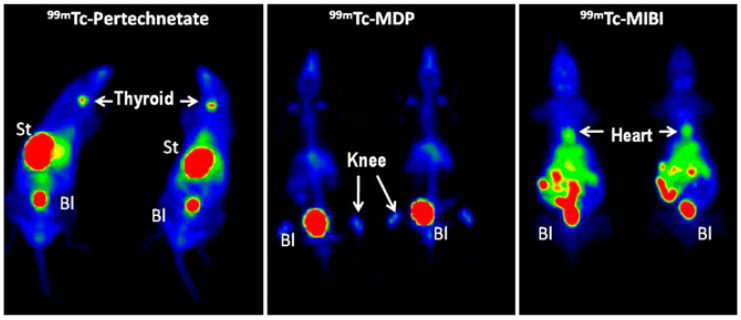

Figure 1. Whole-body scintigrams of two rats 2 h after administration of: 90 MBq of ^{99m}Tc-pertechnetate; 34 MBq of ^{99m}Tc-MDP; 15 MBq of ^{99m}Tc-MIBI, prepared from cyclotron- (right image) and generator-produced ^{99m}Tc (left image).

measure activities of target tissues. Static images obtained 2 h after administration of each of these ^{99m}Tc-radiopharmaceuticals show matching ^{99m}Tc distribution patterns, clearly delineating the thyroid with ^{99m}Tc-pertechnetate, skeleton with ^{99m}Tc-MDP, and heart with ^{99m}Tc-MIBI (Fig. 1). Uptake kinetics calculated over the target organs (thyroid, bones, and heart), show identical uptake patterns for the cyclotron- and generator-produced ^{99m}Tc-radiopharma-ceuticals (Fig. 2). Tissue activities from dissected samples collected 30 min after the end of imaging with ^{99m}Tc-MDP and ^{99m}Tc-MIBI also show matching patterns between cyclotron- and generator-derived ^{99m}Tc preparations (Fig. 3).

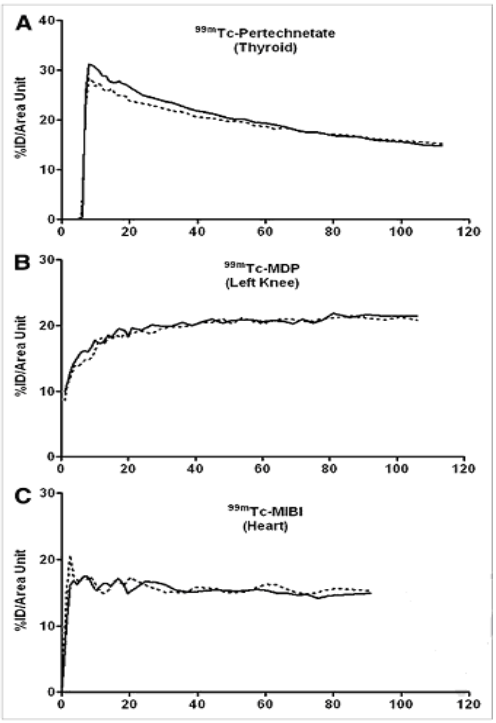

Figure 2. Time/radioactivity curves derived from regions of interest drawn around target organs (Fig.1) Dotted line: cyclotron-produced ^{99m}Tc, Solid line: generator produced ^{99m}Tc. Radioactivity is expressed as percentage of injected dose per unit area, corrected for radioactive decay.

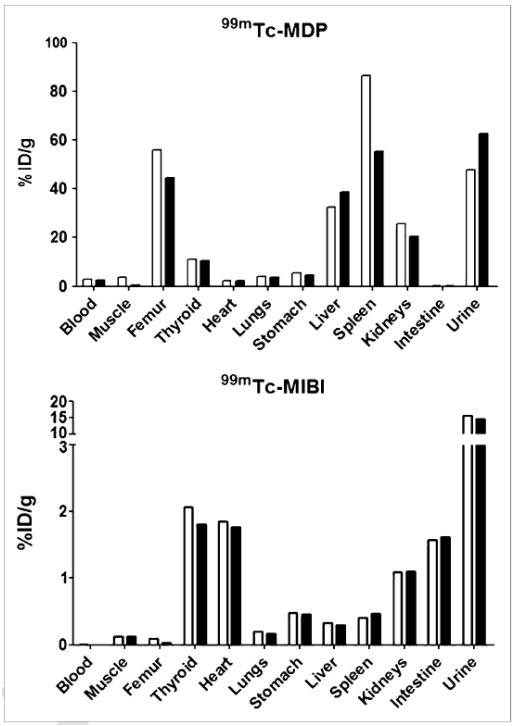

Figure 3. Tissue uptake in healthy rats, expressed as percentage of injected dose per gram of tissue, 2.5 h after intravenous injection of 34 MBq of ^{99m}Tc-MDP or 15 MBq of ^{99m}Tc-MIBI, prepared from cyclotron-produced ^{99m}Tc (open bars) or generator-produced ^{99m}Tc (solid bars).

Conclusion. The results of these *in vivo* experiments and quality control tests support the concept that cyclotron-produced ^{99m}Tc is suitable for preparation of USP-compliant ^{99m}Tc radiopharmaceuticals. Establishing decentralized networks of medium energy cyclotrons capable of producing large quantities of ^{99m}Tc may effectively complement the supply of ^{99m}Tc traditionally provided by nuclear reactors, at a fraction of the cost of a single nuclear reactor production facility, while sustaining the expanding need for other medical isotopes, including short-lived positron emitters for PET imaging.

1. Beaver J., Hupf H. Production of ^{99m}Tc on a medical cyclotron: a feasibility study. J. Nucl. Med. 1971;12:739-741
2. Lagunas-Solar M C. Accelerator production of ^{99m}Tc with proton beams and enriched ^{100}Mo targets. In: IAEA-TECDOC-1065. Vienna, Austria: International Atomic Energy Agency; 1999:87
3. Scholten B, *et al*. Excitation functions for the cyclotron production of ^{99m}Tc and ^{99}Mo. Appl. Radiat. Isotopes. 1999;51:69-80.
4. Takács S, *et al.* Evaluation of proton induced reactions on ^{100}Mo: New cross sections for production of ^{99m}Tc and ^{99}Mo. J. Radioanal. Nuclear. Chem. 2003; 257:195-201
5. Lebeda, O. *et al*. New measurement of excitation functions for (p,x) reactions on ^{nat}Mo with special regard to the formation of ^{95m}Tc, $^{96m+g}$Tc, ^{99m}Tc and ^{99}Mo, Appl. Radiat. Isot., in press
6. Guérin, B. *et al.* Production of ^{99m}Tc: An Approach to the Medical Isotope Crisis J. Nuclear Med., 2010;51:13N-16N
7. Chattopadhyay S, *et al.* Recovery of ^{99m}Tc from $Na_2[^{99}Mo]MoO_4$ solution obtained from reactor-produced (n,γ) ^{99}Mo using a tiny Dowex-1 column in tandem with a small alumina column. Appl. Radiat. Isotopes. 2008; 66:1814-1817

Cyclotron Production of Tc-99m

A. Zyuzin[1], B. Guérin[2], E. van Lier[1], S. Tremblay[2], S. Rodrigue[2], J.A. Rousseau[2], V. Dumulon-Perreault[2], R. Lecomte[2], J.E. van Lier[2] S. McQuarrie[3], K. Gagnon[3], D. Abrams[3], J. Wilson[3]

[1]Advanced Cyclotron Systems Inc., Richmond, BC, Canada
[2]Sherbrooke Molecular Imaging Center, Université de Sherbrooke, QC, Canada
[3]Cross cancer Institute, Edmonton, AB, Canada

History

May 2009	Recent isotope crisis begins: NRU Shutdown
Jun 2009	NRCan calls for Expressions of Interest
	ACSI propose to implement direct Tech production in Canada using network of TR24 cyclotrons
Jul 2009	EOI Submitted to NRCan: National Cyclotron Network for Production of Medical Isotopes
Sep 2009	CIHR/NSERC grant submission
Oct 2009	First production runs and animal scans
Nov 2009	Expert Panel Report
Nov 2009	CIHR awards 1.3M for R&D cyclotron production ^{99m}Tc
Mar 2010	Two Canadian organizations purchase 24 MeV cyclotron
Mar 2010	NRCan commits to develop non-fission solution
June 2010	NRCan calls for proposal on development and demonstration of non-fission methods of ^{99}Tc production

^{100}Mo(p,2n)^{99m}Tc Production Yield

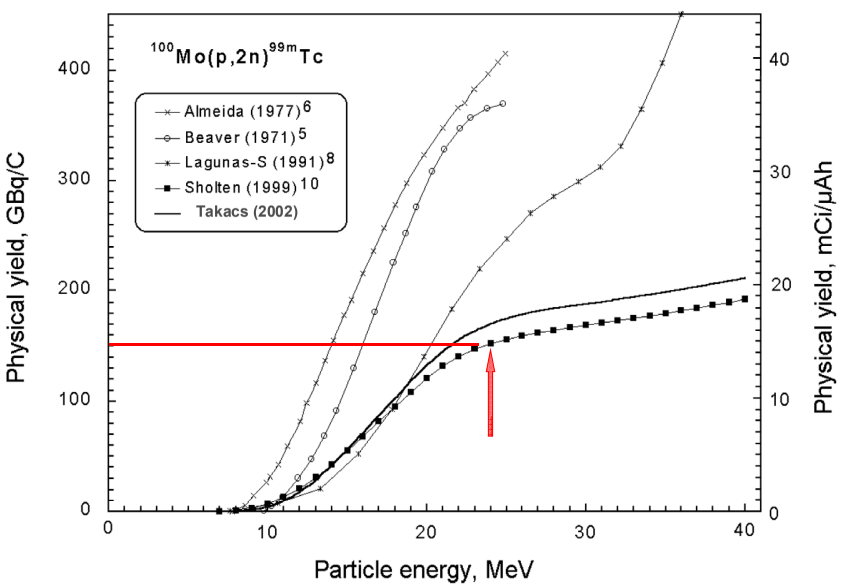

ACSI TR24 Cyclotron

The measured production yields @24 Mev

~150 mCi/μA at saturation

500 μA TR-24 can generate:

56 Ci (one 12 hr run)
75 Ci (two 6 hr runs)

How many ^{99m}Tc doses can we make?

Sat Yield 24 MeV	150	mCi/uA	Measured yields @ 24 MeV
Beam on TA	500	uA	
Hrs / day	12	hrs	
Production	**56**	Ci / day	37 Ci in 6 hours (75 Ci in 2 x 6 hrs)
Av. Dose	25	mCi	20-30 mCi for cardiac and NPT bone scans
Av. t EOB	10	hrs	
Tc losses	15%		
Av. dose @ EOB	93	mCi	
Doses per site	**602**	Dose/day	
Tc-99m Req	**6,500**	Doses/day	Daily requirements for Canada
Tc-99m Req	**600**	Ci/day	For entire Canadian Population

Cost of Production

Cyclotron production of ^{99m}Tc can to be economically viable, it can effectively supplement and possibly compete with reactor based supply:

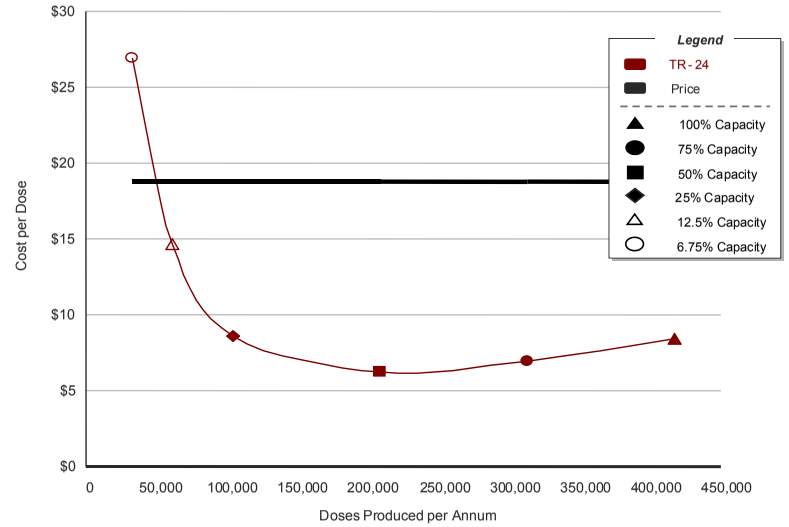

Challenges. Radionuclidic Purity

NUCLIDE	HALF-LIFE	REACTION	COMMENTS
^{99g}Tc	2.1E+5 y	^{100}Mo(p,2n)^{99}Tc ^{99m}Tc decay	Amounts produced at EOB are 2.5-3 times higher than in ^{99m}Tc eluted from generator after 24 hr growth time
^{98}Tc	4.2E+6 y	^{100}Mo(p,3n)^{98}Tc ^{98}Mo(p,n)^{98}Tc	Essentially stable, (p,3n) cross-section is negligible. Mostly produced from ^{98}Mo impurities
^{97m}Tc	91.4 d	^{98}Mo(p,2n)^{97m}Tc ^{97}Mo(p,n)^{97g}Tc	Radioactive impurity. Mostly produced from ^{98}Mo, since ^{97}Mo content is small
^{97g}Tc	4.2E+6 y	^{98}Mo(p,2n)^{97g}Tc ^{97}Mo(p,n)^{97g}Tc ^{97m}Tc decay	Essentially stable, small amount produced from ^{98}Mo impurities
^{96m}Tc	51.5 min	^{98}Mo(p,3n)^{96m}Tc ^{97}Mo(p,2n)^{96m}Tc	Short half-life. Low production cross-section. Small amount produced from ^{98}Mo impurities
^{96g}Tc	4.8 d	^{98}Mo(p,3n)^{96g}Tc ^{97}Mo(p,2n)^{96g}Tc ^{96m}Tc decay	Main radioactive impurity. Production rates 10 times higher on ^{97}Mo (very small content). ^{98}Mo(p,3n)^{96g}Tc is energy sensitive, 50% yield at 23 MeV.
^{99}Mo	2.75 d	^{100}Mo(p,pn)^{99}Mo ^{100}Mo(n,2n)^{99}Mo	Very low production rates. Molybdenum isotope, will be chemically separated.
^{97}Nb	72.1 min	^{100}Mo(p,α)^{97}Nb	Low production rates. Will be chemically separated.
^{96}Nb	23.3 h	^{100}Mo(p,αn)^{96}Nb	Low production rates. Will be chemically separated.
^{95}Nb	35 d	^{98}Mo(p,α)^{95}Nb	Low production rates. Will be chemically separated.

Radionuclidic Purity

Currently available enrichment 99.54 %

For >99.0% enrichment: ^{97m}Tc - 0.012%
^{96g}Tc - 0.2%

For >99.3% enrichment: ^{97m}Tc - 0.008%
^{96g}Tc - 0.11%

For >99.5% enrichment: ^{97m}Tc - 0.006%
^{96g} Tc - 0.08%

USP requirements <0.01% for any γ-emitter with no consideration given to dosimetry

Dosimetry studies will be required to determine dose from radionuclidic impurities. Preliminary estimated dose:

0.5 to 1.5 % for target organs
2-3% for whole body

Challenges. Specific Activity

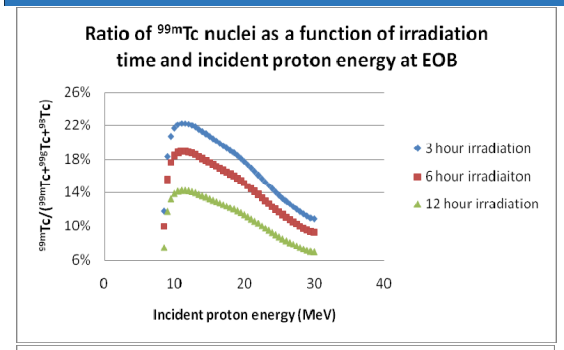

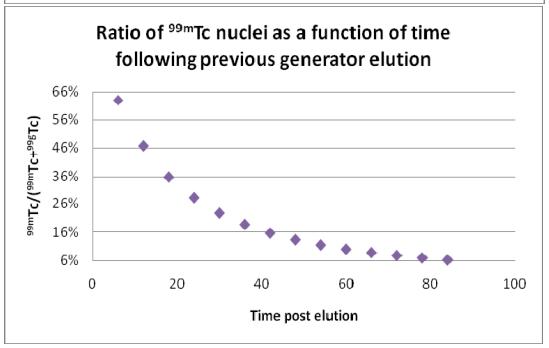

Cyclotron ^{99m}Tc specific activity is 2.5-3 (EOB) times lower than ^{99m}Tc eluted from a generator after 24 hr grow in period

24 hr generator – 28%

12 hr run cyclotron ~ 9%

6 hr run cyclotron ~ 12%

Measured by ICP MS 6 hrs @16.4 MeV

^{99m}Tc/Tc ~19%

equivalent to 36 hr generator

Labeling with specific activity as low as 2.8% has been studied for HMPAO, TF, MAG3, ECD and MIBI, as model compounds. All the standard quality control indicators, radiochemical purity and labeling efficiency values were unaffected.

Urbano, Journal of Radioanalytical and Nuclear Chemistry, Vol 265, No 1 (2005) 7-10.

Work in Progress

First experiments on direct ^{99m}Tc production started in October 2009 at University of Sherbrooke. The main objective was:

1. to demonstrate the feasibility of ^{99m}Tc production using "a cyclotron" and
2. to compared the chemical and radiochemical properties and *in vivo* behavior of cyclotron- and generator-produced technetium

Mo-100 (99.54%) targets were bombarded with 15.5-17.0 MeV protons (14–52 uA) using TR-19 cyclotron.

Radionuclidic purity: 0.0014% ^{96g}Tc, 0.0010% ^{95g}Tc and 0.0003% ^{95m}Tc
no ^{97m}Tc were detected
^{99}Mo and ^{97}Nb were quantitatively separated

Work in Progress

^{99m}Tc was formulated as 3 different radiopharmaceuticals:

- ^{99m}Tc-pertechnetate for thyroid imaging,
- ^{99m}Tc methylene diphosphate (^{99m}Tc-MDP) for bone scanning
- ^{99m}Tc hexakis-2- methoxyisobutyl isonitrile (^{99m}Tc-MIBI) for heart imaging

The radiochemical purity of cyclotron produced [^{99m}Tc]TcO_4^-

99.5% (USP requirement of 95%)

The labeling efficiency (potentially affected by ground state technetium):

98.4% for ^{99m}Tc-MDP
98.0% for ^{99m}Tc-MIBI

90.0% USP requirements

Work in Progress

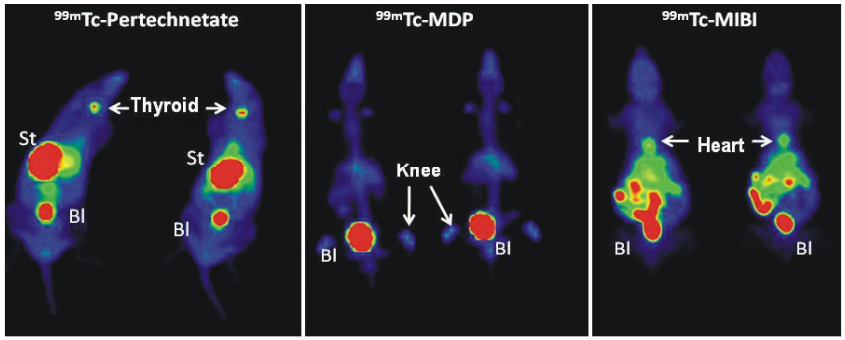

Whole-body scintigrams of two rats 2 h after administration of:

90 MBq of ^{99m}Tc-pertechnetate
34 MBq of ^{99m}Tc-MDP
15 MBq of ^{99m}Tc-MIBI

prepared from cyclotron- (right) and generator-produced ^{99m}Tc (left)

Guerin et al. J Nuclear Med 2010;51:13N-16N

Work in Progress

Time/radioactivity curves derived from ROIs

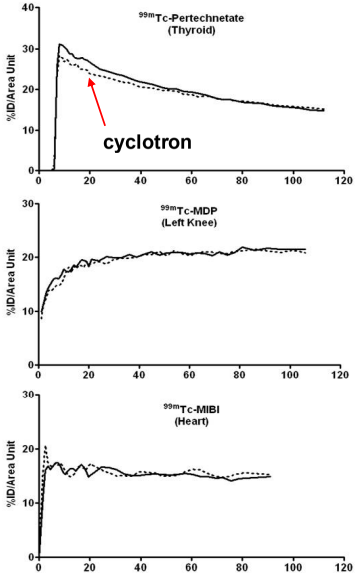

Tissue uptake in healthy rats (%ID/g)

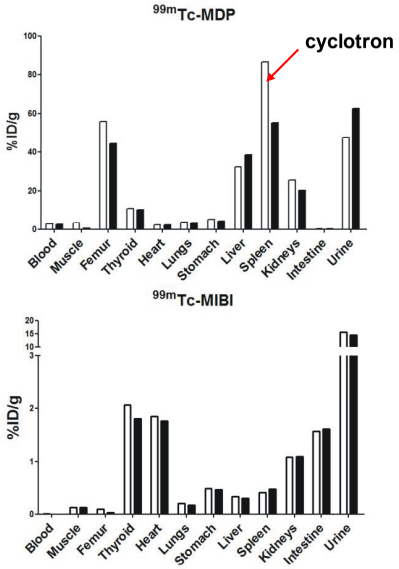

Conclusion

- Make the use of safe and relatively low-cost cyclotron technology is an attractive alternative to regional supply of ^{99m}Tc
- Flexible solution. As production demand changes sites can react to address new demands in a few weeks or even days
- Cyclotron production of ^{99m}Tc can to be economically viable, it can effectively compete with reactor based supply
- Expanding availability for other medical isotopes, including for PET imaging
- World-wide interest in this model

WTTC XIII – Presentation Discussions

1. Specific activity
   - Generator, 24h: 28%
   - Cyclotron 12h: 9%
   - Cyclotron 6h: 12%
   - Carefull with Tc96: bad energy to collimators
2. Supply of Mo100
   - Max 10Kg available worldwide
   - Price will depend on demand
3. Final price
   - Mo100 price decisive in overall process price
   - GMP compliance: 2$ USD / dose
4. Alternative processes
   - Nuclear reactor will start again
   - (n,gamma)M99: 10Ci/g, but still not profit wise for power plants

Targets for Cyclotron Production of Tc-99m

E.J. van Lier[1], J. Garret[2], B. Guerin[3], S. Rodrigue[3], J.E. van Lier[3], S. McQuarrie[4], J. Wilson[4], K. Gagnon[4], M.S. Kovacs[5], J. Burbee[1], A. Zyuzin[1]

[1]Advanced Cyclotron Systems Inc., Richmond, BC, Canada
[2]Brockhouse Institute for Materials Research, McMaster University, Hamilton, ON, Canada
[3]Sherbrooke Molecular Imaging Center, Université de Sherbrooke, QC, Canada
[4] Dept Oncologic Imaging, Cross Cancer Institute, Edmonton, AB, Canada
[5] Department of Medical Biophysics, University of Western Ontario, London, ON, Canada

Introduction: The measured yields of direct ^{99m}Tc production via ^{100}Mo(p,2n)^{99m}Tc suggest that ^{99m}Tc can be produced in quantities sufficient for supplying regional radiopharmacies[i, ii, iii], thereby reducing our reliance on reactor-derived ^{99}Mo. Cyclotron- and generator-produced ^{99m}Tc-radiopharmaceuticals were shown to be radionuclidically, chemically and biologically equivalent, giving matching images and identical kinetic and biodistribution patterns in animals, indicating that a medical cyclotron can produce USP-compliant ^{99m}Tc-radiopharmaceuticals for nuclear imaging procedures.[iv, v] In this work, several different ^{100}Mo target configurations were investigated and thick target yields were measured, validating the production of clinically useful quantities of ^{99m}Tc on a medical cyclotron.

Target Holders: Two different solid target holders were used to measure the thick target yields of the ^{100}Mo(p,2n)^{99m}Tc nuclear reaction. The straight 90° target holder has a heat removal capacity of 1.5 kW and while the 30° tilted solid target holder has a heat removal capacity of 3.0 kW. Two different solid target holders (Advanced Cyclotron Systems Inc., Richmond, BC, Canada) were installed on three compact medical cyclotrons (TR-19, Cross Cancer Institute, Edmonton, AB, TR-19 Centre Hospitalier Universitaire de Sherbrooke, Sherbrooke QC, Canada, GE PETrace, Lawson Health Research Institute, London ON, Canada).

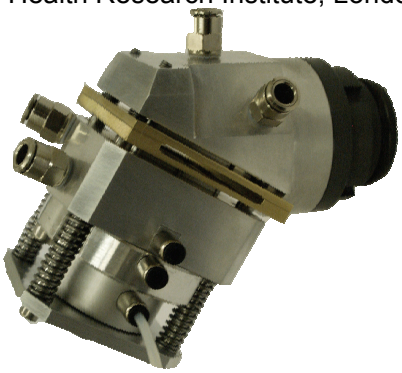

30° Solid Target Holder

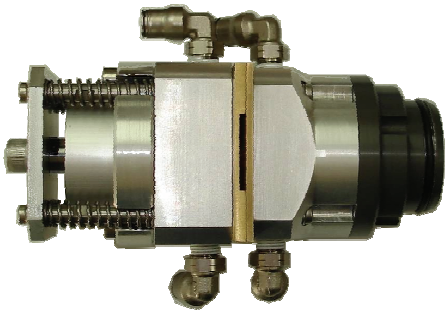

Straight Solid Target Holder

^{100}Mo Targetry. Molybdenum has been a metal of choice in accelerator targetry for several decades. With a high melting point, good thermal conductivity and chemical stability, molybdenum is nearly an ideal material for manufacturing high power targets. While a number of low and medium current cyclotron targets that use natural and enriched molybdenum isotopes have been developed and used for production of technetium isotopes: ^{94}Tc, ^{96}Tc and ^{99m}Tc [vi], a reliable process for preparation of enriched molybdenum targets has not yet been implemented. A number of standard target manufacturing techniques are being evaluated: melting, sintering, pressing/pelletizing, rolling, plating from solutions or molten salts, formation of low melting temperature Mo alloys, brazing or soldering ^{100}Mo to a target substrate, coating molybdenum with a protective layer, development of a thick target, plasma sputtering and other coating techniques.

Mo Target Preparation: Between 100-450 mg natural and enriched ^{100}Mo (99.5%) were pressed into 6 and 9.5 mm pellets at between 25,000 N and 100,000 N. The pellets were sintered in wet or dry hydrogen at 800-900ºC, and subsequently mounted into a tantalum substrate, either by pressing or arc melting or electron beam melting at currents between 40-70 mA with different sweeping / focusing patterns.

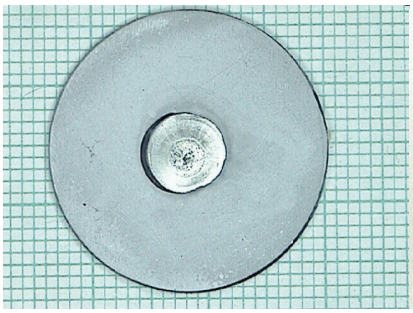

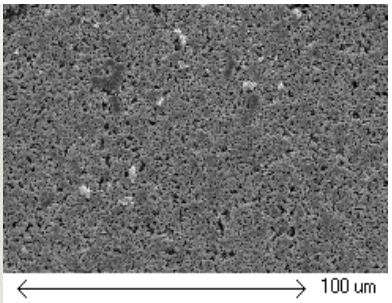

1. Arc Melted Mo in tantalum 2. Pressed Mo in Ta (EOB) 3. SEM of pressed Mo

^{99m}Tc Production: ^{99m}Tc was produced via the ^{100}Mo(p,2n)^{99m}Tc nuclear reaction on a 19 MeV medical cyclotron using an incident proton energy of 15-17 MeV at current between 14-52 µA. After bombardment targets were subjected to electrochemical dissolution, ^{99m}Tc was purified by ion-exchange chromatography and recovered as pertechnetate.

Electron beam melting of Mo to Tatarget substrate

Results: Up to 44.7 GBq (1.2 Ci) (EOB) of ^{99m}Tc was produced after a 6-h bombardment at 16.4 MeV and 39 µA. This corresponds to a thick target production yield of 0.25 GBq/µA/h (6.8 mCi/µA/h) and 2.3 GBq/µA (63 mCi/µA) at saturation and is in good agreement with literature data.[I, II, III] The radionuclide purity of the cyclotron-produced ^{99m}Tc was >99.99%, as assessed by γ spectroscopy, exceeding USP requirements for generator-based ^{99m}Tc. The content of other technetium isotopes was measured after allowing sufficient time (4 days) for ^{99m}Tc decay and was below USP requirements of 0.01% for generator-produced ^{99m}Tc. No other radionuclidic impurities were found. The radiochemical purity of cyclotron-produced $^{99m}TcO_4^-$ was >99.5%, well above the USP requirement of 95%.

Conclusion: This study confirms that clinically useful quantities of ^{99m}Tc can be produced on medical cyclotrons installed worldwide. Extrapolating these results to the optimal energy of 22-24 MeV indicates that over 2 TBq of ^{99m}Tc can be produced daily for regional distribution on a high-current medium-energy cyclotron. Implementing networks of high-current medium energy cyclotrons would reduce reliance on nuclear reactors and attenuate the negative consequences associated with the use of fission technology.

---

[i] Scholten, B., Lambrecht, R.M., Cogneau, M., Vera Ruiz, H., Qaim, S.M., 1999. Excitation functions for the cyclotron production of ^{99m}Tc and ^{99}Mo. Appl. Radiat. Isotopes 51, 69–80

[ii] Takács, S.; Szűcs, Z., Tárkányi, F.; Hermanne, A.; Sonck, M Evaluation of proton induced reactions on ^{100}Mo: New cross sections for production of ^{99m}Tc and ^{99}Mo, J. of Radioanalytical and Nuclear Chemistry, 257,1 , 2003, 195-201(7)

[iii] Lebeda, O.; Pruszynski, M.: New measurement of excitation functions for (p,x) reactions on natMo with special regard to the formation of ^{95m}Tc, $^{96m+g}$Tc, ^{99m}Tc and ^{99}Mo, Appl. Radiat. Isot., in press, (personal communication)

[iv] Guérin, B.; Tremblay, S; Rodrigue, S.; Rousseau, J.A.; Dumulon-Perreault, V.; Lecomte, R.; van Lier, J.E.; Zyuzin, A.; van Lier, E.J. Cyclotron Production of ^{99m}Tc: An Approach to the Medical Isotope Crisis J. Nuclear Med., 2010;51:13N-16N

[v] Zyuzin, A.; Guérin, B.; van Lier, E.J.; Tremblay, S; Rodrigue, S.; Rousseau, J.A.; Dumulon-Perreault, V.; Lecomte, R.; van Lier, J.E.; Cyclotron production of ^{99m}Tc WTTC 13, Abstract

[vi] Qaim, S.M., Production of high purity ^{94m}Tc for positron emission tomography studies, Nuclear Medicine and Biology, 27, 4, 2000, 323-328

Targets for Cyclotron Production of Tc-99m

E.J. van Lier[1], J. Garret[2], B. Guerin[3], S. Rodrigue[3], J.E. van Lier[3], S. McQuarrie[4], J. Wilson[4], K. Gagnon[4], M.S. Kovacs[5], J. Burbee[1], A. Zyuzin[1]

[1] Advanced Cyclotron Systems Inc., Richmond, BC, Canada
[2] Brockhouse Inst. for Mat. Research, McMaster University, Hamilton, ON, Canada
[3] Sherbrooke Molecular Imaging Center, Université de Sherbrooke, QC, Canada
[4] Dept Oncologic Imaging, Cross Cancer Institute, Edmonton, AB, Canada
[5] Dept. of Medical Biophysics, University of Western Ontario, London, ON, Canada

Overview

- Cross-Section measurements
- Target Stations: 40 μA – 500 μA
- Targets for Cyclotron Produced Tc-99m
  - Arc Melting Molybdenum
  - E-Beam Melting Molybdenum
  - Pressed Molybdenum Power
- Thick Target Yields -- Results
- Future Work

^{100}Mo(p,2n)^{99m}Tc Cross Section

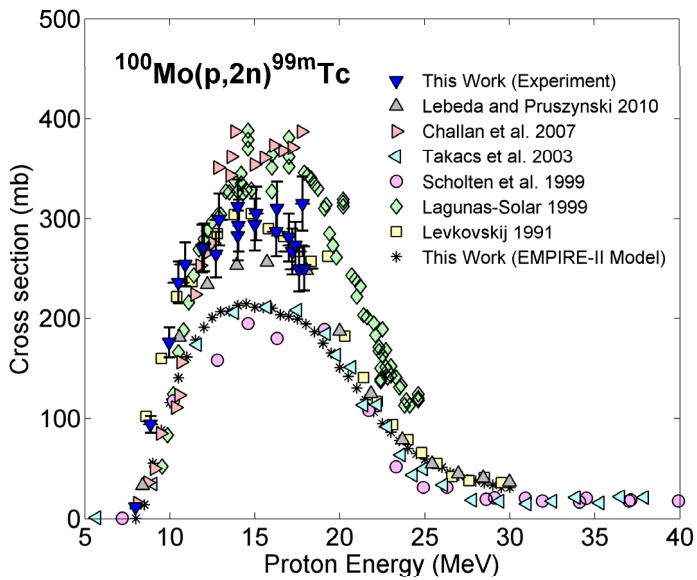

Gagnon et al. WTTC13

Target Stations

Straight Target: 40 μA
PET: 1.3 Ci in 6 hrs
TR24: 2.8 Ci in 6 hrs

30° Target: 80 μA
PET: 2.6 Ci in 6 hrs
TR24: 5.6 Ci in 6 hrs

Medium Current : 200 μA
PET: 6.6 Ci in 6 hrs
TR24: 14 Ci in 6 hrs

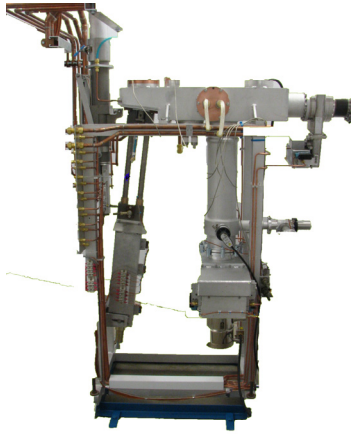

High Current: 500 μA
PET: N/A
TR24: 35 Ci in 6 hrs

Pressed Molybdenum Powder

- 100-450 mg Mo (nat. and enriched ^{100}Mo 99-99.5%)
- 6 and 9.5 mm diameter pellets
- Force: 27-107 kN

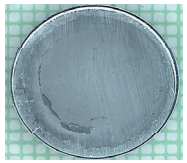

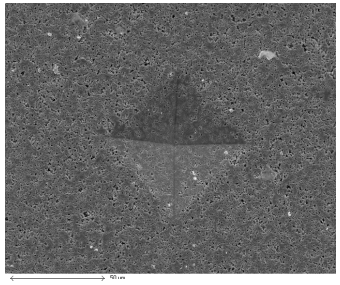

SEM @655x of 27 kN sample

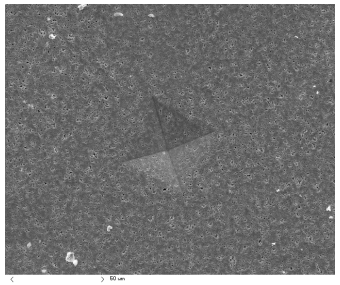

SEM @655x of 107 kN sample

Pressed Molybdenum Powder

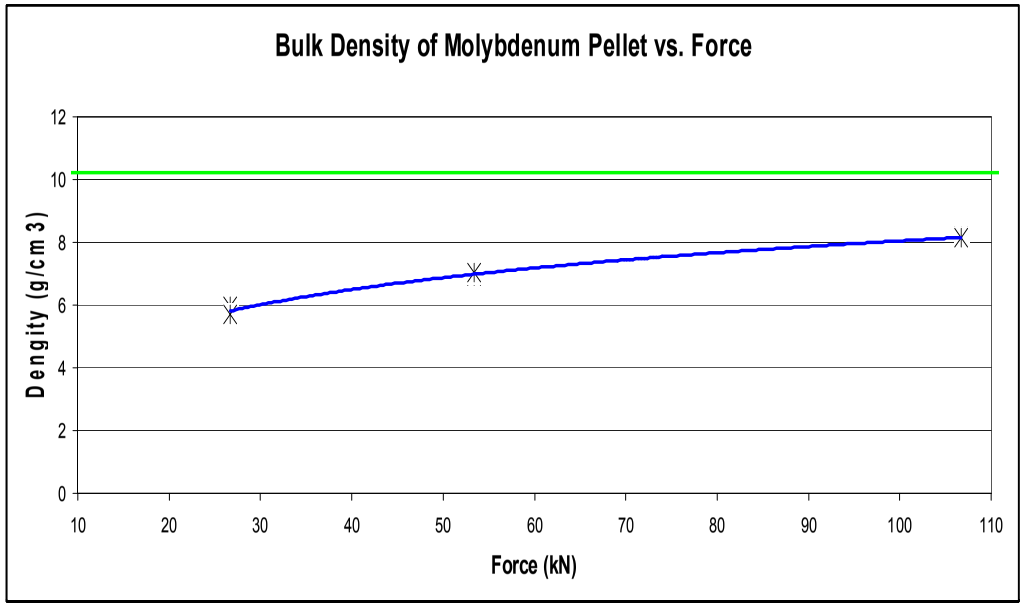

Molybdenum Targets – Arc Melting

- Pressed Mo Pellets Arc Melted to 24 mm tantalum disk
  - Pro:
    - Good thermal contact Mo/Ta
    - Easy to manufacture
    - Can run up to 65 μA
  - Cons:
    - Difficult to control arc
    - Potential alloy formation
    - Slow dissolution of target

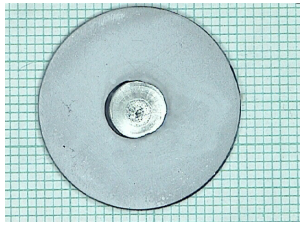

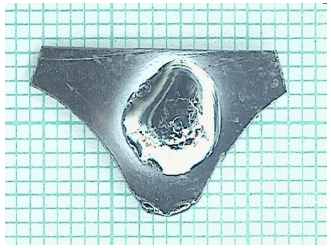

Molybdenum Targets – E-beam

- Mo Disks were Ebeam melted to 24 mm tantalum disk
  - 50-70 mA Electron beam
  - Pros:
    - Accurate control of E-beam
  - Cons
    - No Bonding Mo/Ta
    - Critical Temp Mo melting (mp 2617°C) and Ta deformation (mp 3017°C)

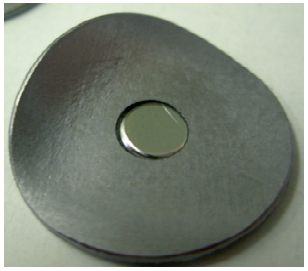

Molybdenum Targets – Pressed

- **Mo pellets pressed into Al ring then to 24 mm Ta disk**
- **Mo pellets pressed directly into 24 mm Al disk**
  - Pros:
    - Relatively Inexpensive
    - Easy to dissolve Mo
    - Can run up to 40 μA
  - Cons:
    - Brittle Mo pellets
    - Poor thermal contact

Results –Thick Target Yields

- **Thick Target, 16.4 MeV → 0 MeV, 39 μA 6 hrs**
  - **44.7 GBq (1.2 Ci) Tc-99m (EOB)**
  - **thick target production yield**
    - **0.25 GBq/μA/h (6.8 mCi/μA/h)**
  - **Saturated yield**
    - **2.3 GBq/μA (63 mCi/μA)**
- **Preliminary results (23.8→ 12.5 MeV, 5 min, 1.94 μA)**
  - **Saturated yield**
    - **4.6 GBq/μA (125 mCi/μA) (measured)**
    - **5.4 GBq/μA (147 mCi/μA) (scaled to 24→10 MeV)**

Results –Thick Target Yields

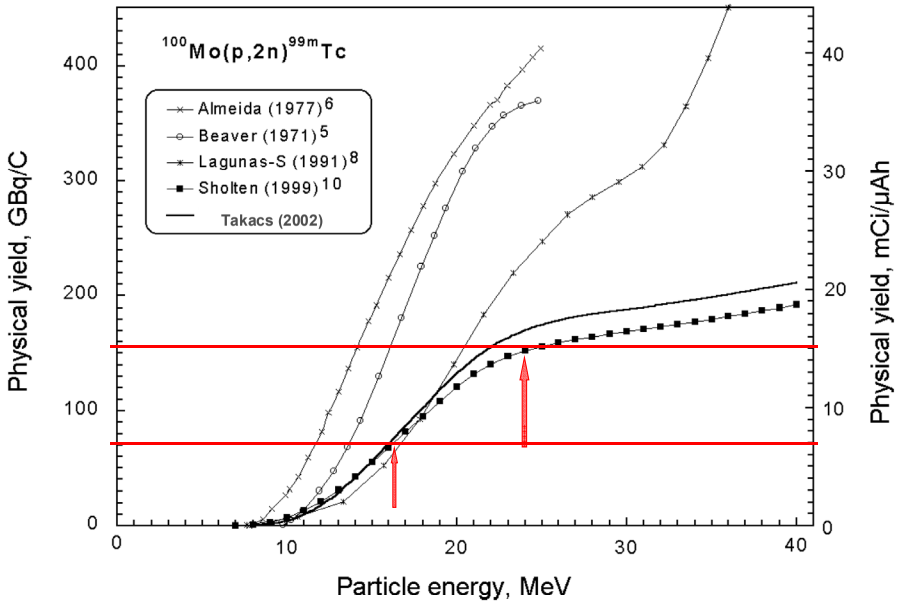

Conclusion

- **Target Yields:**
  - **Thick target yields agreement with previously measured**
  - **PET cyclotrons can produce multi-Ci Tc-99m**
  - **High Current TR24 cyclotron could complement generators**

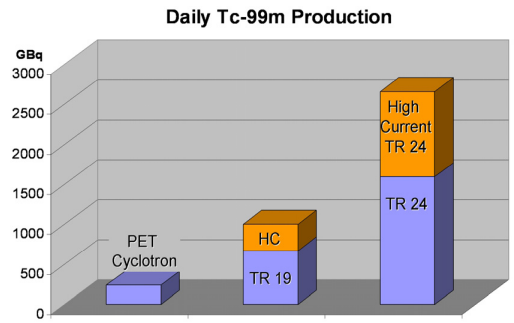

Current	PET	TR24
40 μA	1.3 Ci	2.8 Ci
80 μA	2.6 Ci	5.6 Ci
200 μA	6.6 Ci	14 Ci
500 μA	NA	35 Ci

Future Work

- Continue to study targets:
  - Pressed Targets
  - Ebeam/Arc Melting
  - Foils
  - Plating
  - Vapor deposition / plasma spray
- Select most appropriate method
  - Cost effective
  - Reliable / Robust
  - Scalable with overall process integration

WTTC XIII – Presentation Discussions

1. Tc/Mo separation?
   - Next step.

2. Cyclotrons needed to replace nuclear production of Tc99m?
   - 5-8 TR-24 for Canada, 10x more for the USA
   - But: 500uA cyclotrons…
   - FDA approval? It was approved 3 decades ago…

A further exploration of the merits of a Niobium/Niobium vs Niobium/Havar target body/foil combination for [^{18}F]Fluoride production: A detailed HP γ-spectrometry study

John Sunderland, G Leonard Watkins, Colbin E Erdahl, Levent Sensoy, Arda Konik

PET Imaging Center, University of Iowa Health Care, Iowa City, IA 52242, USA

In the current nuclear medicine environment, both the Molybdenum crisis and FDA regulation, are driving the PET community to look more closely at the production of [^{18}F]NaF for PET imaging. This situation has led the University of Iowa to design and construct a targetry unit and a synthesis/purification module designed to obtain highest purity [^{18}F]NaF. In this study we investigate the radionuclidic purity of [^{18}F]NaF from this module with [^{18}F]NaF produced from both a Nb/Havar and Nb/Nb target/body combination. The rationale for the targetry comes from the recent observations of the Wisconsin and Edmonton groups[1, 2, 3].

As can be seen from the schematic in Figure 2 [^{18}O]H_2O was irradiated in a Nb target body equipped with either a Nb or Havar front foil. The target water was emptied into a target collection vessel (TCV). Under N_2 overpressure the contents were passed sequentially through a CM cation SPE cartridge and a QMA anion SPE cartridge to an [^{18}O]H_2O recovery vessel. Any non-anionic material was then flushed from the QMA with water (5 mL) to waste. The [^{18}F]NaF and any other anionic species were the eluted into the final product vial with isotonic saline (15 mL).

To assess radionuclidic purity, the Nb/Niobium body/foil combination was bombarded at 30 µA for 5, 10, 20 and 80 minutes. The Nb/Havar body/foil combination was bombarded at 30 µA for 80 minutes. In all cases the TCV, CM, QMA, and Product Vial were quantitatively assessed for radionuclidic content using an GEM20P4-70. ORTEC GEM Coaxial P-type HPGe Gamma-Ray Detector. Results are summarized in Figure 2.

The Nb-Nb body/foil combination spectrum was simple; 30 µA for 10 minutes created minute quantities of ^{56,57,58}Co and ^{52}Mn (<0.1 nCi) from the trace quantities of iron and chromium in the Nb foil, but approximately 1 µCi of ^{93m}Mo from the ^{93}Nb(p,n)^{93m}Mo reaction (Figure 1). The CM cation cartridge quantitatively bound the cobalt isotopes, while the ^{93m}Mo, initially trapped by the QMA anion cartridge, eluted quantitatively with the [^{18}F]NaF. Under similar conditions, the Nb/Havar body/foil created 12 radionuclides at 10-100 nCi levels. The CM/QMA cartridge combination served to eliminate 6 of 12 contaminants, and reduce the quantities of the remaining nuclides substantially, but not completely. The product vial from the Nb/Nb combination had only ^{93m}Mo, while the product vial from the Nb/Havar target resulted in [^{18}F]NaF with ^{51}Cr, ^{95,96}Tc,^{181,182}Re, and ^{93m}Mo (from Nb target body) contaminants with activities ranging from 1-30 nCi.

References:

1. SJA Nye, MA Avila-Rodriguez & RJ Nickles. "A grid-mounted niobium body target for the production of reactive [^{18}F]fluoride". *Appl. Radiat. Isot.* (2006);64:536-539

2. JS Wilson, MA Avila-Rodriguez, & SA McQuarrie. "Ionic contaminants in irradiated [^{18}O]water generated with Havar and Havar-Nb foils". *Abstract Book: 12th International Workshop on Targetry and Target Chemistry, Seattle,* 2008: pp31-33.

3. MA Avila-Rodriguez, JS Wilson and SA McQuarrie. "A quantitative and compararative study of radionuclidic and chemical impurities in water samples irradiated in a niobium target with Havar vs niobium-sputtered Havar as entrance foils". *Appl. Radiat. Isot.* (2008);66: 1777-1780

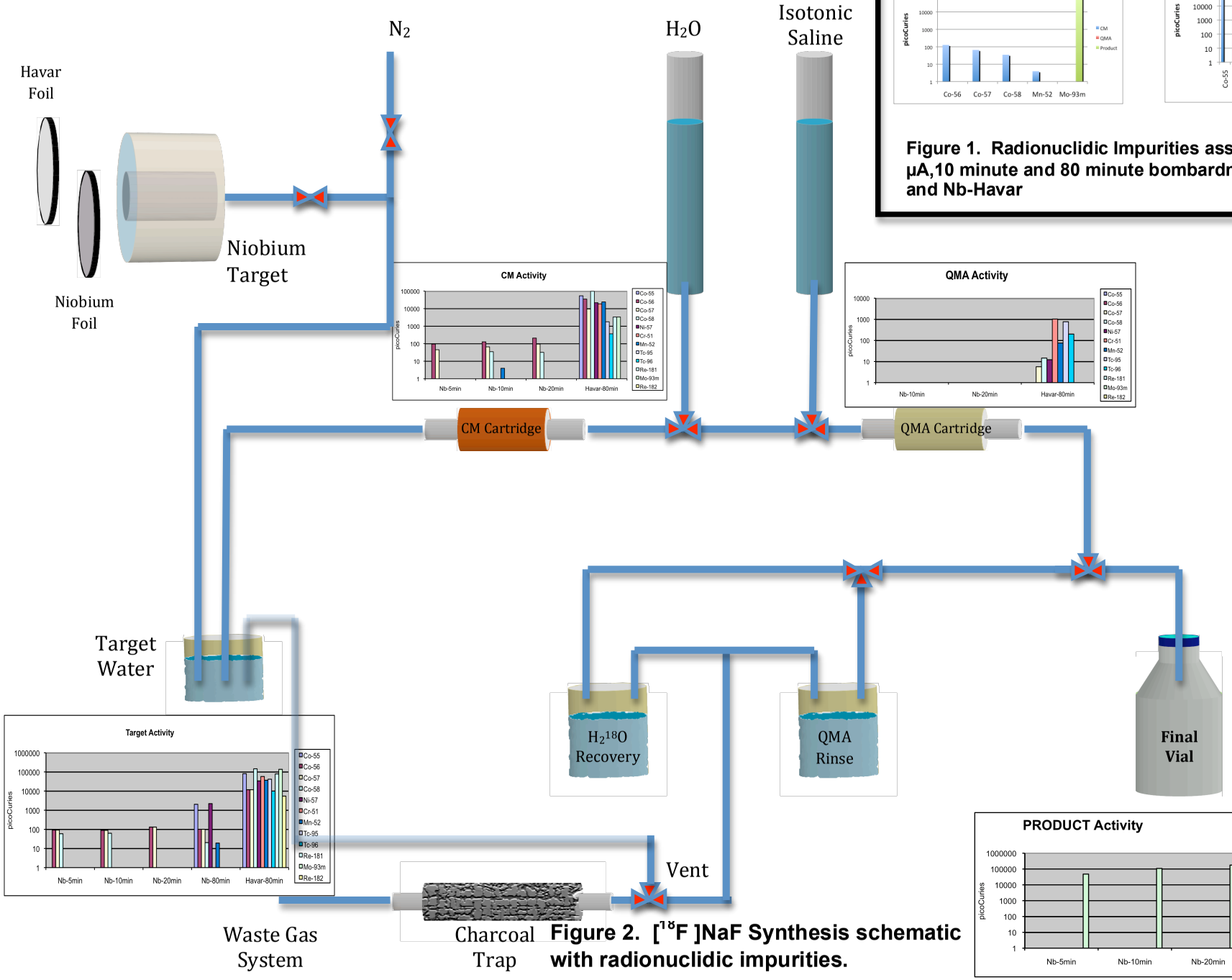

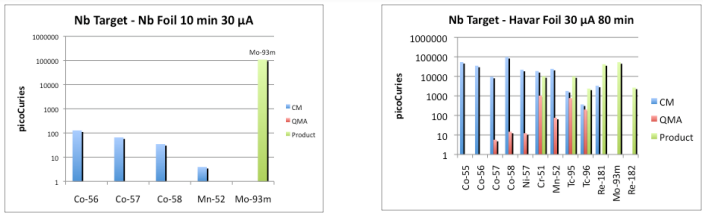

Figure 1. Radionuclidic Impurities associated with 30 µA,10 minute and 80 minute bombardments on Nb-Nb and Nb-Havar

Figure 2. [^{18}F]NaF Synthesis schematic with radionuclidic impurities.

A Further Exploration of the Merits of a Niobium/Niobium vs. Niobium/Havar target body/foil Combination for [^{18}F]Fluoride Production: A detailed HPGe γ-spectrometry study

John Sunderland, G Leonard Watkins, Colbin E Erdahl, Levent Sensoy, Arda Konik. PET Imaging Center, University of Iowa Health Care, Iowa City, IA

Project Rationale

1. In the current nuclear medicine environment, both the Molybdenum crisis and FDA regulation are driving the PET community to look more closely at the production of [^{18}F]NaF for PET imaging. This situation has led the University of Iowa to design and construct a targetry and a synthesis/purification module designed to obtain highest purity [^{18}F]NaF.
2. In this study we investigate the radionuclidic purity of [^{18}F]NaF from this module with [^{18}F]Fluoride produced from both a Nb/Havar and Nb/Nb target/body. combination.

[^{18}F]NaF Synthesis Schematic

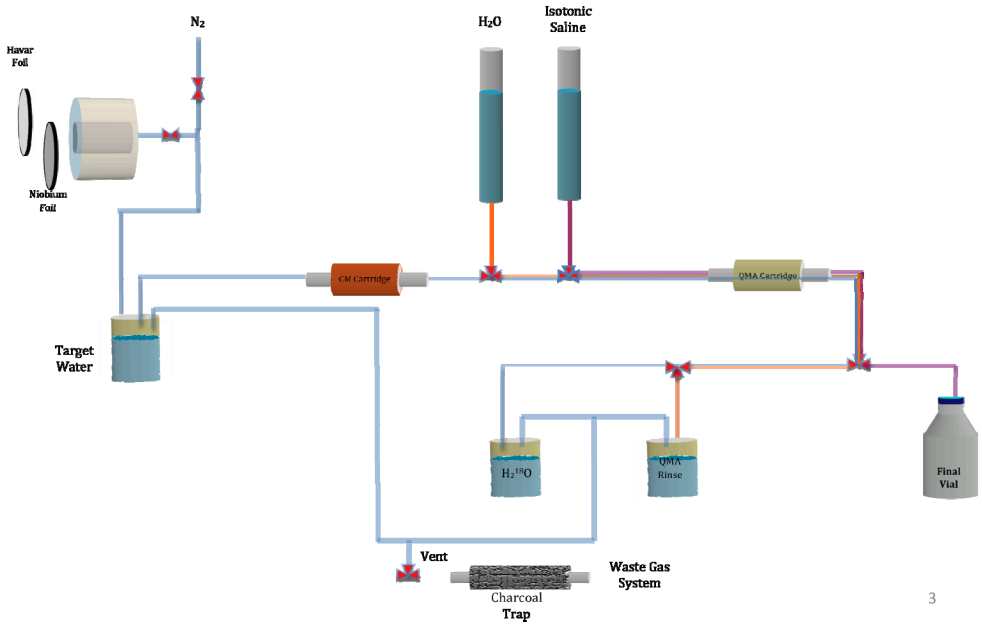

[^{18}F]NaF Synthesis Module

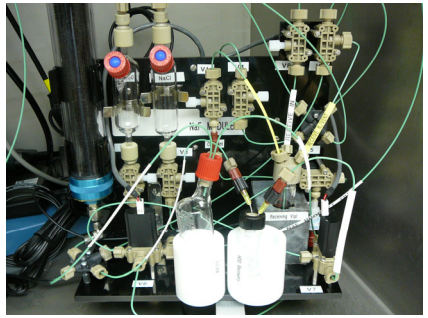

HPGe Counting System

In all cases the Target(TCV), CM cartiridge (CM), QMA cartridge (QMA) and Product Vial were quantitatively assessed for radionuclidic content using a shielded calibrated GEM20P4-70 ORTEC GEM Coaxial P-type HPGe Gamma-Ray Detector.

Typical Target Water Spectra from Nb-Havar Combination

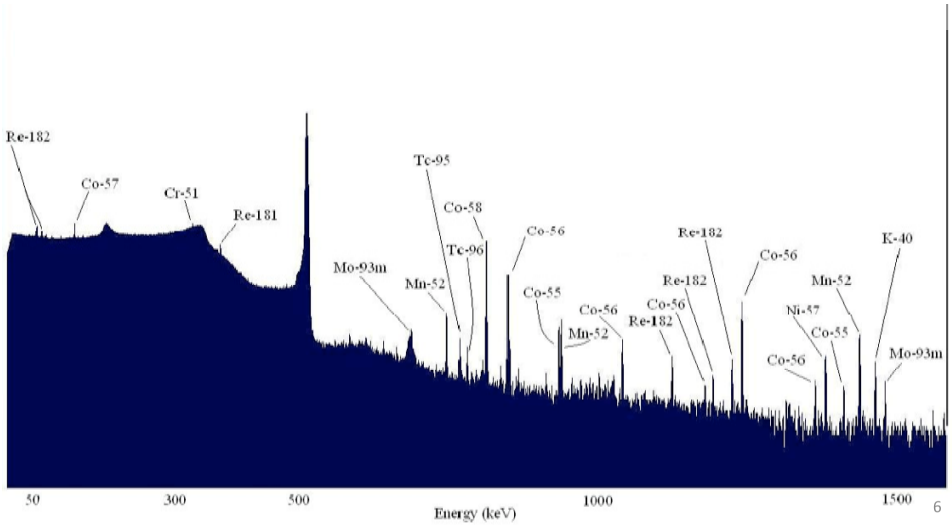

Purification Cartridge and Product Vial Radionuclidic Contents – Nb Target/Havar Foil

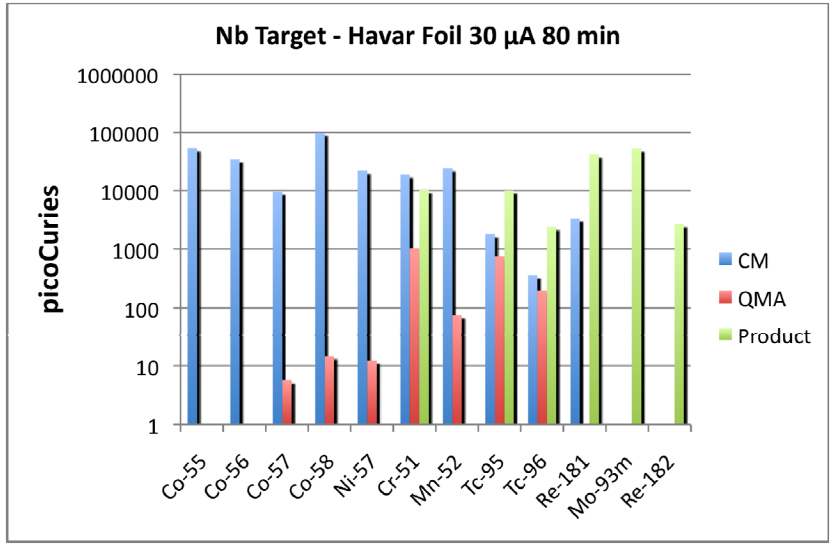

Radionuclidic Contaminants in Synthesis Components & Final Product

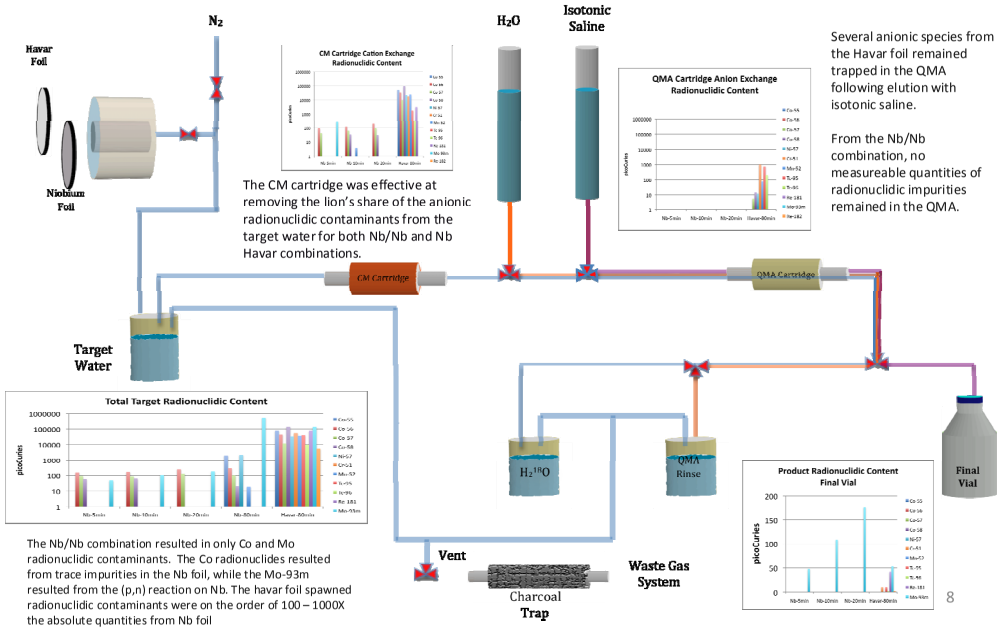

Conclusions

1. The University of Iowa [^{18}F]NaF synthesis/purification system produced a final product with acceptable radionuclidic purity regardless of whether the Nb-Nb or Nb/Havar target body/foil combination was used.

2. Order of magnitude calculations suggest that *additional* radiation dose resulting from the picoCurie levels of radionuclidic contaminants will result in substantially less than 1 mR additional whole body radiation dose for both target body/foil combinations using highly conservative assumptions that.
   a) All particulate and gamma radiation emitted in the body are absorbed.
   b) Biological half-lives are infinite.
   c) No attempt to model biodistribution was included in the calculation.

Conclusions

3. It is NOT clear which of the two target body/foil systems is optimal. Mo-93m has a short half-life (6.85 hours) but it also has three relatively energetic gamma emissions of approximately 1 MeV. The radionuclides from Havar have generally longer half-lives, but lesser quantities. Havar has the additional advantage of having more desirable physical properties that make it the foil of choice for many targetry applications.

4. As the University of Iowa [^{18}F]NaF synthesis/purification system removes the vast majority of radionuclidic contaminants from Havar, and the system fails to remove the Mo-93m produced by the Nb foil from the final product. It is likely that we will revert to the Nb target body/Havar foil model due to the physical robustness of the system.

WTTC XIII – Presentation Discussions

1. Which one is the best foil?
   - Ni vs. Havar: no yield difference
   - Careful with impurities in foil material
   - Ti can be used, Va trapped in Sep-pak
   - Niobium-Havar preferred to Niobium-Niobium (experience)

A multi-wire proportional counter for measurement of positron-emitting radionuclides during on-line blood sampling

H. T. Sipila[1], A. Roivainen[1] and S-J. Heselius[2]
[1] Turku PET Centre, Turku University Hospital, P.O. Box 52, FI-20520 Turku, Finland
[2] Turku PET Centre, Accelerator Laboratory, Porthansgatan 3, FI-20500 Turku, Finland

Introduction. Pharmacokinetic analyses of PET data require the exact determination of the input function, i.e. the determination of radioactivity concentrations in blood and plasma. Silicon diodes have been used for the measurement of blood radioactivity during PET imaging of rodents [1]. Conventional BGO detectors are widely used for blood radioactivity measurements in human studies (Allog Ab, Sweden). The purpose of the present study was to develop a flow-through multi-wire proportional counter with high sensitivity for positrons emitted from the commonly used positron emitters ^{11}C, ^{15}O, ^{18}F and ^{68}Ga. The proportional counter used in this work was a multi-wire flow-through detector filled with argon-methane gas (P10). The detector system was tested for measurements of ^{11}C, ^{15}O, ^{18}F and ^{68}Ga with mean positron energies in the energy interval 250 - 830 keV. Although the sensitivity of a gas-filled detector is low for 511 keV photons, positrons in the mentioned energy range will give an efficient signal when they interact with the detector fill gas. This type of detector requires only light lead shielding and the detector system can be installed very close to the animal or patient. The detector was used in studying time-activity curves in rats after i.v. injection of [^{15}O]water. Our measurements indicate that the conventional proportional counter technique is useful for routine on-line analyses of blood samples obtained during PET studies of rodents and humans.

Materials and Methods. The multi-wire proportional counter (Fig. 1) was constructed in our laboratory. The electronics was purchased from Oxford Instruments Analytical Oy (Finland). The detector was equipped with an aluminium tube window (thickness 100 µm, diameter 13 mm, length 78 mm). The detector was filled with argon-methane gas (P10) and closed at 1060 mbar pressure. The counter electronics, preamplifier, linear amplifier and high-voltage power supply were all placed in the same aluminium box. The counter A/D converter and software for data collection were custom made. The detector was shielded with 50 mm of lead (25 kg). The background count rate was 2-4 cps. The stability and working conditions of the detector were tested with a ^{241}Am X-ray source. The performance of the multi-wire proportional counter was tested with known activities of ^{11}C, ^{15}O, ^{18}F and ^{68}Ga in water solutions. Oxygen-15 was produced with the Cyclone 3 cyclotron (IBA, Belgium) of the Turku PET Centre. [^{15}O]water was produced with a Hidex Radiowater Generator (Hidex Oy, Finland). ^{11}C and ^{18}F sources were produced with the MGC-20 and CC-18/9 cyclotrons of the Turku PET Centre. ^{68}Ga-chloride solution was obtained from a $^{68}Ge/^{68}Ga$ generator (Obninsk, Russia).

The rats were anesthetized with isoflurane. [^{15}O]water (50 - 60 MBq, 500 µL) was manually injected via tail vein using a cannula. The blood sampling tube (Teflon, i.d. 0.5 mm, o.d. 1.0 mm) was installed through the detector. A peristaltic pump was used for blood sampling from the arteria femoralis. The blood-flow rate through the detector was 500 µL/min. The animals were placed in a PET scanner (HRRT, Siemens) in order to get a reference input function from the heart left ventricle.

Results and Discussion. Fig. 2 shows the detector efficiency as a function of the mean energy of positrons. The radionuclides ^{11}C, ^{15}O, ^{18}F and ^{68}Ga in water solutions in the Teflon tubing (i.d. 1.5 mm, o.d. 2.5 mm) were used as positron sources. The graph reflects a linear relationship between the detector efficiencies and the mean energies for positrons of the four radionuclides (R^2 = 0.9982). The multi-wire proportional counter responses to ^{11}C, ^{15}O, ^{18}F and ^{68}Ga activities in the Teflon tubing are shown in Fig. 3. The detector response was linear for ^{15}O in the range 5 - 80 kBq/mL with the i.d. 1.5 mm Teflon tubing and in the range 100 - 1300 kBq/mL with the i.d. 0.5 mm Teflon tubing. These ranges cover the radioactivity concentrations for both human and

rat studies. Radioactivity levels in humans are about 20 times lower but still well above the signal to noise level.

Blood time-activity curves (arteria femolaris) were recorded for [^{15}O]water in rat studies. Our results show that a multi-wire proportional counter setup can be used for measurements of blood time-activity curves in PET studies with [^{15}O]water. Blood radioactivities with injection of ^{11}C, ^{18}F and ^{68}Ga labelled tracers can also be measured. The detector efficiency for ^{18}F is low (0.9 - 4.0 %, depending on wall thickness and i.d. of sampling tubing), which limits the use of the detector in ^{18}F applications. Taking into account the abundance of positron decay of ^{68}Ga (86%) the actual detector efficiency for ^{68}Ga is slightly less than for ^{15}O (positron decay 100%).

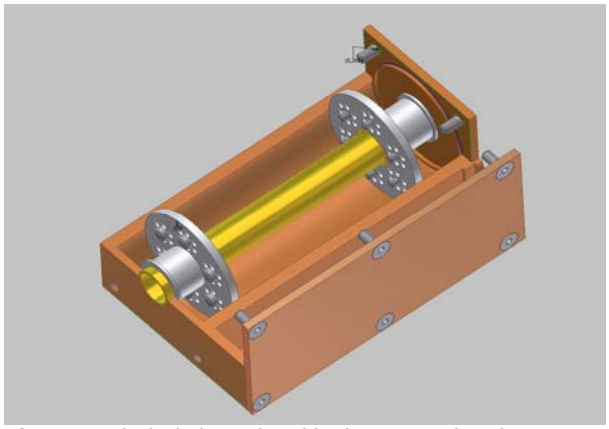

Fig. 1. Exploded view of multi-wire proportional counter.

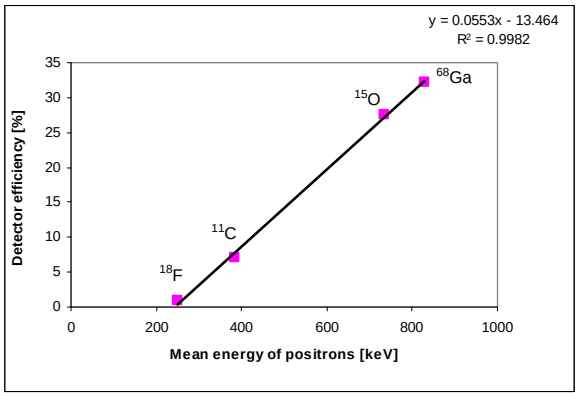

Fig. 2. Detector efficiency versus mean energy of positrons. Radionuclides ^{11}C, ^{15}O, ^{18}F and ^{68}Ga were used as positron sources.

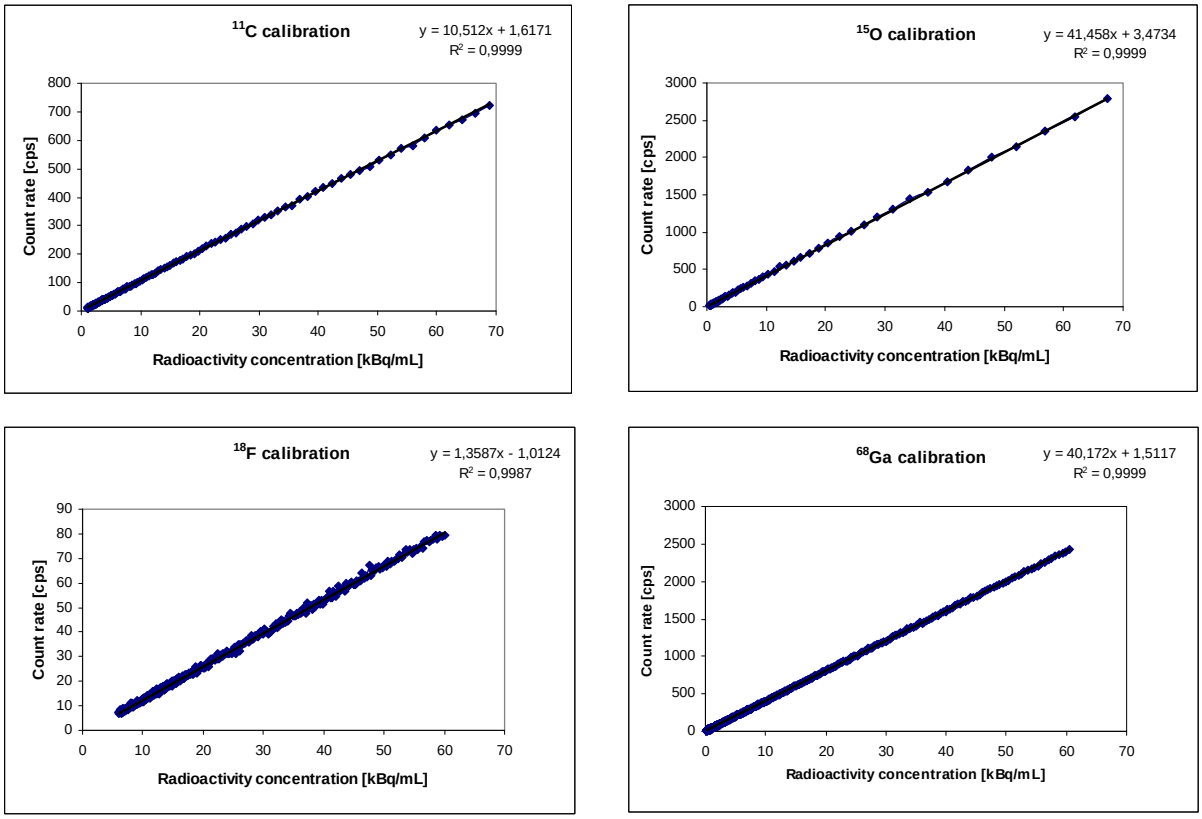

Fig. 3. Multi-wire proportional counter response to ^{11}C, ^{15}O, ^{18}F and ^{68}Ga activities in Teflon tubing.

Reference. 1. Jean-Marc Reymond, David Guez, Sophie Kerhoas, Philippe Mangeot, Raphael Boisgard, Sebastien Jan, Bertrand Tavitian and Regine Trebossen, Nuclear Instr. Meth. **A571** (2007) 358–361.

A multi-wire proportional counter for measurement of positron-emitting radionuclides during on-line blood sampling

H. T. Sipila[1], A. Roivainen[1] and S-J. Heselius[2]
1 Turku PET Centre, Turku University Central Hospital, PO Box 52, FI-20500 Turku , Finland
2 Turku PET Centre, Accelerator Laboratory, Porthaninkatu 3, FI-20500 Turku, Finland

- low activity
- high 511keV photon background

- low 511keV photon sensitivity
- good geometry - flowthrough detector
- positrons, prositron sensitive dector

- gas proportional counter = positron sensitive
- low sensitivity for 511keV photons
- low background,

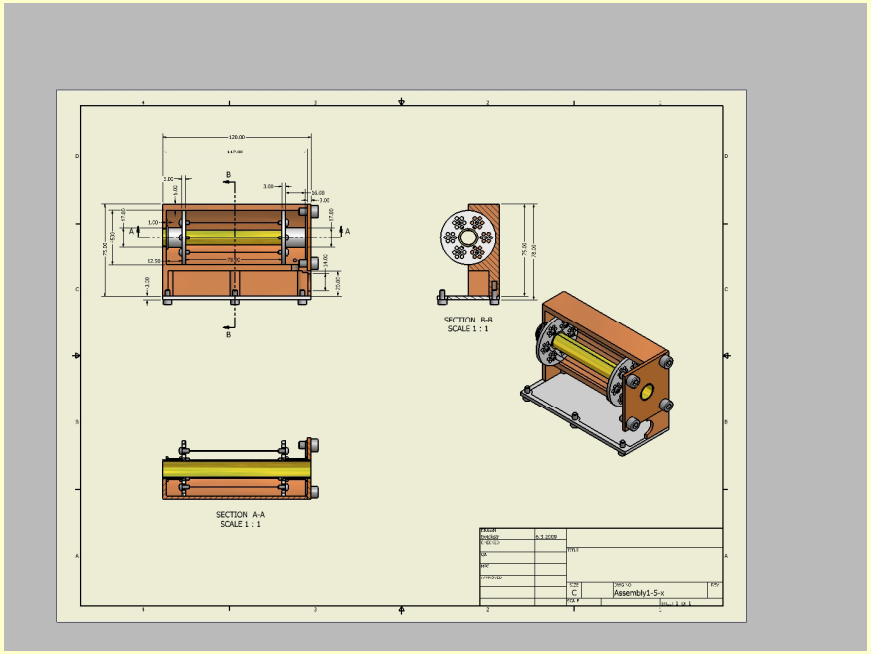

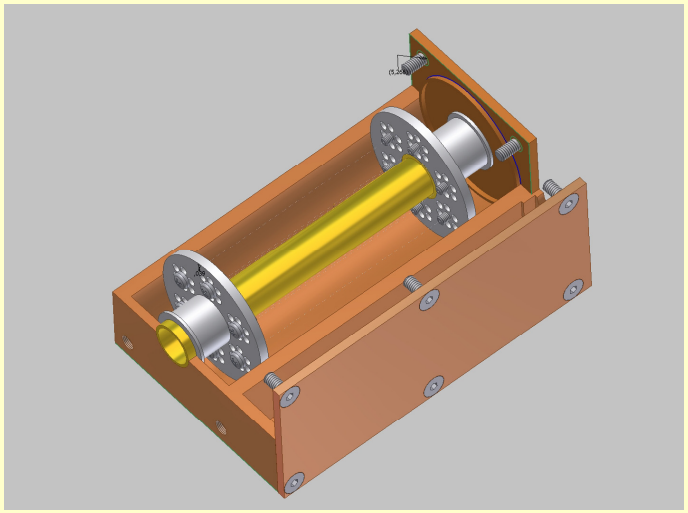

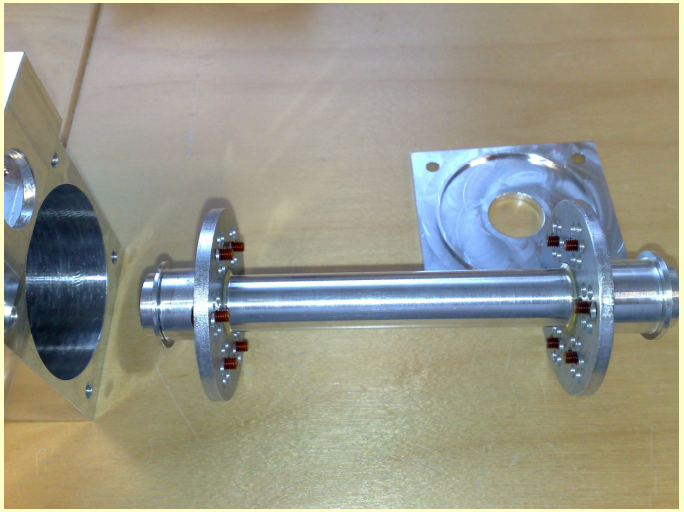

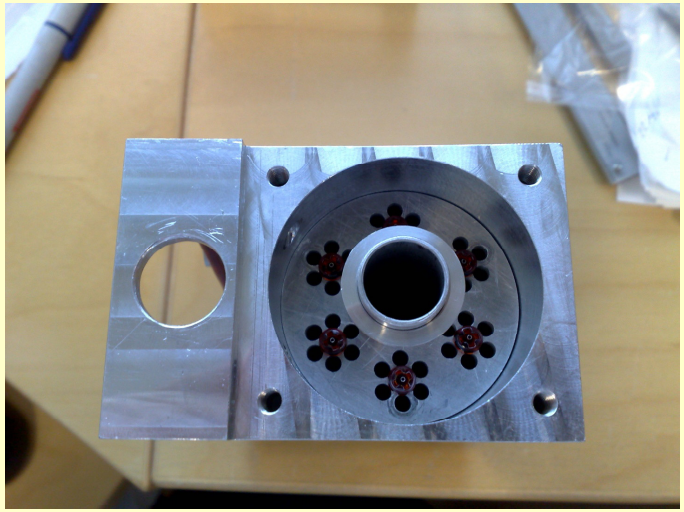

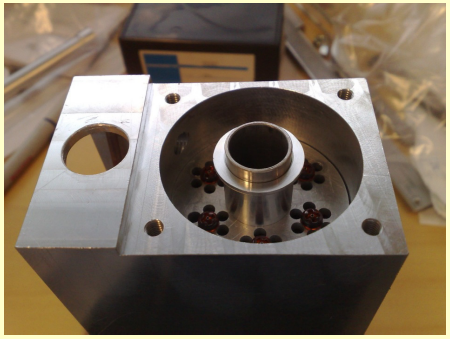

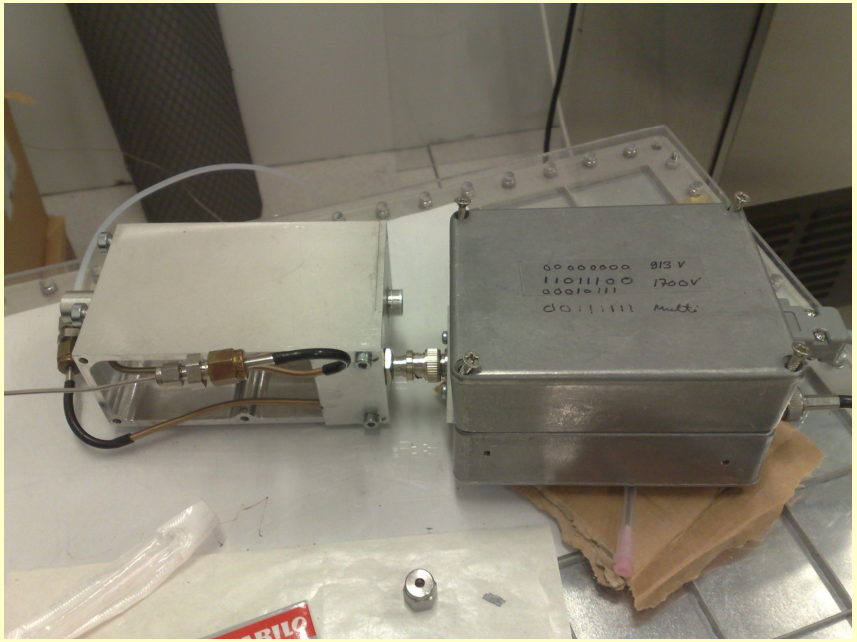

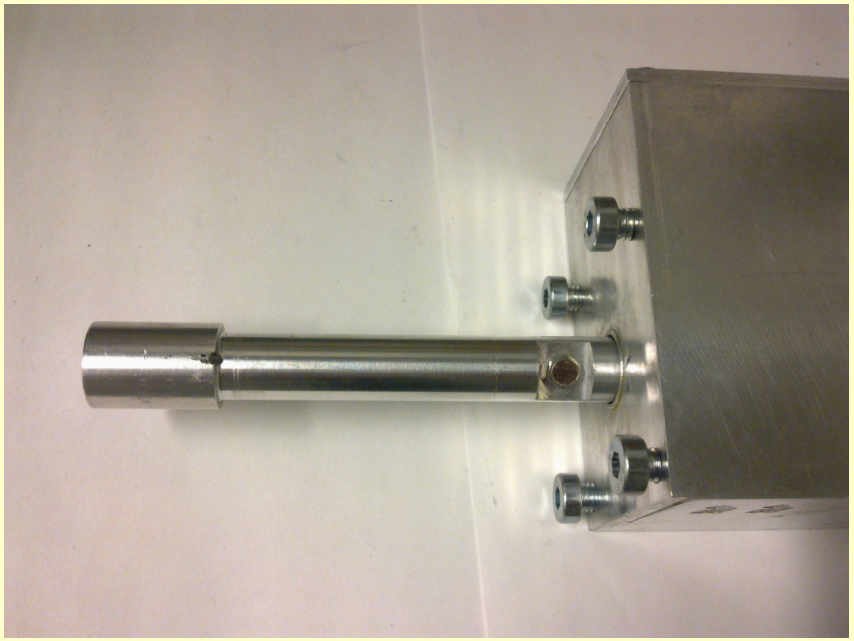

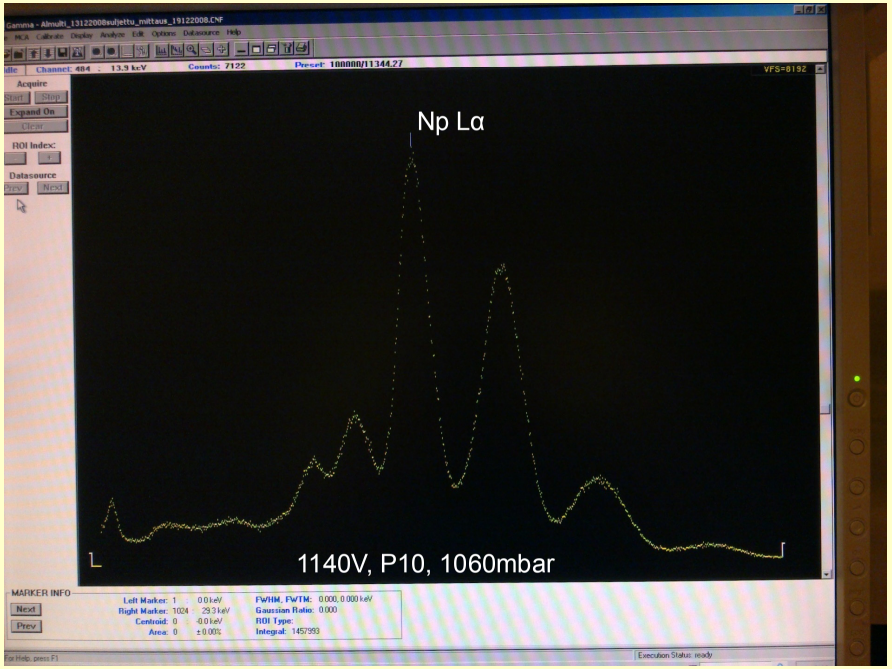

X-ray spectrum of ^{241}Am

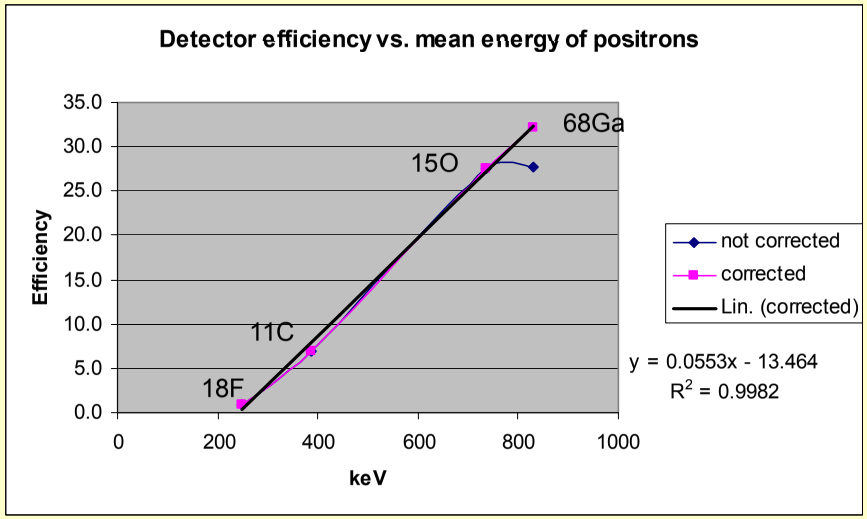

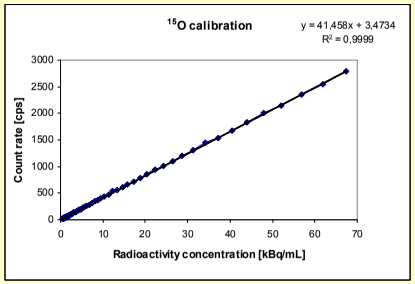

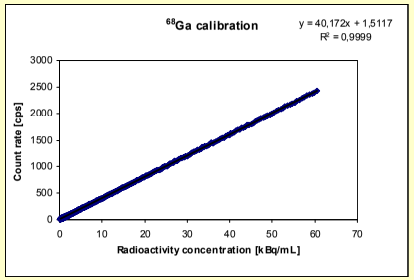

PTFE tubing o.d. 2.5mm. i.d. 1.5mm

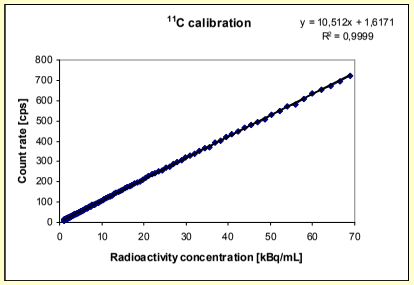

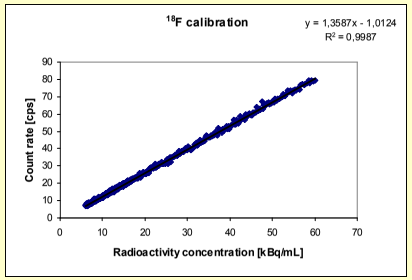

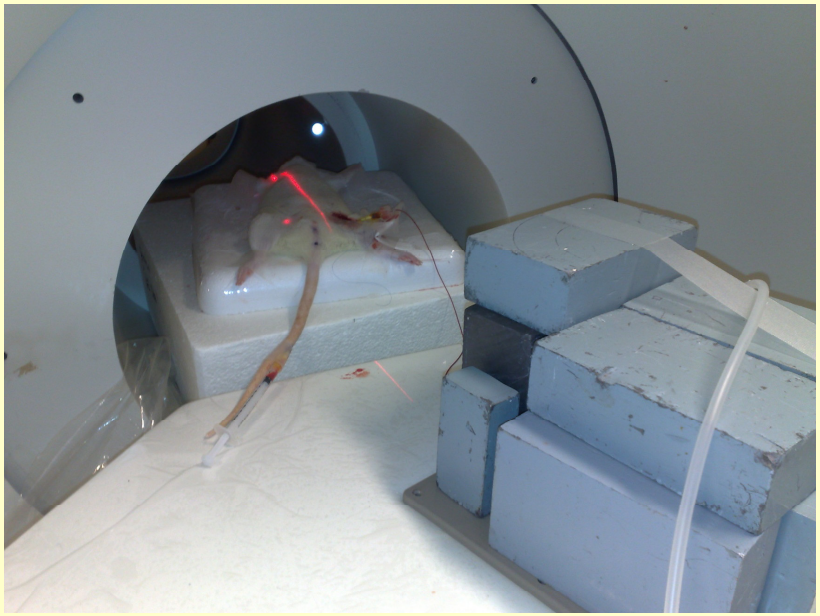

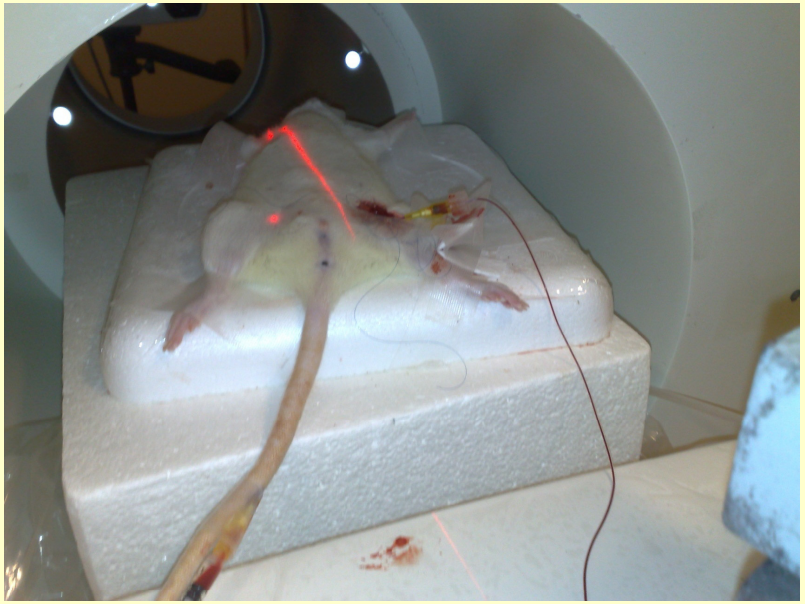

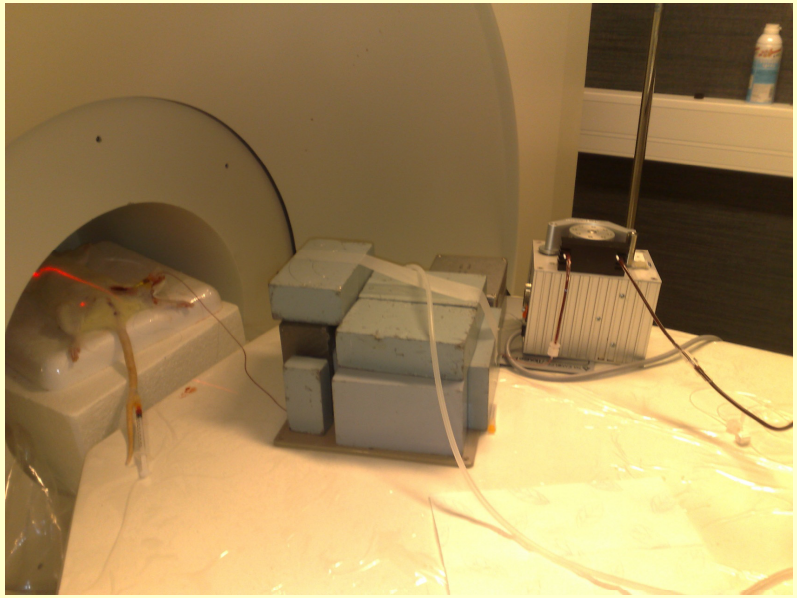

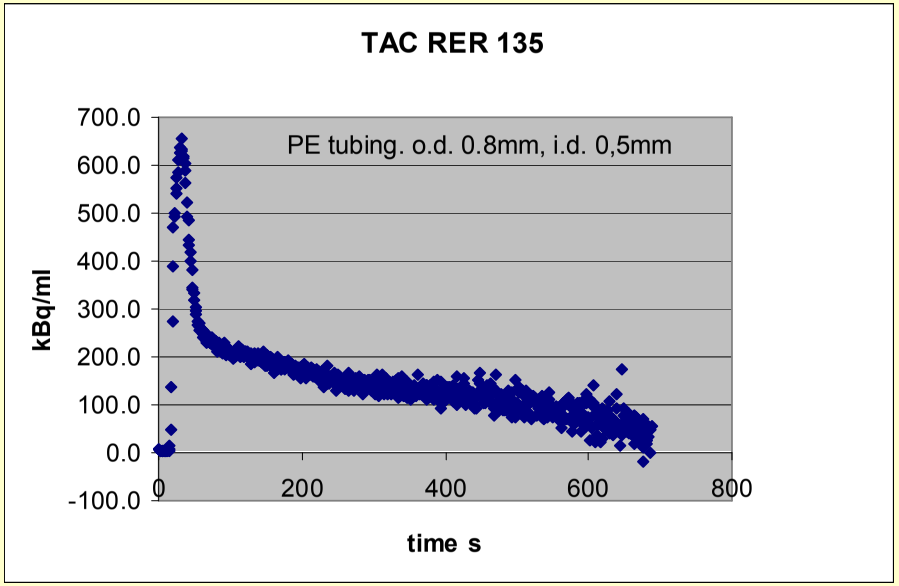

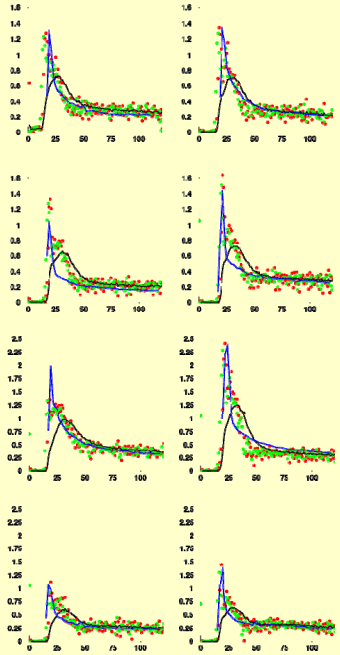

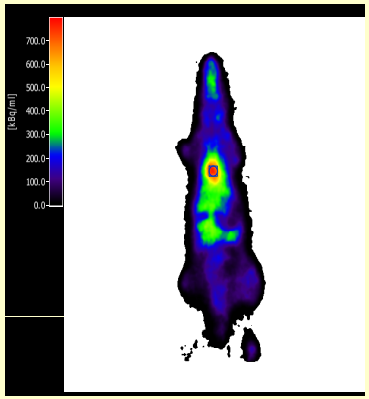

Black line: measured blood curve; Red and green plot: measure blood curve with dispersion correction by Munk's and Iida's methods, respectively. Blue line: Image based input. by Nobu Kudomi

Liquid target system for production of ^{86}Y

Jan Ráliš, Ondřej Lebeda and Josef Kučera

Nuclear Physics Institute of the Academy of Sciences of the Czech Republic, public research institution, Husinec-Řež 130, 250 68 Husinec-Řež, Czech Republic

Introduction Radionuclide ^{90}Y is a widely used tool for cancer therapy due to its suitable half-life, ready availability in high specific activities at relatively low cost. As it is a pure β^{-} emitter with no associated γ rays, there is a need for a tracer of ^{90}Y. Promising candidate for these purposes is ^{86}Y, since it is a positron emitter with half-life of 14.74 h. This radionuclide has been usually produced by the (p,n) reaction on enriched ^{86}Sr solid targets ($SrCO_3$) [1]. Handling and processing of those targets have several disadvantages. There is an interesting alternative to this approach, namely irradiation of a liquid target filled with aqueous solution of strontium nitrate [2]. It makes the target processing significantly easier and allows for automation of the process. Separation step can be also simplified, since usual electrolysis can be replaced by filtration of yttrium colloid in alkaline milieu [3].

Materials and methods Strontium carbonate (96.3% ^{86}Sr) was purchased from JV Isoflex, Moscow. Trace select ultra grade HNO_3, HCl and NH_4OH were purchased from Sigma-Aldrich. Puratronic grade $(NH_4)_2CO_3$ was purchased from AlfaAesar. High purity de-ionized water was used (specific resistance 18.2 MΩ/cm).

The main part of target asembly was water cooled chamber (volume 2.4 ml) made out of pure Nb with Ti entrance foil. The concentration of irradiated solution of strontioum nitrate was 35% (w/w). After irradiation, the solution was transfered to separation unit, target was washed with 10 mM nitric acid and water. All parts were collected together, pH was set to 10, filtered through PVDF filter and washed with 50 ml water. Filtrate was collected for Sr recovery. Yttrium was eluted from the filter with 10 ml 1M HCl. Eluate was evaporated to dryness and re-disolved in 100–300 µl of 0.05M HCl as a stock solution for labelling.

Radionuclidic purity and activity of produced yttrium was measured with γ-ray spectrometry (HPGe detector GMX45, Ortec).

Content of chemical impurities (for ^{86}Y – Fe, Cu, Zn, Al, ^{86}Sr) was determined via ICP-MS at the Institute of Chemical Technology Prague. We used two alternative methods for determination of the purity of the produced ^{86}Y: differential pulse voltametry and labelling efficiency of DOTATOC. Ca. 40 MBq of ^{86}Y stock solution was mixed with 20 µg of DOTATOC in 300 µl of 0.4 M sodium acetate and heated in for 30 min at 80 °C. The labelling yield was monitored with TLC, using silica gel plates (Merck, Germany) developed with 10 % NH_4OAc aq. / MeOH = 1:1, R_f = 0.46, and measured on a Cyclone autoradiography system (Perkin-Elmer).

Enriched ^{86}Sr was recovered by precipitation of strontium carbonate with ammonium carbonate [1]. The precipitate was decanted with water and acetone. Strontium carbonate was than dissolved in concentrated nitric acid, evaporated to dryness and re-dissolved in water for further irradiations.

Results The yield of irradiation was 33 MBq/µAh. It corresponds well to the published data [1] and given content of ^{86}Sr in the target matrix. Radionuclide purity was excellent (^{86}Y>99.4 %, ^{87}Y<0.55 %, ^{88}Y<0.025 %). Separation yield was more than 90 %, about 4–5 % is left on the filter. Less than 0.1 % of ^{86}Y stays in filtrate. Also losses during evaporation of 1M HCl are under 1 %. Table 1 shows comparison of methods used for determination of copper concentration as a example of impurity. Labelling efficiency reflects well the copper concentration.

TABLE 1 Comparison of different analytical methods for estimating the copper content in the product

Batch	Polarography [µg/ml]	ICP-MS [µg/ml]	Labelling efficiency
1	8.7	8.9	51.0 %
2	5.7	5.3	77.3 %
3	0.5	0.4	96.6 %

Recovery of enriched strontium was nearly quantitative, all solution used in recycling process were collected and reprocessed.

Discussion/Conclusion This work presents a compact, fully automated system for production of ^{86}Y in activity and quality suitable for radiopharmaceuticals production. Transport of irradiated target matrix via a capillary to a separation unit minimizes problematic handling of radioactive material and losses of expensive enriched ^{86}Sr. It also reduces significantly personnel radiation burden.

Acknowledgement The project was supported by Nuclear Physics Institute under the NPI research plan AV0Z10480505 and Ministery of Education, Youth and Sports, grant no. 2B061665.

[1] Rösch F, Qaim SM, Stöcklin G (1993): Appl. Radiat. Isot. 44(4): 677-681.
[2] Vogg, A.T.J., Scheel, Solbach, C., Neumaier, B. (2007): J. Label. Compounds and Radiopharmaceuticals 50, S105
[3] Kurbatov, J.D., Kurbatov, M.H. (1942): J. Phys. Chem. 46, 441

LIQUID TARGET SYSTEM FOR PRODUCTION OF ^{86}Y

Jan Ráliš, Ondřej Lebeda and Josef Kučera

Nuclear Physics Institute
Academy of Sciences of the Czech Republic, public research institution,
Řež near Prague

Yttrium-86

- ^{90}Y is a widely used radionuclide for cancer therapy due to its suitable half-life ($T_{1/2}$ = 64 h, $I_{\beta-}$ = 100 %, $E_{\beta-,max}$ = 0.98 MeV) and availability in high activities in carrier-free state at relatively low cost
- because ^{90}Y is a pure ß$^-$ emitter, there is a need for a diagnostic yttrium
- ^{86}Y is good choice, since it is a positron emitter with suitable half-life (14.74 h)

Decay properties of ^{86}Y

- half-life 14.74 h
- 33 % β^+
- $E_{\beta-,max}$ = 3141.3 keV
- $E_{\beta-,ave}$ = 213.1 keV

Eγ (keV)	Iγ (%)
443.14	16.9
627.72	32.6
777.35	22.4
1076.64	83
1153.01	30.5
1854.38	17.2
1920.72	20.8

Design of the Liquid Target System

- water cooled chamber (volume 2.4 ml) made out of pure Nb with Ti entrance foil
- helium cooling of target foils
- an integrated colimator at the beam entrance
- automated operation (filling and processing after irradiation)

Liquid Target System

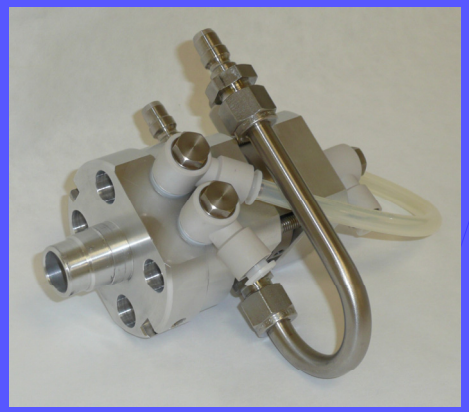

Liquid Target System

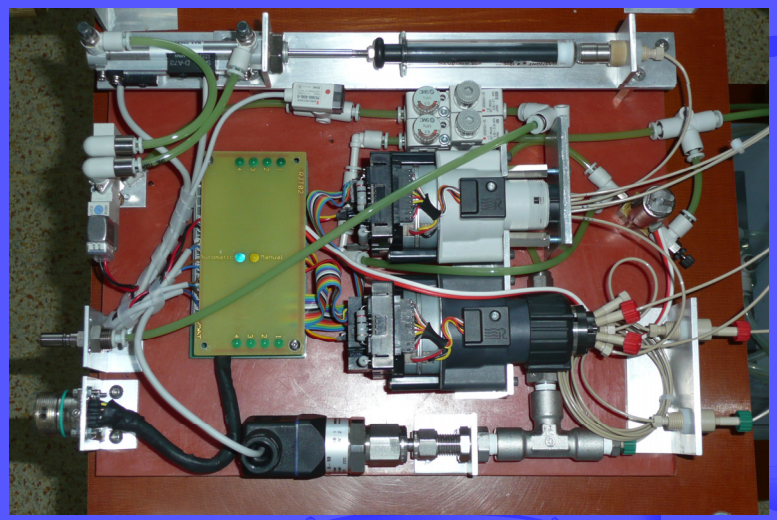

Production

- $^{86}Sr(p,n)^{86}Y$ – excitation function well-known since 1993 (Rösch, Qaim and Stöcklin)
- 2.4 ml of 35% solution of $^{86}Sr(NO_3)_2$, enrichment 96.3 % (JV Isoflex)
- the achieved thick target yield was 33 MBq/µAh, what corresponds well with to the published data and the content of ^{86}Sr in the target matrix
- irradiation on beam line of U-120M isochronous cyclotrone
- typical irradiation conditions were 1 – 2 hours, 10 – 15 µA, A_{EOB} 500 – 1000 MBq

Separation of ^{86}Y

- irradiated solution was transferred to separation unit, target was washed with 10mM nitric acid and water
- pH was set to 10, filtered through PVDF filter and washed with 50 ml of water
- filtrate was collected for Sr recovery
- yttrium was eluted from the filter with 10 ml 1M HCl
- eluate was evaporated to dryness and re-dissolved in 100–300 µl of 0.05M HCl (stock solution ready for labelling)

Separation of ^{86}Y

Recovery of ^{86}Sr

- all solutions with enriched strontium were collected together and evaporated to aprox. 30 ml
- strontium carbonate was precipitated with ammonium carbonate
- the precipitate was decanted with water and acetone
- strontium carbonate was dissolved in concentrated nitric acid, evaporated to dryness and re-dissolved in water for further irradiations

Methods for quality control of ^{86}Y

- polarographic estimation of metal impurities (Cu and Fe)
- ICP-MS estimation of metal impurities (Al, Fe, Sr, Cu, Zn)
- SLT (standard labelling test) based on the determination the labelling efficiency of the producted ^{86}Y with DOTATOC (DOTA-Tyr^3-Octreotide)(20 µg of DOTATOC in 300 µl of 0.4 M sodium acetate, heated for 30 min at 80 °C)

Sensitivity of SLT

Batch No.	Cu detm. by polarography [µg/ml]	Cu detm. by ICP-MS [µg/ml]	Labelling efficiency using SLT [%]
1	8.7	8.9	51.0
2	5.7	5.3	77.3
3	0.5	-	93.6

- According to the sensitive reactivity of DOTATOC with various metal impurities in the producted ^{86}Y, SLT is a suitable method for quality control

Conclusion

- fully automated system for production of ^{86}Y in amounts and quality appropriate to usual requirements for labelling
- very fast and efficient
- possibility transport of irradiated target matrix via a capillary to a separation unit
- minimizes problematic handling of radioactive material and losses of expensive enriched ^{86}Sr
- it also reduces significantly personnel's radiation burden

Acknowledgements

Department of Radiopharmaceuticals

MSc. K. Eigner Henke
MSc. Ondřej Lebeda, Ph.D.
MSc. Jan Kučka
Assoc. Prof. František Melichar, D.Sc.

Department of Accelarators

MSc. Jan Štursa
MSc. Jan Kučera

Vakuum Praha s.r.o.

The project was supported by the Academy of Sciences of the Czech Republic under the NPI research plan AV0Z10480505 and by the Ministry of Education, Youth and Sports, grant no. 2B061665.

WTTC XIII – Presentation Discussions

1. What happens to nitrates?
   - Some "hydrolyses"
   - Some stays in the solution
   - No salt precipitation from high concentration

Can Half-life Measurements Alone Determine Radionuclidic Purity of F-18 Compounds?

Thomas Jørgensen[1], Mille Ankerstjerne Micheelsen[2], and Mikael Jensen[1]

[1]*Hevesy Lab, Risoe-DTU,Technical University of Denmark, DK-4000 Roskilde, Denmark*
[2]*Dept.Clinical Physiology and Nuclear Medicine, Koege Hospital, DK-4600 Koege, Denmark*

Current revisions of monographs for F-18 pharmaceuticals in the European Pharmacopoeia call for a radionuclidic purity (RNP) of or better than 99.9%. If (debatably) this requirement is put at end of shelf life, typically 10 hours EOS , the requirement can be very difficult to assure by actual measurements, if all possible radionuclide contaminations should be considered. Clearly, gamma spectroscopy can do much, but only if the contaminant has strong gamma emissions above 511 keV. We have tried to analyse mathematically to what extent that half-life measurements alone can establish RNP for F-18 compounds. The method could in principle be extended to other isotopes. The current method of half-life determination in the Ph.Eur with two measurements at 6h interval is not sufficient nor effective for testing the required RNP level.

We present a theoretical model leading to a practical procedure for testing RNP of F-18 compounds with a confidence of 95%.

We look at a batch of F-18 contaminated with one other isotope with a half-life of βT_{18F}. The contamination level is α at time 0. The recorded number of counts, $N(t)$, for a sample, that contains one other isotope, is described by

$$N(t) = \frac{N(0)}{(1+\alpha)}\left(\left(\frac{1}{2}\right)^{t/T_{18F}} + \alpha\left(\frac{1}{2}\right)^{t/\beta T_{18F}}\right)$$

with N(0) as the total number of counts at t = 0.

RNP is defined by the expression

$$RNP = \frac{A_{18F}}{A_{\text{tot}}} \Rightarrow RNP(0) = \frac{1}{1+\alpha} \simeq 1-\alpha, \quad \alpha = \frac{A_{18F}(0)}{A_{\text{other}}(0)}$$

If all measured impulses are converted to initial point values (t = 0 min.), the curve should give a straight line with constant value (the initial value of counts) for a pure F-18 sample. Due to the stochastic nature of the F-18 nuclide, the data points will deviate from this line. If the sample is contaminated the curve will increase rapidly. The condition for the pure and unpure curves to be separated is, the difference of the

measurements must be equal to (or larger than) the sum of 1.96 standard deviations for the two curves (confidence of 95%). An approximated expression for the limit of α is

$$\alpha \simeq \frac{3.92\left(\frac{1}{2}\right)^{t/2T_{18_F}}}{\sqrt{N(0)}\left(\left(\frac{1}{2}\right)^{t/\beta T_{18_F}} - \left(\frac{1}{2}\right)^{t/T_{18_F}}\right)}$$

In the figure below a contour plot of RNP(0) ($\simeq 1-\alpha$) is plotted against β and recording time for a total amount of initial counts of 10^6 (the limit of the Liquid Scintillation Counter). We can readily see that after 6 hours, we cannot detect a contamination with $\alpha \leq 0.1\%$ (RNP(0) $\geq 99.9\%$), but after another 6 hours we should be able to detect a RNP(0) of 99,95% or smaller (for $\beta = 20$). However at very low β values there is a strong divergence in the time needed to detect these small RNP's, which in practice sets a lower limit for a detectable β. In the case below this lower β value is ~ 3.

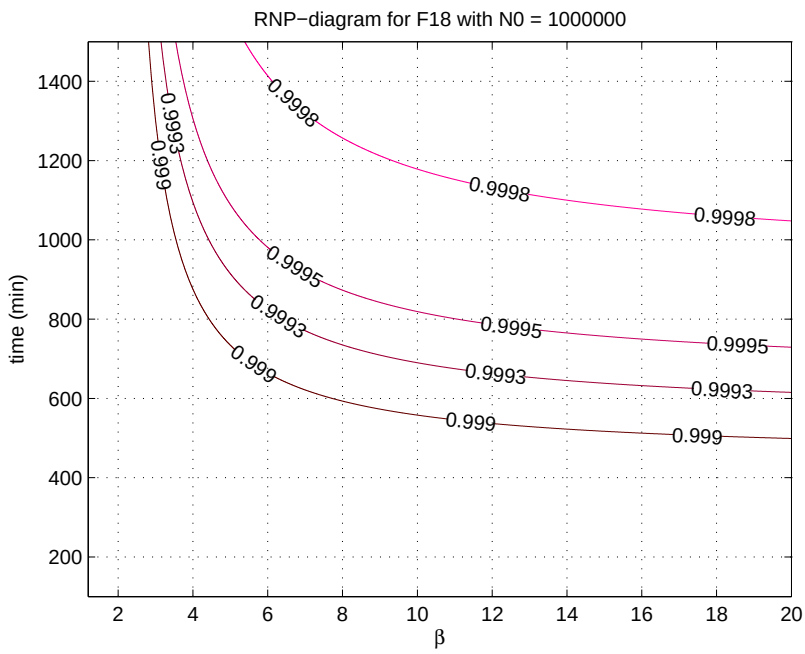

Figure 1: RNP plotted against β and recording time. The confidence is 95%.

In the above method, the lower level of the recording time and β is set by the inherent poisson noise. By using a series of recordings in a method that looks at the mean, rather than just two single points (start and stop), the statistical noise is lowered and consequently the lower limit of β is reduced to approximately 1.5 (recording time of $\sim$ 800 min). In conclusion we cannot find any contaminating isotope with half-lives shorter than 1.5 times 109.77 min. for RNP(0) = 0.9990 and a confidence of 95%.

Radio Nuclidic Purity (RNP)

Red-necked Phalaropes (another RNP)

Thomas Jørgensen[1], Mille Micheelsen[2], Mikael Jensen[1]

[1]Hevesey Lab, Risoe-DTU, Technical Universtiy of Denmark
[2]Dep. of Nuclear Medicine, Køge University hospital

^{18}F as an example

- Determining the RNP of a ^{18}F batch with confidence is non-trivial...
- Current accepted method use half-life determined from decay over 6+ 6 hours...
- We investigate the boundaries of validity for this method and introduce simple methods that both improve accuracy as well as optimize time consumption

^{18}F as an example

- A possible byproduct from silver (Ag) as target is ^{107}Cd
- ^{107}Cd has a half-life that is 3.6 times longer than ^{18}F
- With 1% impurity at production time the pink and purple lines illustrate how the impure and pure samples behaves.
- Its clear that by this method the impurity would not be detected before well after 800min.
- We can improve on that...

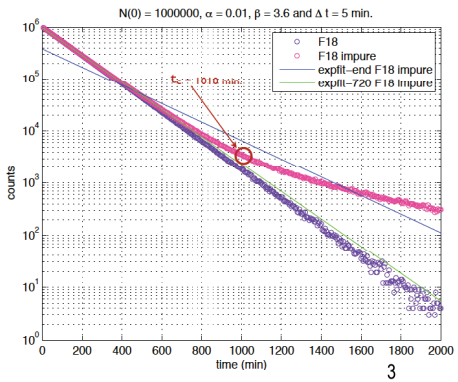

^{18}F as an example

- The time t_c where the impurity starts to dominate is given by:

$$t_c = \frac{\ln(1=®)}{\ln(2)} \frac{-}{-_i 1} T_{18F}$$

- So for α=0.01 t_c=1010min (17h)
- for α=0.001 t_c=1515min (25h)

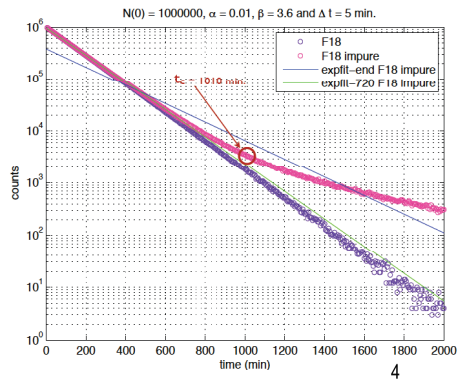

Simple method 1

- We compare a pure and an impure decay curve.
- Both are converted into initial point values (multiplied by $(½)^{(-t/T)}$).
- First we identify the time where the separation of the two curves (pure and impure) become statistically significant, this is the minimum time our sample needs to decay.
- Significance (95%) occurs when:

$$N(t) - 1.96\sigma_{N(t)} = N_p(t) + 1.96\sigma_{N_p(t)}$$

Simple method 1

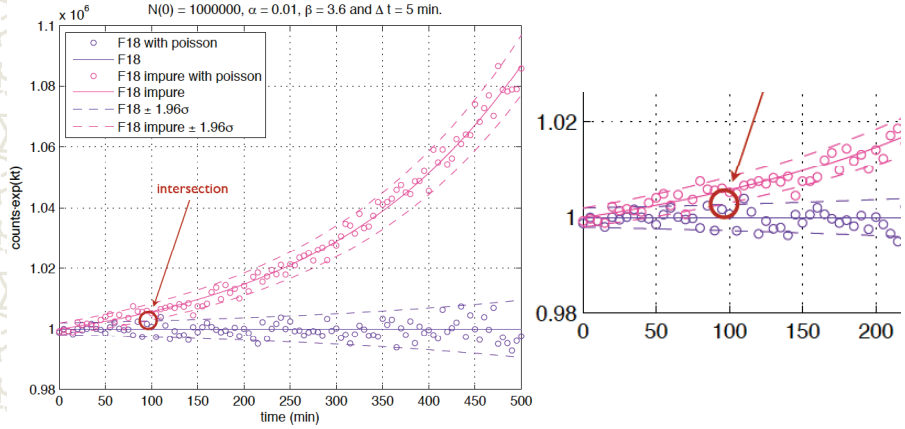

Simple method 1

- If we consider only the poisson noise in the system we can write up the relation between RNP, t and β. This is approximately given by:

$$RNP \approx 1 - \frac{3.92\left(\frac{1}{2}\right)^{\frac{t}{2T}}}{\sqrt{N(0)}\left(\left(\frac{1}{2}\right)^{\frac{t}{\beta T}} - \left(\frac{1}{2}\right)^{\frac{t}{T}}\right)}$$

Simple method 1

- We use this expression to find min t…

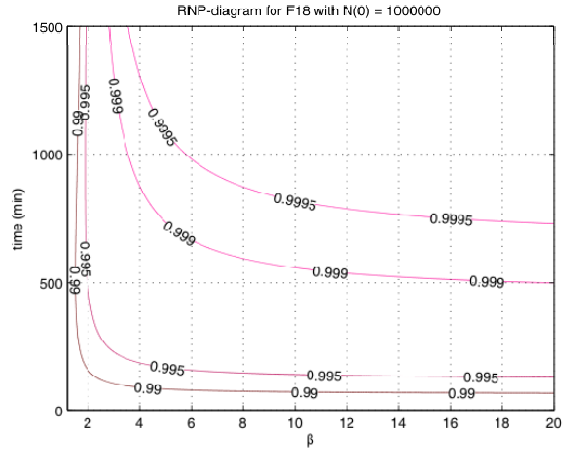

Simple method 1

- From hereon it's a simple YES/NO answer e.g.

$$N(t) > N(0) + 1.96\left(\sqrt{N(0)} + \sqrt{N(t)}\right)$$

- If the answer is YES – then we have a 95% confidence that our sample is not contaminated more than the limit set by RNP…

Simple method 1

Some points to stress:

- β dependence only at small β (but strong here)…
- Lower detection limit for β (depend on RNP)…
- For lower RNP – impurity is detected earlier, so we find every impurity > RNP
- Time depends on N0 – so this should be as large as possible without distorting measurements (dead time etc…)

Simple method 2

- We can increase efficiency (lower detectable β and t_c at given RNP) by taking more data points in a time frame and use the mean and the standard deviation of the mean:
- This way statistical noise is lowered to:

$$\sigma_{\overline{X}} = \frac{\sigma_X}{\sqrt{n}}$$

where n is the number of data points

- In this method to find t_c we generate the time, β curve by computational method.

Simple method 2

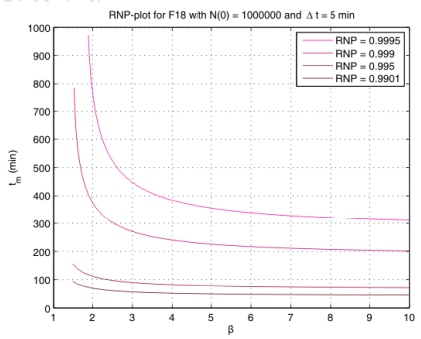

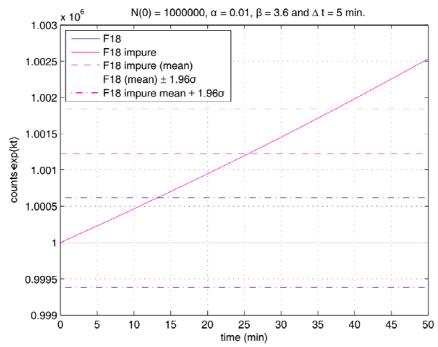

Summary

Summary of example with contamination of ^{18}F with ^{107}Cd

Method \ RNP(0)	0.99	0.999
Current	1000min	1500min
I	100min	1000min
II	50min	250min

Methods have been verified computationally but not yet experimetally

WTTC XIII – Presentation Discussions

1. Example: 107Cd
   - Ag targets by-product
   - Different half-life, but impossible to distinguish before 800mins
2. HPGe spectroscopy need
   - Requirement: 0,1% RNP: not trivial (if possible) using HPGe

PC-controlled radiochemistry system for preparation of NCA ^{64}Cu

Adam Rebeles R., Van den Winkel P., De Vis L., Waegeneer R.
Cyclotron Laboratory, Vrije Universiteit Brussel (VUB), Brussels, Belgium

Due to the rapid increase of the use of nuclear medicine techniques in modern clinical diagnosis and in a selected series of therapies, researchers' efforts are focusing for the standardization and optimization of different production routes for a series of emerging radioisotopes like ^{64}Cu, ^{67}Cu, ^{114m}In, ^{211}At.

In particular the EC/β^+/β^- decay of ^{64}Cu makes it a promising candidate for both PET imaging and internal targeted radio therapy. In the last decades several groups studied different production routes like for this radio nuclide, i.e. ^{64}Ni(p,n), ^{64}Ni(d,2n),^{64}Zn(d,2p).

Taking into account the wider availability of the medium energy proton beam machines, the (p,n) reaction on ^{64}Ni seems to be the most attractive one, although ^{64}Zn(d,2p) may be considered as an alternative where lower activity is necessary, as it may require less investment in enriched material.

The production of large activities of ^{64}Cu on regular basis requires a fast and reliable chemistry system. Based on the experience gathered in the last decades in our laboratory we present here and efficient, remote controlled chemistry system for production of the non carrier added ^{64}Cu via ^{64}Ni(p,n) reaction.

To avoid excessive investment in a gold target carrier, a good practice is to coat the copper target carrier with a thin inert material, i.e. 5-6 μm of gold, followed by electrodeposition of the ^{64}Ni target layer. In that way, the cross contamination of the non carrier added ^{64}Cu with the copper present in the target carrier is excluded. In general the irradiations are performed with protons having incident energy of about 15 MeV, and, depending on irradiation condition, may lead to curie amount of induced activity of ^{64}Cu. To reduce the thickness of the ^{64}Ni target layer, and, as consequence, to minimize the problems related with the plating and dissolution of the target layer, a low beam/target angle geometry (6 degrees) is desired. Nevertheless, the separation of target / activation product is required. Upon irradiation, our chemistry system proposes the dissolution of the ^{64}Ni layer in a heated flow trough stripper by means of diluted nitric acid. Next, the non carrier added ^{64}Cu is selective extracted into benzene (containing 0.1 M benzoylacetone) at pH 4.5, leaving the enriched ^{64}Ni and possible Co induced isotopes in the inorganic phase. The back extraction of ^{64}Cu is done in a small volume of diluted hydrochloric acid (6 N). The final purification step is achieved using an anion exchange column Dowex 1X8. Finally, the NCA ^{64}Cu is eluted with a small volume (10 ml), diluted hydrochloric acid (1 N).

The overall yield of the chemistry is estimated as being higher than 95% with a short total chemistry time, less than 2 hours, while the gold plated target carriers can be reused as long as the thin gold layer remains intact, meaning that scratches and cracking by careless handling are avoided.

PC-controlled radiochemistry system for preparation of NCA ^{64}Cu

Adam Rebeles R., Van den Winkel P., A. Hermanne, De Vis L., Waegeneer R.

Cyclotron Laboratory, Vrije Universiteit Brussel (VUB), Brussels, Belgium

Introduction

- **EC/β^+/β^- decay of ^{64}Cu**
  - **promising candidate for PET imaging**
  - **internal targeted radiotherapy.**
- **Different production routes**
  - ***$^{64}Ni(p,n)^{64}Cu$***
  - **$^{64}Ni(d,2n)^{64}Cu$**
  - **$^{64}Zn(d,2p)^{64}Cu$**
- **Chemistry – separation of NCA isotope**

Target preparation

- **IBA Cyclone 30 solid target carrier**
  - **copper preplated with a thin Au layer (5 μm)**
- **Plating baths:**
  - **Watts ($NiSO_4$*$6H_2O$,$NiCl_2$*$6H_2O$,H_3BO_3)**
  - **Chloride bath ($NiCl_2$*$6H_2O$, H_3BO_3)**
  - **Sulfamate ($Ni(NH_2SO_3)_2$, H_3BO_3)**
  - ***Alkaline bath ($NiSO_4$*$6H_2O$, $(NH_4)_2SO_4$, NH_3 , pH 9-11)***

Target preparation

Example of gold preplated target carrier

Target preparation

Example of nickel plated target

Target preparation

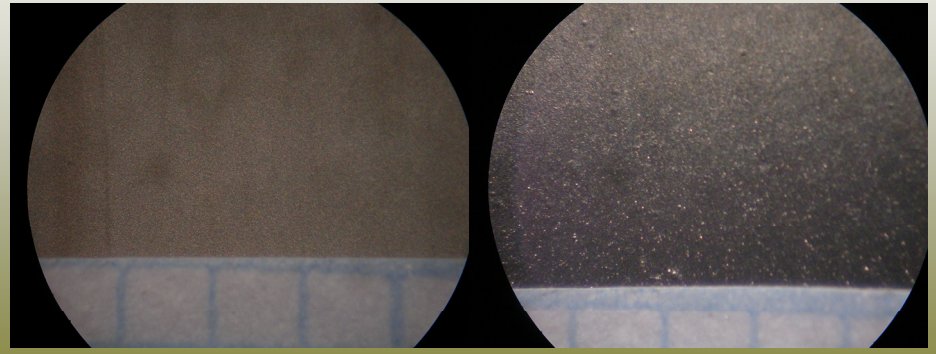

Good *Poor*

Surface area granulometry(50X)

Overview of PC-controlled radiochemistry system for ^{64}Cu production

Chemistry – separation of NCA ^{64}Cu

- **Dissolution of the ^{64}Ni layer in diluted nitric acid**
- **Selective extraction of ^{64}Cu into tert-Butyl Methyl ether (containing 0.1 M benzoyltrifluoroacetone) at pH 2.7- 3**
  - **Enriched ^{64}Ni and possible Co induced isotopes remain in the inorganic phase (NH_4NO_3 - HNO_3)**
  - **Other solvents like isoamyl acetate or ethyl acetate may be used**

Chemistry – separation of NCA ^{64}Cu

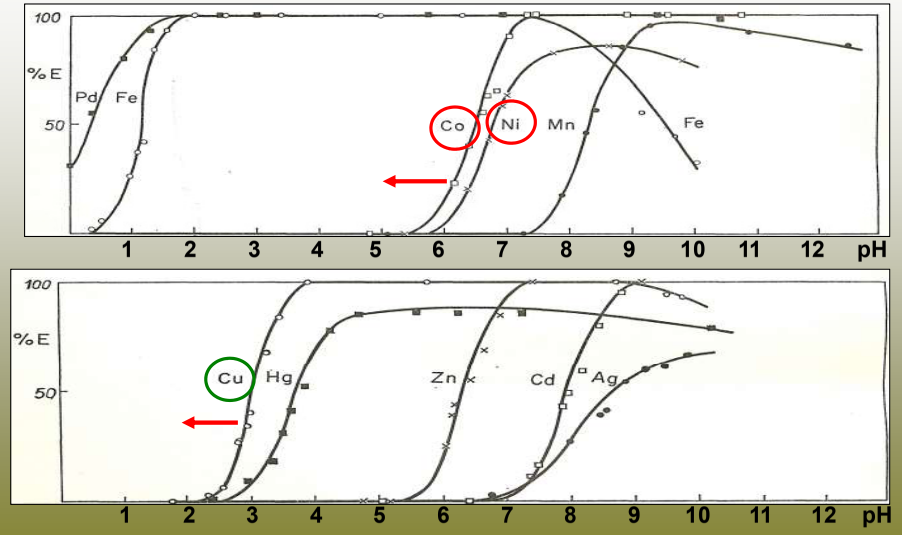

G. N. Rao,J. S. Thakur, (1974), Z. Anal. Chem., 271:286

Effect of the pH on the extraction (J. Starý, E. Hladký, (1963) Analyt. Chim. Acta, 28:227)

Chemistry – separation of NCA ^{64}Cu

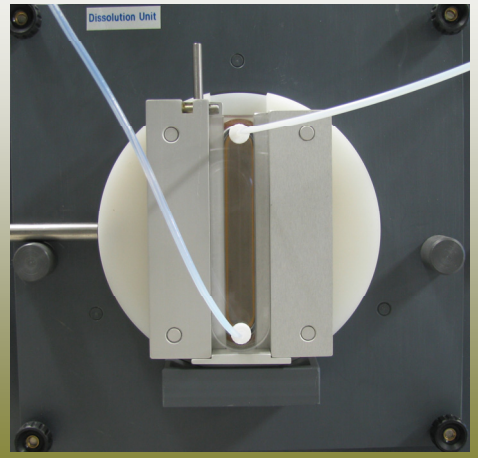

Flow through stripper

Extraction unit

Chemistry – separation of NCA ^{64}Cu

- Back extraction of ^{64}Cu is done in a small volume of diluted hydrochloric acid (6 N)
- Final purification step - anion exchange column Dowex 1X8.
  - The NCA ^{64}Cu is eluted with a small volume diluted hydrochloric acid (0.05 N).

Chemistry – separation of NCA ^{64}Cu

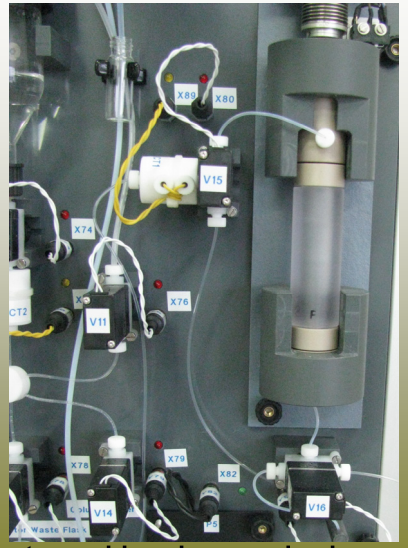

Chromatographic column and volume measuring unit

Target Dissolution

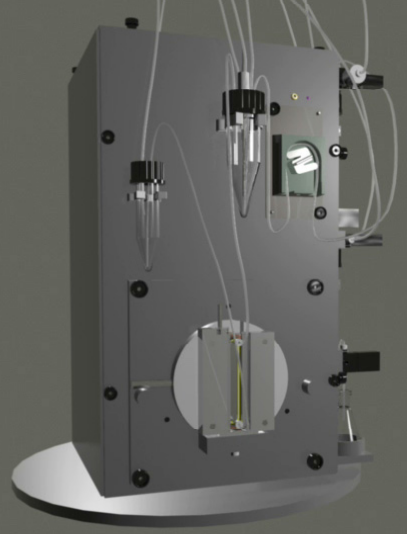

Conclusions

- Based on the experience gathered in our laboratory in developments on solid target chemistry systems, a robust modular system for the separation of NCA ^{64}Cu was developed.
- Analytical separation techniques:
  - *solvent/solvent extraction*
  - *ion exchange chromatography*
- High chemistry yield >95%
- Total chemistry time <2 hours
- The user friendly Visual Basic interface - allows the full control over each step of the chemistry with a minimum risk of operator errors and of radiation exposure for the staff.

Acknowledgements

- The authors would like to thank the IBA - Ion Beam Applications - Louvain-la-Neuve company for providing the enriched ^{64}Ni

Conclusions

- Based on the experience gathered in our laboratory in developments on solid target chemistry systems, a robust modular system for the separation of NCA ^{64}Cu was developed.
- Analytical separation techniques:
  - *solvent/solvent extraction*
  - *ion exchange chromatography*
- High chemistry yield >95%
- Total chemistry time <2 hours
- The user friendly Visual Basic interface - allows the full control over each step of the chemistry with a minimum risk of operator errors and of radiation exposure for the staff.

WTTC XIII – Presentation Discussions

1. Fe?
   - Extracted in ion exchanger

2. Reuse of golden plated back
   - Reused 10x, without big activation
   - Careful: Cu/Au dissolve in each other: hotspots=activation
   - Worst: Cu dissemination = low specific activity

Production of ^{124}I, ^{64}Cu and [^{11}C]CH_4 on an 18/9 MeV cyclotron

M.Leporis, M.Reich, P.Rajec, O.Szöllős
Biont a.s., Karloveska 63, SK-842 29 Bratislava, Slovakia

Iodine-124 ($T_{1/2}$ = 4.18 d) and copper-64 ($T_{1/2}$ = 12.7 h) are two very important radionuclides for radiopharmaceuticals production for preclinical research in a positron emission tomography (PET). The method for producing ^{124}I was based on a dry distillation of ^{124}I from a solid [^{124}Te]TeO_2 target technique. The platinum target disk was used as a base for TeO_2 melt and irradiated on COSTIS target station installed at the end of the external beam line of the IBA Cyclone 18/9 cyclotron. The target station was equipped with a 25 µm aluminum or 250 µm Nb window foil in front of the target, which results in a final beam energy of 17.7 or 13.5 MeV respective.

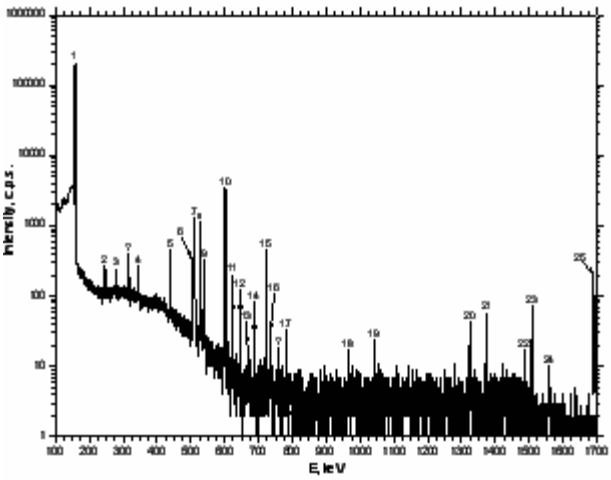

γ-spectra of the ^{124}I product at EOS

Peak	Nuclide	E, keV	Intensity, %	Peak	Nuclide	E, keV	Intensity, %
1	123I	158.97	83.3	14	123I	687.95	0.0267
2	123I	247.96	0.071	15	124I	722.78	10.35
3	123I	281.03	0.079	16	123I	735.78	0.062
4	123I	346.35	0.126	17	123I	783.59	0.059
5	123I	440.02	0.428	18	124I	968.22	0.435
6	123I	505.33	0.316	19	124I	1045.0	0.441
7	124I (annih.)	511.0	46.0	20	124I	1325.50	1.561
8	123I	528.96	1.39	21	124I	1376.0	1.75
9	123I	538.54	0.382	22	124I	1488.9	0.199
10	124I	602.72	62.9	23	124I	1509.49	3.13
11	123I	624.57	0.083	24	124I	1559.8	0.165
12	124I	645.82	0.988	25	124I	1691.02	10.88
13	124I	662.4	0.056				

γ-lines of the spectra with their energies and intensities

The $^{64}Ni(p,n)^{64}Cu$ reaction route was used for ^{64}Cu ($T_{1/2}$ = 12.7 h) preparation because its entrance channel is accessible at low energies and yield of the reaction is quite high. Disadvantage of the reaction used is high price of enriched ^{64}Ni. Gold and platinum targets were used for a thick ^{64}Ni target preparation by electro deposition. Because the external beam line of the cyclotron has no beam diagnostic devices, several aluminum plates were irradiated in the COSTIS target station with a 5 µA proton beam for 5 min with different settings for the beam focusing quadrupole magnets. After 15 minutes decay time the plates were scanned by a TLC scanner along the horizontal and vertical central axes of the plates in order to visualize the beam shape. The settings providing the most homogeneous beam spot on the target were selected and used further for the actual target irradiations. The radionuclidic purity of the product was determined by γ-spectrometry.

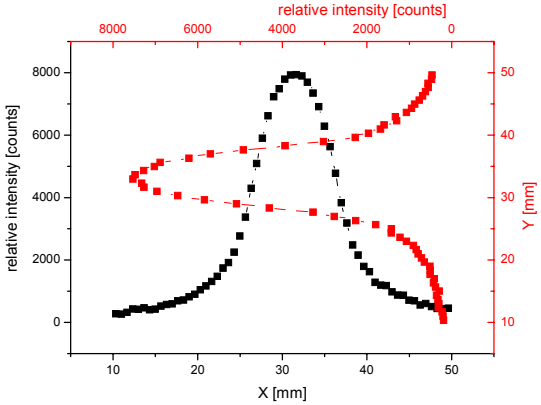

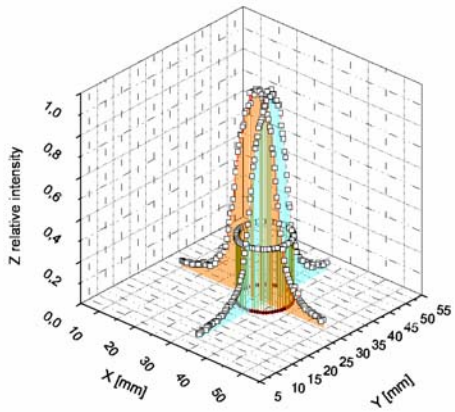

Beam profile measured on Al disk; Nb window 0.30 mm

Carbon-11 ($T_{1/2}$ = 20.39 min) was prepared in the form of methane in aluminum target made by IBA. Total irradiated volume of the gas mixture (90% N_2 +10%H_2) was 50 cm^3. Reaction used at irradiation was $^{14}N(p,\alpha)^{11}C$. Aluminum and niobium windows were used during irradiation. The irradiations were performed first without and then with niobium foil inside the target with purpose to eliminate the surface influence of aluminum. During the optimization of irradiation, different pressures of gas were tested as well as the beam currents. Produced methane was sorbed on Carboxen 1000 column at the temperature of -150 °C on TracerLab FX_C module made by GE Medical Systems.

Acknowledgement

The authors are indebted to IAEA Vienna for financial support during realization of TC Project SLR/4/010 Production of the Positron Emitting Radionuclides and the work connected with Cu-64 production was supported by the Slovak Research and Development Agency under the contract No. VMSP-P-0075-09

Production of 124I, 64Cu and [11C]CH4 on 18/9 MeV cyclotron

V. Csiba[1], M.Leporis[1], M.Reich[1], P.Rajec[1,2], O.Szöllős[1], J. Ometákova[2]

1 Biont a.s., Karloveska 63, Bratislava, Slovakia
2 Faculty of Natural Science, Department of Nuclear Chemistry, Comenius University, Mlynská dolina, Bratislava, Slovakia

Preparation and characterization of nickel targets for cyclotron production of 64Cu

Increase of production of the radiopharmaceuticals labeled with 64Cu can be seen in the last years. This interest is related to physical properties of 64Cu (T1/2=12.7 h; β- 37.1%, β+ 17.9%) and easy radiopharmaceuticals preparation. 64Cu can be used for both the therapeutic (β-) and for a diagnostic (β+) applications. For example, 64Cu was used for hypoxia tumor diagnosis, for labeling of peptides for diagnostic and therapy of non-oncological illnesses and other cases.

There are more reaction routes for 64Cu production, for example 64Zn(d,2p), 66Zn(d,α), 68Zn(p,αn), 64Zn(n,p), 64Ni(d,2n), 64Ni(p,n). However, the 64Ni(p,n) is very suitable due to the large cross-section for energy of protons which can be easily reached in small biomedical cyclotrons.

Preparation and characterization of nickel targets for cyclotron production of 64Cu

The aim of this study was development an electroplating method for preparation of a nickel target suitable for COSTIS assembly. The desired product is a thick layer of metallic nickel on a gold disc.

Production of 64Cu can be described in these steps:

- Preparing of a target by electrodeposition – a galvanostatic or potentiostatic electroplating of Ni on thick gold or platinum target
- irradiating the target
- dissolving of a target material and separation of 64Ni and 64Cu
- preparing of a 64CuX solution

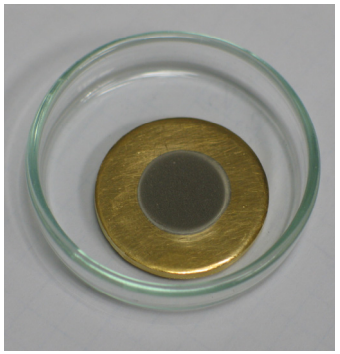

Preparation and characterization of nickel targets for cyclotron production of 64Cu

Our bath, containing 0.5 g NiSO4.6H2O, 0.056 g H3BO3 and 0.5 g NH4Cl in 5 ml H2O, was brought to pH 9. Simultaneously, NH4Cl/NH4OH buffer was added to keep pH at 9 during the whole electrodeposition process. As the electroplating process continued, the color of the electrolytic bath turned from dark blue to colorless. The full loss of color indicates that electrodeposition is finished. The efficiency of electroplating in this bath was 96%.

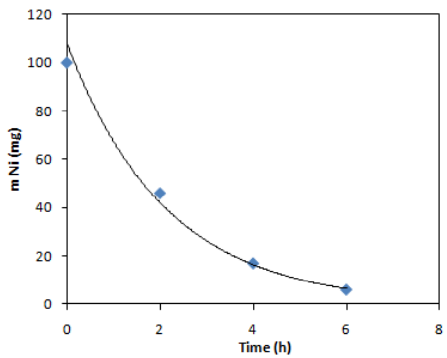

Decrease of nickel in the bath during the electrodeposition

Preparation and characterization of nickel targets for cyclotron production of 64Cu

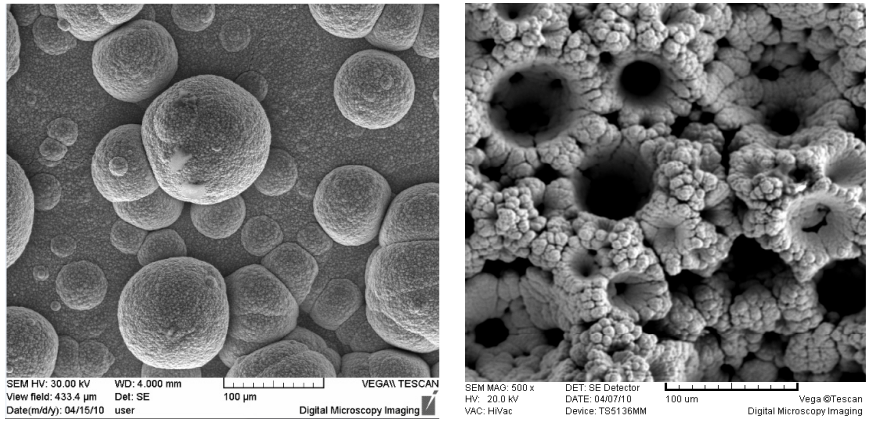

Ni surface on gold disk in x 500 SEM (electroplating by 30 and 100 mA)

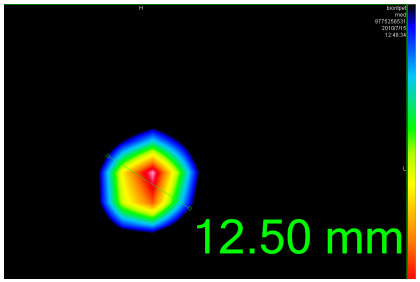

PET scan of the Ni-64 target after irradiation

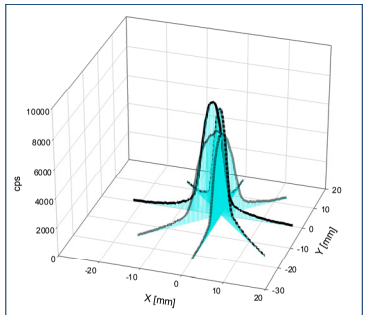

TLC scan on MiniGita Raytest of the Ni-64 target after irradiation

Gamma- spectrum of the 64Cu

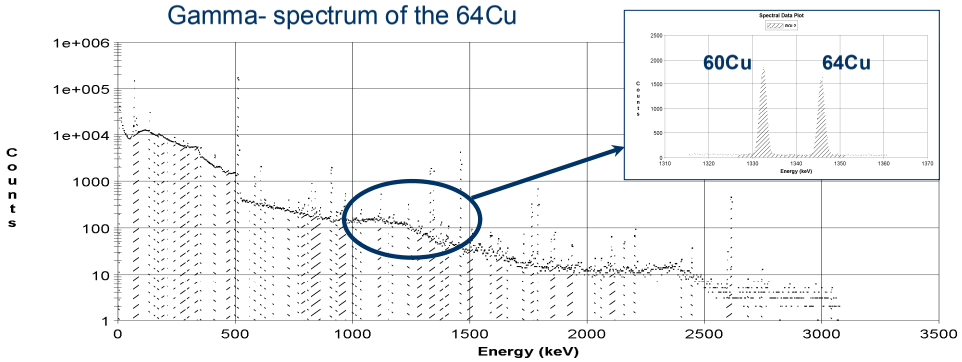

Yield of ^{64}Cu in the EOB time

	64Ni plated, [mg]	Current [µA]	Yield EOB [mCi/µAh]
Our results	100	5	2.77
[1]	60-110	15-30	2.6-4.2
[2]	50-250	30	1-3.4

[1] Journal of Radioanalytical and Nuclear Chemistry, Vol. 257, No. 1 (2003) 175-177
[2] M. Matarreseetal,AppliedRadiationandIsotopes68(2010)5–13

Production of 11C[CH4]

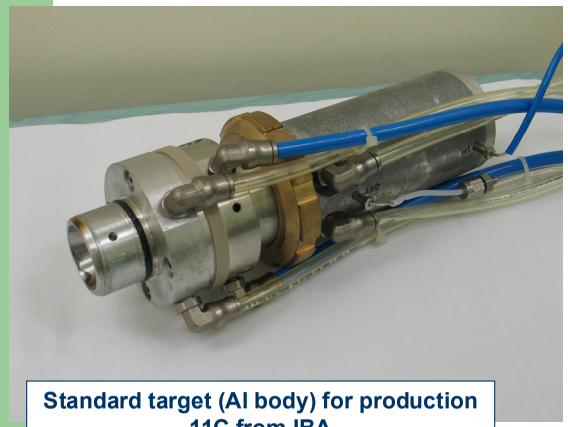

Standard target (Al body) for production 11C from IBA

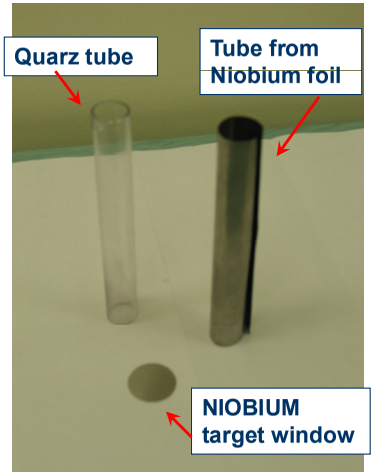

Production of 11C[CH4]

We used standard alumina-body target (50cm^3) made by IBA in these three modification:

- without changes (Al-body)
- With tube made from NIOBIUM foil inside
- With tube from quartz-glass inside (will be realize in near future)

Modified parameters:

- Input gas-pressure (from 10-30 barr)
- Beam current (10-30 μA)

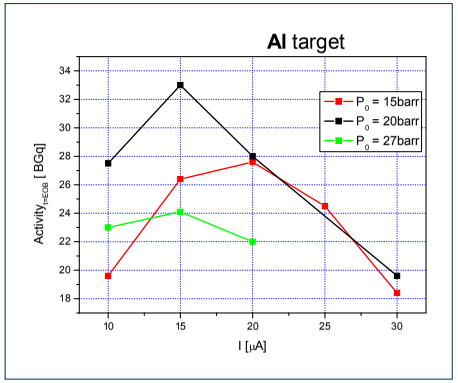

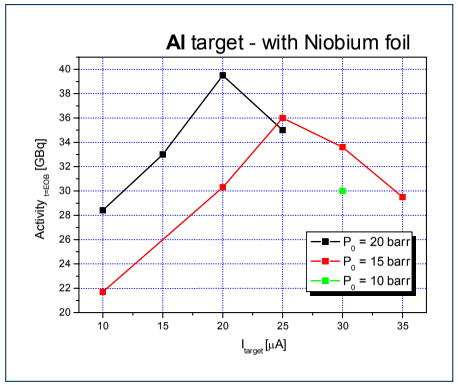

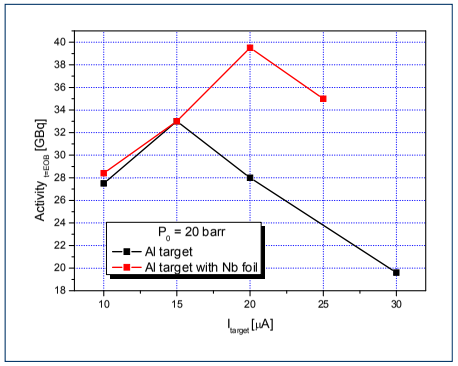

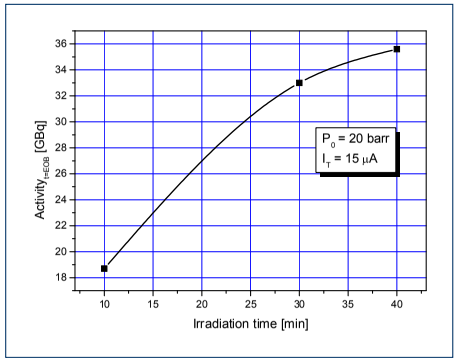

Production of 124I

The method for producing 124I was based on a dry distillation of 124I from a solid [124Te]TeO2 target technique. The platinum target disk was used as a base for TeO2 melt and irradiated on COSTIS target station installed at the end of the external beam line of the IBA Cyclone 18/9 cyclotron. The target station was equipped with a 25 μm aluminum window foil in front of the target, which results in a final beam energy of 17.7 MeV.

Production of 124I

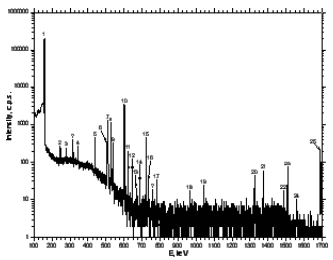

Peak	Nuclide	E, keV	Intensity, %	Peak	Nuclide	E, keV	Intensity, %
1	123I	158.97	83.3	14	123I	687.95	0.0267
2	123I	247.96	0.071	15	124I	722.78	10.35
3	123I	281.03	0.079	16	123I	735.78	0.062
4	123I	346.35	0.126	17	123I	783.59	0.059
5	123I	440.02	0.428	18	124I	968.22	0.435
6	123I	505.33	0.316	19	124I	1045.0	0.441
7	124I (annih.)	511.0	46.0	20	124I	1325.50	1.561
8	123I	528.96	1.39	21	124I	1376.0	1.75
9	123I	538.54	0.382	22	124I	1488.9	0.199
10	124I	602.72	62.9	23	124I	1509.49	3.13
11	123I	624.57	0.083	24	124I	1559.8	0.165
12	124I	645.82	0.988	25	124I	1691.02	10.88
13	124I	662.4	0.056				

γ-lines of the spectra with their energies and intensities

CONCLUSIONS

- 64Cu
  - More than 95% efficiency of the electroplating depositions
  - First irradiation with yield 2.8mCi/microAh
  - Future – radiochemical separation of 64Cu and 64Ni
    – design and realization of the automatic production system
- 11C[CH4]
  - Increasing yield up to 30% using Niobium foil
  - In the future continue with Quartz-tube
- 124I
  - Successful synthesis of 124I
  - works were stopped for stopping financial support

Thanks for an attention

Acknowledgement

The authors are indebted to IAEA Vienna for financial support during realization of TC Project SLR/4/010 Production of the Positron Emitting Radionuclides and APVV Slovakia for financial support project VMSP-P-0075-09

WTTC XIII – Presentation Discussions

1. Niobium foil
   - Why does it improve yield? Temperature?

A simple and flexible device for LabView applications

A. Hohn, E. Schaub, S. Ebers, R. Schibli

Paul Scherrer Institut, 5232 Villigen PSI, Switzerland

LabView is the state of the art programming tool for measurement and control applications and the market offers a wide range of sophisticated data acquisition tools (DAQ). However, for radionuclide separation purposes a high sample rate and a high accuracy is often not necessary. Therefore, we were looking for a low-cost DAQ with a USB interface for maximum flexibility and sufficient I/O lines. Finally, we decided to use the USB-6008 by National Instruments. This small size, low-cost DAQ has 8 analog inputs, 2 analog outputs and 12 digital I/O lines. Mounted on a print together with a transistor for each digital line (Fig. 1) this DAQ is the base of our device.

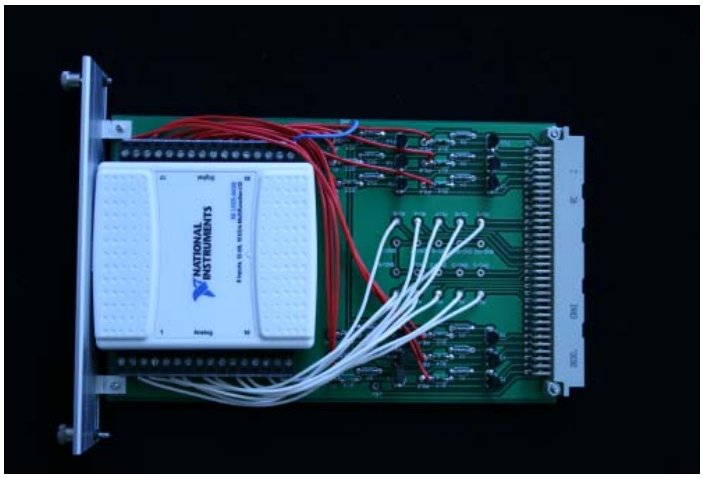

Fig. 1 USB DAQ mounted on a print

For the portable version of our device (Fig.2) the USB DAQ module is mounted in a desktop rack together with a power supply module (24 V, 120 W) and a relay module containing 12 relays. Additional slots are available for other modules. Each single module can be replaces easily in case of a failure. If more slots are needed all modules can be mounted as well in a 19'' rack

Fig. 2 Portable device for LabView applications with a mounted PC

Several additionally modules like a temperature module and a pulse-width-modulator (PWM) are available. An amplifier for pH measurements and for activity measurements with photodiode radiation detectors (Fig.3) was developed. This amplifier with a variable gain is a modified version of the amplifier described by Zeisler et al. Another module is a mini PC including a hard drive. In combination with a touch screen the device can be used without an external PC or notebook.

Fig. 3 Amplifier with photodiode radiation detector

The described devices are used in our group for the routine production of radionuclides (^{89}Zr and ^{64}Cu) for several years without any problems.

Literature:

Zeisler, S. K., Ruth, T. J., Rektor, M. P. (1994). "A Photodiode Radiation Detektor for PET Chemistry Modules." Appl. Radiat. and Isotopes **45**(3): 377-378.

A simple and flexible device for LabView applications

A. Hohn, E. Schaub, S. Ebers, R. Schibli

WTTC XIII
2010
Roskilde

Data Acquisition Tool (DAQ)

- USB-6008 by National Instruments
- 8 analog inputs, 2 analog outputs and 12 digital I/O lines
- USB-DAQ mounted on a print for plug and play

Computer

- Alix3d3 single board PC
- CPU: 500 MHz AMD Geode LX800
- DRAM: 256 MB DDR DRAM
- Storage: 8 GB CompactFlash
- OS: Windows XP

Amplifier for activity and pH measurements

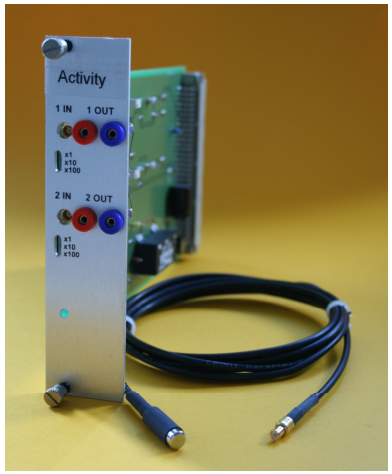

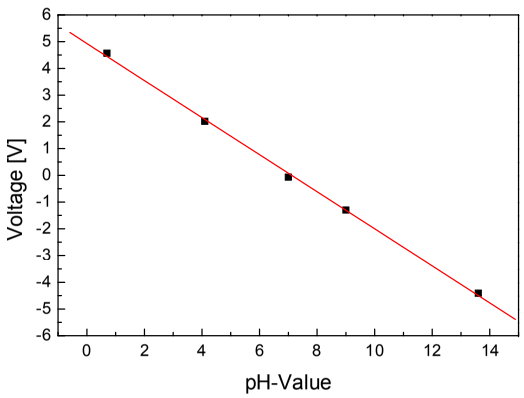

Building Block System

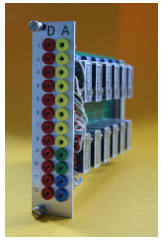

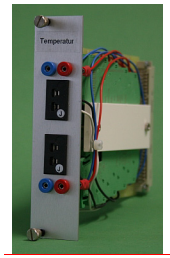

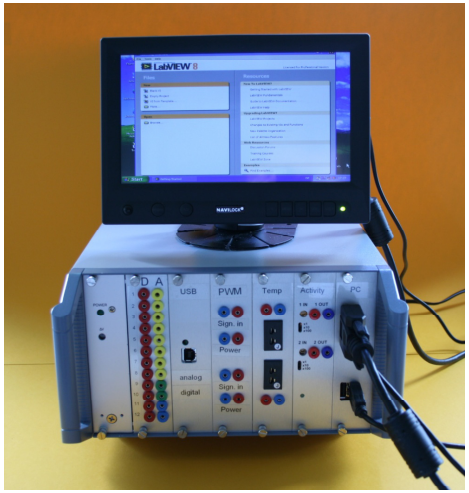

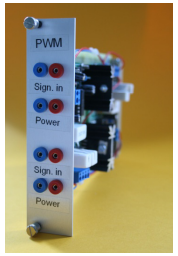

^{89}Zr-Separation with LabView

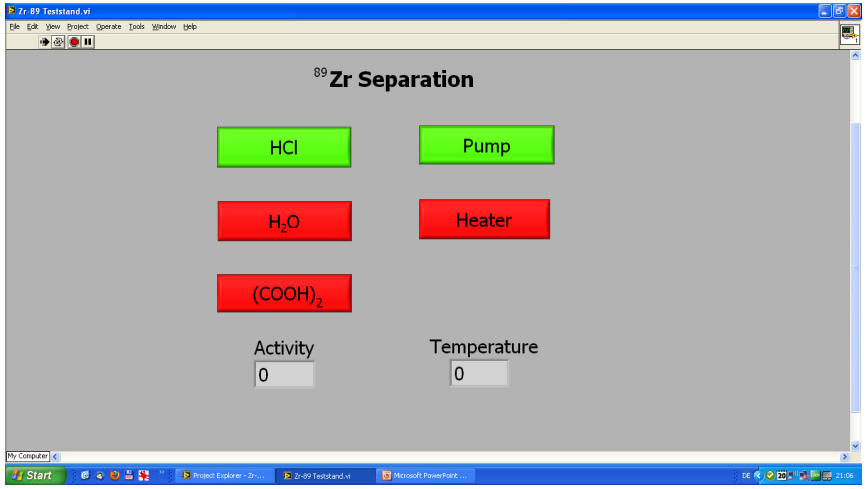

Three years experience in operation and maintenance of the $[^{18}F]F_2$ proton target at the Rossendorf Cyclone® 18/9 cyclotron

St. Preusche, F. Fuechtner, J. Steinbach
Forschungszentrum Dresden-Rossendorf, Institute of Radiopharmacy, P.O. Box 51 01 19, 01314 Dresden, Germany

Introduction

An increasing demand of radiopharmaceuticals based on electrophilic reaction with $[^{18}F]F_2$ gas (for instance $[^{18}F]$FDOPA) led to an upgrade of the IBA $[^{18}F]F_2$ gas target system in summer 2007. The more than 10 years operated $[^{18}F]F_2$ deuteron target $[^{20}Ne(p,\alpha)^{18}F]$ was not able to meet the increasing requirements in terms of activity anymore and was thus replaced by an IBA $[^{18}F]F_2$ proton gas target $[^{18}O(p,n)^{18}F]$ based on the so-called "double-shot" 'irradiation method by R.J. Nickles [1]. The upgrade itself was done by IBA.
We run the Cyclone® 18/9 cyclotron in routine operation for more than 14 years. One of the specific features of the Rossendorf PET Center is the Radionuclide transport system (RATS) [2], 500 m in length that bridges the distance from the cyclotron to the radiopharmaceutical laboratories. The activity at the end of bombardment (EOB) is calculated taking in account the transfer time and experimental data of activity losses (about 30%) in the transfer tube [2].

The target and its supply

The $[^{18}F]F_2$ proton gas target is connected directly to the vacuum chamber of the cyclotron inside the return yoke. Target body: aluminium; target volume: 35 cm^3 of conical shape; target window: aluminium, thickness 500 µm; vacuum window: titanium, thickness 12.5 µm.
As target gases are used for the first bombardment: ^{18}O (enrichment: > 97%; cartridge volume: 75 ml, gas volume: 5250 ml, pressure: 70 bar, manufacturer: Cambridge Isotopes Laboratories, Inc./USA, distributor: ABX/Germany) and for the second bombardment: (Ne/2% F_2), filled up with pure Ne (both: Air Liquide/Germany) to achieve (N_2/0.45% F_2).

Experience in operation and maintenance of the target

First bombardment: $^{18}O_2$: 20 - 22 bar, 40 or 60 or 80 minutes at 22 µA target current
Second bombardment: Ne/F_2: 20 - 22 bar, 15 minutes in each case at 22 µA

Hints for operation:

- Keep the target cavity in standby always under (Ne/F_2) atmosphere
- Prior to the first bombardment of the $[^{18}F]F_2$ production a pre-irradiation (5 minutes, 10 µA) with (Ne/F_2) and transfer of the irradiated gas to the radiopharmaceutical laboratory for the conditioning of the target cavity and the transfer tube is useful.
- After deposition of the irradiated ^{18}O gas into the liquid nitrogen cooled trap: A careful pump down of the target cavity for some minutes is mandatory before filling it for the second bombardment to prevent the formation of $[^{18}F]F - O$ species.
- One ^{18}O cartridge is sufficient for (100 – 120) irradiations. An average gas loss of less than 5% per bombardment has to be compensated by filling from the ^{18}O cartridge. It is possible to use the ^{18}O gas (from the cooling trap and the cartridge) until the residual pressure of the ^{18}O cartridge is around 10 bars.

A slight but permanent drop in the target yield is an indication for a target cleaning procedure to be necessary (see Fig. 1).
After target opening it is observed that the surface of the target cavity did not have a metallic sheen anymore. We added a grinding procedure of the cavity with very fine sand paper to the IBA cleaning procedure [3]. After the cleaning the surface of the cavity should look as metallic. We found this procedure necessary to be done after 100 to 120 runs and perform it once a year.
The handling of the target system is not easy because the results of any kind of changes are often not well reproducible. The highly-reactive $[^{18}F]F_2$ gas at the µmol level is difficult to handle due to the large surfaces of the target cavity, the transfer tube and the synthesis module.

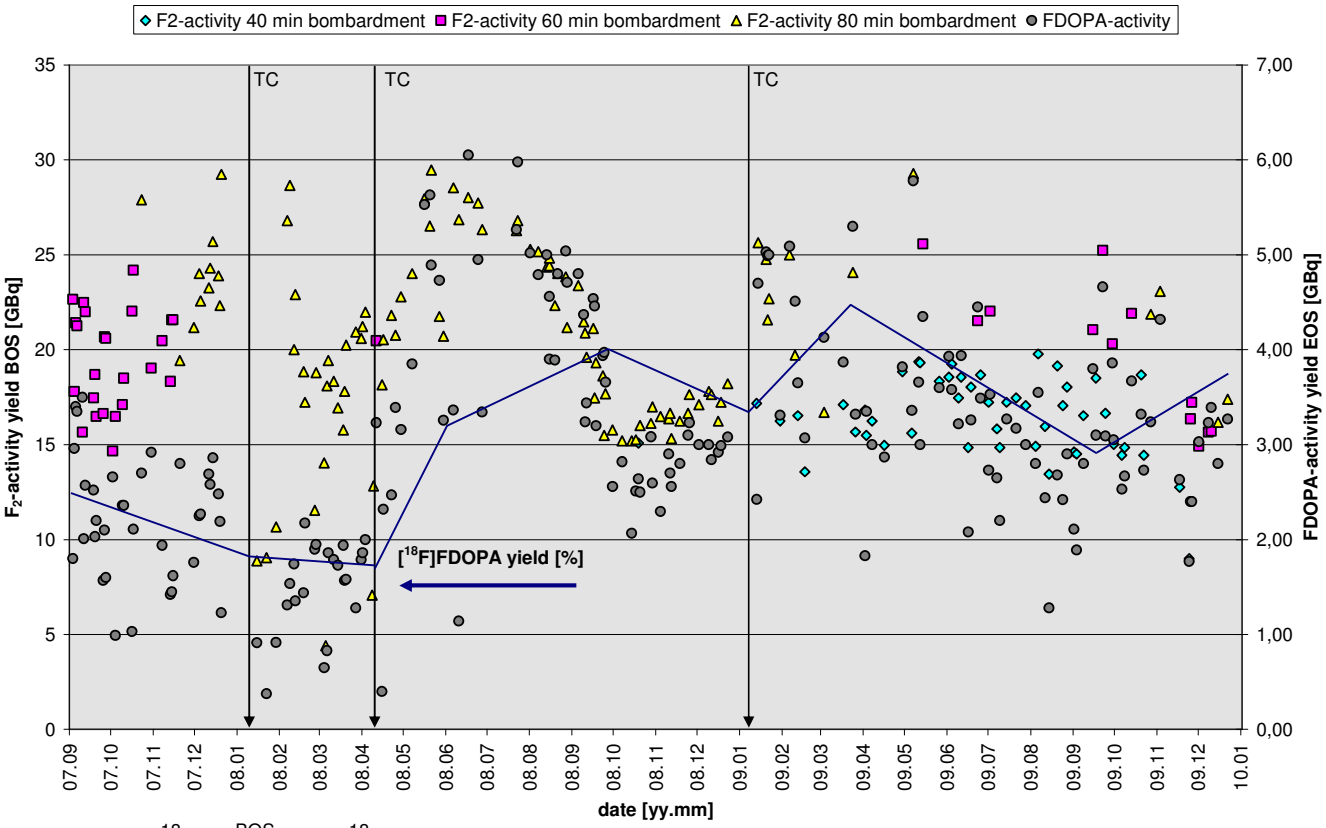

Fig. 1: $[^{18}F]F_2^{BOS}$ and $[^{18}F]$FDOPA activity yields in 2007 – 2009,
TC: target cleaning, line: $[^{18}F]$FDOPA yield

Results

- Dependence of produced $[^{18}F]F_2^{BOS}$ activity on the irradiation time of first bombardment: 40 minutes - 16 ± 2 GBq, 60 minutes - 20 ± 3 GBq, 80 minutes - 20 ± 5 GBq ➔ no increase of $[^{18}F]F_2^{BOS}$ activity increasing the irradiation time of first bombardment from 60 to 80 minutes,
- Besides the produced absolute $[^{18}F]F_2$ activity, the reactivity of the F_2 gas is important for the $[^{18}F]$FDOPA activity yields.
- Target cleaning is recommended if:
  - The absolute $[^{18}F]F_2^{BOS}$ activity yield drops down to about 15 GBq or
  - The $[^{18}F]$FDOPA yield is near or below 15 %.

The advantages of the new $[^{18}F]F_2$ proton target are:

- Higher efficiency in terms of $[^{18}F]F_2$ activity and resulting $[^{18}F]$FDOPA activity yields,
- Operating conditions far from limitations of the target current; that results in less wear of the cyclotron.

A comparison of the $[^{18}F]F_2$ deuteron and proton targets is given in the table.

	Deuteron target	Proton target
Max. target current	18 µA	30 µA
Irradiating conditions time average /common current	120 min 18 µA	First bombardment: 60 min Second bombardment: 15 min 22 µA
A^{EOB}, GBq	7 - 11	34 ± 5

References

[1] R.J. Nickles, M.E. Daube, T.J. Ruth; An $^{18}O_2$ target for the production of $[^{18}F]F_2$ Int. J. Appl. Radiat. Isot. 35 (1984) 117-122

[2] St. Preusche, F. Füchtner, J. Steinbach, J. Zessin, H. Krug, W. Neumann; Long-distance transport of radionuclides between PET cyclotron and PET radiochemistry, The Journal Applied Radiation & Isotopes 51 (1999) 625-630

[3] IBA, $[^{18}F]F_2$ proton target, maintenance procedure, 2007

Cancer Research

Three years experience in operation and maintenance of the $[^{18}F]F_2/[^{18}O]O_2$-gas target at the Rossendorf Cyclone® cyclotron

St. Preusche, F. Füchtner, J. Steinbach

Forschungszentrum Dresden Rossendorf

Institute of Radiopharmacy • St. Preusche et al. • www.fzd.de • Member of the Leibniz Association

Content

1. Introduction

Why change from $[^{18}F]F_2$-deuteron target to $[^{18}F]F_2$-proton target?

- increasing demand of radiopharmaceuticals based on electrophilic reaction with $[^{18}F]F_2$ gas (for instance $[^{18}F]$FDOPA)
  - ➔ Not enough $[^{18}F]F_2$ activity with $[^{18}F]F_2$ deuteron target $[^{20}Ne(d,\alpha)^{18}F]$

Measure

- $[^{18}F]F_2/[^{18}O]O_2$-gas target $[^{18}O(p,n)^{18}F]$:
  "double-shot" 'irradiation method by R.J. Nickles [1]
- upgrade done by IBA

Rossendorf conditions

- 500 m RN transport system: losses of $[^{18}F]F_2$ activity ~ 30% [2]
- routine operation of Cyclone® 18/9 for 14 years

2. The target and its supply

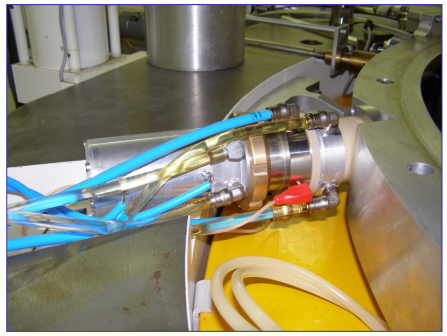

$[^{18}F]F_2/[^{18}O]O_2$-gas target
connected directly to vacuum chamber

target body:	aluminium
target volume:	35 cm^3 of conical shape
target window:	aluminium, thickness 500 µm
vacuum window:	titanium, thickness 12.5 µm

Target supply

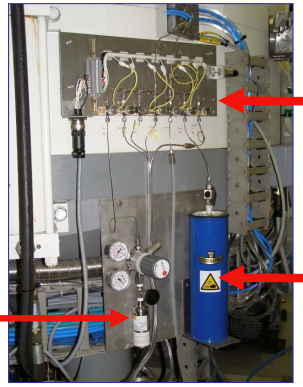

target gas for 1st bombardment: **^{18}O**
enrichment: > 97%
cartridge volume: 75 ml
gas volume: 5250 ml
pressure: 70 bar
manufacturer: Cambridge Isotopes Laboratories, Inc./USA
distributor: ABX/Germany

target gases for 2nd bombardment:
Ne/2% F_2 (4.5 bar)
filled up with **pure Ne** to 20 bar
➔ 140 µmol F_2

both: Air Liquide/Germany

3. Experience in operation and maintenance of the target

Irradiating conditions

1st bombardment: $^{18}O_2$: 20 - 22 bar, 40 or 60 or 80 minutes at I_T = 22 µA
2nd bombardment: Ne/F_2: 20 - 22 bar, 15 minutes at I_T = 22 µA

Hints for operation

- Keep the target cavity in standby always under (Ne/F_2) atmosphere
- Conditioning of the target cavity and the 500 m transfer tube prior to 1st bombardment
  ➔ pre-irradiation (5 minutes, 10 µA) with (Ne/F_2)
- Prevent the formation of $[^{18}F]F$ – O species
  ➔ After deposition of the irradiated ^{18}O gas into the trap:
  careful pump down of the target cavity for some minutes, incl. Ne-flush (20 sec)
- ^{18}O cartridge
  ➔ sufficient for 100 - 120 irradiations
  ➔ average gas loss per bombardment: < 5%, compensated by filling from ^{18}O cartridge
  ➔ use of ^{18}O gas (trap, cartridge) until residual pressure of ^{18}O cartridge: ~ 10 bars.

Maintenance

A slight but permanent drop in the target yield ➔ indication for target cleaning

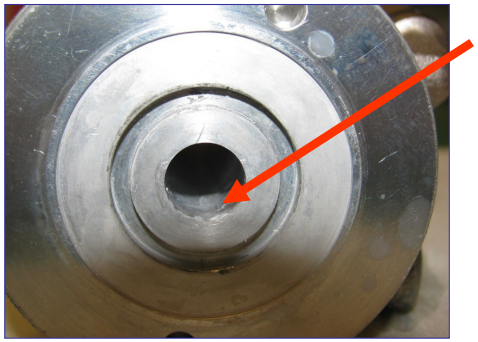

front

Before cleaning
➔ target cavity:
no metallic sheen anymore

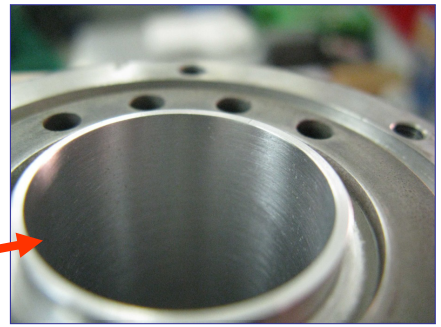

rear

After cleaning
➔ target cavity: should look as metallic

Conclusion of operation and maintenance

Handling of target system is not easy
➔ results of any kind of changes are often not well reproducible

Highly-reactive $[^{18}F]F_2$ gas at the µmol level is difficult to handle
➔ large surfaces of target cavity, transfer tube and synthesis module

4. Results

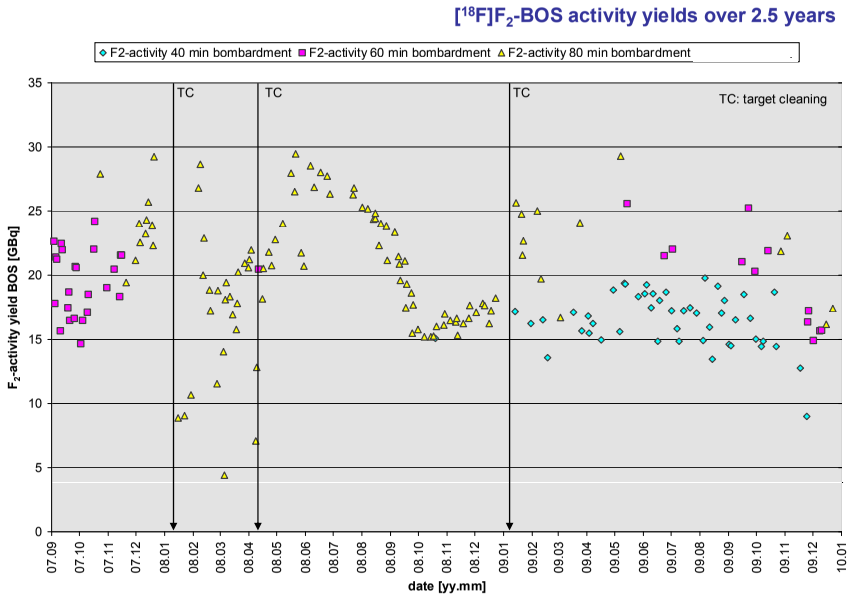

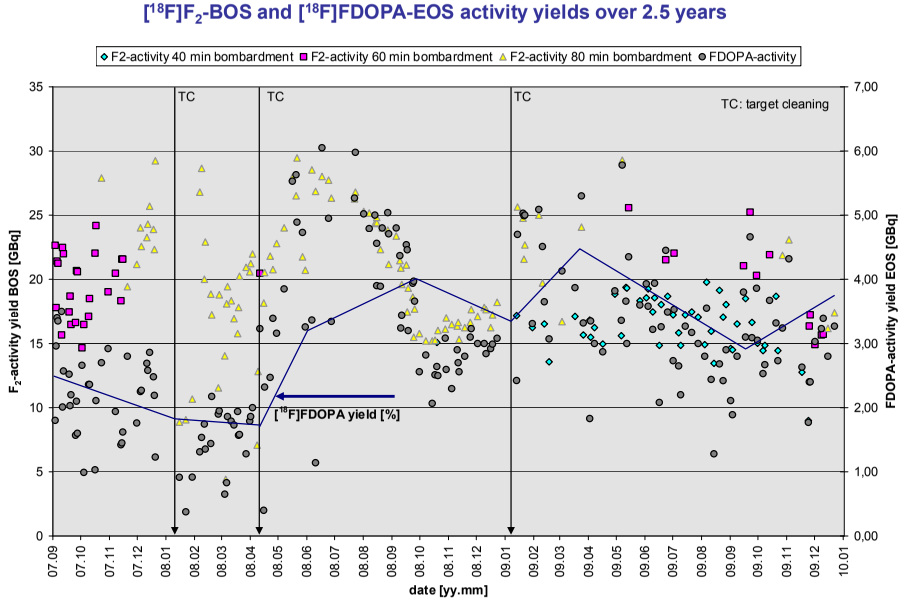

Summary

[18F]F2-BOS activity as function of 1st bombardment

40 minutes: 16 ± 2 GBq
60 minutes: 20 ± 3 GBq
80 minutes: 20 ± 5 GBq

➔ hardly increase in [18F]F2-BOS activity from 60 to 80 minutes

Besides the produced absolute [18F]F2 activity:
the reactivity of the F2 gas is important for the [18F]FDOPA activity yields

Target cleaning is recommended if:
- slight but permanent drop in the target yield
- [18F]F2-BOS activity yield drops down to an activity level where the [18F]FDOPA-EOS yield is not sufficient for the numbers of patients planned to be investigated
- [18F]FDOPA yield is near or below 15 % over a certain period

Summary

Advantages of the new [18F]F2/[18O]O2-gas target

➔ Higher efficiency in terms of [18F]F2 activity and resulting [18F]FDOPA activity yields

➔ Operating conditions far from limitations of the target current; that results in less wear of the cyclotron

Comparison of [18F]F2 deuteron target (old) and proton target (new)

	Deuteron target	Proton target
Max. target current, µA	18	30
Irradiating conditions: irradiating time, minutes target current, µA	120 18	1st bombardment: 60 min 2nd bombardment: 15 min 22
A_{EOB}, GBq	7 – 11	34 ± 5

5. References

[1] R.J. Nickles, M.E. Daube, T.J. Ruth; An $^{18}O_2$ target for the production of $[^{18}F]F_2$; Int. J. Appl. Radiat. Isot. 35 (1984) 117-122

[2] St. Preusche, F. Füchtner, J. Steinbach, J. Zessin, H. Krug, W. Neumann; Long-distance transport of radionuclides between PET cyclotron and PET radiochemistry, The Journal Applied Radiation & Isotopes 51 (1999) 625-630

[3] IBA, $[^{18}F]F_2$ proton target, maintenance procedure, 2007

6. Some more details

6.1 Target cleaning procedure

1. Dismount the target completely (rear plate too)
2. Grinding the target cavity with very fine sand paper
3. IBA cleaning procedure (solvents, water, dry) [3]
4. Pray for good results

Cleaning tools

Important

Dose rate of grinding water after use: **> 500 µSv/h**

➔ work carefully!

6.2 Further maintenance hints

A) Radiation protection in the working area

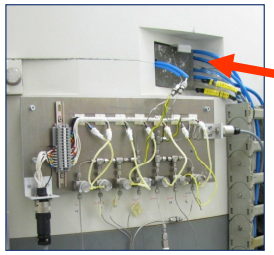

Lead brick (5 cm)
reduces dose rate in front of the gap

EOB + 2 hrs	
without leak brick	> 28.000 µSv/h
with lead brick	6.400 µSv/h
EOB + 24 hrs	
without leak brick	330 µSv/h
with lead brick	75 µSv/h

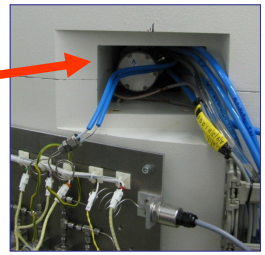

B) Parker valves of valve tableau

problems with inserts (= poppets):

drop in target pressure: valves not leak-proof anymore

➔ keep poppets as spare parts
➔ change poppet during He-flush through target
➔ some pre-irradiations after changing poppets

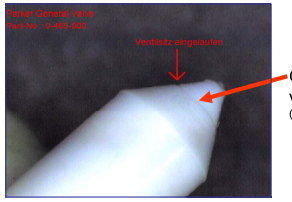

Grove by valve seat
(photo: Parker)

WTTC XIII – Presentation Discussions

1. Transfer lines
   - Cu 1,5mm diameter used
   - Careful with cleaning
   - Valve poppets that can handle 18F (IBA has new ones)

Non-HPLC Methods for the Production of F-18, C-11 and Ga-68 PET Tracers

Alexander Yordanov[1], Damion Stimson,[2] Didier Le Bars,[5] Seth Shulman[1], Matthew J. Combs[1], Ayfer Soylu,[4] Hakan Bagci,[4] and Marco Mueller[3]

[1] Bioscan, Inc., Washington, DC, U.S.A.
[2] Royal Brisbane Hospital, Brisbane, Queensland, Australia
[3] ABX, Radeburg, Germany
[4] Ezcacibasi-Monrol, Ankara, Turkey
[5] CERMEP, Lyon, France

The most popular PET radionuclides in routine clinical use are C-11 and F-18, although other radionuclides, such as Ga-68, continue to make headlines. This is due to their well established chemistry, their utility for labeling low molecular weight compounds, and their ease of production in modern PET cyclotrons or via commercially available generators. Their relatively short half-lives, along with the global trend toward Good Manufacturing Practice in PET drug production has necessitated the development of aseptic, robust and rapid labeling methodologies. This is achieved by the use of automated radiochemistry systems, which, in turn, has allowed radiosynthesis scale-up and multiple dose preparation.

Major impediments to routine production of a number of useful C-11, F-18 and Ga-68 PET tracers, and to new tracer development, remain: 1) the necessity of thorough system clean up in between consecutive runs; and 2) inconsistent yields and prolonged synthesis time when using HPLC methods for final product separation and purification. To address these issues, new radiochemistry applications have been developed for the radiochemistry modules:

a) for F-18: FLT Lite, F-MISO Lite, F-Choline Lite, and FET Lite;
b) for C-11: Acetate, Methyl Iodide, Methionine, Choline;
c) for Ga-68: DOTA-Peptides.

These methods utilize sterile disposable kits, and allow for the PET tracers to be purified and isolated with SPE cartridges only, thus eliminating the need for HPLC separation. The processes and the radiochemical yields obtained with these methods will be presented, and their utility discussed.

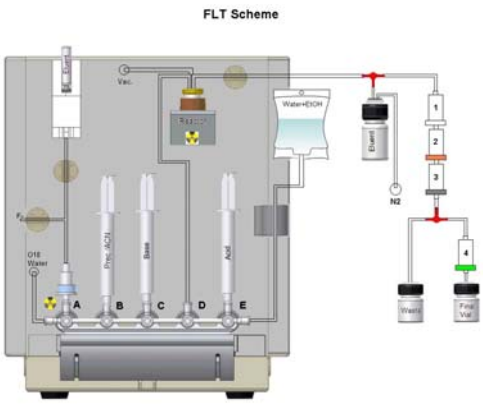

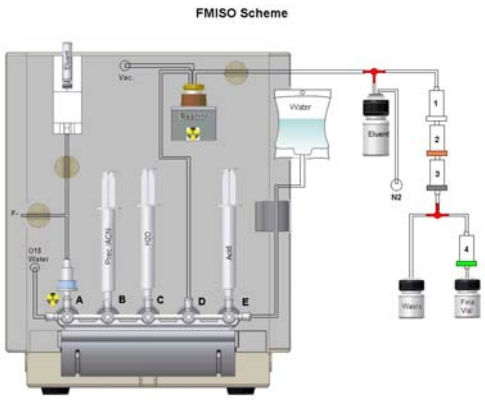

FET Scheme

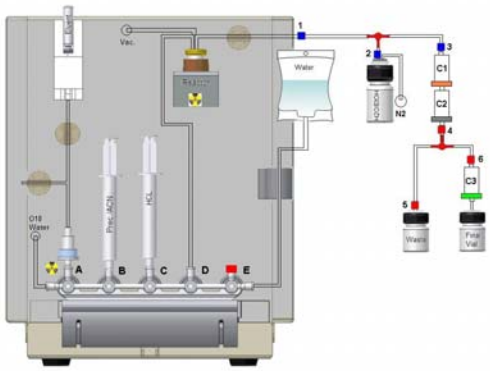

18F-Choline Scheme

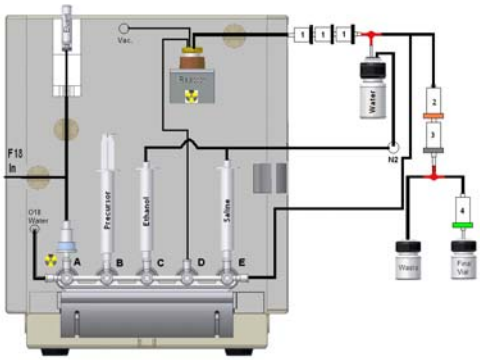

C-11 Acetate

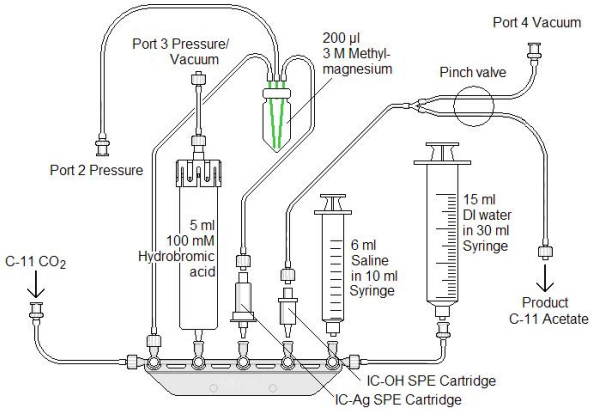

C-11 Methyl Iodide

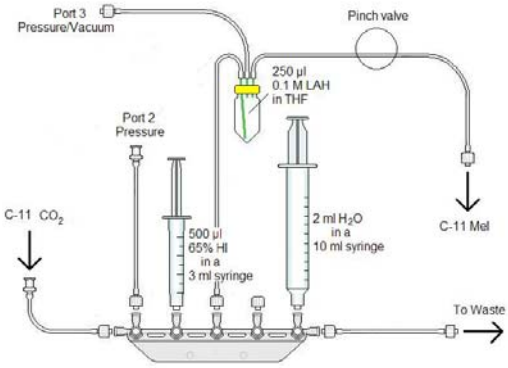

C-11 Choline

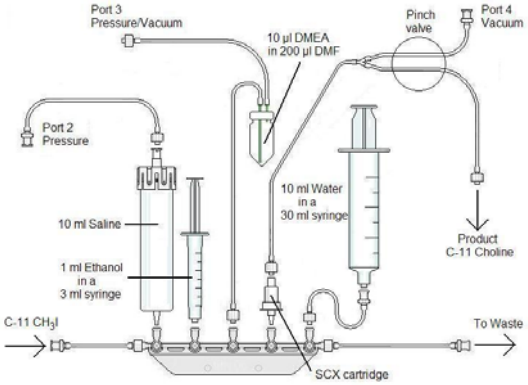

C-11 Methionine

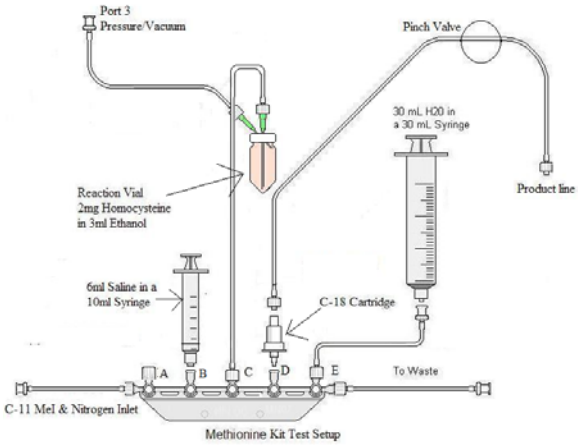

Non-HPLC Methods for the Production of F-18, C-11, Ga-68, Cu-64 and Sc-44 Radiopharmaceuticals

- A. Yordanov, M. Combs, S. Shulman Bioscan, Inc., Washington DC, U.S.A.
- D. Stimson, Royal Brisbane Hospital, Brisbane, Queensland, Australia
- M. Müller - ABX GmbH, Radeberg, Germany
- H. Bağci, A. Soylu - Eczacibasi-Monrol, Ankara, Turkey
- D. LeBars, CERMEP, Lyon, France

BIOSCAN

Disclaimer

This presentation is solely intended to provide and disseminate the authors' scientific results, interpretation and views in the nuclear medicine community. It does not constitute an endorsement of any Bioscan or other commercial manufacturers' products listed, displayed on mentioned hereof.

BIOSCAN

2010 – Good Year for the PET Radiopharmaceutical Industry

- WILEX - IBA Molecular Phase III Clinical Trial of REDECTANE(R) was successfully completed; NDA filing expected by the beginning of year
- Lantheus Phase III clinical trial to begin
- AVID Phase III clinical trial near completion
- Bayer Schering Pharma AG Phase III

BIOSCAN

2010 – Good Year for PET Radiopharmaceutical Industry (cont.)

- IBA Molecular – Aposense Phase III Clinical Trial
- Fluoropharma
- NuView Pharmaceuticals
- Lantheus, AVID – next leads in the pipeline
- More PET Tracer Start-ups

BIOSCAN

Is There Future for New Radionuclides in Imaging and Therapy?

- Yes if (among other factors) the radionuclide:
  - has a convenient half-life
  - is available in commercial quantities and at reasonable cost
  - has optimal radio-labeling chemistry
  - has established an optimal target – targeting vector – radionuclide match

BIOSCAN

Is There Future for New Radionuclides in Imaging and Therapy (cont.)?

- Yes if (among other factors) the imaging or therapeutic drug candidate:
  - is manufactured by a process easy to scale up
  - has demonstrated sufficient *in vitro* and *in vivo* stability
  - provides high quality image or superior therapeutic effect
  - clinical indication with few alternatives

BIOSCAN

Is There Future for New Radionuclides in Imaging and Therapy (cont.)?

- And last but not least :
  - **enterpreneurship** (the right person doing the right thing at the right time)
  - availability of funding for clinical trials
  - it is a trial-and-error process (out of every 12 radiolabeled molecules only one will become a drug on the market)

BIOSCAN

Radionuclides Status from Industry Point of View

- Existing or under construction manufacturing network – C-11, N-13, O-15, F-18, I-124, Cu-64, Zr-89, Tc-99m, I-123, I-131, Y-90
- Manufacturing issues that are expected to be solved during the next few years - for Ga-68, Re-188, Y-86, At-211, Cu-67, Ho-166, Lu-177, Bi-213
- Other radionuclides not mentioned here – may be available in large quantities in 10 years or more

BIOSCAN

Standard Purification Tools for Pharmaceuticals

- Crystallization
- Sublimation
- Filtration
- Distillation
- Liquid-liquid or solid phase extraction
- **Preparative HPLC purification ???**

BIOSCAN

Pros and Cons of HPLC separation

Pros:

- Provides universal separation method in complex mixtures

Cons:

- Lengthens radiosynthesis time
- Column packing material is variable
- Radiolytic damage to column packing with high activity

BIOSCAN

Ga-68, Cu-64 and Sc-44 Peptide Radiolabeling

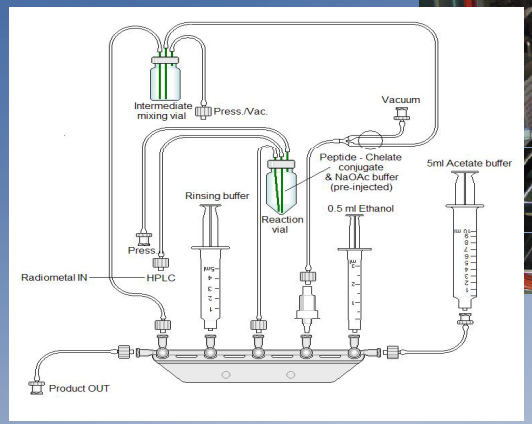

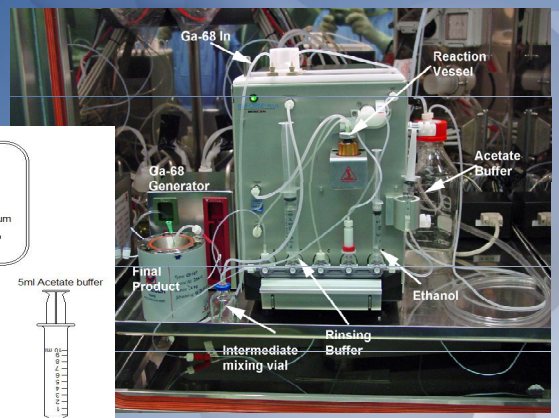

BIOSCAN

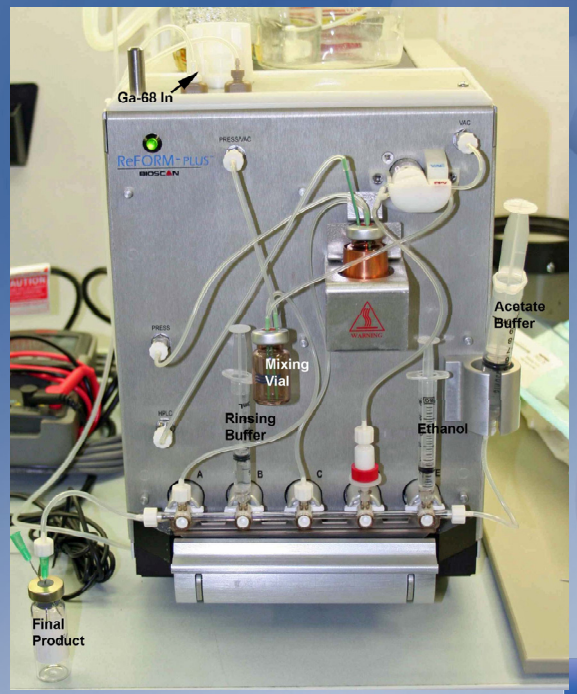

Ga-68 DOTA-TATE

- Elute Generator into top of box
- Capture eluent in reactor that contains precursor
- Heat Mixture
- Trap on SPE
- Elute with Ethanol into mixing vial
- Rinse with Acetate Buffer
- Collect product

BIOSCAN

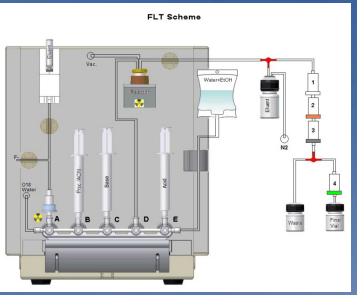

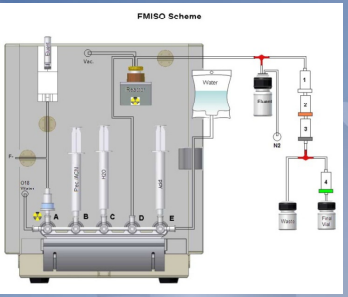

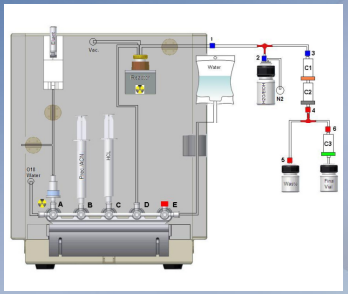

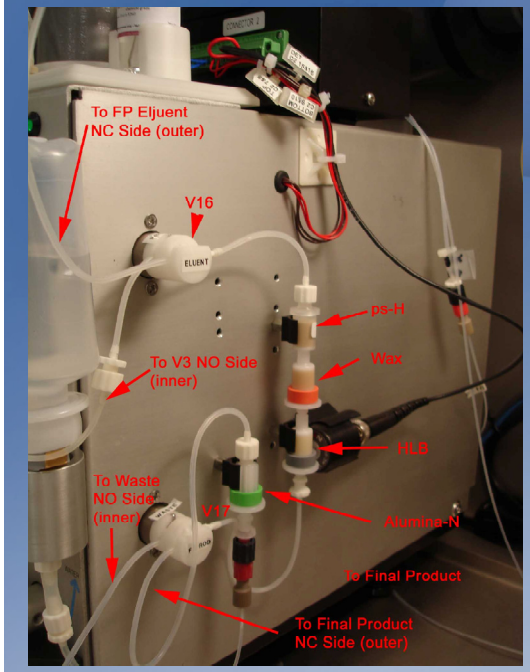

PS-H: Bu_4N^+,

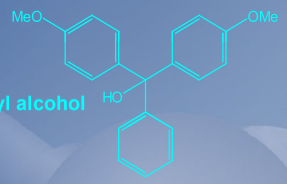

4,4'-dimethoxytrityl alcohol

WAX:

Nosylate anion

HLB:

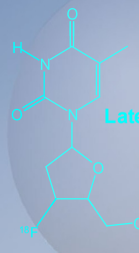

Later eluted with 10% aq. EtOH

FLT

FLT-Lite Hot Runs

Date	Beam	Duration of Bombardment (Minutes)	Activity (mCi)	FLT Activity (mCi)	Corrected Yield	Precursor
10.02.2009	Single	18	557	61	15.2	25 mg
14.02.2009	Single	198	1256	106	11.7	25 mg
18.02.2009	Single	168	3155	493	21.4	25 mg
13.04.2009	Single	50	852	153	24.8	20 mg
15.04.2009	Dual	88 – 91	3587	483	19.1	25 mg
16.04.2009	Dual	128 – 77	4290	531	17.9	20 mg
17.04.2009	Single	90	2409	215	12.9	20 mg*

*The precursor was dissolved the previous day and kept in a fridge overnight

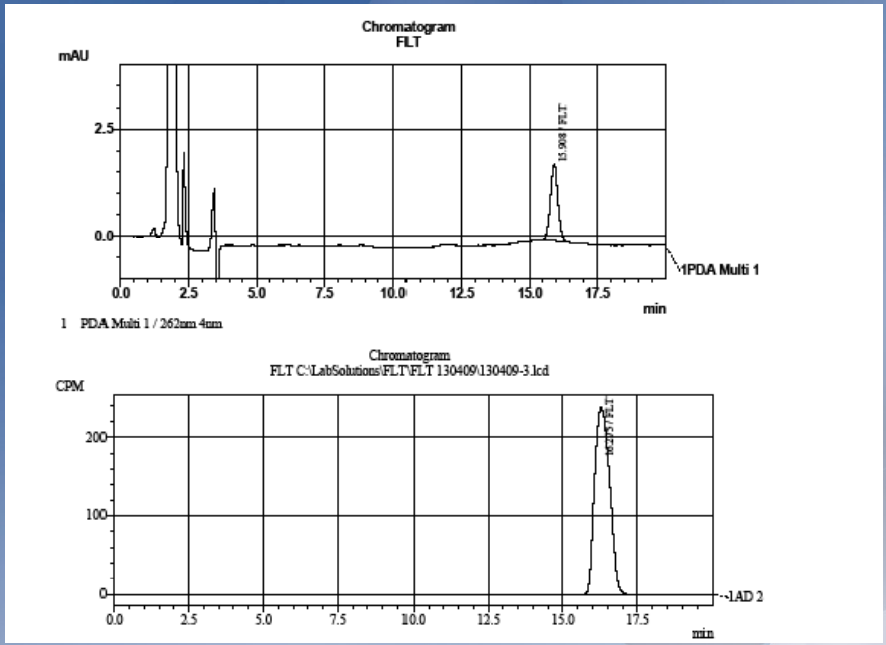

FMISO Scheme

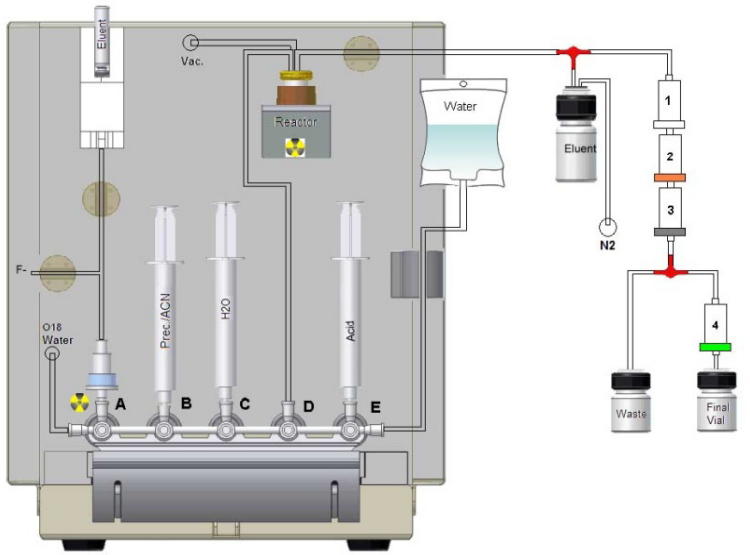

BIOSCAN

C-11 Acetate

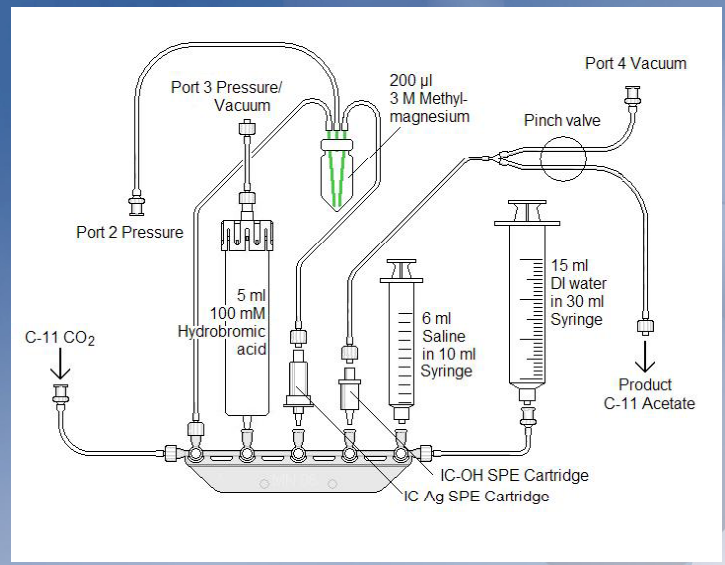

BIOSCAN

C-11 Choline

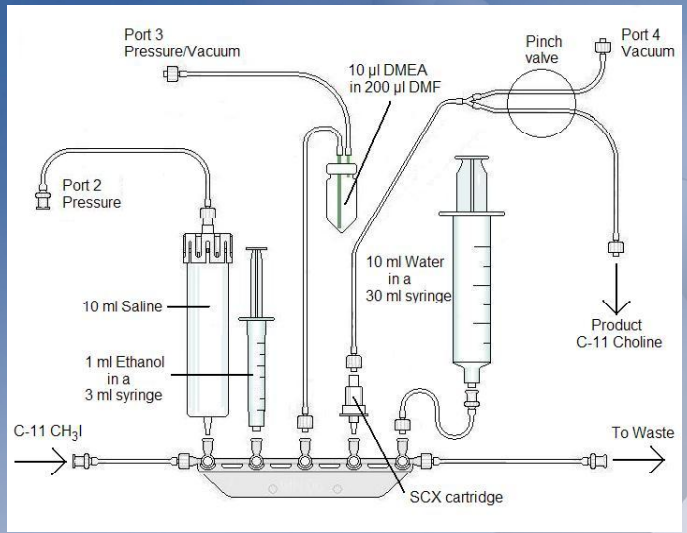

BIOSCAN

C-11 Methionine

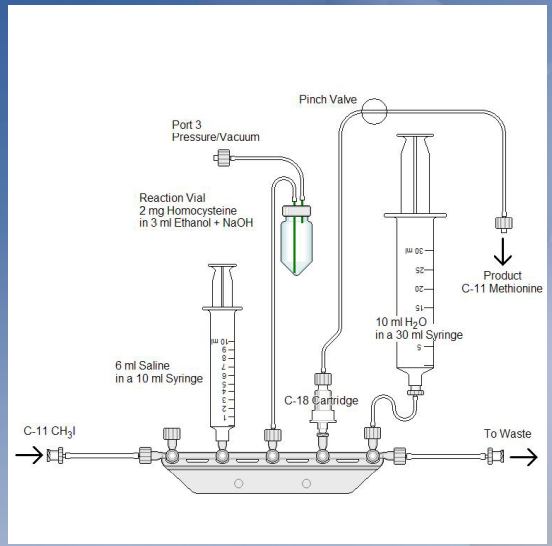

BIOSCAN

C-11 Methyl Iodide (MeI)

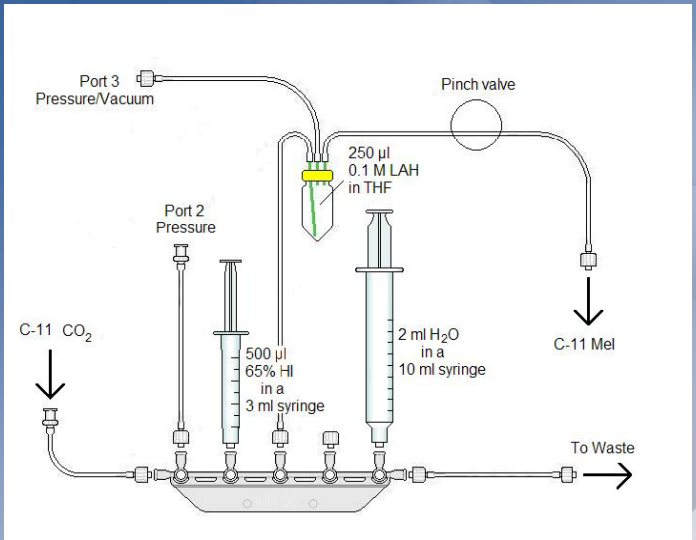

BIOSCAN

C-11 Methyl Iodide (MeI)

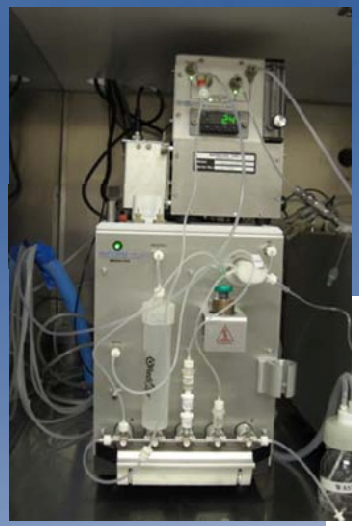

Average Yield: 50 % EOS

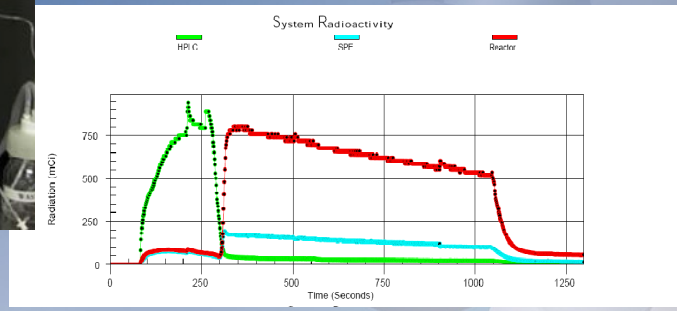

BIOSCAN

Clearly, there is a lot of work to be done. More challenges ahead:

- Target processing automation
- Alternative suppliers for enriched target materials
- Antibody and antibody fragments radio-labeling automation
- What about the future of targeted radiotherapy?
  - At-211 chemistry automation

BIOSCAN

WTTC XIII – Presentation Discussions

1. FLT: system by-products
   - Peak always there, maybe just cold FLT
2. Sep-pak vs. HPLC
   - Sep-pak not GMP… regulators can see a problem
   - Sep-pak easier than HPLC
3. Challenge: collaboration target/chemistry/manufacturers

Evaluation on metallic Sc as target for the production of ^{44}Ti on high energy protons

K. Zhernosekov[1,2], A. Hohn[1], M. Ayranov[2], D. Schumann[2], R. Schibli[1], A. Türler[1,2]

[1] Center for Radiopharmaceutical Science, Paul Scherrer Institute, 5232 Villigen, PSI, Switzerland

[2] Labor für Radio- und Umweltchemie Departement Chemie und Biochemie Universität Bern Switzerland

Radionuclide generators provide an alternative and often more convenient source of radionuclides compared to the direct production routes at accelerators and nuclear reactors. Especially generator produced positron emitters are of increased interest for development of novel PET-radiopharmaceuticals [1]. Thus ^{68}Ge/^{68}Ga radionuclide generator is successfully introduced into the clinical PET for routine production of ^{68}Ga-PET tracers. Due to rather short half-life ($T_{½}$ 68 min) ^{68}Ga is useful, however, only for the investigations on fast *in vivo* processes.

With 3.97 h half-life and 94.27 % positron branching ^{44}Sc is a very attractive alternative for applications in clinical PET. The major advantage is the production possibility of this radionuclide *via* ^{44}Ti/^{44}Sc radionuclide generator (^{44}Ti $T_{½}$ = 60.0 y). The limited availability of the long-lived mother nuclide ^{44}Ti complicates further development in the radionuclide generator technique and ^{44}Sc-radiolabelled compounds.

^{44}Ti can be produced by the ^{45}Sc(p,2n) nuclear reaction. The long half-life of the accumulating nuclide and a low cross section (Fig. 1) result in a very low production rates and long-term high-current irradiations must be performed. The irradiation facility at Paul Scherrer Institute provides up to 72 MeV and 70 µA proton beam. For the production of ^{44}Ti we are evaluating massive metallic ^{45}Sc targets for the long-term irradiation with protons up to 40 MeV. Up to 10 mm thick scandium blocks are encapsulated in an electron-beam welded thin Al-foil. For the possible routine production the water-cooled target system is supposed to withstand up to 7000 µAh resulting in 50 – 100 MBq of ^{44}Ti. In this respect, the preliminary results on the irradiation yields and optimizations as well as stability of the system are presented.

[1] Rösch, F., Knapp, F. F. Radionuclide Generators. In: Vértes, A., Nagy, S., Klencsár, Z. Handbook of Nuclear Chemistry. Amsterdam, 2003; 4: 81 – 118;

[2] Experimental Nuclear Reaction Data (EXFOR) http://www-nds.iaea.org/exfor/exfor.htm

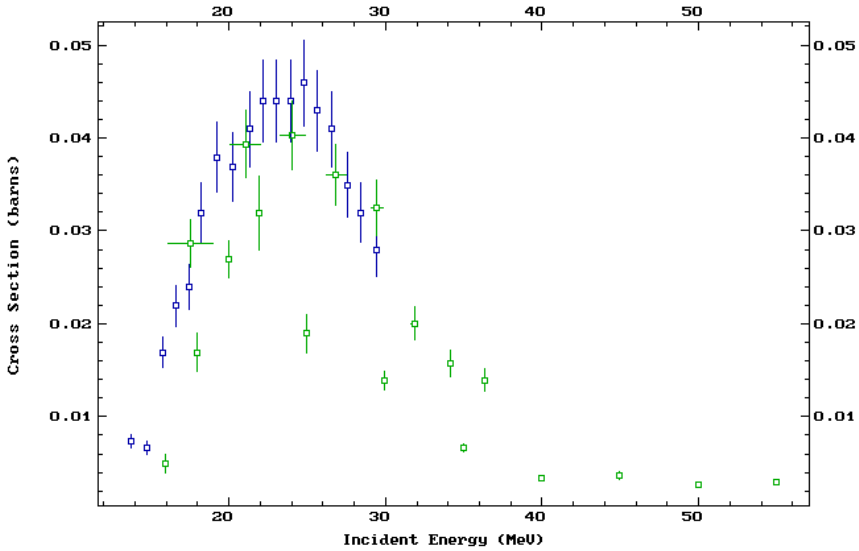

Figure 1. Excitation function of $^{45}Sc(p,2n)^{44}Ti$ reaction [2]

Operating RbCl Targets Beyond the Boiling Point? – Work in progress

F.M. Nortier[1], H.T. Bach[1], M. Connors[1], K.D. John[1], J.W. Lenz[2], F.O. Valdez[1], J.W. Weidner[1]

[1]Los Alamos National Laboratory, Los Alamos, New Mexico, USA
[2]John W. Lenz & Associates, Waxahachie, Texas, USA

The 100 MeV Isotope Production Facility (IPF) at Los Alamos National Laboratory produces the medical isotope Sr-82 on a large-scale. For routine production runs, RbCl salt targets are encapsulated in electron beam welded Inconel® 625 capsules and irradiated in a typical target stack consisting of two RbCl targets for Sr-82 production and one gallium target for Ge-68 production [1] (see Fig.1). These two-inch diameter targets are cooled on their faces with water flowing through 5 mm wide cooling channels that separate the targets. Systematic target performance studies of similar encapsulated targets under extended bombardment with intense proton beams are not available in the literature. Routine production experience at LANL shows that while the unexpected failure of a gallium target after an extended irradiation is often associated with radiation damage and other cumulative effects in the niobium capsule material [2], the abrupt early failure of a RbCl target is usually associated with the thermal effects occurring in the encapsulated target material. Numerous Sr-82 production runs were performed at IPF over a period of six years. Almost one hundred RbCl targets were irradiated with production beam currents of up to the facility administrative limit of 250 µA. Target performance statistics indicate that these targets can reliably accept production beam currents of between 230 µA and 240 µA. At higher beam currents, occasional early target failures are likely to occur. Excessive bulging of the two adjacent RbCl target capsules interrupts the water flow in the cooling channel between the targets and leads to sudden loss of cooling, causing the two target capsules to fuse together (see Fig. 2).

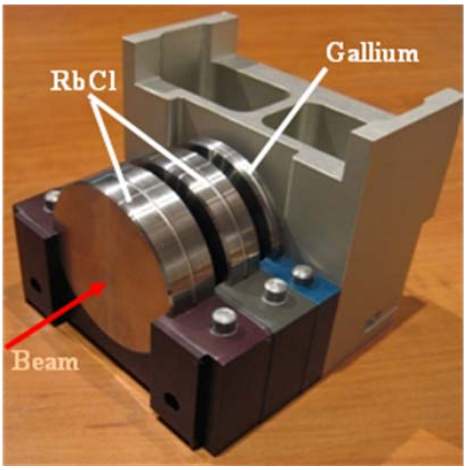

Fig. 1. Typical target stack for production of Sr-82 and Ge-68

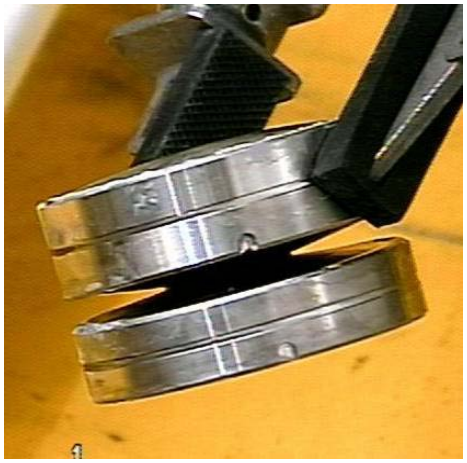

Fig. 2. Failed RbCl targets

In a recent development, the administrative limit of the IPF facility was increased from 250 µA to 450 µA, increasing the production capacity of the facility by almost a factor of two. In December of 2009 a preliminary high current test was conducted using a test stack consisting of three aluminium targets. During this test, the IPF demonstrated that the facility can safely operate at 360 µA. A follow-up high current test is now planned for the 2010 run cycle in order to demonstrate facility operation at the authorized current limit of 450 µA. Since most of the facility beam time is consumed by the large scale production of Sr-82, this new development sparked the desire to

better understand the RbCl target failure mechanisms in order to push the in-beam performance of the targets beyond their present beam current limit.

The existing failure theory assumes that the observed target bulging results from internal pressure driven by localized boiling of the RbCl salt, which has a boiling point of 1390 °C. In one controlled experimental irradiation, a set of RbCl targets were driven to the point of failure by systematically increasing the beam current. The targets were inspected before each beam current increase. During this experiment, a thermal performance limit for the RbCl targets was established at 275 μA. It should be noted that occasional thermal failure under production conditions could occur at beam currents as low as 245 μA. In a separate, more theoretical effort, a detailed thermal analysis (see Fig. 3) predicted localized RbCl boiling at a beam current of 250 μA, suggesting that the thermal performance limit should be at 250 μA. The analysis took into account the major coupled thermal processes outside and inside the target, such as the water cooling of the target faces by means of forced convection, heat conduction through the solid and molten materials, and natural convection in the molten part of the salt. These results, together with data gained from the few target failures experienced during production runs, tend to support the theory that failure occurs when the maximum temperature reaches the boiling point of RbCl.

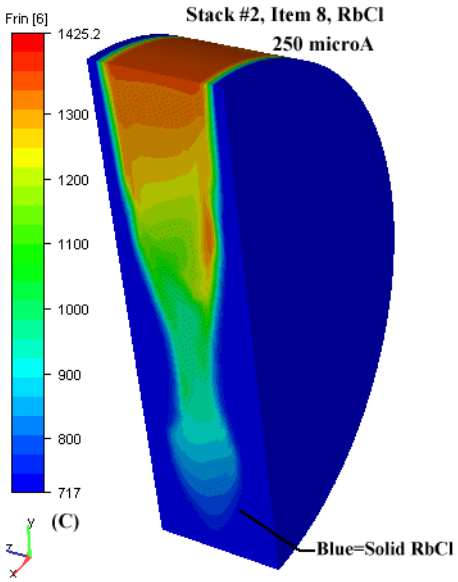

Fig. 3. Predicted temperature distribution in a RbCl target

However, some evidence also suggests that the maximum temperature must be much higher than the boiling point at the time of failure. For example, it is known that bulging is observed in most of the production targets but that abrupt target failure occurs only when the cooling channel is sufficiently disturbed. This suggests that failure occurs when the bulging windows of the two adjacent RbCl targets touch, meaning the deflection of a single window reaches 2.5 mm. Based upon hydraulic deflection tests of capsule windows, a deflection of 2.5 mm corresponds to an internal capsule pressure in excess of 30 bar. Assuming that the internal pressure is caused by RbCl vapour, the high pressure value suggests a maximum internal target temperature in excess of 2100 °C, which does not correlate with the thermal analysis results.

Considering the growing demand for Sr-82 and the recent increase in the IPF administrative beam current limit, there is renewed interest in increasing the existing beam current limit imposed on our RbCl targets. Efforts to gain a still better understanding of the failure mechanisms occurring in these high-power targets through improved analysis and capsule design changes are in progress.

[1] F. M. Nortier, J. W. Lenz, C. Moddrell and P. A. Smith, “Large-scale Isotope Production with an Intense 100 MeV Proton Beam: Recent Target Performance Experience”, Proceeding 18th International Conference on Cyclotrons and their Applications, edited by D. Rifuggiato and L.A.C Piazza, Presso la C.D.B. di Ragusa (2008) 257.

[2] H.T. Bach, T.N. Claytor, J.F. Hunter, B.E. Dozier, F.M. Nortier, D.M. Smith, J.W. Lenz, C. Moddrell, and P.A. Smith, Ultrasonic and Radiographic Imaging of Niobium Target Capsules for Radioisotope Production. Proc. 35th Annual Review of Progress in Quantitative Nondestructive Evaluation; AIP Conference Proceedings 1096 (2009) 674.

Operating RbCl Targets Beyond the Boiling Point? A work in progress

F.M. Nortier[1]
H.T. Bach[1], M.A. Connors[1], M.S. Gulley[1], K.D. John[1], J.W. Lenz[2], E.R Olivas[1], F.O. Valdez[1], J.W. Weidner[1]

[1]*Los Alamos National Laboratory, Los Alamos, New Mexico, USA*

[2]*Facility for Rare Ion Beams, East Lansing, Michigan, USA*

IPF Targetry Facts

- Generally targets are irradiated with 100 MeV protons up to 250 μA.
- Production occurs simultaneously in 3 energy ranges
- Three targets in a stack with cooling channels in between
- Pulsed beam with ring-shaped beam profile

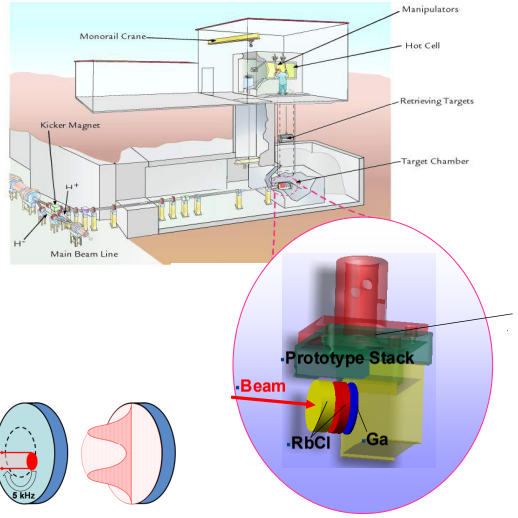

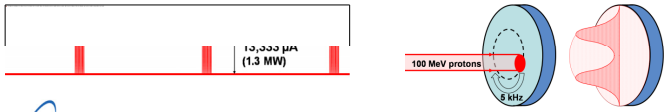

Sr-82 and Ge-68 production facts

- RbCl targets are encapsulated in inconel and Ga target is encapsulated in niobium
- Sr-82 production consumes more than 90% of available beam time
- Recently demonstrated that beam currents up to 360 μA available (future 450 μA) – taking advantage of this will open up beam time for R&D isotopes

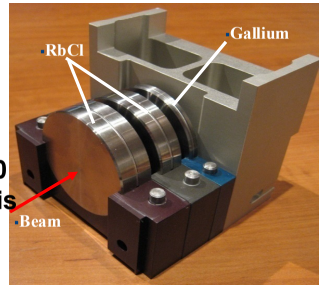

IPCM000D01 CM inst value	355.979	uA
IPCM000D02 IP 1 Minute Running Av	355.560	uA
IPCM001I06 H+ Avg Crnt (IPTM)	356.938	UA
IPCM002I06 H+ Avg Crnt	356.698	UA
IPCM003I06 H+ Avg Crnt	358.856	UA
IPCM004I06 H+ Avg Crnt	356.219	UA

- Thermal performance of RbCl salt targets is significantly lower than most metals
- Routine productions use beam currents between 230 and 240 μA – occasional failures beyond 240 μA

Improving RbCl Salt Target Performance

What to do?

- Understand what is going on
- Learn how to control each individual parameter in order of decreasing significance
- Success!!!!!

Exhibit A – Routine Production experience

- Six years of production experience
- >100 production targets irradiated at beam currents up to 250 μA
- Occasional failures at currents >240 μA
- Excessive bulging due to internal pressure
- Targets fuse together due to obstruction of the cooling water channel
- Thermal performance limit assumed to be 240 μA

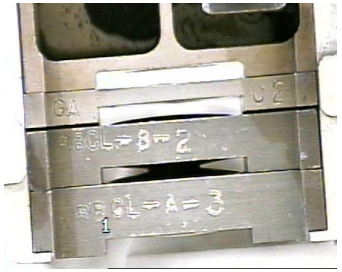

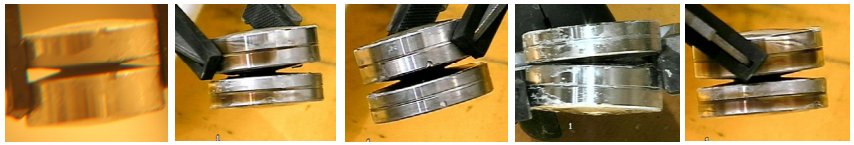

Exhibit B – Controlled experiment

- Set of RbCl targets driven to failure by increasing the beam current incrementally
- Targets were inspected for bulging after each increment
- Targets failed at 275 μA
- Thermal performance limit assumed to be 275 μA
- Supports production experience to some extent

Bulging at 270 μA

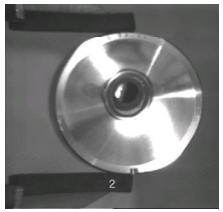

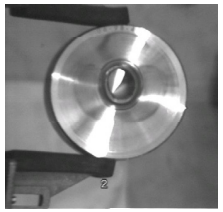

Exhibit C – Thermal analysis results

- Parallel, more theoretical effort
- Takes into account major thermal processes
  - Forced convection cooling with turbulent water
  - Conduction through solid- and molten materials
  - Natural convection in the molten part of the RbCl salt
- Results predict local boiling of the RbCl at beam currents beyond 250 μA
- Thermal performance limit around 250 μA
- Tend to support Exhibits A&B

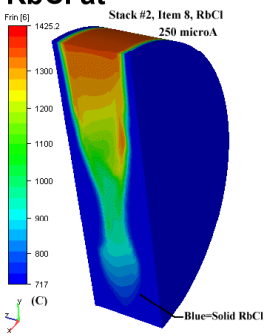

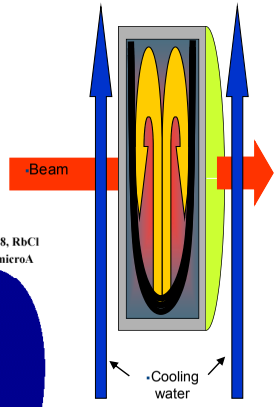

Exhibit D – Structural analysis results

- Targets fail when internal pressure cause 2.5 mm window deflection
- Structural analysis predicts an internal pressure of ~25 bar

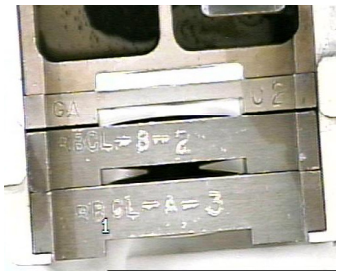

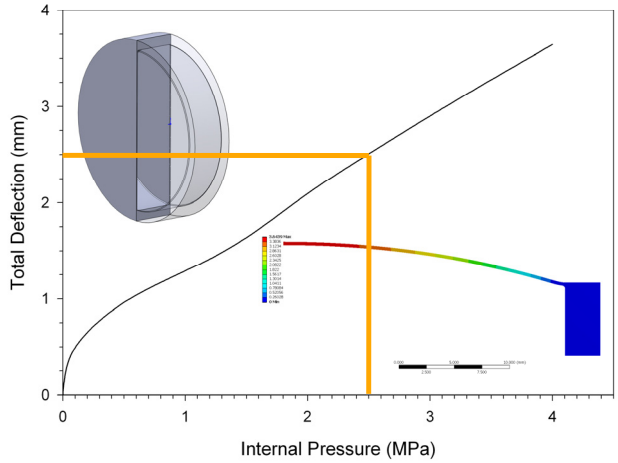

Exhibit D – Structural analysis results

- RbCl Vapour Pressure reaches 25 bar at 2200 ºC
- Much higher than suggested by Exhibits A, B & C (~1400 ºC)

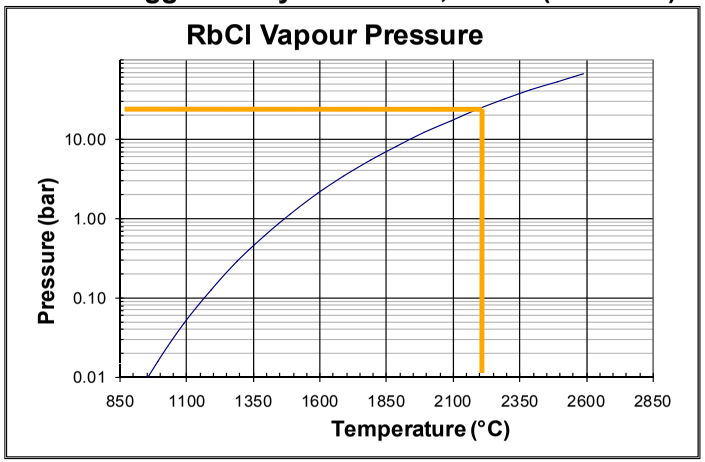

Conclusions

1) Production experience anticipates occasional target failure beyond 240 µA.
2) A controlled experimental irradiation confirms target failure at 275 µA.
3) A thermal analysis expects the maximum local internal temperature in the RbCl to exceed boiling point at 250 µA. This may be interpreted as supporting evidence for the results in 1 & 2.
4) A structural analysis of the target capsule expects target failure to occur at local internal temperatures far beyond the boiling point of RbCl. This does not correlate with the thermal analysis results.

Are we operating our RbCl targets beyond the boiling point?
How do these targets fail exactly?
Why discrepant results from the thermal and structural analysis results?
Which is more realistic?

Are we the first to routinely operate a solid-liquid-gas target?

To be continued…..

WTTC XIII – Presentation Discussions

1. RbCl vs metallic Rb
   - "Burocracy" favours RbCl
   - Why not RbF?
2. Gas sealing
   - Electron beam welding
3. Beam shape
   - Focused to 12mm
   - Rotated 5 kHz
4. RbCl changes in density
   - Solid to liquid : 30% change
   - Changes by pressure

[^{18}O]Water Target Design for Production of [^{18}F]Fluoride at High Irradiation Currents

Alex D. Givskov[1,2], **Mikael Jensen**[1]
[1]Radiation Research Division, Risø National Laboratory for Sustainable Energy, DK-4000 Roskilde, Denmark
Email: [2]algi@risoe.dtu.dk

Abstract

The current standard for [^{18}F]fluoride production is proton irradiation on a [^{18}O]water target. Heat removal is the main obstacle to achieve a higher production. The 16.5 MeV proton cyclotron at Risø has a maximum [^{18}F]fluoride production rate at an irradiation current of 55 μA. The aim of this target design is to irradiate at a proton current not below 100 μA while maintaining a [^{18}O]water volume close to 5 mL and a yield better than 80% compared with theoretical. The theoretical yield is calculated by cross section data [1] and using SRIM [2] H_2O stopping power calculation. At 55 μA the production yields 84% $\pm$ 4% of theoretical yield. This corresponds to an average of 140 GBq [^{18}F]fluoride for 1 hour of irradiation. A higher intensity beam will further reduce the efficiency of the [^{18}F]fluoride production. Still much remains in understanding the physics inside the currently used water target. However it is claimed that current water targets operating at maximum yield contain saturated steam vapor phase region(s) which are not constant in volume over time [3]. We propose a new target design which is a deep narrow cylindrical/cone shaped silver[i] target, see figure 1. The target has a depth of over 80 mm and width of about 10 mm near the target front. The width decreases as the target deepens. Its chosen shape is based on our model, which simulate the extent of the claimed steam/water matrix. This target is designed to operate at 30 bar of helium pressure and it is cooled by water at the sides and back and not by helium at the front. Introducting fins inside the target cavity will increase the [^{18}O]water-target wall surface and the heat transfer over this boundary is assumed to be the limiting factor in transfering heat from the [^{18}O]target water. Possible nucleate boiling heat transfer by conduction via convection may increase the heat conduction of up by a factor 10^2.

References

[1] E. Hess, S. Takacs, B. Scholten, F. Tarkanyi, H. H. Coenen, and S. M. Qiam. Excitation Function of the [O-18](p,n)[F-18] Nuclear Reaction from Threshold up to 30 MeV. *Radiochim. Acta 89, 357*, 2001.

[2] SRIM The Stopping and Range of Ions in Matter. Homepage: http://www.srim.org. World Wide Web.

[3] J. Michael Doster. New Cyclotron Targetry to Enhance F-18 Clinical Positron Emission Tomography. Homepage: http://www.osti.gov/bridge/servlets/purl/945375-HKLadR/945375.pdf. World Wide Web.

[i]Silver is chosen as target chamber material during this stage og modelling and prototype development, because of the good mechanical and thermal characteristics, its reasonable low price and universal availability. Once cavity design is optimized other target chamber materials will be used, i.e. noble metal plated silver.

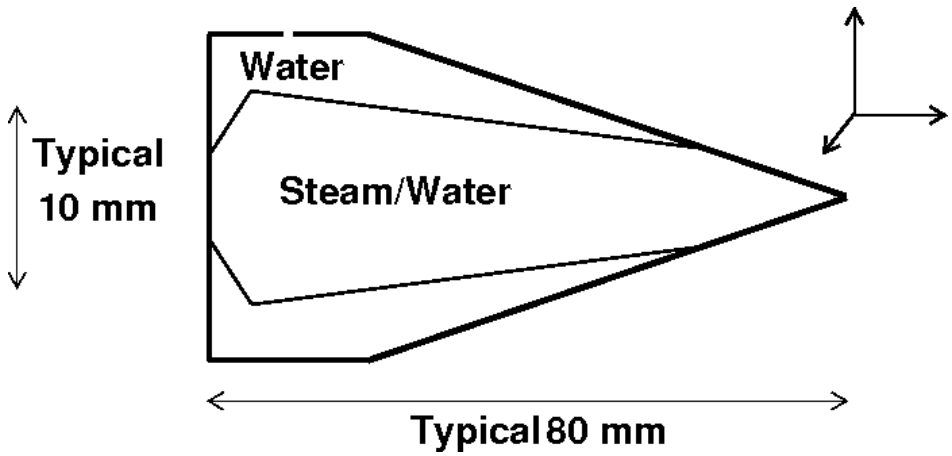

Figure 1: The target cavity of the [^{18}O]water target design is illustrated in the figure. The typical dimension of the target is 80 mm deep and 10 mm wide. A schematic extent of an assumed steam/water matrix (Steam/Water) is also shown. In the rest of the cavity is water.

[^{18}O]Water Target Design for Production of [^{18}F]Fluoride at High Irradiation Currents

Alex D. Givskov & Mikael Jensen
Hevesy Lab, Risø National Laboratory for Sustainable Energy,
DK-4000 Roskilde, Denmark.
Email: algi@risoe.dtu.dk

Poster Presentation
Tuesday 27th of July 2010 14:00
in the Niels Bohr Auditorium, Risø DTU

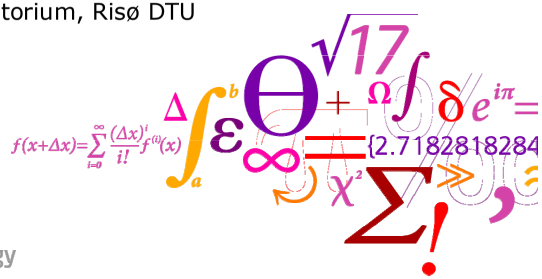

Risø DTU
National Laboratory for Sustainable Energy

The Targets

Present and new design

The Aim:

- Increase the beam current from 55 µA to **100+ µA** and maintaining high sat. yield/µA (presently 8.3 GBq/µA)

The New Taget Design:

- Deep narrow cylindrical/cone shaped target
- 30 bar (unchanged) He pressure (T_b = 234°C)
- Water density(T_b) = 0.8219 g/cm^3
- No helium cooling in front
- Max 5 mL of [^{18}O]water when filled

- What should be its dimensions?

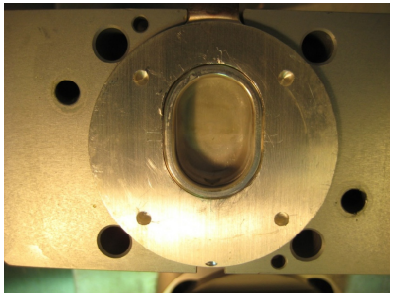

Target cavity of Risø's **present target**(s) seen from the front. Lateral extent of cavity is larger than new design, but not as deep

Established knowledge

So far …

We know:

- Liquid volume in target cavity is not constant over time

-> Target water highly governed by dynamics

- We loose production rate as increase beam current

-> Target cavity must contain steam vapor

Most likely:

A liquid phase
and
a phase of steam with water droplets
(steam/water matrix)

Where we go for a new target design?:

-> Simulation!

- Finite element analysis?
- Or can we do with less?

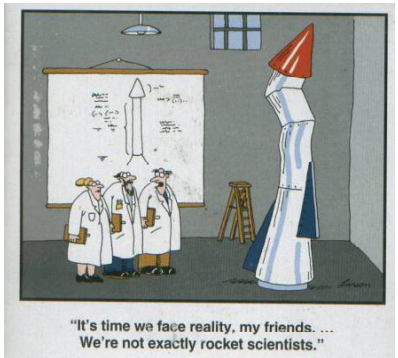

A Theoretical Phase State: Steam/Water Matrix

Fitting with Experimental Data

Consider a volume element in the target cavity:

- Initially: Water
- Irradiate -> deposit heat to the water
- Heat is transported away

At T_b:

If total heat load is transported away:

- Stays water

Else -> Phase transition

We set a value for heat removal for the entire water cavity!

-> Determines what is water and what is steam/water matrix

Constraints of the Steam/Water Matrix:

- Worst case density(T_b) close to saturated steam vapor at 30 bar (0.0150 g/cm^3) , i.e. mostly steam vapor
- The heat load **must** be transferred to the surrounding water

-> What regions have steam/water matrix?

Steam/Water Matrix

A Static Scenario

Mostly in the center of the impinging beam!

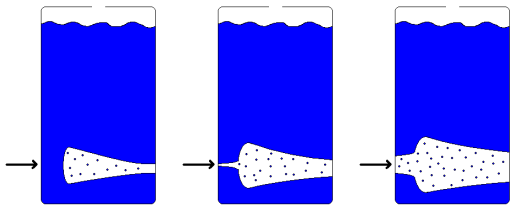

Initial guess of the extent of the steam/water matrix for different irradiation currents for Risø's present target (~55 µA and below)

White with blue droplets: Steam/Water Matrix

Blue: Water

Conditions for the Steam/Water Matrix:

- The target cavity is assumed only radially cooled
- We simulate a static target performance (the dynamics is there, but we do not calculate it!)
- A constant value for heat removal is set

-> Regions heated above **threshold** are considered steam/water matrix

- The **threshold** level: Calculated to match yields of Risø's present targets , but scaled to higher irradiation currents

Simulation of the Steam/Water Matrix

Simulation Tools and Data Used

Protons are simulated in ROOT using SRIM and cross section data

SRIM + Cross Section Data:

- SRIM H_2O stopping power calculation → Ionization, range and lateral range.
- We use desity reduction for water (ρ_{water} = 0.8219 g/cm^3) **and** a steam/water matrix ($\rho_{steam/water\ matrix}$ = 0.0150 g/cm^3)
- Cross section data from E. Hess et al. *Radiochim. Acta 89, 357, 2001*

Cern ROOT Simulation:

- Used to simulate the extent of the steam/water matrix
- An Object Orientated Data Analysis Framework. Homepage: ***http://root.cern.ch***

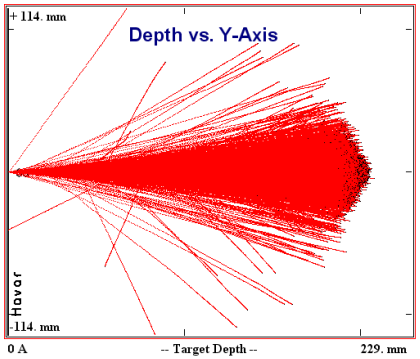

SRIM simulation of 16.5 MeV protons impinging on a 25 µA Havar, steam/water matrix. Average proton range is 195 mm.

Simulation of Heat Transfer

Out of the Steam/Water Matrix

Direction of Heat Transfer:

- Hottest in the center of the proton beam.
- Heat is transfered radially from the beam center **and** longitutionally in the steam/water matrix until it reaches the water / steam/water matrix boundary (left picture).
- At the boundary the heat is distributed to nearby water (right picture).

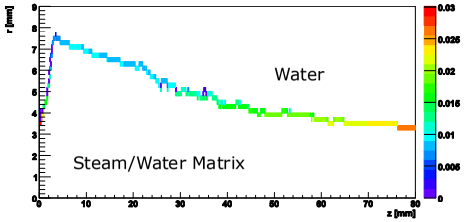

Transferred heat **to** the imminent boundary

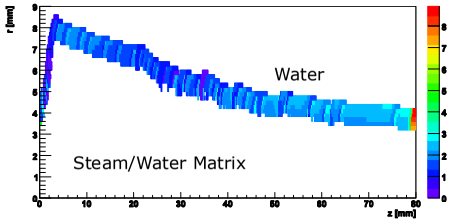

Transferred heat **from** the imminent boundary to nearby water

Simulated Results

Risø's Present Standard Target(s)

Beam current 55 µA, Depth 10 mm , 2D axial symmetric view

This matches our day in and day out yields

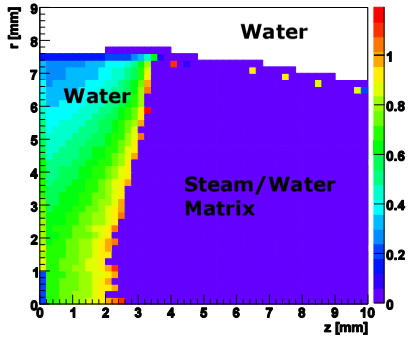

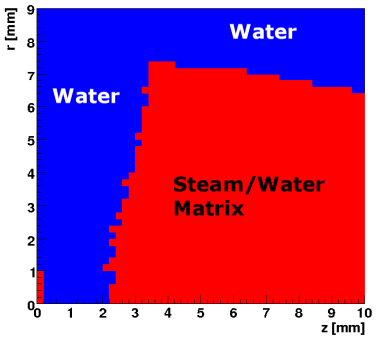

Left: Energy deposited due to ionization is transported from the water / steam/water matrix boundary

Right: Extent of the steam/water matrix (red) in the water (blue)

Simulated Results

The New Target

Beam current 100 μA, Depth 80 mm , 2D axial symmetric view
~80% of theoretical sat yield

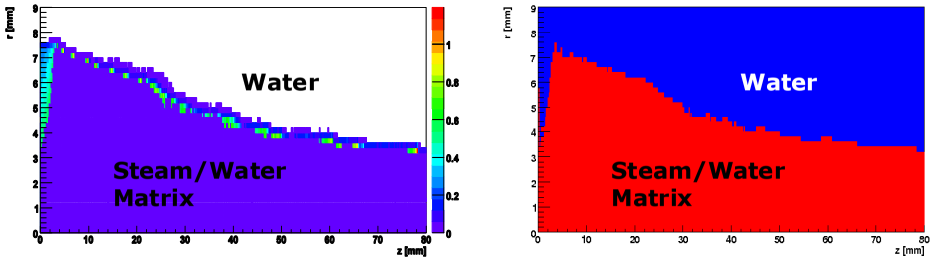

Left: Energy deposited due to ionization is transported from the water / steam/water matrix boundary

Right: Extent of the steam/water matrix (red) in the water (blue)

The New Design

A sketch

Very thin, very efficiently cooled metal surface

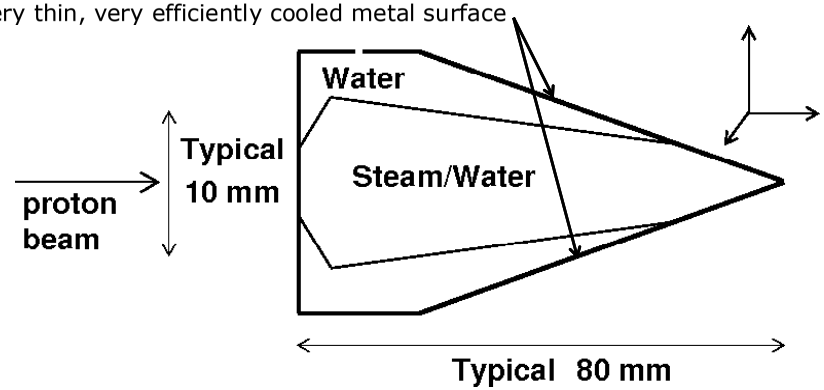

We still wait for experiments…

Thank you!

WTTC XIII – Presentation Discussions

1. Simulation results
   - Steam observed close to the target window
   - Coincident with experience
   - Why not a water mixer inside target?

Direct production of Ga-68 from proton bombardment of concentrated aqueous solutions of [Zn-68] Zinc Chloride.

Mikael Jensen, The Hevesy Laboratory, Risoe-Technical University of Denmark
kmje@risoe.dtu.dk
John Clark, University of Edinburgh, College of Medicine and Veterinary Medicine, UK
jcc240@gmail.com

Expecting a drastic increase in use of Ga-68 in the coming years, we have reconsidered the possibilities for direct production by small cyclotrons. Although the Ge-68 generator is widely available and easily used, it often does suffer problems from limited lifetime (shorter than the physical T½ of Ge-68) , high price and limited activity output. It is also our concern that a global creep from Tc-99m examinations towards Ga-68 PET-CT counterparts could rapidly exhaust the present global supply of Ge-68.

The direct production by electroplated, solid, highly enriched Zn-68(p,n)Ga-68 is well known and closely mimics the production of the blockbuster isotope Ga-67. Same target, same chemistry, just a little more energy to give the (p,2n) reaction. However the prospect of doing an enriched electroplated solid target, bombardment, etching, ion exchange separation and target material recovery chemistry for a single patient dose of Ga-68 does not seem feasible for routine use.

For this reason we have tested a “solution target”, where we bombard ZnCl2 in high concentration in water. Of course, the water does “eat up” some useful cross section and gives more stopping, but for a high yield “easy” (p,n) reaction and with a short lifetime product, this is certainly possible.
From the outset, we only had four concerns:

1. Can highly concentrated zinc chloride solutions be contained in a metal target and behind a target foil during bombardment? It is, after all, strongly acidic, and popularly used as strong soldering flux, dissolving many metal oxides.
2. Can the yield be predicted and is it high enough for routine application?
3. Will zinc remain as zinc chloride during the rather unusual conditions during proton bombardment? And will Ga-68 come out in solution from the target?
4. Can the Ga-68 be extracted rapidly from the target solution and will it be possible to reuse the enriched zinc chloride solutions directly?

We have addressed all four problems experimentally, and will report the very satisfying outcome.
As target we used a slightly modified Niobium target body (designed for F-18 production), kindly provided with very few questions by Tomas Eriksson of GE Medical Systems in Uppsala. As target foil we chose 100 micrometer thick Niobium foil, partly to degrade 16.5 MeV proton beam of our PETtrace down to more optimal (p,n) energies, partly because we wanted to lower the risk of getting foil breaks and loss of the brine solution into a routinely used cyclotron.

We have kept a piece of this Nb foil in a concentrated ZnCl2 solution for 6 months without any signs of attack, loss of luster or change of weight. The target has survived many bombardments at 5, 10 uA and a single 20 uA run. We have not yet pressurised the target beyond atmospheric, and we thus did get boiling through the target filling line at 20 uA. But pressurisation should allow higher currents. After bombardments, the target body chamber and the foil look completely untouched.

Clear ZnCl2 solutions at room temperature can be prepared with more than 3 grams of ZnCl2 to 1 gram of water. We did the early target testing with 2 grams of ZnCl2 to 1 gram of water. When testing with enriched Zn-68, we used 1 gram ZnCl2 to 1 gram water.

The cross section for Zn-68(p,n)Ga-68 is well known (F.Szelecsneyi *et al.* JARI, **49**,1005 (1998). Using this and a straight forward stopping power calculation made by SRIM (version 2008.04, J.F.Ziegler *et al 2008* WWW.SRIM.ORG) we predicted a saturation yield for 1µA of 1500 MBq for a one-to-one ZnCl2 solution. This again corresponds to 1500 MBq at EOB after 20 minutes bombardment at 5 µA.

Experimentally we found values at little higher than this (1800 MBq Ga-68 @ EOS), measured by both dose calibrator after 1 hour and by gamma spectroscopy and thus corrected for influence of other positron emitters. With pressurisation of target, higher current on target and a higher Zn concentration, yields above 10 Gbq EOS should be obtainable.

We have used a batch of Zn-68 from Campro with 99% enrichement for our target solution. The only observed radionuclic impurity (after chemical separation of the Gallium, see below) was Ga-67 (probably from the (p,2n) process), and this accounted for less than 0.1% of total activity EOB.

To extract the Ga-68 from the target solution (still having a pH around 2 after bombardment) we passed it through a preconditioned Waters C-18 sep-pak. From old literature, it is known that Gallium chloride complexes behave “lipophilic”, - but the success of this was still a pleasant surprise to us. Zinc chloride passes through while more than 90% of Ga-68 sticks on the seppak.
The seppak was washed by 2 fractions of 10 ml water to remove effectively the remaining Zinc. The primary eluate and the water washings were collected and concentrated by simple boiling up the original ZnCl2 concentration. Another successful production with same yield was done on this solution. The Ga-68 could be eluted from the seppak in a small volume of 0.1 Molar HCl. Thus, both activity extraction and target material recovery can be done rapidly and simple.

Ga-68 activity will be of limited use, if it cannot be reclaimed in more or less metal free form. The large initial load of Zinc on the column is however effectively washed out by the water fractions. Using Zn-63 and Zn-65 as indicators, the Zinc “decontamination” factor of this process is better than 5000. Other metals, like for example Iron impurities in target solution, can be more difficult to separate out by this method and should thus be avoided.

We believe that this method with some more development can be of value for local production of large activities of Ga-68 for subsequent radiopharmaceutical production. It also looks like the “solution target” with Niobium body and Niobium foil is a viable approach to a broader class of metal radioisotopes, bypassing the need for electroplating and solid targets.

"Instant Ga-68"

Direct production of Ga-68 from proton bombardment of concentrated aqueous solutions of [Zn-68] Zinc Chloride.

Mikael Jensen, The Hevesy Laboratory, Risø-DTU,Denmark kmje@risoe.dtu.dk

John Clark, University of Edinburgh, College of Medicine and Veterinary Medicine, UK jcc240@gmail.com

Why ?

Ga-68 is the PET radionuclide of the future:

It can work the " bifunctional chelator game"
It is easy to make
It is easy to get
It labels nicely (Ga+++)
It has excellent imaging
It gives low doses

You could imagine Ga-68 replacing Tc-99m f or many purposes

Zn68(p,n)Ga-68 is an excellent high yield nuclear reaction

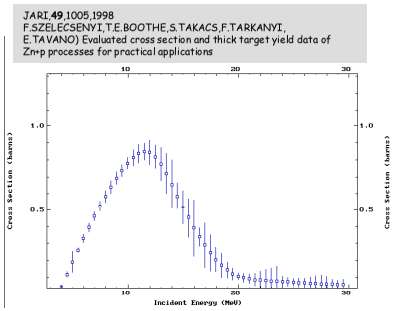

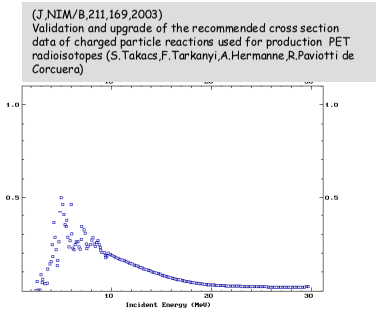

dE/dx =0.025 MeV/mg/cm2

Target nuclides/mg=9E18

0.04MeV/mg/cm2

Target nuclides/mg=3E22

Target:

4 gram of 99% enriched Zn68-Cl_2 dissolved in 4 ml of water

SRIM and EXFOR gives a saturation yield 1500 MBq/ 1μA

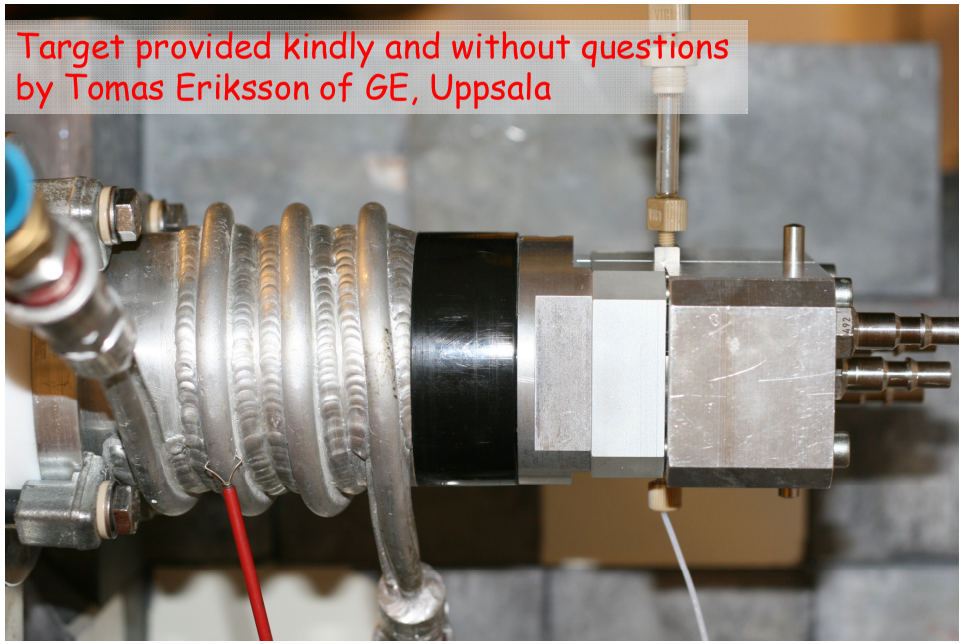

Experimental yield 1800 MBq /1μA
corresponds to 1500 MBq at EOB after 20 minutes bombardment at 5 μA.

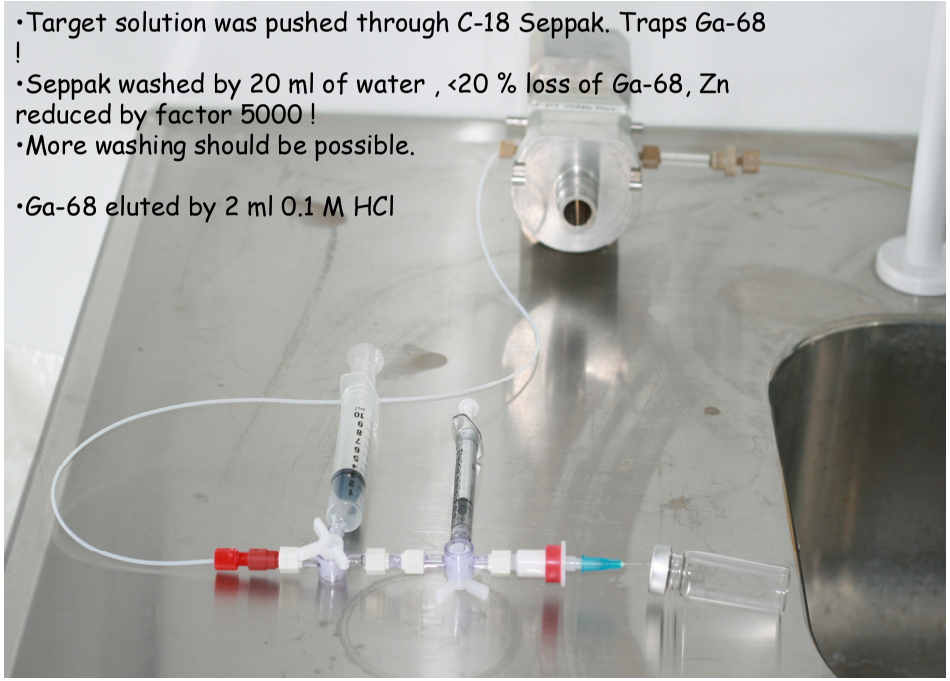

Zinc salts out in water wash,- but can be reclaimed by boiling.

We had problems with Iron,- from the Zn-68 !
(our DOTA-Octreotate turned purple!)

Target chamber and foil unchanged

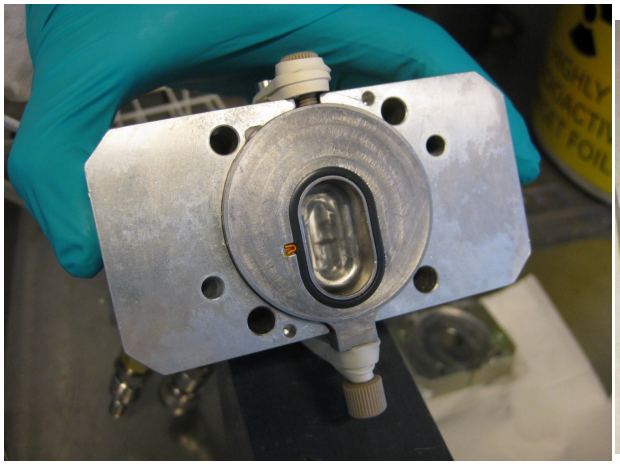

WTTC XIII – Presentation Discussions

1. Irradiation conditions and yields
   - 10uA OK; 20uA=boiling
   - 10GBq in saturation

Using the Neutron Flux from p,n Reactions for n,p Reactions on Medical Cyclotrons

Jonathan Siikanen[a,b] and Anders Sandell[b]
[a]Lund University, Medical Radiation Physics, Barngatan 2:1, 221 85 Lund, Sweden
[b]University Hospital in Lund, Radiation Physics, Klinikgatan 7, 221 85 Lund, Sweden

The formation of the isomeric pair $^{58}Co^{m,g}$ can be reached via the $^{58}Ni(n,p)$, $^{59}Co(n,2n)$, $^{59}Co(p,pn)$, $^{58}Fe(p,n)$, $^{57}Fe(d,n)$, $^{55}Mn(a,n)$, and $^{61}Ni(p,a)$ reactions. Natural nickel (68.1% ^{58}Ni) foils were placed behind a [^{18}F]Flouride water target to produce ^{58}Co[**1**] ($T_{1/2}$=70.86 d, β^+=14.9%, Eγ=811 keV, 99.4%) through the $^{58}Ni(n,p)^{58}Co$ reaction. The water target is mounted on a MC 17 Scanditronix cyclotron (15.5 MeV protons on water). To quantify the ^{58}Co activity the irradiated foils were measured after four days (after EOB) for a full conversion of the co-produced metastable state ^{58m}Co ($T_{1/2}$=9 h).

Nickel foils (~20x20 mm) with different thicknesses were placed between the water cooling tubes on the backside of the water target according to figure 3. The foils were irradiated with ejected neutrons from the $^{18}O(p,n)^{18}F$ reaction for different accumulated proton charges (µAh) in the water target.

So far, ^{58}Co-activities of about 0.1-0.15 kBq/µAh have been produced in 0.25 mm thick foils and approximately 1 kBq/µAh in a 2 mm thick foil. The ^{58}Co activities were quantified with an HPGe detector against a known 511 keV peak in same geometry. More results will be presented at the conference.

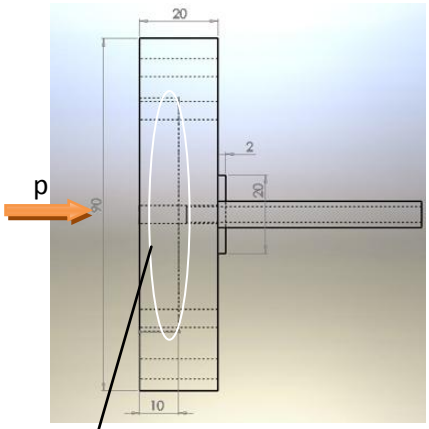

Fig 1: Backplate, side view

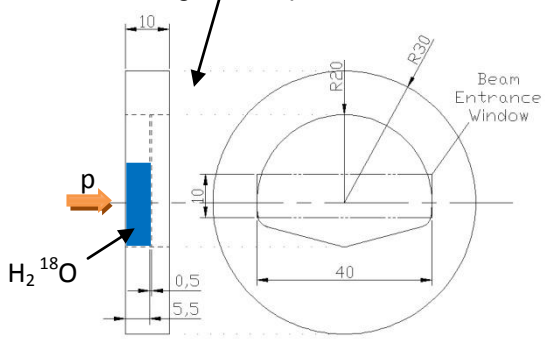

Fig 2: niobium insert

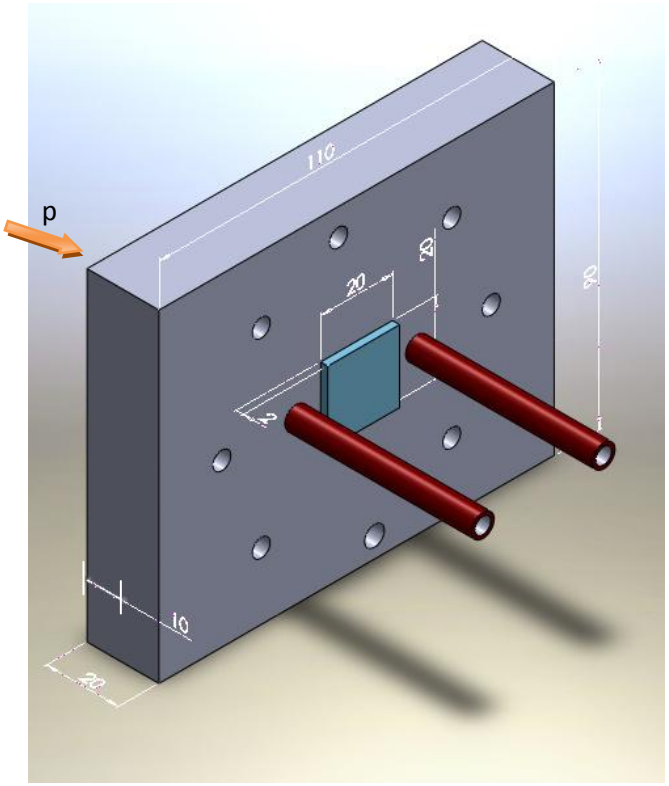

Fig 3: Backplate housing the niobium-insert with a 2 mm nickel foil on the rearside between water tubes

References:
C.E. Mellish & J.A. Payne, Nature Vol 187/275-276/1956
H.-J. Lincke, Radioanal.Nucl.Chem.,Letters 87/5/311-316/1984

Using the Neutron Flux from p,n Reactions for n,p Reactions on Medical Cyclotrons

Jonathan Siikanen[a,b] and Anders Sandell[b]
[a]Lund University, Medical Radiation Physics, Barngatan 2:1, 221 85 Lund, Sweden
[b]University Hospital in Lund, Radiation Physics, Klinikgatan 7, 221 85 Lund, Sweden

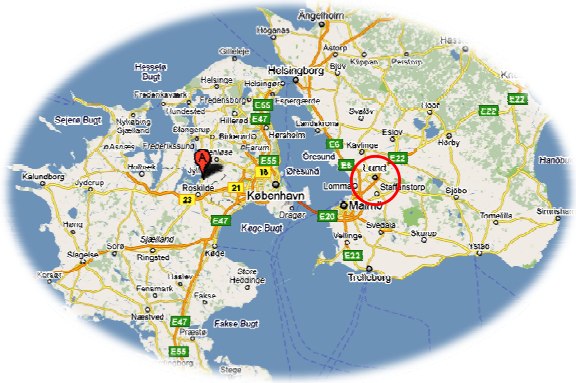

LUND UNIVERSITY

Background

- We were asked if we could produce ^{58}Co activity
- Can be used for labeling of organo metallic compounds for biomedical studies
- Available is a MC 17 Scanditronix cyclotron

Introduction

- Routes to ^{58}Co production:
  $^{59}Co_{(100\,\%)}(n,2n)$, $^{59}Co_{(100\,\%)}(p,pn)$, $^{58}Fe_{(0.28\,\%)}(p,n)$, $^{57}Fe_{(2.2\,\%)}(d,n)$, $^{55}Mn_{(100\,\%)}(a,n)$, $^{61}Ni_{(1.14\,\%)}(p,a)$ and $^{58}Ni_{(68.08\,\%)}(n,p)$
- The preferred way may be d,n on ^{57}Fe
- Requires enriched ^{57}Fe (only 2.2 % abundance) and a dedicated target
- We currently have no access to deuterons

Introduction

- Curiosity about the ejected neutrons from p,n-reactions
- For those who have routine production targets a parasitic/hitch hiking n,p-mode can be useful
- [^{18}F]Flouride target are normally the most used
- Natural $Ni_{(68.08\,\%\ Ni\text{-}58)}$ (n,p) $^{58}Co^{m,g}$

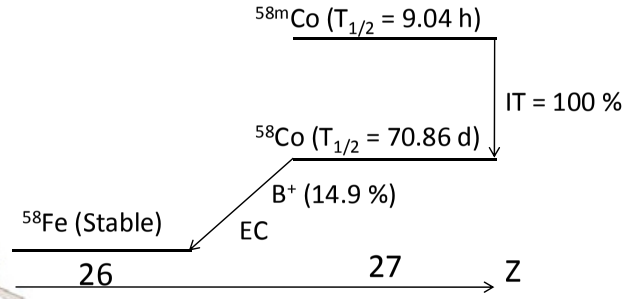

Neutron Source: Home made [^{18}F]Flouride target

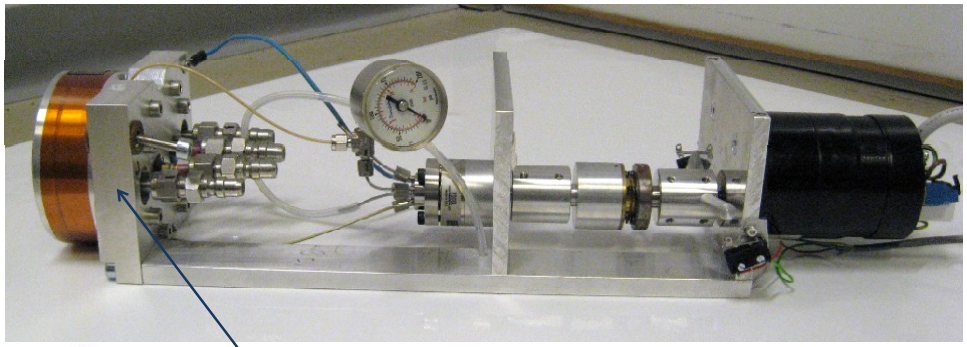

- A_sat = 8 GBq/µA at 15.5 MeV
- Runs with 45 µA p at 3.5 bars (50 psi)
- No pre pressure
- 4 ml $H_2{}^{18}O$

Advantage is the short distance to target material (Ni)

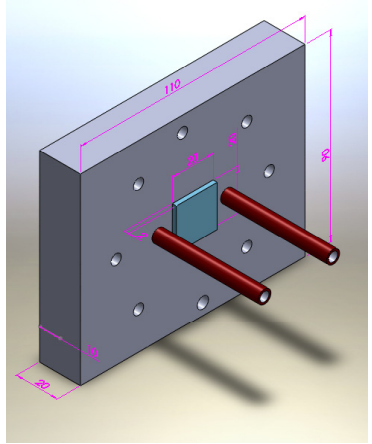

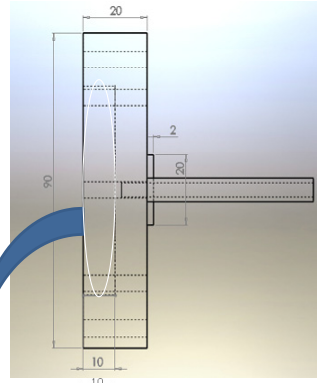

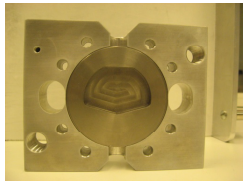

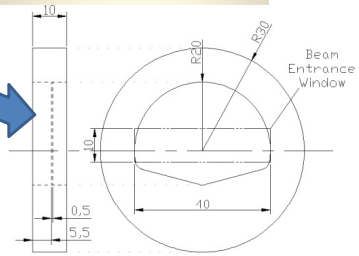

Target Design

+ No cooling
+ No dedicated target
+ No heat deposition problems

Estimation: Neutron Flux on 20x20 mm^2 nickel plate

- Estimation of the total neutron flux
- use experimental A_sat yield for the water target (~8 GBq/µA)
- At 45 µA the total n flux is > 3.6×10^{11} S^{-1} (only p,n considered)

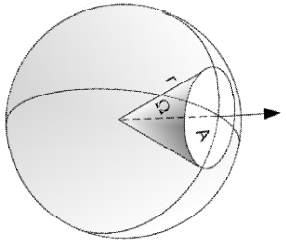

- p,n-reactions at r= 1.5-2 cm away from Ni-foil
- A=4 cm^2 covers 8-14 % of sphere area

> 3.6×10^{10} s^{-1}

L. R. Carroll, 9:th WTTC Turku Finland, 2002

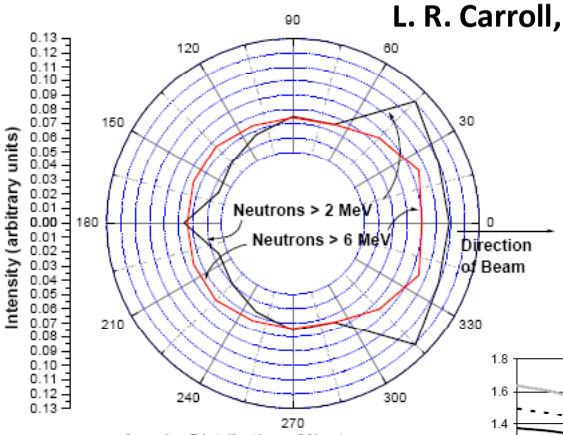

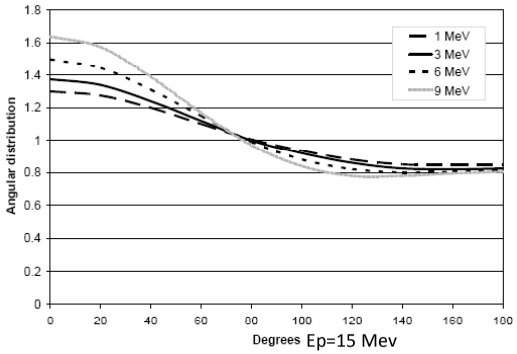

Lundgren and Ingemannson, GE, 2001 (from a dissertation by ANDREY BOSKO)

Experiments

- Nickel foils (~20x20 mm) different thicknesses and set-ups
- Two 20x20x2 Ni foils separated by 20 mm
- Irradiated with neutrons from F-18 target (about 50 µAh)

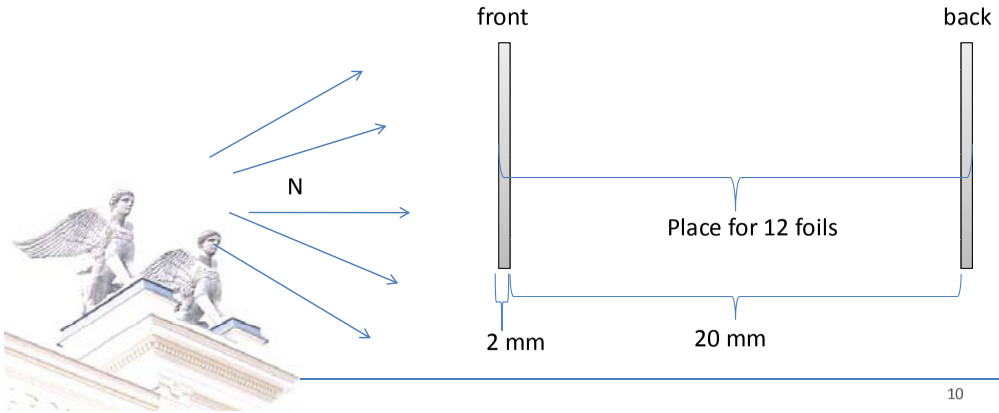

Results-Single Foils

- 0.25 mm foils give ~ 0.1-0.15 kBq/µAh
- 2 mm foils give ~ 1-1.3 kBq/µAh

$$A_{\frac{Month}{2mm\ Ni}} = 50\ \frac{\mu Ah}{day} \cdot 1\ \frac{kBq}{\mu Ah}\left(e^{-T_{1/2}\cdot 31\ d} + \cdots + e^{-T_{1/2}\cdot 1\ d}\right) \approx 1\ MBq$$

No productions Saturdays and Sundays

Results- Two Separated Foils

- Front foil ~ 1.3 kBq/µAh Back foil ~ 0.4 kBq/µAh

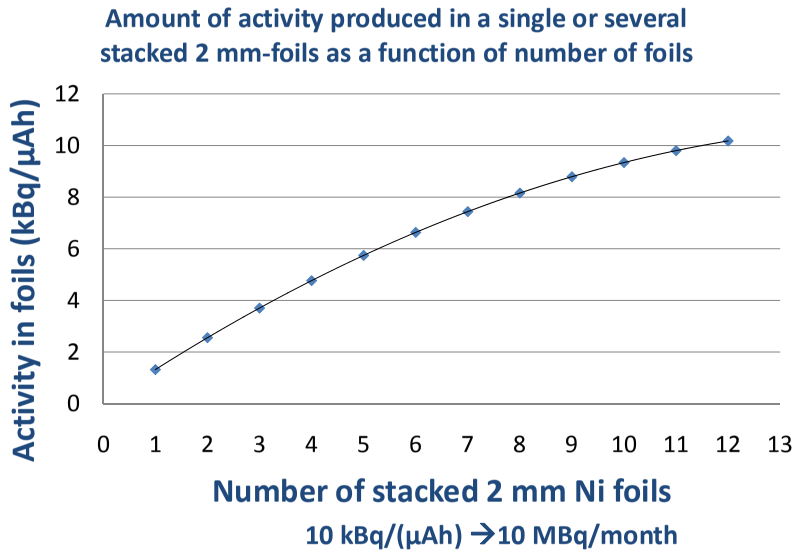

WTTC XIII – Presentation Discussions

1. Irradiation conditions
   - Ni foils and “a usual F18 target”
   - 45uA : neutron flux > 3,6 x 1011 Sr-1 (from p,n alone)

2. Other isotopes?
   - Co58, Co57, Co60

3. Thermalisation?
   - Would produce Ni59, Ni60
   - 1010 neutrons: too little

Abstract 054

Repairing water leaks in the TR-19 cyclotron: A case study in what not to do. MJ Schueller, DJ Schlyer. Medical Department, Brookhaven National Laboratory, Upton, NY 11973, USA.

In early September, 2009, a water leak opened up in one of the dees of BNL's ACSI TR-19/9 cyclotron. Attempts to patch the leak in place failed, so the dee was removed, repaired and replaced. After a week of operation, a nearly identical leak opened in the other dee. This began a chain of failures in the cyclotron, leading to approximately 8 months of down time in the human PET program at BNL. Multiple water leaks, burned internal components, and two new dees later, the machine is back to running stably.

A time sequence of events will be presented, with cascading problems, and a discussion of what steps were taken and why, with a particular focus on in house repairs that "seemed like a good idea at the time."

Some highlights:

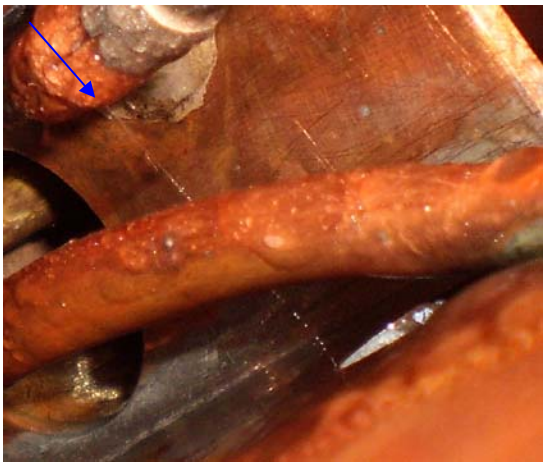

The first leak, in an elbow near the dee stem.

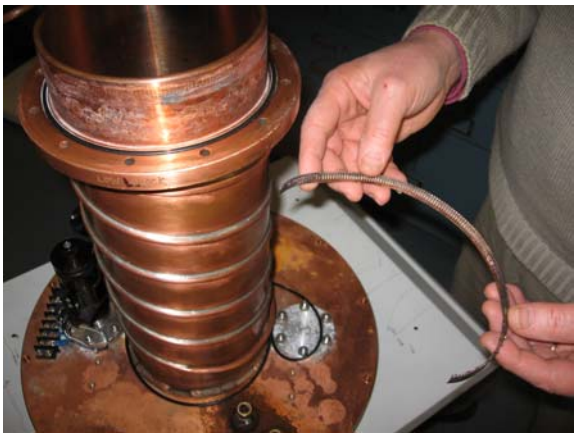

An attempt by BNL to replace burned fingerstock in situ failed. The cold solder joint held for a few weeks.

Fingerstock shouldn't look like this. When we opened the vacuum tank and smelled burned flux we knew we had a problem.

This issue was finally resolved with ACSI providing a replacement part with factory-soldered fingerstock.

The new lower dee was installed and aligned, then removed to replace the burned fingerstock. At some point, it became bent ~2mm at the dee tip. Made of 7mm copper, it did not bend back easily. The cause is unknown.

Improved High Current Liquid and Gas Targets for Cyclotron Produced Radioisotopes

AlJammaz I., AlRayyes A., Chai J., Ditroi F., Jensen M., Kivrakdal D., Nickles J., Ruth T., Schlyer D., H. Schweickert., Solin O., Winkel P., M.Haji-Saeid, M. Pillai

Coordinated Research Project, International Atomic Energy Agency
P.O. Box 100, Wagramer Straße 5, A-1400 Vienna

Radiopharmaceuticals utilizing cyclotron produced radionuclides have already been shown to be extremely valuable in basic medical research, disease diagnosis and radiotherapy. IAEA Member States world-wide have acquired more than 600 cyclotrons employed for nuclear medicine applications and the number is growing every year. In the past, cyclotrons and the related targetry systems were mainly operated by dedicated professionals situated either within academic physics research institutions, large university hospitals or industrial scale radionuclide manufacturers. However, because of the rapidly spreading use of PET and PET/CT, the number of cyclotron installations is rapidly growing and target technology needs to be appreciated by a much larger group of professionals. Although many of the new cyclotrons are primarily erected for the production of a single isotope (F-18) in the form of a single, well defined radiopharmaceutical (FDG) a sizeable fraction of these new installations have declared and started active research programs in C-11 and other non-traditional positron emitting radiotracers. As part of International Atomic Energy Agency (IAEA) activities to disseminate knowledge for member states, a three year Coordinated Research Project (CRP) was organized. The overall goal of this CRP was the development of new and reliable cyclotron targetry technology for the production of high specific radioactivity for the most widely used radionuclides.

Significant advances have been made under this CRP in the development and standardization of high power gas and liquid targets. The primary focus of this CRP was to develop targets and methods to increase specific activity, radionuclidic purity and production reliability for several radionuclides including F-18, C-11, I-123, and Rb-81/Kr-81m. These advances applied in several facilities have minimized the unnecessarily operator exposure to radiation. A particular area of interest for this group was the recovery and characterization of enriched $H_2{}^{18}O$ focusing on the reuse of the water and several important conclusions were reached. It was determined that the tritium introduced by the inevitable nuclear reactions does not pose any health physics problems either during the tracer manufacturer or during potential water reclamation. It was further determined that radionuclides produced in the metal foil during irradiation are found in the target water at very low concentrations. These impurities can be essentially eliminated by using noble metal plated foils and by the separation used for fluorine extraction from the O-18 water. In no case were the radionuclides produced in the foil found in the final product. Moreover, a survey of target maintenance procedures has been carried out and the results of this survey are reported in this CRP. In spite of these findings, the knowledge that has been gained needs to be transferred to the countries and facilities where it will help to optimize the production of radionuclides used for PET and SPECT. In this regard, a book will be published focusing on two of the most widely used target systems (F-18 and C-11) and including both fundamental knowledge and practical advice on the operation of these target systems. In addition to this book, lectures have been planned to convey both the knowledge gained in this CRP and the problems identified by the expert panel to the wider radionuclide production community with the idea that further research on these problems will benefit all the member states and the community in general.

120+ μA Single $^{18}F^{-}$ Target and Beam Port Upgrade for the RDS/Eclipse

Matthew H. Stokely[1], Thomas M. Stewart[2] and Bruce W. Wieland[1]

[1]Bruce Technologies, Inc., Chapel Hill, NC, USA, 27514
[2]D-Pace, Inc., PO Box 201, Nelson, BC, Canada, V1L 5P9

A high power (>1.3 kW) target platform has been developed for the RDS-111/Eclipse and RDS-112 cyclotrons. This fully engineered solution includes upgrades to four subsystems: target, beam port, target support unit and deionized water cooling system. This platform has been in service 6 days per week since August 2009. The target is operated within an intensity range of 100 to 120 μA with a mean ^{18}F saturation yield of 121 mCi/μA. Only 2300 μL of [^{18}O]enriched water is consumed each irradiation, resulting in one of the highest aqueous ^{18}F target power densities to date (570 W/cc). In addition to offering unprecedented performance, the single target platform greatly simplifies operation and improves the overall robustness of the cyclotron system.

The water target model CF-1000 is a conventionally pressurized cousin to the highly optimized, bottom pressurized *Thermosyphon* target. Due to the small volume of the target and the simplicity of using the OEM target support unit software, bottom pressurization was not viable. The target insert is constructed of either EB melted or arc cast tantalum or niobium, and is housed in a 6061 aluminum body. The conduction layer between cooling water and target medium is less than 0.030" for all chamber surfaces except the target window, and the flow regime is fully developed turbulent in all cooling water passages. To achieve turbulent conditions a conservative minimum flow rate of 2.5 GPM is required for this specific geometry. Window cooling is provided by nucleate boiling in the target medium.

The single target port replaces the rotating "turret" target changer on the 111/Eclipse cyclotron. The port includes a beam tube, vacuum isolation valve, water cooled graphite collimator, and vacuum roughing line. The assembly is constructed primarily of hard anodized 6061 aluminum for ruggedness and electrical isolation. Some PEEK is used sparingly in high wear areas and critical insulating layers. The ring collimator is made of very low porosity ATJ grade graphite to mitigate water absorption during target changes. This greatly shortens subsequent pump down time. The graphite is baked out at 150C under 10 microns partial vacuum prior to installation. The assembly mounts to the cyclotron steel via the carrier plate which allows for independent adjustment in x and y via small lead screws. The collimator, port and beam tube section interface with the carrier plate via a spherical bearing, which is clamped in place after alignment

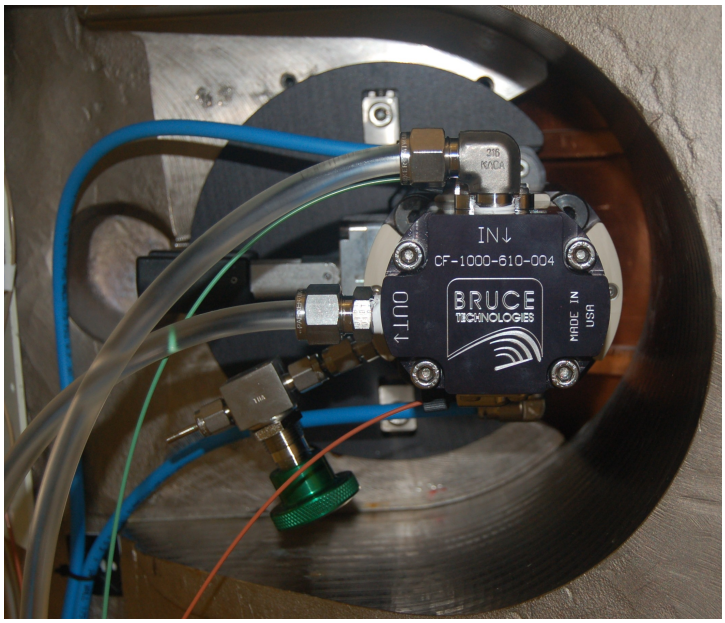

Figure 1: CF-1000 Installed on RDS-111 Cyclotron

adjustments are made. This ensures that the collimator and target are coaxial at all times and provides an extremely rigid yet easily adjustable mount.

A larger recirculation pump is installed in the water system to accommodate the additional flow requirements. To ensure that proper flow balance is maintained, adjustable distribution manifolds are installed at the recirculation pump inlet and outlet. The supply manifold has a back-pressure regulating valve to allow bypass flow. This prevents both dead heading and overpressure conditions when the cyclotron is shut down. The upgrades to the water system are a small fraction of the total system fabrication cost and critical to high performance operation.

The target support unit(TSU) geometry was redesigned to mitigate the pressure rise from elevated vapour fraction at high intensity and to improve liquid recovery. The OEM software is used to operate the TSU so the functionality remained the same. Significant improvement is made from a maintenance perspective as a much more suitable pressure transducer is used resulting in smaller hysteresis, increased robustness and a reduction in replacement cost of more than a factor of five.

The performance history of the target system is shown in figure 2. The product was used exclusively for clinical ^{18}FDG, and showed radiochemical yields consistently within specifications for both synthesis modules used. Note that the discontinuity at run number 65 is due to change in the Capintec CRC-15PET dose calibrator settings. This is the result of a technical bulletin issued by Capintec in 2009.

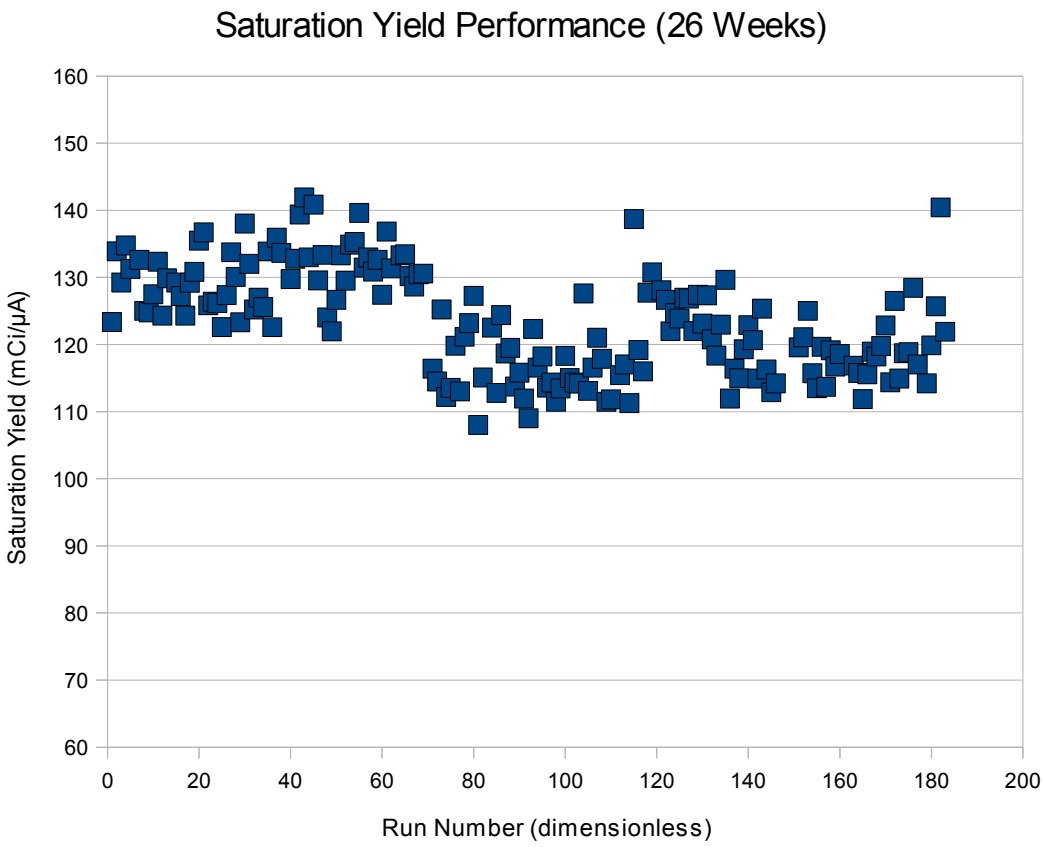

Figure 2: Operational Performance from DV3

AUTHOR INDEX

TOPIC INDEX

Risø DTU is the National Laboratory for Sustainable Energy. Our research focuses on development of energy technologies and systems with minimal effect on climate, and contributes to innovation, education and policy. Risø has large experimental facilities and interdisciplinary research environments, and includes the national centre for nuclear technologies.

Risø DTU
National Laboratory for Sustainable Energy
Technical University of Denmark

Frederiksborgvej 399
PO Box 49
DK-4000 Roskilde
Denmark
Phone +45 4677 4677
Fax +45 4677 5688

www.risoe.dtu.dk